The design and synthesis of drug-like trypanosome alternative oxidase inhibitors for the treatment of African trypanosomiasis

Ryan West

Submitted for the degree of Doctor of Philosophy

University of Sussex

August 2018

I hereby declare that this thesis has not been and will not be, submitted in whole or in part to another University for the award of any other degree.

……

Acknowledgements

I would like to thank my supervisors Professor Simon Ward and Professor John Atack for their help, encouragement and enthusiasm. You have made my PhD a thoroughly enjoyable and challenging experience and have enabled me to develop into an independent, free-thinking scientist. I am grateful to the BBSRC and Novartis for funding this research project.

I would like to thank my industrial supervisors Dr. Paul Smith, Dr. Jan Jiricek and Dr. Srinivasa Rao, for all their input and guidance to aid the progression of this project. I'd like to thank Novartis for hosting me in their research labs in Emeryville, California and especially thank Debjani Patra, Nila Johnson and Rima Palkar for teaching me how to culture *T. b. brucei* parasites and for generating parasite inhibition data for all my compounds. I'd also like to thank Tom Kirrane and Michael Turner, for helping me get set up in the chemistry labs and helping me make my time there productive.

I am extremely grateful to the members (past and present) of the Sussex Drug Discovery Centre - special thanks to Trevor Askwith, Gareth Williams, Sarah Walker, Dawn Field, Lucas Kraft, Chloe Koulouris, James Noble and Tori Miller for teaching me practical biochemistry over the course of my project. It has been a pleasure working with you all. Special thanks to Lewis Pennicott, it has been fantastic to chat medicinal and synthetic chemistry with you over the past four years; Ben Wahab, I've learnt so much computer aided drug design with your help; Mark Honey and Tristan Reuillon, it has been great working with you, I've even enjoyed being challenged by the synthetic and medicinal chemistry problem sessions that you ran; Tom Cunningham, thank you for all of your efforts in helping synthesise some of these TAO inhibitors, I wish you well in your future endeavours. The rest of the chemistry team, Kam Bala, Alex Ashall-Kelly, Scott Henderson, Marco Derudas, Michael Paradowski, Mo Benchkouran, Oran O'Doherty, Katie Duffel it has been a joy working with you all.

Finally, I'd like to thank my wonderful family for their support, Mum, Dad, Hayley, Craig, Felicity, Antonia and Elouisa, along with Drifter and Merlin. I'd especially like to thank my fiancée Katie for your love and help getting me through these past four years, I look forward to our future together.

Abstract

Trypanosome alternative oxidase (TAO) is the sole terminal oxidase responsible for the aerobic respiration of the parasite *T. b. brucei*. Specific strains of this parasite cause the neglected tropical disease Human African trypanosomiasis (HAT), and thus TAO is an interesting target for the potential treatment of this disease.

Inhibition of TAO with the natural product inhibitors colletochlorin B or ascofuranone has been shown to clear infections of *T. b. brucei* in mice at high concentrations. However, these natural product inhibitors contain undesirable chemical functionality and have poor physicochemical properties, preventing adequate drug exposure to effectively treat HAT.

Robust protocols for the expression and purification of recombinant TAO were developed, which enabled the development of biochemical assays to identify inhibitors of TAO function. Single point inhibition screening of the Medicines Malaria Venture 'kinetoplastid collection' of 400 compounds identified a range of micro-molar inhibitors of TAO.

A program of chemical optimisation was carried out around the natural product inhibitor colletochlorin B, with the aim to improve the physicochemical properties and retain inhibitory potency against TAO. The structure activity relationships generated over the course of this exploration identified a dependency on high lipophilicity to retain potent TAO inhibition. The TAO inhibitors synthesised were also assessed for parasite growth inhibition and mammalian cell cytotoxicity to correlate inhibition data with cellular efficacy, in collaboration with Novartis. The physicochemical properties of these novel compounds showed improvement over the natural product colletochlorin B and prompted further assessment of leading compounds in advanced parasite kill kinetic and parasite clearance assays at Novartis. The data generated in these assays for compounds synthesised in this thesis determined that TAO inhibition results in a trypanostatic response, and not a preferred trypanocidal response in *T. b. brucei.*

Abbreviations

-ve	Negative
+ve	Positive
°C	Degree Celcius
δ	Chemical shift
δ	Difference
Δ	Heat
µ	micro
Å	Angstrom
A_{278}	Absorbance at 278 nm
AAT	African animal trypanosomiasis
ADP	Adenosine diphosphate
AF	Ascofuranone
ALA (A)	Alanine
AOX	Alternative oxidase
AQP	Aquaporin transporter
ArBr	Aromatic bromide
ARG (R)	Arginine
ASN (N)	Asparagine
ATP	Adenosine triphosphate
B.C.	Before Christ
BBB	Blood brain barrier
Bn	Benzyl
BTEAT	Benzyl triethylammonium tribromide
BTMAT	Benzyl trimethylammonium tribromide
C10E8	Octaethylene glycol monodecylether

CAR	Central African Republic
CATT	Card aggultination test for trypanosomiasis
CC_{50}	Half maximal cytotoxic concentration
CCB	Colletochlorin B
CNS	Central nervous system
CNS-MPO	Central nervous system multi-parameter optimisation
CSF	Cerebrospinal fluid
CYP	Cytochrome P450 oxidase
CYS	Cysteine
Da	Dalton
DALY	Disability adjusted life years
DBU	1,8-Diazabicyclo[5.4.0]undec-7-ene
DDM	n-Dodecyl β-D-maltoside
Deoxofluor®	Bis(2-methoxyethyl)aminosulfur Trifluoride
DHAP	Dihydroxy acetone phosphate
DMF	*N,N*-dimethyl formamide
DMSO	Dimethyl sulfoxide
DNA	Deoxyribonucleic acid
DNDi	Drugs for neglected diseases initiative
E	Enzyme
E	Glutamic acid
EC_{50}	Half maximal efficacious concentration
E. coli	*Escherichia coli*
EI	Electron ionisation
ES	Enzyme substrate complex
ESI	Electrospray ionisation

Et	Ethyl
Et_2O	Diethyl ether
EtOH	Ethanol
F	Fraction absorbed
FAD	Flavin adenine dinucleotide
FIND	Foundation for innovative new diagnostics
FPLC	Fast protein liquid chromatography
FT	Flow through
g	gram
g	gravity
G3P	Glycerol-3-phosphate
GK	Glycerol kinase
GLN (Q)	Glutamine
GPCR	G-protein coupled receptor
GPDH	Glycerol phosphate dehydrogenase
GPI	Glycosyl-phosphatidylinositol
GSH	Glutathione
h	hour
HAT	Human African trypanosomiasis
HATU	O-(7-azabenzotriazole-1-yl)-1,1,3,3-tetramethyluronium hexafluorophosphate
HBA	Hydrogen bond acceptor
HBD	Hydrogen bond donor
HepG2	Hepatocellular carcinoma cell line
HMBC	Heteronuclear multiple bond correlation spectroscopy
HPLC	High performance liquid chromatography
HSQC	Heteronuclear single quantum correlation spectroscopy

Hz	Hertz
IC_{50}	Half maximal inhibitory concentration
IMAC	Immobilised metal affinity chromatography
i.p.	Intraperitoneal injection
IPA	2-propanol
IPTG	Isopropyl-β-D-1-thiogalactopyranoside
IR	Infra-red
kDa	Kilodaltons
kDNA	Kinetoplastid DNA
K_M	Michaelis-Menten constant
L	Litre
LB	Lysogeny broth
LCMS	Liquid chromatography mass spectrometry
LEU (L)	Leucine
LLE	Lipophilic ligand efficiancy
M	Molar (moles per Litre)
m	Meter
m	Meta
Me	Methyl
MeCN	Acetonitrile
MeOH	Methanol
mg	Milligram
min	Minute
mL	Millilitre
mM	Millimolar
MMV	Medicines for malaria venture

MOA	Mechanism of action
mol	Mole
MPO	Multi-parameter optimisation
mRNA	Messenger RNA
MS	Mass spectrometry
Mwt	Molecular weight
n	Nano
NAD^+	Nicotinamide adenine dinucleotide
NBS	*N*-bromosuccinimide
NCS	*N*-chlorosuccinimide
NECT	Nifurtimox Eflornithine combination therapy
NHC	*N*-heterocyclic carbene
nm	Nanometer
NMP	1-Methyl-2-pyrrolidinione
NMR	Nuclear magnetic resonance
NMT	*N*-myristoyl transferase
NOE	Nuclear Overhauser effect
NOESY	Nuclear Overhauser effect spectroscopy
NTR	Nitro reductase
o	Ortho
OD_{600}	Optical density, measured at 600 nm
OG	*n*-Octylglucoside
OPLS3	Optimised potentials for liquid simulations
p	Para
P	Product
P2	Aminopurine transporter

p.o.	*Per os* (oral delivery)
PAR2	Protease activator receptor 2
PDB	Protein data bank
P-gp	P-glycoprotein
Ph	Phenyl
PHE (F)	Phenylalanine
ppm	parts per million
PSA	Polar surface area
PVDF	Polyvinylidene fluoride
Q1	1-ubiquinol
Q9	9-ubiquinol
rcf	Relative centrifugal force
RNAi	RNA interference
RO5	Rule of 5
RuPhos	2-Dicyclohexylphosphino-2',6'-diisopropoxybiphenyl
s	Seconds
S	Substrate
SAR	Structure activity relationship
s. d.	Standard deviation
SDDC	Sussex drug discovery centre
SDS-PAGE	Sodium dodecyl sulphate polyacrylamide gel electrophoresis
SEM	Standard error of mean
SHAM	Salicyl hydroxamic acid
t	Time
TAO	Trypanosome alternative oxidase
T. b. b.	*Trypanosoma brucei brucei*

TBD	1,5,7-Triazabicyclo[4.4.0]dec-5-ene
TBST	Tris buffered saline
TCEP	Tris(2-carboxyethyl)phosphine hydrochloride
TEA	Triethylamine
TFA	Trifluoroacetic acid
TFAA	Trifluoroacetic acid anhydride
THF	Tetrahydrofuran
THP	Tetrahydropyran#
THR (T)	Threonine
TMS-Cl	Chloro(trimethyl)silane
TMS-I	Iodo(trimethyl)silane
t_R	Retention time
Tris	Trisamine, 2-amino-2-hydroxylmethyl-propane-1,3-diol
TYR (Y)	Tyrosine
UPLC	Ultra performance liquid chromatography
UV	Ultraviolet
V	Velocity
V	Volt
VAL (V)	Valine
V_{max}	Maximal velocity
VSG	Variant surface glycoprotein
v/v	volume / volume
WHO	World health organisation
w/v	weight / volume

Index of Figures

Index of Tables

Table of Contents

Chapter 1

Chapter 1 - Introduction

1.1 The diseases

Human African trypanosomiasis (HAT), also known as African sleeping sickness, and African animal trypanosomiasis (AAT), are caused by the protozoan trypanosome parasite *Trypanosoma brucei* (Figure 1).[1] The earliest documented description of the disease dates back to Egypt in the 2nd millennium B.C. Further records of the disease in Africa have been identified from the middle ages.[2] It was first proposed by David Livingstone that 'Nagana' (now known as AAT) was transmitted by Tsetse flies in 1852; however, it wasn't until the late 19th century that the infection of *Trypanosoma brucei* was shown to cause AAT. Sir David Bruce showed that AAT was transmitted by the Tsetse fly vector in the early 20th century.[2,3] Further inspection of HAT patient samples by both Dutton and Castellani in 1902 showed the presence of trypanosomes, which were attributed to the cause of the disease.[4]

Figure 1 - *Trypanosoma spp.* parasites in blood smear from a patient with African trypanosomiasis.[5]

1.1.1 Human African trypanosomiasis

HAT is prevalent in sub Saharan Africa and in the most recent figures available from 2012 there were 20,000 estimated cases with an at risk population of 60 million.[1] In 2000 it was estimated that 1.34 million disability adjusted life years (DALY's) are lost to HAT annually.[6]

Two strains of the parasite, *Trypanosoma brucei gambiense* and *T. b. rhodesiense,* are responsible for HAT. *T. b. gambiense* is estimated to be responsible for 95% of cases endemic

in Western and Central Africa. The remaining cases of HAT are attributed to the *T. b. rhodesiense* strain which is prevalent in Eastern and Southern Africa.[1] The two strains have differences in epidemiology, symptoms and progression of the disease.

The disease has two stages: the first is haemo-lymphatic, which then progresses into the second meningo-encephalitic stage where more severe symptoms present themselves.[7] After initial contraction of HAT a chancre (a primary sore or ulcer) may appear at the sight of infection. Stage one disease symptoms include intermittent fever, headaches, itching and musculoskeletal pain. Enlargement of the cervical lymph nodes are also common, referred to as Winterbottom's sign. The second stage of the disease arises once the trypanosomes traverse into the central nervous system (CNS), which causes neurological symptoms. Sleeping dysfunction arises from the disruption of the circadian rhythm.[8] Sensory disorders and tremor are also often observed. The disease progresses to coma and death resulting from organ haemorrhage if left untreated.[7]

Diagnosis of the disease is not straightforward, relying on serological and parasitological screening. Samples from aspirated lymph nodes or blood are used to diagnose stage one of the disease. Diagnosis of stage 2 of the disease requires cerebrospinal fluid (CSF) samples taken from lumbar puncture.[1] Samples are analysed using the card agglutination test for trypanosomiasis (CATT) originally developed by Magnus *et al.* in 1978.[9] The CATT diagnosis is used to detect *T. b. gambiense* specific antibodies from the blood, serum or CSF fluid of patients. Positive identification of specific antibodies is then confirmed by parasitological screening. An updated thermostable version of the CATT detection antibodies has recently been developed.[10] The test is also only available for *T. b. gambiense*; *T. b. rhodesiense* diagnosis continues to rely on parasitological screening. The non-profit Foundation for Innovative New Diagnostics (FIND) is working with The World Health Organisation (WHO) to more accurately determine levels of HAT. Early diagnosis improves treatment for HAT and can identify areas at high risk for preventative measures. Reported cases of HAT in the Democratic Republic of Congo are now below 4,000, the lowest levels observed for 75

years.[11] Global annual cases are estimated to be 20,000. Currently, screening for HAT is not carried out in Nigeria[12] or Ghana and the environment is too unstable to carry out effective screening in the Central African Republic (CAR).[13] Improved diagnostic devices are now available for *T. b. gambiense* HAT,[14] facilitating future screening campaigns for the disease.

T. b. rhodesiense causes an acute disease progressing to stage two within a few weeks of transmission. Infection from *T. b. gambiense* progresses more slowly, developing to the second stage nine months to two years post infection.[1] This has been attributed to the greater number of trypanosomes being present in *T. b. rhodesiense* infection over *T. b. gambiense*.[7] Without treatment HAT is considered fatal;[15] existing therapies require complicated, prolonged administration of compounds that have poor pharmacokinetic and CNS penetration properties, or are drugs that are highly toxic resulting in unacceptable side effects.[16]

1.1.2 African animal Trypanosomiasis

Trypanosomal diseases are also observed in other vertebrates and referred to as Nagana or AAT. Cattle and other livestock are the most frequently infected animals due to the feeding patterns of Tsetse flies. AAT in domestic animals is observed as a wasting disease; animals appear extremely thin, have anaemia and are in general poor condition. AAT is often fatal without intervention for domestic animals. *Trypanosoma* infections have also been observed in a range of wild animals. However, wild animals are less affected by the trypanosome and have developed some evolutionary trypanotolerance.[17]

A larger range of *Trypanosoma* species are responsible for AAT; the most common are *T. b. spp., T. vivax* and *T. congolense.* AAT parasites are not only detected in Africa; *T. vivax* is also found across South and Central America along with areas of the Caribbean that do not have Tsetse flies, where it is thought to be transmitted mechanically by other biting insects.[2,18] *T. evansi* has been identified in areas of Vietnam following an investigation into a human case, where infected cattle were identified as the source of the parasite.[19]

In Africa it is estimated that the economic burden of AAT in cattle loss alone is 1 to 1.2 billion US dollars per year.[20] The extra cost of reduced productivity of livestock, and in treating infected animals along with preventative measures in affected regions of farming is also a detriment of the disease.[20] The infected animal populace also provides a reservoir of *T. b. rhodesiense,* from which HAT can be contracted in a zoonotic manner.[1]

Diagnosis of AAT is also through parasitological investigation from blood smears taken from animals that show symptoms of anaemia and emaciation. Confirmation of trypanosome infection and species is often carried out by antibody analysis or xenodiagnoses.[21,22] Current attempts to control AAT consist of Tsetse fly traps and spray on livestock insecticides.[1,7,23] Tsetse habitat removal has also been employed as a means of controlling infection rates with some success, along with a range of veterinary treatments and prophylactics.[24]

1.1.3 *Trypanosoma brucei* spp.

Protozoa are a varied group of eukaryotic unicellular organisms that have been sub divided into 8 phyla.[25] Trypanosoma are of the Kinetoplastea class of Euglenozoa as they contain a kinetoplast, a circular structure of mitochondrial DNA,[26] located at the base of the flagellum, a whip like organelle used for propulsion.[27] One of the first recorded observations of flagellated protozoan blood parasites was by Gruby in 1843, whilst microscopically studying the blood from a frog.[28] 170 years of further research and study have given a detailed perspective of the trypanosome life cycle and biology.

Trypanosoma b. spp. (all *Trypanosoma brucei* species) have a complex life cycle (Figure 2), where adaptations in metabolism and immune evasion are vital for the survival and transmission of the parasite. Metacyclic trypomastigotes are initially injected into the mammalian host from a Tsetse blood meal. Once in the mammalian blood stream, they transform into long slender bloodstream trypomastigotes that rely on glycolysis for respiration. No evidence of a functional tricarboxylic acid cycle or respiratory chain has been observed.[29] Trypanosomes multiply asexually by binary fission to increase parasite load in

the host, and can move throughout blood and tissue. Some trypanosomes differentiate into short stumpy trypomastigotes which can then be ingested by another Tsetse fly taking a blood meal from an infected mammal. Once in the Tsetse mid gut the trypanosome sheds its variant surface glycoprotein (VSG) coat, replacing its coat with glycosyl phosphatidylinositol (GPI)-anchored procyclins differentiating into procyclic trypomastigotes. This change is thought to be a response to the increased levels of proteases and higher pH of the Tsetse gut.[30] Once the procyclic trypomastigote is established the trypanosome can migrate to the anterior of the midgut. The respiratory pathways of procyclic trypanosomes also change; the mitochondrion re-establishes tricarboxylic acid cycle enzymes and electron transport chain complexes.[29] The procyclic forms elongate into mesocyclic trypomastigotes where upon they transfer to the Tsetse salivary glands and develop into epimastigotes, attaching to the epithelium of the salivary gland wall with their flagella. Over time these epimastigotes transform into short infective metacyclic trypomastigotes regenerating their VSG coat ready for reinfection of a mammalian host and completing their life cycle (Figure 2).

Trypanosomes have adapted to thrive in both Tsetse and mammalian hosts. Without intervention the parasites can multiply to high levels and are one of only a few parasites that are able to cross into the CNS. It has been shown that trypanosomes can exploit host derived inflammatory mediators such as cytokines, chemokines and adhesion molecules to move across membranes.[31,32] Trypanosomes also generate cysteine proteases that interact with protease-activator receptor 2 (PAR2) a G-coupled protein coupled receptor (GPCR) on endothelial cells that can increase blood brain barrier (BBB) permeability.[31,33] Once a host has been infected, trypanosomes are able to avoid host immune response by antigenic variation of their VSG coat.[34,35] The VSG coating not only enables the variation of antigen expression on the surface of the trypanosome but also sterically blocks recognition of other surface proteins. The extent to which trypanosomes are able to alter their surface protein expression makes vaccine development extremely difficult,[36] highlighting the need for identification of safe treatments for HAT and AAT.

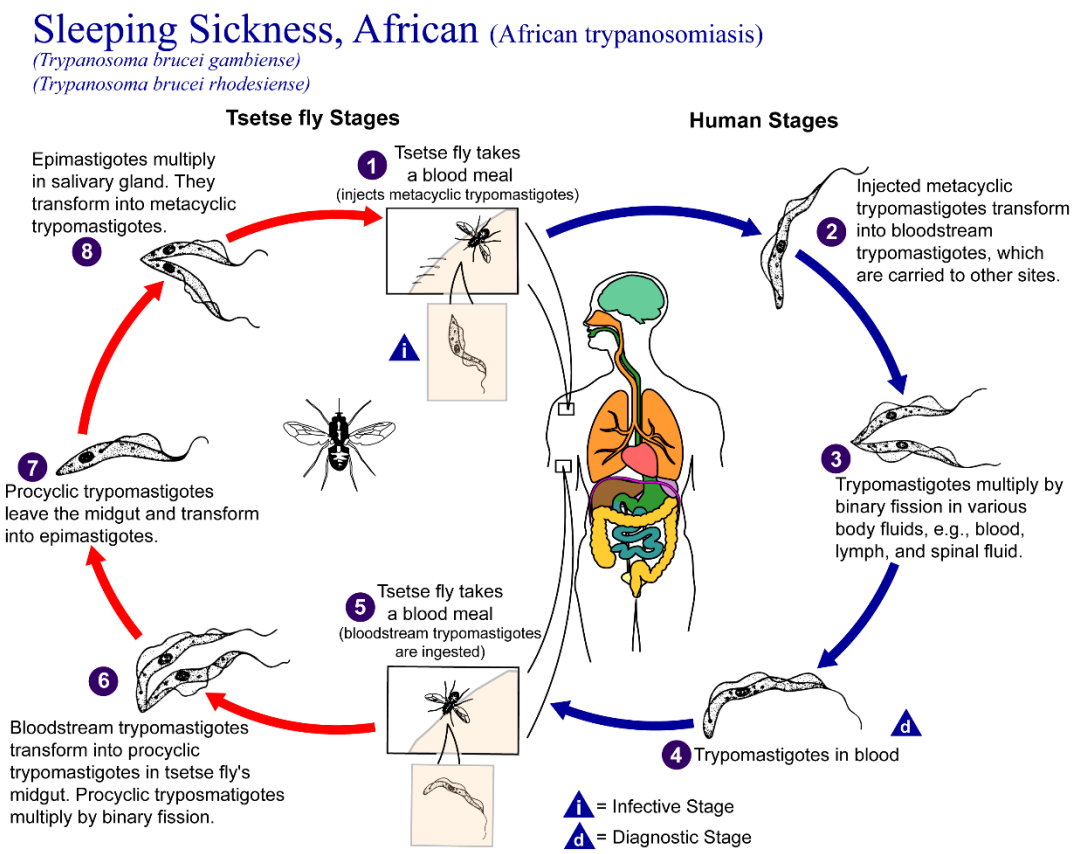

Figure 2 - Trypanosoma life cycle – image from Centre for Disease Control and Prevention – copyright free Public Health Image Library (image 3418), da Silva and Moser 2003[37]

1.2 Current Treatments

1.2.1 Human African trypanosomiasis

There are currently four treatments for HAT, their use is specific to the strain of infective parasite and the stage of disease diagnosis. Many of the drugs used to treat the disease have undesirable side effects or complex requirements for administration summarised in Table 1.

Suramin

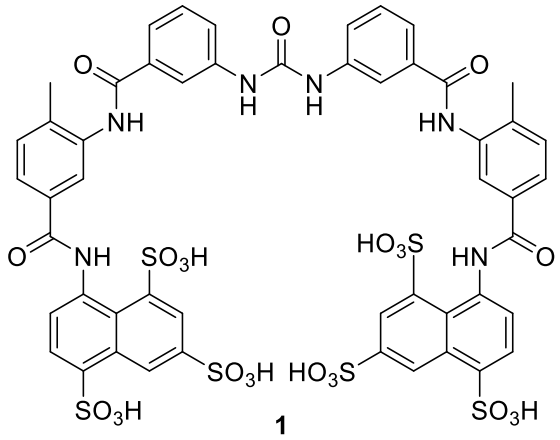

Figure 3 – Suramin – **1**

Suramin (**1** - Figure 3) has been the standard of care for Stage 1 HAT caused by *T. b. rhodesiense* since 1920. Suramin was developed by Bayer in the early 1900s, following the discovery of the trypanocidal activity of the azo dye trypan red.[38] It is administered as five intravenous injections of 20 mg/kg every 5 - 7 days.[39] Mild kidney toxicity and fever are often seen as adverse reactions.[16] It has a very high topological polar surface area (PSA) of 430 Å^2 that is likely responsible for its inability to pass through biological membranes. In general compounds with PSA above 140 Å^2 have been shown to be poorly passively permeable through biological membranes.[40] This could be the reason that Suramin has low oral bioavailability and requires intravenous administration. It could also give reason for why the treatment isn't effective against stage two of the disease, where the parasite has penetrated the CNS.[41,42] It has been shown that Suramin binds to serum proteins and is taken up by

trypanosomes *via* receptor mediated endocytosis.[43] Suramin is a multi-action kinase and dehydrogenase inhibitor, inhibiting all glycolytic enzymes in trypanosomes more potently than the mammalian counterparts leading to its efficacy and observed local toxicity upon dosing.[44] Resistance to suramin has not been frequently observed, supporting the idea that it inhibits trypanosomes *via* multiple mechanisms of action (MOA).[45]

Melarsoprol

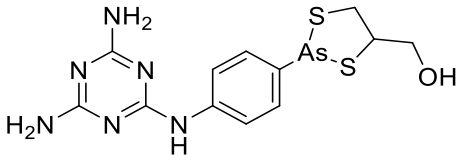

2

Figure 4 – Melarsoprol - **2**

The meningo-encephalitic stage of HAT caused by *T. b. rhodesiense,* can presently only be effectively treated with Melarsoprol (**2** - Figure - 4). It is administered intravenously at 3.6 mg/kg in a series of 4 injections separated by at least one week.[39] Organo-arsenides have inherently high levels of toxicity. 5 – 10% of patients treated with the Melarsoprol suffer brain injury as a side effect, and in these patients the side effects cause are fatal for approximately 1 – 5%.[46] Melarsoprol inhibits phosphofructokinase, leading to the depletion of fructose-2,6-bisphosphate that halts the activity of pyruvate kinase, glycolysis and overall energy production within the trypanosome.[47] Uptake of Melarsoprol has been shown to be *via* the P2 amino purine transporter. Melarsoprol resistance can occur in trypanosome strains that lack this transporter.[48,49] Increasing incidences of resistance have been observed and in the early 2000's failure rates for Melarsoprol treatment had reached 20 – 30%.[50]

Pentamidine

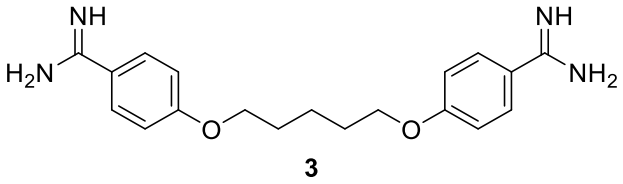

3

Figure 5 – Pentamidine - **3**

Stage 1 HAT caused by *T. b. gambiense* is currently treated with a drug developed in the early 1940s, Pentamidine (**3** - Figure 5). It has been shown that Pentamidine has an affinity for kinetoplast DNA.[51] The mechanism of trypanocidal activity of this molecule is as yet unknown. It is hypothesised that pentamidine could have an inhibitory effect on mRNA trans-splicing, although further experimental evidence is needed to prove this MOA.[45] The uptake of pentamidine has also been shown to rely on P2 amino purine and two other similar transporters. Resistance against the drug has been observed and attributed to trypanosomes having reduced drug uptake.[49,52] Pentamidine is administered *via* a deep muscular injection at 4 mg/kg in 7 - 10 daily injections, as it is not orally bioavailable. However, intravenous administration results in hypotensive side effects.[16,39] The drug has limited effect against the second stage of the disease linked to its poor BBB permeability.[45] Work into generating a pro-drug of di-amidine compounds has been undertaken by Midgley *et al.* to improve drug permeability and tissue distribution, particularly CNS penetration.[53] Although improvements in permeability and CNS penetration were achieved, compound related toxicity was observed in *in vivo* experiments and further studies into alternative dosing regimens resulted in a lack of efficacy in primate models.[54,55]

Eflornithine

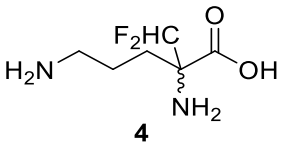

4

Figure 6 – Eflornithine – **4**

Stage 2 HAT caused by *T. b. gambiense,* is now standardly treated with a Nifurtimox (**5**), Eflornithine (**4**) combination therapy (NECT) replacing the use of Melarsoprol (**2**). Eflornithine (**4** - Figure 6) is a suicide inhibitor of orthinine decarboxylase, an enzyme that catalyses the first stage of polyamine biosynthesis.[56] Polyamines are important for cell growth, proliferation, chromatin structure and stability and are involved in gene expression, along with ion channel regulation.[57] In particular, the polyamine spermidine plays an important role in trypanosomes, conjugating two molecules of glutathione into trypanothione which regulates redox homeostasis in the parasite.[58] Resistance to Eflornithine has been observed and attributed to decreases in the expression of specific amino acid transporters that are responsible for trypanosomal uptake of drug.[59] Eflornithine is administered *via* slow intravenous infusion of 200 mg/kg every 12 h for 7 days with oral administration of nifurtimox.[39] Side effects most frequently observed are bone marrow toxicity and related anaemia.[60]

Nifurtimox

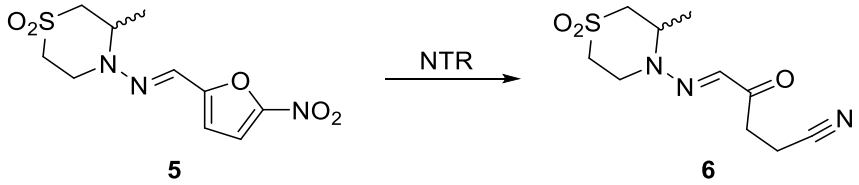

5 **6**

Figure 7 – Nifurtimox – **5** and structure of active trypanocide **6**

Nifurtimox (**5** - Figure 7) has been used for the past 40 years to treat another trypanosomatid infection, Chagas disease, and has only recently been approved for stage 2, *T. b. gambiense* HAT infections in a combination therapy with Eflornithine (**4**).[61] Nifurtimox is administered

orally 5 mg/kg every 8 h for 10 days. It was originally thought to induce oxidative stress in the parasite; however, recent data reported by Hall *et al.* has shown that Nifurtimox is acting as a pro-drug. Nifurtimox is reduced by a trypanosomal nitro-reductase (NTR) resulting in an open-chain nitrile product (**6**) that is cytotoxic and able to inhibit trypanosomal growth.[62] The combination therapy has proven highly successful, with a cure rate of 95% in studies of patients with meningo-encephaltic HAT caused by *T. b. gambiense.*[61] The combination therapy provides an improved adverse event profile over Eflornithine alone, and reduces treatment time from 2 weeks to 1.[63] Unfortunately, due to the rapid regeneration of orthinine decarboxylase in *T. b. rhodesiense*, Eflornithine has limited utility against this strain and thus the combination therapy is only recommended for *T. b. gambiense* infections.[64]

Table 1 - Summary of HAT treatments

Treatment	Date introduced	Parasite Species	Stage of disease	Dosing	Pros	Cons
Suramin (**1**)	1922	*T. b. rhodesiense*	1	5 x 20 mg/kg every 5 - 7 d	No resistant strains observed	Stage 1 only Kidney toxicity
Pentamidine (**3**)	1940's	*T. b. gambiense*	1	4 mg/kg, 7 – 10 daily injections	Effective at treating stage 1 *T. b. gambiense*	Stage 1 only Resistant strains observed
Melarsoprol (**2**)	1949	*T. b. rhodesiense*	2	4 x 3.6 mg/kg every 7 d	Effective against stage 2 of both *T. b. gambiense* and *T. b. rhodesiense*	High toxicity (0.5% clinical fatalities) Resistant strains observed Failures in the clinic
NECT (**5** + **4**)	2009	*T. b. gambiense*	2	(E) 200 mg/kg 12 h infusion for 7 d (N) 5 mg/kg every 8 h 10 d	Effective against stage 2	Prolonged administration for 1 week. Requires cold storage and transport.

New Approaches

The issues with current HAT treatment options summarised in table 1 have resulted in the involvement of the Drugs for Neglected Diseases initiative (DNDi), a non-profit public private partnership organisation. The DNDi collaborates with a variety of academic and industrial partners to aid the identification and progression of new HAT treatments. They have released an ideal product profile for new compounds (Table - 2), to ensure that potential treatments have the desired features to improve upon the options presently available in the clinic.[65] There are currently two treatments under investigation, in phase I and phase II/III clinical trials, for *T. b. gambiense* HAT with the DNDi.[66]

Table 2 - DNDi product profile criteria[65]

Ideal	Acceptable: improvement to current
Effective against stage 1 & 2	Effective against stage 1 & 2 (used stage 2 only)
Broad Spectrum (*T. b. gambiense* and *T. b. rhodesiense*)	Efficacy against *T. b. gambiense* only
Clinical efficacy > 95% at 18 months follow up	
Effective in melarsoprol refractory patients	
< 0.1% drug related mortality	< 1% drug related mortality
Safe during pregnancy and for lactating women	
Adult and paediatric formulations	
No monitoring for Adverse Events	Weekly simple lab testing (field testing)
< 7 d oral dosing, once daily (Directly Observed Treatment)	10 d oral dosing (up to three times a day)
< 7 d i.m. once daily	10 d i.m. once daily
Stability in Zone 4 (tropical – heat and humidity) for > 3 years	Stability in Zone 4 for > 12 months
Trypanocidal	
Multitarget	Unique target (but not uptake *via* P2-transporter only)
< 30 € per patient drug course	< 100 € per patient drug course

Fexinidazole

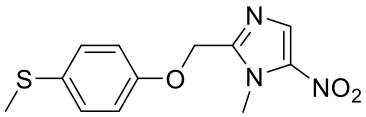

7

Figure 8 – Fexinidazole – **7**

Fexinidazole (**7** - Figure 8) was developed in the 1970s as a broad spectrum antimicrobial agent, in the 1980s was shown to have *in vivo* efficacy against stage 2, *T. b. brucei* infections in mice.[67] Further evaluation demonstrated that the compound was acting as a pro-drug, being oxidised by a range of CYP450 enzymes to both the sulfone and sulfoxide active metabolites.[68] Although its mode of action is unknown, there are other nitro-hetero-aromatic chemotherapeutics that function as pro-drugs, being reduced by target nitro-reductases to generate cytotoxic agents.[69] Some evidence supporting this has been reported. A down regulation in the nitro-reductive enzymatic pathway of *T. b. brucei*, has been shown to increase parasite resistance to both Fexinidazole and Nifurtimox.[70] An extensive pharmacokinetic study has shown that Fexinidazole is suitable for oral administration. The parent compound is well absorbed and the active metabolites show long half-lives *in vivo*, producing cures in infected rodents after treatment with 100 mg/kg dosed daily for four days.[71] The compound was recently assessed in a phase II/III non-inferiority to NECT clinical trial, dosing orally for 10 days. The results from the trial showed that a similar efficacy to NECT could be achieved with Fexinidazole, with no observed differences in treatment-emergent adverse events between the two arms of the study.[72] Fexinidazole is currently undergoing a phase IIIb study investigating home administration of the treatment compared to hospitalisation and dosing (ClinicalTrials.gov Identifier: NCT03025789).[73]

SCYX-7158 Oxaborole

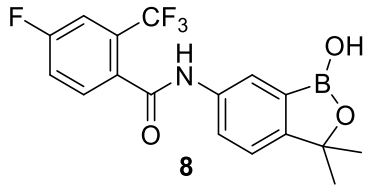

8

Figure 9 - SCYX-7158 Oxaborole - **8**

The other compound currently being assessed in the clinic is the oxaborole SCYX-7158 (**7** – Figure - 9). The oxaborole chemotype was first identified from a phenotypic screen against *T. b. brucei*. Further work to optimise the pharmacokinetic properties of these compounds identified SCYX-7158 as having improved blood brain barrier permeability. This compound was progressed to *in vivo* pharmacokinetic models, where good oral bioavailability and long duration were observed.[74–76] *In vivo* mouse models indicated that a daily oral dose of 25 mg/kg for seven days could clear a stage 2 infection of *T. b. brucei* in mice.[75] The compound's MOA is unknown, but initial work has shown that removal of the boron atom resulted in complete loss of activity.[75] The compound was successfully assessed in healthy volunteers in a phase I clinical trial; clinicaltrials.gov NCT01533961.[77] A follow-up efficacy phase II/III study is currently underway; ClinicalTrials.gov Identifier: NCT03087955.[78]

NMT inhibitors

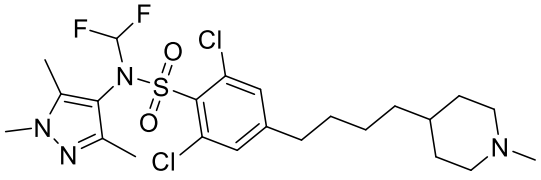

9

Figure 10 - NMT Pyrazole sulphonamide – **9**

Further to this, academic and industrial groups have looked into new effective treatments for HAT either *via* inhibiting parasite specific targets or through phenotypic screening.[44,79,88,89,80–87] N-myristoyltransferase (NMT) has been shown to be vital for

trypanosome survival by RNA interference (RNAi) gene knockdown experiments.[90] The screening of a diverse set of 62,000 compounds by the Dundee Drug Discovery Unit identified a class of pyrazole sulfonamide compounds that were inhibitors of this enzyme. They were shown to inhibit trypanosome growth, resulting in clearance of a haemo-lymphatic infection in mice.[83] Further work to optimise BBB penetration resulted in compounds with reduced polar surface area (PSA) and increased lipophilicity (**9** – Figure 10). Although CNS penetration was achieved with these compounds, off target activity attributed to poor tolerability in *in vivo* studies and further work on this target has been halted.[81]

1.2.2 African animal trypanosomiasis

Homidium

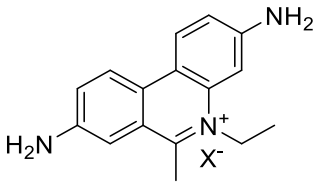

10

Figure 11 – Homidium – **10**

The phenanthridine homidium bromide or chloride (**10** - Figure 11) can be used to clear *T. vivax, T. b. spp and T. congolense* infections in cattle and horses.[91] Homidium has some action as a prophylactic, preventing trypanosomal infections for 17 to 19 weeks.[92] The phenanthridine chemical class was first identified as a trypanocide in 1938 by Browning *et al.*[93] Further development of the class by Watkins and Woolfe identified that the quaternary ethyl phenanthridine Homidium was much less toxic than the quaternary methyl phenanthridine Dimidium.[94] It has been suggested that the phenanthridine class of trypanocides act by intercalating DNA base pairs.[95] Unfortunately, decades of administration of Homidium as a prophylactic has given rise to parasite resistance to the phenanthridine class of trypanocides.[96,97] Due to the lack of sufficient research funding into these agrochemicals, minimal exploration of the resistance mechanisms in AAT has been performed. Resistant cases of AAT are alternatively treated with Isometamidium or Diminazene. Homidium is now only used as a prophylactic due to observed resistance, and not a treatment option for AAT.[98]

Diminazene

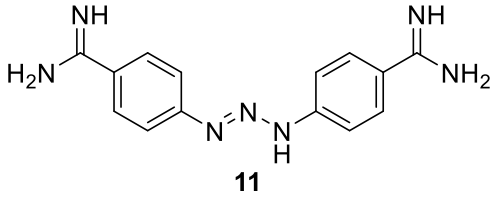

11

Figure 12 – Diminazene – **11**

Diminazene (**11** - Figure 12) is a diamidine trypanocide, similar in structure to HAT treatment pentamidine.[99] The compound was introduced to treat infections of *T. congolense, T. b.* spp*., T. vivax* and babesiasis in 1955.[100] It is not recommended for use as a prophylactic, as evidence has shown that its protective effect is short lived, lasting for a maximum of 7 days as it is excreted rapidly.[99] Diminazene acts on binding to kinetoplastid DNA (kDNA) by direct interaction with sites rich in thymine-adenine base pairs.[101] This blocks the generation of RNA primers and inhibits kDNA replication. The inhibition of mitochondrial type II topoisomerase has also been shown with Diminazene, which also prevents the replication of DNA.[51] Resistance to Diminazene is seen to a lesser extent than to Homidium (**10**) and Isometamidium (**12**). The resistance mechanism is unknown but postulated to be similar to that of Pentamidine, as it is reliant on P2 amino transport for uptake by the trypanosome.[102]

Isometamidium

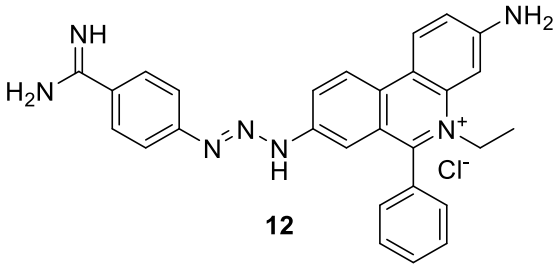

12

Figure 13 – Isometamidium – **12**

Isometamidium (ISM) (**12** - Figure 13), also a phenanthridine, is currently used as both a prophylactic and treatment for cattle infections of *T. congolense, T. vivax* and *T. b.* spp. The

compound was designed in 1961, combining the moieties from the earlier discovered trypanocides, Homidium and Diminazene. ISM has been shown to localise in kinetoplastid DNA to a greater extent than homidium.[103] The compound can act prophylactically for up to 5 months against single or multiple *T. congolense* challenges.[104] However, resistance to ISM by *T. congolense* has also been observed. Studies carried out by Delespaux *et al.* identified a mutated trypanosomal protein structurally similar to ABC-multidrug transporters as a potential mechanism for resistance, that resulted in reduced parasite concentrations.[105]

Quninapyramine

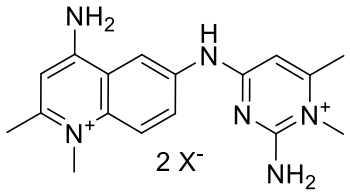

13

Figure 14 – Quinapyramine – **13**

Quinapyramine, otherwise known as antrycide (**13** Figure 14), was discovered in 1950 by Curd and Davey as a curative and prophylactic treatment for *T. congolense* and *T. Evansi.*[106] It is widely used for infections in horses, camels, pigs and dogs due to its cross reactivity against a wide range of trypanosome species: *T. vivax; T. congolense; T. evansi; T. b. spp.; T. equiperdum*; and *T. simiae.* It has been shown that Quinapyramine inhibits trypanosome cell division but not nuclear division and is not itself a trypanocide.[107,108] The trypanostatic response that it produces presumably enables the host immune system to clear the parasite infection.[109,110] Resistance to Quinapyramine has been observed in some species of trypanosome, but the mechanisms behind this resistance are not well understood.[111]

New Approaches

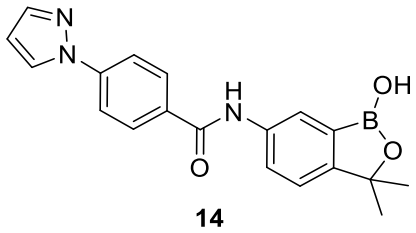

14

Figure 15 - AN7973 Oxaborole – **14**

Following on from the apparent success of the oxaborole compound SCYX-7158 as a potential treatment option for HAT, the pharmaceutical company Anacor have initiated investigations into identifying an oxaborole compound suitable for treating AAT. One compound (AN7973 – **14** - Figure 15) was identified to successfully clear *T. congolense* infections *in vivo*. Efficacy against the *T.* vivax strain was however not observed at a similar dosage. Further follow up compounds are currently being explored to increase potency against other strains, specifically *T. vivax*, and efforts to improve metabolic stability are ongoing.[112]

1.3 Trypanosome alternative oxidase

1.3.1 The Enzyme

Despite the recent successes of new approaches towards the treatment of HAT and AAT, alternative therapies are needed that are less toxic to the host and that provide efficacy in emerging drug-resistant parasite strains. Targeting a trypanocidal mechanism that is absent in the host is an attractive strategy to avoid on target host selectivity issues. Trypanosome alternative oxidase (TAO) has been investigated by a variety of academic groups as a potential target for treating HAT.[84–87] The oxidase is the sole aerobic respiratory terminal oxidase located in the mitochondria of the long slender bloodstream form of *T. b.* spp.[113,114]

TAO oxidises two equivalents of ubiquinol to ubiquinone, in tandem carrying out the four-electron reduction of oxygen to water. Ubiquinone is reduced by mitochondrial glycerol

phosphate dehydrogenase (GPDH) as part of the glycerol phosphate oxidase system to generate flavin adenine dinucleotide (FAD). FAD is further utilised by GPDH to recycle glycerol-3-phosphate (G3P) back into dihydroxyacetone phosphate (DHAP). DHAP can return to the glycolytic pathway *via* triose phosphate isomerase to enable the net generation of 2 molecules of ATP from each molecule of glucose. ATP is essential for cellular respiration, survival and growth of the trypanosome (Red - Figure 16).[113,115,116] A compensatory anaerobic mechanism of glycolysis is available to *T. b. brucei* (Blue – Figure 16). Under anaerobic conditions, or when TAO is inhibited, G3P accumulates from the breakdown of fructose-1,6-biphosphate. Under these increased concentrations of G3P, glycerol kinase (GK) can function in reverse to allow the generation of 1 molecule of ATP, facilitating survival of the parasite. It has been shown that once glycerol, the by-product from the reverse action of GK, accumulates trypanosome viability is compromised and parasites are unable to survive.[116] Both the aerobic and anaerobic pathways exploit DHAP and cytosolic glycerol phosphate dehydrogenase to generate NAD^+, which is also essential for parasite energy production and function (Figure 16).

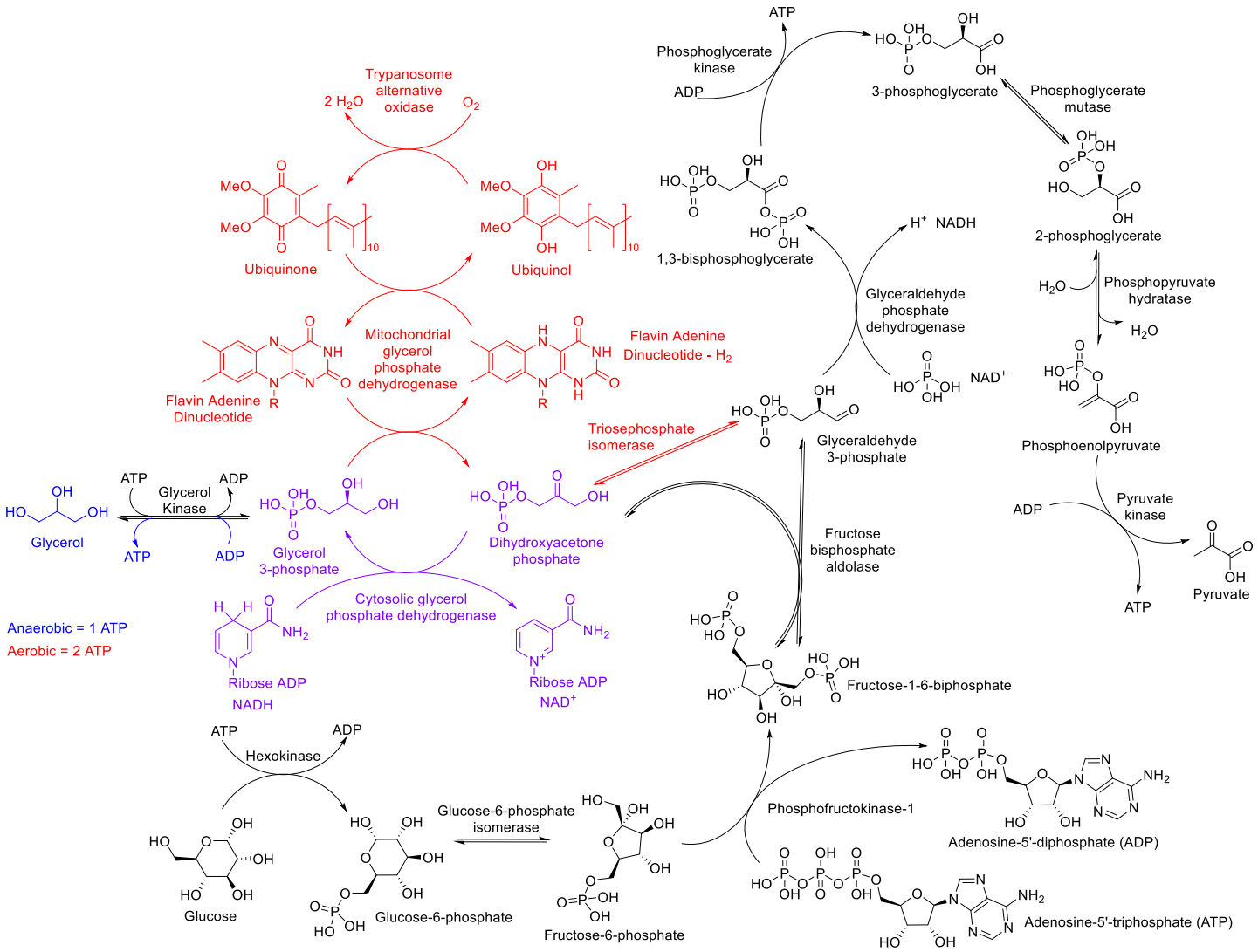

Figure 16 - Glycolysis in *T. b. brucei*

TAO was first observed by Chaudhuri *et al.* whilst immunoblotting mitochondrial proteins isolated from *T. b. brucei*, with monoclonal and polyclonal antibodies that had been raised against voodoo lily and skunk cabbage plant alternative oxidases.[117] Two protein bands were identified, one a dimer that could only be denatured under rigorous conditions. Further immunofluorescent studies with the monoclonal antibody showed the protein to be localised in the mitochondria of the blood stage long slender trypomastigote and absent in the insect stage procyclic trypomastigote. The mitochondrial fraction of the trypanosomes was solubilised with lauryl maltoside or NP-40 detergents and fractionated by size exclusion gel filtration chromatography to isolate the ~33 kDa protein where TAO enzymatic activity resided.[117] In a follow up article from the same group cDNA cloning was carried out and the mitochondrial protein was characterised as TAO.[118]

Ever since the identification of TAO, and the establishment of its role in trypanosome respiration,[113,119] the generation of purified recombinant trypanosome alternative oxidase (rTAO) was a focus of many groups.[120–124] The identification of the gene responsible for the expression of TAO provided the means to clone and transfect DNA into *E. coli* for the recombinant expression of functionally active TAO.[118,122] Different groups have used various *E. coli* expression strains to aid production of active protein. Initially, haem deficient *E. coli* that lack cytochrome respiratory pathways were employed to show that alternative oxidase expression could rescue the growth of bacteria and that this could be fully inhibited with the plant alternative oxidase inhibitor salicylhydroxamic acid (Figure 20).[118] Some groups continued to use haem deficient *E. coli* for recombinant expression of rTAO to remove the interference of other ubiquinol oxidases, primarily cytochrome bo and bd, useful for assessing the enzymatic activity of crude membrane fractions.[120,122,125] Other groups have preferred to express rTAO in standard BL21 *E. coli* strains. Primarily, these were used to reduce the effect of disruption of the succinate dehydrogenase complex, a key haem enzyme that regulates the energy metabolism of *E. coli*, that had resulted in poor growth of the *E. coli* cultures and prevented their large scale preparation.[126]

Further screening and optimisation of detergents for the efficient solubilisation of *E. coli* inner membrane fractions and rTAO protein has enabled the isolation of larger amounts of

higher purity protein.[120] This has facilitated biochemical studies of the enzyme and the generation of robust functional assays. It has also enabled structure elucidation through protein crystallisation to a 2.9 Å resolution, and hence structure based design of new inhibitors.[127–130]

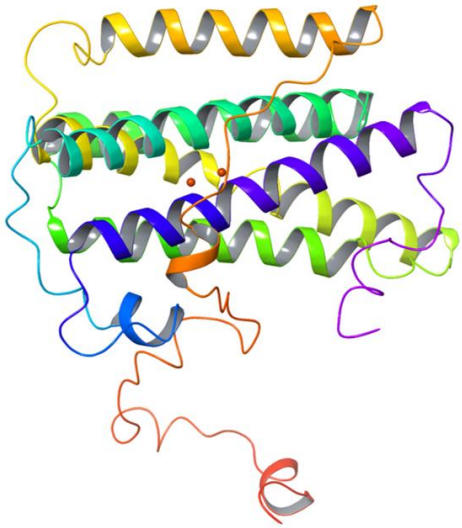

Figure 17 - Trypanosome alternative oxidase - Apo structure adapted from crystal structure PDB 3VV9, Shiba *et al.*[129], coloured by helix using Maestro – Schrodinger drug discovery suite

The structure of TAO has 6 α-helices 4 of which are arranged in a 4-α-helix bundle that accommodates the di-iron catalytic centre of the enzyme (Figure 17 - orange spheres).[131] The di-iron nature of TAO was first elucidated by inductively coupled plasma mass spectrometry (ICP-MS) experiments that confirmed the initial suggestion of a di-iron centre from the similar electron paramagnetic resonance spectroscopy (EPR) signals that were observed between analysis of TAO and other di-iron carboxylate proteins. [120,132] Site directed mutagenesis of the residues around the di-iron active site have shown large detriments to the enzymatic activity. Specifically, A216L/N, E213A, E215A, L122A/N, R118A/Q, T219V and Y220F mutations lead to complete loss of enzymatic activity (Figure 18).[129]

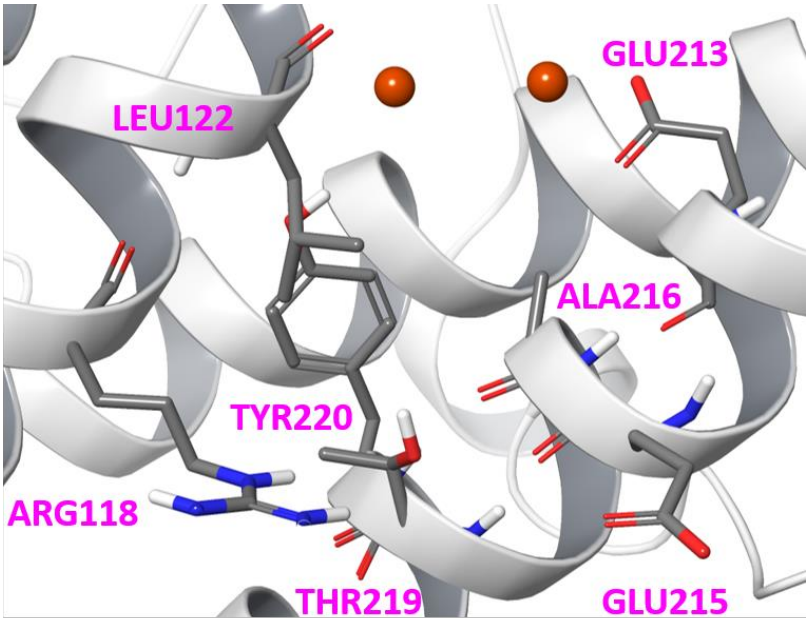

Figure 18 - Key residues of TAO established by site directed mutagenesis - Apo structure adapted from crystal structure PDB 3VV9, Shiba *et al.*[129], mutated residues displayed and labelled, iron atoms coloured orange using Maestro – Schrodinger drug discovery suite.

The binding pocket of TAO has been characterised with inhibitor-protein crystal structures to 2.5 Å resolutions.[129] The natural product inhibitor colletochlorin B (CCB) (Figure – 23) is shown to bind close (within 3 - 4 Å) to the di-iron centre of TAO and occupy a lipophilic chamber formed inbetween 4 of the α-helices (Figure – 19).

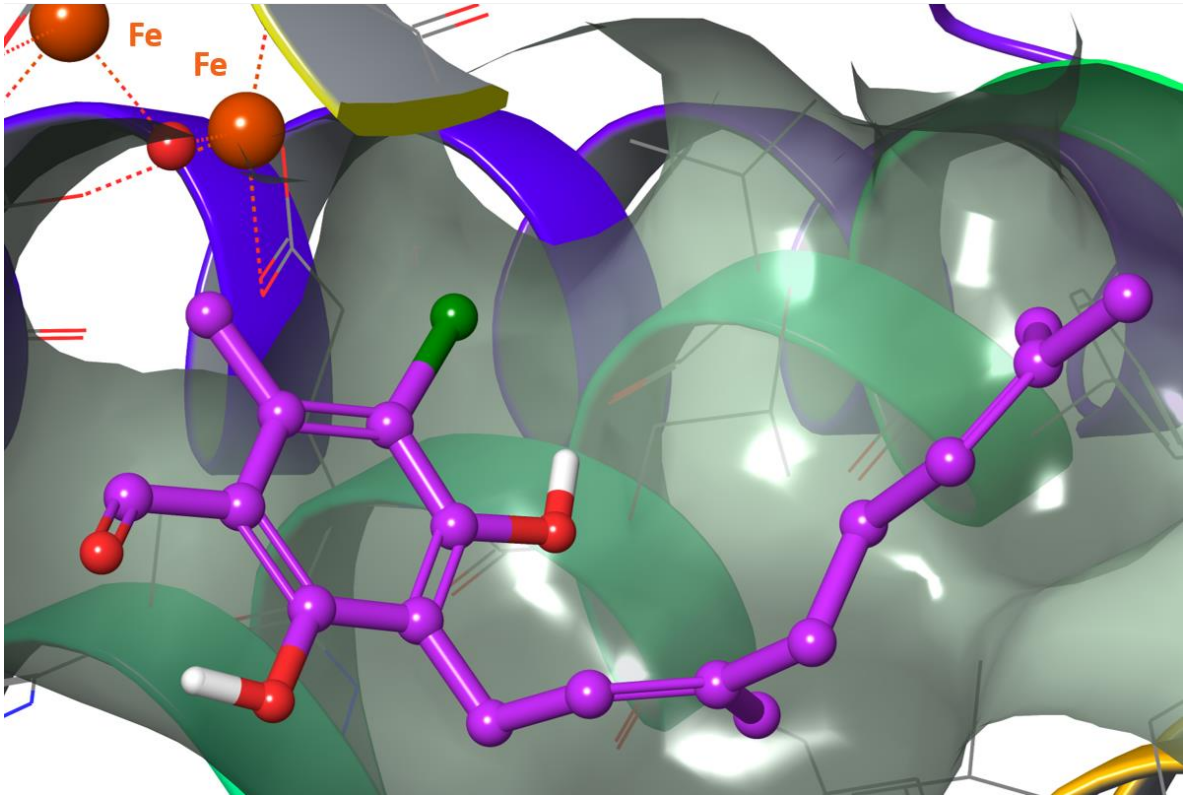

Figure 19 - TAO binding pocket adapted from crystal structure PDB 3W54 Shiba *et al.*[129], protein-ligand surface displayed grey, CCB in pink, di-iron centre orange spheres. Generated in Maestro – Schrodinger drug discovery suite.

The alternative oxidase is a desirable drug target as it is not present in mammalian host cells and is specific to the long slender blood stream form of *T. b.* spp.[86] Genetically engineered trypanosomes that overexpress TAO show increased resistance to Suramin and reactive oxygen species.[133,134] A recent study on the AQP2 amino purine drug resistant strains of *T. b. gambiense* and a laboratory generated *T. b. brucei* AQP1-2-3 mutant have shown a heightened sensitivity to TAO inhibition. This has been linked to the parasites reduced capacity to effectively efflux glycerol, resulting in faster accumulation, inhibition of anaerobic respiration and parasite growth inhibition.[135]

1.3.2 Trypanosome alternative oxidase inhibitors

Salicylhydroxamic acid

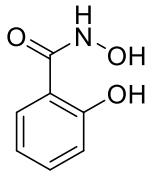

15

Figure 20 - Salicylhydroxamic acid (SHAM) – **15**

The first identified inhibitor of TAO was salicylhydroxamic acid (**15** – SHAM - Figure 20). It was discovered that the target of SHAM's respiratory inhibition was a non-cytochrome alternative oxidase, insensitive to cyanide and antimycin A. [136–138] Similar alternative oxidases have been observed in a variety of plants, fungi and the parasitic protozoa *T. b. brucei.*[116] Due to TAO's role in respiratory function within the long slender blood stream form of trypanosomes, several groups have investigated inhibiting the proliferation of the parasite with SHAM analogues.[84,85,87] It has been shown that inhibition of TAO with SHAM and the inhibition of the anaerobic glycolysis pathway by mass action with glycerol could clear an infection of *T. b. brucei* in rats.[138] The importance of the combination of a TAO inhibitor being co-administered with a high concentration of glycerol has been the subject of some debate. It is generally thought that glycerol is acting by shutting down the anaerobic glycolytic pathway, by stopping the function of glycerol kinase *via* mass action.[138–140] Excipient effects on solubility, absorption and distribution of alternative oxidase inhibitors with and without glycerol has not been reported in the literature. SHAM is reported to have high micromolar affinity for inhibiting TAO.[87]

Ascofuranone

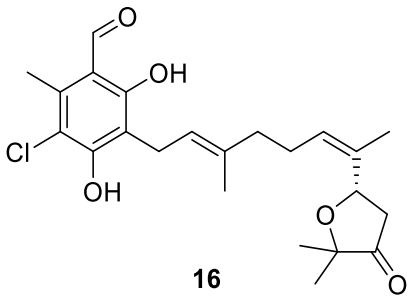

Figure 21 - Ascofuranone (AF) – **16**

Ascofuranone (16 - Figure 21), a natural product isolated from the fungus *Ascochyta viciae* was first identified as an antibiotic in the 1970's.[141,142] It was identified from the same fungus from which a similar natural product, ascochlorin was isolated.[143]

The first synthesis of ascofuranone was reported by Mori and Fujioka, along with its hypolipidemic and anti-tumour properties (Figure - 22).[144] Treatment of the THP-protected intermediate (17) that had previously been utilised by Mori *et al*. with a preformed lithium enolate in an aldol type reaction provided the diol intermediate (18). This could be cyclised under acidic conditions to provide the furanone ring (19). Swapping the THP protecting group on the terminal alcohol with acetate and protection of the ketone as a cyclic ketal (20) allowed, conversion of the terminal alcohol to a geranyl bromide (21) *via* a tosylated intermediate and nucleophilic substitution with LiBr. This intermediate could be reacted with the anion of 1,3-dimethoxy-5-methylcyclohexa-1,4-diene to provide (22). Treatment of this intermediate with *N*-chlorosuccinimide (NCS) provided the di-α-chlorinated cyclohexanedione intermediate (23). Aromatisation, utilising 1,8-diazabicyclo[5.4.0]undec-7-ene (DBU) to eliminate HCl and introduction of the diethyl acetal, aldehyde equivalent provided ascofuranone upon hydrolysis (16).

The isolation of enantiomerically pure ascofuranone enantiomers was subsequently reported by the same group. The isolation was carried out *via* the chromatographic separation of a diastereomeric mixture of a derivatised intermediate, which provided the

individual enantiomers of ascofuranone after cleavage of the chiral auxiliary and completion of the synthesis.[145]

Further investigation into AF's anti-tumour properties highlighted the inhibition of respiration in macrophages.[146] ascofuranone was subsequently identified as a potent inhibitor of glucose dependent respiration, specifically inhibiting the glycerol-3-phosphate oxidase system in trypanosomes. ascofuranone was identified to inhibit TAO at sub-nanomolar and low single digit nanomolar concentrations.[86,115,147]

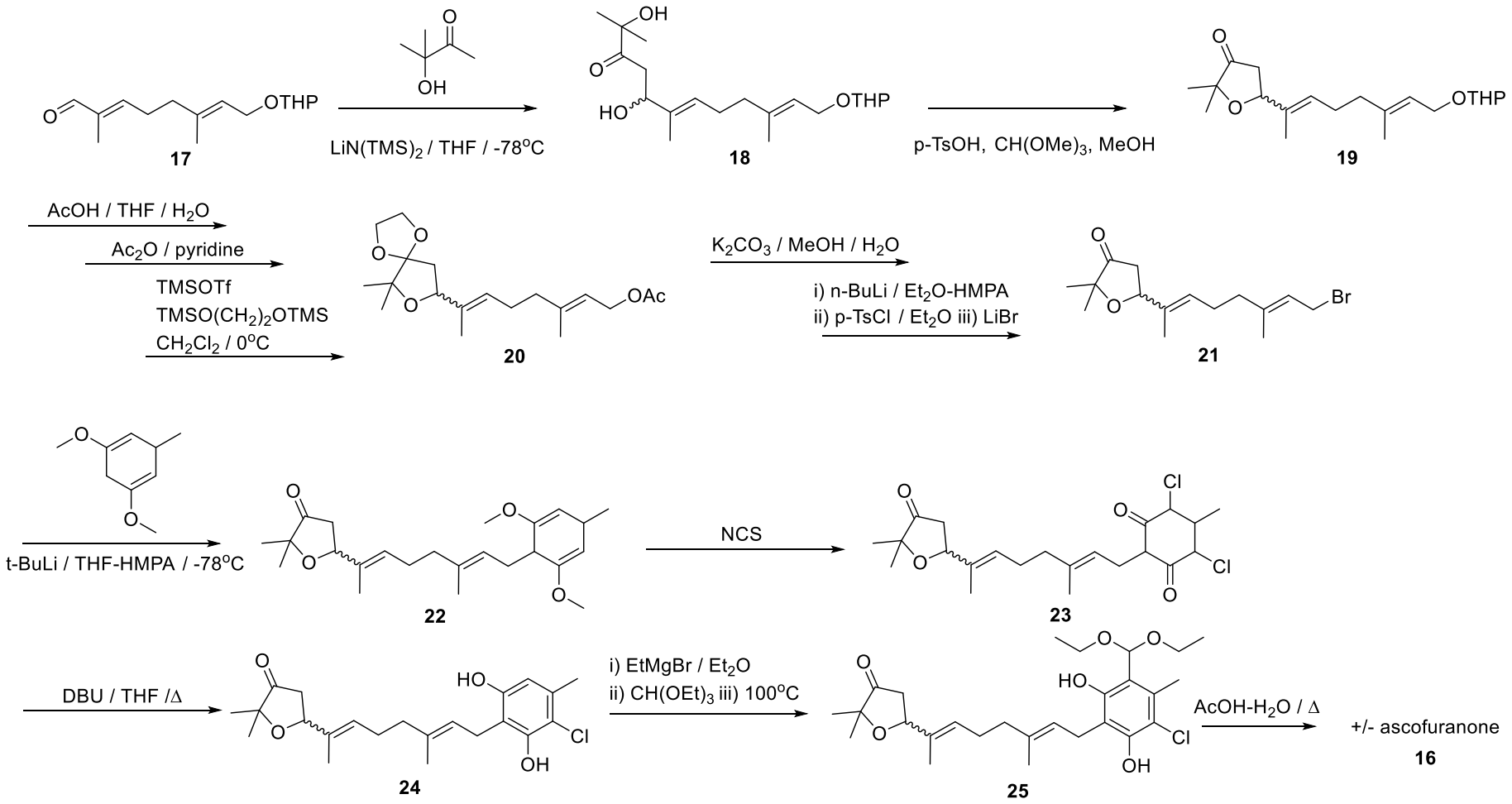

Figure 22 - Ascofuranone synthesis reported by Mori and Fujioka[144]

Colletochlorin B (CCB)

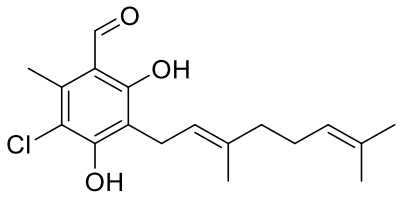

26

Figure 23 - Colletochlorin B (CCB) – ***26***

Colletochlorin B (**26** – Figure 23) was similarly identified in the 1970s, isolated from the fungus *Colettotrichum nicotianae*.[148] The first synthesis was again described by Mori *et al.*[149] The original biological activity was reported to be as a potent cytotoxin of the human leukaemia cell line HL-60.[150] It was later found to be a potent inhibitor of TAO in similar studies to ascofuranone and its analogues.[128] Colletochlorin B's synthesis is somewhat more tractable than that of ascofuranone, partly due to its reduced complexity and absence of a chiral centre. It shows very similar low nanomolar inhibition of TAO and thus is a preferred starting point for analogue synthesis and structure activity relationship (SAR) exploration.[128]

Saimoto *et al.* reported an initial SAR exploration following their groups published crystal structure of a colletochlorin B : TAO complex (PDB 3W54 – Figure 19).[128,129] They showed that the benzaldehyde could be replaced with nitrile or nitro electron withdrawing groups without much detriment to activity. Replacement with ketone and ester electron withdrawing groups showed 10 - 100-fold decreases in inhibitory potency against TAO, and greater than 100-fold decreases observed when replacing the aldehyde with chloro (turquoise - Figure 24 - A). They also showed that methylation of one of the phenols was tolerated with a small detriment to potency; however, the compound was rendered effectively inactive if the phenol ortho to the chloro atom was removed completely (blue - Figure 24 - A). Single removal of the chloro atom resulted in a compound with similar potency to CCB (orange - Figure 24 - A); however, once this was combined with removal of the methyl substituent a 10 to 100-fold decrease in inhibitory activity was observed (red/orange - Figure 24). The phenol *ortho* to the aldehyde in the crystal structure (3w54), is expected to form hydrogen bond interactions with an arginine residue close to the active di-iron site (ARG118

– depicted in Figure 19). The addition of a terminal hydroxy on the geranyl chain resulted in a small decrease in potency against TAO and terminal carboxylic acid showed larger detriments in potency. Potencies similar to CCB and ascofuranone could be achieved when the acid was capped as a large lipophilic ester. (green - Figure 24 - A). When considering these extended compounds with regards to the crystal structure reported by the same group (3w54), it is likely that these terminal chain modifications are accessing the periphery of the enzyme and occupying solvent exposed regions of the protein.

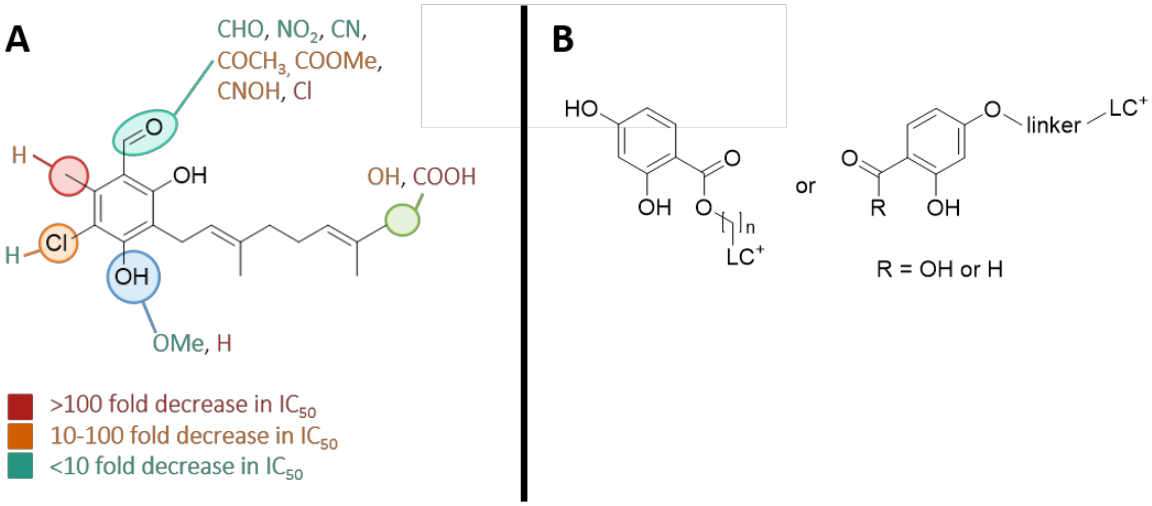

Figure 24 - **A** SAR summary from Saimoto *et al.*[128], **B** Koning and Dardonville exploration of targeting TAO inhibitors to mitochondria.

Recent reports by the groups of Koning and Dardonville on structurally similar TAO inhibitors have shown improvement in efficacy against *T. b. brucei* and *T. congolense* parasites (Figure 24 – B). This has been achieved by targeting the compounds to the parasite mitochondria through cross linking inhibitors to cationic lipids, which have an affinity to the parasite mitochondria.[151–153] However, the phenol ether linked analogues (Figure 24 - B – right), have shown increased cytotoxicity in mammalian cells and are yet to show an improvement in selectivity over the non-targeting inhibitors.[151] The ester linked analogues (Figure 24 - B - left) have shown some susceptibility to cleavage in serum and higher than expected efficacy in parasites indicating alternative mechanisms of action than TAO inhibition alone.[152]

The initial SAR data around the colletochlorin B analogues and the availability of a protein-inhibitor crystal structure provided an attractive starting point for the further investigation and optimisation of this chemotype. The overall aim of this project was to identify drug-like inhibitors of TAO, for use as tool compounds to validate TAO inhibition as a suitable target for the treatment of African trypanosomiasis. Therefore, colletochlorin B was used as a scaffold to investigate the lipophilic tail and aromatic substitution patterns to improve compound physicochemical properties. This thesis describes the SAR exploration undertaken around this natural product. The first step for this investigation required a source of active TAO, to enable the development of robust screening assays, described in the following chapters.

Chapter 2

Chapter 2 – TAO Protein Expression and Isolation

2.1 Recombinant Protein Expression and Purification Introduction

Recombinant protein expression has significantly advanced the biochemical sciences. This area has been reviewed extensively; for example advancements in bacterial expression systems such as *Escherichia coli* (*E. coli*) has most recently been reviewed by Rosano and Ceccarelli.[154] Bacterial expression systems have many strengths: *E.* coli are able to achieve fast growth kinetics and reach high cell densities relatively quickly; the media required for culture is easy to prepare from cheap readily available materials; and transformation of exogenous DNA is facile.

Typically, a specific gene of interest is inserted into *E. coli* cells for expression by mixing a plasmid containing the gene, with a competent strain of *E. coli* and subjecting the mixture to a mild heat shock. The short heat shock creates a temporary pressure imbalance between the inside and outside of the cell, causing the formation of pores in the cell membrane and enables the passage of the supercoiled plasmid DNA into the cell. Following this, the bacteria is recovered in super optimal broth with catabolite repression medium to maximise the transformation efficiency.[155] Antibiotic resistance markers are often also included in the plasmid, and allow selection for cells containing the gene of interest.[156] Once the gene has been transformed into the bacterial strain, large scale cultures of the *E. coli* can be carried out to overexpress the protein of interest.

Bacterial expression systems often utilise T7 RNA polymerase promoters to activate protein expression. T7 RNA polymerase is activated by the lactose operon (lac operon). The lac operon is repressed under standard culture conditions by a lac repressor. Isopropyl β-D-1-thiogalactopyranoside (IPTG) is used as a metabolically stable analogue of allolactose, the lac repressor's endogenous ligand, and remains present at a constant concentration. Once IPTG disrupts the binding of the lac repressor to the lac operon, protein synthesis from the T7 polymerase is initiated, resulting in the recombinant expression of the inserted gene.[157]

Expression of recombinant proteins as fusions with purification handles is common in biochemical protein preparations, and has enabled the isolation of tagged proteins to a high purity.[154] Purification often utilises affinity chromatography where the tag has a high affinity to an immobilised resin, allowing the capture of the tagged protein, and removal of other protein impurities. The tagged protein can subsequently be eluted from the resin with a resin competitive reagent. Tagged recombinant proteins often contain an enzyme cleavable linker, which allows the subsequent removal of the purification tag following protein isolation. This is important as the tag may interfere with later enzyme function assessment.[158]

Following the discovery of the TAO encoding gene by Chaudhuri *et al.*, numerous protocols have been established detailing the recombinant expression of TAO in a variety of *E. coli* expression systems.[117] Initially, expression systems similar to that used to express plant and fungus alternative oxidases were employed.[121,122,159] These *E. coli* were haem deficient, and provided the advantage that they could not express respiratory cytochromes, that would interfere with the functional assessment of TAO, upon crude purification and isolation. However, haem deficient strains are impacted by low growth yields. Fukai *et al* also developed TAO expression systems in standard BL21 *E. coli* strains to improve yields and overcome this problem. These conditions have also been used to generate TAO by other groups,[87,126] and Fukai's protocol provided a basis for the recombinant expression of TAO described in this thesis.

2.2 TAO Expression and Purification Methods

2.2.1 TAO cDNA Transformation into Rosetta2® *E. Coli*

A pET15b TAO plasmid (Figure 25), supplied by Anthony Moore at the University of Sussex, was transformed into Rosetta2® BL21 *E. coli* cells (Novagen). Cells were thawed on ice and treated with 1 µL of plasmid, and incubated on ice for 5 min. The cells were then heat shocked at 42 °C for 30 s in a water bath then placed back on ice for 2 min. Super optimal broth with catabolite repression medium (250 µL) was added and incubated at 37 °C with shaking for 1 h. The cell medium (50 µL) was then spread over lysogeny broth (LB) agar media

plates containing 50 µg/mL ampicillin and 35 µg/mL chloramphenicol. Plates were incubated at 37 °C overnight. A starter culture was made by picking a single colony into LB media (200 mL) containing 50 µg/mL ampicillin and 35 µg/mL chloramphenicol and incubated over night at 37 °C. Starter cultures of transformed *E. coli* were used for inoculating large scale cultures (1 L) and for the generation of glycerol stocks by mixing 1:1 with 50% glycerol in water. Glycerol stocks were stored at -80 °C for future use.

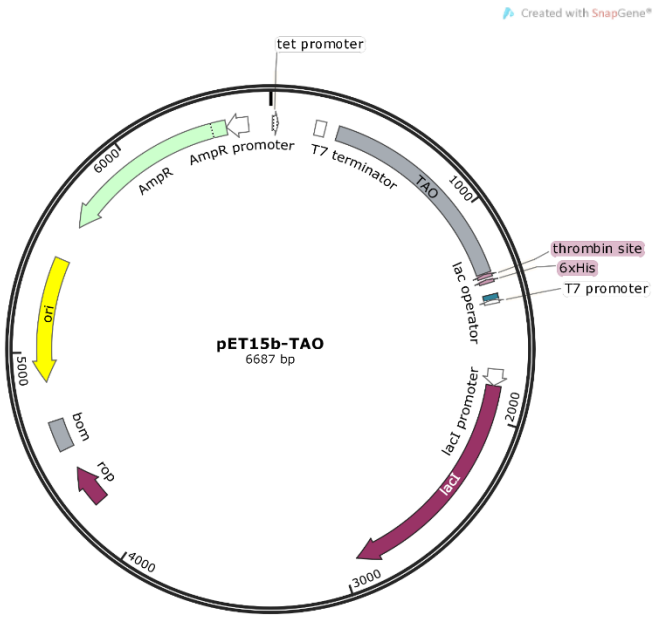

Figure 25 - pET15b-TAO expression plasmid

2.2.2 TAO Plasmid Amplification and Isolation

To amplify and isolate plasmid DNA, a Qiagen maxi-prep was performed. The plasmid was transformed into *E. coli* (Rosetta2® BL21 DE3 cells). A single colony was picked into LB media (100 mL) containing antibiotics as before and grown at 37 °C overnight. The culture was centrifuged (4000 rcf, Beckman Coulter Allegra X30R centrifuge, SX4400 rotor) at 4 °C for 20 min. The maxi-prep was performed using a Qiagen kit according to manufacturer's instructions. The DNA was air dried before being re-suspended in TE buffer pH 8.0 (30 µL). The concentration of DNA was measured (NanoDrop Lite double stranded DNA setting) to be 1049 ng/µL. The plasmid was sequence confirmed (Eurofins Genomics, Figure 26) before storage.

2.2.3 TAO Expression Tests

A pre-culture was prepared by inoculating LB medium (200 mL), containing ampicillin (50 μg/mL) and chloramphenicol (35 μg/mL), with the glycerol stock (200 μL) of TAO transformed Rosetta2® *E. coli* cells. The culture was incubated at 37 °C overnight to provide sufficient starter culture to inoculate 8 x 1 L test cultures described overleaf (Table 3), 2 x 1 L for each condition. Each test culture (1 L) was inoculated with starter culture (1 mL) and incubated at 37 °C, 150 rpm until an OD_{600} of 0.2 was achieved. Each culture was continued at 18 °C, 150 rpm until OD_{600} of 0.6 was achieved. Cultures were cooled at 4 °C for 15 min and one sample for each condition was induced, by the addition of IPTG to give a final concentration of 500 μM. The other culture was not induced for comparison. Each culture was grown at 18 °C. Samples were taken at time points 2 h, 4 h and overnight for comparison of expression outcomes (Figure 27).

Table 3 - Expression test conditions

Test Culture Conditions	Expression media contents
LB Media	LB media (20 g/L) Chloramphenicol (35 µg/mL) Ampicillin (50 µg/mL)
Supplemented LB (Haem deficient *E. coli* conditions)[122]	LB media (20 g/L) Chloramphenicol (35 µg/mL) Ampicillin (50 µg/mL) K_2HPO_4 (10.4 g/L) KH_2PO_4 (3 g/L) trisodium-citrate·$2H_2O$ (0.75 g/L) $(NH_4)_2SO_4$ (2.5 g/L) $MgSO_4 \cdot 7H_2O$ (0.05 g/L) $FeSO_4 \cdot 7H_2O$ (0.025 g/L) $FeCl_3$ (0.025 g/L) glucose (0.2% w/v)
Betaine, sorbitol medium	LB media (20 g/L) Chloramphenicol (35 µg/mL) Ampicillin (50 µg/mL) Sorbitol (120 g/L) Betaine (2.5 µM)
Turbo broth	Turbo broth (16 g/L) glycerol (4 mL/L) Chloramphenicol (35 µg/mL) Ampicillin (50 µg/mL)

2.2.4 *E. coli* Inner Membrane Fraction Isolation and Solubilisation

A pre-culture was prepared as in the expression tests and used to inoculate 4 × 1 L of betaine sorbitol media containing the appropriate antibiotics as described in section 2.2.3. The culture was incubated at 37 °C, 150 rpm until an OD_{600} of 0.2 was achieved, then the temperature was reduced to 18 °C until OD_{600} of 0.6 was achieved. The culture was cooled to 4 °C for 15 min, then induced by the addition of IPTG (0.5 mL of 1 M stock, to give a final concentration of 500 µM). The cultures were grown at 18 °C overnight.

The cells were harvested by centrifugation (Beckman Coulter Avanti J26S, JLA9.1000 rotor, at 8000 rpm for 1 h at 4 °C) and lysed for purification of TAO immediately. The pellet was resuspended in lysis buffer (50 mL, 50 mM Tris HCl, 20% (w/v) sucrose pH 7.4, 1 × protease inhibitor cocktail tablet and 2 µL of Benzonase / DNAse® Sigma). Cells were lysed by sonication (Sonics Vibracell, 13 mm probe, 35% intensity, 180 s, 5 seconds pulse), then cell debris and unbroken cells were removed by centrifugation (Beckman Coulter Avanti J26S, JA 25.50 rotor, 8000 g, 10 min, 4 °C) to provide the supernatant as the crude fraction for inner membrane isolation.

The crude supernatant was overlaid onto 45% sucrose solution (3 × 20 mL, 50 mM Tris-HCl, 45% (w/v) sucrose, pH 7.4) and ultra-centrifuged (Beckman Coulter L-80, SW28, 141000 rcf max, 1 h, 4 °C) to isolate the *E. coli* inner membranes as the buoyant supernatant fraction. The supernatant from this was diluted 1:1 (50 mM Tris HCl, pH 7.4) to give a 15-20% sucrose solution reducing the density of the media and enabling the sedimentation of the inner membranes as a pellet by further ultracentrifugation (Beckman Coulter L-80, SW28, 141000 rcf max, 1 h, 4 °C).

The inner membrane pellet was solubilised by a re-suspension buffer (37 mL, 50 mM Tris-HCl, 1.4% OG (w/v), 20% glycerol (v/v), 200 mM $MgSO_4$, pH 7.4) followed by ultra-centrifugation (Beckman Coulter L-80, SW28, 141000 rcf max, 1 h, 4 °C) to remove un-solubilised proteins and debris to provide the solubilised inner membrane fraction.

2.2.5 TAO Purification

Purification of the solubilised inner membrane fraction was carried out by immobilised metal ion affinity chromatography (IMAC), using the cobalt affinity resin TALON® (6 mL of suspended resin). The resin was equilibrated with buffer (50 mL, 20 mM Tris HCl, 1.4% OG, 20% glycerol, 100 mM $MgSO_4$ pH 7.4) before being incubated with the solubilised supernatant for 30 min on a roller shaker at 4 °C. The flow through was collected and the resin was washed with buffer 1 (2 × 50 mL 20 mM Tris-HCl, 20 mM imidazole, 0.042% (w/v) *n*-dodecyl-β-D-maltopyranoside (DDM), 20% (v/v) glycerol, 50 mM $MgSO_4$, pH 7.4) and buffer 2 (1 × 50 mL 20 mM Tris-HCl, 160 mM imidazole, 0.042% (w/v) n-dodecyl-β-D-maltopyranoside (DDM), 20% v/v glycerol, 50 mM $MgSO_4$, pH 7.4). rTAO was eluted with elution buffer (10 × 10 mL 20 mM Tris-HCl, 200 mM imidazole, 0.042% w/v n-dodecyl-β-D-maltopyranoside (DDM), 20% v/v glycerol, 50 mM $MgSO_4$, 60 mM NaCl, pH 7.4). Fractions were concentrated through a 10 kDa molecular weight cut off Amicon Ultra-15 filter unit yielding IMAC-purified rTAO protein to a concentration of approximately 8 mg/mL. This sample was further purified by size exclusion chromatography (Hiload Superdex 75 pg 26/600 XK column, GE healthcare) with the (AKTA FPLC, GE Healthcare). The gel filtration column was pre-equilibrated with 1 x CV phosphate buffered saline and 2 x CV elution buffer (20 mM Tris HCl, 250 mM NaCl, 20% (v/v) glycerol, 0.042% (w/v) DDM). Protein sample was loaded in a 10 mL load loop and eluted with 1 x CV of elution buffer (20 mM Tris HCl, 250 mM NaCl, 20% (v/v) glycerol, 0.042% (w/v) DDM) at 0.75 mL/min.

2.2.6 TAO Western Blot

TALON purified TAO protein was run on SDS-PAGE, loading 100 ng per well. The gel was transferred onto a 0.45 micron PVDF membrane using a Bio-Rad plate electrode transfer kit (30 min at 100 V, 4 °C). The membrane was blocked with 5% milk in tris-HCl buffered saline (TBST) for 2 h at 4 °C, then incubated with a primary rabbit polyclonal anti-body raised against plant AOX-1/2 supplied by Agrisera (AS04054) at 1:5000 dilution in 5% milk TBST for 16 h at 4 °C. The membrane was washed three times with 5% milk TBST (30 min incubations), then incubated with goat anti rabbit IgG-HRP secondary antibody, supplied by Santa Cruz (sc-2004) in a 1:5000 dilution in 5% milk TBST for 1 h at 4 °C. The membrane was again

washed three times with 5% milk TBST (30 min incubations) before treatment with ECL detection reagent (3 mL). The membrane was developed onto X-RAY film with 3 min exposure time.

2.2.7 TAO Trypsin Digest Mass-Spectrometry

Affinity-chromatography (TALON) purified TAO protein (100 ng per lane) was run on SDS-PAGE. The gel was stained with Coomassie blue, and then the bands correlating to 38 kDa and 74 kDa were excised from the gel with a scalpel and cut into small pieces. The gel pieces were processed for an in-gel trypsin digestion, according to manufacturer's instructions (Thermo Scientific). The gel pieces were initially de-stained with a solution of ammonium carbonate in water and acetonitrile (1:1), to remove the Coomassie stain and residual SDS. The de-stained gel pieces were then reduced with a 50 mM TCEP solution to allow the alkylation of free cysteine residues with a 500 mM iodoacetamide solution. Acetonitrile was removed from the gel by air-drying to facilitate the absorption of the trypsin digestion buffer. Mass spectrometry grade trypsin (10 ng/µL) buffer (25 µL, Thermo Scientific) was incubated with the gel pieces overnight at 30 °C. Addition of 1% TFA solution (10 µL) inhibited trypsin activity before the samples were analysed by mass spectrometry. A sample (8 µL) from each band was injected onto a peptide Acclaim™ PepMap™ 100 C18 column. Different constituent peptides were separated *via* reverse phase chromatography, and eluent from the nano-HPLC was directed into the LTQ-OrbitrapXL mass spectrometry. Unique protein mass-spectrometry profiles were obtained.

2.3 Results and discussion

For this project, a standard BL21 *E. coli* recombinant expression strain was used, to obtain high growth yields.[126] A Qiagen maxi-prep isolated plasmid DNA from the culture and genomic sequencing confirmed that TAO encoding gene (Figure 25) had been successfully transformed into the BL21 Rosetta2® *E. coli* (Figure 26).

Figure 26 - Sequencing results from Eurofins Genomics, of DNA obtained from Qiagen maxi-prep section 2.2.2

With the plasmid containing the TAO gene successfully transformed into *E. coli*, expression tests were carried out to ascertain which conditions provided adequate production of TAO. Four conditions were tested; standard LB expression media, turbo broth, supplemented LB media (used in the haem deficient *E. coli* expression systems) and betaine sorbitol expression media (Figure 27).

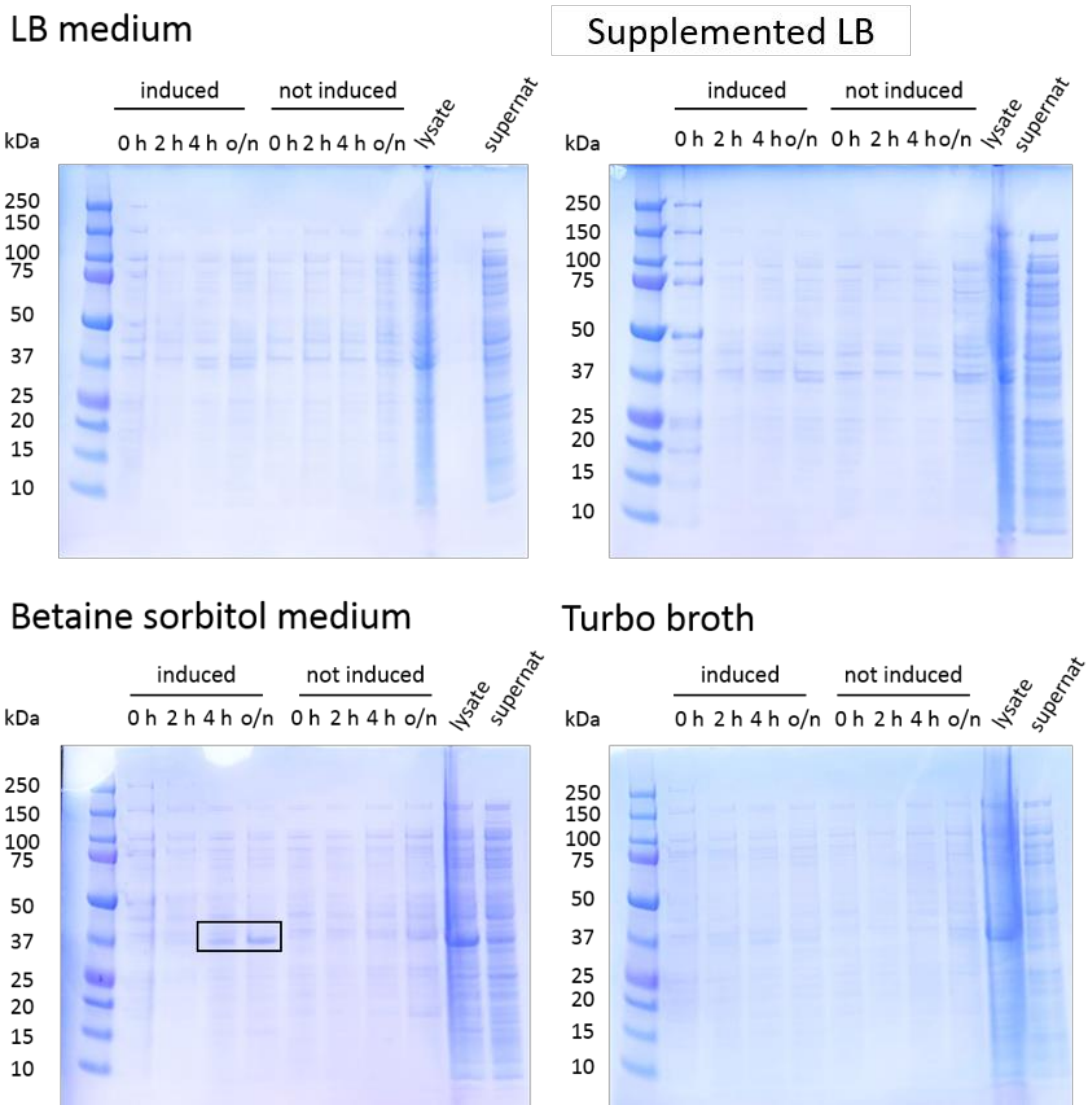

Figure 27 - Expression test SDS-PAGE results Expressed rTAO has an expected mw of 38.5 kDa (box), Novex Nupage 4-12% Bis-Tris gel, staining with quick Coomassie stain, run for 40 min at 200 V and 1.25 A. Lysate and supernatant following overnight expression.

The highest yielding conditions determined qualitatively by SDS-PAGE were from the betaine, sorbitol medium. The supplemented LB conditions reported by Kido *et al.*[120] along with standard LB media and standard Turbo broth all showed less intense bands for TAO expression (Figure 27). High concentrations of sorbitol and betaine have been shown to aid the stability of recombinant proteins, when supplemented in expression media.[160,161] Under these conditions the cellular concentration of osmolytes and chaperones are increased,

promoting recombinant protein stability by reducing the likelihood of protein precipitation and the formation of insoluble inclusion bodies.

Plant alternative oxidases reside on the inner leaf of the mitochondrial membrane,[162] and this is similarly observed in trypanosomes.[113] *E. coli* do not have mitochondria, and in previous recombinant expressions of TAO in bacteria the enzyme has been observed in the cytoplasmic membrane fraction.[126] Isolation of the inner membrane fraction of the *E. coli* cells has previously been reported as a key step in the purification of TAO.[120]

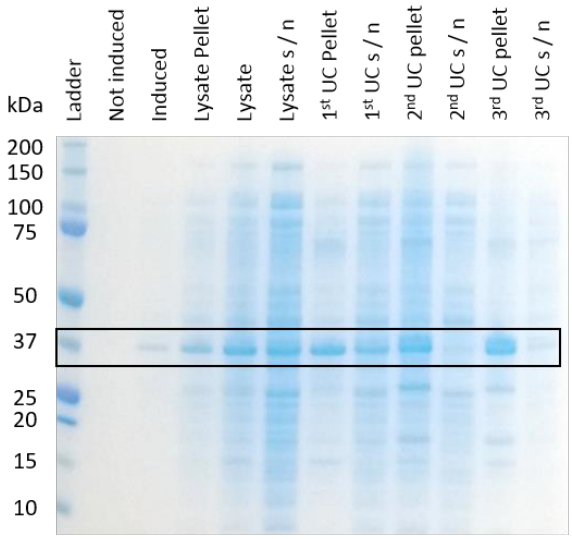

Figure 28 - Inner membrane isolation SDS-PAGE Expressed rTAO has an expected mw of 38.5 kDa (box), Novex Nupage 4-12% Bis-Tris gel, staining with quick Coomassie stain, run for 40 min at 200 V and 1.25 A

A variety of groups have commented on the necessity to isolate the inner membrane fraction of *E. coli* to adequately solubilise and purify large amounts of rTAO.[120,122] Isopycnic centrifugation provides a suitable method for achieving this; however, some protein is lost at every stage of the separation as seen in the SDS-PAGE of the isolated fractions. The 1st ultracentrifuge supernatant fraction (lane 8 - Figure 28) contains buoyant inner membranes, where TAO resides. Some rTAO was potentially lost, that was not separated in the first lysate low speed centrifugation and was retained in the remaining debris (lane 7 – figure 28). These isolated membranes are then successfully pelleted by dilution of the media and further ultra-centrifugation to give the inner membrane pellet (lane 9 - Figure 28), less dense cytosolic

proteins should remain in the supernatant of this ultra-centrifugation step (lane 10 – figure 28).

Solubilisation of TAO from the inner membrane is vital for isolation of rTAO. Nihei *et al.* carried out a detergent screen to identify suitable detergents for the solubilisation of TAO, and found that the only detergent that solubilised active TAO was digitonin, a non-ionic surfactant.[122] Further screening to find the optimal detergent for TAO solubilisation was carried out by Kido *et al.* and identified octylglucopyranoside (OG) as a preferred detergent.[120] This successfully solubilised rTAO from the inner membrane fraction (lane 12 – Figure 28). Some protein was not successfully solubilised from this step, as the pellet contained a visible band for TAO (lane 11 – 28). Further attempts in extracting this pellet with more washings of OG detergent provided only small amounts of TAO, and thus more than one extraction was not performed routinely.

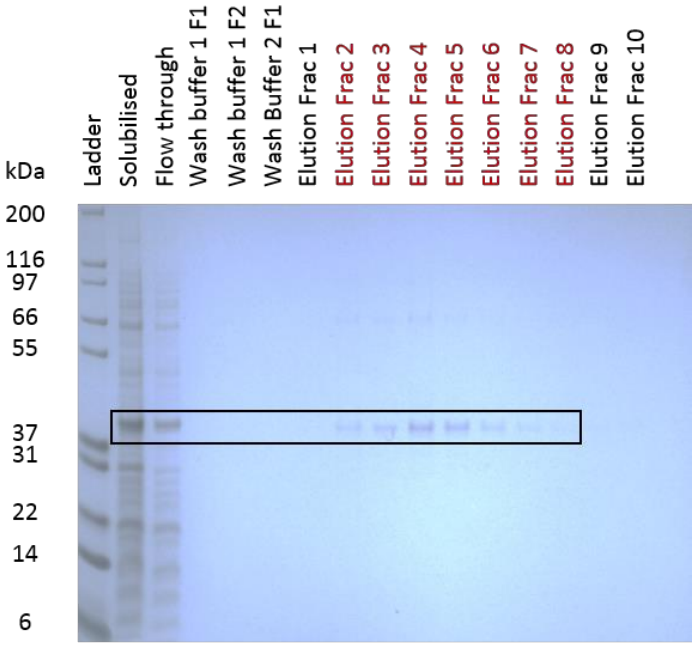

Figure 29 - TAO IMAC purification - SDS-PAGE Expressed rTAO has an expected mw of 38.5 kDa (box), Novex Nupage 4-12% Bis-Tris gel, staining with quick Coomassie stain, run for 40 min at 200 V and 1.25 A

rTAO was expressed with a thrombin linked poly-histidine tag to facilitate purification by IMAC. Analysis of the flow through, wash and elution fractions of the IMAC purification by SDS-PAGE showed that some rTAO was lost in the initial flow through over the resin with

other protein impurities (lane 3 - Figure 29). Kido *et al.* had observed that upon IMAC purification rTAO was retained on the resin when using OG detergents and that the use of *n*-dodecyl-β-D-maltopyranoside (DDM) resulted in the successful elution of rTAO.[120] These conditions were implemented successfully to elute rTAO from the TALON resin.

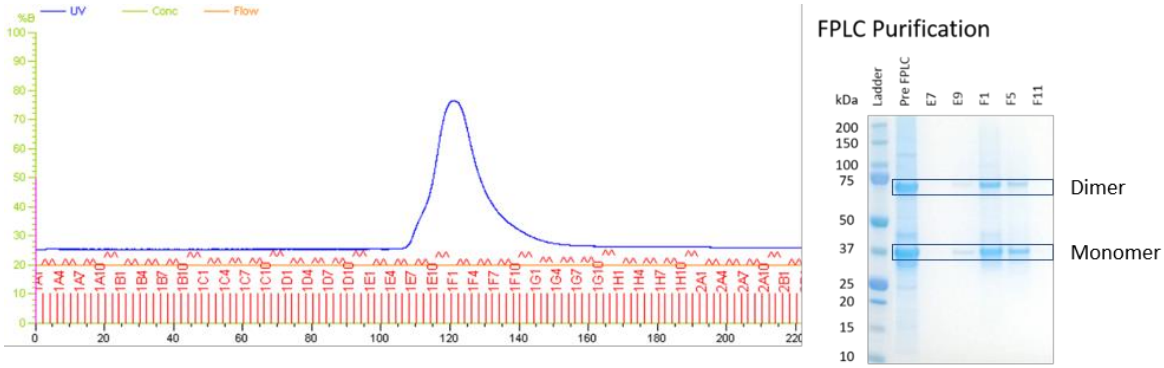

Figure 30 - FPLC purification and SDS-PAGE analysis of rTAO, dimer and monomer fractions box

Size exclusion chromatography was performed on this sample to further purify the isolated rTAO. Proteins are separated through interaction with a stationary phase, dependant on the extent that proteins penetrate into the pores of the stationary phase. Smaller protein molecules penetrate to a greater extent and are retained on the stationary phase for longer, thus effectively separating proteins by their relative size. Both monomer and dimer bands co-eluted from the gel filtration column. Analysis of the elution fractions showed rTAO had been successfully isolated, in good purity for downstream applications (lanes 4-6 – Figure 30). Concentration of the combined fractions provided approximately 9 mg of rTAO from the 8 L culture, that corresponds to a 3-fold increase in protein yield from the reported expression using haem deficient mutant *E. coli* expression systems.[120]

Western blot analysis was carried out to confirm the protein isolated was rTAO. Western-blot or immunoblotting was originally reported by Towbin *et al.*[163] The technique relies on the transfer of proteins separated using SDS-PAGE onto a membrane, followed by antibody recognition of an epitope of a specific part of a protein, then detection with a secondary antibody and chemiluminescent reagent.

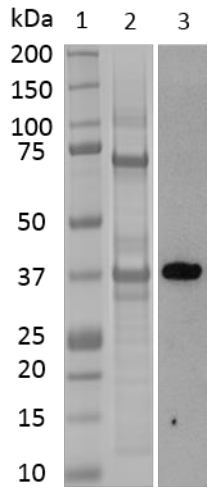

Figure 31 - SDS-PAGE and Western-blot analysis of rTAO

Analysis of the western blot (lane 3 – figure 30) and SDS-PAGE gel (lane 2 – figure 31) of the purified rTAO, showed recognition for the 37-38 kDa band isolated. The primary antibody used was raised against a plant alternative oxidase that shares > 75% sequence homology to TAO. The other high concentration protein band at ~ 74 kDa observed in the SDS-PAGE was not detected in the western blot. We had previously thought this band to be a homo-dimer of TAO, that has similarly been reported in the literature by a variety of groups.[116,117,124] If the epitope recognition site for the antibody is between the dimer interface antibody binding would be inhibited and result in no detection in the immunoblot. To confirm that the second band was attributed to a dimer of TAO, a trypsin digest of bands excised from the SDS-PAGE gel was performed and analysed by protein mass-spectrometry.

Advances in mass-spectrometry resolution, accuracy and detection limits have improved proteomic mass-spectrometry, and have been recently reviewed by Cardoza *et al.*[164] It is possible to identify proteins by searching unique individual protein mass spectrometry fragmentation profiles against large databases of calculated and experimentally determined data sets.

The mass spectrum data generated was searched against the Mascot mass-spectrometry database supplied by Matrix Scientific. Both the ~ 37 kDa and the ~ 74 kDa excised bands,

following trypsin digest, identified TAO as the predominant protein in both samples with 60% and 61% sequence coverage of peptide fragments, respectively. Found fragments are highlighted in red for the 37 kDa (Figure 32) and 74 kDa (Figure 33) excised bands. The mass spectrometry analysis highlighted that rTAO protein was isolated in good purity for further assay development.

```
  1 MFRNHASRIT AAAAPWVLRT ACRQKSDAKT PVWGHTQLNR LSFLETVPVV
 51 PLRVSDESSE DRPTWSLPDI ENVAITHKKP NGLVDTLAYR SVRTCRWLFD
101 TFSLYRFGSI TESKVISRCL FLETVAGVPG MVGGMLRHLS SLRYMTRDKG
151 WINTLLVEAE NERMHLMTFI ELRQPGLPLR VSIIITQAIM YLFLLVAYVI
201 SPRFVHRFVG YLEEEAVITY TGVMRAIDEG RLRPTKNDVP EVARVYWNLS
251 KNATFRDLIN VIRADEAEHR VVNHTFADMH EKRLQNSVNP FVVLKKNPEE
301 MYSNQPSGKT RTDFGSEGAK TASNVNKHV
```

Figure 32 - 37 kDa excised band from mass spectrometry analysis

```
  1 MFRNHASRIT AAAAPWVLRT ACRQKSDAKT PVWGHTQLNR LSFLETVPVV
 51 PLRVSDESSE DRPTWSLPDI ENVAITHKKP NGLVDTLAYR SVRTCRWLFD
101 TFSLYRFGSI TESKVISRCL FLETVAGVPG MVGGMLRHLS SLRYMTRDKG
151 WINTLLVEAE NERMHLMTFI ELRQPGLPLR VSIIITQAIM YLFLLVAYVI
201 SPRFVHRFVG YLEEEAVITY TGVMRAIDEG RLRPTKNDVP EVARVYWNLS
251 KNATFRDLIN VIRADEAEHR VVNHTFADMH EKRLQNSVNP FVVLKKNPEE
301 MYSNQPSGKT RTDFGSEGAK TASNVNKHV
```

Figure 33 - 74 kDa excised band from mass spectrometry analysis

Chapter 2 - Protein Expression and Isolation Conclusions

In conclusion, rTAO has been successfully expressed in *E. coli* BL21 cells, and isolated from the inner membrane fraction. The protein was further purified using IMAC, and analysis by Western blot and mass spectrometry confirmed protein identity. Other quinol-oxidase proteins (that may have been present from recombinant expression in *E. coli*) were not observed in the protein analyses performed, suggesting that the rTAO produced was sufficiently pure for use in assay development and characterising TAO activity. rTAO production in sufficient quantity and quality was a vital step for this project, to enable the set up and development of robust assays. Chapter three describes the optimisation of a bio-chemical assay for the determination of the inhibitory activity of synthesised compounds, and to perform kinetic studies on rTAO.

Chapter 3

Chapter 3 – Biochemical Assay Development

3.1 Activity Assessment of TAO

TAO functions by catalysing the 4-electron reduction of oxygen to water, utilising the substrate ubiquinol by oxidising it to ubiquinone (Figure 34).[165] This process can be monitored photochemically by UV absorbance. The wavelength at which ubiquinol has the strongest absorbance (lambda max) is at 272 nm whereas ubiquinone's is at 275 nm. This small difference makes it hard to achieve a good assay signal window, and because of this, the oxidation of ubiquinol is regularly measured at 278 nm, where the absorbance spectra are at their largest divergence.[87,122,126,166,167] The principal Beer-Lambert law dictates that absorbance is linear with concentration if pathlength and molar absorptivity are kept constant, therefore absorbance measurements can be used to monitor ubiquinol turnover.

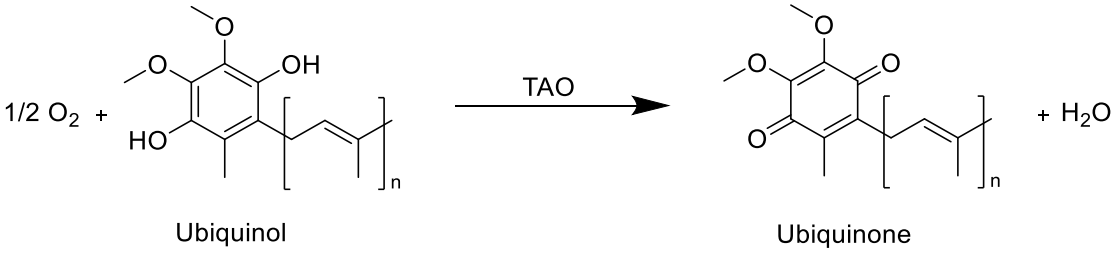

Figure 34 - Ubiquinol / Ubiquinone structure

TAO is a membrane associated protein; in trypanosomes it is located in the inner membrane of the mitochondria.[113] In order to carry out a biochemical assessment of the enzymatic activity using absorbance it is necessary to have a homogeneous solubilised sample of enzyme, substrate and inhibitor. In nature, ubiquinol / ubiquinone contains 9 isoprene units (Q9) in trypanosomes (Figure 34 – n = 9). Unfortunately, the aqueous solubility of Q9 is too low to use in a biochemical assay format with aqueous buffer. Many groups have circumvented this problem by utilising shorter chain ubiquinol / ubiquinone analogues', most commonly 1-ubiquinol (Q1) (Figure 34 – n = 1).[120] It has been observed that when assessing the biochemical activity of TAO and other plant alternative oxidases (AOX) inadequate substrate concentrations were achieved to reliably measure kinetic parameters without detergents.[120,122,168] The use of decyl octaethylene glycol ether (C10E8) specifically has

enabled standard Michaelis-Menten kinetic parameters and accurate measurements of apparent K_M and V_{max} to be recorded.[120] Using these reported studies as a basis, the assessment of the enzymatic function of rTAO described in chapter 2 was undertaken.

3.2 Methods

3.2.1 rTAO Activity Assessment - Absorbance Measurements

The assessment of TAO activity was carried out in single wells of a Greiner 96-well, UV-star flat bottom plate suitable for absorbance measurements at 278 nm. Initially, 150 µL of assay buffer was added to the wells. 1 µL DMSO was then added to each well as a baseline control or a solution of CCB in DMSO to give a final in well concentration of 1000 nM as a positive control. This was followed by the addition of rTAO (10 µL) diluted with enzyme dilution buffer to give an accurate in-well concentration of enzyme (detailed in the tables below), or with buffer alone for a no enzyme control. 1-Ubiquinol (150 µL) was then added, made up from a dilution in assay buffer from a 100 mM DMSO stock solution to give an accurate final in-well concentration of substrate (detailed in the tables below) and a total assay well volume of 311 µL. Each condition (enzyme, no enzyme and enzyme and inhibitor (CCB)) was plated in triplicate unless otherwise described and the experiment repeated three times to report mean and standard error. Absorbance measurements at 278 nm were taken every 90 s following a 5 s shake on the BMG Pherastar plate reader.

Table 4 - Biochemical assay buffers

Assay Buffer	**Enzyme dilution buffer**
Tris HCl 50 mM	Tris HCl 50 mM
C10E8 0.05% (w/v)	NaCl 60 mM
pH 7.4	$MgSO_4$ 50 mM
	Glycerol 20% (v/v)
	DDM 0.042% (w/v)
	pH 7.4

3.2.2 TAO Inhibition 10-point Inhibition Assay

Enzyme function was measured as described above in 3.2.1. CCB at a 1 µM top concentration was used as a positive control inhibitor and a further 3 test compounds (Table 5, A, B, C) at 32 µM top concentrations were diluted as depicted in the plate map (Table 5). Negative control wells had DMSO only, to ensure the final assay plate content was uniform.

Table 5 - TAO 10-point IC_{50} plate map, compound concentration indicated in nM

No Enzyme	CCB 1000	333.3	111.1	37.0	12.3	4.1	1.4	0.5	0.2	0.1	Enzyme
	CCB 1000	333.3	111.1	37.0	12.3	4.1	1.4	0.5	0.2	0.1	
	A 32000	10666.7	3555.6	1185.2	395.1	131.7	43.9	14.6	4.9	1.6	
	A 32000	10666.7	3555.6	1185.2	395.1	131.7	43.9	14.6	4.9	1.6	
Enzyme	B 32000	10666.7	3555.6	1185.2	395.1	131.7	43.9	14.6	4.9	1.6	No Enzyme
	B 32000	10666.7	3555.6	1185.2	395.1	131.7	43.9	14.6	4.9	1.6	
	C 32000	10666.7	3555.6	1185.2	395.1	131.7	43.9	14.6	4.9	1.6	
	C 32000	10666.7	3555.6	1185.2	395.1	131.7	43.9	14.6	4.9	1.6	

1 µL from each well of this compound plate was then transferred into a Greiner 96-well, UV-star flat bottom plate containing assay buffer with enzyme (160 µL) to give a final 3 nM enzyme concentration, or blank assay buffer for no enzyme control (Table 5 – red) addition *via* an automated liquid handling robot (Fluid Xpp-721). This was incubated at 22 °C for 10 min to allow equilibration. The reaction was then initiated by addition of assay buffer containing 1-ubiquinol (150 µL) to give a final concentration of 15 µM. Absorbance at 278 nm was measured immediately after 1-ubiquinol addition, and then every 90 s following a 5 s shake, for a total of 15 min on the BMG Pherastar plate reader.

3.2.3 TAO Inhibition Single Point Inhibition Assay

A 96-well DMSO compound plate was manually prepared, to enable compound addition *via* an automated liquid handling robot (Fluid Xpp-721). CCB (1 µM) was used as a positive control inhibitor and a further 80 compounds were tested at 10 µM, depicted in the plate

map (Table 6). Control wells had DMSO only, to ensure final assay plate content was uniform. TAO activity assessment was carried out by measuring absorbance at 278 nm as described above in section 3.2.2.

Table 6 - TAO Single Point Inhibition Plate Map

No Enzyme	A1	A2	A3	A4	A5	A6	A7	A8	A9	A10	Enzyme
	B1	B2	B3	B4	B5	B6	B7	B8	B9	B10	
	C1	C2	C3	C4	C5	C6	C7	C8	C9	C10	
CCB	D1	D2	D3	D4	D5	D6	D7	D8	D9	D10	CCB
	E1	E2	E3	E4	E5	E6	E7	E8	E9	E10	
Enzyme	F1	F2	F3	F4	F5	F6	F7	F8	F9	F10	No Enzyme
	G1	G2	G3	G4	G5	G6	G7	G8	G9	G10	
	H1	H2	H3	H4	H5	H6	H7	H8	H9	H10	

3.2.4 TAO 5-Point Inhibition Assay

A 96-well DMSO compound dilution plate was set up to enable compound addition *via* an automated liquid handling robot (Fluid Xpp-721). A 5 point 1:5 serial dilution was performed for each compound, manually changing tips between each dilution step. CCB at a 250 nM top concentration was used as a positive control inhibitor, and a further 7 compounds were tested at 10 µM top concentration (Table 7). Control wells had neat DMSO, to ensure final assay plate content was uniform. TAO activity assessment was carried out by measuring absorbance at 278 nm as described above in section 3.2.2 and 3.2.3

Table 7 - TAO 5-point IC50 plate map, compound concentration indicated in nM

No Enzyme	CCB 250	50	10	2	0.4	D 10000	2000	400	80	16	Enzyme
	CCB 250	50	10	2	0.4	D 10000	2000	400	80	16	
	A 10000	2000	400	80	16	E 10000	2000	400	80	16	
	A 10000	2000	400	80	16	E 10000	2000	400	80	16	
Enzyme	B 10000	2000	400	80	16	F 10000	2000	400	80	16	No Enzyme
	B 10000	2000	400	80	16	F 10000	2000	400	80	16	
	C 10000	2000	400	80	16	G 10000	2000	400	80	16	
	C 10000	2000	400	80	16	G 10000	2000	400	80	16	

3.3 Results and discussion

Initial assessment of rTAO activity showed that the rTAO isolated could efficiently catalyse the oxidation of 1-ubiquinol to 1-ubiquinone, and this process could be inhibited by CCB. These results indicated a good turnover of substrate; however, substrate depletion or product inhibition was observed in the uninhibited reaction after approximately 20 mins (Figure 35 – green), as the line began to curve downwards, and turnover become non-linear. For that reason, the concentration of enzyme used in further kinetic characterisation experiments was decreased to 3 nM, to allow steady state measurements at initial velocity to be taken.

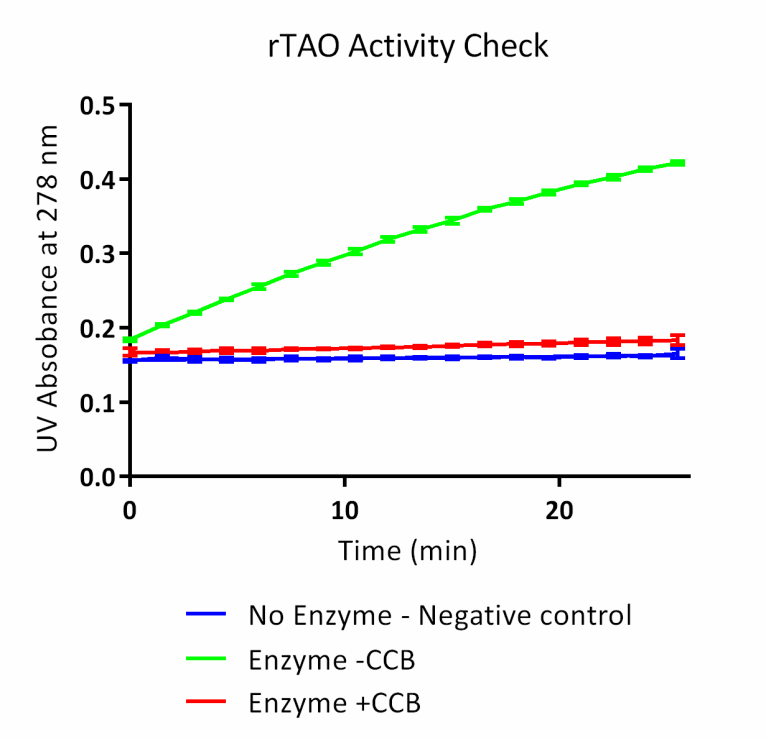

Figure 35 - rTAO activity assessment - rTAO (10 nM), 1-ubiquinol (150 µM), CCB (1000 nM), UV absorbance profile at 278 nm over 30 min. Mean of data and ± SEM reported.

Michaelis-Menten kinetic experiments are a valuable tool for characterising enzymes and for setting up robust screening assays. The Michaelis-Menten model of enzyme kinetics is based on Equation 1 and was described by Michaelis and Menten in the early 1900s. Equation 1 describes the relationship between reaction rate and substrate concentration (Equation 1).

Equation 1 - Michaelis-Menten Equation

$$E + S \underset{k_r}{\overset{k_f}{\rightleftharpoons}} E\text{-}S \xrightarrow{k_{cat}} E + P$$

$$V = \frac{\delta [P]}{\delta t} = \frac{V_{max} [S]}{K_M + [S]}$$

E corresponds to the enzyme, S to the substrate, ES to the enzyme substrate complex and P to the product. K_f is the forward rate of ES formation and K_r the reverse rate, as this process is viewed as reversible (the reverse rate has a negligible contribution). K_{cat} is the rate limiting process that corresponds to the breakdown of the ES complex and product formation, in the process releasing the free enzyme. By measuring the formation of product over time or velocity (V), over a range of substrate concentrations, it is possible to calculate the maximal velocity (V_{max}) of the enzyme and the K_M for the substrate that is being consumed. The maximal rate achieved by the enzyme (V_{max}) assumes that there is a saturated supply of substrate so that it does not affect the rate of reaction. K_M is the Michaelis-Menten constant and is the substrate concentration required for ½ V_{max}.[169]

Historically, graphical plots of the linearisation of this data by performing 1/[S] and 1/V manipulations allowed the calculation of both V_{max} and K_M. Extrapolation of this data to the Y intercept gives $1/V_{max}$ and either the gradient (K_M/V_{max}) or extrapolation to the X-axis ($-1/K_M$) would allow K_M to be determined. This method was pioneered by Hans Lineweaver and Dean Burk, and allowed early enzyme kinetic parameters to be generated without the use of computers, hence these graphs are often known as Lineweaver-Burk plots.[170] However, this method suffers from some disadvantages: the double reciprocal plot generates a distortion of the error of measured velocities when the reciprocal is taken; errors in velocity measurement are more often observed at low velocities and can therefore significantly affect the gradient and estimation of V_{max} and K_M; and the distribution of graphical data is often skewed as low 1/[S] values are not easily obtained, as these are limited by substrate solubility at high concentrations.[171]

As a result, Lineweaver-Burk plots have since become disfavoured for generating enzyme kinetic data, and improvements in computing have allowed instead the facile generation of non-linear regression analysis to determine V_{max} and K_M values. These values allow the comparison of enzyme preparations and are of importance when developing screening assays. It is vital to measure enzyme reaction rates at their initial velocity, determined to be before substrate is 10% consumed in the reaction and the generation of product is in a linear

phase. This allows the assumption that the rate of reaction is not affected by substrate depletion or product inhibition.

To ensure that measurements were taken in the initial 10% of the reaction progression a 1-ubiquinone concentration *vs* absorbance at 278 nm correlation was carried out. Future absorbance reads were correlated to this data to ensure measurements were within the linear phase of reaction progression. The reaction rate initial velocities were measured over a variety of substrate concentrations (1000, 750, 500, 250, 100, 75, 50, 25, 10, 5, 2.5, 1 μM, Figure 36) with 3 nM TAO enzyme.

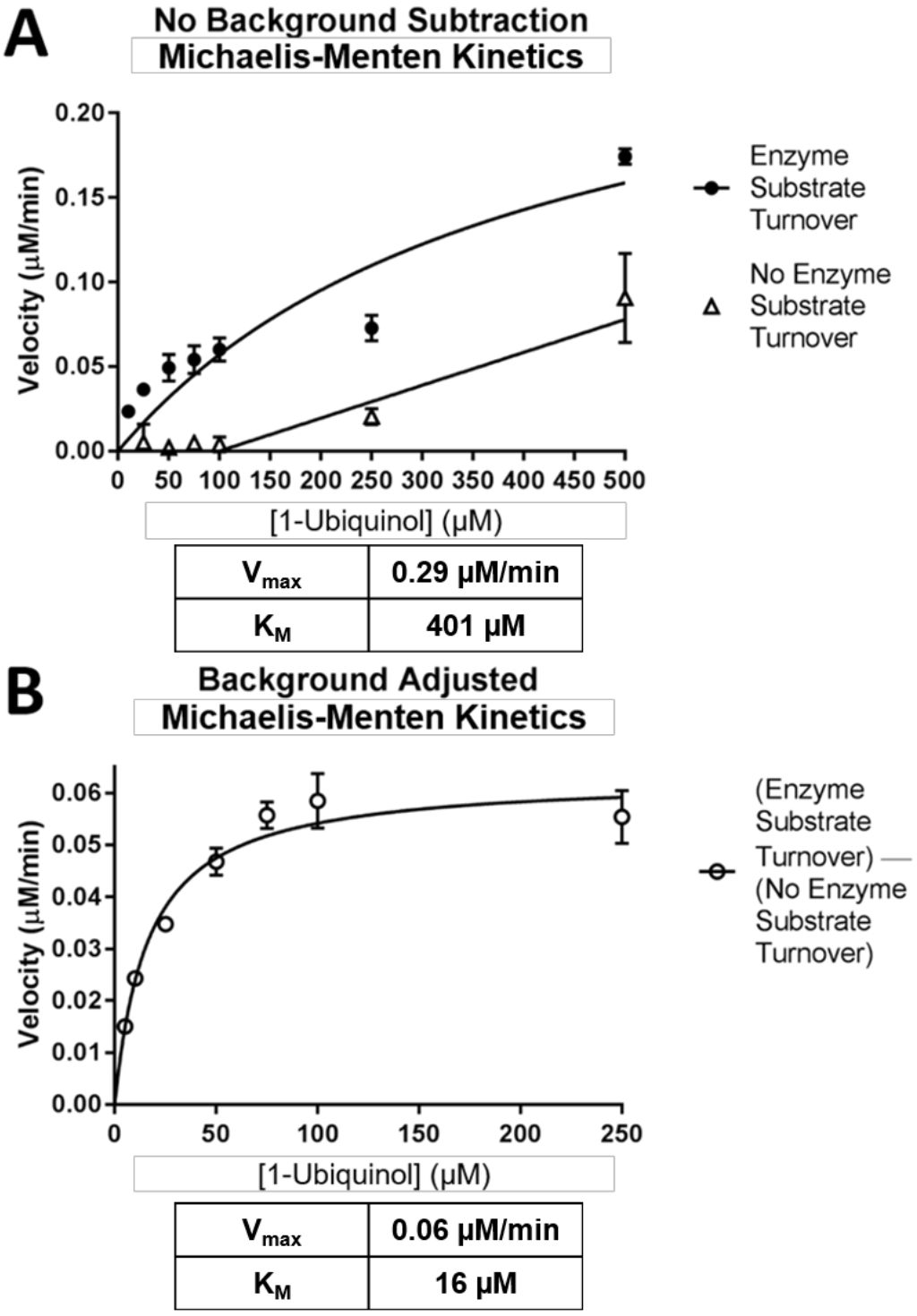

Figure 36 - Michaelis-Menten data, A – Non-linear regression plot of initial velocities obtained with 3 nM rTAO (filled circles). Auto-oxidation of 1-ubiquinol observed without TAO (unfilled triangles). B – Background velocity corrected Michaelis-Menten kinetics, generated from subtracting unfilled triangles from filled circles – (A). Mean and ± SEM reported of n = 3 data.

When looking at the initial data, measurements at high substrate (> 500 µM) concentrations showed a large variability. This had similarly been reported in the literature, and attributed to the low solubility of substrate 1-ubiquinol at these concentrations.[120] Upon closer inspection of these assay wells there was indeed precipitation visible at both 750 µM and 1000 µM. These points were therefore excluded in the following Michaelis-Menten kinetic calculations.

Measurements at 1 µM and 2.5 µM also proved problematic, as velocities here could not be accurately measured at initial velocity due to the turnover being greater than 10% of total substrate concentration after two time points. Sensitivity of the reader was also an issue, as the lower detection limits for the signal were reached at these low concentrations. This data was too close to background absorbance, and as a result these concentrations were also excluded from the Michaelis-Menten kinetic calculations.

Further investigation of the data following a non-linear regression fit using Graph-pad Prism v7.03, highlighted a poor curve fit to the data (Figure 36 – A, circles), although similar K_M values were obtained to what had been previously reported in the literature.[87,120,122,126] Upon closer inspection of the data generated from the substrate turnover without enzyme (Figure 36 – A, triangles), interference was observed from the auto-oxidation of substrate at higher (> 250 µM) concentrations. Detergent effects on the auto-oxidation of ubiquinol substrates had previously been reported by Hoefnagel *et al.*[172] Subtraction of the observed substrate turnover without enzyme (Figure 36 – A, triangles) from the turnover observed with enzyme (Figure 36 – A, circles) improved the data fitting for graphical Michaelis-Menten calculations (Figure 36 – B). Calculations for the Michaelis-Menten constant K_M at 16 µM were however, lower than previous literature reports, resembling data more closely observed with 2-ubiquinol.[87,115,120,127,167] This could be due to the auto-oxidation of substrate not being accounted for in previous studies. The choice of detergent can greatly affect the availability of both the enzyme and substrate of the alternative oxidase system and hence impact the resulting kinetics observed. The kinetic parameters are taken as apparent measurements under the conditions used, as different detergents have been shown to impact the effective concentration of substrate available to the enzyme.[172] To confirm that the activity and kinetic

parameters measured from these studies was from rTAO and not an undetected quinol oxidase impurity, an azide inhibition assay was performed.

TAO is insensitive to respiratory poisons such as cyanide and azide.[113] These respiratory poisons commonly chelate to the metal centres in essential haem cofactor proteins like cytochrome quinol oxidases and fully inhibit their function.[173]

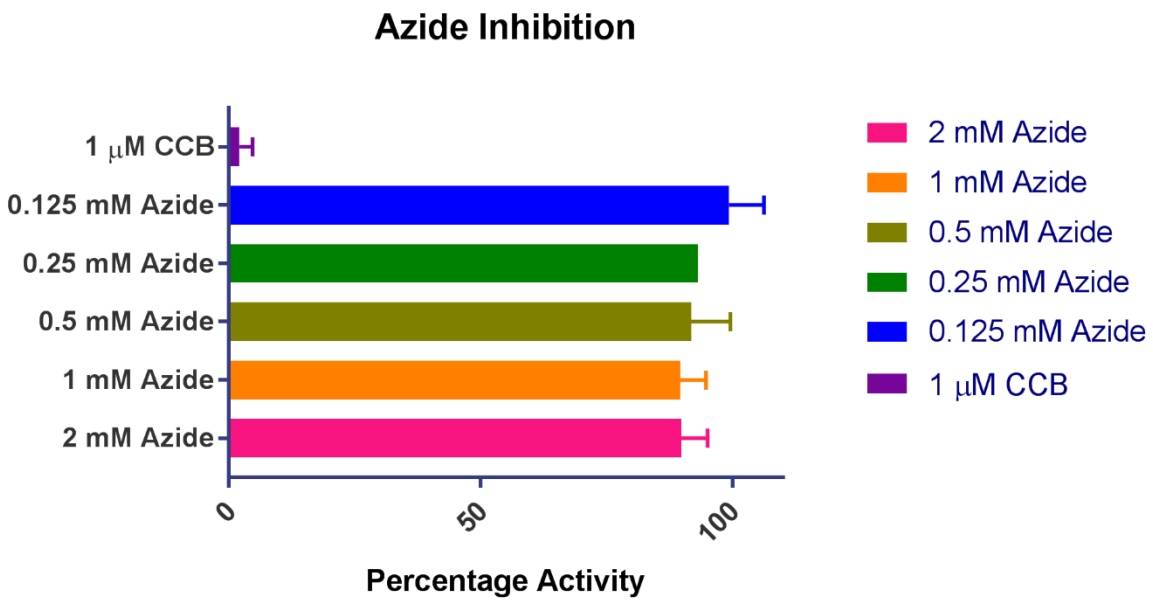

Figure 37 - Azide inhibition of rTAO (3 nM), turnover of 1-ubiquinol (15 μM), CCB (1000 nM) as a positive control. Data normalised to in-plate no-enzyme and no-azide controls, mean and ± SEM reported (n = 3).

Analysis of the data generated from the azide inhibition experiment showed that 1-ubiquinol turnover was not inhibited by any concentration of sodium azide up to 2 mM (Figure 37 – pink). This confirmed that the 1-ubiquinol oxidation activity that was observed is from the function of rTAO and not an undetermined quinol oxidase impurity. On the other hand, 1-ubiquinol oxidation could be completely inhibited with the addition of 1 μM CCB (Figure 37 – purple).

With calculated Michaelis-Menten kinetic measurements in-hand, a substrate concentration close to the K_M was required for maximising detection of substrate competitive inhibitors.[174] Performing inhibition assays at higher than K_M substrate concentrations can cause

competitive inhibitors to be inaccurately detected as false negatives, as a high concentration of substrate can effectively out compete a competitive inhibitor. A concentration of 15 µM 1-ubiquinol was used for assay development, as this was close to the measured K_M. To ensure that velocity measurements from future assays were taken in the linear range of reaction progression an enzyme concentration experiment was conducted to give reaction progression profiles to find the optimal concentration of enzyme.

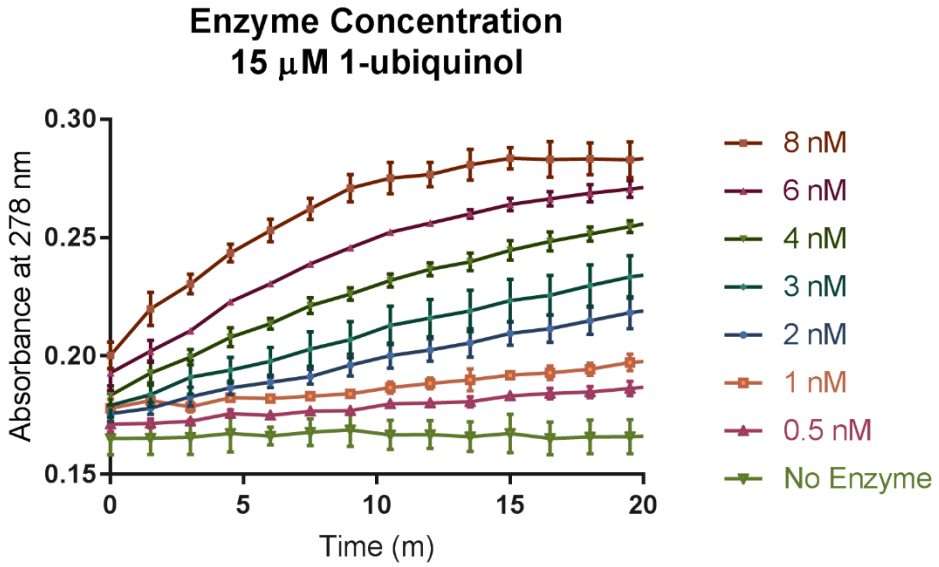

Figure 38 - Enzyme concentration – 1-ubiquinol (15 µM) oxidation measured by UV absorbance at 278 nm, with increasing concentrations of rTAO.

Analysis of the progression curves over 20 min showed that 3 nM of rTAO gave a good compromise between 1-ubiquinol turnover and achieving linear conversion over the course of the assay (Figure 38 – blue). Concentrations below 1 nM enzyme would require a longer assay time to achieve a significant signal window, whereas concentrations above 4 nM would require short plate read times to ensure kinetic measurements were within a linear initial velocity time frame. Going forward, a final concentration of 3 nM enzyme and 15 µM 1-ubiquinol were used for rTAO inhibitory assay development experiments.

As test compounds will be dissolved and diluted from DMSO it was important to test the assay's tolerance to this solvent, to ensure that any observed effects were due to the test compound and not a component solvent.

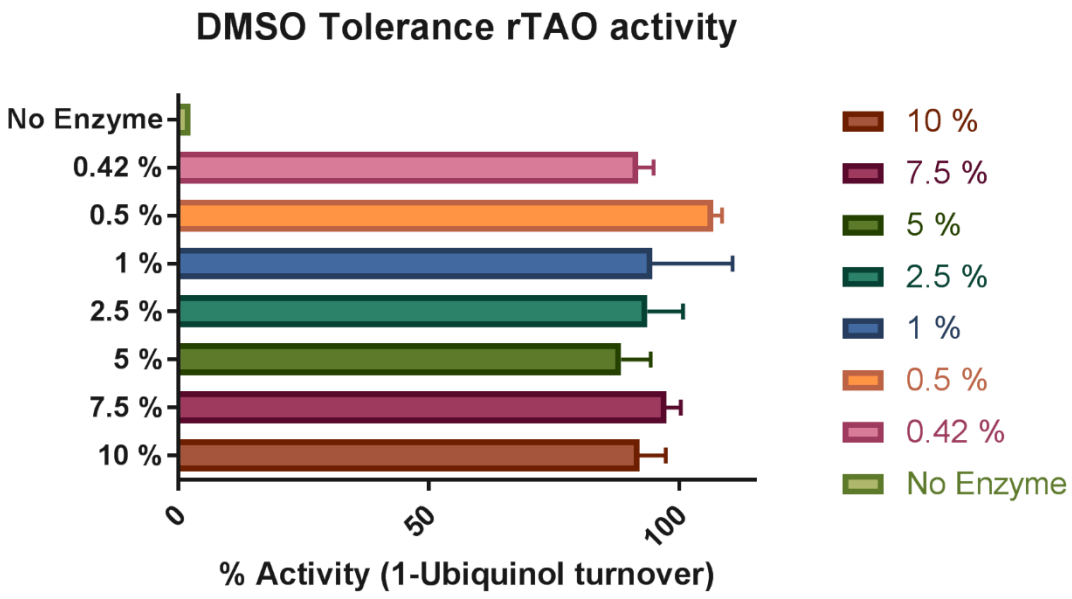

Figure 39 - DMSO tolerance

Analysis of the rTAO activity in the presence of increasing amounts of DMSO showed a good tolerance, with no observed effect on enzymatic performance (Figure 39). Final DMSO concentration in the assay going forward will be kept to the minimum possible concentration of 0.42%. This is determined from the combined content of 1 µL of DMSO from compound addition and the DMSO carried through from the dilution of the 1-ubiquinol substrate that is made up in DMSO at 100 µM.

Determination of IC_{50} (the concentration that causes 50% inhibition of maximal enzyme activity) values is the preferred method to compare different molecules and assess their ability to inhibit an enzyme. Standardly, a 10-point 1:3 serial dilution of compound is carried out and the relative activity of enzyme is measured at each inhibitor concentration. A 4-parameter non-linear plot of this data provides an IC_{50}, Hill-slope, and maximum and minimum inhibition values. The maximum and minimum values can be normalised to the

positive and negative controls within the assay, and IC_{50} data compared between different compounds. The Hill-slope or coefficient gives an indication of the stoichiometry and co-operativity of binding. Ideally the Hill-coefficient should be close to 1, which is indicative of 1 molecule of inhibitor binding to 1 molecule of enzyme. Enzymes however, often exist in oligomeric forms. In these cases, the binding of one ligand may have a positive or negative impact on the binding of a second ligand to another structural oligomeric enzyme. This can cause the Hill coefficient to deviate either positively or negatively from 1 respectively. Compounds that show unusually high Hill slopes are often indicative of protein denaturants, tight binding inhibitors or covalent enzyme inhibitors, highlighting the necessity for further characterisation when these results arise. Hill slope values less than 1 are indicative of the presence of two non-equivalent ligand binding sites in the same enzyme, in which both need to be occupied to fully inhibit enzyme activity. Alternatively, Hill coefficients lower than 1 also arise from the presence of non-equivalent proteins, for example dimers and monomers may have differential affinities for ligands generating a shallow Hill slope (< 1).

To maximise the generation of these data, a 96-well DMSO compound dilution plate was set up (Table 5) to enable compound dilution *via* an automated liquid handling robot (Fluid Xpp-721). Initially a 10-point 1:3 serial dilution was prepared for each compound by the liquid handling robot. Analysis of the initial data set showed an unusually shallow linear IC_{50} curve for the CCB control, suggesting that the serial dilution had not been correctly carried out. Performing automated serial dilutions of highly lipophilic compounds can prove challenging, due to the compound affinity for plastics. This in turn creates a carryover of higher concentrated material into the next well and disrupts the serial dilution. Modification of the method by performing compound serial dilution manually and changing the tips of the multi-channel pipette after each dilution step resolved this issue. Manual preparation of compound stocks afforded reproducible IC_{50} curves for the literature natural product CCB with similar values (2.8 ± 2 nM) to what had previously been reported (Figure 40).[128] The Hill coefficient for CCB was calculated to be 0.6, indicating the presence of two non-equivalent ligand binding sites. This could be from differential affinities of dimeric and monomeric forms of the enzyme or from the binding of CCB to the two hydrophobic cavities that ubiquinol has

been reported to interact with.[129] Using this assay format, historical compounds that showed structural similarity to CCB synthesised by members of the research group of Professor Simon Ward at the University of Sussex were assessed for TAO inhibition. These data will be discussed in chapter 4 of this thesis.

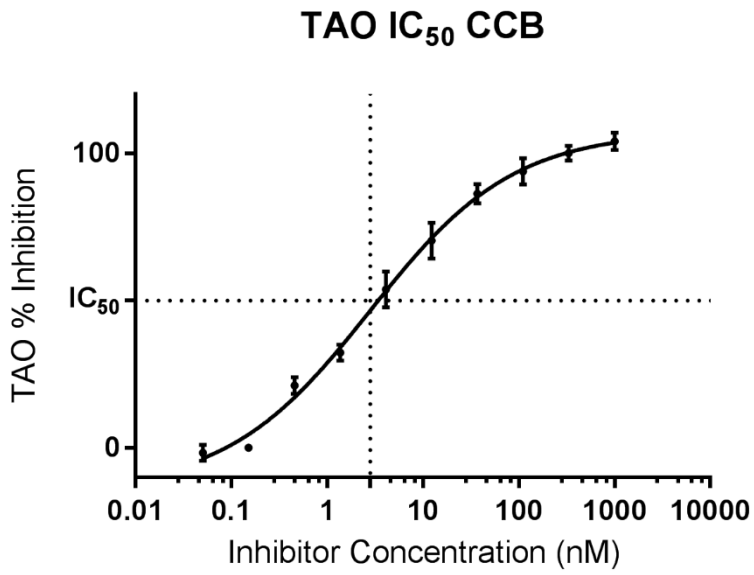

Figure 40 - IC_{50} curve CCB, generated from 3 nM TAO and 15 μM 1-ubiquinol, normalising to no enzyme and no inhibitor in plate controls. Data reported is mean ± SEM (n = 3)

To support screening activities of numerous compounds, it was desirable to have a higher throughput assay. Single point inhibition assays are routinely used to screen large compound collections. The disadvantage of these assays is that each compound is only assessed once per plate, so discrepancies in individual wells that are sometimes observed may result in some false positive or false negative results. Hits that are identified from these screening activities require further assessment to confirm inhibitory activities. Medicines malaria venture (MMV), provided a set of 400 compounds that had been identified from the phenotypic screening of a range of kinetoplastid parasites. These compounds were tested against rTAO at a single concentration of 10 μM, with the aim of identifying a structurally distinct class of TAO inhibitor described in section 3.2.3.

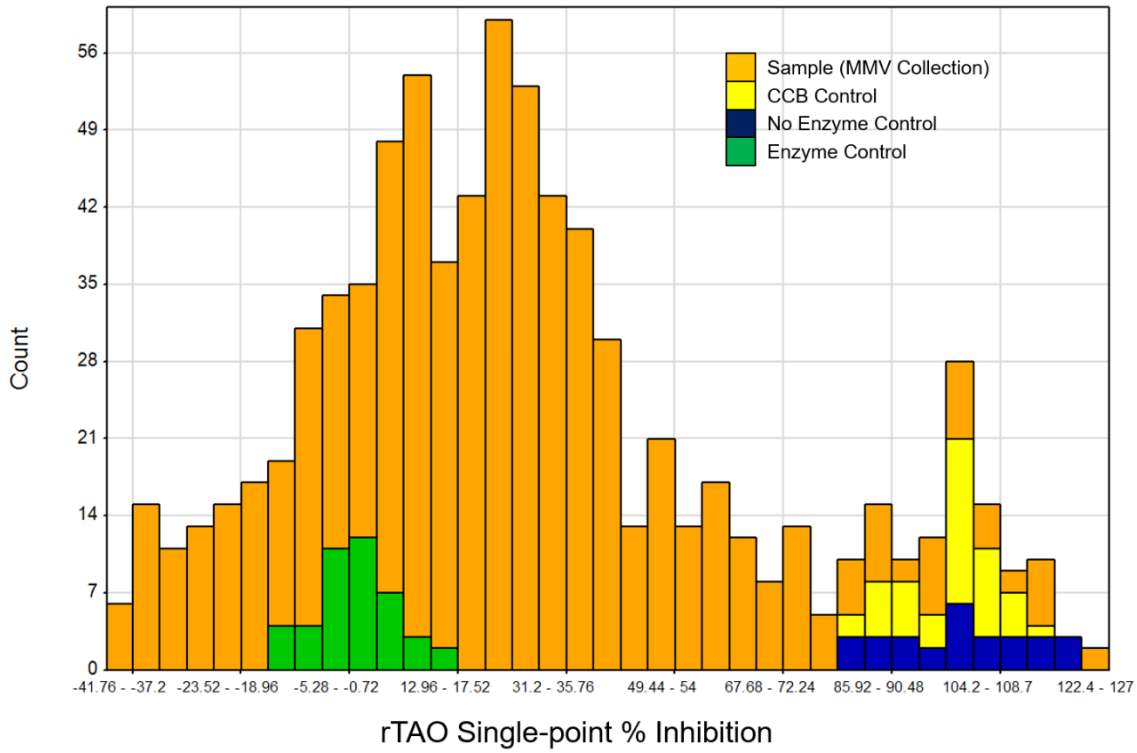

Figure 41 - Single-point inhibition summary (MMV collection). Binned inhibition data of number of compounds, green is enzyme control (DMSO only, no inhibition of TAO), blue is no enzyme control (complete inhibition), yellow is CCB in plate positive control. Data is fitted to in-plate controls 0% inhibition is mean of enzyme only control, 100% inhibition is mean of no enzyme control.

Analysis of the single point inhibition data generated with the MMV collection identified new hits for further validation. Assessment of assay robustness was carried out by calculating Z scores for the assay plates. Z prime values are calculated from the mean and standard deviation of the high and low controls and are indicative of assay window and variance.[175] Optimal Z prime values above 0.5 indicate a robust assay, and the calculated Z prime scores of the single point inhibition assay ranged from 0.52 to 0.66. Compounds that showed greater than 50% inhibition at 10 µM were deemed a significant response that warranted further testing to confirm inhibition. 70 compounds inhibited rTAO by ≥ 50% at 10 µM (green circles, Figure 42, mean value from two assay runs). These compounds were further assessed by performing a 5-point IC_{50} determination described in section 3.2.4. The distribution of the data showed a higher than expected number of active compounds, this could be due to these compounds already being identified as inhibitors of parasite growth.

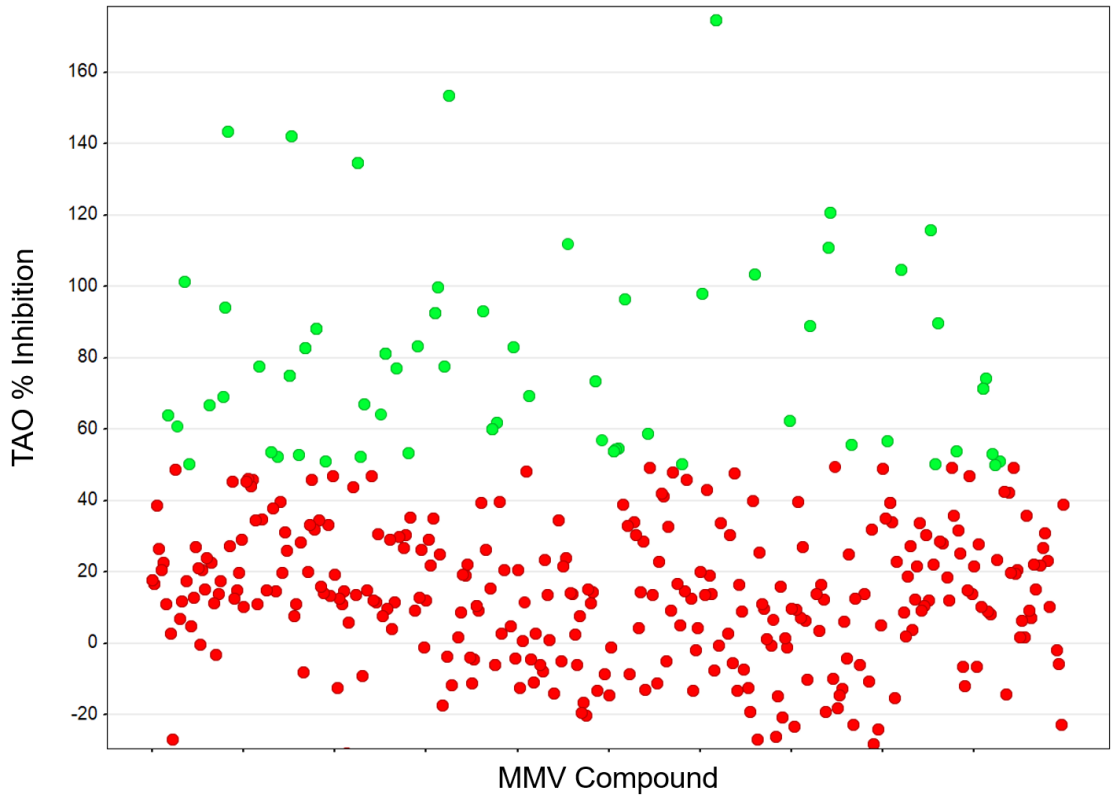

Figure 42 - MMV TAO Mean Single Point Inhibition data, compounds in green showed > 50% inhibition and were confirmed in in 5-point IC_{50} screening assays

It was clear from this analysis that the single point data generated suffered from a reasonable amount of interference, with some measured inhibitions of > 100 and < 0%. Absorbance assays are prone to interference due to insoluble particulates or absorbance of analyte compounds. It is important to verify any identified hits from single point assays in more robust multiple point inhibition screens.[176]

Analysis of the 5-point IC_{50} curves showed that 20 compounds had reproducible IC_{50}s below 10 µM (Table 8). From these 20 compounds, 10 were available to re-purchase as solids from MMV. These compounds were re-ordered to perform full 10-point IC_{50} determinations, which were carried out as described in section 3.2.2. These data are discussed in chapter 4.

Table 8 - MMV Hits Summary 5-point IC_{50} confirmation

Structure	#	TAO% Inhibition (at 10 µM)[b]	5-point TAO (pIC_{50})[b]
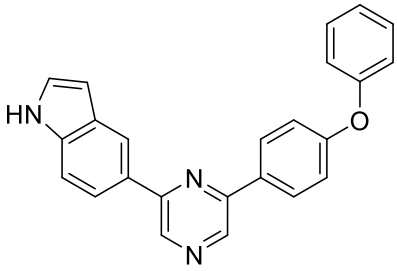	27*	175 ± 56	5.7 ± 0.3
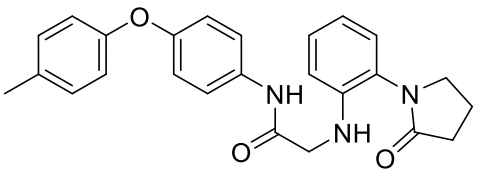	28*	135 ± 100	5.5 ± 0.1
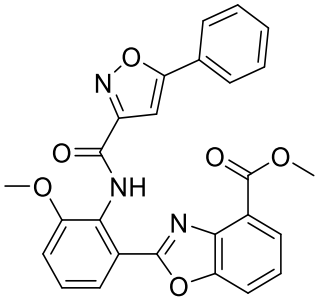	29	121 ± 17	5.2 ± 0.2
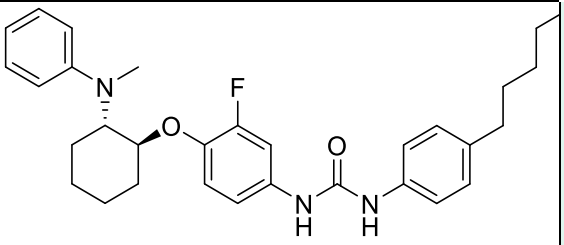	30	111 ± 29	5.2 ± 0.1
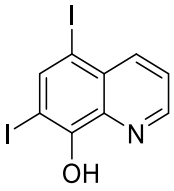	31	100 ± 20	5.1 ± 0.1

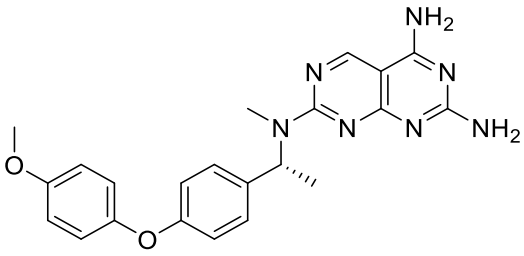	**32**	96 ± 42	5.3 ± 0.1
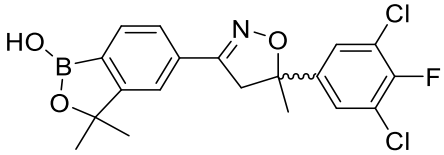	**33***	93 ± 4	5.8 ± 0.1
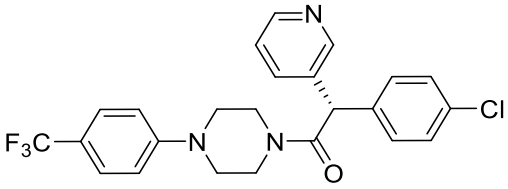	**34**	90 ± 15	5.1 ± 0.1
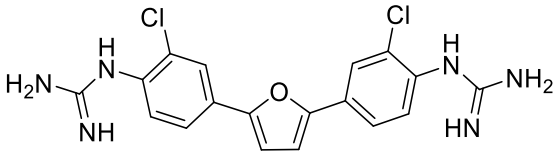	**35**	89 ± 99	5.4 ± 0.2
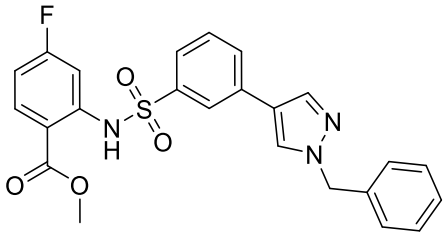	**36***	88 ± 12	5.4 ± 0.1
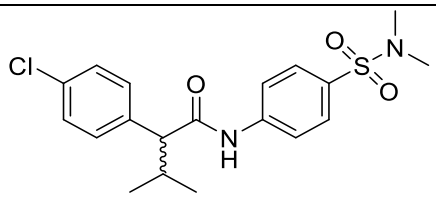	**37**	83 ± 14	5.1 ± 0.1
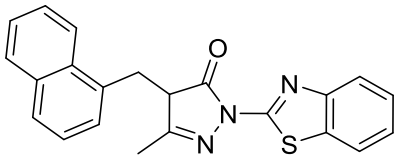	**38***	83 ± 18	5.6 ± 0.2

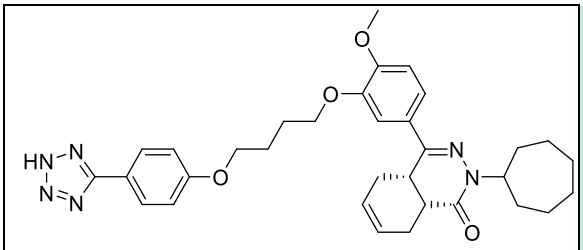	**39***	81 ± 22	5.5 ± 0.1
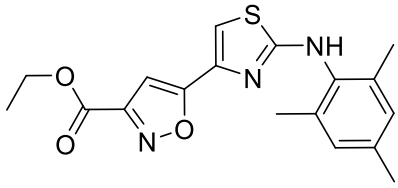	**40***	75 ± 38	5.5 ± 0.1
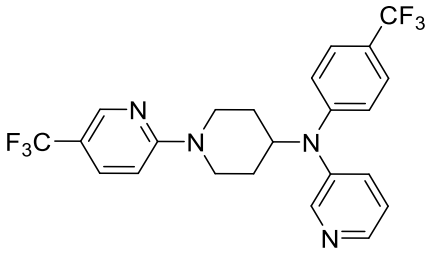	**41***	71 ± 49	5.7 ± 0.1
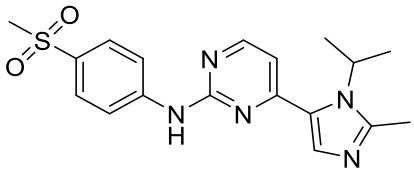	**42**	67 ± 3	5.3 ± 0.1
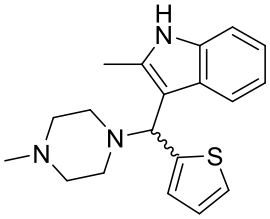	**43***	60 ± 9	5.7 ± 0.1
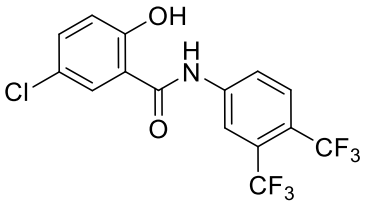	**44**	59 ± 3	6.0 ± 0.1
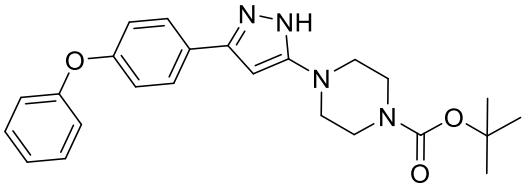	**45***	54 ± 24	5.4 ± 0.1

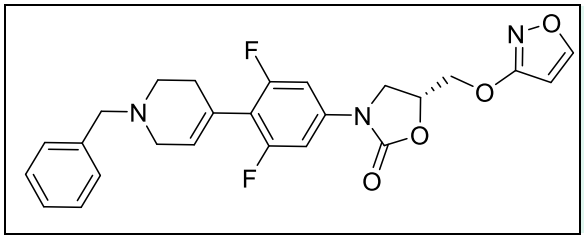	46	53 ± 37	5.0 ± 0.1

[a]% Inhibition of rTAO activity at 10 μM compound concentration, with s.d. (n = 2). [b] 5-point pIC_{50} calculated from negative log of IC_{50} value from 5-point 4-parameter non-linear regression fit of inhibition data, with s.d. (n = 2). * Indicates compound availability for confirmation in 10-point IC_{50} experiments from solid sample.

Chapter 3 - Biochemical Assay Development Conclusions

In conclusion, the isolated rTAO that was described in chapter 2 showed functional activity, catalysing the oxidation of 1-ubiquinol to 1-ubiquinone. Robust assays were developed to determine the enzymatic activity of rTAO, allowing the kinetic characterisation of rTAO. It was of interest that the Michaelis Menten enzyme kinetics observed with rTAO expressed in Rosetta® BL21 *E. coli* vary from previous reports of other expressions of TAO from alternative strains of *E. coli.* This discrepancy could be due to other laboratories not observing and correcting for the auto-oxidation of 1-ubiquinol. This could also be linked to the use of C10E8 as a detergent in the assay, as detergents have similarly been shown to have an effect on the auto-oxidation of ubiquinol substrates.[172] Alternatively, the expression described here may contain higher concentrations of co-factors that may improve the kinetics observed in these experiments. For example, pyruvate has previously been shown to affect the activity of TAO.[168]

It was important to show that the enzyme was insensitive to azide, to give confidence that the 1-ubiquinol turnover observed was not from an undetected quinol oxidase impurity, and due to rTAO. A range of screening assays were developed, that allowed the single point inhibition screening of the MMV 'kinetoplastid box' collection of 400 compounds. This identified a range of compounds that inhibited TAO at micro-molar concentrations. One important outcome from the development of the 10-point inhibition assay highlighted the need to change pipette tips between each dilution step during the preparation of the compound dilution series. This ensured that accurate dilutions were performed and made sure that there was no erroneous transfer of compound. This supplemented the single point screening assay allowing inhibitor confirmation in robust 5 and 10-point IC_{50} determination assays. TAO was shown to be sensitive to colletochlorin B at similar concentrations to what had previously been reported in the literature,[128] allowing the inclusion of a positive control in assay plates when assessing future compounds. The next steps for this project were to design and synthesise drug-like inhibitors of TAO, that are described in chapters 4, 5 and 6.

Chapter 4

Chapter 4 – TAO inhibitor – lead compound identification

A suitable starting point for lead optimisation, amenable for high throughput synthetic exploration, was required to progress this project. A variety of hit molecules had been identified as potential lead compounds. Both the MMV single point screen and initial SAR described in the literature around the natural products ascofuranone and CCB provided interesting compounds for potential exploration. Some structurally similar analogues of CCB had also been synthesised in house prior to the initiation of this work. The activity of these compounds was tested in the 10-point TAO IC_{50} assay described in chapter 3, which provided some direction for further analogue design.

An ideal lead compound would be a synthetically amenable molecule allowing for further analogue design and synthesis. The lead should show potency against the target enzyme, that correlates to activity in cellular assays. It is important that cellular efficacy tracks to enzyme inhibition and the compound is specific for parasite inhibition and not acting as a general cytotoxin. Before embarking on analogue synthesis and further exploration of chemical hits, it is vital to confirm and validate the biological activity of hit molecules from pure characterised material, as often erroneous data can be generated from poor quality samples that exist in screening libraries.[177]

4.1 MMV Screening follow up

Screening of the MMV 'pathogen box' identified 20 compounds with reproducible binding curves and $pIC_{50} > 5.0$, when assessed by a 5-point IC_{50} determination. As part of follow up investigations, 10 compounds could be reordered from MMV as solids. Compounds **27**, **28**, **33**, **36**, **38**, **39**, **40**, **41**, **43** and **45** (Table 9) were available and were re-ordered to perform validation assays. For each compound, 10-point TAO IC_{50} determination and in collaboration with Novartis, *T. b. brucei* growth inhibition (EC_{50}) determination and cytotoxicity evaluation in mammalian HepG2 cells (CC_{50}), were performed, these data are summarised in Table 9.

Table 9 - MMV hit follow up

Structure	#	TAO (pIC_{50})[a]	*T. b. brucei* (pEC_{50})[b]	HepG2 (pCC_{50})[c]
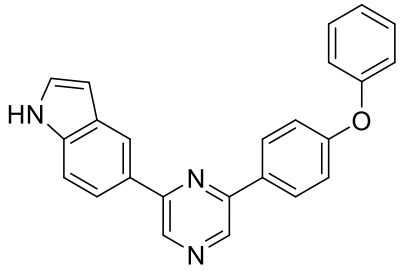	27	< 4.5	4.5 ± 0.1	4.8 ± 0.1
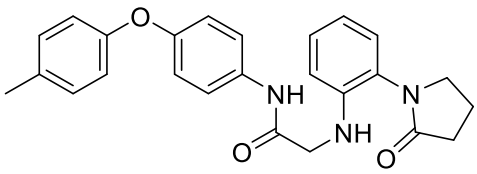	28	5.5 ± 0.1	4.6 ± 0.1	5.4 ± 0.1
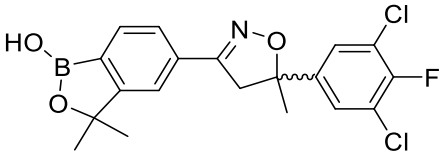	33	5.8 ± 0.1	5.3 ± 0.1	4.8 ± 0.1
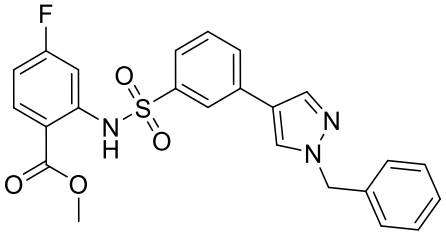	36	< 4.5	4.7 ± 0.1	4.9 ± 0.1
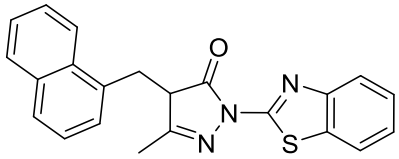	38	5.6 ± 0.1	5.1 ± 0.1	5.5 ± 0.1
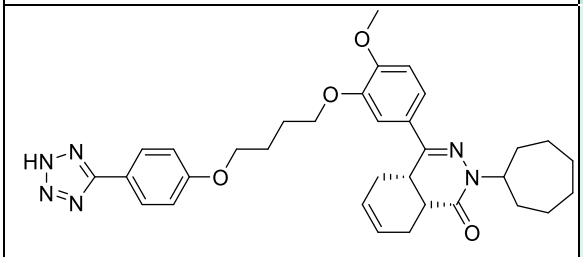	39	5.5 ± 0.3	7.4 ± 0.1	4.9 ± 0.1

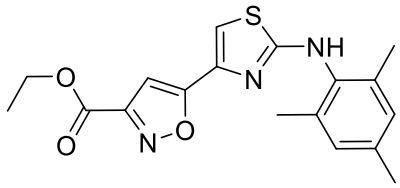	**40**	4.9 ± 0.1	4.8 ± 0.1	5.1 ± 0.1
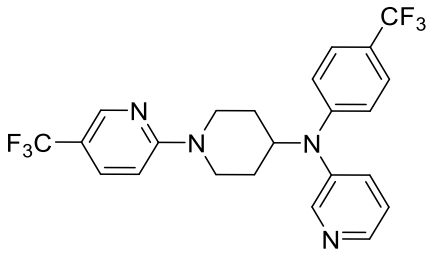	**41**	5.6 ± 0.2	5.2 ± 0.1	5.3 ± 0.1
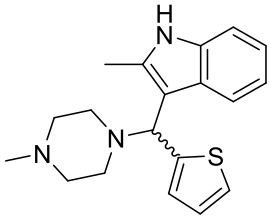	**43**	5.7 ± 0.1	5.7 ± 0.1	5.4 ± 0.1
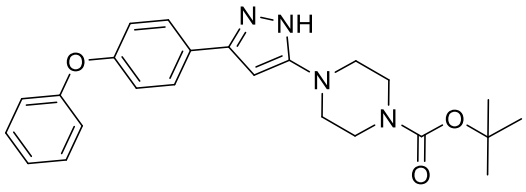	**45**	5.0 ± 0.1	5.8 ± 0.1	5.6 ± 0.1

[a] Negative log concentration and standard deviation of compounds required for 50% inhibition of trypanosome alternative oxidase. [b] Negative log concentration and standard deviation of compounds required for 50% growth inhibition of T. b. brucei Lister427. [c] Negative log concentration and standard deviation of compounds required for 50% growth inhibition of HepG2 cell line.

Examination of these data generated against the 10 MMV hit compounds showed that two compounds did not reconfirm activity against TAO in a 10-point IC_{50} assessment (**27, 36**). Compound **39** showed excellent inhibition of parasite growth; however, this was at a higher potency than TAO inhibition, indicating that this compound is inhibiting parasite growth by an alternative mechanism. The remaining compounds showed similar inhibitory activities against TAO and the parasite, with a slight decrease in potency observed from the biochemical enzymatic assay to the parasite assay. This is thought to be due to compound permeability into the parasite, leading to the effective internal parasite concentration being lower. Unfortunately, when the growth inhibition of the parasite is compared to the growth

inhibition of mammalian HepG2 cells there seems to be negligible selectivity for parasite inhibition with these identified compounds. This could be due to compound inhibition of similar quinol oxidases, necessary respiratory function in the mammalian cell. Compounds 33 and 43 showed a small window of selectivity for parasite inhibition although this was deemed too narrow to warrant further exploration. On the other hand, CCB showed 2 to 3 orders of magnitude selectivity for parasite growth inhibition over mammalian cells, and so the compounds identified from the MMV screen were not taken forward, and CCB was explored as an alternative starting point for inhibitor design.

4.2 CCB Profile

CCB showed high potency for inhibiting TAO (TAO pIC_{50} 8.5), which corresponded to similar high potency for *T. b. brucei* parasite growth inhibition (*T. b. b.* pEC_{50} 8.4) (Figure 43). CCB also showed good selectivity for parasite growth inhibition over mammalian cells with a > 1000-fold selectivity window (HepG2 pCC_{50} 5.1).[178]

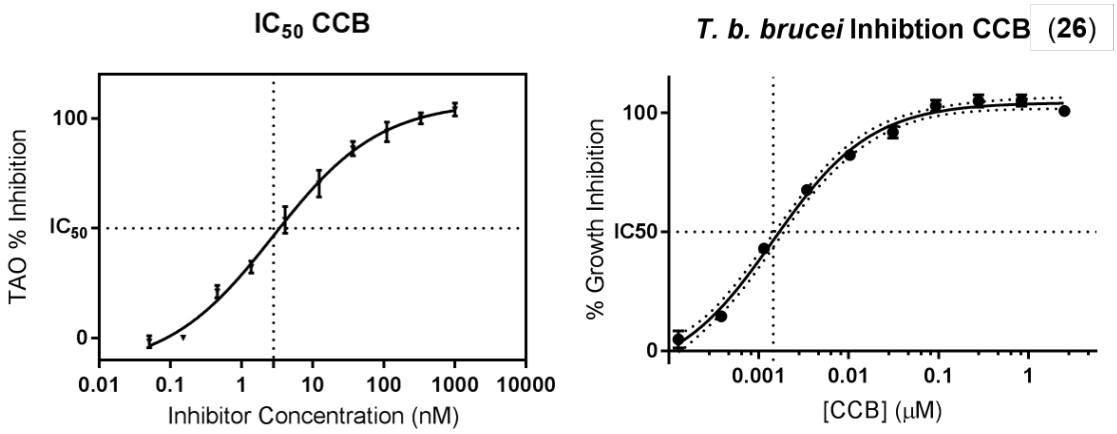

Figure 43 -- CCB TAO IC_{50} and *T. b. brucei* EC_{50}

In consideration of the high enzymatic inhibitory activity, high efficacy in the parasite growth inhibition assay, favourable selectivity over mammalian cells, a published crystal structure of CCB with TAO (PDB: 3W54), and the basic SAR previously described; further optimisation of the CCB chemotype was undertaken with an aim to identify a synthetically amenable lead

compound that could be developed into a more drug-like tool compound to enable the validation of TAO as a potential treatment for African trypanosomiasis.

A number of CCB analogues had previously been synthesised in the Sussex Drug Discovery Centre (SDDC) at the University of Sussex; however, biological data on these compounds were limited. These compounds were screened in the 10-point TAO inhibition assay to give an initial insight into the SAR around CCB, these data are summarised in Table 10 and published in the European Journal of Medicinal Chemistry.[178]

Table 10 – SAR summary of CCB analogues previously synthesised at the SDDC.

Structure	#	TAO (pIC_{50})[a]	*T. b. brucei* (pEC_{50})[b]	HepG2 (pCC_{50})[c]
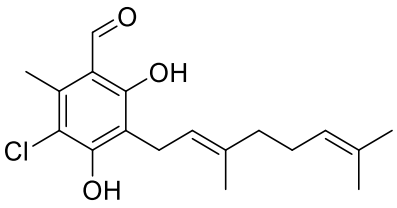	**26** CCB	8.5 ± 0.3	8.4 ± 0.1	5.1 ± 0.1
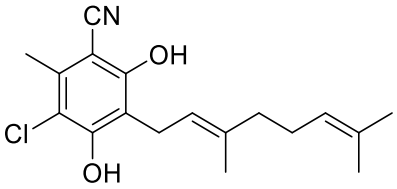	**47**	8.4 ± 0.2	6.4 ± 0.1	4.9 ± 0.1
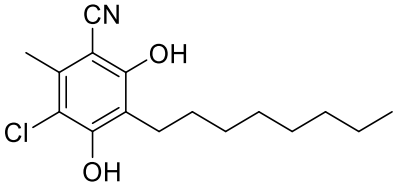	**48**	7.3 ± 0.1	5.6 ± 0.1	-
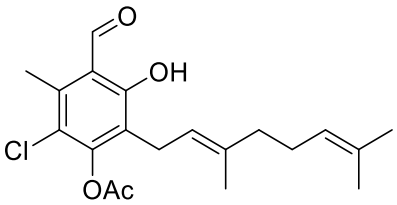	**49**	6.5 ± 0.2	7.4 ± 0.7	4.8 ± 0.1

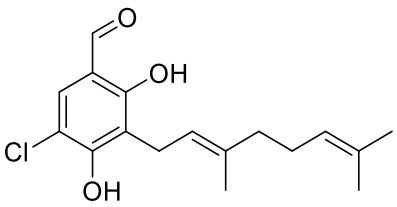	**50**	7.0 ± 0.2	6.6 ± 0.1	< 4.8
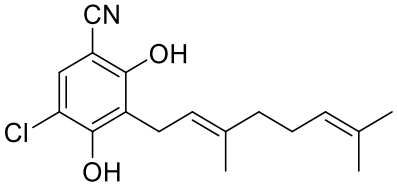	**51**	7.6 ± 0.3	5.2 ± 0.1	4.4 ± 0.1
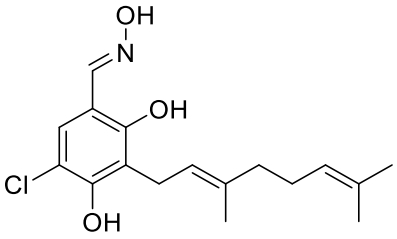	**52**	6.1 ± 0.3	5.7 ± 0.1	5.0 ± 0.1
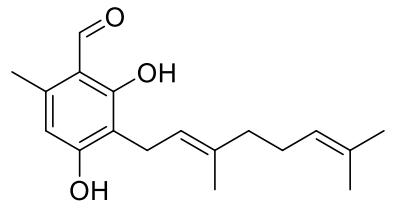	**53**	5.5 ± 0.2	5.8 ± 0.1	4.4 ± 0.1
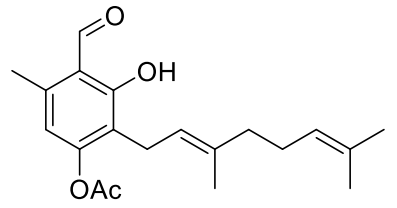	**54**	5.4 ± 0.2	-	-
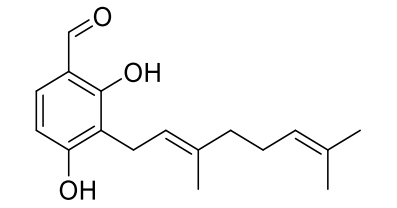	**55**	5.4 ± 0.2	-	-
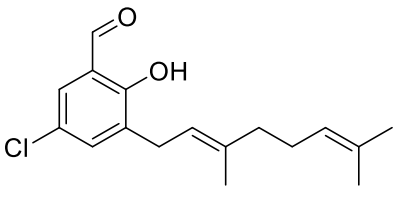	**56**	5.4 ± 0.1	-	-

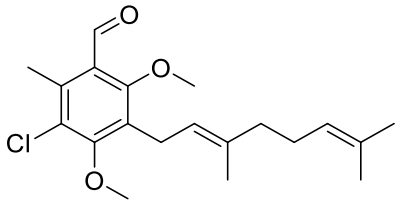	**57**	6.9 ± 0.2	4.9 ± 0.1	4.9 ± 0.1
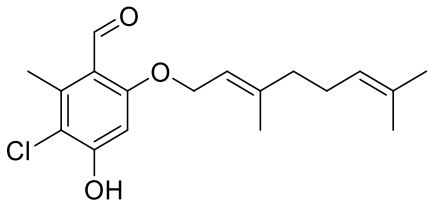	**58**	6.6 ± 0.2	5.5 ± 0.2	4.7 ± 0.1
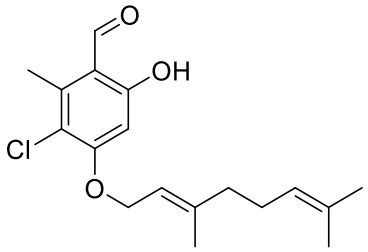	**59**	6.0 ± 0.1	4.9 ± 0.2	5.0 ± 0.1
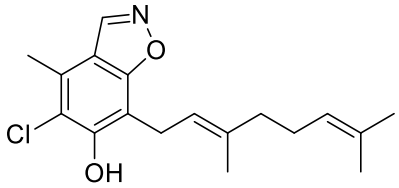	**60**	8.1 ± 0.1	7.0 ± 0.2	5.3 ± 0.1
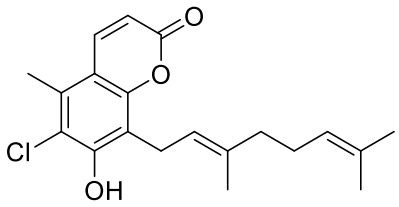	**61**	7.2 ± 0.1	6.2 ± 0.1	5.1 ± 0.1

[a] Negative log concentration and standard deviation of compounds required for 50% inhibition of trypanosome alternative oxidase. [b] Negative log concentration and standard deviation of compounds required for 50% growth inhibition of T. b. brucei Lister427. [c] Negative log concentration and standard deviation of compounds required for 50% growth inhibition of HepG2 cell line.

Substituting the benzaldehyde of CCB (**26**) for the nitrile (**47**) showed minimal detriment to TAO inhibitory activity. A benzonitrile moiety is preferred over a benzaldehyde group in a drug molecule, as hard electrophiles such as aldehydes are metabolic weak spots for oxidation.[179] Aldehydes can also readily form adducts with glutathione (GSH), or cysteine, creating toxic liabilities, *via* GSH depletion or nonspecific interaction with proteins.[180] The

removal of the aromatic methyl group provided 10-100-fold drop in potency against TAO (**50** & **51**). A key requirement for potent inhibitory activity of TAO was the chloro group; removal of this in compound **53** led to a 100 to 1000-fold decrease in potency. Results concerning the availability of the hydrogen bond donor phenols were mixed. Compound **57** surprisingly still inhibited TAO with reasonable potency. Potency was also retained with compounds **58** and **59** where the geranyl tail point of attachment was explored, albeit with around 100-fold detriment in potency.

In addition to the data that was published in the European Journal of Medicinal Chemistry,[178] two other bicyclic inhibitors of TAO had been synthesised in Simon Ward's group. The 1,2-benzisoxazole intermediate (**60**) was converted *via* a Kemp elimination to the nitrile analogue **47**.[181] Compound **60** showed good inhibitory activity of TAO and warranted further synthetic exploration. The coumarin analogue (**61**) had also been synthesised and showed respectable potency against TAO.

The initial project strategy was to identify a synthetically tractable lead compound that would facilitate late stage diversification and generation of SAR. The nitrile analogue was preferred to the benzaldehyde as TAO inhibition of both analogues were shown to be similar and the nitrile had a reduced metabolic and toxic liability. The other advantage that the nitrile provided was an improved chemical stability, allowing a wider range of reaction conditions to be employed at later stage synthetic steps. The 1,2-benzisoxazole was also of interest, as it provided a means to remove of one of the HBDs, improving the likelihood of achieving CNS penetrantration.[182]

4.3 Resorcinol analogue synthesis and TAO activity assessment

The established synthetic routes to analogues of CCB are not trivial and often require multiple synthetic steps, with a variety of protection and deprotection strategies. Previous work from the Ward group has highlighted the difficulties in the generation of advanced intermediates for late stage diversification of this chemotype.[183] A synthetic route to an advanced intermediate was developed to investigate late stage diversification of the 'lipophilic tail' region of the CCB chemotype (Figure – 44). It was anticipated that

intermediate **66** could provide access to tail modifications through electrophilic aromatic substitution. Previous efforts from our group had focused on diversification through halogenation and subsequent transition metal mediated cross couplings, Lewis acid mediated rearrangement or directed lithiation chemistries. Unfortunately these methods had not been fruitful in providing analogues of CCB.[183]

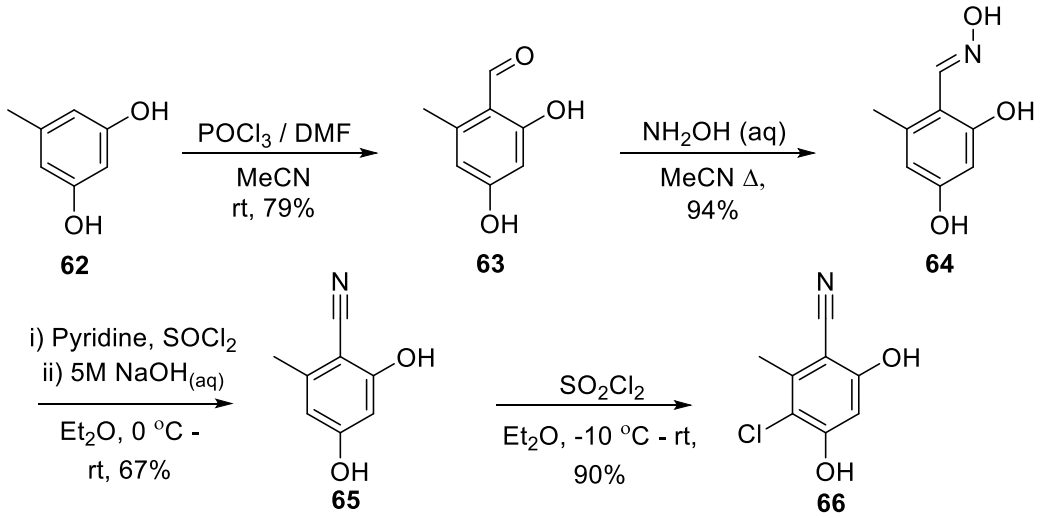

Figure 44 - Resorcinol advanced intermediate synthesis

The readily available resorcinol starting material (**62**) could be formylated under Vilsmeier-Haack conditions in high yield (79%).[184] Generation of the Vilsmeier intermediate (**67** – Figure 45) by the dehydration and chlorination of DMF, provided the species that underwent electrophilic aromatic substitution with the electron rich resorcinol. Subsequent hydrolysis of the dimethyl iminium species afforded the benzaldehyde (**63**).

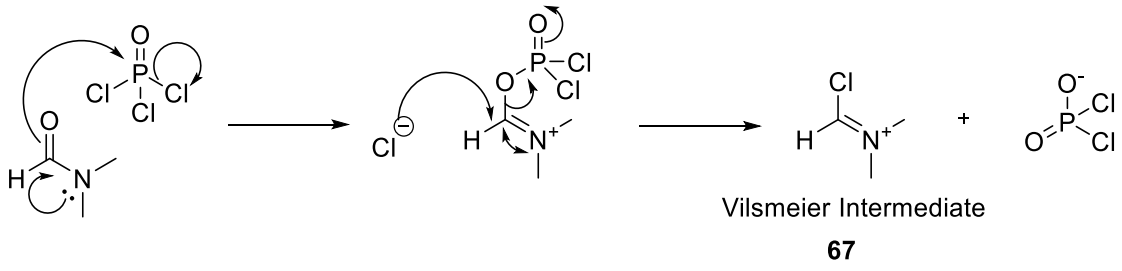

Figure 45 - Vilsmeier-Haack intermediate formation

To aid isolation of the compound on large scale the reaction was performed in acetonitrile. Quenching the reaction with water provided small amounts of solid product and then removal of acetonitrile by concentration under *vacuum* afforded the desired product as a yellow solid in satisfactory purity for continuation of synthesis. In contrast, conducting the reaction in neat DMF provided crude material that had to be purified by flash chromatography, limiting isolation on a large scale. The characteristic aldehyde proton signal at 10.04 ppm and the shift of the *ortho*-phenol to 12.05 ppm (due to the intramolecular hydrogen bond formation between the aldehyde) were indicative of formation of the benzaldehyde (**63**). Oxime formation was carried out by the addition of an aqueous solution of hydroxylamine in acetonitrile under reflux to provide (**64**). This could be dehydrated through chlorination with thionyl chloride then cyclisation with the adjacent phenol. *In situ* Kemp elimination with aqueous sodium hydroxide provided nitrile intermediate (**65**), with a characteristic band at 2225 cm^{-1} for the CN triple bond stretch in the infra-red (IR) spectrum. Treatment of this with an electrophilic chlorination reagent (**68**), generated from sulfuryl chloride and diethyl ether (Figure 46) as described by Masilamani *et al*.[185], provided the desired chloro nitrile resorcinol intermediate (**66**) for further synthesis.

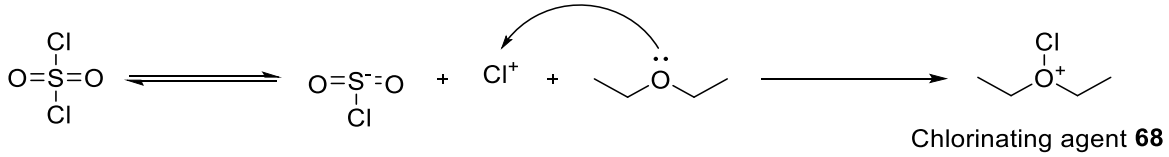

Figure 46 - Electrophilic chlorinating agent generation as reported by Masilamani *et al*.[185]

Chlorination of the benzaldehyde intermediate (**63**) under identical chlorination conditions provided the comparative chloro benzaldehyde (**69**) for further synthetic exploration (Figure 47).

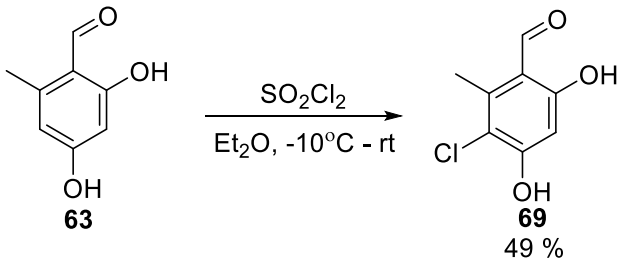

Figure 47 - chlorination of benzaldehyde

It was envisaged that Mannich-phenol chemistry could be employed to furnish the aromatic system with a tail containing a benzylic amine as a final step diversification. The inclusion of a hetero atom in the lipophilic chain was desirable, as the introduction of polarity improves cLogP and cLogD, thus significantly improving the CNS MPO score (discussed later) for these molecules. The target benzylamine molecule was modelled in the binding cavity of TAO in complex with CCB (PDB: 3W54).[129] Replacing CCB present in the 3W54 crystal structure with the benzyl amine analogue (**71**) and performing an energy minimisation with the OPLS3 (Optimized Potentials for Liquid Simulations 3) forcefield showed good structural similarity to CCB (Figure 48), using Schrödinger drug discovery suite - Maestro. OPLS is a forcefield that is used to calculate the molecular dynamics of biomolecules. Recent refinements to the latest forcefield OPLS3 have included the description of aryl nitrogen lone pairs, halogen bonding *via* off atom charge sites and refined dihedral parameters of peptide bonds. This has allowed more accurate simulations, calculations and model generation, which compare to experimentally observed binding modes.[186]

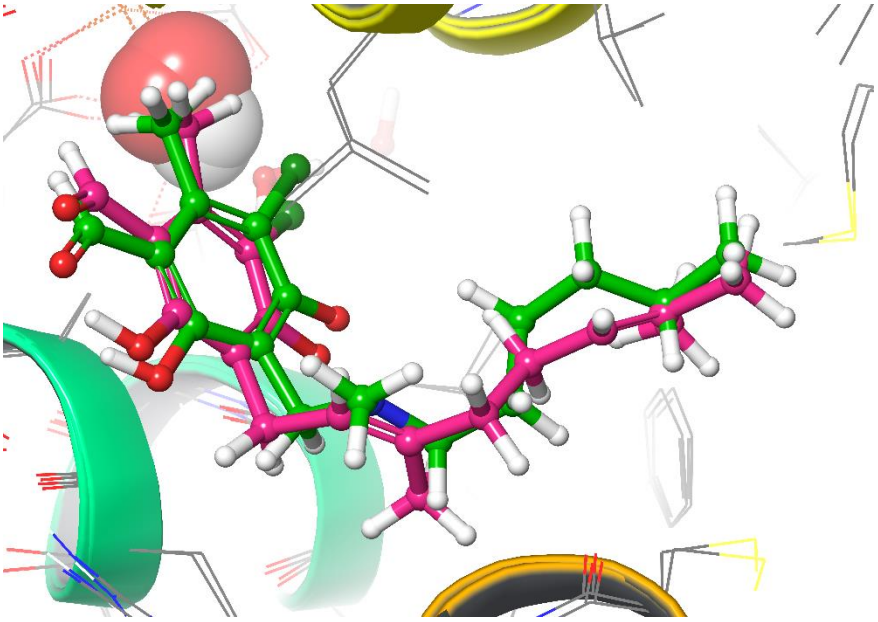

Figure 48 - Modelled benzylamine analogue (green) compared to CCB (pink), overlayed energy minimised structures, using OPLS3 forcefield in Maestro – Schrodinger drug discovery suite. Strucutral data from published crystal structure PDB: 3W54, Shiba *et al.*[129]

Formation of the iminium species (**70**) following the dehydration of paraformaldehyde with *N*-hexylmethylamine in ethanol and subsequent electrophilic aromatic substitution with the benzaldehyde resorcinol intermediate (**69**), provided the desired benzylamine derivative (**71**) (Figure 49). Similarly, analogues of the benzonitrile intermediate (**66**) were synthesised by a Master's student (Thomas Cunningham) under my supervision with the same reaction conditions to provide compounds **72** & **73** (Table 11).

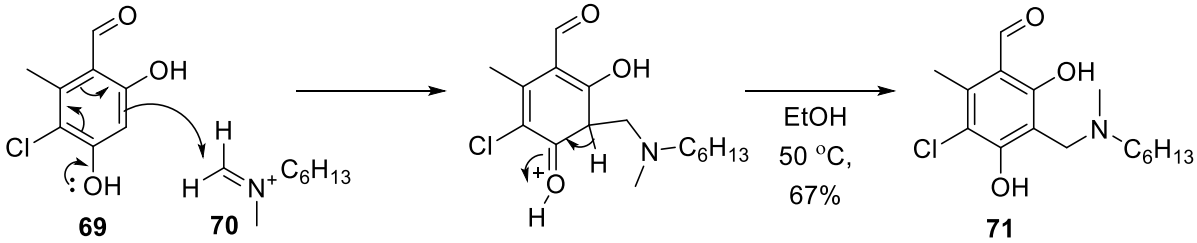

Figure 49 - Mannich Phenol Chemistry

Table 11 - TAO inhibition of resorcinol benzylamine analogues

Structure	#	TAO (pIC_{50})[a]	cLogP[b]	cLogD7.4 [c]	CNS MPO [d]
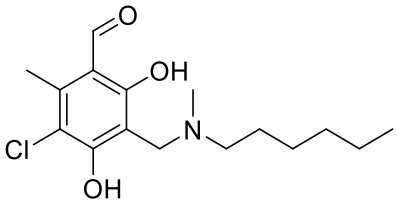	71	< 4.5	5.0	3.3	4.4
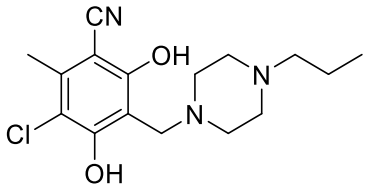	72	< 4.5	3.0	1.4	5.3
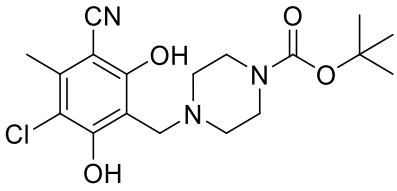	73	< 4.5	3.0	1.3	5.1

[a] Negative log concentration and standard deviation of compounds required for 50% inhibition of trypanosome alternative oxidase. [b, c, d] Calculated using ChemAxon MarvinSketch 17.25.0.

Assessment of the TAO inhibitory activity of these compounds was disappointing, with no inhibition of TAO observed, despite the improvement of calculated physicochemical properties (Table 11). These data suggest that inclusion of a basic centre in this part of the molecule is disfavoured. Due to the extensive synthetic effort of accessing these resorcinol aromatic systems, these targets were deprioritised in favour of investigating the bicyclic compounds that had been identified, in particular the 1,2-benzisoxazole (60).

4.4 Synthesis and activity assessment of bicyclic analogues

Compound 60 showed promising inhibitory activity against TAO (Table 10). The synthesis of a halogenated advanced intermediate was devised to facilitate the exploration of the tail region of these molecules through transition metal cross coupling.

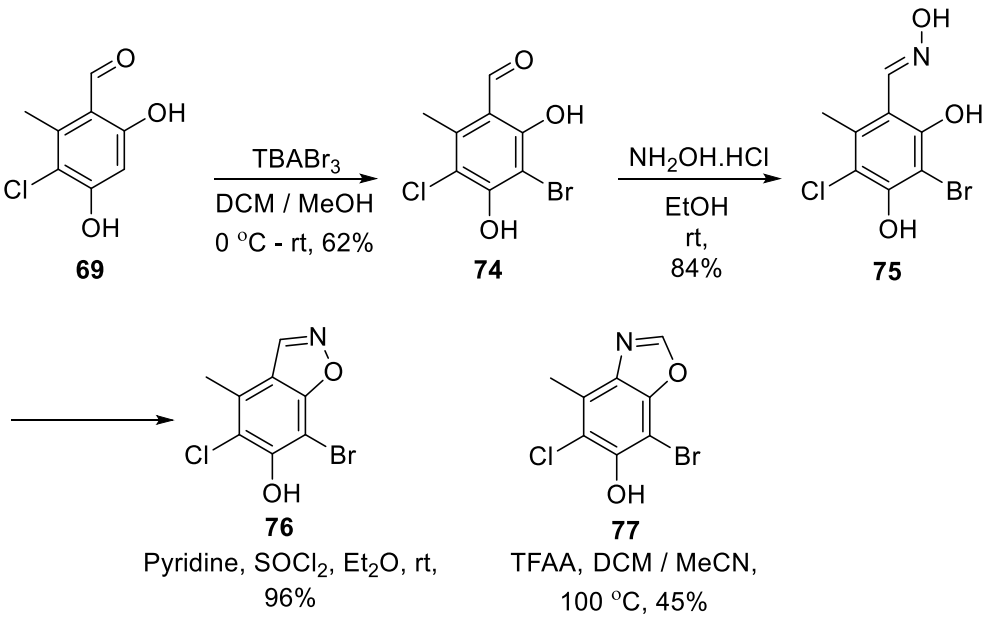

Figure 50 - Benzisoxazole / benzoxazole synthesis

Electrophilic bromination of **69** with tetrabutylammonium tribromide at 0 °C provided compound **74** in reasonable yield. Oxime formation was carried out under similar conditions as used for non-halogenated analogue **64**. Cyclisation of this intermediate was initially carried out in the presence of trifluoroacetic anhydride in dichloromethane reported by Kalkhambkar *et al*.[187] However, the poor solubility of **75** in dichloromethane prevented any reaction in neat solvent. Modification of the solvent system to 10:1 dichloromethane acetonitrile provided small amounts of product at room temperature following prolonged reaction times. Heating the reaction in the microwave to 100 °C expediated the reaction, and after 1 hour the reaction had proceeded to completion (Figure 50). Initial analysis by LCMS showed the correct molecular ion of the 1,2-benzisoxazole (**76**). However, upon analysis of the 2D NMRs of the purified material, nuclear Overhauser effect experiments failed to show expected correlations between the methyl C-H and the aromatic C-H and hetero-nuclear multi-bond correlation spectroscopy experiments also failed to show correlation between the aromatic C-H and the aromatic carbon bearing the methyl group (Figure 51).

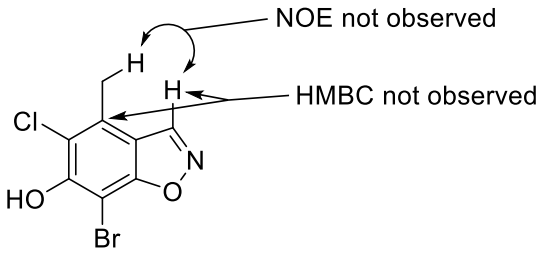

Figure 51 - NOE, HMBC correlation

Previously the non-chlorinated 1,2-benzisoxazole synthesis was carried out *via* dehydration of the oxime with thionyl chloride in pyridine. This promoted intra-molecular cyclisation with the adjacent phenol, that upon Kemp elimination with NaOH provided compound **65**. These initial cyclisation conditions were attempted with analogue **76**. This reaction provided a product that had a different retention time by LCMS to the microwave conditions but contained the desired product molecular weight. Analysis of the purified material from this reaction showed NOE correlation between the methyl C-H and the aromatic C-H at 9.40 ppm and 2.53 ppm (Figure 52) confirming that the correct product had been isolated.

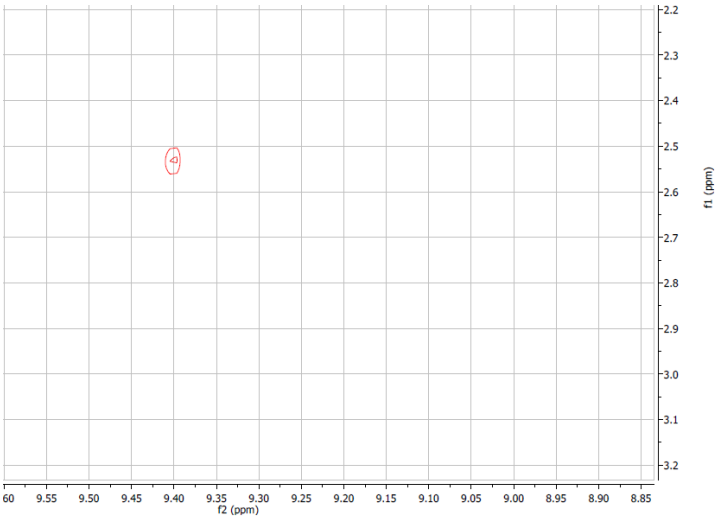

Figure 52 - NOE correlation for 1,2-isoxazole

It was suspected that conducting the reaction at elevated temperatures promoted a Beckman rearrangement of the oxime that had previously been reported by Thomas *et al*

(Figure 53).[188] This would give rise to the 1,3-benzoxazole (**77**) upon cyclisation, which matched the NMR data obtained for this compound. To provide further evidence that the correct assignment of the benzisoxazoles was made, the products were subjected to Kemp elimination conditions. The products were dissolved in acetonitrile and treated with 3 M aqueous sodium hydroxide. In agreement to the NMR studies, the 1,2-isoxazole product underwent Kemp elimination[181] to give the nitrile phenol product, whereas the product isolated from the initial trifluoroacetic acid anhydride, dichloromethane, 100 °C reaction was stable to these conditions.

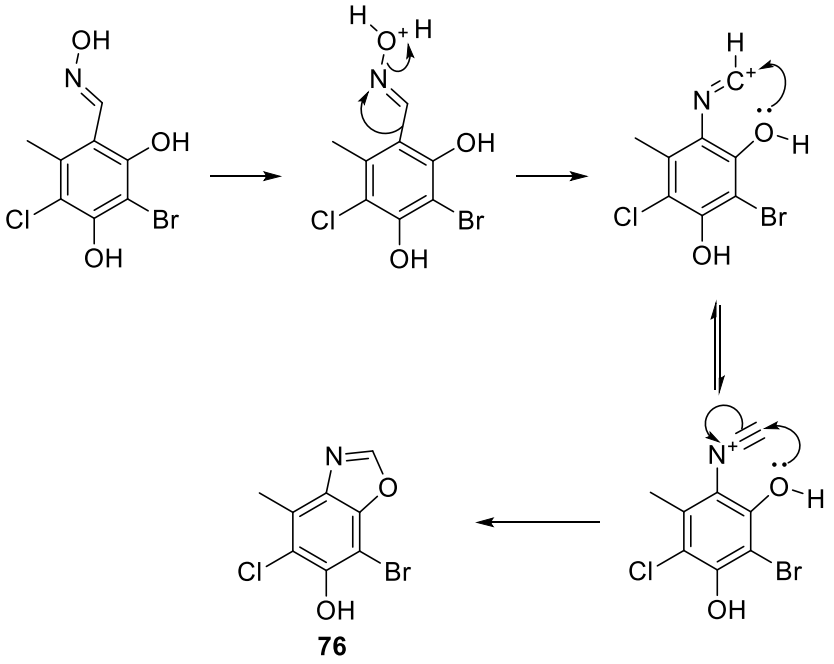

Figure 53 – Plausible mechanism of Beckmann rearrangement to 1,3-benzoxazole

With the 1,2-benzisoxazole (**76**) now in hand, a variety of palladium mediated cross-couplings were attempted to furnish substituents of the lipophilic tail. Unfortunately, despite screening a matrix of 3 bases (K_2CO_3, K_3PO_4 and triethylamine) and 3 catalysts [$Pd(PPh_3)_2Cl_2$, $Pd(dppf)Cl_2$ and $Pd(dptpf)Cl_2$], Suzuki-Miyaura cross coupling with 3,4-difluorophenyl boronic acid was unsuccessful.[189,190] Under these basic reaction conditions at elevated temperatures, Kemp elimination was predominant, and the starting material degraded to the nitrile phenol. Similarly, attempts at Mizoroki-Heck cross coupling with 1-octene were also

unsuccessful,[191,192] again providing the ring opened starting material. At this point an alternative strategy was sought for two reasons. Firstly, any future base mediated reactions would likely provide Kemp eliminated products, creating purification and elucidation problems, that would limit the synthetic versatility of this intermediate. Secondly, the long-term chemical stability of these compounds is uncertain, especially regarding the demanding stability requirements that had been set out for new treatments for HAT by DNDi (Table 2). These chemical stability issues could also prove problematic in more advanced *in vivo* pharmacokinetic and pharmacodynamic studies.

4.5 Mono phenol analogue synthesis and biological assessment

The TAO inhibitory activity of the 1,2-benzisoxazole (60) and compounds 57, 58 and 61 provided an interesting observation: removal of the hydrogen bond donating phenol *ortho* to the aldehyde or nitrile appeared to be tolerated, as these compounds retained potent inhibition of TAO. The hydrogen bond donor had previously been suggested as important for the interaction with the enzyme, forming hydrogen bonds with arginine (R118) and threonine (T219) residues.[128,129] However, analogues challenging this hypothesis had not previously been synthesised or reported. The data generated here was of particular interest and looked to challenge this assumption. Removal of the other phenol *para* to the aldehyde however was not tolerated well resulting in a 40-fold reduction in potency (51 & 56 – table 7).

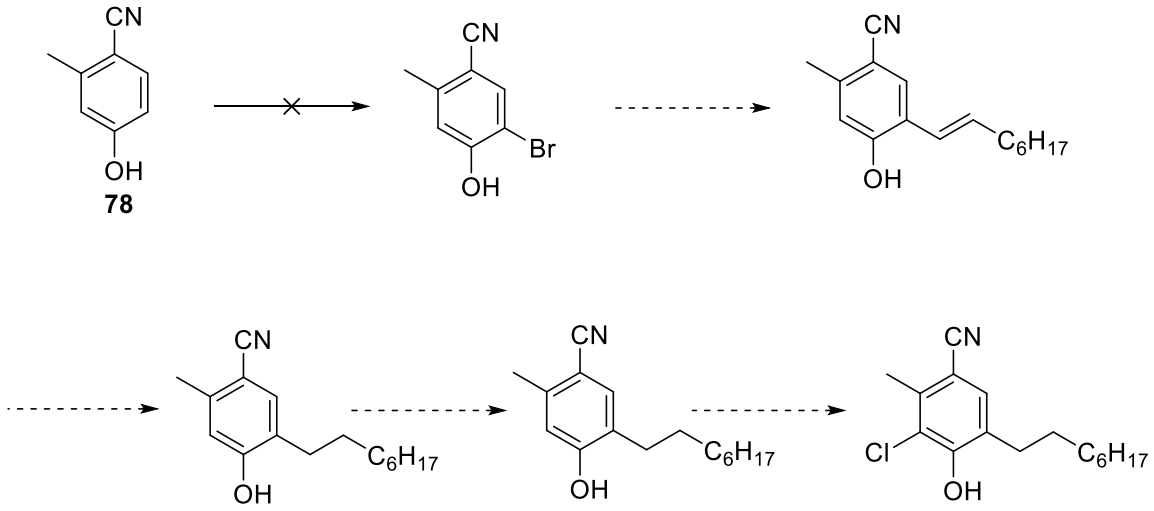

Figure 54 - Proposed synthesis of mono-phenol analogue

A synthesis to the mono phenol analogue was devised (Figure 54). Pourmoursavi *et al.* had described the use of benzyl triethylammonium tribromide (BTEAT) to selectively brominate a range of substituted phenols.[193] Unfortunately attempts at mono bromination using similar conditions with benzyl trimethylammonium tribromide (BTMAT), provided a mixture of brominated products at room temperature. Efforts to optimise the mono bromination of the commercially available benzonitrile (**78**) were also unsuccessful. Modification of reaction temperature, addition order and speed provided a mixture of brominated products that could not be easily separated. Alternative brominating agents (Br_2, tetrabutylammonium tribromide and *N*-bromosuccinimide) were also trialled to no avail providing mixtures of the brominated products; therefore, an alternative synthesis was sought.

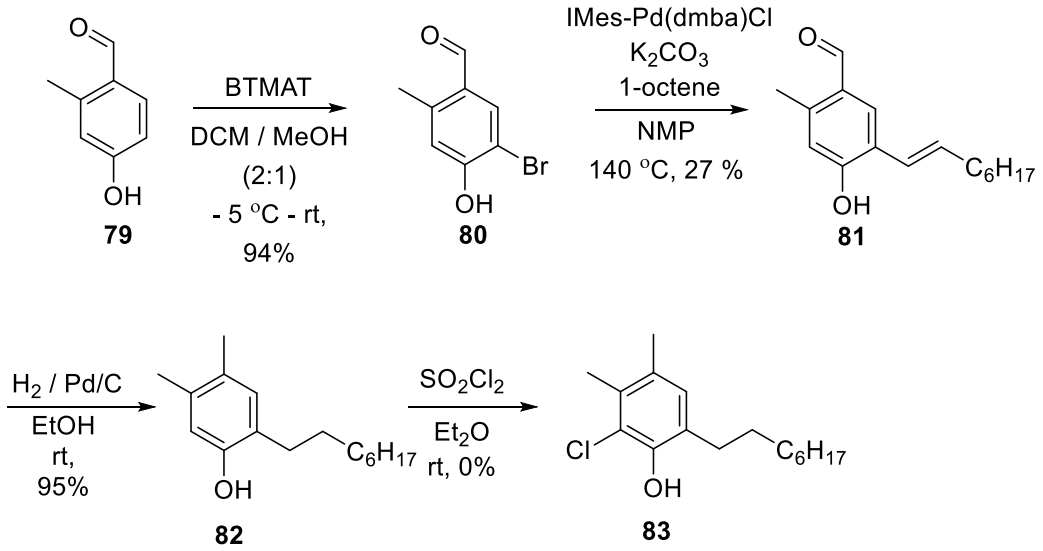

Figure 55 - Proposed mono-phenol benzaldehyde synthesis

Selective mono-bromination of the benzaldehyde (**79**) was however successful with the BTMAT conditions and the desired product (**80**) could be isolated in high yield (94%) and on scale (Figure 55). A reaction condition screen was performed around the subsequent Mizoroki-Heck reaction. It was found that reaction with 1-octene afforded the alkene intermediate (**81**) in 27% yield, utilising conditions reported by Peh *et al.*[194] These conditions utilise a *N*-heterocyclic carbene (NHC) ligand for the palladium catalyst. NHC ligands have been shown to have advantages over phosphine ligands: they show higher stability at elevated reaction temperatures than bulky phosphine ligands and have strong σ-donating properties that aid oxidative addition of the metal into the carbon-halogen bond.[195,196] These conditions allowed the isolation of the tail derivatised analogue (**81**). The next step required hydrogenation of the alkene double bond, which proved challenging. The benzaldehyde was shown to be susceptible to hydrogenation and the resulting benzylalcohol readily underwent hydrogenolysis to provide the undesired dimethyl analogue (**82**) that showed 2 methyl signals in the ^{1}H NMR at 2.18 and 2.19. The crude material isolated from this reaction was however taken on in synthesis to provide the chlorinated dimethyl analogue **83** unfortunately due to an error on the purification this compound was not isolated to allow for future SAR comparison. Adaption of the synthesis to provide the more attractive benzonitrile was devised (Figure 56).

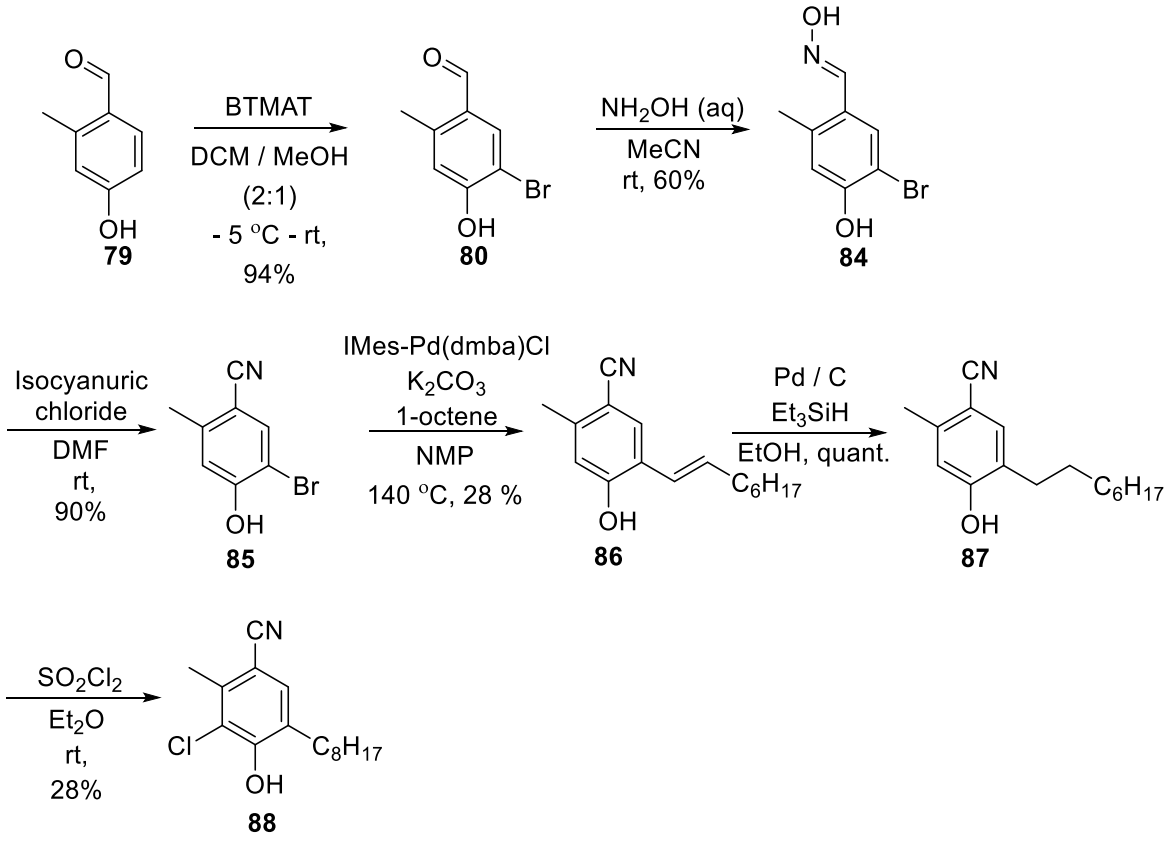

Figure 56 - Successful monophenol analogue synthesis

A variety of routes were investigated to interconvert the aldehyde **80** into the nitrile **85**. Vatèle *et al.* had reported the facile conversion of primary alcohols to their corresponding aldehydes, with subsequent reaction to the nitrile *via* an aldimine intermediate using TEMPO, diacetoxyiodobenzene and ammonium formate in a one-pot procedure.[197] Bag *et al*. had also reported the oxidation of an aldimine to the nitrile using diacetoxyiodobenzene.[198] Unfortunately, under both of these conditions the nitrile product **85** was not isolated and the material underwent a highly exothermic degradation to unidentified products. This was likely due to the phenol, that has previously been reported to react with hyper-valent iodine reagents.[199,200] Although initial attempts were unsuccessful *via* the aldimine, there was promise in generating the aldoxime with hydroxylamine, and carrying out a subsequent dehydration. Conditions reported by De Luca *et al,*[201] describe the reaction between cyanuric chloride and DMF to generate a Vilsmeier-like intermediate. This electrophilic intermediate

is suggested to undertake nucleophilic attack from the oxygen of the aldoxime, which breaks down to generate the nitrile. These reaction conditions successfully provided the nitrile **85** with an indicative carbon-13 NMR shift at 117.7 ppm and the presence of CN triple bond stretch at 2232 cm^{-1} in the IR spectrum. The nitrile could be cross coupled using the same conditions previously identified in the synthesis of aldehyde **81**, with similar yields. The vinylic intermediate **86** was isolated and confirmed as the trans-alkene from a proton coupling constant of 16 Hz. This could be successfully reduced by transfer hydrogenation using conditions reported by McMurray.[202] Over-reduction of the nitrile was not observed, as the quaternary nitrile carbon was still present at 118.4 ppm in the NMR analysis of **87**. Final electrophilic aromatic chlorination with sulfuryl chloride in diethyl ether was slow, requiring the addition of extra equivalents of the chlorinating component and the extension of reaction time to provide sufficient material for isolation of compound **88**.

The mono-phenol analogue **88** was isolated successfully through the implementation of the synthesis described (Figure 56). Compound **88** was assessed in the 10-point TAO inhibition assay and sent for *T. b. brucei* parasite growth inhibition and mammalian HepG2 cytotoxicity assessment at Novartis (Figure 57). Compounds **47** – **53**, **57** - **61** and **83** were at this point sent to Novartis for evaluation in the same assays, summarised in Table 7. Data generated against *T. b. brucei* showed that the change from aldehyde to nitrile was not as well tolerated as in the enzyme inhibition assay. Direct comparison of compounds **47** to CCB (**26**) and compounds **50** to **51** show between 10-100-fold loss in potency against parasite growth with the nitrile. In addition, the nitrile did not result in any loss of cytotoxicity in the mammalian HepG2 cell and as a result the favourable selectivity profile observed with CCB was diminished to 10-100-fold. The replacement of the geranyl chain with a straight *n*-octyl chain correlated to a 10-fold decrease in potency against the enzyme and a 10-fold decrease in efficacy against the parasite (**47** & **48**). Interestingly the potency of the acylated phenol analogue (**49**) showed improved potency in the parasite compared to the enzyme. It was hypothesised that the acetyl group was labile, either under assay conditions or due to parasite enzyme activity, and so degraded to the more potent CCB (**26**) *in situ*.

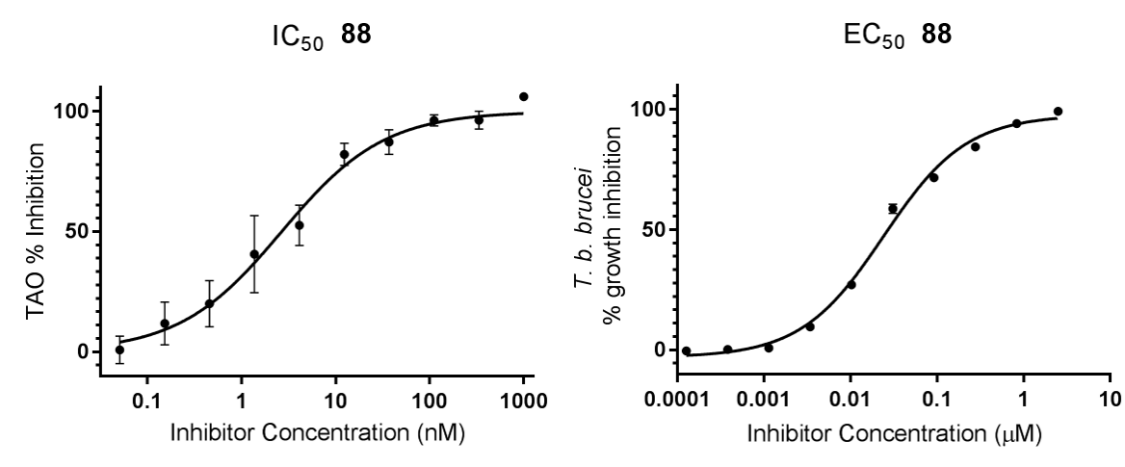

Figure 57 - TAO IC_{50} and *T. b. brucei* EC_{50} assessment of mono-phenol **88**, s.d. shown (n = 3).

The mono phenol compound **88** potently inhibited TAO with a pIC_{50} 8.5 (3 nM), which correlated to potent inhibition of parasite growth with a pEC_{50} of 7.6 (27 nM). The compound still retained selectivity of parasite inhibition (~ 300-fold) over mammalian HepG2 cells with a corresponding pCC_{50} of 5.1 (7.8 μM). Compound **88** provided a synthetically amenable lead that would allow further chemical property exploration and SAR investigation. Comparison of this compound to the matched pair **48** was of interest, as removal of the phenol had resulted in a 10-fold increase in potency against the enzyme, and also retention of parasite growth inhibition, resulting in reasonable selectivity against the parasite over mammalian cells. Overall this compound provided a chemically tractable lead, which retained good biochemical and cellular potency.

Chapter 4 - TAO Inhibitor – Lead Compound Identification Conclusions

The focus of this chapter was to highlight the screening and chemistry efforts aimed at identifying a synthetically amenable lead compound. The compounds identified from screening the MMV kinetoplastid box initially detected several structurally novel TAO inhibitors. Unfortunately, following the confirmation of these compounds activity in 10-point TAO inhibition, *T. b. brucei* parasite growth inhibition and HepG2 cytotoxicity assessment, no lead like molecules were identified and no improvements to CCB were observed. Extensive exploration of synthetic routes to analogues of CCB had previously been carried out in the

SDDC with variable success.[178,183] The synthesis of hexa-substituted aromatic systems is not trivial, especially with an aim to carry out a late stage diversification of these molecules.[203] The combination of the complex electronic nature of these highly functionalised molecules and the steric hindrance of neighbouring substituents limits the viability of using these molecules as chemically tractable lead molecules.

Further analysis of TAO inhibition data of historical compounds challenged the hypothesis that both hydrogen-bonding phenols were required for potent TAO inhibition. The synthesis of a mono phenol analogue was carried out and confirmed our previous observations verifying that the phenol ortho to the aldehyde / nitrile was not required for potent TAO inhibition. The synthesis that was developed on route to this compound had potential to be used in a late stage diversification strategy, towards additional analogues that would facilitate further exploration of SAR and lipophilic tail modification, discussed in chapter 5.

Chapter 5

Chapter 5 – SAR Exploration of Lipophilic Tail

5.1 Introduction

To develop a TAO inhibitor into a potential treatment for HAT it is important to consider the target product profile set out by the DNDi (Table 2). Some features of this profile can be achieved through astute compound design. Firstly, to effectively treat the second stage of the disease it is important that the compound will achieve efficacious concentrations in a range of tissues including the brain, so blood brain barrier (BBB) permeability is a requirement. An oral dosing strategy is also the preferred route for administration due to limited accessibility of health care in sub-Saharan Africa.

Oral dosing has well studied barriers, which limit effective drug delivery. Solubility and dissolution along with absorption, distribution, metabolism and excretion, often referred to as ADME, are all important parameters to optimise during the development of orally bioavailable drugs.[204] There have been many studies that relate compound physicochemical properties to ideal pharmacokinetic profiles for oral dosing. Lipinski's rule of five (RO5) was derived from the analysis of approved oral drug molecules and their physicochemical parameters. The RO5 states that in order to obtain a compound that has a high chance of being orally bioavailable it should not fail more than one of the following parameters: higher than 500 molecular weight (MWt), have more than 5 hydrogen bond donors (HBD), more than 10 hydrogen bond acceptors (HBA) and a lipophilicity (LogP) above 5.[205]

Other studies have looked at the effects of physicochemical properties on measured parameters like absorption.[40] Palm and co-workers have shown the close relationship that polar surface area (PSA) has with human fraction absorbed (F); compounds with PSA of below 63 Å are > 90% absorbed and compounds with PSA above 140 Å are < 10% absorbed.[40] These observations have been further employed, along with other calculated parameters like cLogP and MWt, in models to predict absorption.[206–208]

Similar explorations of the relationship between solubility and physicochemical properties have been attempted. However, correlations between high solubility and calculated physical

chemical properties are not clear-cut, making predications of solubility from compound structure imprecise. Many parameters have to been taken into account, and solubility models that contain a measured melting point often predict more accurately.[209] More recent models have since been developed that include descriptors for structural shape, including number of rotational bonds and dihedral angles, which can better predict solubility when combined with other physicochemical parameters.[210,211]

Metabolism of xenobiotics is a vital mechanism for organism survival, that facilitates the excretion of potentially harmful substances from the body. External molecules that are absorbed are subjected to a variety of metabolising enzymes in the liver. A large class of these enzymes are cytochrome P450 oxidases (CYP), that display recognition for a broad range of substrates and facilitates their mono-oxygenation.[212] The rate and extent of compound metabolism can have a large impact on *in vivo* efficacy. Compounds that are rapidly metabolised and excreted will have a limited capacity to reach and maintain efficacious concentrations in the body. Metabolites that arise from enzymatic phase one processes such as oxidation, often undergo further 2nd phase metabolism through conjugation with molecules such as glucuronic acid. This furnishes the metabolite with polar functionality, which allows for efficient elimination and excretion. One common strategy to reduce metabolism, is to block the specific site of metabolic liability with a functional group that is less reactive or not recognised by metabolic enzymes.[213,214] Recent reports of metabolic stability improvement strategies have involved utilising specific CYP enzymes to bio-transform advanced drug candidates on a preparative scale, then utilise fluorination chemistry to transform the oxidised drug molecule into a fluorine blocking group, specific to the site of metabolising enzyme action. This resulted in the generation of more metabolically stable molecules in some cases. However, the study also showed that stabilisation was only effective if the site of metabolism was the predominant weak spot. There are variations in metabolic pathways between species, and stability with one species' CYP enzymes did not always correlate to stability across species. It was also highlighted that not all drug molecules will be suitable for late stage fluorination, as this depends on the tolerability of other functional groups present.[215]

Another general strategy to promote metabolic stability is to lower compound lipophilicity,[214,216,217] as compounds with higher lipophilicity have been shown to have higher affinity for CYP enzymes.[218] A common method employed to reduce lipophilicity is to introduce polarity into molecules through structural modification such as inclusion of heteroatoms and replacement of lipophilic groups.[217] Adoption of compound optimisation metrics like lipophilic ligand efficiency (LLE) in early drug discovery programs is also becoming popular.[219] LLE facilitates program advancement through the simultaneous optimisation of target potency and lipophilicity. This allows the identification of compounds that attain potency through enthalpic protein interactions and not lipophilic entropic interactions, reducing the risk of compounds having poor solubility or high metabolism.[220]

The design of CNS penetrant compounds requires further optimisation of orally bioavailable molecules to permeate the blood brain barrier (BBB). The BBB provides an additional obstacle preventing xenobiotics from entering the CNS. The BBB comprises an endothelial cell membrane with tight junctions that restricts paracellular diffusion.[221] The BBB also contains a range of efflux transporters that transport lipophilic molecules back into the blood stream, preventing their absorption and protecting the CNS from a variety of toxins.[222]

A number of physicochemical properties have been assessed with regards to achieving high BBB permeability, previously reviewed by Clark.[223] Interestingly, as with intestinal permeability predictions, HBD, HBA, PSA, lipophilicity and molecular size all have a correlative effect on BBB penetration. It is of note that compounds that have a lipophilicity in the range LogD 1-3, have fewer hydrogen bonding atoms (< 5), lower PSA (< 90 Å) and MWt (< 450 Da) are more BBB permeable. Further observations that the majority of CNS drugs have high permeability, low metabolic clearance and low efflux have recently been developed into a model deemed ‘multi-parameter optimisation’ (MPO) for CNS penetration.[182,224] In this study the physicochemical parameters for a range of CNS approved drugs and CNS drug candidates were correlated to measured human liver microsome (HLM) clearance, passive permeability and P-glycoprotein (P-gp) efflux. Compounds that had cLogP < 5, cLogD < 4, HBD < 3.5, PSA (20-120 Å) and pKa (8 – 10) scored positively (the scoring function changed linearly depending on the distance from the cut off parameter). The combined scores for each

compound were shown to correlate to the measured clearance, P-gp efflux and passive permeability rates. It is interesting to see that the MPO scoring function does not have a lower limit for lipophilicity score, as previous studies looking at BBB penetration had highlighted that this was an issue for permeability.[225] These methods have been implemented in CNS drug discovery to attain molecules with improved BBB permeability and efficacy.[224] It is worth noting that BBB penetration and total brain concentration does not infer biological efficacy alone. Total brain concentration often poorly correlates to efficacy in pharmacodynamic models. The unbound fraction of drug in the brain has been shown to better correlate to *in vivo* efficacy, making this an important consideration when designing new drugs for CNS disorders.[226]

Designing TAO inhibitors whilst considering and optimising the physicochemical parameters outlined above will facilitate the identification of tool compounds suitable for validating TAO as a target to clear trypanosome infections *in vivo*. It is of interest that the use of ascofuranone and glycerol has been shown to clear infections of trypanosomes in mice.[227] A single oral dose of 200 mg/kg without glycerol was unsuccessful in clearing the infection. However, a single dose of ascofuranone at 100 mg/kg with glycerol (3 g/kg) could cure parasitaemia. Glycerol could be functioning in two ways in this study. Firstly glycerol can inactivate the anaerobic respiratory pathway of glycerol kinase by mass action (discussed in chapter 1).[135] Secondly glycerol could be acting as an excipient and improve the effective concentration of ascofuranone enhancing its efficacy.[228] A second study of ascofuranone without glycerol was conducted by the same group; here, it was observed that consecutive daily dosing of ascofuranone at 100 mg/kg (i.p.) for four days or 400 mg/kg (p.o.) for eight days in mice could clear a trypanosome infection.[229] Pharmacokinetic data was not reported in this study, but a high oral dose did show efficacy in models of the 1st stage of the disease. Another interesting observation in this study was that following 3 days of consecutive treatment, only short stumpy forms of the parasite were found in the isolated trypanosomes, and long slender blood stage forms were not identified. This is important as short stumpy forms of the trypanosome are unable to proliferate, and have lost their ability to alter their VSG coat expression, and could be subsequently cleared by host immune mechanisms.[230,231]

Obtaining TAO inhibitors with improved pharmacokinetic profiles could improve *in vivo* efficacy, reduce compound burden and improve therapeutic potential.

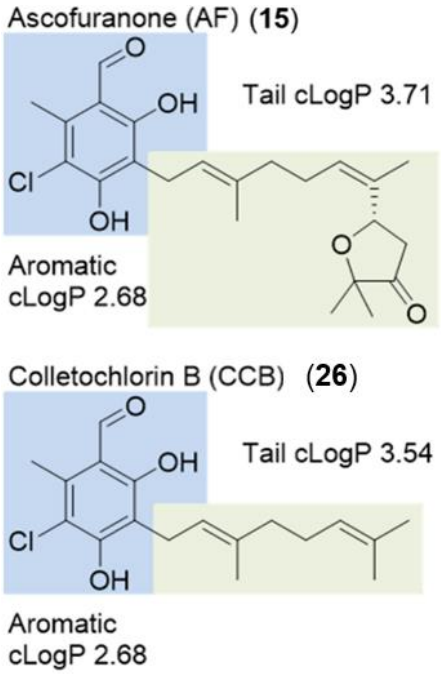

Figure 58 - Ascofuranone and CCB structural contribution to lipophilicity

Initial calculations of physicochemical properties of ascofuranone and CCB highlight the extremely high lipophilicity of both molecules (Figure 58). As previously highlighted, lipophilic compounds have a tendency to be highly metabolised,[217,218] poorly soluble in aqueous and physiological fluids and show off-target promiscuity often resulting in toxic side effects.[232,233] High lipophilicity has also been shown to contribute to a poor MPO CNS score, compounds with an MPO > 4 are predicted to permeate the BBB. This effectively penalises highly lipophilic compound twice, once for cLogP and once for cLogD, resulting in MPO scores of < 4 for both ascofuranone and CCB. Further investigation into the contribution of the constituent parts of CCB and ascofuranone show that the majority contribution (> 3.5 cLogP) to lipophilicity is the tail portion of the molecule (Figure 43). The presence of two hydrogen bond donors also affects the CNS MPO score negatively. These aspects of the molecule would need to be explored and optimised to identify inhibitors of TAO with improved

physicochemical parameters, which would maximise the potential to attain ideal pharmacokinetic exposure *in vivo* for treating African trypanosomiasis infections.

With the aim to improve the drug likeness and CNS penetration MPO score of the TAO inhibitors identified in chapter 4, the physicochemical properties of the synthetically amenable lead compound **88** were investigated (Table 12).

Table 12 - Physicochemical properties and MPO score of compound **88**

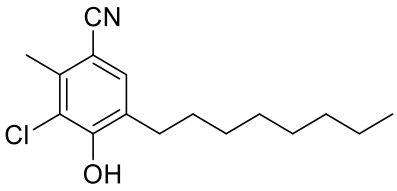

Compound Number		PSA (Å²)	HBD	Basic pKa	cLogD$_{7.4}$	cLogP	MWt	CNS MPO Score
88	Value	44	1	- 7.9	5.5	6.3	279	-
	MPO score	1	0.8	1	0	0	1	3.8
CCB (**26**)	Value	58	2	- 7	4.8	6.2	322	
	Score	1	0.5	1	0	0	1	3.5

Parameters calculated using Chemaxon Marvin Sketch 17.25.0 and JChem extensions for Knime

Analysis of the physicochemical properties reported in table 12 show that compound **88** is penalised for being highly lipophilic, having a cLogP of > 5 and a cLogD$_{7.4}$ > 4, generating an overall CNS MPO score of below 4. This result is similar to the calculated properties of CCB (**26**), which is further penalised in the CNS MPO calculation as it contains two hydrogen bond donors. As discussed previously, the main contribution to high lipophilicity in these molecules arises from the lipophilic tail. The identification of compound **88** was anticipated to facilitate the synthesis of a wider variety of analogues to explore the SAR and reduction of lipophilicity in this region. Inspection of the enzyme-inhibitor crystal structure (Figure 59), highlighted the lipophilic nature of this part of the inhibitor-binding pocket. No available polar residues were present that could be targeted for improving enthalpic interactions between the

protein and the ligand. The lipophilic tunnel of TAO was also shown to be narrow at only 7.1 Å between leucine residues LEU122 and LEU212. This could potentially limit the size of the inhibitor that can be accommodated in the binding site.

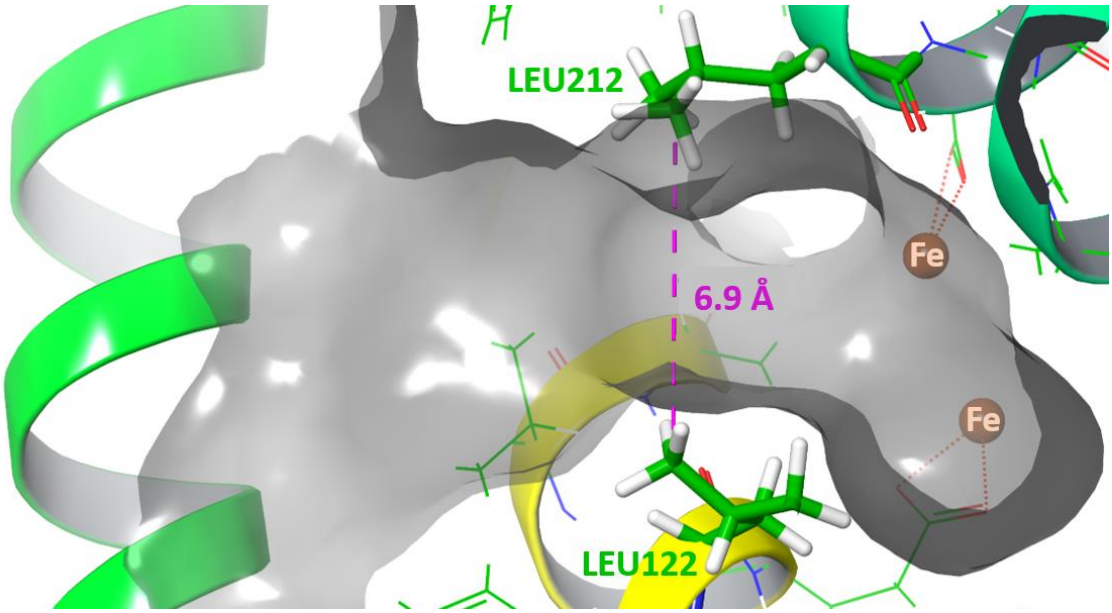

Figure 59 - Narrow lipophilic tunnel - Leucine residues (LEU122 and LEU212) shown in green, Iron centre shown in orange towards the back of TAO inhibitor binding pocket (right), exterior of TAO left, molecular binding surface in grey. Image generated from Protein preparation of PDB 3W54 structure using energy minimisation (OPLS3 forcefield) and receptor binding surface generation in Maestro, Schrodinger drug discovery suite. 3W54 deposited by Shiba *et al.*[129]

In consideration of this a range of polar tail analogues were designed, focused on minimising the steric and electronic impact that these molecules would have on inhibitor binding to TAO (Table 13).

Table 13 - Designed tail modifications of TAO inhibitors with reduced lipophilicity, Chemaxon v17.25.0 was used to calculate properties, utilising consensus model (Chemaxon, Klopp *et al.* and PhysProp data base) for calculation of cLogP and $cLogD_{7.4}$

Structure	#	cLogP[a]	$cLogD_{7.4}$ [b]	CNS MPO [c]
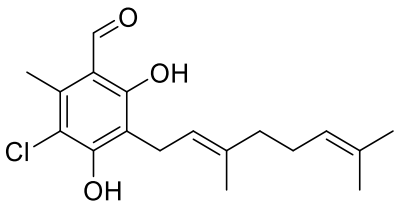	26	6.2	4.8	3.5
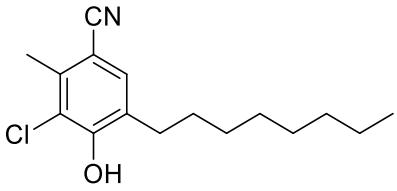	88	6.3	5.5	3.8
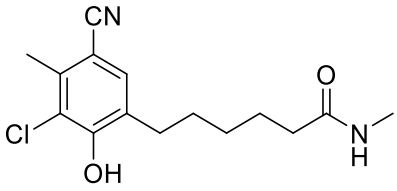	89	3.5	2.7	4.9
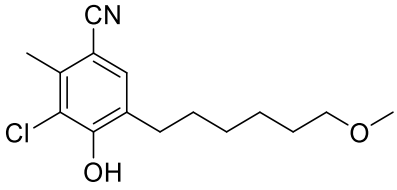	90	4.6	3.8	4.1
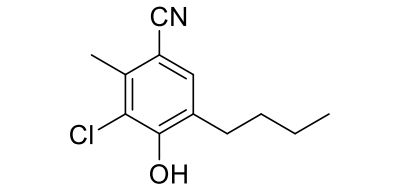	91	4.5	3.7	4.2

Parameters calculated using Chemaxon Marvin Sketch 17.25.0 and JChem extensions for Knime

5.2.1 Polar Tail Modifications Synthesis

Analysis of the calculated properties of these designed inhibitors showed that the reduction in lipophilicity from these molecules resulted in CNS MPO scores of above 4. If these compounds retained inhibitory activity against TAO and parasite growth they would provide analogues that had potential for improved CNS penetration over CCB. The synthesis of

analogues containing amide, and ether functionality was initially prioritised, as these modifications improved the compound lipophilicity profiles to the greatest extent. The synthetic route to compound **88** provided a good basis for the synthesis of these analogues in the most economical fashion. Electrophilic chlorination of intermediate **85** would enable the final synthetic step to be the installation of the tail.

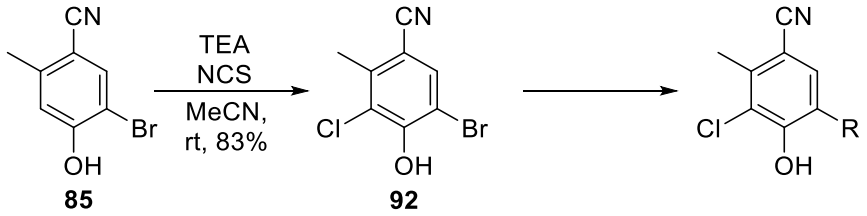

Figure 60 - Chlorination of advanced intermediate **85**

Chlorination of **85** to **92** was however, not trivial (Figure 60). The sulfuryl chloride in diethyl ether conditions that were previously employed to synthesise compounds **83** and **88** and the intermediates **66** and **69** formed product, but an unidentified compound related impurity was also produced in around 20% yield. This impurity could not be easily separated through crystallisation or chromatography. A variety of electrophilic chlorinating conditions were screened, with an aim to identify optimal conditions to provide pure material for diversification. The impurity profile was improved in two sets of reaction conditions providing the compound in >90% purity: NCS in tetrahydrofuran; or NCS in acetonitrile with 1.1 equivalents of triethylamine. However, the unidentified impurity was still present at around 5 – 10%.

To mitigate the risk of slowing the progression of the project, the synthesis of the des-methyl intermediate (**94**) was performed in parallel (Figure 61). The chlorophenol (**93**) starting material was commercially available and could be readily brominated with *N*-bromosuccinimide in acetonitrile to give **94** in good yield. The 25-fold reduction in TAO potency observed with the des-methyl CCB analogue (**50** – Table 10) was deemed acceptable for future analogue comparison.

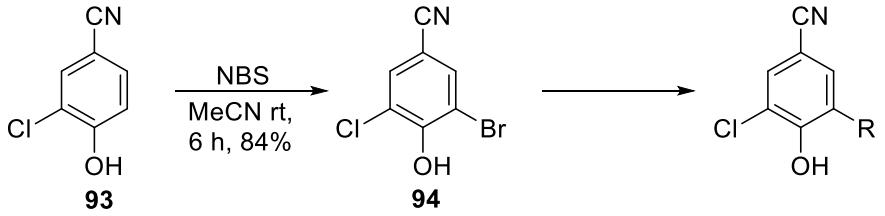

Figure 61 – Bromination of des methyl intermediate (**94**) synthesis

A Mizoroki-Heck coupling was carried out with the methylated intermediate **92**,[191,192] utilising the I-Mes NHC catalyst that had previously been identified.[195] Some desired product was synthesised in the reaction; however, the reaction profile showed the formation of other structurally related impurities. The product required isolation by reverse-phase preparative high-performance liquid chromatography (HPLC) to provide compound **95** in a low 7% yield. Utilising Mizoroki-Heck conditions to install the tail meant that a subsequent reduction of the resulting alkene was required. Conducting this reduction *via* hydrogenation would provide the desired saturated carbon chain analogues, although aromatic hydro-dehalogenation is often observed under hydrogenation conditions and would be a likely side-reaction of this route. Dehalogenation has been reported to be suppressed when conducting the hydrogenation under acidic conditions. However, hydrogenation of **95** in an ethanolic HCl solution resulted in the formation of the hydro-dehalogenated product, an intermediate that had been previously synthesised (**87** - figure 62).

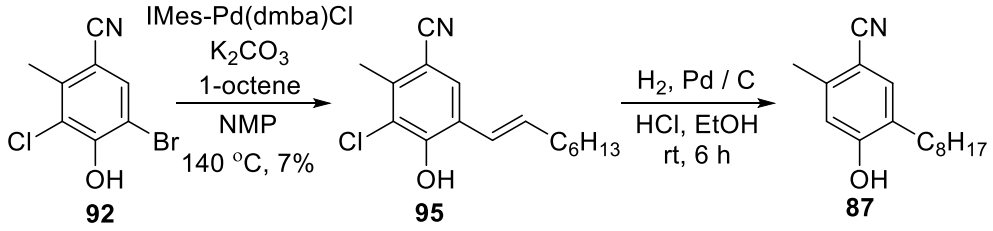

Figure 62 - Mizoroki-Heck installation of lipophilic tail

At this point alternative cross-coupling reactions were investigated to install the tail modifications. Li *et al*. had recently reported the Suzuki-Miyaura cross coupling of trialkylboranes with aryl halides, and had showed good utility with a variety of aromatic and

hetero aromatic substrates.[234] A point of interest with this chemistry was that the trialkylborane coupling partner could be easily synthesised *in situ* from the hydroboration of a terminal alkene with a solution of borane in THF. The only perceived limitation of this chemistry was that there were no examples of substrates containing acidic hydrogens. Perhaps unsurprisingly, when attempting these reaction conditions with the free phenol intermediates **92** and **94,** no product was observed. Li *et al.* had exemplified an array of anisole substrates with high isolated yields, prompting the investigation of protecting the phenol and retrying the chemistry (Figure 63).

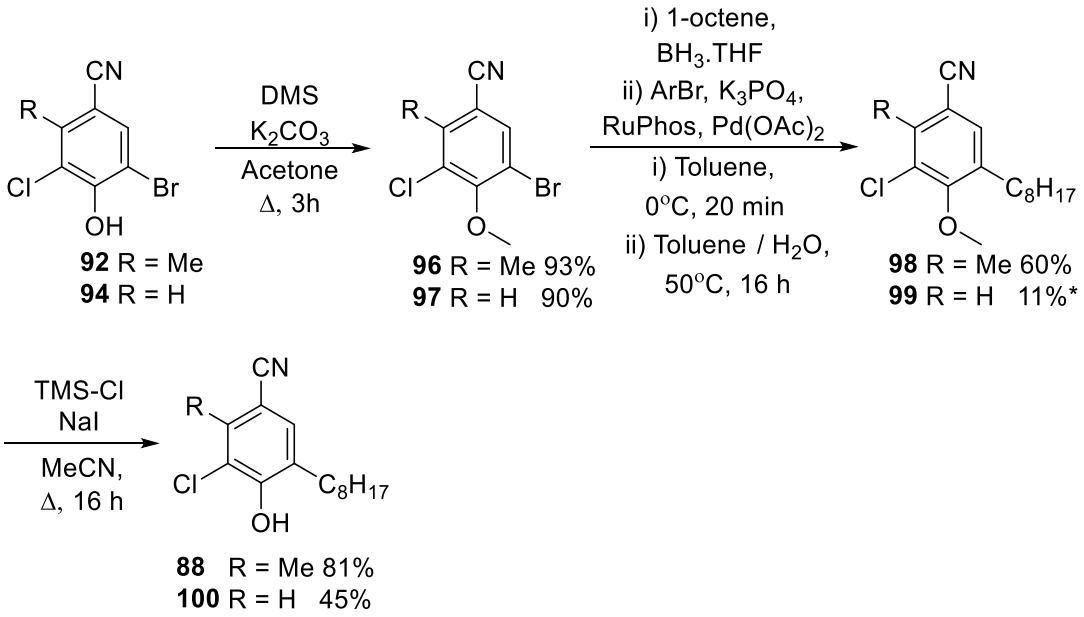

Figure 63 - Suzuki-Miyaura chemistry to install lipophilic tail, based on Li *et al.* conditions[234] * Formation of **99** conducted at 100 °C. However, the formation of bis Suzuki coupled material through Cl and Br, led to a reduced yield.

Methylation of the intermediate **92** and **94** could be carried out with dimethyl sulphate (DMS) in acetone in high yield to provide compounds **96** and **97**. Attempting the chemistry reported by Li *et al.* on this substrate proved very successful. Trioctylborane was pre-formed by hydroboration of 1-octene with a solution of borane in THF at 0 °C. The excess borane reagent was quenched by the addition of water, the arylbromide (**96** or **97**) was successfully Suzuki cross-coupled. This route enabled the installation of the lipophilic tail in a high yield, although the phenol was now protected as an anisole (**98** and **99**) and would require

deprotection to provide the desired analogues. The reaction to form the des-methyl analogue (**99**) was conducted at a higher temperature of 100 °C in an attempt to expedite the reaction. At this elevated temperature, formation of the *bis* Suzuki cross-coupled product was observed as a major by-product of the reaction. The by-product was formed by the reaction of the aryl chloride with a further equivalent of alkyborane and resulted in a lower isolated yield of the desired mono-coupled product (**99**). A range of deprotection conditions were screened to remove the anisole and furnish the desired product as the free phenol. The best conditions identified were trimethylsilyl chloride (TMS-Cl) and sodium iodide at 80 °C, giving the free phenols (**88** and **100**) in respectable 45-81% yields. With these conditions in hand the syntheses of the amide and ether tails were carried out. The des-methyl intermediate **94** was used for this initial exploration as the small impurity that was present in **92** provided a difficult final purification of each analogue. Suzuki-Miyaura cross-couplings were carried out using methyl ester trialkyl boranes that were pre-formed by the hydroboration of the corresponding alkene ester with borane in THF. The ester products **101**, **102**, **103**, **104** were isolated in good yields ranging from 54 – 80%. Two synthetic strategies were developed to synthesise the amide analogues (Figure 64).

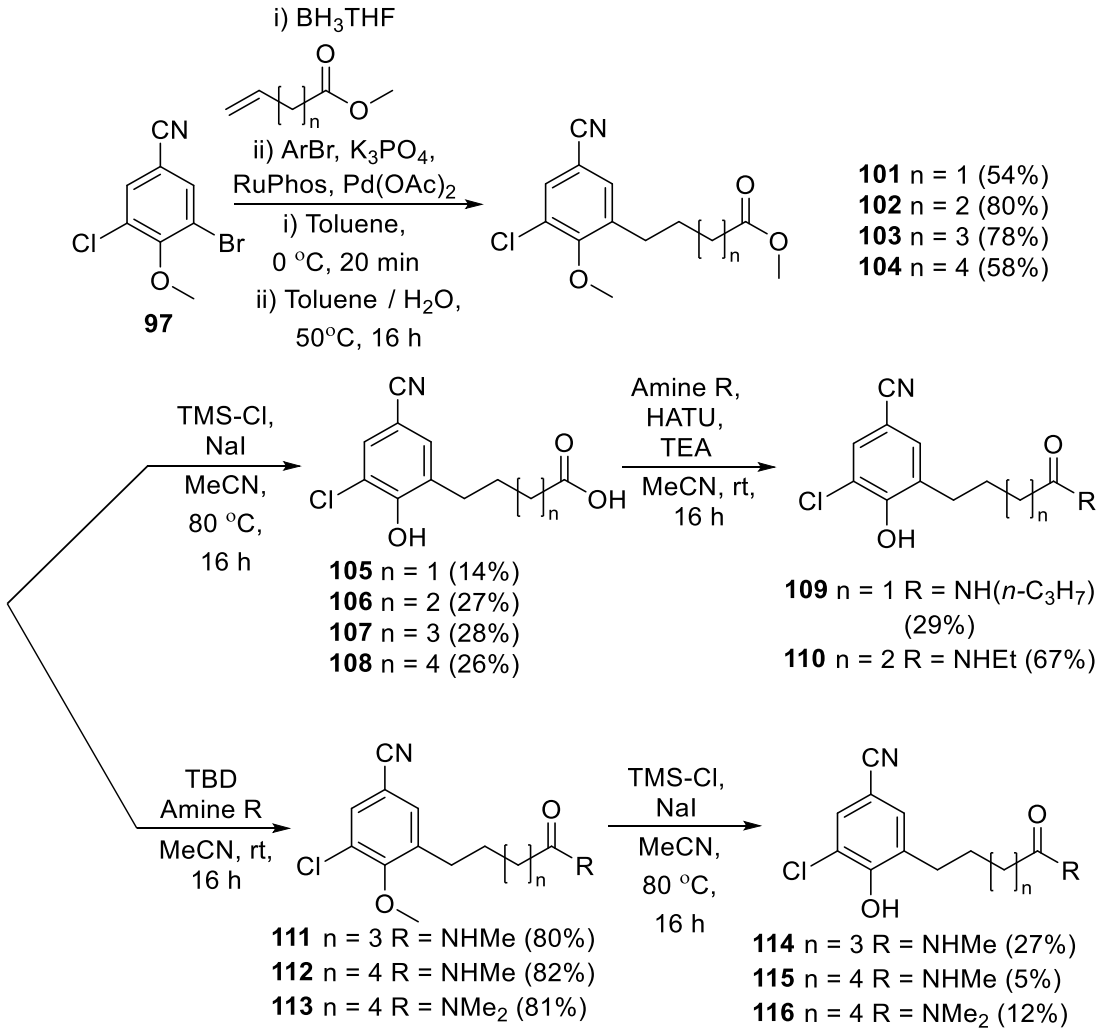

Figure 64 - Amide tail synthesis

The isolated esters (101-104) were initially treated with the demethylation conditions (TMS-Cl and sodium iodide) to give the free phenol and free acid products. These molecules were poorly soluble in organic solvent and required reverse-phase purification to isolate the material at sufficient purity. The acid could be reacted using the amide coupling reagent HATU, to provide the final products 109 and 110. The longer chain amides were not isolated in sufficient purity from the HATU reactions. Due to the purification difficulties and resulting lower yields observed with TMS-Cl, sodium iodide demethylation of the esters (101-104), an alternative synthetic route to these amides was investigated. Sabot *et al.* had reported the efficient aminolysis of esters catalysed with the reagent 1,5,7-triazabicyclo[4.4.0]dec-5-ene

(TBD) under solvent free conditions.[235] In view of using these conditions, ester intermediate **103** was treated with methylamine and TBD and intermediate **104** with methylamine and dimethylamine with TBD, in acetonitrile at room temperature. These reactions provided clean conversion to the amide products and were readily isolated in high yields to provide compounds **111**, **112** and **113**. These anisoles could be successfully demethylated using the TMS-Cl sodium iodide conditions to provide the other amide analogues (**114**, **115** and **116**).

The Suzuki-Miyaura cross coupling reaction failed with the ethyl acrylate, possibly due to the reduced electron density of the alkene in ethyl acrylate. Studies of the reaction between borane and ethyl acrylate have been shown to form an unexpected product. The electron withdrawing effect of the ester is thought to direct the borylation to the α carbon, through stabilisation of the negative charge of the transition state. This unstable product is reported to then undergo a rapid 1,2-rearrangement and yield ethyl propionate upon hydrolysis with water (Figure 65).[236]

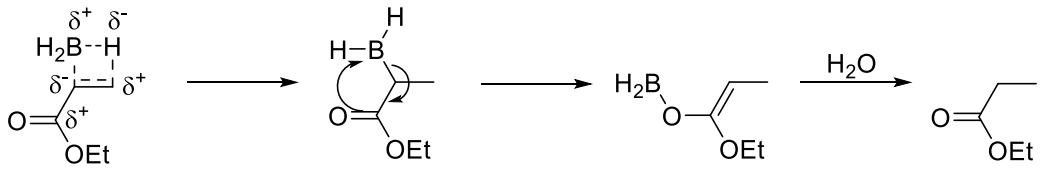

Figure 65 - Hydroboration of ethylacrylate reported by Brown *et al*.[236]

With the aim to synthesise amide **120** a Mizoroki-Heck cross coupling was utilised. The brominated benzonitrile (**85**) was successfully cross coupled using the I-Mes NHC ligand previously identified for the synthesis of **87** and provided the alkene intermediate **117**. This alkene was successfully hydrogenated to the saturated analogue **118**, and then electrophilic aromatic chlorination of the phenolic ring using sulfuryl chloride in diethyl ether afforded compound **119**. The amide (**120**) was successfully synthesised by treatment with TBD and *n*-butylamine in acetonitrile (Figure 66).

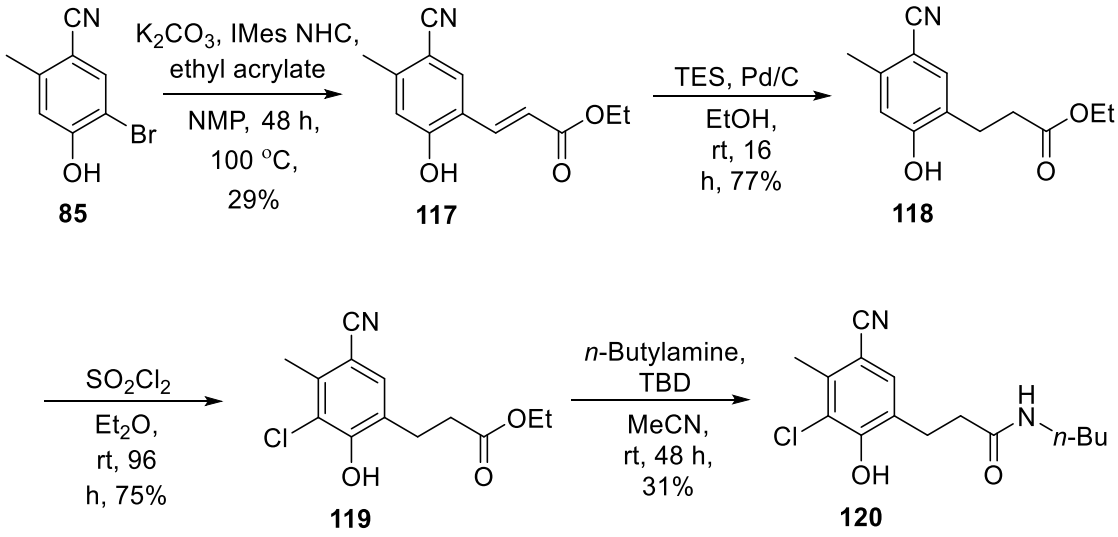

Figure 66 - Synthesis of ethyl acrylate analogue

The synthesis of ether containing tail modifications was carried out by a master's student, Thomas Cunningham whilst under my supervision (Figure 67). These analogues proved to be more of a synthetic challenge than their amide equivalents. An alternative phenol protection was required to enable the successful Suzuki-Miyaura coupling, as the deprotection of the aryl ether could not be conducted selectively without the tail alkyl ethers also reacting. A small screen of protecting groups highlighted some initial success with acetyl phenol protection (**121** – Figure 66). Larger silyl protecting groups appeared to restrict the successful coupling, as the tri-isopropylsilyl phenol ether provided no product. The acetyl protected phenol on the other hand looked to provide approximately 25% conversion to the cross-coupled phenol analogues directly. The major by-product of this reaction was however the deprotected starting material that could not be progressed further with addition of extra substrate, catalyst and ligand, or with prolonged reaction times at higher temperatures. The desired ether tail analogues (**122**, **123** and **124**) could however be isolated by reverse-phase chromatography, albeit in low yield.

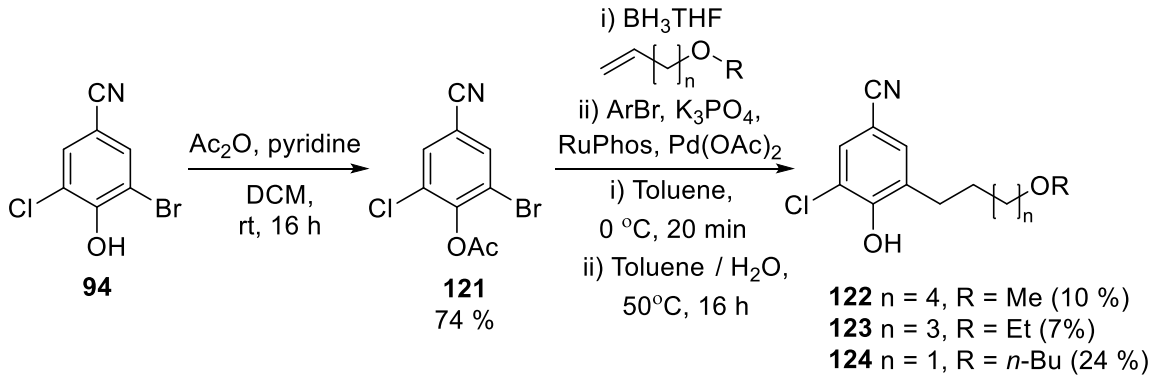

Figure 67 - Ether tail analogues synthesised by master's student Thomas Cunningham

5.2.2 Polar Tail Modifications Biological Activity Assessment

The TAO inhibitory activity of the amide and ether analogues synthesised above were assessed in the biochemical ubiquinol assay. Intermediates **87**, **95**, **98**, **99**, **119** and comparison compound **100** were also assayed for inhibitory activity (data summarised in table 14).

Table 14 - SAR of polar tail modifications

Structure	#	TAO (pIC_{50})[a]	*T. b. b.* (pEC_{50})[b]	cLogP[c]
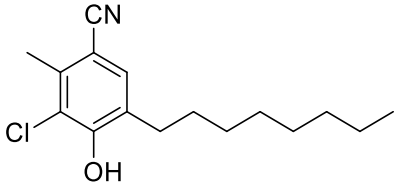	**88**	8.5 ± 0.2	7.6 ± 0.1	6.3
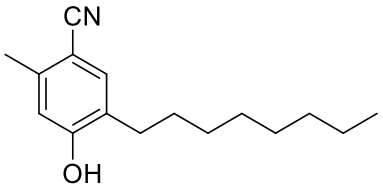	**87**	5.9 ± 0.2	4.9 ± 0.1	5.7
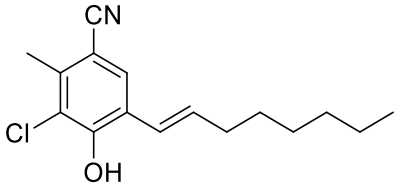	**95**	8.3 ± 0.2	5.9 ± 0.1	6.0

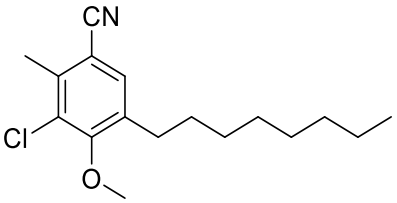	**98**	< 4.5	< 4.3	6.4
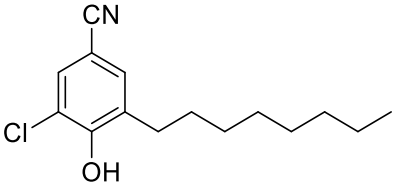	**100**	7.0 ± 0.1	-	5.8
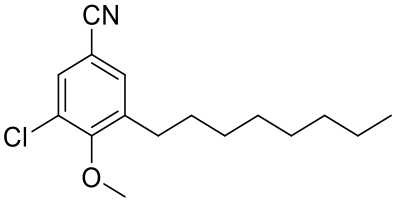	**99**	4.6 ± 0.1	-	5.9
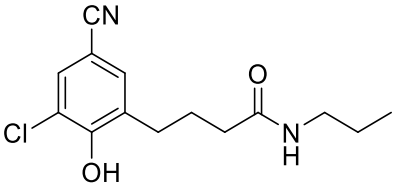	**109**	< 4.5	-	3.0
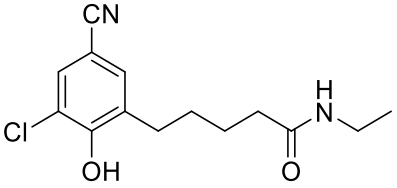	**110**	< 4.5	< 4.3	2.9
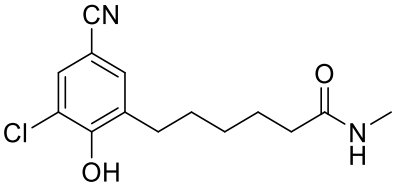	**114**	< 4.5	-	3.0
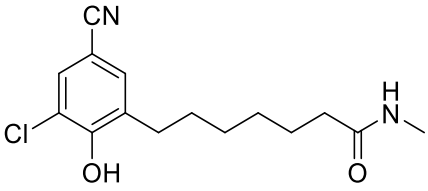	**115**	5.1 ± 0.1	< 4.3	3.6

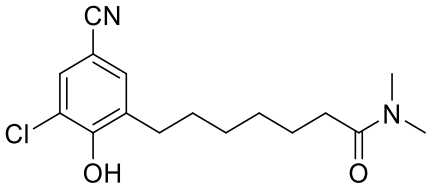	**116**	5.5 ± 0.2	< 4.3	3.8
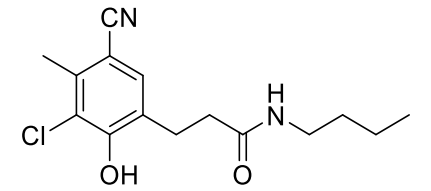	**120**	5.5 ± 0.2	< 4.3	3.5
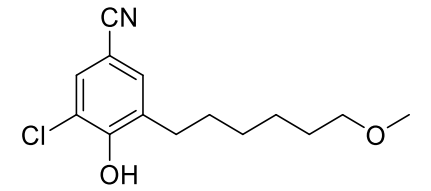	**122**	5.2 ± 0.1	< 4.3	4.1
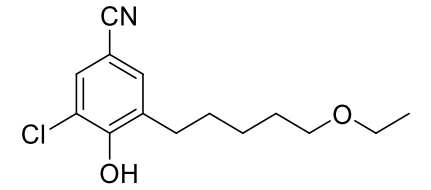	**123**	5.6 ± 0.1	4.6 ± 0.1	4.0
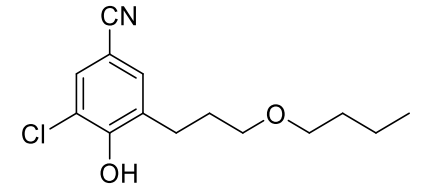	**124**	4.8 ± 0.1	4.7 ± 0.1	4.1
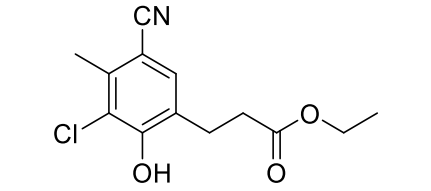	**119**	5.8 ± 0.1	4.5 ± 0.1	3.2

[a] Negative log concentration and standard deviation of compounds required for 50% inhibition of trypanosome alternative oxidase. [b] Negative log concentration and standard deviation of compounds required for 50% growth inhibition of *T. b. brucei* Lister427. [c] Parameters calculated using Chemaxon Marvin Sketch 17.25.0 and JChem extensions for Knime

Analysis of the inhibition data generated with these more polar analogues disappointingly looked to have significantly reduced TAO inhibition. Assessment of the polar tail analogues in the *T. b. brucei* assay also correlated with poor TAO inhibition. In consideration of these

data an alternative option was considered to reduce the lipophilicity of the tail, as minor changes in the tail resulted in large reductions in potency. Saimoto *et al.* had previously highlighted that a reduction in carbon chain length was tolerated with the complete CCB aromatic head group linked *via* a trans-alkene. On the other hand, a greater than 100-fold loss of potency was observed with tail analogues of 3 carbon atoms or below.[128] The synthesis of analogues to investigate the required tail length was carried out utilising the same cross-coupling chemistry described above. Due to the decrease in potency observed in the parasite growth assay with the des-methyl analogues, intermediate **96** was used for this exploration.

5.3 Tail Chain Length Modifications Synthesis

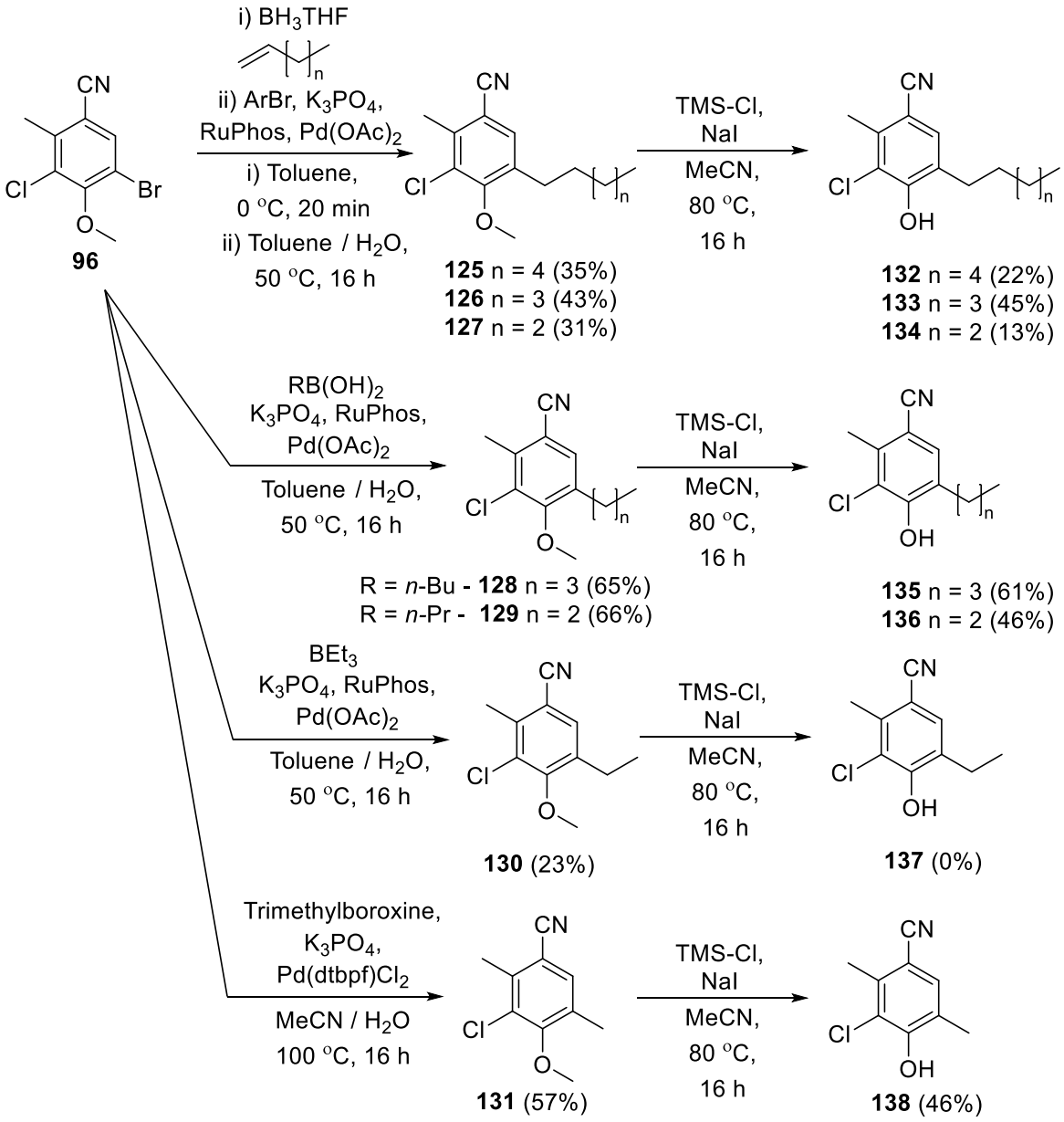

Figure 68 - Chain length exploration synthesis

Analogues with chain lengths greater than 5 were synthesised *via* the same cross coupling conditions utilised previously to synthesise intermediates **125**, **126** and **127**, as the alkenes were readily available (Figure 68). The alkenes of shorter carbon chains are gaseous at room temperature and require specialist reaction equipment for use. These alkenes were also not readily available from commercial sources. The methyl analogue (**131**) was synthesised by a

Suzuki-Miyaura cross coupling with trimethylboroxine, using a recently developed palladium catalyst dichloro [1,1'- bis(di-tertbutylphosphino)ferrocene]palladium(II) (Pd-118), that has shown good activity and application in difficult Suzuki-Miyaura cross couplings.[237] The ethyl analogue (**130**) was synthesised using the conditions that had been reported by Li *et al.* using a solution of reagent grade triethyl borane.[234] The *n*-propyl and *n*-butyl analogues were synthesised using the respective alkyl boronic acids with the catalyst conditions utilised for the coupling of the tri-alkyl boranes to provide intermediates **128** and **129**. Attempted Suzuki cross-couplings with Pd-118 and these alky boronic acids were not successful, but alkyltrifluoroborates have previously been shown to Suzuki cross-couple well using RuPhos and palladium acetate catalyst systems.[238] The deprotection of these anisole intermediates was carried out using TMS-Cl and NaI, and compounds **132** – **136** and **138** were isolated successfully. The ethyl analogue (**137**) however, was isolated in poor yield due to a technical issue upon purification. Compounds **132**-**136** and **138** were assessed for inhibitory activity of TAO and growth inhibition of *T. b. brucei*, data summarised in table 15.

5.3.2 Alkyl Chain Length Analogues Biological Activity Assessment

Table 15 - SAR of chain length analogues

Structure	#	TAO (pIC_{50})[a]	*T. b. b.* (pEC_{50})[b]	cLogP [c]	LLE [d]
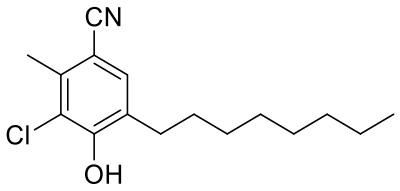	**88**	8.5 ± 0.2	7.6 ± 0.1	6.3	2.2
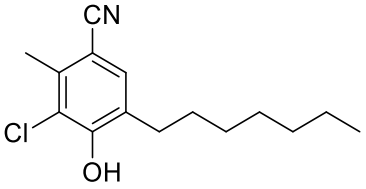	**132**	8.5 ± 0.1	6.6 ± 0.1	5.8	2.7
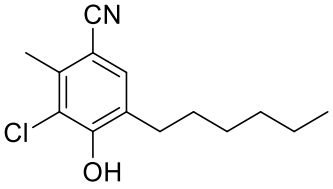	**133**	8.2 ± 0.1	6.1 ± 0.1	5.4	2.8

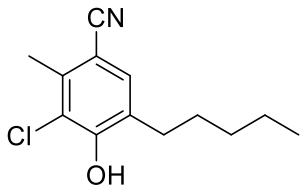	**134**	7.8 ± 0.1	5.9 ± 0.1	4.9	2.9
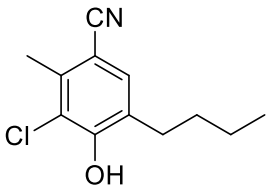	**135**	7.7 ± 0.1	5.3 ± 0.1	4.5	3.2
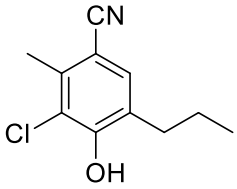	**136**	7.1 ± 0.1	4.7 ± 0.1	4.1	3.0
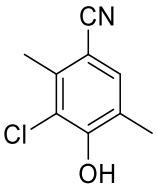	**138**	6.2 ± 0.1	4.7 ± 0.1	3.2	3.0

[a] Negative log concentration and standard deviation of compounds required for 50% inhibition of trypanosome alternative oxidase (n = >2). [b] Negative log concentration and standard deviation of compounds required for 50% growth inhibition of *T. b. brucei* Lister427 (n = >2). [c] Parameters calculated using Chemaxon Marvin Sketch 17.25.0 and JChem extensions for Knime. [d] LLE calculated from TAO pIC_{50} – cLogP.

Interestingly the inhibition of TAO appeared to track with the decrease in lipophilicity (cLogP) and reduction of tail length with a lipophilic ligand efficiency (LLE) of around 3. Lipophilic ligand efficiency is a calculated compound metric that is used to optimise and correlate compound lipophilicity and potency (pIC_{50} – cLogP). LLE is useful to help identify potency improvements that arise from enthalpic protein ligand interactions such as hydrogen bonding or electrostatic contacts, with lead like compounds often achieving an LLE of 4.[220] *T. b. brucei* growth inhibition correlated with the observed inhibition of TAO and calculated lipophilicity; however, parasite growth inhibition tracked to around a 100-fold decrease from the biochemical inhibition of TAO, resulting in LLE in the cellular assay of around 1. Compounds with a carbon chain length of 4-5 still showed good inhibition of TAO in the low nM range, with parasite growth inhibition of around 1 μM. These compounds also had a

cLogP of below 5 and MPO scores of around 4, meaning they were predicted to have improved CNS penetration. The shorter chain analogues showed promise, and further exploration was carried out with the aim to further improve LLE and identify an optimal tail for this class of TAO inhibitor.

5.4.1 Diverse Tail Analogues Synthesis

At this point a scale-up of the synthesis of the brominated intermediate **92** was conducted. Unfortunately, final purification of this intermediate was not achieved on scale, with the close running impurity that had previously been observed co-eluting on chromatography and co-crystallising with the desired product. The initial batch of this intermediate (**92**) also contained a small amount of this impurity that provided a challenge for the isolation of the final compounds previously synthesised. An alternative synthesis of tail analogues was conducted (Figure 69) to circumvent the issues with the isolation of intermediate **92**.

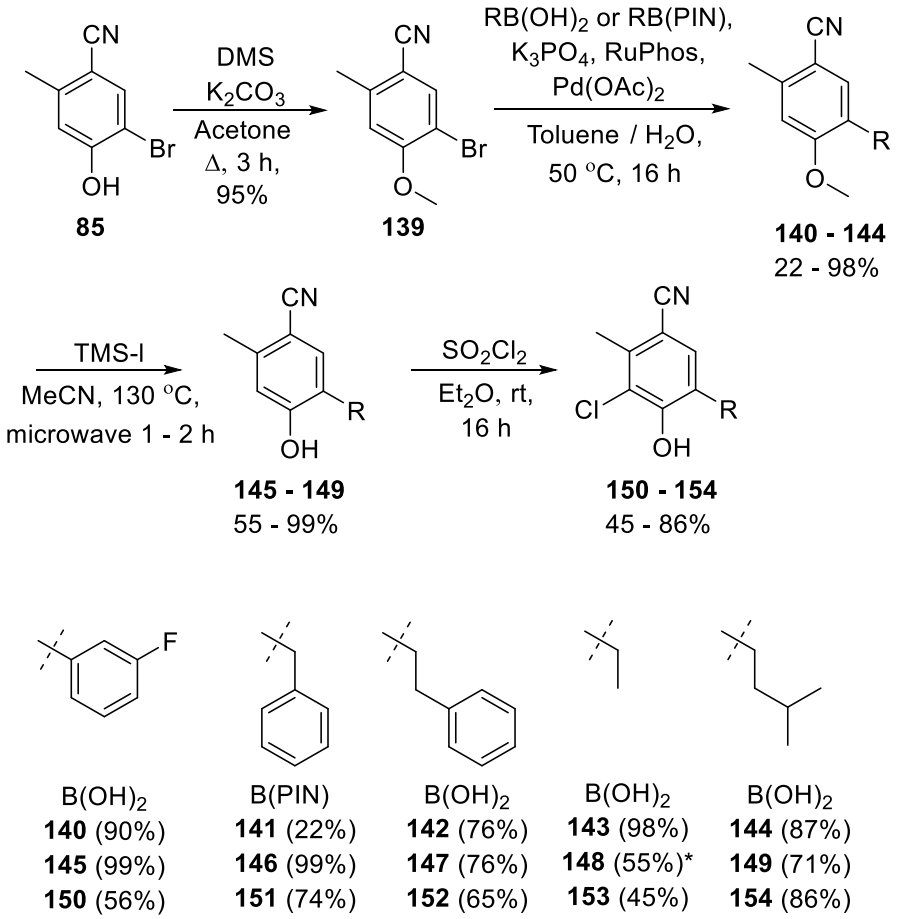

Figure 69 - Adapted synthesis of tail analogues to overcome impurity profile of chlorination. * Demethylation carried out with NaI and TMS-Cl.

The synthesis of analogues **150** – **154** by this method avoided the problematic impurity profile of the chlorination reaction. Carrying out the chlorination in the final step yielded a single product with no other contaminants. Unfortunately, sp^3 di-alkyl boronates (cyclohexane, cyclopentane, cyclobutane) failed to cross-couple with these Suzuki coupling conditions. To overcome this issue, sp^2 alkenyl boronic acids were utilised to furnish cyclic tail analogues **163** and **164.** The alkenyl cyclopropyl ethene boronic ester was also commercially available and was of interest to synthesise to compare with analogues **134**, **135** and **154** (Figure 70).

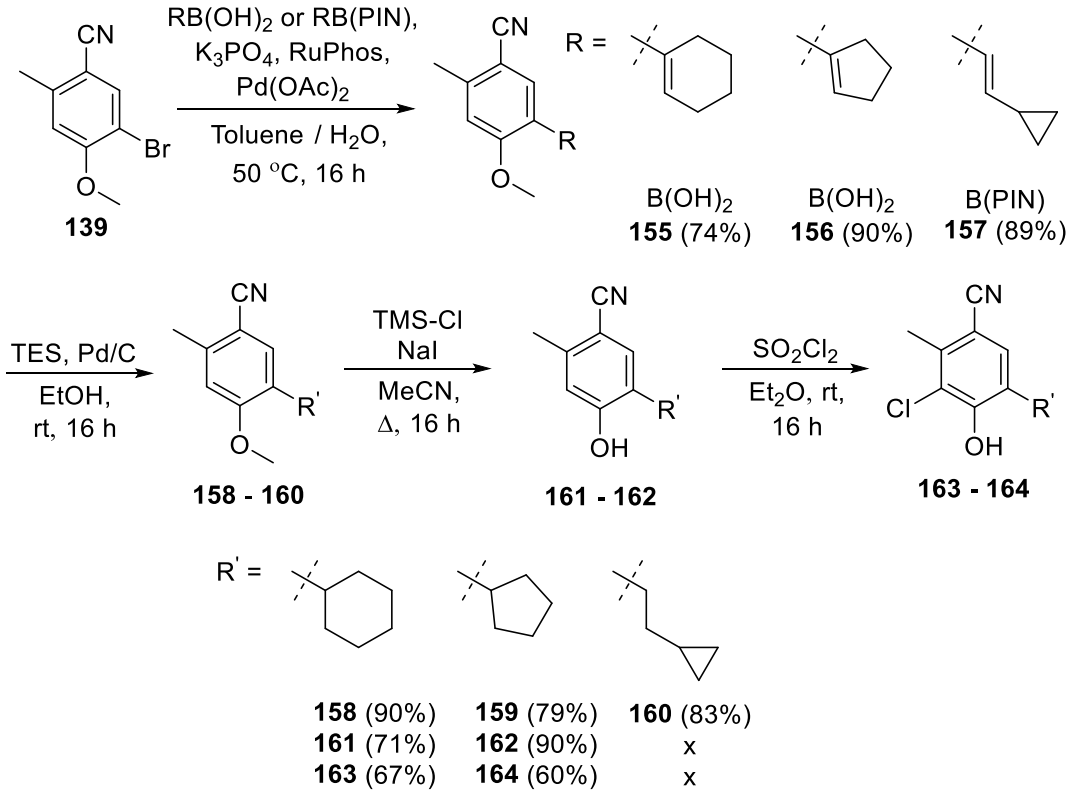

Figure 70 - Cyclic tail analogue synthesis

Both the cyclohexyl (158) and cyclopentyl (159) analogues were synthesised successfully, utilising the transfer hydrogenation conditions reported by McMurray *et al.* to reduce the alkene following the Suzuki cross-coupling.[202] Under hydrogenation some of the cyclopropane ring of 160 was also reduced, resulting in a mixture of desired product and a ring opened impurity. Attempts at demethylation of the isolated intermediate 160 resulted in the degradation of starting material and no observed product, so an alternative synthesis of this analogue was sought (Figure 70).

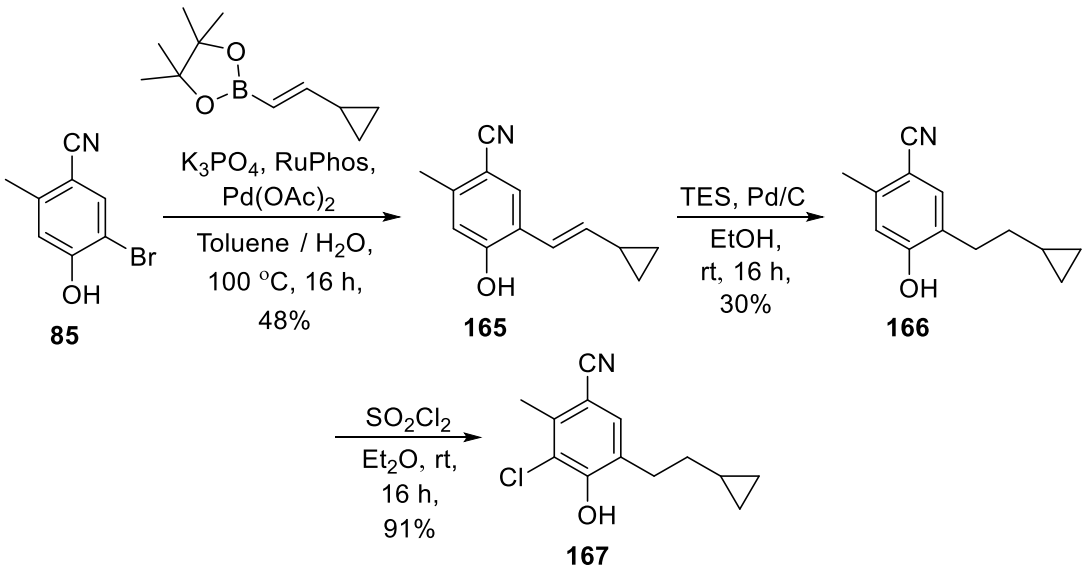

Figure 71 - Synthesis of cyclopropyl ethyl analogue **167**

Attempting the Suzuki cross-coupling on the direct phenol bromide intermediate (**85**) showed formation of product **165** at an elevated temperature of 100 °C, **165** could be isolated in a reasonable yield of 48%. Transfer hydrogenation of this using the McMurray conditions previously employed again provided the desired product **166** but with an impurity of the hydrogenated cyclopropane ring. The impurity could be separated with reverse-phase chromatography to provide intermediate **166**, this was successfully chlorinated with sulfuryl chloride to provide analogue **167** (Figure 71). Analogues **150** - **154**, **163**, **164** and **167** were assessed in TAO inhibition and *T. b. brucei* growth inhibition assays, data summarised in table 16.

5.4.2 Diverse Tail Analogues Biological Activity Assessment

Table 16 - SAR of follow up tail analogues

Structure	#	TAO (pIC_{50})[a]	*T. b. b.* (pEC_{50})[b]	cLogP[c]
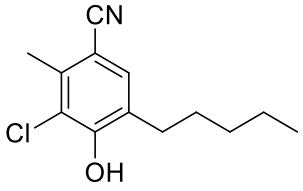	**134**	7.8 ± 0.1	5.9 ± 0.1	4.9

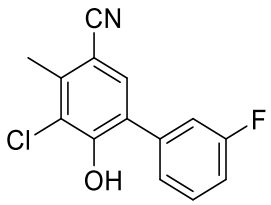	**150**	7.4 ± 0.1	< 4.3	4.4
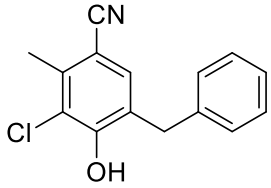	**151**	8.0 ± 0.2	6.1 ± 0.1	4.7
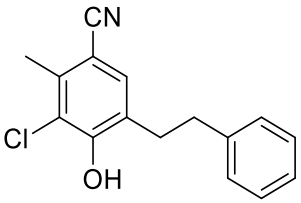	**152**	8.2 ± 0.2	5.5 ± 0.1	5.2
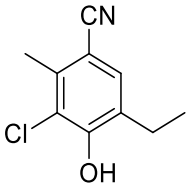	**153**	6.4 ± 0.1	4.4 ± 0.1	3.6
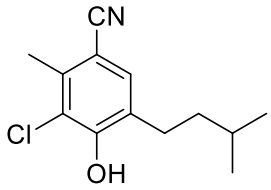	**154**	8.1 ± 0.1	6.5 ± 0.1	4.8
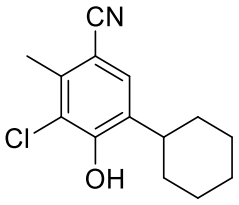	**163**	7.3 ± 0.1	< 4.3	4.8
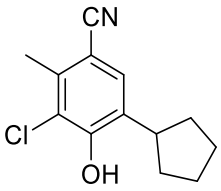	**164**	7.8 ± 0.1	4.3 ± 0.1	4.3

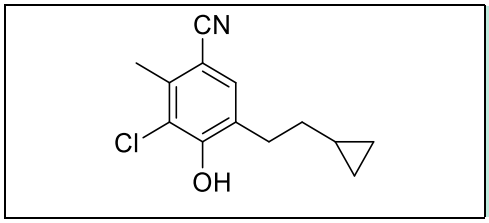	167	7.6 ± 0.1	5.6 ± 0.1	4.3

[a] Negative log concentration and standard deviation of compounds required for 50% inhibition of trypanosome alternative oxidase (n = >2). [b] Negative log concentration and standard deviation of compounds required for 50% growth inhibition of T. b. brucei Lister427 (n = >2). [c] Parameters calculated using Chemaxon Marvin Sketch 17.25.0 and JChem extensions for Knime.

Analysis of these analogues showed good TAO inhibition profiles and highlighted one compound that showed a half log increase in potency for the inhibition of *T. b. brucei* growth. Compound **154**, with the isopentyl tail, showed an increase in TAO inhibition that transferred to inhibition of parasite growth. This compound had small improvements in calculated physicochemical properties, with a cLogP of 4.8 and a $cLogD_{7.4}$ of 3.8, which resulted in a CNS MPO score of 4.2. This compound was of sufficient quality for assessment in more advanced parasite-kill kinetic and parasite reversibility assays, to determine the time dependency and efficacy of compound treatment. Preliminary solubility and rat microsomal clearance turnover were also studied. It was of interest that the benzyl analogue **151** also showed an improvement in parasite growth inhibition potency and reduction of lipophilicity. Analogues **150**, **163** and **164** were shown to be active against TAO, but this potency was not retained in the parasite growth inhibition assays. The phenol of **150** has an increased acidity, as the fluorophenyl substituent is electron withdrawing, lowering the phenolic pKa. This could cause a reduction in the compounds' passive permeability into the parasite, as only un-ionised compound will be able to passively permeate a cell membrane. This is unlikely to explain the loss of potency observed with analogues **163** and **164**, as these analogues will have similar pKa's to that of the other alkyl analogues. There may be a number of reasons why these analogues are less potent in the trypanosome, including their reduced TAO inhibition and lower lipophilicity, that could result in a reduced membrane affinity and effective concentration of compound in the parasite inner membrane. The cyclopropylethyl

(**167**) and phenethyl (**152**) analogues showed similar profiles against TAO and parasite inhibition, as observed previously.

5.5.1 Fluorinated Alkyl Chain Analogue Synthesis

A final attempt was made to reduce the lipophilicity of the tail portion of this chemotype. An alternative method to introduce polarity into an alkyl chain is to incorporate a fluorine atom. Although fluorine is more lipophilic than hydrogen, the resulting polarity that is introduced from the highly electronegative fluorine atom, induces a polarisation of the carbon chain. This method has been used to reduce the lipophilicity of alkyl chain containing molecules and resulted in the identification of compounds with improved *in vitro* and *in vivo* pharmacokinetic profiles.[239–241] A synthesis to incorporate fluorine atoms into the carbon chain of these analogues was devised (Figure 71).

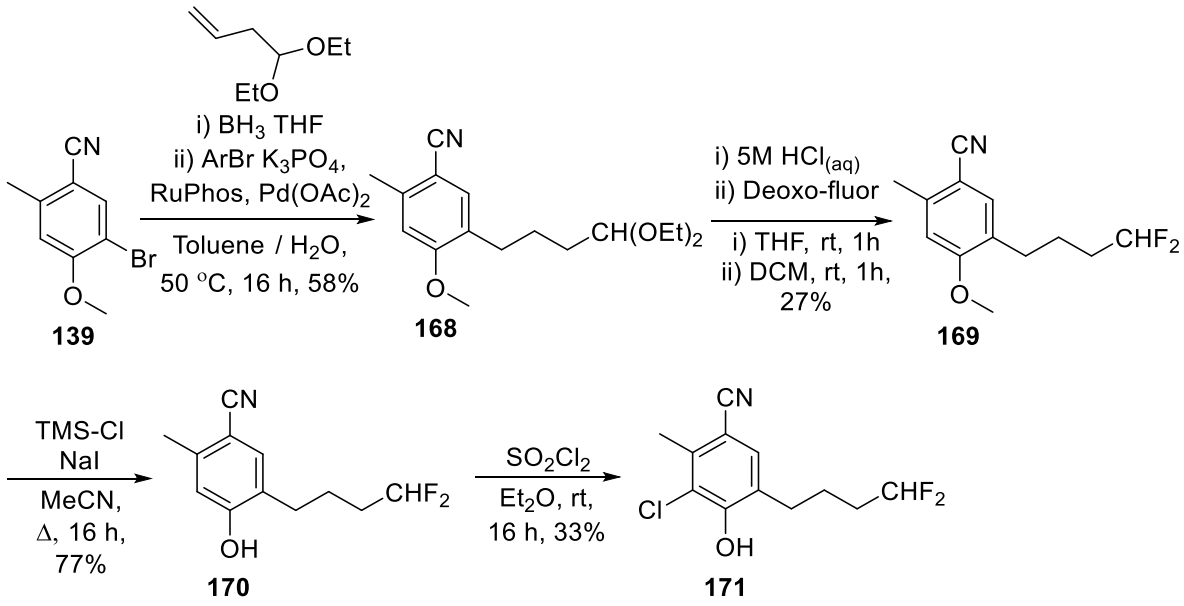

Figure 72 - Synthesis of di-fluoro butyl analogue **171**

The butyl alkene containing a terminal ethyl acetal was commercially available and was successfully cross-coupled *via* formation of the trialkyl borane, as previously discussed, to form **168**. The acetal was converted to the terminal aldehyde in aqueous acid, and isolated by extraction into ethyl acetate, then concentration. This crude material was treated with a

solution of Deoxo-fluor® to generate the difluorinated intermediate (**169**). Removal of the anisole protecting group and subsequent electrophilic aromatic chlorination, provided the desired di-fluorinated butyl tail analogue (**171** – Figure 72).

A synthesis towards a fluorinated analogue of the most potent molecule in the parasite growth inhibition assay (compound **154**) was also planned (Figure 73), with the aim to maintain the parasite growth potency and further reduce the lipophilicity of the molecule. The boron pinacol ester of methyl propanoate was available, which was cross-coupled utilising the conditions previously identified to provide **172**. Compound **172** was then treated with two equivalents of methyl magnesium bromide to afford the tertiary alcohol **173**. This intermediate was fluorinated with Deoxo-fluor® to provide the fluorinated chain analogue **174**. Unfortunately, upon demethylation of the anisole the compound self-cyclised to form **175**, and the desired compound was not isolated.

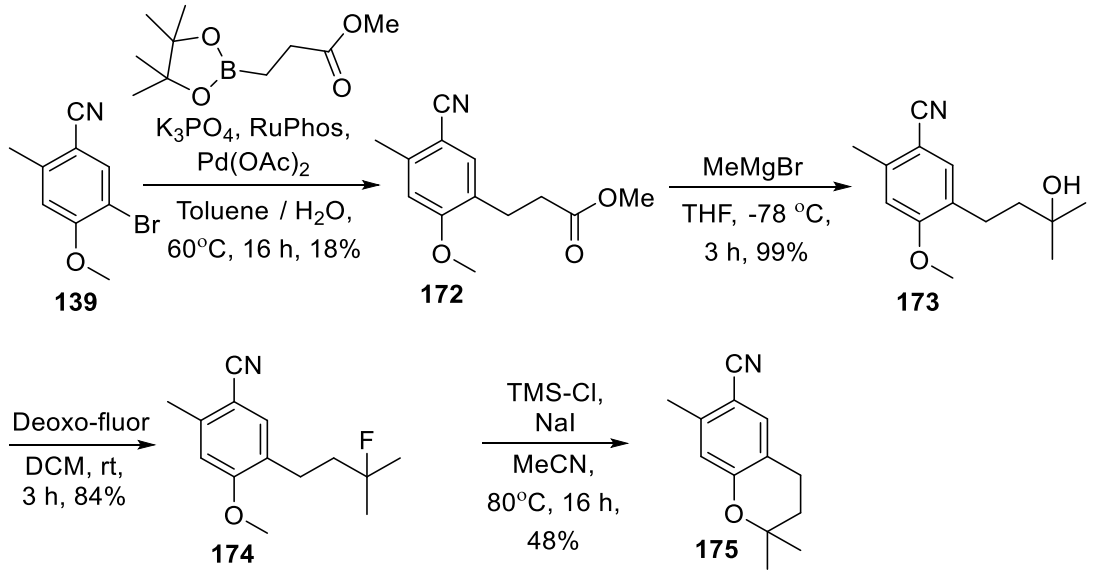

Figure 73 - Attempted synthesis of fluorinated analogue of **154**.

5.5.2 Fluorinated Alkyl Chain Analogue Biological Activity Assessment

Analogue **171** was assessed in the TAO inhibition assay and in the parasite growth inhibition assays with pIC_{50} (6.7 ± 0.1) and pEC_{50} (5.3 ± 0.1) respectively. A 10-fold decrease in TAO inhibition was observed when comparing this result to the butyl chain analogue (**135**). This

reduction in potency was however not as pronounced in the inhibition of parasite growth, with comparable activities observed. The inclusion of these two terminal fluorine atoms had resulted in a half log unit reduction of lipophilicity and provided a future avenue for further investigation.

Chapter 5 – SAR Exploration of Lipophilic Tail Conclusions

An overview of the analogues synthesised in this chapter is highlighted in figure 74. The isopentyl analogue **154** showed the most promising LLE profile out of the compounds synthesised in this chapter. The isopentyl chain may achieve a lipophilic interaction similar to the natural substrate ubiquinol. It is also of interest that the benzylic chain analogue **151** also showed a marked improvement for inhibition of parasite growth and lower lipophilicity. This could provide a further point for future exploration. The aromatic system could be substituted further to attain greater binding interactions with TAO. Heteroatoms could also be introduced to further reduce the lipophilicity of these compounds. The final compound that was of interest is the difluorinated analogue **171**. This compound has a reduced lipophilicity profile with a similar retention of parasite inhibition. Again, this strategy provides another area for future exploration that could be carried out in combination to identify more potent and less lipophilic TAO inhibitors.

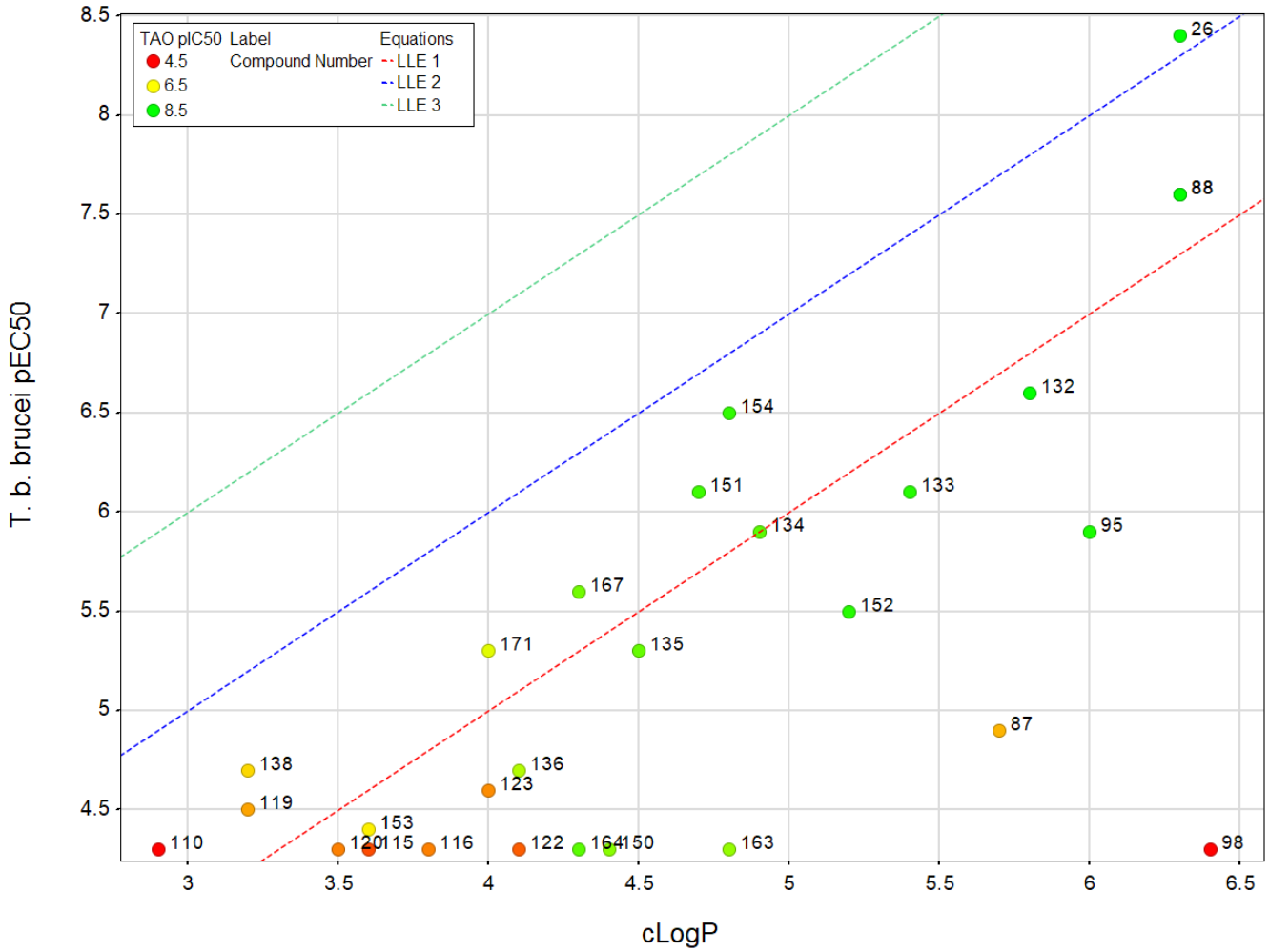

Figure 74 – Mean *T. b. brucei* pEC_{50}, cLogP and LLE Plot of tail modification analogues, LLE 1 = red line, LLE 2 = blue line, LLE 3 = green line. Labelled by compound number, and points coloured by mean TAO pIC_{50} (Green 8.5, lime green 7.5, yellow 6.5, orange 5.5 and red 4.5). cLogP generated using Chemaxon Marvin Sketch 17.25.

The focus of this chapter was to explore the lipophilic tail region of the synthetically amenable lead compound **88** that was identified in chapter 4. In summary, the introduction of polarity by inclusion of heteroatoms and polar functionality was not tolerated, with modest changes in structure in this region resulting in a complete loss of activity in both TAO inhibition and parasite growth assays. Tail analogue synthesis was optimised to remove a persistent impurity and following this the investigation into the tail length was carried out showing that adequate parasite inhibition could be attained with shorter carbon chain analogues. This highlighted the pentyl chain analogue (**134**), which retained micromolar inhibition of parasite growth with a reduction in cLogP to below 5. Further analogues were synthesised to explore more spatially diverse SAR in this region. This identified both the isopentyl analogue (**154**) and the benzyl analogue (**151**) to have improved LLE profiles, potently inhibiting TAO function with resultant parasite growth inhibition at concentrations of below 1 μM. Finally, the synthesis of fluorinated alkyl chain analogues was carried out resulting in analogue **171**. This analogue had a reduced lipophilicity and showed similar inhibitory potency in parasite growth assays to its direct matched-pair **135**. The isopentyl tail compound **154** showed sufficient quality for assessment in more advanced parasite assays, the results from these assays will be discussed chapter 7.

Chapter 6

Chapter 6 – Aromatic Head Group Substituent Exploration

The synthetic exploration of the CCB chemotype had thus far focused on modulating the lipophilicity of the tail portion of the molecule. Inclusion of polarity in this region was poorly tolerated and resulted in poorly active TAO inhibitors. It was therefore decided to investigate alternative substitution vectors from the aromatic ring, with the aim to identify molecules that were less lipophilic or that had the potential to improve binding interactions with TAO. Evaluation of the TAO : CCB crystal structure (PDB: 3W54) highlighted two vectors that could potentially be exploited and will be discussed in the following sections.[129]

6.1 Chloro replacement analogues

Analysis of the data generated from the initial lipophilic tail modification showed that polarity was not tolerated in this region of the molecule without loss of potency against TAO and therefore loss of parasitic inhibition. An alternative strategy was investigated to introduce polar functionality into the molecule and explore the SAR of the aromatic head group. Analysis of the TAO inhibitors that had been previously synthesised showed that the chloro substituent was required. Comparison of match pairs (**26**, **53** and **87**, **88**) indicated a 2.5 log drop in potency against TAO for the des-chloro analogues. Apart from removal of the halogen atom, no further exploration of the aromatic head group had been reported in the literature.[128] On review of the protein crystal structure in complex with CCB (PDB:3W54),[129] the chloro substituent looks to occupy the opening of a small channel present in TAO (Figure 75).

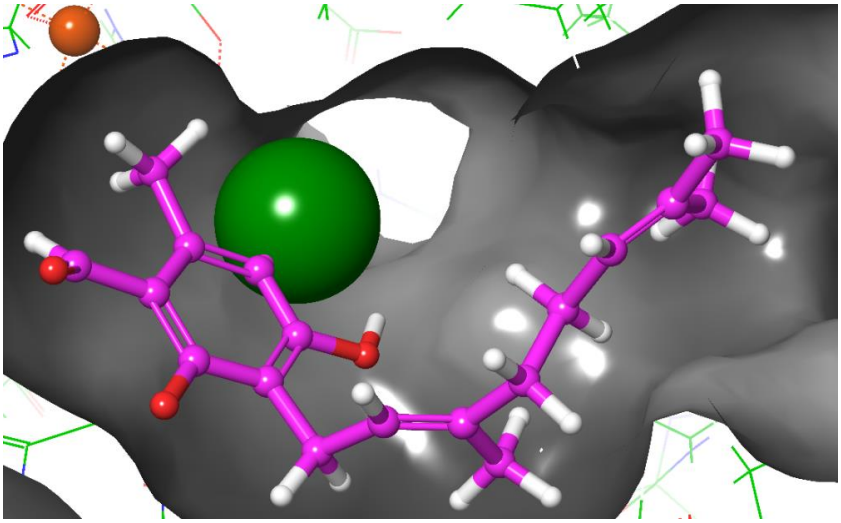

Figure 75 - Chloro-substituent exploration PDB: 3W54 structure, prepared and energy minimised using OPLS3 forcefield, Maestro - Schrodinger drug discovery suite. CCB coloured pink, chloro-atom depicted in Corey Pauling and Koltun (CPK) representation (green ball), at opening of small tunnel.

Closer inspection of the channel present in the crystal structure (PDB: 3W54) showed the presence of structural water molecules, that form interactions with TAO (Figure 76). This channel also has potential to introduce ligand contacts through electrostatic interaction (Figure 76 - surface coloured by electrostatic potential – calculated computationally by the Poisson-Boltzmann equation).

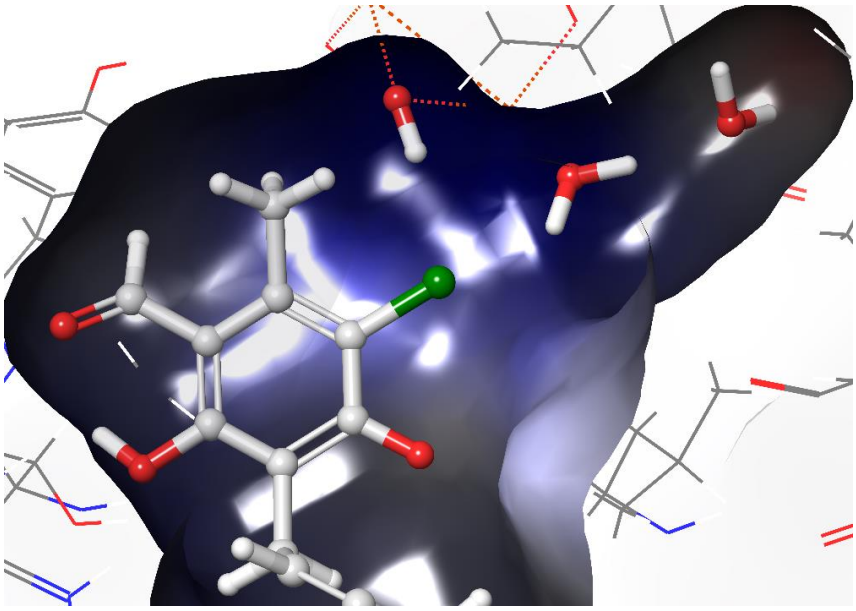

Figure 76 - Chloro-substituent exploration PDB: 3W54 structure, prepared and energy minimised using OPLS3 forcefield, Maestro - Schrodinger drug discovery suite. CCB coloured white, with chloro atom in green, surface of binding pocket without water removal, coloured by electrostatic potential - red to blue.

The chloro atom appeared vital for inhibition of TAO, therefore further analogues were planned to investigate whether this interaction could be further exploited to maximise TAO ligand interactions. This round of optimisation was initialised following the identification of the potent shorter *n*-pentyl carbon chain analogue **134**, and so the first step to facilitate exploration of this vector was the preparation of the *n*-pentyl chain intermediate (**177**). The deprotection of **176** with TMS-I at reflux in MeCN showed reduced conversion to **177** following lengthy reaction times of 96 h. Performing the reaction at a higher temperature in a sealed system in the microwave expediated the reaction to completion after 2 h (Figure 77).

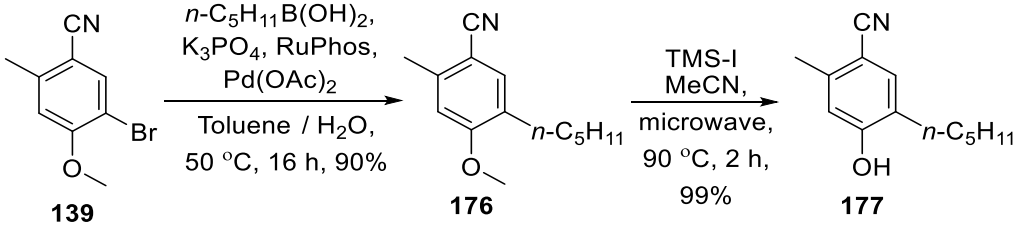

Figure 77 - Synthesis of *n*-pentyl intermediate for aromatic chloro head group exploration

With a bulk amount of intermediate **177** in hand, a range of analogues was planned to investigate replacement of the chloro atom. Preparation of the bromo analogue (**178**) by electrophilic aromatic bromination was carried out with NBS in acetonitrile. It was anticipated that the brominated intermediate (**178**) would provide access to a range of analogues through cross-coupling chemistry (Figure 78).

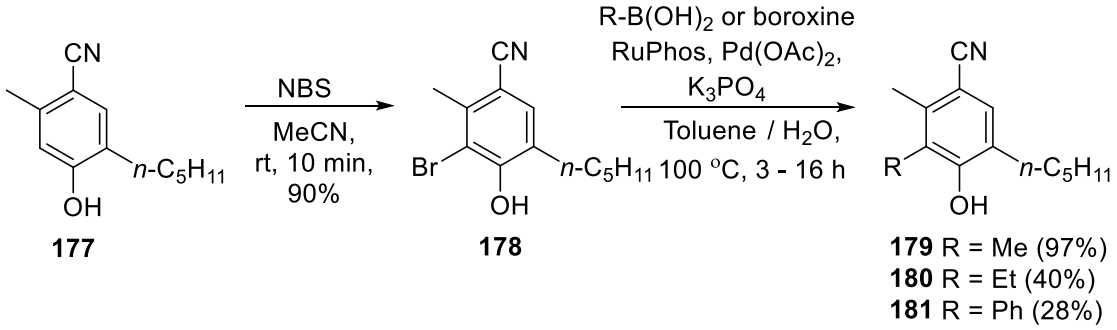

Figure 78 - Bromination of **177** to provide access to cross-coupled chloro replacement analogues

To probe the nature of interaction of the chlorine atom to the protein, the methyl (**179**), ethyl (**180**) and phenyl (**181**) analogues were prepared *via* Suzuki-Miyaura cross-coupling, utilising similar reaction conditions to those used to install the tail modifications. The methyl compound provides a similar overall lipophilicity profile and is of interest to determine whether an electrostatic or lipophilic interaction is being formed with the halogen. A range of Buchwald and Ullmann cross-couplings were attempted to furnish the aromatic with *N*-linked heterocycles, unfortunately these were not successful. Attempts at cross-coupling **178** with heterocyclic boronic acids under these cross-coupling conditions were also unsuccessful. A substituted 5-membered heterocycle was of interest, as *in silico* modelling suggested that 2,5-substitution would enable access to the narrow pocket *via* this vector (Figure 79). In particular, 1,3,4-oxadiazoles have recently been shown to provide some of the best improvements in compound solubility over other heterocycles.[242]

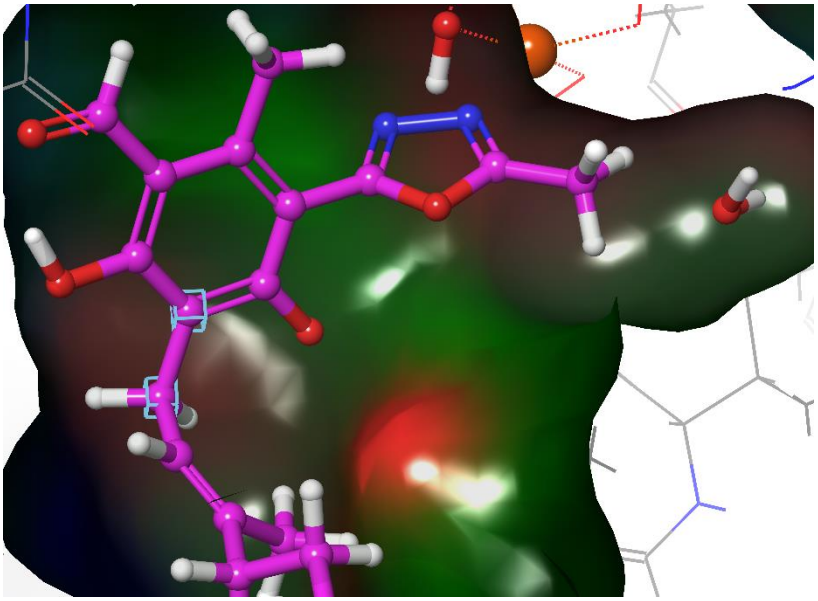

Figure 79 – 1,3,4-oxadiazole heterocyclic replacement of aromatic chloro substituent. Virtual molecule (pink) built in Maestro – Schrodinger drug discover suite from PDB:3W54 (TAO : CCB crystal structure) and energy minimised. Surface generated of binding pocket of TAO.

Following the failure to introduce these heterocycles from cross-coupling chemistries an alternative synthetic strategy was sought. The synthesis of 1,3,4-oxadiazoles can be performed from the dehydrative cyclisation of diacyl hydrazides at high temperatures.[243,244]

To access these intermediates, synthesis of the ethyl ester of intermediate **178** was carried out by palladium mediated carbonylation. The carbonylation of aromatic halides, utilising inorganic carbon monoxide sources such as molybdenum hexacarbonyl has been extensively reported in the literature.[245–247] The use of the catalyst developed by Herrmann and Beller,[248] with $Mo(CO)_6$ and DBU in ethanol provided the ethyl ester (**182**) in good yield following microwave irradiation. Hydrolysis of intermediate **182** required heating at 60 °C for 96 h to progress the reaction to completion and isolate the free acid (**183**). Attempts to form the diacyl hydrazide through the formation of the acid chloride or HATU activated ester, then reaction with acyl hydrazine were however unsuccessful (Figure 80).

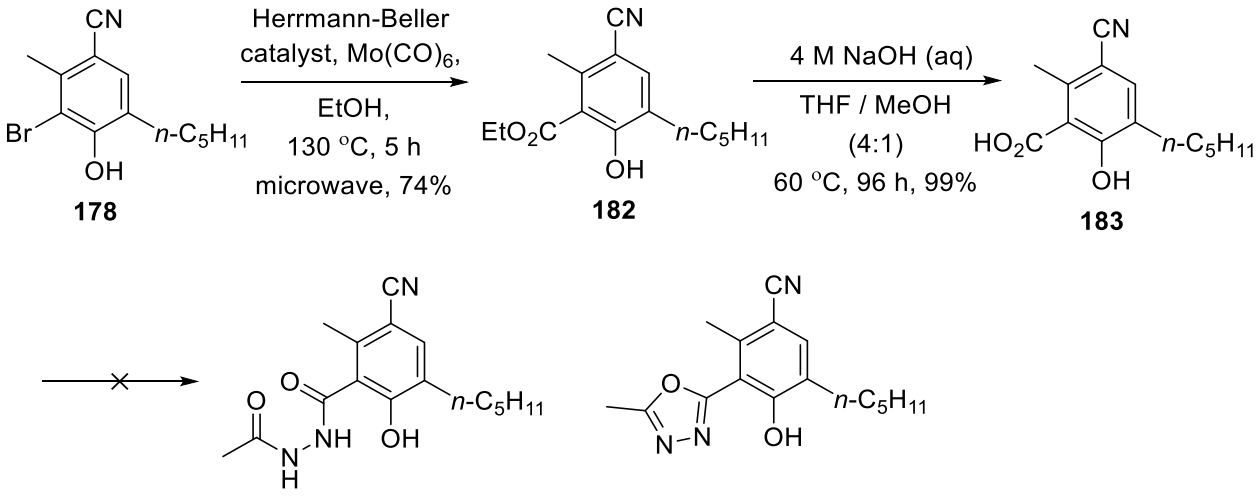

Figure 80 - 1,3,4-oxadiazole synthesis

Introduction of the carboxylic acid in this position also provided the opportunity to introduce amidic functionality with an aim to lower the overall lipophilicity of the molecule. Modelling of the dimethyl amide looked to also provide a vector to access the narrow tunnel present in the TAO : CCB crystal structure (PDB:3W54),[129] (Figure 81).

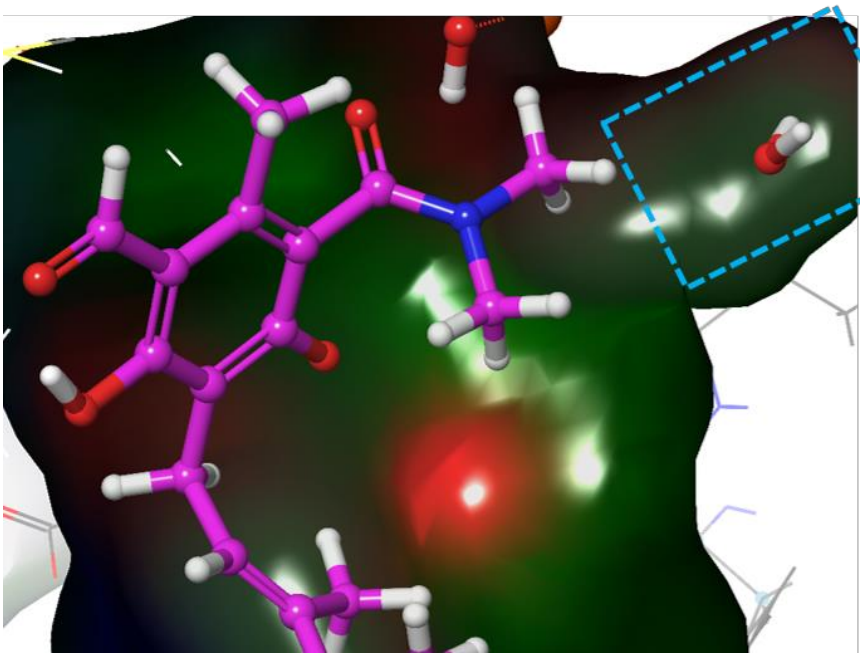

Figure 81 - Dimethylamide replacement of aromatic chloro substituent. Virtual molecule (pink) built in Maestro – Schrodinger drug discover suite from PDB:3W54 (TAO : CCB crystal structure) and energy minimised. Surface generated of binding pocket of TAO – narrow tunnel blue dotted box.

Formation of the acid chloride from intermediate **183** was obtained by reaction with oxalyl chloride and a catalytic amount of DMF. The acid chloride was quenched by the addition of dimethylamine in THF, to provide the dimethyl amide (**184**) in good yield (Figure 82).

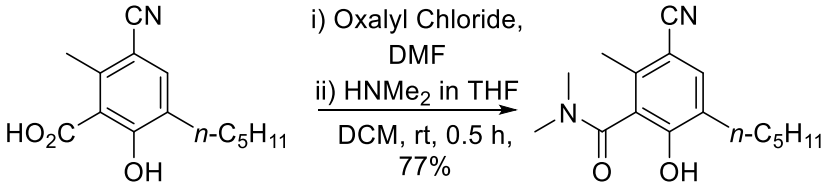

183 **184**

Figure 82 - Synthesis of dimethyl amide chloro replacement analogue

A final attempt to synthesise a heterocyclic replacement for the chloro substituent was attempted. Sangshetti *et al.* had reported the successful synthesis of 1,3,4-oxadiazoles from the reaction of aldehydes with acyl hydrazides, utilising a sodium bisulphite catalyst.[249] A synthesis to the intermediate benzaldehyde (**185**) was attempted. Initially, a Vilsmeier-Haack reaction was trialled by refluxing intermediate **177** with $POCl_3$ in DMF; no product could be

identified from this reaction. An alternative method of formylation was investigated, as chemistry developed in 1876 by Reimer and Tiemann had shown the successful formylation of phenols using chloroform and sodium hydroxide.[250] The Reimer-Tiemann reaction has been extensively studied and is understood to react through the formation of an electrophilic di-halo carbene species formed from the reaction of chloroform and hydroxide, that is then attacked by the electron rich phenol.[251] The treatment of intermediate **177** with sodium hydroxide and chloroform at reflux showed the formation of the desired formylated product (**185**), albeit with a range of other by-products. Optimisation of this reaction through modification of reaction temperature and time provided no improvement in the yield or purity of **185**. The reaction profile by LCMS showed formation of multiple side products, and the reaction never proceeded to completion. Approximately half of the starting material could be readily recovered from the chromatographic purification of **185**. Unfortunately, the subsequent attempts of synthesising heterocycle replacements for the chloro substituent from the benzaldehyde were unsuccessful (Figure 83).

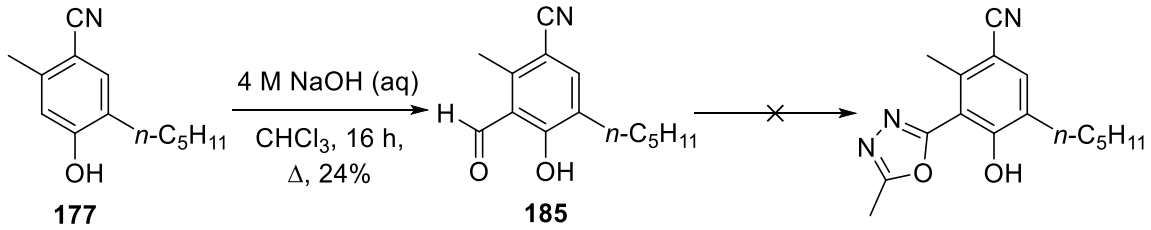

Figure 83 - Formation of benzaldehyde intermediate **185**

A range of chloro replacement analogues and intermediates had been synthesised (**177** - **185**). These compounds were assessed in TAO inhibition and *T. b. brucei* growth inhibition assays before further synthetic exploration was initiated in this area, data summarised in Table 17.

Table 17 - Chloro replacement analogues

Structure	#	TAO (pIC_{50})[a]	*T. b. b.* (pEC_{50})[b]	cLogP [c]
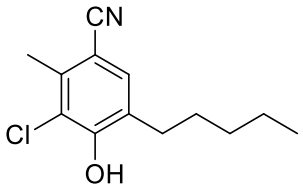	**134**	7.8 ± 0.1 (LLE 2.9)	5.9 ± 0.1 (LLE 1.0)	4.9
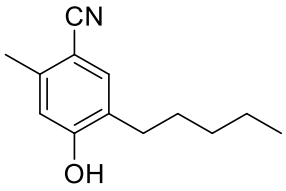	**177**	5.7 ± 0.1	4.4 ± 0.1	4.3
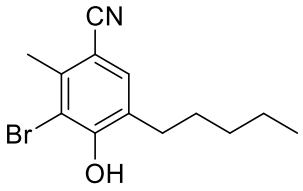	**178**	8.4 ± 0.1 (LLE 3.3)	6.5 ± 0.1 (LLE 1.4)	5.1
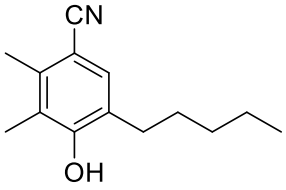	**179**	6.7 ± 0.1	5.1 ± 0.1	4.8
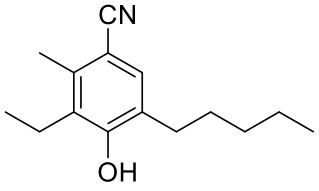	**180**	6.4 ± 0.1	4.8 ± 0.1	5.3
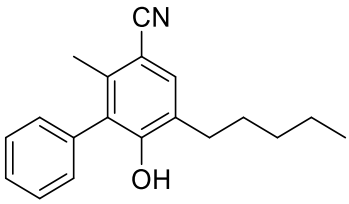	**181**	6.0 ± 0.2	< 4.3	6.0
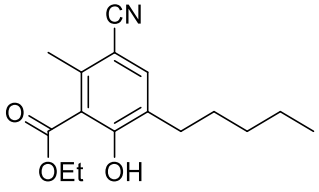	**182**	-	< 4.3	5.3

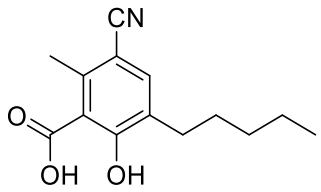	**183**	5.0 ± 0.1	< 4.3	4.6
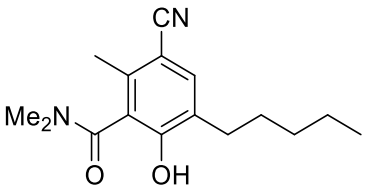	**184**	5.3 ± 0.1	< 4.3	4.3
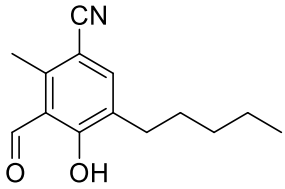	**185**	< 4.5	< 4.3	4.7

[a] Negative log concentration and standard deviation of compounds required for 50% inhibition of trypanosome alternative oxidase (n = >2). [b] Negative log concentration and standard deviation of compounds required for 50% growth inhibition of *T. b. brucei* Lister427 (n = >2). [c] Parameters calculated using Chemaxon Marvin Sketch 17.25.0.

Inspection of these data suggested that the introduction of polar functionality was again detrimental to potency, particularly in the parasite growth inhibition assay. Introduction of a carbonyl *ortho* to the phenol also provided poorly active compounds (**182** - **185**) with TAO pIC_{50}s below 6. Interestingly, replacement of the chloro atom with other lipophilic moieties appeared to be tolerated, with compounds **178** – **181** retaining sub-micro molar inhibition profiles of TAO, suggesting that the chloro interactions were predominately lipophilic. This potency tracked well with the observed inhibition of *T. b. brucei* growth apart from the phenyl replacement (**181**), that showed no inhibition of parasite growth. Again, a reduction in activity of approximately 1.5 log units was observed from inhibition of TAO to parasite growth. A 0.6 pIC_{50} improvement in TAO inhibition and a 0.6 pEC_{50} improvement in parasite growth inhibition was observed with the bromo analogue (**178**). This increase in potency was driven with only a small 0.2 increase in cLogP, and as a result had a marked 0.4 improvement in LLE (compounds **134** and **178** - Table 17). It would be of interest to see if this improvement in potency and LLE could be combined with the improvement in potency that were observed with the introduction of the isopentyl tail analogue (**154**). In review of the data in this section,

a halogen atom looked to be required for potent TAO inhibition, the introduction of other functional groups had resulted in a large detriment to potency, and thus alternative aromatic substitutions were explored.

6.4 Benzonitrile exploration

Inspection of the parasite growth inhibition data generated thus far had shown a lower potency for benzonitrile analogues over the benzaldehyde substituent compounds (**47** to CCB **26** and **51** to **50**). The benzaldehyde analogue containing the shorter *n*-pentyl chain (**187**) was synthesised to investigate whether this potency observation still held with the mono-phenol aromatic system. The synthesis of the cyclopropyl ethyl analogue (**167**) had been performed utilising Suzuki-Miyaura cross-coupling of the free phenol with a boronic acid, and so this route was successfully implemented to install the *n*-pentyl chain directly to provide **186**. Subsequent chlorination of **186** with conditions previously utilised provided the desired benzaldehyde analogue (**187**) for matched-pair comparison (Figure 84).

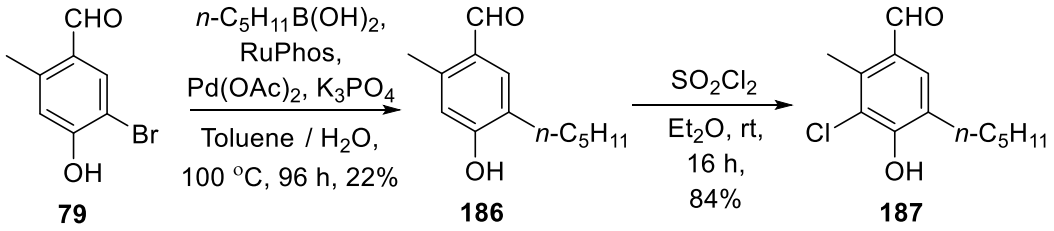

Figure 84 - Synthesis of *n*-pentyl benzaldehyde analogue

Analogue **187** showed good inhibitory potency of TAO (pIC_{50} 8.7 ± 0.1), that correlated to an increased inhibition of *T. b. brucei* growth (pEC_{50} 6.7 ± 0.2), displaying a six to eight-fold improvement in potency in both enzyme and parasite inhibition assays. Due to the superior potency observed with these benzaldehyde analogues, the published crystal structure was further inspected to ascertain the potential interactions that the benzaldehyde was making with TAO (Figure 85).

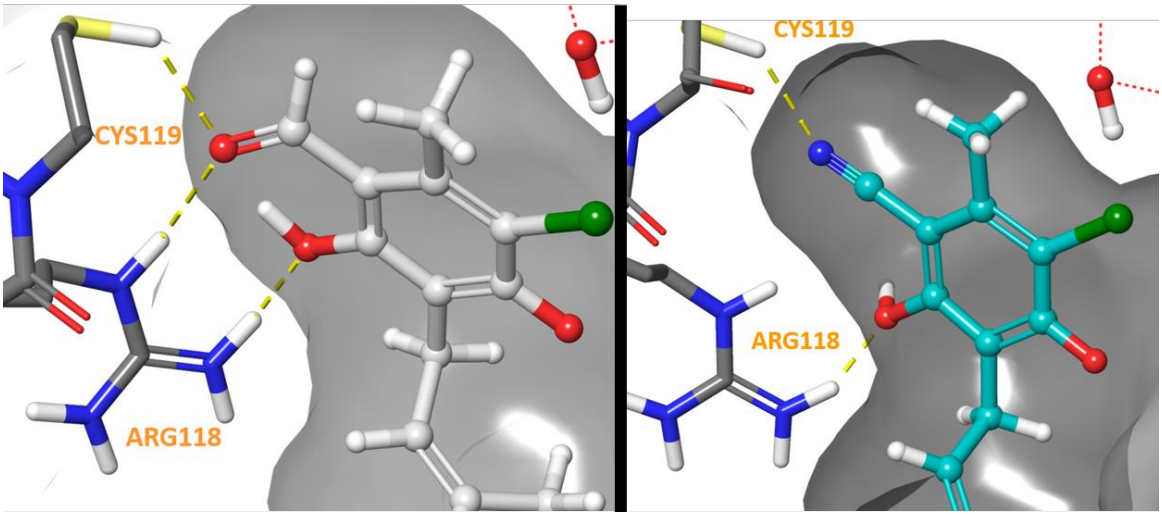

Figure 85 - Aldehyde (left) and Nitrile (right) TAO interactions observed in crystal structure (PDB: 3W54)[129] and virtual molecule built in Maestro – Schrodinger drug discovery suite energy minimised structure using OPLS3 forcefield. CCB (white - left), virtual nitrile analogue of CCB (teal - right), protein binding surface (grey), CYS119 and ARG118 amino acid residues displayed and labelled with hydrogen bonds to aldehyde or nitrile (yellow hash lines).

The published crystal structure shows the formation of potential hydrogen bonds with both cysteine (CYS119) and arginine (ARG118) residues with the aldehyde (Left - Figure 85). The nitrile replacement analogue was predicted to occupy an area further from the arginine residue (ARG118) due to the linear orientation and vector from the aromatic ring. The nitrile was predicted to retain the hydrogen bond interaction with the cysteine residue, however the loss of interaction with ARG118 could help to explain the reduced inhibitory activity of TAO (Right – Figure 85). The synthesis of other carbonyl containing analogues was planned, to determine whether this interaction could be retained with a more chemically desirable functional group. Initially, electrophilic bromination of the methyl ester intermediate (**188**) was attempted. Similar results to the unsuccessful bromination of the benzonitrile intermediate (**78**) were observed, with the formation of a mixture of multiple bromination products under these conditions. Carrying out the addition of brominating reagent at lower temperatures, and as a dilute solution in reaction solvent, provided no improvement in reaction profile. Alternative electrophilic brominating reagents (Br_2, NBS, dibromoisocyanuric acid and tetrabutyl ammonium tribromide) were also investigated; however, these showed similar reaction profiles to BTMAT and did not provide the desired

mono brominated analogue in sufficient purity for continuation of the synthesis (Figure 86). Therefore, an alternative synthesis to these analogues was sought.

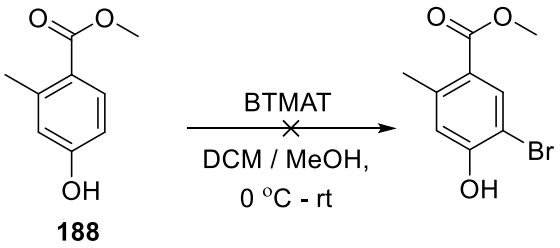

Figure 86 - Attempted bromination of methyl ester intermediate

As selective mono bromination of the benzaldehyde had previously been carried out in good yield to provide intermediate **80**, this intermediate was used as a starting point for further synthetic exploration (Figure 86). Oxidation of the aldehyde to the carboxylic acid (**189**) was performed using Pinnick oxidation conditions.[252] This mild oxidation was originally reported by Kraus and Roth,[253] in the partial synthesis of the natural product verrucarol. Sodium chlorite acts as the oxidant to generate the carboxylic acid from the aldehyde, producing hypochlorous acid as a by-product. This can further react with other functional groups, so 2-methyl-2-butene is commonly used as a scavenger to prevent undesired side reactions. Intermediate **189** was successfully di-methylated with dimethyl sulphate in acetone, utilising potassium carbonate as a base to provide **190**. The isopentyl chain was installed *via* Suzuki-Miyaura cross coupling, utilising the same conditions that were previously employed to append the alkyl chain to provide intermediate **191**. This intermediate was doubly de-protected using chlorotrimethyl silane and sodium iodide in the microwave to provide the free phenol and carboxylic acid (**192**). Electrophilic aromatic chlorination of **192** with sulfuryl chloride in diethyl ether as discussed previously, provided the chlorinated intermediate (**193**). This material was used to generate primary (**196**), secondary methyl (**195**) and tertiary dimethyl (**196**) amides for comparison to the benzaldehyde analogue (**187**) (Figure 87).

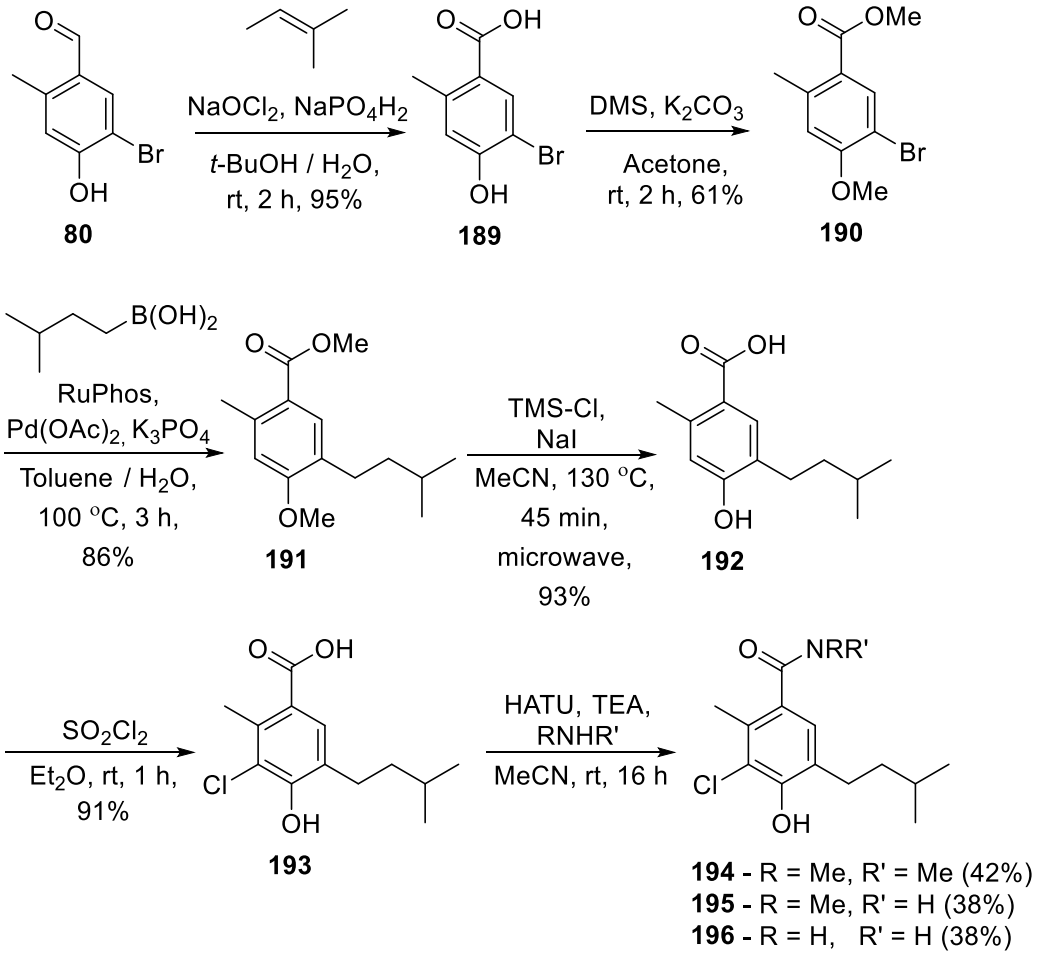

Figure 87 - Synthesis of benzaldehyde replacement analogues

Analogues **193** – **196** were assessed in TAO and *T. b. brucei* growth inhibition assays. Unfortunately, these analogues showed a large reduction in potency in both assays. The most potent analogue was the primary amide (**196**), which showed 3-fold higher potency than the other analogues in the TAO inhibition assay (pIC_{50} 5.8), compared to pIC_{50}s of around 5.2 for **193** – **195**. In review of these data, further synthetic exploration around this functional group was deprioritised.

6.3 Combination compounds

With deadline limitations approaching for the conclusion of this project, examination of all the analogues that had been synthesised around the CCB chemotype was carried out. This highlighted potential amalgamations for some of the successful structural modifications that

had been identified. The isopentyl analogue (**154**), had shown a decrease in lipophilicity and an improvement in parasite growth inhibition potency in comparison to the *n*-pentyl analogue (**134**). Replacement of the chlorine with a bromine atom (**178**) had also provided an analogue with improved potency against TAO, with a minimal increase in lipophilicity. It was therefore decided to combine these two structural modifications to ascertain whether they could be combined to obtain a molecule that had improved parasite growth inhibition potency and LLE profile.

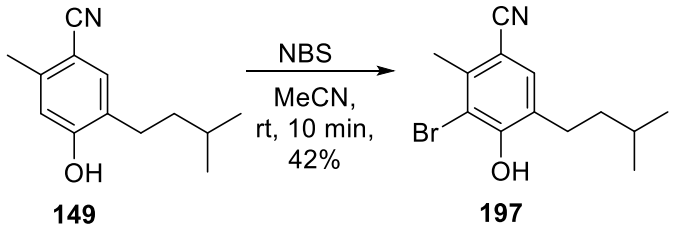

Figure 88 - Synthesis of combination bromo isopentyl analogue (**197**)

Analogue **197** was successfully synthesised by the electrophilic aromatic bromination of intermediate **149** (Figure 88). The compound required further purification by reverse-phase chromatography that resulted in a lower than expected yield. Assessment of the biological activity of this compound was promising with TAO pIC50 8.3 ± 0.1 and *T. b. brucei* inhibition pEC_{50} 6.9 ± 0.1, correlating to a 0.4 pEC_{50} increase in potency for parasite growth inhibition and a resultant LLE of 2.0. The CNS MPO score for **197** is 3.9 close to the desired score required for optimal predicted CNS penetration. The comparison of **197** to the chloro analogue however, shows a 0.3 decrease (CNS MPO score 4.2). The increase in lipophilicity from the bromine atom has again negatively influenced the cLogP and $cLogD_{7.4}$ scoring functions for the total MPO score. The compound was still regarded to be of sufficient quality for assessment in advanced kill kinetic and parasite cure assays at Novartis and *in vitro* pharmacokinetic profiling, that should highlight metabolism and permeability issues of these compounds. These data will be discussed in the next and final chapter of this thesis, along with comparative data generated with the *n*-pentyl benzaldehyde (**187**) and CCB (**26**) analogues.

Chapter 6 - Aromatic Head Group Substituent Exploration Summary and Conclusions

The aim of the work performed in this chapter was to explore the SAR of the aromatic substituents of the CCB chemotype. A synthesis was developed to allow introduction of alternative functionality in place of the chloro and nitrile substituents. Unfortunately, many of the analogues synthesised in this exploration resulted in major reductions in inhibition of TAO and parasite growth. A highlight of this exploration was the identification of the brominated analogue (178) that achieved improved parasite inhibition potency with a minor increase in lipophilicity. Bromine atoms can potentially form stronger electrostatic halogen bond interactions than chlorine atoms. This arises from the increased size of the σ-hole present in bromine due to the electron anisotropy. As halogen atoms increase in size, the σ-hole becomes larger and more electron deficient allowing stronger electrostatic interactions with Lewis bases.[254] However, inspection of the crystal structure reported by Shiba *et al*.[129] (PDB: 3W54) does not identify a Lewis basic amino acid residue to be present in this part of TAO, that could potentially form this type of head on interaction. A halogen bond to a water molecule present in the narrow channel is observed in the crystal structure 3W54. Structural water molecules have previously been observed to partake in protein-water-inhibitor binding interactions that result in positive affinities for inhibitors.[255] The combination of chloro replacement with bromo, and the improvement in potency observed with the isopentyl analogue resulted in additive potency improvements for analogue 197. This analogue was considered to be of sufficient quality for assessment in further parasite kill kinetic and cure assays along with basic *in vitro* pharmacokinetic profiling assays conducted at Novartis. Further exploration into the benzonitrile substituent resulted in the identification of compounds with reduced potency against TAO. The aldehyde analogues continued to show higher potency against TAO, which correlated to an improvement in parasite growth inhibition. The benzaldehyde 187 was therefore also assessed in the advanced parasite inhibition and *in vitro* pharmacokinetic assays. These data will be discussed in the concluding chapter.

Chapter 7

Chapter 7 – Final Compound Profiling, Conclusions and Future Work

7.1 Final Compound Profiling

Several interesting TAO inhibitors were identified and characterised over the course of this research project. Compound **88** provided a synthetically amenable starting point, to explore the lipophilic tail region of the CCB (**26**) chemotype. Shorter carbon chain tail analogues had improved physicochemical properties and retained micromolar parasite growth inhibition. Further synthetic exploration of these shorter chain analogues (**134** and **135**) identified the isopentyl analogue **154,** a compound with reduced lipophilicity, a significant improvement in potency against TAO inhibition and improved parasite growth inhibition.

The investigation into replacing the chloro substituent highlighted that the larger bromo halogen analogue **178** had improved parasite growth inhibition, with only a marginal increase in lipophilicity. This compound showed little improvement in CNS MPO score over the natural product CCB (**26**) as the cLogP and $cLogD_{7.4}$ were still below the parameter scoring limit. Synthesis of the combination isopentyl bromo compound **197** was synthesised and demonstrated additive potency improvements in the parasite inhibition assay, resulting again in a compound with slightly lower lipophilicity, and improvement in LLE. Following further exploration of the benzonitrile, it was apparent that the benzaldehyde analogues retained higher potency in the parasite inhibition assay. This led to the synthesis of the *n*-pentyl benzaldehyde analogue **187** for further assessment in parasite kill kinetic and reversibility studies and enabled in *in vitro* pharmacokinetic profiling which is currently ongoing.

Table 18 - SAR overview of key TAO inhibitors

Structure	#	TAO (pIC_{50}) [a]	*T. b. b.* (pEC_{50}) [b]	HepG2 (pCC_{50}) [c]	*T.b.b* LLE [d]	CNS MPO [e]
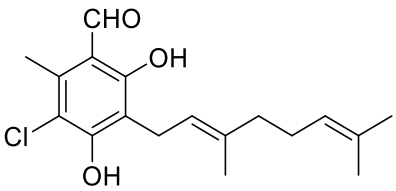	**26**	8.5 ± 0.2	8.4 ± 0.1	5.1 ± 0.1	2.2	3.5

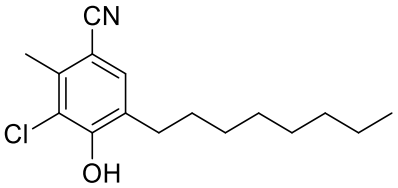	**88**	8.5 ± 0.2	7.6 ± 0.1	5.1 ± 0.1	1.3	3.8
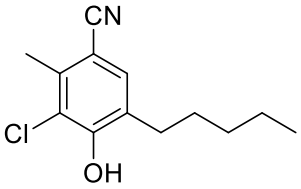	**134**	7.8 ± 0.1	5.9 ± 0.1	4.4 ± 0.1	1.0	3.9
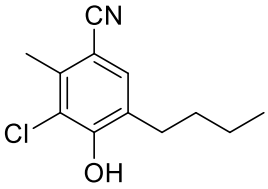	**135**	7.7 ± 0.1	5.3 ± 0.1	-	2.1	4.2
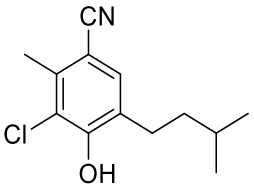	**154**	8.1 ± 0.1	6.5 ± 0.1	4.1 ± 0.1	1.7	3.9
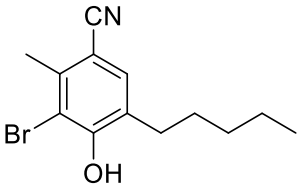	**178**	8.4 ± 0.1	6.5 ± 0.1	4.4 ± 0.1	1.4	3.8
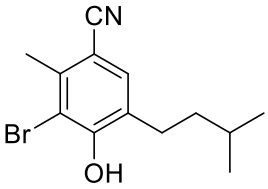	**197**	8.3 ± 0.1	6.9 ± 0.1	-	1.8	3.9
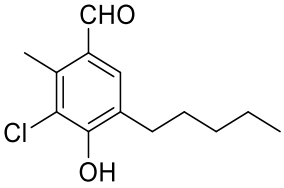	**187**	8.7 ± 0.1	6.7 ± 0.1	-	1.9	4.0

[a] Negative log concentration and standard deviation of compounds required for 50% inhibition of trypanosome alternative oxidase (n = >2). [b] Negative log concentration and standard deviation of compounds required for 50% growth inhibition of *T. b. brucei* Lister427 (n = >2). [c] Negative log concentration and standard deviation of compounds required for 50% growth inhibition of T. b. brucei Lister427 (n = >2). [d] Parameters calculated using Chemaxon Marvin Sketch 17.25.0. LLE *T. b. brucei* pEC_{50} – cLogP. [e] Calculated in Knime workflow using ChemAxon JChem nodes.

Analysis of these data indicated that the shorter alkyl chain analogues had a reduced cytotoxicity in mammalian HepG2 cells, compared to the more lipophilic, longer alkyl chain analogues. An improvement in LLE was observed with the isopentyl chain (**154**), the bromo substituent (**178**) and the benzaldehyde analogues (**187**). The benzaldehyde (**187**) has stronger electron-withdrawing properties over the benzonitrile (**134**), decreasing the calculated pKa of the phenol. This decreased the calculated $cLogD_{7.4}$ by 0.6 units, which improves the CNS MPO scoring function. The *T. b. brucei* LLE and TAO inhibition profiles for the TAO inhibitors synthesised over the course of this project are highlighted in figure 88. From this plot it is apparent that the later synthesised compounds (**154**, **178**, **187**) have improved LLE. The combination of these structural modifications in compound **197** attained an LLE of 2. Incorporation of the benzaldehyde moiety together with the structural modifications previously identified may improve the LLE to higher than the natural product CCB (**26**), approaching a more desirable LLE value of 3 (Figure 89 - green line).

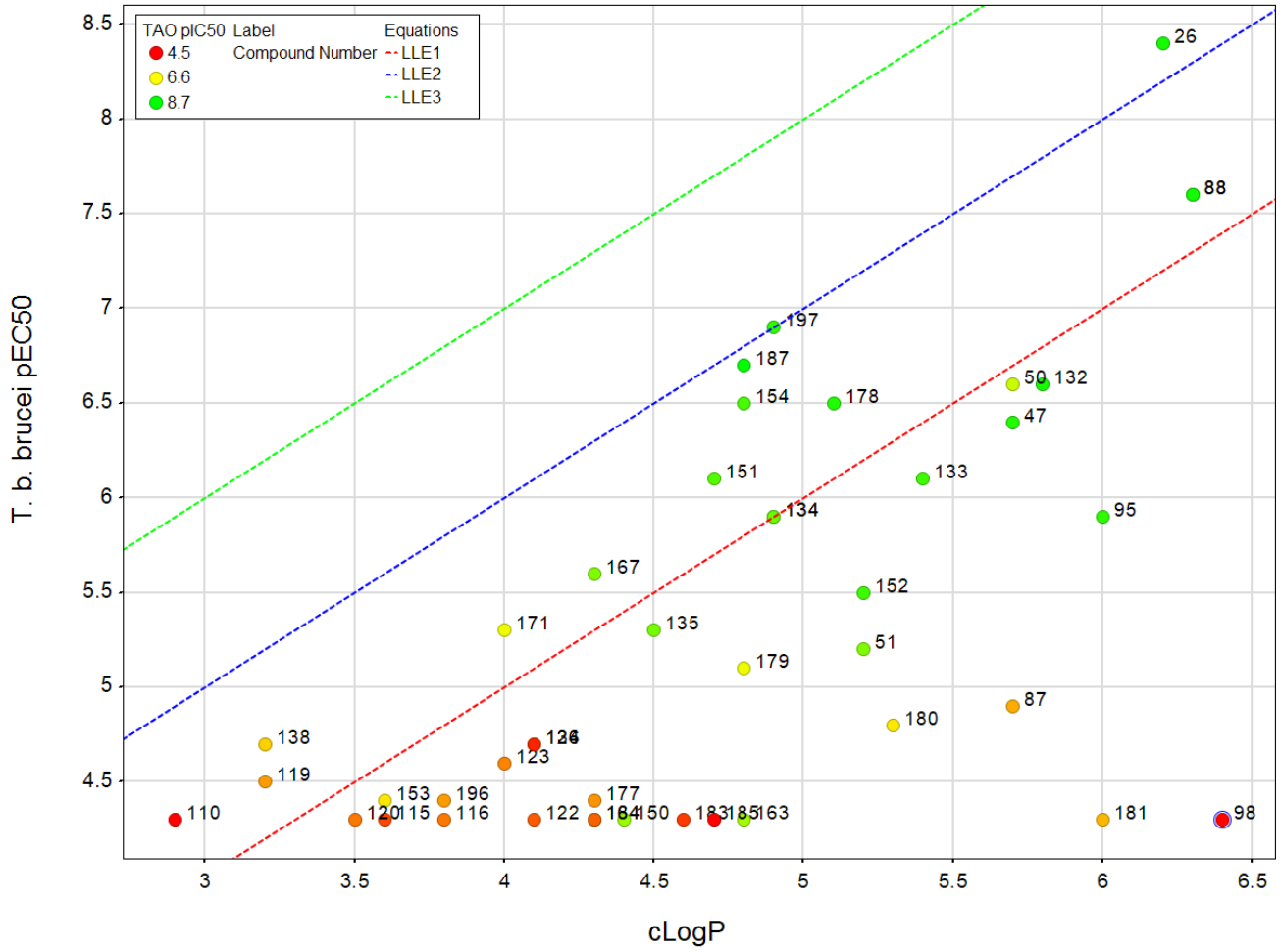

Figure 89 - LLE Plot of *T. b. brucei* growth inhibition activity of all compounds, generated in Vortex. Mean *T. b. brucei* pEC_{50}, cLogP and LLE Plot of tail modification analogues, LLE 1 = red line, LLE 2 = blue line, LLE 3 = green line. Labelled by compound number, and points coloured by mean TAO pIC_{50} (Green 8.7, lime green 7.5, yellow 6.6, orange 5.5 and red 4.5). cLogP generated using Chemaxon Marvin Sketch 17.25.

7.2 Parasite Kill Kinetics and Reversibility Assessment

The parasite kill kinetic assay determines the concentration of compound that is required to reduce parasite levels over a time course of 6, 24 and 48 h. This data is used to show compound cidality, which is determined to be a 1 log order reduction in parasite concentration. This assay was conducted by research associates at Novartis. A *T. b. brucei* culture is initiated at a 1×10^5/mL parasite density at 10 concentrations of inhibitor. Parasite density is then assessed using cell-titre glow reagent at the time points stated to allow analysis of the time dependent inhibition profile and cidality assessment. The data for compounds **26**, **134**, **154**, **178**, **187** is summarised in figure 89. Analysis of these data show that the kill kinetic profiles of these TAO inhibitors require 24 h to reach maximal inhibition. Unfortunately, the TAO inhibitors show poor trypanocidal efficacy in this assay, instead showing a trypanonstatic effect. Much higher concentrations of compound are required to instigate parasite clearance than was necessary to inhibit parasite growth. A CCB (**26**) concentration of 1.8 μM was required for a cidal response in this assay. This equates to a concentration approximately 25 × greater than the concentration required to inhibit 90% of parasite growth. These types of inhibition profile are indicative of a non-cidal mechanism of action. The target product profile set out by the DNDi (Table 2), highlights the preference for progressing trypanocidal compounds into the clinic as potential HAT treatments.[65] This data suggests that TAO inhibitors predominately act *via* a trypanostatic mechanism, and would therefore be a less desirable class of compounds to progress into further drug development. However, TAO inhibition does show a marked increase in potency for the Melarsoprol and Pentamidine drug resistant strains.[135] Assessment of cidal activity against these drug resistant strains may re-new interest in TAO inhibitors for the potential treatment of HAT. The data generated here also showed the need for compounds with much higher potency in the parasite growth inhibition assays due to the significant decrease observed in the parasite kill kinetic assay. Attaining such a high compound concentration in an *in vivo* setting would be difficult especially over the prolonged time period required to attain parasite clearance, highlighted in this experiment (Figure 90). The therapeutic window of these compounds

would also likely be diminished as CC_{50} in mammalian HepG2 cells is close to the micromolar concentrations that would be required to clear parasite infections.

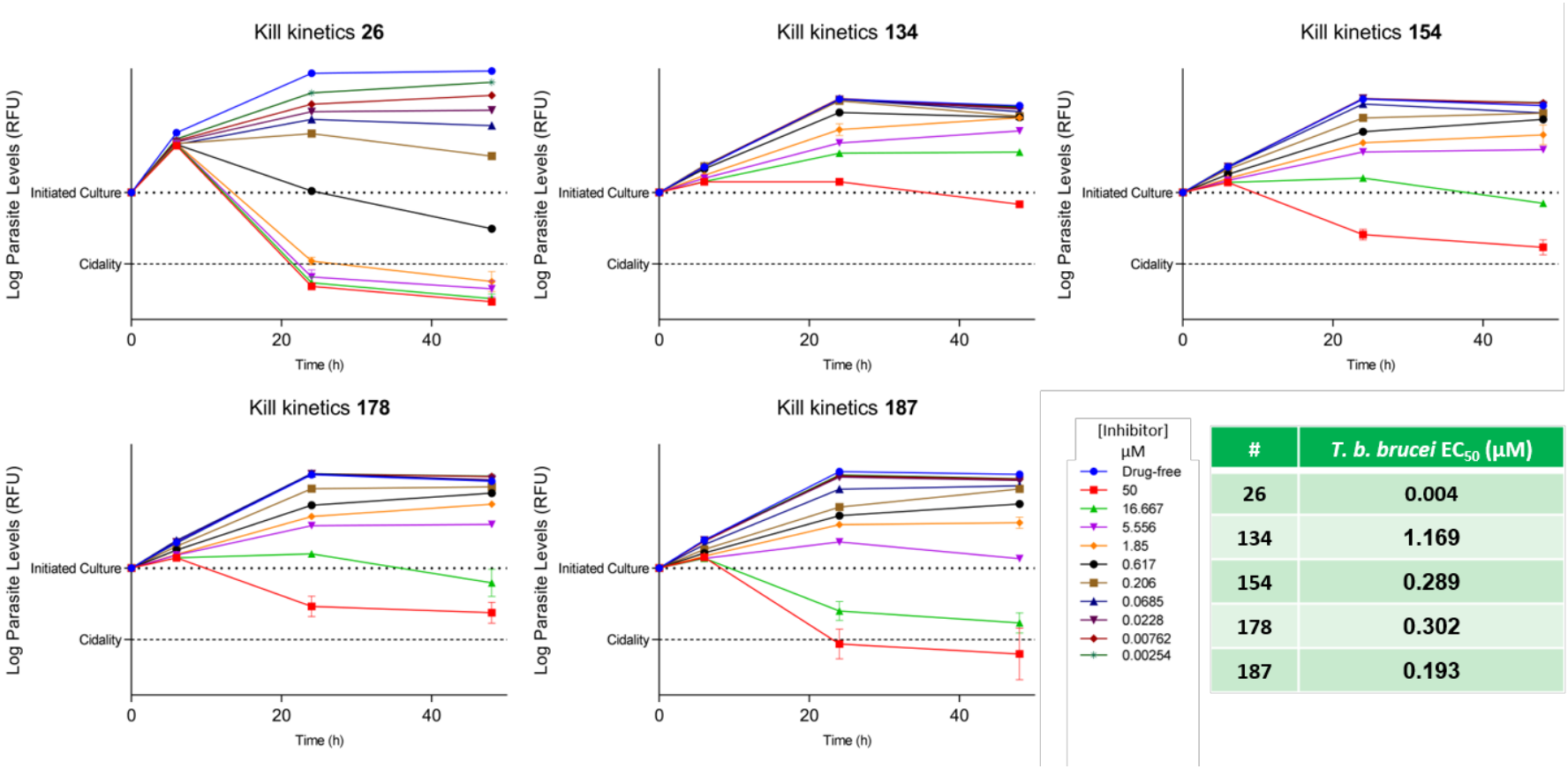

#	*T. b. brucei* EC_{50} (µM)
26	0.004
134	1.169
154	0.289
178	0.302
187	0.193

Figure 90 - Kill Kinetic data for TAO inhibitors

These compounds were also assessed in parasite cure reversibility assays, also conducted at Novartis. These assays are used to determine the concentration of compound that is required to irreversibly clear a parasite culture. In this assay a 1×10^5 per mL of *T. b. brucei* culture is inoculated with inhibitor at 10 concentrations (3-fold serial dilution from 50 µM). Each culture is incubated for 48 h with compound at 37 °C, 5% CO_2. The supernatant is then removed, and the parasites are washed 3-times with media before placing under culture conditions for 72 h. Parasites levels are then assessed with celltitre glo® reagent to determine the compound concentration required to clear parasites irreversibly. Parasite clearance is determined when a response below the limit of detection is observed (Figure 91).

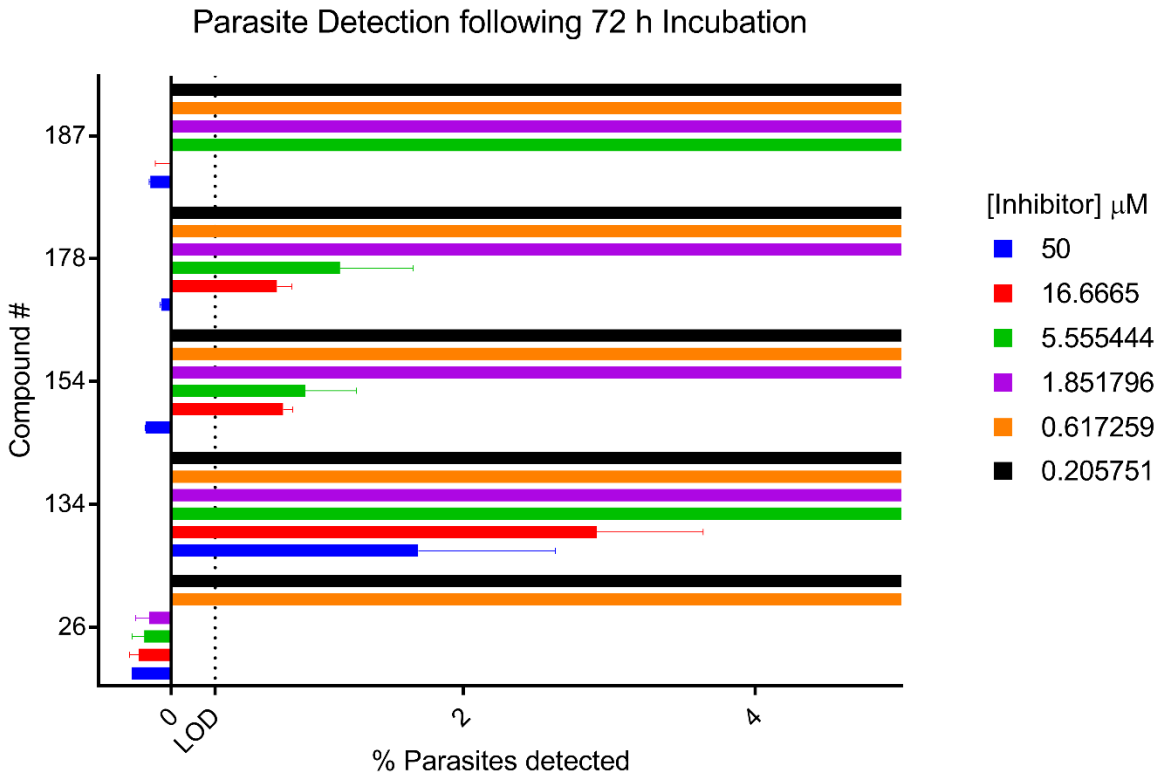

Figure 91 - *T. b. brucei* reversibility / cure assay

Again, a similar result to the kill kinetic profiles was observed. Very high concentrations of TAO inhibitor were required to observe parasite clearance. The benzaldehyde compound **187** looks to show higher potency for clearance than the direct nitrile comparison **134**. The iso-

pentyl chain analogue (**154**) and the bromo analogue (**178**) also showed improved parasite clearance profiles in this assay format. The natural product CCB (**26**) again showed to cure at the lowest concentrations; however, this again tracked to a significantly higher concentration than that was required to inhibit *T. b. brucei* growth. These data support the hypothesis that TAO inhibition causes a trypanostatic response and that inhibition of TAO does not cause cidality of the *T. b. brucei* parasite. The increase in potency observed with CCB (**26**) in all of the parasite assays could be due to a number of reasons. The compound may be acting on a complimentary un-identified inhibition pathway. The higher lipophilicity of CCB may also increase compound affinity to the parasites mitochondrial inner-membrane, where TAO is located. Unfortunately, the generation of parasite genetic mutants for trypanostatic compounds is not trivial and was therefore not pursued at this point to identify alternative targets that CCB may be inhibiting through.

7.2 Conclusions

Over the duration of this research project robust methods to generate functionally active recombinant TAO have been established. This enabled the development of medium throughput biochemical assays that were used to identify inhibitors of TAO. With these assays in place, the optimisation of drug like properties of compounds similar to the natural product CCB (**26**) was initiated. This highlighted the difficulties of synthesis of hexa-substituted aromatic molecules. The synthetically amenable mono-phenol analogue (**88**) was identified and found to have good TAO inhibition that correlated to potent *T. b. brucei* growth inhibition. The high lipophilicity observed with **88** and the parent CCB natural product contributed to poor physicochemical properties and predicted CNS penetration profiles, so a focus was made to identify potent TAO inhibitors that had lower lipophilicity and improved predicted CNS penetration profiles. This investigation highlighted that polar functionality was not well tolerated in the lipophilic tail portion of CCB based TAO inhibitors, and that shorter alkyl chain analogues (**134** and **135**) retained adequate potency with reduced lipophilicity. This instigated the synthesis and evaluation of further diverse tail analogues and identified the isopentyl tail compound (**154**) to have improved activity for inhibiting both TAO and *T. b. brucei* growth, and also lower lipophilicity. Further attempts to lower these TAO

inhibitors' lipophilicity showed that polar functionality was also not tolerated on the chloro substituent vector. Evaluation of the bromo intermediate (178) that was synthesised to facilitate this exploration showed increased inhibition of TAO, which correlated to a higher inhibition of *T. b. brucei* growth with only a minor increase in lipophilicity. This observation led to the synthesis of the iso-pentyl bromo analogue (197), which showed an additive potency increase in *T. b. brucei* inhibition. Replacement of the benzonitrile with amide functionality was poorly tolerated and resulted in reduced potency against TAO. On review of the data generated with the TAO inhibitors synthesised over the course of this project, it was obvious that the benzaldehyde analogues showed higher inhibition of *T. b. brucei* growth. The synthesis and evaluation of the pentyl chain benzaldehyde analogue 187 followed this observation. More advanced parasite kill kinetic and reversibility assays were conducted at Novartis. Data from these assays showed that the compounds act as trypanostatic inhibitors, as a much higher compound concentration is required to cause a cidal response in the parasite, compared to the concentration required to inhibit parasite growth. The parasite kill kinetic and reversibility assays tracked to the potency trends observed in the *T. b. brucei* growth inhibition assays, with the benzaldehyde (187), bromo analogue (178) and isopentyl chain analogue (154) all showing improved concentration responses than the matched pair (134). Unfortunately, the trypanostatic response observed with these TAO inhibitors will restrict interest in the further development of these compounds, as the desired target product profile set out by the DNDi states a preference for development of trypanocidal molecules.

I have successfully synthesised compounds based on the natural product CCB to validate TAO as a potential target for the treatment of HAT. TAO inhibitors were synthesised with improved calculated physicochemical properties to CCB; however, these compounds were shown to be trypanostatic, rather than trypanocidal. These results indicate that TAO inhibition is a poor target as a single agent for widespread HAT treatment.

7.3 Future Work

An interest in developing and studying TAO inhibitors may still exist for treating HAT and AAT in some cases. *In vivo*, clearance of *T. b. brucei* may be improved over what is observed in these *in vitro* assays. In animals, a host immune response can clear infections of *T. b. brucei* that are in an arrested state.[229] This is also observed with the trypanostatic compound Eflornithine, which was used in the clinic as a monotherapy prior to the introduction of combination therapies for treatment of HAT *T. b. gambiense* infections.[60] Combination of Eflornithine with the trypanocide Nifurtimox is now the standard of care for *T. b. gambiense* infections. Similarly, the combination of a TAO inhibitor with a trypanocide may also prove interesting for treatment of HAT or AAT infections. NECT treatment is not used for treatment of *T. b. rhodesiense* infections as the ornithine decarboxylase enzyme turns over much more readily than in *T. b. gambiense*.[64] TAO inhibitors may provide an alternative trypanostatic mechanism that could be useful in *T. b. rhodesiense* treatment.

Further optimisation of these TAO inhibitors could identify a molecule that has a similar *T. b. brucei* growth inhibition profile to CCB, with lower lipophilicity and an improved predicted CNS penetration. The combination compound **197** is currently being tested in the kill kinetic and parasite clearance assays. Combination of the structural modifications present in **197** with the potency improvements observed with the benzaldehyde analogue **187** would likely result in a low nanomolar inhibitor of TAO and of *T. b. brucei* growth. This compound (**198**) would also have an improved CNS MPO score, lower $LogD_{7.4}$ and lower lipophilicity (Figure 92).

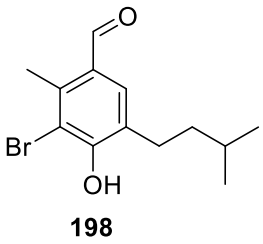

198

cLogP	$cLogD_{7.4}$	Predicted TAO pIC_{50}	Predicted *T. b. b.* pEC_{50}	Predicted *T.b.b.* LLE	CNS MPO
4.8	3.8	> 8.5	> 7.5	> 2.7	4.0

Figure 92 - Design and predicted activity of compound 198 – Predicted potency from pEC50 increment observed with benzaldehyde analogue (134 to 187 = 0.8, 47 to 26 = 2.0, 51 to 50 = 1.4). Parameters calculated using Chemaxon Marvin Sketch 17.25.0

Compound **198** however, would however contain the benzaldehyde motif. As discussed previously, compound metabolism and reactivity would have to be assessed before committing to further synthesis of molecules containing the benzaldehyde moiety.

The TAO inhibitors synthesised may also be of interest for the treatment of other parasitic infections. *Cryptosporidium* parasites are reliant on a similar alternative oxidase for their respiratory function, and share approximately 50% sequence homology to TAO.[256] An *in silico* homology model built from the FASTA sequence of *cryptosporidium homonis* and the crystal structure of *T. b. brucei* (PDB: 3W54), shows good homology of the predicted binding site of CCB (Figure 93 - Identical residues – red, similar residues – orange and dis-similar residues - white). A range of microsporidian parasites also rely on similar alternative oxidases for their function.[257] Compounds designed for TAO inhibition may show inhibitory activity against the alternative oxidase enzymes of these parasites and provide chemically tractable starting points for further development.

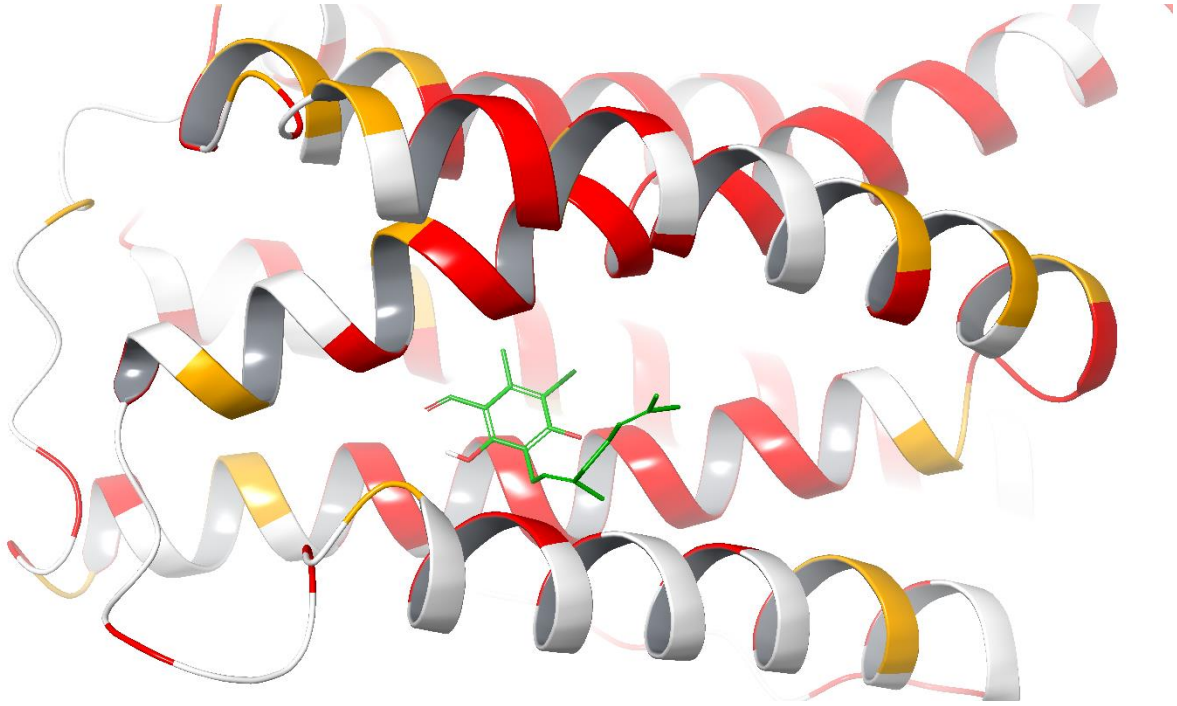

Figure 93 - *Cryptosporidium homonis* homology model built on *T. b. brucei* crystal structure (PDB: 3W54) in Maestro – Schrodinger Drug Discovery Suite. Identical residues coloured red, similar residues coloured orange, dis-similar residues coloured white, CCB coloured green.

This project has generated several TAO inhibitors that have improved drug like properties over the natural product inhibitors colletochlorin B and ascofuranone. The evaluation of these molecules in advanced parasite assays has enabled the discovery that TAO inhibition causes a trypanostatic response in *T. b. brucei* parasites. This will be of interest for the future development of treatments for HAT and AAT. In consideration of these data, TAO inhibition may be deprioritised in preference for trypanocidal compounds. Further *in vitro* and *in vivo* pharmacokinetic and pharmacodynamic experiments would be required to show that these TAO inhibitors could achieve high CNS exposure following oral dosing and are able to clear *T. b. brucei* parasite infections to renew an interest in TAO as a target for treating HAT and AAT.

Chapter 8

Chapter 8 – Experimental

General Experimental

Reactions were performed under an atmosphere of nitrogen unless otherwise stated, using anhydrous solvents as purchased or dried over molecular sieves and degassed with nitrogen flow. Flash chromatography was performed using pre-packed silica gel cartridges, supplied by Biotage, Grace or Teledyne ISCO and performed on ISCO Combiflash RF or Biotage Isolera Prime purification systems. Reverse-phase chromatography was performed with pre-packed C_{18} silica carstridges supplied by Grace and purification performed on a Biotage Isolera Prime purification system. Proton NMR spectra were recorded at 500 or 600 MHz, on either a Varian 500 or 600 spectrometer (at 30 °C) or a Bruker 500 spectrometer (at 25 °C), using the residual isotopic solvent shift as an internal reference ($CHCl_3$ δ_H – 7.27 ppm, DMSO δ_H – 2.50 ppm, MeOH δ_H 3.31 ppm). Chemical shifts are quoted in parts per million (ppm), coupling constants are recorded in Hertz (Hz). Carbon 13 NMR were recorded at 125 MHz on a Varian 500 or 600 spectrometer or a Bruker 500 spectrometer. Residual isotopic solvent shifts were used as an internal reference ($CHCl_3$ δ_C – 77.00 ppm, DMSO δ_C – 39.52 ppm). Infra-red spectra were recorded on a Perkin Elmer FT-IR Spectrum One spectrometer as a neat sample. Absorption maxima are reported in wavenumber (cm^{-1}). Distinguishable and significant absorptions were recorded in wave numbers (cm^{-1}), with key stretches identified in brackets. LCMS (LCQ) data was recorded on Waters 2695 HPLC using a Waters 2487 UV detector and Thermo LCQ ESI-MS, eluting through a Phenomenex Lunar 3 µ C_{18} column (50 mm × 4.6 mm column) with a water to acetonitrile gradient with a formic acid modifier (0.1%). LCMS (MDAP) data was recorded on a Shimatzu Prominence Series coupled to a LCMS-2020 ESI and APCI mass spectrometer. Samples were eluted through a Phenomenex Gemini 5 µ C18 110A 250 mm × 4.6 mm column, using water and acetonitrile gradient with a 0.1% formic acid modifier at 1 ml/min and detected at 254 nm. UPLC data was recorded on a Waters Acuity UPLC and Waters ZQ ESI mass spectrometer. Samples were eluted through a Kinetex 2.6 µ C_{18} column (50 mm × 2.1 mm), using water and acetonitrile gradient with a 0.1% trifluoro acetic acid modifier. High resolution mass-spectrometry (HRMS) data was recorded on Bruker Daltonics, Apex III, ESI source: Apollo ESI with methanol as spray

solvent. Only molecular ions, fractions from molecular ions and other major peaks are reported as mass/charge (*m/z*) ratios. All reported yields refer to chromatographically and spectroscopically pure compounds, unless otherwise specified. Reagents were used as supplied from Manchester Organics, Sigma-Aldrich, Acros, Fluorochem, Combi-blocks or Tokyo Chemical Industry unless otherwise stated. Compound **27** – **46** were supplied by Medicines Malaria Venture (MMV), compounds **26** and **47** – **61** were synthesised by members of the Sussex Drug Discovery Centre (SDDC) prior to the start of this project. Compounds **72**, **73** and **121** – **124** were synthesised by Thomas Cunningham who was a Masters' student under my supervision for his research project.

2,4-Dihydroxy-6-methylbenzaldehyde (63)[258]

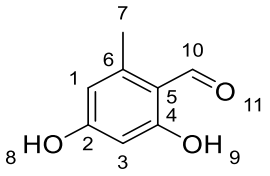

To a solution of $POCl_3$ (26.3 mL, 282 mmol) in acetonitrile (250 mL) was added DMF (21.8 mL, 282 mmol) at 0 °C. After 10 min, 5-methylresorcinol (**62**) (20.0 g, 161 mmol) in acetonitrile (200 mL) was added at 0 °C. The reaction mixture was allowed to warm to RT and stir for 1 hour before being quenched by addition to water (1000 mL). The solution was concentrated under reduced pressure, precipitating a pale-yellow solid. Collection by reduced pressure filtration and drying afforded the title compound as a pale-yellow solid (19.4 g, 79%): m.p. 118–121 °C, (water / acetonitrile). IR (neat, ν_{max}) cm^{-1} 3086, 1623, 1204. ^1H NMR (500 MHz, D_6-DMSO) δ_H 12.05 (br s, 1H, OH-8/9), 10.67 (br s, 1H, OH-8/9), 10.04 (s, 1H, CH-10), 6.20 (s, 1H, CH-1), 6.12 (s, 1H, CH-3), 2.44 (s, 3H, CH_3-7). ^{13}C NMR (126 MHz, D_6-DMSO) δ_C 193.4 (CH-10), 165.8 (C4), 165.7 (C2), 145.2 (C6), 113.1 (C5), 111.2 (CH-1), 100.7 (CH-3), 19.0 (CH_3-7). HRMS (ESI^-) *m/z* $[M-H]^-$ calculated for $C_8H_7O_3$ 151.0401, found 151.0394. LCMS Analytical LCQ, Method 2, t_R 3.48 min, $[M+H]^+$ 153.3 *m/z*, LCMS MDAP, Method 4, t_R 15.14 min, (>95%), $[M-H]^-$ 151.1 *m/z.*

2,4-Dihydroxy-6-methylbenzaldoxime (64)

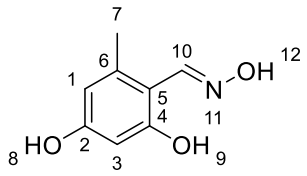

A suspension of 2,4-dihydroxy-6-methylbenzaldehyde (**63**) (4.25 g, 27.9 mmol) in acetonitrile (50 mL) was added hydroxylamine hydrochloride (2.14 g, 30.7 mmol) and heated to reflux for 16 h. The cooled reaction was partitioned between water and ethyl acetate. The organic layer was separated, washed with brine, dried over $MgSO_4$, filtered and concentrated under reduced pressure, to provide the title compound as a pale-yellow solid (4.38 g, 94%). m.p. 196.4-200.7 °C. IR (neat, ν_{max}) cm^{-1} 3237, 1609, 1585, 1302, 1149. ^1H NMR (500 MHz, D_6-DMSO) δ_H 11.12 (s, 1H, OH-8/9/12), 10.65 (s, 1H, OH-8/9/12), 9.68 (s, 1H, OH-8/9/12), 8.36 (s, 1H, CH-10), 6.16 (s, 1H, CH-1), 6.12 (s, 1H, CH-3), 2.38 (s, 3H, CH_3-7). ^{13}C NMR (126 MHz, $CDCl_3$) δ_C 159.7 (C2/4), 159.6 (C2/4), 149.1 (CH-10), 139.5 (C), 110.0 (CH-1), 108.0 (C5), 101.0 (CH-3), 20.0 (CH_3-7). HRMS-ESI *m/z* $[M-H]^-$ calculated for $C_8H_8NO_3$ 166.0510, found 166.0505. LCMS Analytical LCQ, Method 3, t_R 4.15 min, $[M+H]^+$ 168.1 *m/z*. LCMS Analytical MDAP, Method 4, t_R 9.17 min, $[M+H]^+$ 168.0 *m/z* (>95%).

2,4-Dihydroxy-6-methylbenzonitrile (65)[259]

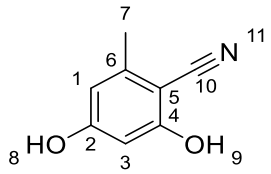

A solution of 2,4-dihydroxy-6-methylbenzaldoxime (**64**) (3.00 g, 18.0 mmol) in diethyl ether (100 mL) was added pyridine (0.97 mL, 11.2 mmol) and cooled to 0 °C. The cooled solution was dropwise added thionyl chloride (1.96 mL, 26.9 mmol) over 10 min. To the reaction mixture was allowed to warm to rt and stir for 16 h. The reaction was concentrated under reduced pressure and the residue dissolved in ethanol (30 mL) and added 2 M NaOH (aq) (20 mL). The reaction mixture was stirred at rt for 96 h. The reaction mixture was acidified with 5 M HCl (aq) (20 mL) and extracted with ethyl acetate. The organic layers were separated,

washed with brine, dried over $MgSO_4$, filtered and concentrated under reduced pressure. The residue was purified by flash silica chromatography. To provide the title compound as a pale-yellow solid. (1.82 g, 67%). m.p. 188.8-194.2 °C. IR (neat, ν_{max}) cm^{-1} 3142, 2225, 1749, 1602, 1468, 1274, 1152. ^1H NMR (500 MHz, D_6-DMSO) δ_H 10.65 (s, 1H, OH-8/9), 10.21 (br s, 1H, OH-8/9), 6.23 (s, 1H, CH-1/3), 6.21 (s, 1H, CH-1/3), (s, 3H, CH_3-7). ^{13}C NMR (126 MHz, D_6-DMSO) δ_C 162.5 (C2+4), 144.2 (C6), 117.3 (C10), 109.3 (CH-1), 100.3 (CH-3), 91.2 (CH-5), 20.6 (CH_3-7). HRMS-ESI *m/z* $[M-H]^-$ calculated for $C_8H_6NO_2$ 148.0404, found 148.0401. LCMS analytical LCQ, Method 2, t_R 0.61 min, $[M+H]^+$ - no ionisation. LCMS analytical MDAP, Method 4, t_R 8.58 min, $[M-H]^-$ 147.9 *m/z* (>95%).

2,4-Dihydroxy-5-chloro-6-methylbenzonitrile (66)

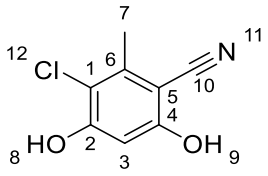

A solution of 2,4-dihydroxy-6-methylbenzonitrile (**65**) (1.76 g, 11.8 mmol) in diethyl ether (10 mL) was cooled to -10 °C, the reaction mixture was dropwise added a solution of sulfuryl chloride (0.96 mL, 11.8 mmol) in diethyl ether (10 mL) over 30 min. The reaction mixture was allowed to warm to rt and stir for 2 h. To the reaction mixture was added 1 M HCl (aq) and extracted with ethyl acetate. The organic layers were separated, washed with brine, dried over $MgSO_4$, filtered and concentrated under reduced pressure. The residue was purified by recrystallization from methanol, water (8:2) to provide the title compound (1.96 g, 90%). m.p. 199.2-204.6 °C. IR (neat, ν_{max}) cm^{-1} 3335, 2226, 1592, 1441, 1330, 1274. ^1H NMR (500 MHz, D_6-DMSO) δ_H 11.07 (s, 1H, OH-8/9), 10.96 (s, 1H, OH-8/9), 6.51 (s, 1H, CH-3), 2.37 (s, 3H, CH_3-7). ^{13}C NMR (126 MHz, D_6-DMSO) δ_C 160.5 (C4), 158.3 (C2), 141.0 (C6), 116.7 (C1), 112.2 (C10), 101.3 (CH-3), 92.7 (C-5), 19.0 (CH_3-7). HRMS-ESI *m/z* $[M-H]^-$ calculated for $C_8H_5{}^{35}ClNO_2$ 182.0014, found 182.0009. LCMS analytical MDAP, Method 4, t_R 15.67 min, $[M-H]^-$ 182.0 *m/z* (>95%).

2,4-Dihydroxy-5-chloro-6-methylbenzaldehyde (69)[149]

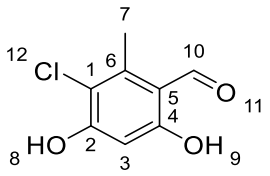

To a solution of 2,4-dihydroxy-6-methylbenzaldehyde (**63**) (9.50 g, 62.4 mmol) in diethyl ether (300 mL) was drop wise added sulfuryl chloride (5.06 mL, 62.4 mmol) as a solution in diethyl ether (20 mL) at -5 °C over 30 min. After 10 min the reaction mixture was allowed to warm to rt and stir for 2 h before the addition of petroleum ether (150 mL) and precipitation of a pale-yellow solid. Collection by reduced pressure filtration and drying afforded the title compound as a pale-yellow solid (5.65 g, 49%): m.p. 172–175 °C (diethyl ether / petroleum ether). IR (neat, ν_{max}) cm^{-1} 2981, 1581, 1307, 1256, 1217. ^{1}H NMR (500 MHz, D_6-DMSO) δ_H 11.93 (br s, 1H, OH-8/9), 11.46 (br s, 1H, OH-8/9), 10.15 (s, 1H, CH-10), 6.40 (s, 1H, CH-3), 2.55 (s, 3H, CH_3-7). ^{13}C NMR (126 MHz, D_6-DMSO) δ_C 193.6 (CH-10), 163.5 (C2), 161.07 (C4), 141.44 (C6), 113.86 (C1/5), 113.82 (C1/5), 101.46 (C3), 15.49 (CH_3-7). HRMS (ESI^-) *m/z* $[M-H]^-$ calculated for $C_8H_6{}^{35}ClO_3$ 185.0011, found 185.0005. LCMS Analytical LCQ, Method 2, t_R 2.62 min, $[M+H]^+$ 187.2 *m/z*. LCMS MDAP, Method 4, t_R 16.89 min, (>95%), $[M-H]^-$ 185.0 *m/z*.

5-Chloro-3-[[hexyl(methyl)amino]methyl]-2,4-dihydroxy-6-methyl-benzaldehyde (71)

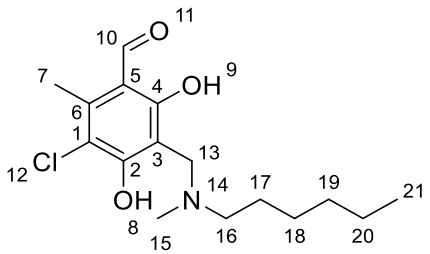

A solution of *N*-methylheptylamine (0.23 mL, 1.30 mmol) in ethanol (5 mL) was added paraformaldehyde (40 mg, 1.30 mmol) and heated to 50 °C for 30 min. The solution was added 2,4-dihydroxy-5-chloro-6-methylbenzaldehyde (**69**) (0.20 g, 1.10 mmol) and heated to 50 °C for 10 min. The reaction mixture was added water and extracted with ethyl acetate. The organic layers were separated, washed with brine, dried over $MgSO_4$, filtered and

concentrated under reduced pressure. The residue was recrystallized from methanol and water (10:1) to provide the title compound as a cream solid (0.226 g, 67%). m.p. 119.2-121.3 °C. IR (neat, vmax) cm^{-1} 2949, 1715, 1621, 1421, 1249, 1227. ^{1}H NMR (500 MHz, $CDCl_3$) δ_H 13.14 (s, 1H, OH-9), 9.95 (s, 1H, CH-10), 3.99 (s, 2H, CH_2-13), 2.75 (t, *J* = 7.9 Hz, 2H, CH_2-16), 2.57 (s, 3H, CH_3-7/15), 2.50 (s, 3H, CH_3-7/15), 1.68 (m, 2H, CH_2-17), 1.37-1.29 (m, 6H, CH_2-18/19/20), 0.89 (t, 3H, CH_3-21). ^{13}C NMR (126 MHz, $CDCl_3$) δ_C 191.5 (CH-10), 167.51 (C2), 162.2 (C4), 139.9 (C6), 110.6 (C1), 110.0 (C5), 104.8 (C3), 56.5 (CH_2-16), 53.9 (CH_2-13), 40.3 (CH_3-15), 31.4 (CH_2-17/18/19/20), 26.5 (CH_2-17/18/19/20), 25.7 (CH_2-17/18/19/20), 22.4 (CH_2-17/18/19/20), 14.4 (CH_3-7), 13.9 (CH_3-21). HRMS-ESI *m/z* $[M-H]^-$ calculated for $C_{16}H_{23}{}^{35}ClNO_3$ 312.1372, found 312.1359. LCMS analytical MDAP, Method 4, t_R 13.28 min, $[M+H]^+$ 314.1 *m/z* (95%).

2,4-Dihydroxy-3-bromo-5-chloro-6-methylbenzaldehyde (74)

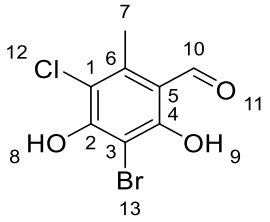

To a solution of 2,4-dihydroxy-5-chloro-6-methylbenzaldehyde (**69**) (5.50 g, 29.5 mmol) in CH_2Cl_2, methanol (4:1, 150 mL) was added tetrabutylammmonium tribromide (14.9 g, 31.0 mmol) as a solution in CH_2Cl_2, methanol (4:1) (20 mL). After 30 min the reaction mixture was concentrated under reduced pressure. The residue was dissolved in methanol (55 mL), addition of water (110 mL) afforded a pale-yellow precipitate. Collection by reduced pressure filtration and drying afforded the title compound as a pale-yellow solid (4.85 g, 62%): m.p. 169–174 °C, (methanol / water). IR (neat, v_{max}) cm^{-1} 3179, 1606, 1405, 1273. ^{1}H NMR (500 MHz, D_6-DMSO) δ_H 13.16 (s, 1H, OH-8/9), 10.10 (s, 1H, CH-10), 2.58 (s, 3H, CH_3-7). ^{13}C NMR (126 MHz, D_6-DMSO) δ_C 195.4 (CH-10), 160.3 (C2/4), 157.8 (C2/4), 140.7 (C6), 114.6 (C1/5), 113.5 (C1/5), 110.0 (C3), 15.1 (CH_3-7). HRMS (ESI^-) *m/z* $[M-H]^-$ calculated for $C_8H_5{}^{79}Br{}^{35}ClO_3$ 262.9116, found 262.9168. LCMS Analytical LCQ, Method 2, t_R 2.97 min, $[M+H]^+$ 267.1 *m/z*, LCMS analytical MDAP, Method 4, t_R 19.11 min, (90%) $[M-H]^-$ 264.9 *m/z*.

2,4-Dihydroxy-3-bromo-5-chloro-6-methylbenzaldoxime (75)

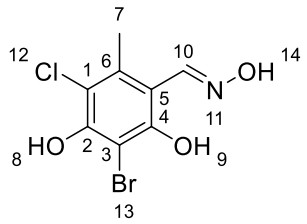

To a suspension of 2,4-dihydroxy-3-bromo-5-chloro-6-methylbenzaldehyde (**74**) (4.85 g, 18.3 mmol) in ethanol (50 mL) was added hydroxylamine hydrochloride (1.90 g, 27.4 mmol). After 16 h the resulting precipitate was collected by reduced pressure filtration, washed with water and cold ethanol to afford the title compound as a white solid (4.40 g, 86%): m.p. 231-234 °C, (ethanol / water). IR (neat, vmax) cm^{-1} 3383, 3347, 1605, 1417, 1400, 1189. ^{1}H NMR (500 MHz, D_6-DMSO) δ_H 11.87 (br s, 1H, OH-8/9/14), 11.67 (s, 1H, OH-8/9/14), 10.19 (br s, 1H, OH-8/9/14), 8.53 (s, 1H, CH-10), 2.38 (s, 3H, CH_3-7). ^{13}C NMR (126 MHz, D_6-DMSO) δ_C 154.6 (C4), 152.0 (C2), 149.4 (CH-10), 135.1 (C6), 113.9 (C1), 109.7 (C5), 98.0 (C3), 16.5 (CH_3-7). HRMS (ESI^-) *m/z* $[M-H]^-$ calculated for $C_8H_6{}^{79}Br^{35}ClNO_3$ 277.9225, found 277.9219. LCMS Analytical LCQ, Method 2, t_R 2.48 min, $[M+H]^+$ 282.5 *m/z.* LCMS analytical MDAP, Method 4, t_R 17.41 min, (>95%), $[M-H]^-$ 279.9 *m/z*.

4-Methyl-5-chloro-6-hydroxy-7-bromo-[1,2]benzisoxazole (76)

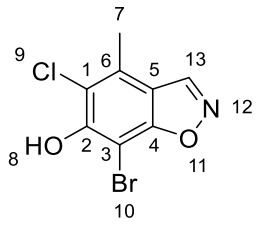

To a suspension of 2,4-dihydroxy-3-bromo-5-chloro-6-methylbenzaldoxime (**75**) (1.13 g, 4.00 mmol) in diethyl ether (100 mL) was added pyridine (0.65 mL, 8.10 mmol) and $SOCl_2$ at 0 °C. After 10 min the reaction mixture was allowed to warm to rt. After 16 h the reaction mixture was partitioned between ethyl acetate (200 mL) and 1 M HCl (aq) (100 mL). The phases were separated, the aqueous phase was extracted with ethyl acetate (3 × 50 mL) and the combined organic extracts were washed with brine (50 mL), dried over $MgSO_4$, filtered and concentrated under reduced pressure. The residue was purified by flash

chromatography (petroleum ether to 30% ethyl acetate in petroleum ether over 25 min) to afford the title compound as a white solid (1.01 g, 96%): m.p. 176–181 °C, (petroleum ether / ethyl acetate). IR (neat, ν_{max}) cm^{-1} 3202, 1594, 1320, 1194. ^{1}H NMR (500 MHz, D_6-DMSO) δ_H 10.97-10.85 (br s, 1H, OH), 9.40 (s, 1H, CH-13), 2.53 (s, 3H, CH_3-7). ^{13}C NMR δ_C (126 MHz, D_6-DMSO) 158.9 (C4), 152.8 (C2), 147.6 (CH-13), 130.8 (C6), 120.1 (C1), 115.8 (C5), 88.0 (C3), 17.3 (CH_3-7). HMBC – observed between H-13 and C-5. HRMS (ESI^-) *m/z* $[M-H]^-$ calculated for $C_8H_4{}^{79}Br^{35}ClNO_2$ 259.9119, found 259.9113. LCMS analytical LCQ, Method 3, t_R 5.78 min, $[M+H]^+$ 264.0 *m/z.* LCMS analytical MDAP, Method 4, t_R 18.37 min, (88%), $[M-H]^-$ 261.9 *m/z*.

4-Methyl-5-chloro-6-hydroxy-7-bromo-[1,3]benzoxazole (77)

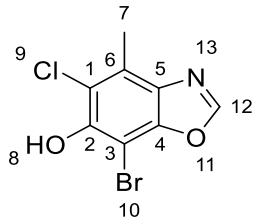

To a solution of 2,4-dihydroxy-3-bromo-5-chloro-6-methylbenzaldoxime (**75**) (1.40 g, 5.0 mmol) in CH_2Cl_2 and acetonitrile (10:1, 10 mL) was added trifluoroacetic anhydride (2.02 mL, 12.0 mmol). After heating the reaction mixture by microwave (Biotage® Initiator) for 1 h at 100 °C the reaction mixture was diluted with CH_2Cl_2 (100 mL) and washed with aqueous sodium bicarbonate (50 mL), brine (50 mL), dried over $MgSO_4$, filtered and concentrated under reduced pressure. The residue was triturated in CH_2Cl_2 and filtered afford the title compound as a tan solid (0.58 g, 45%): m.p. 209–211 °C, (CH_2Cl_2). IR (neat, ν_{max}) cm^{-1} 3144, 1384, 1289. ^{1}H NMR (500 MHz, D_6-DMSO) δ_H 10.24 (br s, 1H, OH-8), 8.64 (s, 1H, CH-12), 2.73 (s, 3H, CH_3-7). ^{13}C NMR (126 MHz, D_6-DMSO) δ_C 153.5 (CH-12), 149.1 (C2), 147.2 (C4), 132.8 (C5), 128.1 (C6), 120.3 (C1), 90.1 (C3), 14.8 (CH_3-7). HMBC observed from H-12 to C4 and C5. HRMS (ESI^-) *m/z* $[M-H]^-$ calculated for $C_8H_4{}^{79}Br^{35}ClNO_2$ 259.9119, found 259.9113. LCMS MDAP, Method 4, t_R 17.86 min, (>95%), $[M-H]^-$ 261.9 *m/z*.

2-Methyl-4-hydroxy-5-bromo-benzaldehyde (80)[260]

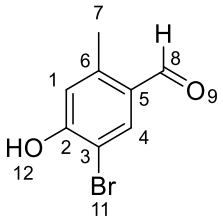

To a solution of 2-methyl-4-hydroxy-benzaldehyde (**79**) (10.0 g, 73.5 mmol) in CH_2Cl_2 (100 mL) and methanol (50 mL) was added a solution of phenyltrimethylammonium tribromide (30.1 g, 77.1 mmol) in CH_2Cl_2: methanol (1:1, 100 mL) at -5 °C. The reaction was warmed to ambient temperature and stirred for 16 h. The reaction was concentrated under reduced pressure and the residue was added 1 M HCl (aq) (200 mL) to precipitate a white solid, the solid was collected by filtration and dried under reduced pressure to give the title compound as a cream precipitate (14.7 g, 94%): m.p. 160–165 °C, (methanol / water). IR (neat, v_{max}) cm^{-1} 3063, 1384, 1310. ^1H NMR (500MHz, D_6-DMSO) δ_H 11.35 (1H, br s, OH-12), 9.95 (1H, s, CH-8), 7.91 (1H, s, CH-4), 6.83 (1H, s, CH-1), 2.49 (3H, s, CH_3-7). ^{13}C NMR (126 MHz, D_6-DMSO) δ_C 190.8 (CH-8), 159.2 (C2), 142.3 (C6), 137.1 (CH-4), 128.0 (C5), 119.1 (CH-1), 107.4 (C3), 19.1 (CH_3-7). HRMS (ESI^-) *m/z* $[M-H]^-$ calculated for $C_8H_6{}^{79}BrO_2$ 212.9557, found 212.9550. LCMS analytical LCQ, Method 2, t_R 2.51 min, $[M+H]^+$ 217.1 *m/z*. LCMS analytical MDAP, Method 4, t_R 16.54 min, (94%), $[M-H]^-$ 213.0 *m/z.*

2-Methyl-4-hydroxy-5-oct-1-enyl-benzaldehyde (81)

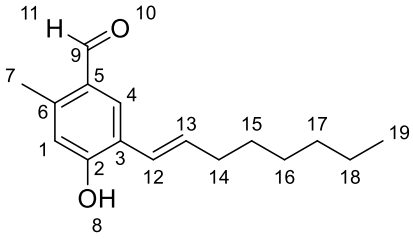

A stirring suspension of chloro[(1,3-dimesitylimidazol-2-ylidene)(n,n-dimethylbenzylamine)palladium(II)] (0.03 g, 0.05 mmol), potassium carbonate (0.96 g, 7.0 mmol), 2-methyl-4-hydroxy-5-bromo benzaldehyde (**80**) (0.50 g, 2.30 mmol) and 1-octene (0.65 g,

0.60 mmol) in *N*-methyl-2-pyrrollidinone (10 mL) was heated in a sealed vial at 140 °C for 2 h. The reaction mixture was cooled to rt, diluted with ethyl acetate (50 mL), washed with water (20 mL), LiCl (aq) (0.5 M, 20 mL) and brine (50 mL). The organic phase was separated, dried over $MgSO_4$, filtered and concentrated under reduced pressure. The residue was purified by flash chromatography (petroleum ether to 15% ethyl acetate in petroleum ether over 20 min) to afford the title compound as a yellow oil (0.147 g, 26%). ^{1}H NMR (500 MHz, $CDCl_3$) δ_H 10.11 (s, 1H, CH-11), 7.79 (s, 1H, CH-4), 6.69 (s, 1H, CH-1), 6.53 (d *J* = 16.1, 1H, CH-12), 6.27 (dt *J* = 16.1, 6.8 Hz, 1H, CH-13), 6.09 (s, 1H, OH-8), 2.61 (s, 3H, CH_3-7), 2.26 (m, 2H, CH_2-14), 1.56-1.18 (m, 8H, CH_2-15/16/17/18) 0.90 (m, 3H, CH_3-19). ^{13}C NMR (126 MHz, D_6-DMSO) δ_C 191.4 (CH-9), 157.1 (C2), 141.6 (C6), 134.8 (CH-4), 132.4 (CH-13), 127.9 (C5), 123.4 (C3), 122.6 (CH-12), 118.6 (CH-1), 33.4 (CH_2-14/17), 31.7 (CH_2-14/17), 29.2 (CH_2-15/16), 28.9 (CH_2-15/16), 22.6 (CH_2-18), 19.2 (CH_3-7), 14.0 (CH_3-19). HRMS (ESI$^-$) *m/z* $[M-H]^-$ calculated for $C_{16}H_{21}O$ 245.1547, found 245.1539. LCMS analytical LCQ, Method 3, t_R 8.14 min, $[M+H]^+$ 247.2 *m/z*. LCMS analytical MDAP, Method 4, t_R 24.10 min, (94%), $[M-H]^-$ 245.2 *m/z*.

4,5-Dimethyl-2-octyl-phenol (82)

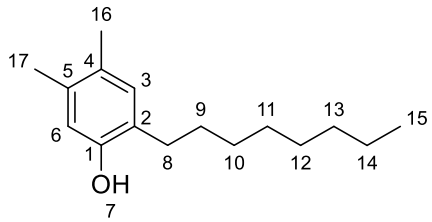

Triethylsilane (0.05 g, 0.43 mmol) was added to a solution 4-hydroxy-2-methyl-5-[(E)-oct-1-enyl]benzaldehyde (**81**) (0.05 g, 0.20 mmol) and 10% palladium on carbon (0.002 g, 0.02 mmol) in ethyl acetate (2 mL). The reaction mixture was stirred at rt for 16 h. The reaction mixture was purged with nitrogen and was filtered through a pad of celite, the filtrate was partitioned between HCl (aq) (1 M, 10 mL) and ethyl acetate (2 x 20 mL). The combined organics were separated, dried over $MgSO_4$, filtered and concentrated under vacuum. The residue was purified by flash silica chromatography, eluting with petroleum ether to 50% ethyl acetate in petroleum ether to provide the title compound

as an orange oil (0.045 g, 95%). ^{1}H NMR (500 MHz, $CDCl_3$) δ_H 6.86 (s, 1H, CH-6/3), 6.57 (s, 1H, CH-6/3), 4.41 (br s, 1H, OH-7), 2.53 (t, *J* = 7.8 Hz, CH_2-8), 2.18 (s, 3H, CH_3-16/17), 2.17 (s, 3H, CH_3-16/17), 1.66-1.55 (m, 2H, CH_2-9), 1.40-1.23 (m, 10H, CH_2s-10-14) 0.88 (t, *J* = 6.7 Hz, 3H, CH_3-15). LCMS - Analytical LCQ (10 min) 30-95% MeCN:Water (0.1% Formic), tR 9.26 min, $[M+H]^+$ 235.1 *m/z* (> 95%).

2-Methyl-4-hydroxy-5-bromo-aldoxime (84)

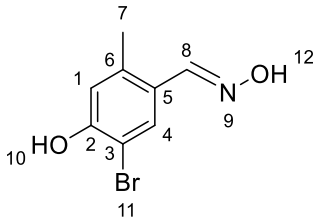

A solution of 2-methyl-4-hydroxy-5-bromo-benzaldehyde (**80**) (6.00 g, 27.9 mmol), in acetonitrile (100 mL) was added hydroxylamine hydrochloride (2.33 g, 33.5 mmol). The reaction mixture was stirred for 3 h at ambient temperature. The resulting solid collected by vacuum filtration. The solid was washed with water (100 mL) and dried under reduced pressure to provide the title compound as a white solid (3.79 g, 59%): m.p. 143–146 °C (acetonitrile / water). IR (neat, vmax) cm^{-1}, 3352, 1594, 1416, 1265. ^{1}H NMR (500MHz, D6-DMSO) δ_H 11.05 (1H, s, OH-12), 10.44 (1H, s, OH-10), 8.15 (1H, s, CH-8), 7.67 (1H, s, CH-4), 6.77 (1H, s, CH-1), 2.26 (3H, s, CH_3-7). ^{13}C NMR (126MHz, D6-DMSO) - δ_C 154.9 (C-2), 146.4 (CH-8), 137.5 (C-6), 130.9 (CH-4), 124.4 (C-5), 118.6 (CH-1), 107.3 (C-3), 19.7 (CH_3-7). HRMS (ESI^-) *m/z* $[M-H]^-$ calculated for $C_8H_7{}^{79}BrNO_2$ 227.9666, found 227.9660. LCMS MDAP, Method 4, t_R 15.15 min, (86%), $[M-H]^-$ 229.9 *m/z*.

4-Hydroxy-2-methyl-5-octyl-benzonitrile (85)

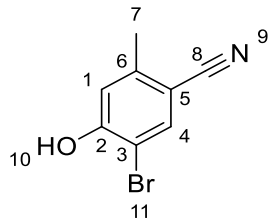

A pre-stirred solution of cyanuric chloride (2.53 g, 13.7 mmol), in DMF (50 mL) was added a solution of 2-methyl-4-hydroxy-5-bromo-aldoxime (**84**) (3 g, 13.0 mmol) in DMF (25 mL) over 15 min. The reaction mixture was stirred at rt for 3 h. The reaction mixture was added water (150 mL) and stirred at rt for 1 h. The resulting white solid was collected by filtration and dried under vacuum to provide the title compound as a white solid (2.77 g, 90%): m.p. 194-199 °C (DMF / water). IR (neat, $\bar{\nu}_{max}$) cm^{-1} 3203, 2232, 1595, 1402, 1386, 1260, 1221. ^{1}H NMR (500MHz, D6-DMSO) - δ_H 11.38 (1H, br s, OH-12), 7.90 (1H, s, CH-4), 6.92 (1H, s, CH-1), 2.49 (3H, s, CH_3-7). ^{13}C NMR (126MHz, D6-DMSO) δ_C 158.6 (C-2), 143.4 (C-6), 137.1 (CH-4), 117.9 (CH-1), 117.7 (C-8), 107.3 (C-3), 103.8 (C-5), 19.1 (CH_3-7). HRMS (ESI^-) *m/z* $[M-H]^-$ calculated for $C_8H_5{}^{79}BrNO$ 209.9560, found 209.9554. LCMS analytical LCQ, Method 2, t_R 2.43 min, $[M+H]^+$ 215.0 *m/z.* LCMS MDAP, Method 4, t_R 17.34 min, (>95%), $[M-H]^-$ 212.0 *m/z*.

4-Hydroxy-2-methyl-5-oct-1-enylbenzonitrile (86)

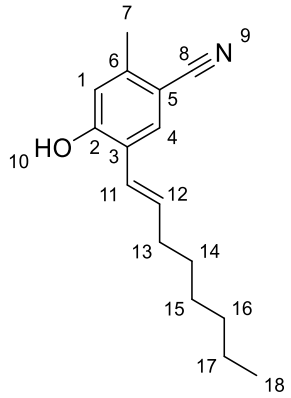

A stirring suspension of chloro[(1,3-dimesitylimidazol-2-ylidene)(n,n-dimethylbenzylamine)palladium(II)] (0.03 g, 0.05 mmol), potassium carbonate (0.39 g, 2.83 mmol), 4-hydroxy-2-methyl-5-octyl-benzonitrile (**85**) (0.20 g, 0.94 mmol) and 1-octene (1.06 g, 9.43 mmol) in *N*-methyl-2-pyrrolidinone (10 mL) was heated in a sealed vial at 140°C for

2 h. The reaction mixture was cooled to rt, diluted with ethyl acetate (50 mL), washed with HCl (aq) (1 M, 20 mL), LiCl (aq) (0.5 M, 10 mL) and brine (25 mL). The organic phase was separated, dried over $MgSO_4$, filtered and concentrated under reduced pressure. The residue was purified by flash chromatography (petroleum ether to 10% ethyl acetate in petroleum ether over 20 min) to afford the title compound as a clear oil (0.066 g, 28%): ^{1}H NMR (500 MHz, $CDCl_3$) δ_H 7.54 (s, 1H, CH-4), 6.73 (s, 1H, CH-1), 6.45 (d J = 16.0 Hz, 1H, CH-12), 6.20 (dt *J* = 16.0 Hz, 7.0 Hz, 1H, CH-13), 5.62 (s, 1H, OH-8), 2.46 (s, 3H, CH_3-7), 2.24 (m, 2H, CH_2-13), 1.56-1.18 (m, 8H, CH_2-14/15/16/17) 0.90 (m, 3H, CH_3-18). ^{13}C NMR (126MHz, $CDCl_3$) δ_C 155.9 (C-2), 142.1 (C-6), 135.5 (CH-4), 131.9 (CH-12), 123.9 (C-3), 122.0 (C-11), 118.4 (CH-8), 117.3 (CH-1) 110.0 (C-8), 33.3 (CH_2-13/16), 31.7 (CH_2-13/16), 29.1 (CH_2-14/15), 28.9 (CH_2-14/15), 22.6 (CH_2-17), 19.2 (CH_3-7), 14.0 (CH_3-18). HRMS (ESI$^-$) *m/z* $[M-H]^-$ calculated for $C_{16}H_{20}NO$ 242.1541, found 242.1541. LCMS MDAP, Method 4, t_R 24.58 min, (91%), [M-H] 242.2 *m/z*.

4-Hydroxy-2-methyl-5-octyl-benzonitrile (87)

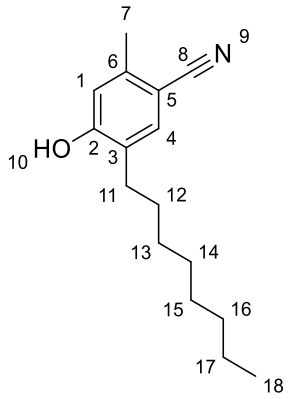

A stirring solution of 4-hydroxy-2-methyl-5-oct-1-enylbenzonitrile (**86**) (0.066 g, 0.27 mmol) in ethanol (5 mL) was added 10% palladium on carbon (0.003 g, 0.03 mmol). Triethylsilane (0.034 g, 0.05 mmol) was added to the stirring suspension. The reaction was sealed and stirred at rt for 2 h. The reaction mixture was filtered through a pad of celite, the filtrate concentrated under reduced pressure to provide the title compound as a colourless oil (0.064 g, quantitative): IR (neat, v_{max}) cm^{-1} 3308, 2917, 2848, 2222, 1608, 1415, 1269. ^{1}H NMR (500 MHz, $CDCl_3$) δ_H 7.35 (s, 1H, CH-4), 6.69 (s, 1H, CH-1), 5.47 (s, 1H, OH-10), 2.56 (m,

2H, CH_2-11), 2.45 (s, 3H, CH_3-7), 1.59 (m, 2H, CH_2-12), 1.56-1.18 (m, 10H, CH_2-13/14/15/16/17) 0.89 (t, *J* = 6.7 Hz, 3H, CH_3-18). ^{13}C NMR (126 MHz, $CDCl_3$) δ_C 157.2 (C2), 141.6 (C6), 134.3 (CH-4), 127.4 (C3), 118.7 (C8), 116.8 (CH-1), 104.3 (C5), 31.8 (CH_2-16), 29.4 (CH_2-11), 29.3 (CH_2-12/13/14/15), 29.3 (CH_2-12/13/14/15), 29.2 (CH_2-12/13/14/15), 29.1 (CH_2-12/13/14/15), 22.6 (CH_2-17), 20.0 (CH_2-7), 14.0 (CH_3-18). HRMS (ESI^-) *m/z* $[M-H]^-$ calculated for $C_{16}H_{22}NO$ 244.1707, found 244.1701. LCMS MDAP, Method 4, t_R 25.14 min, (93%), $[M-H]^-$ 244.2 *m/z*.

3-Chloro-4-hydroxy-2-methyl-5-octyl-benzonitrile (88)

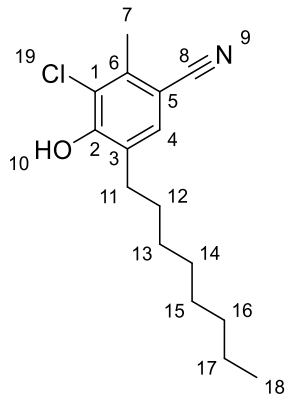

A solution of 4-hydroxy-2-methyl-5-octyl-benzonitrile (**87**) (0.067 g, 0.27 mmol) in diethyl ether (5 mL) was added sulfuryl chloride (0.03 mL, 0.33 mmol) and stirred at rt for 16 h. Further sulfuryl chloride (0.22 mL, 2.70 mmol) was added and the reaction was stirred at rt for 96 h. The reaction was quenched with HCl (aq) (1 M, 20 mL) and extracted with ethyl acetate (50 mL). The organic layer was separated, washed with brine, dried over $MgSO_4$, filtered and concentrated under reduced pressure. The residue was purified by silica flash chromatography, eluting with petroleum ether to 10% ethyl acetate to provide the title compound as a yellow gum. (0.021 g, 28%) IR (neat, ν_{max}) cm^{-1} 3360, 2928, 2850, 2222, 1601, 1473, 1461, 1163. ^{1}H NMR (500 MHz, $CDCl_3$) δ_H 7.31 (s, 1H, CH-4), 6.08 (s, 1H, OH-10), 2.64 (t, *J* = 7.7 Hz, 2H, CH_2-11), 2.56 (s, 3H, CH_3-7), 1.59 (m, 2H, CH_2-12), 1.45-1.20 (m, 10H, CH_2-13/14/15/16/17) 0.91 (t, *J* = 7.2 Hz, 3H, CH_3-18). ^{13}C NMR (126 MHz, $CDCl_3$) δ_C 153.0 (C2), 138.2 (C6), 132.2 (CH-4), 128.9 (C3), 121.0 (C8), 118.0 (C1), 110.0 (C5), 31.8 (CH_2-16), 29.9 (CH_2-11), 29.3 (CH_2-12/13/14/15), 29.3 (CH_2-12/13/14/15), 29.2 (CH_2-12/13/14/15), 29.1

(CH_2-12/13/14/15), 22.6 (CH_2-17), 18.7 (CH_2-7), 14.0 (CH_3-18). HRMS (ESI^-) *m/z* $[M-H]^-$ calculated for $C_{16}H_{21}{}^{35}ClNO$ 278.1317, found 278.1303. LCMS MDAP, Method 4, t_R 26.76 min, (>95%), $[M-H]^-$ 278.1 *m/z*.

5-Bromo-3-chloro-4-hydroxy-benzonitrile (92)

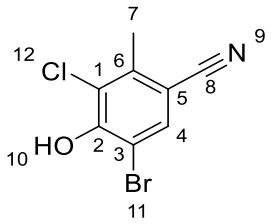

Triethylamine (0.83 mL, 5.97 mmol) was added to a solution of 5-bromo-2-methyl-4-hydroxybenzonitrile (**85**) (1.15 g, 5.42 mmol) in acetonitrile (50 mL). 1-chloropyrorolidine-2,5-dione (1.52 g, 11.38 mmol) was added portion wise to the stirring solution. The reaction mixture was added water precipitating a pale-yellow solid, that was collected by filtration to provide the title compound (1.11 g, 83%) that was used without further purification. m.p. 166.0-168.7 °C. IR (neat, vmax) cm^{-1} 3239, 2236, 1581, 1468, 1384, 1294, 1224. ^1H NMR (500MHz, $CDCl_3$) δ_H 7.70 (s, 1H, CH-4), 6.39 (s, 1H, OH-10), 2.58 (s, 3H, CH_3-7). ^{13}C NMR (126 MHz, $CDCl_3$) δ_C 152.5 (C2), 140.9 (C6), 134.4 (CH-4), 122.1 (CH-1), 116.4 (C8), 107.5 (CH-3), 106.9 (C5), 19.0 (CH_3-7). HRMS-ESI *m/z* $[M-H]^-$ calculated for $C_8H_4{}^{79}Br{}^{35}ClNO$ 243.9170, found 243.9165. LCMS - Analytical MDAP 5-95% MeCN:Water (0.1% Formic), tR 18.99 min, $[M-H]^-$ 245.7 *m/z* (89%)

3-Bromo-5-chloro-4-hydroxybenzonitrile (94)

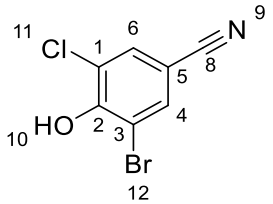

N-bromosuccinimide (0.30 g, 1.71 mmol) was added to a solution of 3-chloro-4-hydroxybenzonitrile (**93**) (0.25 g, 1.63 mmol) in acetonitrile (5 mL). The reaction mixture was added water (15 mL), precipitating a white solid, this was collected by filtration and dried

under reduced pressure to provide the title compound as a white solid (0.36 g, 84%). m.p. 165.9-169.2 °C. IR (neat, vmax) cm^{-1} 3411, 2229, 1471, 1327, 1294, 1245, 1204. ^{1}H NMR (500MHz, $CDCl_3$) δ_H 7.75 (s, 1H, CH-4/6), 7.64 (s, 1H, CH-4/6), 6.37 (s, 1H, OH-8). ^{13}C NMR (126 MHz, $CDCl_3$) δ_C 152.8 (C2), 135.0 (CH-4/6), 132.6 (CH-4/6), 121.7 (C1), 116.3 (C7), 110.9 (C3), 106.1 (C5). HRMS-ESI *m/z* $[M-H]^-$ calculated for $C_7H_2{}^{79}Br^{35}ClNO$ 229.9014, found 231.8984. LCMS - Analytical MDAP 5-95% MeCN:Water (0.1% Formic), tR 18.07 min, [M-H] 231.9 *m/z* (> 95%).

3-Chloro-4-hydroxy-2-methyl-5-oct-1-enylbenzonitrile (95)

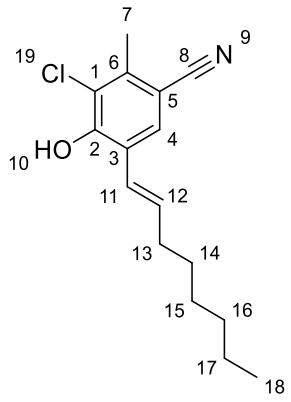

A stirring suspension of chloro[(1,3-dimesitylimidazol-2-ylidene)(n,n-dimethylbenzylamine)palladium(II)] (0.03 g, 0.05 mmol), potassium carbonate (0.39 g, 2.83 mmol), 4-hydroxy-2-methyl-5-octyl-benzonitrile (**92**) (0.20 g, 0.94 mmol) and 1-octene (1.06 g, 9.43 mmol) in *N*-methyl-2-pyrrolidinone (10 mL) was heated in a sealed vial at 110 °C for 16 h. The reaction mixture was cooled to rt, diluted with ethyl acetate (50 mL), washed with HCl (aq) (1 M, 20 mL), LiCl (aq) (0.5 M, 10 mL) and brine (25 mL). The organic phase was separated, dried over $MgSO_4$, filtered and concentrated under reduced pressure. The residue was purified by mass directed prep Shimadzu 0-95% MeCN in water (0.1% formic acid) title compound as a clear oil (0.008 g, 7%): IR (neat, v_{max}) cm^{-1} 3321, 2917, 2851, 2228, 1596, 1468, 1416. ^{1}H NMR (500 MHz, $CDCl_3$) δ_H 7.56 (s, 1H, CH-4), 6.55 (d, *J* = 16.1 Hz, 1H, CH-11), 6.30 (dt, *J* = 16.1 Hz, 7.0 Hz, 1H, CH-12), 6.20 (s, 1H, OH-10), 2.57 (s, 3H, CH_3-7), 2.25 (dt, *J* = 7.0 Hz, 7.4 Hz, 2H, CH_2-13), 1.49 (m, 2H, CH_2-14), 1.42-1.24 (m, 6H, CH_2-15/16/17), 0.91 (m, 3H, CH_3-18). ^{13}C NMR (126MHz, $CDCl_3$) δ_C 151.5 (C2), 138.2 (C6), 135.2 (CH-12), 129.0 (CH-

4), 124.8 (C3), 122.0 (CH-11), 121.6 (C1), 117.8 (C8), 105.6 (C5), 33.3 (CH_2-13), 31.7 (CH_2-16), 29.7 (CH_2-14/15), 29.1 (CH_2-14/15), 22.6 (CH_2-17), 18.8 (CH_2-7), 14.1 (CH_3-18). HRMS (ESI^-) *m/z* $[M-H]^-$ calculated for $C_{16}H_{19}{}^{35}ClNO$ 276.1161, found 276.1152. LCMS MDAP, Method 4, t_R 26.40 min, (>95%), $[M-H]^-$ 276.1 *m/z*.

5-Bromo-3-chloro-4-methoxy-benzonitrile (96)

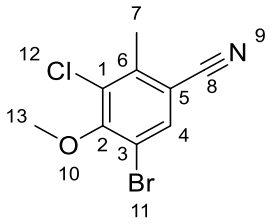

Dimethyl sulphate (0.85 mL, 8.95 mmol) was added to a suspension of 5-bromo-3-chloro-4-hydroxy-benzonitrile (**92**) (2.10 g, 8.52 mmol), and potassium carbonate (1.41 g, 10.22 mmol) in acetone (80 mL). The reaction mixture was heated to reflux for 3 h, the reaction was cooled to rt and added water (160 mL) precipitating a white solid that was collected by filtration to give the title compound (2.07 g, 93%). m.p. 118.5-119.8 °C. IR (neat, vmax) cm^{-1} 2229, 1457, 1372, 1275, 1048, 946. ^1H NMR (500 MHz, $CDCl_3$) δ 7.74 (s, 1H, CH-4), 3.94 (s, 3H, CH_3-12), 2.58 (s, 3H, CH_3-7). ^{13}C NMR (126 MHz, $CDCl_3$) δ_C 157.4 (C2), 141.7 (C6), 134.9 (CH-4), 131.3 (C1), 116.3 (C3), 116.0 (C8), 111.0 (C5), 61.0 (CH_3-12), 19.2 (CH_3-7). HRMS-ESI *m/z* no ionisation observed with +ve or -ve ion mode LRMS only EI^+ 261 *m/z*. LCMS - Analytical MDAP 50-95% MeCN:Water (0.1% Formic), tR 15.41 min, $[M+H]^+$ - poor ionisation (>95%).

3-Bromo-5-chloro-4-methoxybenzonitrile (97)

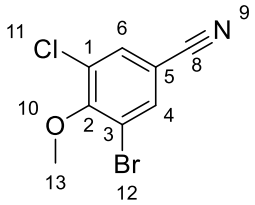

Dimethyl sulphate (0.15 mL, 1.61 mmol) was added to a suspension of potassium carbonate (0.22 g, 1.61 mmol) and 3-bromo-5-chloro-4-hydroxy-benzonitrile (**94**) (0.30 g, 1.29 mmol) in acetone (10 mL). The reaction mixture was heated to reflux for 30 min, cooled to rt and

added water (20 mL). The resulting precipitate was collected by filtration and dried under reduced pressure to provide the title compound as a white solid (0.29 g, 90%). m.p. 114.7-116.1 °C. IR (neat, vmax) cm^{-1} 2236, 1539, 1470, 1419, 1272. ^{1}H NMR (500MHz, $CDCl_3$) δ_H 7.78 (s, 1H, CH-4/6), 7.66 (s, 1H, CH-4/6), 3.97 (s, 3H, CH_3-12). ^{13}C NMR (126 MHz, $CDCl_3$) δ_C 157.6 (C2), 135.4 (CH-4/6), 133.2 (CH-4/6), 130.4 (C1), 119.5 (C3), 116.0 (C9), 109.9 (C5), 61.0 (CH_3-12). HRMS-ESI *m/z* $[M-H]^-$ calculated for $C_8H_5{}^{79}Br{}^{35}ClNO$ 243.9170, found 243.9165. LCMS - Analytical MDAP 5-95% MeCN:Water (0.1% Formic), tR 20.90 min, $[M+H]^+$ - no ionisation, (>95%).

3-Chloro-4-methoxy-2-methyl-5-octylbenzonitrile (98)

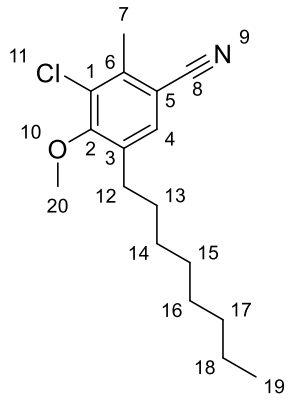

1-Octene (0.6 mL, 3.84 mmol) was dropwise added to an ice cooled solution of 1 M borane in THF (1.44 mL, 1.44 mmol). This solution was warmed to rt and stirred for 15 min. The solution was quenched with the addition of water (0.5 mL) and diluted with toluene (2.5 mL). Potassium phosphate tribasic (0.44 g, 1.92 mmol), 5-bromo-3-chloro-4-methoxy-2-methyl-benzonitrile (96) (0.25 g, 0.96 mmol), palladium (II) acetate (0.02 g, 0.02 mmol) and 2-dicyclohexylphosphino-2'-6'-diisopropoxybiphenyl (0.02 g, 0.05 mmol) were added. The reaction mixture stirred at 50 °C for 16 h. The reaction mixture was partitioned between water (10 mL) and ethyl acetate (20 mL). The organic layer was separated, dried over $MgSO_4$, filtered and concentrated under reduced pressure. The residue was purified by flash silica chromatography, eluting with petroleum ether to 10% ethyl acetate followed by purification by reverse-phase chromatography 75% MeCN in water to 100% MeCN to provide the title compound as a colourless oil, that solidified upon standing (0.18 g, 60%). m.p. 53.9 – 55.2 °C.

IR (neat, v_{max}) cm^{-1} 2913, 2849, 2226, 1468, 1291. ^{1}H NMR (500 MHz, $CDCl_3$) δ_H 7.36 (s, 1H, CH-4), 3.87 (s, 3H, CH_3-20), 2.62 (t, *J* = 7.9 Hz, 2H, CH2-13), 2.57 (s, 3H, CH_3-7), 1.61-1.55 (m, 2H, CH_2-14), 1.36-1.27 (m, 10H, CH_2s 15-19), 0.89 (t, *J* = 6.8 Hz, 3H, CH_3-20). ^{13}C NMR (126 MHz, $CDCl_3$) δ_C 158.2 (C2), 139.4 (C6), 136.3 (C3), 132.0 (CH-4), 129.7 (C1), 117.7 (C11), 109.4 (C5), 60.9 (CH_3-20), 31.8 (CH_2-17), 30.2 (CH_2-12), 29.7 (CH_2-13), 29.4 (CH_2 14/15/16), 29.3 (CH_2 14/15/16), 29.1 (CH_2 14/15/16), 22.6 (CH_2 18), 18.8 (CH_3-7), 14.0 (CH_3-19). HRMS-ESI *m/z* no ionisation observed with +ve or -ve ion mode LRMS only EI^+ 293 *m/z*. LCMS - Analytical MDAP 70-95% MeCN:Water (0.1% Formic), tR 26.07 min, $[M+H]^+$ no ionisation (>95%).

5-Chloro-4-methoxy-5-octylbenzonitrile (99)

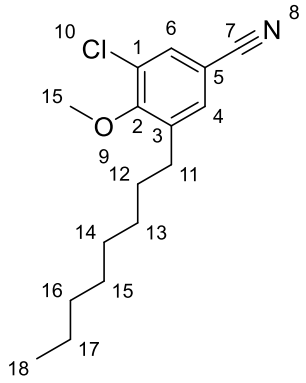

1-Octene (0.40 mL, 2.54 mmol) was dropwise added to an ice cooled solution of 1 M borane in THF (0.91 mL, 0.91 mmol). This solution was warmed to rt and stirred for 15 min. The solution was quenched with the addition of water (0. 5 mL) and diluted with toluene (2.5 mL). Potassium phosphate tribasic (0.43 g, 2.03 mmol), 5-bromo-3-chloro-4-methoxy-benzonitrile (**97**) (0.25 g, 1.01 mmol), palladium (II) acetate (0.02 g, 0.03 mmol) and 2-dicyclohexylphosphino-2'-6'-diisopropoxybiphenyl (0.02 g, 0.05 mmol) were added. The reaction mixture sealed and heated 100 °C for 16 h. The reaction mixture was partitioned between water (10 mL) and ethyl acetate (20 mL). The organic layer was separated, dried over $MgSO_4$, filtered and concentrated under vacuum. The residue was purified by flash silica chromatography, eluting with petroleum ether to 10% ethyl acetate followed by purification by reverse-phase chromatography 75% MeCN in water to 100% MeCN to provide the title compound as a pale brown oil, that solidified upon standing (0.03 g, 11%). m.p. 55.8-58.2 °C. IR (neat, vmax) cm^{-1} 2925, 2854, 2232, 1470, 1426, 1275. ^{1}H NMR (500 MHz, $CDCl_3$) δ_H 7.53

(s, 1H, CH-6), 7.40 (s, 1H, CH-4), 3.90 (s, 3H, CH_3-19), 2.66 (t, *J* = 7.9 Hz, 2H, CH_2-11), 1.60 (m, 2H, CH_2-12), 1.40 – 1.26 (m, 10H, CH_2s-13/1/15/16/17), 0.90 (t, *J* = 6.8 Hz, 3H, CH_3-18). ^{13}C NMR (126 MHz, $CDCl_3$) δ_C 158.2 (C2), 139.7 (C3), 132.4 (CH-4), 131.7 (CH-6), 128.9 (C1), 117.7 (C7), 108.5 (C5), 61.1 (CH_3-19), 31.8 (CH_2-16), 30.2 (CH_2-12), 30.0 (CH_2-11), 29.4 (CH_2-13/14/15), 29.3 (CH_2-13/14/15), 29.1 (CH_2-13/14/15), 22.6 (CH_2-17), 14.0 (CH_3-18). HRMS-ESI *m/z* $[M-H]^-$ calculated for $C_{15}H_{19}{}^{35}ClNO$ 264.1161, found 264.1153. LCMS - Analytical MDAP 5-95% MeCN:Water (0.1% Formic), tR 28.59 min, $[M+H]^+$ no ionisation (94%).

5-Chloro-4-hydrox-5-octylbenzonitrile (100)

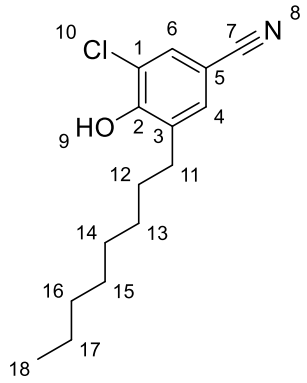

Chlorotrimethyl silane (0.25 mL, 2.00 mmol) was added to a suspension of sodium iodide (0.30 g, 2.00 mmol) and 3-chloro-4-methoxy-5-octyl-benzonitrile (0.14 g, 0.50 mmol) in acetonitrile (2 mL). The reaction mixture was sealed and heated at 80 °C for 16 h. The reaction mixture was partitioned between HCl (aq) (1 M, 20 mL) and ethyl acetate, the organics were separated, washed with sodium thiosulfate (aq) (0.1 M, 5 mL), brine (5 mL), dried over $MgSO_4$, filtered and concentrated under reduced pressure. The residue was purified by reverse-phase chromatography, eluting with water to MeOH, to provide the desired product as a pale tan solid (0.060 g, 42%). m.p. 60.1 – 61.8 °C. IR (neat, ν_{max}) cm^{-1} 3362, 2927, 2849, 2230, 1595, 1471, 1316, 1241, 1168. ^{1}H NMR (500 MHz, $CDCl_3$) δ_H 7.49 (s, 1H, CH-6), 7.34 (s, 1H, CH-4), 6.07 (s, 1H, OH-9), 2.66 (m, 2H, CH_2-11), 1.59 (m, 2H, CH_2-12), 1.49-1.17 (m, 10H, CH_2-13/14//15/16/17), 0.88 (m, 3H, CH_3-18). ^{13}C NMR (126 MHz, $CDCl_3$) δ_C 153.4 (C2), 132.9 (C4), 132.2 (CH-1), 130.4 (CH-6), 120.5 (C3), 118.2 (C7), 104.6 (C5), 32.0 (CH_2-16), 30.3 (CH_2-11), 29.5 (CH_2-13/14/15), 29.5 (CH_2-13/14/15), 29.4 (CH_2-4), 29.2 (CH_2-13/14/15), 22.8 (CH_2, 17), 14.3 (CH_3-18). HRMS-ESI *m/z* $[M-H]^-$ calculated for $C_{15}H_{19}{}^{35}ClNO$

264.1161, found 264.1151. LCMS - Analytical MDAP 50-95% MeCN:Water (0.1% Formic), tR 21.67 min, $[M-H]^-$ 265.0 *m/z* (> 95%).

Methyl 4-(3-chloro-5-cyano-2-methoxy-phenyl)butanoate (101)

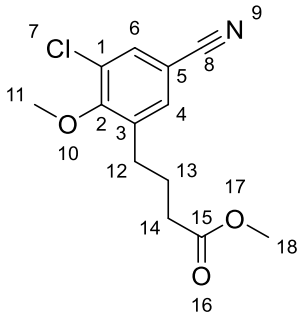

A solution of 1 M borane in THF (3.04 mL, 3.04 mmol) was added dropwise to a 40% solution methyl but-3-enoate in diethyl ether (2.03 g, 8.11 mmol) at 0 °C. This solution was warmed to rt and stirred for 15 min. The solution was quenched with the addition of water (1 mL) and diluted with toluene (5 mL). Potassium phosphate tribasic (1.17 g, 5.07 mmol), 5-bromo-3-chloro-4-methoxy-benzonitrile (**97**) (0.50 g, 2.03 mmol), palladium (II) acetate (0.05 g, 0.05 mmol) and 2-dicyclohexylphosphino-2'-6'-diisopropoxybiphenyl (0.05 g, 0.10 mmol) were added. The reaction mixture was sealed and heated to 50° C for 16 h. The cooled reaction mixture was filtered through a pad of celite, the filtrate partitioned between water (10 mL) and ethyl acetate (20 mL). The organic layer was separated, dried over $MgSO_4$, filtered and concentrated under reduced pressure. The residue was purified by flash silica chromatography, eluting with petroleum ether to 15% ethyl acetate followed by purification by preparative HPLC 75% MeCN in water to 100% MeCN to provide the title compound as a light-yellow oil (0.330 g, 54%). IR (neat, vmax) cm^{-1} 2952, 2231, 1732, 1427, 1276. ^1H NMR (500 MHz, $CDCl_3$) δ_H 7.55 (d, J = 2.1 Hz, 1H, CH-4/6), 7.40 (d, *J* = 2.1 Hz, 1H, CH 4/6), 3.90 (s, 3H, CH_3-11/18), 3.68 (s, 3H, CH_3-11/18), 2.70 (t, *J* = 7.7 Hz, 2H, CH_2-12/14), 2.36 (t, *J* = 7.3 Hz, 2H, CH_2-12/14), 1.92 (m, 2H, CH_2-13).^{13}C NMR (126 MHz, $CDCl_3$) δ_C 158.2 (C2), 139.7 (C3), 132.4 (CH-4), 131.7 (CH-6), 128.9 (C1), 117.7 (C7), 108.5 (C5), 61.1 (CH_3-19), 31.8 (CH_2-16), 30.2 (CH_2-12), 30.0 (CH_2-11), 29.4 (CH_2-13/14/15), 29.3 (CH_2-13/14/15), 29.1 (CH_2-13/14/15), 22.6 (CH_2-17), 14.0 (CH_3-18). HRMS-ESI *m/z* no ionisation observed with +ve or -ve ion mode

LRMS only EI+ 267 *m/z*. LCMS - Analytical MDAP 30-95% MeCN:Water (0.1% Formic), tR 18.30 min, $[M+H]^+$ no ionisation (94%).

Methyl 5-(3-chloro-5-cyano-2-methoxy-phenyl)pentanoate (102)

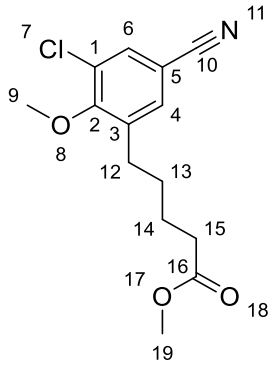

A solution of 1 M borane in THF (3.04 mL, 3.04 mmol) was added dropwise to a 31% solution methyl but-3-enoate in diethyl ether (2.99 g, 8.11 mmol) at 0 °C. This solution was warmed to rt and stirred for 15 min. The solution was quenched with the addition of water (1 mL) and diluted with toluene (5 mL). Potassium phosphate tribasic (1.17 g, 5.07 mmol), 5-bromo-3-chloro-4-methoxy-benzonitrile (**97**) (0.50 g, 2.03 mmol), palladium (II) acetate (0.05 g, 0.05 mmol) and 2-dicyclohexylphosphino-2'-6'-diisopropoxybiphenyl (0.05 g, 0.10 mmol) were added. The reaction mixture was sealed and heated 50 °C for 16 h. The cooled reaction mixture was filtered through a pad of celite, the filtrate partitioned between water (10 mL) and ethyl acetate (20 mL). The organic layer was separated, dried over $MgSO_4$, filtered and concentrated under vacuum. The residue was purified by flash silica chromatography, eluting with petroleum ether to 15% ethyl acetate followed by purification by preparative HPLC 75% MeCN in water to 100% MeCN to provide the title compound as a light-yellow oil (0.460 g, 80%). IR (neat, vmax) cm^{-1} 2951, 2233, 1733, 1472, 1275. ^1H NMR (500 MHz, $CDCl_3$) δ_H 7.53 (s, 1H, CH-6/4), 7.38 (s, 1H, CH-6/4), 3.89 (s, 3H, CH_3-9/19), 3.67 (s, 3H, CH_3-9/19), 2.67 (m, 2H, CH_2-12/15), 2.35 (m, 2H, CH_2-12/15), 1.65 (m, 4H, CH_2-13/14). ^{13}C NMR (126 MHz, $CDCl_3$) δ 173.8 (C16), 158.2 (C2), 139.9 (C3), 132.4 (C6/4), 132.0 (C6/4), 128.9 (C1), 117.6 (C10), 108.5 (C5), 61.1 (CH_3-9), 51.6 (CH_3-19), 33.7 (CH_2-15), 29.7 (CH_2-12/13), 29.5 (CH_2-12/13), 24.6 (CH_2-14). HRMS-ESI *m/z* no ionisation observed with +ve or -ve ion mode LRMS only EI+

281 *m/z*. LCMS - Analytical MDAP 30-95% MeCN:Water (0.1% Formic), tR 19.60 min, $[M+H]^+$ no ionisation (95%).

Methyl 6-(3-chloro-5-cyano-2-methoxy-phenyl)hexanoate (103)

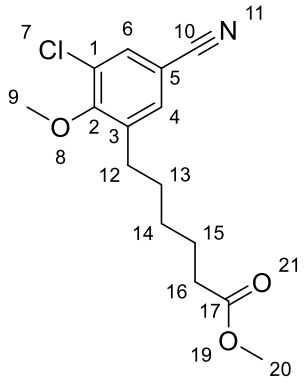

A solution of 1 M borane in THF (3.04 mL, 3.04 mmol) was added dropwise to methyl hex-5-enoate (1.04 g, 8.11 mmol) at 0 °C. This solution was warmed to RT and stirred for 15 min. The solution was quenched with the addition of water (1 mL) and diluted with toluene (5 mL). Potassium phosphate tribasic (1.17 g, 5.07 mmol), 5-bromo-3-chloro-4-methoxy-benzonitrile (**97**) (0.50 g, 2.03 mmol), palladium (II) acetate (0.05 g, 0.05 mmol) and 2-dicyclohexylphosphino-2'-6'-diisopropoxybiphenyl (0.05 g, 0.10 mmol) were added. The reaction mixture was sealed and heated 50 °C for 16 h. The cooled reaction mixture was filtered through a pad of celite, the filtrate partitioned between water (10 mL) and ethyl acetate (20 mL). The organic layer was separated, dried over $MgSO_4$, filtered and concentrated under vacuum. The residue was purified by flash silica chromatography, eluting with petroleum ether to 15% ethyl acetate to provide the title compound as a light-yellow oil (0.470 g, 78%). IR (neat, vmax) cm^{-1} 2948, 2232, 1733, 1472, 1275. ^1H NMR (500 MHz, $CDCl_3$) δ_H 7.53 (s, 1H, CH-6/4), 7.38 (s, 1H, CH-6/4), 3.89 (s, 3H, CH_3-9), 3.67 (s, 3H, CH_3-20), 2.65 (m, 2H, CH_2-12), 2.32 (m, 2H, CH_2-16), 1.70-1.57 (m, 4H, CH_2s 13/15), 1.39 (m, CH_2-14). ^{13}C NMR (126 MHz, $CDCl_3$) δ_c 174.0 (C20), 158.2 (C2), 139.2 (C3), 132.4 (CH-6/4), 131.9 (CH-6/4), 128.9 (C1), 117.7 (C10), 108.5 (C5), 61.1 (CH_3-9), 51.5 (CH_3-20), 33.83 (CH_2-16), 29.82 (CH_2-12/13/14), 29.80 (CH_2-12/13/14), 28.8 (CH_2-12/13/14), 24.6 (CH_2-15). HRMS-ESI *m/z* no ionisation observed with +ve or -ve ion mode LRMS only EI+ 295 *m/z*. LCMS - Analytical MDAP 30-95% MeCN:Water (0.1% Formic), tR 20.99 min, $[M+H]^+$ no mass ion (85%).

Methyl 7-(3-chloro-5-cyano-2-methoxy-phenyl)heptanoate (104)

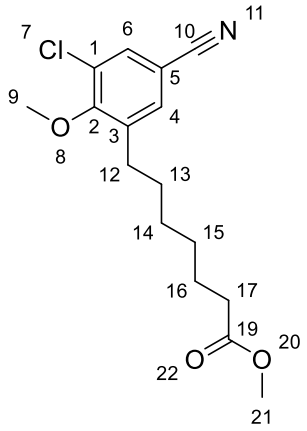

A solution of 1 M borane in THF (3.04 mL, 3.04 mmol) was added dropwise to methyl hept-6-enoate (1.15 g, 8.11 mmol) at 0 °C. This solution was warmed to rt and stirred for 15 min. The solution was quenched with the addition of water (1 mL) and diluted with toluene (5 mL). Potassium phosphate tribasic (1.17 g, 5.07 mmol), 5-bromo-3-chloro-4-methoxy-benzonitrile (**97**) (0.50 g, 2.03 mmol), palladium (II) acetate (0.05 g, 0.05 mmol) and 2-dicyclohexylphosphino-2'-6'-diisopropoxybiphenyl (0.05 g, 0.10 mmol) were added. The reaction mixture was sealed and heated 50 °C for 16 h. The cooled reaction mixture was filtered through a pad of celite, the filtrate partitioned between water (10 mL) and ethyl acetate (20 mL). The organic layer was separated, dried over $MgSO_4$, filtered and concentrated under vacuum. The residue was purified by flash silica chromatography, eluting with petroleum ether to 15% ethyl acetate to provide the title compound as a light-yellow oil (0.360 g, 58%). IR (neat, vmax) cm^{-1} 2933, 2232, 1734, 1472, 1276. ^{1}H NMR (500 MHz, $CDCl_3$) δ_H 7.52 (s, 1H, CH-6/4), 7.38 (s, 1H, CH-6/4), 3.88 (s, 3H, CH_3-9), 3.66 (s, 3H, CH_3-21), 2.64 (m, 2H, CH_2-12), 2.31 (m, 2H, CH_2-17), 1.66-1.55 (m, 4H, CH_2s-13/16), 1.36 (m, 4H, CH_2s 14/15). ^{13}C NMR (126 MHz, $CDCl_3$) δ_C 174.3 (C19), 158.4 (C2), 139.6 (C3), 132.6 (CH-6/4), 132.0 (CH6/4), 129.1 (C1), 117.9 (C10), 108.6 (C5), 61.3 (CH_3-9), 51.7 (CH_3-21), 34.1 (CH_2-17), 30.14 (CH_2-12/13/14/15), 30.08 (CH_2-12/13/14/15), 29.2 (CH_2-12/13/14/15), 29.0 (CH_2-12/13/14/15), 24.9 (CH_2-16). HRMS-ESI *m/z* $[M+Na]^+$ calculated for $C_{16}H_{20}{}^{35}ClNNaO_3$ 332.1024, found 332.1019. LCMS - Analytical MDAP 30-95% MeCN:Water (0.1% Formic), tR 22.46 min, $[M+H]^+$ 310.1 *m/z* (86%).

4-(3-Chloro-5-cyano-2-hydroxy-phenyl)butanoic acid (105)

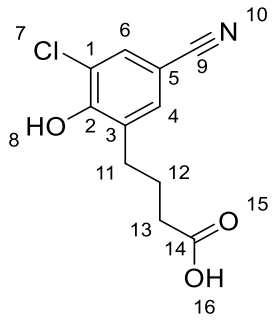

Sodium iodide (1.12 g, 7.47 mmol) was added to a solution of methyl 4-(3-chloro-5-cyano-2-methoxy-phenyl)butanoate (**101**) (0.25 g, 0.93 mmol) and chloro(trimethyl)silane (0.95 mL, 7.47 mmol) in acetonitrile (5 mL). The reaction mixture was sealed and heated to 80 °C for 96 h. The cooled reaction mixture was partitioned between sodium thiosulfate (aq) (1 M, 10 mL) and ethyl acetate (2 x 20 mL). The organic layer was separated, dried over $MgSO_4$, filtered and concentrated under reduced pressure. The residue was purified by flash silica chromatography, eluting with petroleum ether to ethyl acetate to provide the title compound as a colourless waxy solid (0.030 g, 14%). IR (neat, vmax) cm^{-1} 3345, 2569, 2228, 1691, 1474, 1253. ^{1}H NMR (500 MHz, $CDCl_3$) δ_H 12.06 (br s, 1H, COOH-15), 10.43 (br s, 1H, OH-7), 7.81 (d, *J* = 2.0 Hz, 1H, CH-6), 7.51 (d, *J* = 2.0 Hz, 1H, CH-4), 2.61 (t, *J* = 7.5 Hz, 2H, CH_2-11), 2.19 (t, *J* = 7.5 Hz, 2H, CH_2-13), 1.73 (quintet, *J* = 7.5 Hz, 2H, CH_2-12). ^{13}C NMR (126 MHz, $CDCl_3$) δ_C 174.6 (C14), 155.6 (C2), 133.1 (CH-4), 132.4 (C3), 131.9 (CH-6), 121.6 (C1), 118.7 (C9), 102.8 (C5), 33.6 (CH_2-13), 29.5 (CH_2-11), 24.5 (CH_2-12). HRMS-ESI *m/z* $[M-H]^-$ calculated for $C_{11}H_9{}^{35}ClNO_3$ 238.0276, found 238.0266. LCMS - Analytical MDAP 30-95% MeCN:Water (0.1% Formic), tR 11.53 min, $[M-H]^-$ 238.1 *m/z* (95%).

5-(3-Chloro-5-cyano-2-hydroxy-phenyl)pentanoic acid (106)

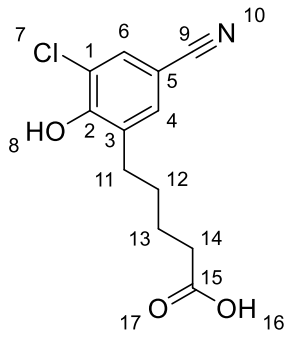

Sodium iodide (1.28 g, 8.52 mmol) was added to a solution of methyl 5-(3-chloro-5-cyano-2-methoxy-phenyl)pentanoate (**102**) (0.30 g, 1.06 mmol) and chloro(trimethyl)silane (1.08 mL, 8.52 mmol) in acetonitrile (5 mL). The reaction mixture was sealed and heated to 80 °C for 96 h. The cooled reaction mixture was partitioned between sodium thiosulfate (aq) (1 M, 10 mL) and ethyl acetate (2 x 20 mL). The organic layer was separated, dried over $MgSO_4$, filtered and concentrated under reduced pressure. The residue was purified by flash silica chromatography, eluting with petroleum ether to ethyl acetate to provide the title compound as a colourless waxy solid (0.070 g, 27%). IR (neat, vmax) cm^{-1} 3093, 2867, 2243, 1723, 1471. ^1H NMR (500 MHz, $CDCl_3$) δ_H 11.98 (br s, 1H, COOH-16), 10.40 (br s, 1H, OH-7), 7.78 (d, *J* = 2.0 Hz, 1H, CH-6), 7.53 (d, *J* = 2.0 Hz, 1H, CH-4), 2.59 (t, *J* = 7.2 Hz, 2H, CH_2-11), 2.20 (m, 2H, CH_2-14), 1.49 (m, 4H, CH_2s-12/13). ^{13}C NMR (126 MHz, $CDCl_3$) δ_C 174.8 (C15), 155.6 (C2), 133.8 (C4), 133.0 (C3), 131.8 (C6), 121.5 (C1), 118.8 (C9), 102.7 (C5), 33.9 (CH_2-14), 29.8 (CH_2-11), 28.7 (CH_2-12), 24.5 (CH_2-13). HRMS-ESI *m/z* $[M-H]^-$ calculated for $C_{12}H_{11}{}^{35}ClNO_3$ 252.0433, found 252.0423. LCMS - Analytical MDAP 30-95% MeCN:Water (0.1% Formic), tR 11.53 min, $[M-H]^-$ 238.1 *m/z* (94%).

6-(3-Chloro-5-cyano-2-hydroxy-phenyl)hexanoic acid (107)

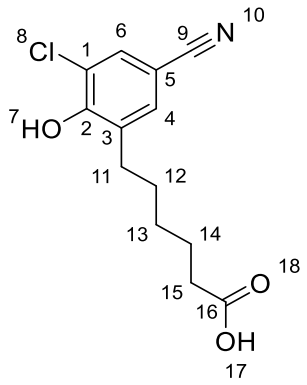

Sodium iodide (1.22 g, 8.11 mmol) was added to a solution of methyl 6-(3-chloro-5-cyano-2-methoxy-phenyl)hexanoate (**103**) (0.30 g, 1.01 mmol) and chloro(trimethyl)silane (1.03 mL, 8.11 mmol) in acetonitrile (5 mL). The reaction mixture was sealed and heated to 80 °C for 96 h. The cooled reaction mixture was partitioned between sodium thiosulfate (aq) (1 M, 10 mL) and ethyl acetate (2 x 20 mL). The organic layer was separated, dried over $MgSO_4$, filtered and concentrated under reduced pressure. The residue was purified by flash silica chromatography, eluting with petroleum ether to ethyl acetate to provide the title compound as a colourless waxy solid (0.070 g, 28%). IR (neat, vmax) cm^{-1} 3365, 2943, 2230, 1699, 1172. ^1H NMR (500 MHz, $CDCl_3$) δ_H 11.97 (br s, 1H, COOH-17), 10.37 (br s, 1H, OH-7), 7.77 (d, *J* = 2.0 Hz, 1H, CH-6), 7.53 (d, *J* = 2.0 Hz, 1H, CH-4), 2.58 (t, *J* = 7.5 Hz, 2H, CH_2-11), 2.18 (t, *J* = 7.3 Hz, 2H, CH_2-15), 1.49 (m, 4H, CH_2s-12/14), 1.27 (m, 2H, CH_2-13). ^{13}C NMR (126 MHz, $CDCl_3$) δ_C 174.9 (C16), 155.5 (C2), 133.1 (C3), 133.0 (C4), 131.7 (C6), 121.5 (C1), 118.8 (C9), 102.8 (C5), 34.0 (CH_2-15), 30.0 (CH_2-11), 29.0 (CH_2-12), 28.7 (CH_2-13), 24.7 (CH_2-14). HRMS-ESI *m/z* $[M-H]^-$ calculated for $C_{13}H_{13}{}^{35}ClNO_3$ 266.0589, found 266.0577. LCMS - Analytical MDAP 30-95% MeCN:Water (0.1% Formic), tR 13.68 min, $[M-H]^-$ 266.2 *m/z* (93%).

7-(3-Chloro-5-cyano-2-hydroxy-phenyl)heptanoic acid (108)

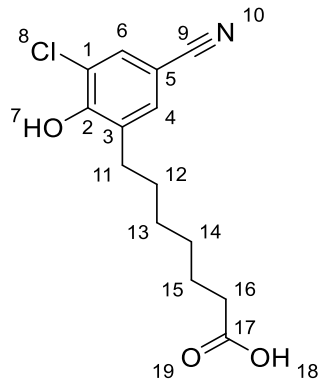

Sodium iodide (1.16 g, 7.75 mmol) was added to a solution of methyl 7-(3-chloro-5-cyano-2-methoxy-phenyl)heptanoate (**104**) (0.30 g, 0.97 mmol) and chloro(trimethyl)silane (0.98 mL, 7.75 mmol) in acetonitrile (5 mL). The reaction mixture was sealed and heated to 80 °C for 96 h. The cooled reaction mixture was partitioned between sodium thiosulfate (aq) (1 M, 10 mL) and ethyl acetate (2 x 20 mL). The organic layer was separated, dried over $MgSO_4$, filtered and concentrated under reduced pressure. The residue was purified by flash silica chromatography, eluting with petroleum ether to ethyl acetate to provide the title compound as a colourless waxy solid (0.070 g, 26%). IR (neat, vmax) cm^{-1} 3401, 2926, 2227, 1699, 1473, 1160, 1113. ^1H NMR (500 MHz, $CDCl_3$) δ_H 11.96 (br s, 1H, COOH-18), 10.36 (br s, 1H, OH-7), 7.77 (d, *J* = 2.0 Hz, 1H, CH-6), 7.52 (d, *J* = 2.0 Hz, 1H, CH-4), 2.57 (t, *J* = 7.6 Hz, 2H, CH_2-11), 2.18 (t, *J* = 7.4 Hz, 2H, CH_2-16), 1.49 (m, 4H, CH_2s-12/15), 1.26 (m, 4H, CH_2s-13/14). ^{13}C NMR (126 MHz, $CDCl_3$) δ_C 174.9 (C16), 155.5 (C2), 133.2 (C3), 133.0 (C4), 131.7 (C6), 121.5 (C1), 118.8 (C9), 102.8 (C5), 34.0 (CH_2-16), 30.1 (CH_2-11), 29.1 (CH_2-12), 28.9 (CH_2-13), 28.8 (CH_2-14), 24.8 (CH_2-15). HRMS-ESI *m/z* $[M-H]^-$ calculated for $C_{14}H_{15}{}^{35}ClNO_3$ 280.0746, found 280.0731. LCMS - Analytical MDAP 30-95% MeCN:Water (0.1% Formic), tR 14.92 min, $[M-H]^-$ 280.2 *m/z* (95%).

4-(3-Chloro-5-cyano-2-hydroxy-phenyl)-*N*-propyl-butanamide (109)

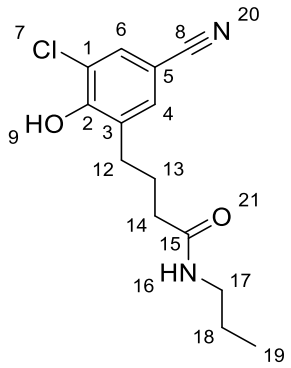

Triethylamine (0.07 mL, 0.52 mmol) was added to a solution of 4-(3-chloro-5-cyano-2-methoxy-phenyl)butanoic acid (**105**) (0.05 g, 0.21 mmol), HATU (0.09 g, 0.23 mmol), and propylamine (0.03 mL, 0.31 mmol) in acetonitrile (0.5 mL). The reaction was stirred at rt for 16 h. The reaction mixture was partitioned between ethyl acetate (0.25 mL) and water (0.25 mL). The organic layer was separated, washed with brine, dried over $MgSO_4$, filtered and concentrated under reduced pressure. The residue was purified by flash silica chromatography eluting with petroleum ether to ethyl acetate, then further purified by reverse-phase chromatography eluting with water to MeOH to provide the title compound as a colourless oil, that solidified upon standing (0.020 g, 29%). m.p. 117-119 °C. IR (neat, vmax) cm^{-1} 2933, 2225, 1727, 1601, 1469, 1289. ^{1}H NMR - (500MHz, $CDCl_3$) δ_H 10.73 (br s, 1H, OH-9), 7.95 (br t, 1H, NH-16), 7.73 (s, 1H, CH-6), 7.45 (s, 1H, CH-4), 2.97, (m, 2H, CH_2-17), 2.56 (t, *J* = 7.4 Hz, 2H, CH_2-12), 2.04 (t, *J* = 7.4 Hz, 2H, CH_2-14), 1.71 (m, 2H, CH_2-13), 1.37 (m, 2H, CH_2-18), 0.81 (t, *J* = 7.4 Hz, 3H, CH_3-19). ^{13}C NMR - (126 MHz, $CDCl_3$) δ_C 172.0 (C15), 155.4 (C2), 132.8 (CH-4), 131.9 (C3), 131.4 (CH-6), 121.2 (C1), 118.3 (C8), 102.12 (C5), 40.3 (CH_2-17), 34.3 (CH_2-14), 29.1 (CH_2-12), 25.0 (CH_2-13), 22.3 (CH_2-18), 11.4 (CH_3-19). HRMS-ESI *m/z* $[M+Na]^+$ calculated for $C_{19}H_{28}{}^{35}ClN_3NaO_2$ 303.0871, found 303.0879. LCMS - Analytical MDAP 30-95% MeCN:Water (0.1% Formic), tR 14.48 min, $[M-H]^-$ 281.0 (95%).

5-(3-Chloro-5-cyano-2-hydroxy-phenyl)-*N*-ethyl-pentanamide (110)

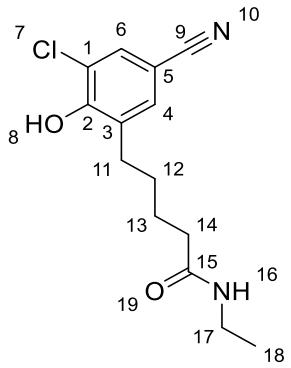

Triethylamine (0.07 mL, 0.49 mmol) was added to a solution of 5-(3-chloro-5-cyano-2-hydroxy-phenyl)pentanoic acid (106) (0.05 g, 0.2 mmol), HATU (0.08 g, 0.22 mmol), and 2 M ethylamine solution in THF (0.02 mL, 0.3 mmol) in acetonitrile (0.5 mL). The reaction was stirred at rt for 16 h. The reaction mixture was partitioned between ethyl acetate (0.25 mL) and water (0.25 mL). The organic layer was separated, brine, dried over $MgSO_4$, filtered and concentrated under reduced pressure. The residue was purified by flash silica chromatography eluting with petroleum ether to ethyl acetate in petroleum ether, then further purified by reverse phase chromatography eluting with water to MeOH to provide the title compound as a colourless oil, that solidified upon standing (0.040 g, 67%). m.p. 113-115 °C. IR (neat, vmax) cm^{-1} 3353, 2945, 2231, 1649, 1560, 1462, 1174. ^{1}H NMR - (500MHz, D_6-DMSO) δ_H 10.16 (br 1H, OH-9), 7.76-7.72 (br m, 2H, CH-6/NH-16), 7.49 (s, 1H, CH-4), 3.02 (m, 2H, CH_2-17), 2.58 (t, *J* = 6.3 Hz, 2H, CH_2-11), 2.02 (t, *J* = 6.3 Hz, 2H, CH_2-14), 1.45 (m, 4H, CH_2-12/13), 0.96 (t, *J* = 7.2 Hz, 3H, CH_3-18). ^{13}C NMR - (126 MHz, D_6-DMSO) δ_C 172.1 (C15), 156.0 (C2), 133.0 (C4), 132.9 (C3), 131.7 (C6), 121.6 (C1), 118.9 (C9), 102.1 (C5), 35.7 (CH_2-14), 33.6 (CH_2-17), 29.9 (CH_2-11), 28.9 (CH_2-12), 25.4 (CH_2-13), 15.2 (CH_3-18). HRMS-ESI *m/z* $[M+Na]^+$ calculated for $C_{14}H_{17}{}^{35}ClN_2NaO_2$ 303.0871, found 303.0865. LCMS - Analytical MDAP 30-95% MeCN:Water (0.1% Formic), tR 12.21 min, $[M-H]^-$ 281.0 (95%).

6-(3-Chloro-5-cyano-2-methoxy-phenyl)-*N*-methyl-hexanamide (111)

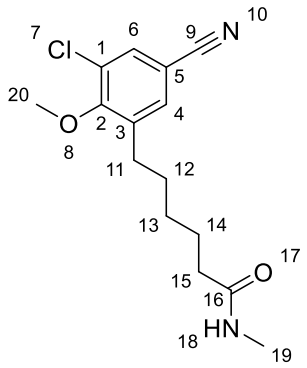

A solution of 2 M methylamine in THF (1.28 mL, 2.57 mmol) was added to a solution of 1,5,7-triazabicyclo[4.4.0]dec-5-ene (0.10 g, 0.71 mmol) and methyl 6-(3-chloro-5-cyano-2-methoxy-phenyl)hexanoate (103) (0.19 g, 0.64 mmol) in acetonitrile (5 mL). The reaction was stirred at rt for 112 h. The reaction mixture was partitioned between ethyl acetate (25 mL) and water (25 mL). The organic layer was separated, washed with brine, dried over $MgSO_4$, filtered and concentrated under reduced pressure. The residue was purified by flash silica chromatography eluting with petroleum ether to ethyl acetate to provide the title compound as a colourless oil, that solidified upon standing (0.15 g, 80%). m.p. 80-81 °C. IR (neat, vmax) cm^{-1} 3300, 2938, 2230, 1639, 1557, 1281. ^{1}H NMR - (500MHz, $CDCl_3$) δ_H 7.52 (d, *J* = 2.0 Hz, 1H, CH-6), 7.37 (d, *J* = 2.0 Hz, 1H, CH-4), 5.44 (br s, 1H, NH-18), 3.88 (s, 3H, CH_3-20), 2.80 (d, *J* = 5.0 Hz, 3H, CH_3-19), 2.65 (t, *J* = 7.6 Hz, 2H, CH_2-11), 2.17 (t, *J* = 7.6 Hz, 2H, CH_2-15), 1.68 (m, 2H, CH_2-14), 1.59 (m, 2H, CH_2-12), 1.37 (m, 2H, CH_2-13). ^{13}C NMR - (126 MHz, $CDCl_3$) δ_C 173.5 (C16), 158.4 (C2), 139.4 (C3), 132.6 (CH-4), 132.0 (CH-6), 129.1 (C1), 117.8 (C9), 108.6 (C5), 61.3 (CH_3-20), 36.6 (CH_2-15), 30.1 (CH_2-11/12), 30.0 (CH_2-11/12), 29.1 (CH_2-13), 26.4 (CH_2-14), 25.5 (CH_3-19). HRMS-ESI *m/z* $[M+Na]^+$ calculated for $C_{15}H_{19}{}^{35}ClN_2NaO_2$ 317.1027, found 317.1019. LCMS - Analytical MDAP 30-95% MeCN:Water (0.1% Formic), tR 14.72 min, $[M+H]^+$ 295.1 (95%).

7-(3-Chloro-5-cyano-2-methoxy-phenyl)-*N*-methyl-heptanamide (112)

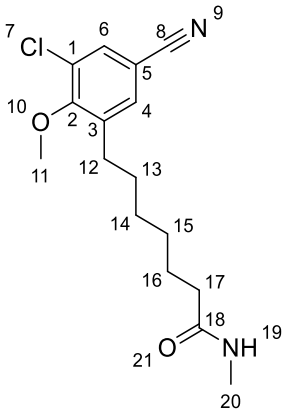

A solution of 2 M methylamine in THF (0.24 mL, 0.48 mmol) was added to a solution of 1,5,7-triazabicyclo[4.4.0]dec-5-ene (0.02 g, 0.17 mmol) and methyl 7-(3-chloro-5-cyano-2-methoxy-phenyl)heptanoate (**104**) (0.05 g, 0.16 mmol) in acetonitrile (1 mL). The reaction was stirred at rt for 16 h. The reaction mixture was partitioned between ethyl acetate (25 mL) and water (25 mL). The organic layer was separated, washed with brine, dried over $MgSO_4$, filtered and concentrated under reduced pressure. The residue was purified by flash silica chromatography eluting with petroleum ether to ethyl acetate to provide the title compound as a colourless oil, that solidified upon standing (0.04 g, 82%). m.p. 95-97 °C. IR (neat, vmax) cm^{-1} 3307, 2934, 2231, 1638, 1554, 1465, 1273. ^{1}H NMR - (500MHz, $CDCl_3$) δ_H 7.52 (d, *J* = 2.0 Hz, 1H, CH-4), 7.37 (d, *J* = 2.0 Hz, 1H, CH-6), 5.41 (br s, 1H, NH-19), 3.88 (s, 3H, CH_3-11), 2.80 (d, *J* = 5.0 Hz, 3H, CH_3-20), 2.64 (t, *J* = 7.9 Hz, 2H, CH_2-12), 2.16 (t, *J* = 7.6 Hz, 2H, CH_2-17), 1.69-1.52 (m, 4H, CH_2-13/16), 1.42-1.28 (m, 4H, CH_2-14/15). ^{13}C NMR - (126 MHz, $CDCl_3$) δ_C 173.5 (C18), 158.2 (C2), 139.4 (C1), 132.4 (C6), 131.8 (C4), 128.9 (C3), 117.7 (C8), 108.4 (C5), 61.1 (CH_3-11), 36.6 (CH_2-17), 30.0 (CH_2-12/13), 29.9 (CH_2-12/13), 29.1 (CH_2-14/15), 29.0 (CH_2-14/15), 26.3 (CH_3-20), 25.5 (CH_2-16). HRMS-ESI *m/z* $[M+Na]^+$ calculated for $C_{16}H_{21}{}^{35}ClN_2NaO_2$ 331.1184, found 331.1176. LCMS - Analytical MDAP 30-95% MeCN:Water (0.1% Formic), tR 16.12 min, $[M+H]^+$ 309.1 *m/z* (95%).

7-(3-Chloro-5-cyano-2-methoxy-phenyl)-*N*,*N*-dimethyl-heptanamide (113)

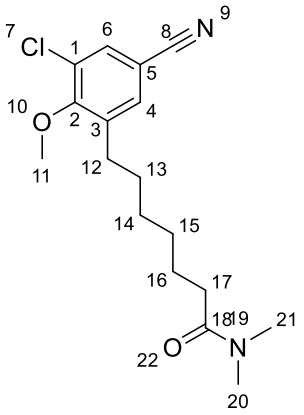

A solution of 2 M dimethylamine in THF (0.24 mL, 0.17 mmol) was added to a solution of 1,5,7-triazabicyclo[4.4.0]dec-5-ene (0.02 g, 0.17 mmol) and methyl 7-(3-chloro-5-cyano-2-methoxy-phenyl)heptanoate (**104**) (0.05 g, 0.16 mmol) in acetonitrile (1 mL). The reaction was stirred at rt for 16 h. The reaction mixture was partitioned between ethyl acetate (25 mL) and water (25 mL). The organic layer was separated, washed with brine, dried over $MgSO_4$, filtered and concentrated under reduced pressure. The residue was purified by flash silica chromatography eluting with petroleum ether to ethyl acetate to provide the title compound as a colourless oil (0.040 g, 81%). IR (neat, vmax) cm^{-1} 2931, 2232, 1639, 1468, 1404, 1272. ^{1}H NMR - (500MHz, $CDCl_3$) δ_H 7.52 (s, 1H, CH-4), 7.37 (s, 1H, CH-6), 3.88 (s, 3H, CH_3-11), 2.99 (s, 3H, CH_3-20/21), 2.94 (s, 3H, CH_3-20/21), 2.64 (m, 2H, CH_2-12), 2.30 (m, 2H, CH_2-17), 1.70-1.53 (m, 4H, CH_2-13/16), 1.43-1.32 (m, 4H, CH_2-14/15).^{13}C NMR - (126 MHz, $CDCl_3$) δ_C 173.0 (C18), 158.2 (C2), 139.5 (C1), 132.4 (C6), 131.8 (C4), 128.9 (C3), 117.7 (C8), 108.4 (C5), 61.1 (CH_3-11), 37.3 (CH_3-20/21), 35.4 (CH_3-20/21), 33.2 (CH_2-17), 30.1 (CH_2-12/13), 29.9 (CH_2-12/13), 29.2 (CH_2-14/15), 29.2 (CH_2-14/15), 25.0 (CH_2-16). HRMS-ESI *m/z* $[M+Na]^+$ calculated for $C_{17}H_{23}{}^{35}ClN_2NaO_2$ 345.1340, found 345.1339. LCMS - Analytical MDAP 30-95% MeCN:Water (0.1% Formic), tR 18.34 min, $[M+H]^+$ 323.1 *m/z* (95%).

6-(3-Chloro-5-cyano-2-hydroxy-phenyl)-*N*-methyl-hexanamide (114)

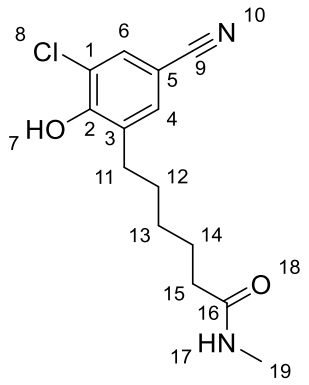

Sodium iodide (0.31 g, 2.04 mmol) was added to a solution of 6-(3-chloro-5-cyano-2-methoxy-phenyl)-*N*-methyl-hexanamide (**111**) (0.15 g, 0.51 mmol) and chloro(trimethyl)silane (0.26 mL, 2.04 mmol) in acetonitrile (2 mL). The reaction mixture was sealed and heated to 80 °C for 16 h. The cooled reaction mixture was partitioned between sodium thiosulfate (aq) (1 M, 10 mL) and ethyl acetate (2 x 20 mL). The combined organics were separated, dried over $MgSO_4$, filtered and concentrated under vacuum. The residue was purified by flash silica chromatography, eluting with CH_2Cl_2 to 5% methanol in CH_2Cl_2, then further purified by reverse phase flash chromatography eluting with water to methanol to provide the title compound as a white solid (0.040 g, 27%). m.p. 123-125 °C. IR (neat, vmax) cm^{-1} 3395, 2941, 2226, 1638, 1559, 1291, 1271. ^1H NMR (500 MHz, D_6-DMSO) δ_H 10.37 (br s, 1H, OH-7), 7.76 (s, 1H, CH-6), 7.67 (br s, 1H, NH-17), 7.51 (s, 1H, CH-4), 2.56 (t, *J* = 7.14 Hz, 2H, CH_2-11), 2.52 (m, 3H, CH_3-19), 2.01 (t, *J* = 7.2 Hz, CH_2-15), 1.47 (m, 4H, CH_2-12/14), 1.22 (m, 2H, CH_2-13). ^{13}C NMR (126 MHz, D_6-DMSO) δ_C 172.9 (C16), 155.6 (C2), 133.2 (C3), 133.0 (CH-4), 131.7 (CH-6), 121.5 (C1), 118.8 (C9), 102.6 (C5), 35.6 (CH_2-15), 29.9 (CH_2-11), 29.0 (CH_2-12), 28.8 (CH_2-13), 25.8 (CH_3-19), 25.5 (CH_2-14). HRMS-ESI *m/z* $[M+H]^+$ calculated for $C_{14}H_{17}{}^{35}ClN_2NaO_2$ 303.0871, found 303.0865. LCMS - Analytical MDAP 30-95% MeCN:Water (0.1% Formic), tR 11.92 min, $[M+H]^+$ 281.0 *m/z* (95%).

6-(3-Chloro-5-cyano-2-hydroxy-phenyl)-*N*-methyl-heptanamide (115)

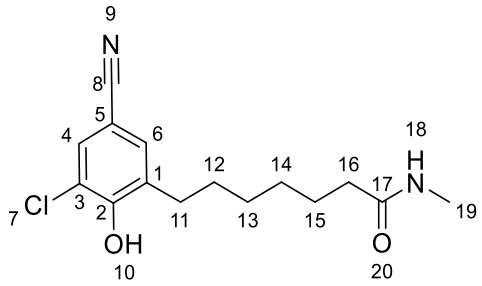

Sodium iodide (0.08 g, 0.52 mmol) was added to a solution of 6-(3-chloro-5-cyano-2-methoxy-phenyl)-*N*-methyl-heptanamide (**112**) (0.04 g, 0.13 mmol) and chloro(trimethyl)silane (0.07 mL, 0.52 mmol) in acetonitrile (1 mL). The reaction mixture was sealed and heated to 80 °C for 16 h. The cooled reaction mixture was partitioned between sodium thiosulfate (aq) (1 M, 10 mL) and ethyl acetate (2 x 20 mL). The combined organics were separated, dried over $MgSO_4$, filtered and concentrated under vacuum. The residue was purified by flash silica chromatography, eluting with CH_2Cl_2 to 5% methanol in CH_2Cl_2, then further purified by reverse phase flash chromatography eluting with water to methanol to provide the title compound as a colourless oil (0.002 g, 5%). m.p. 123-125 °C. IR (neat, vmax) cm^{-1} 3315, 2935, 2227, 1622, 1474, 1168. ^{1}H NMR (500 MHz, MeOD) δ_H 7.57 (d, J = 2.0 Hz, 1H, CH-4), 7.40 (d, J = 2.0 Hz, 1H, CH-6), 2.69 (s, 3H, CH3-19), 2.66 (t, J = 7.4 Hz, 2H, CH2-11), 2.16 (t, J = 7.6 Hz, 2H, CH2-16), 1.70-1.50 (m, 4H, CH2-12/15), 1.44-1.22 (m, 4H, CH2-13/14). ^{13}C NMR (126 MHz, MeOD) δ_C 172.4 (C17), 155.2 (C2),132.9 (C1), 132.1 (CH-6), 130.8 (CH-4), 121.0 (C3), 117.8 (C8), 102.8 (C5), 35.5 (CH_2-15), 29.8 (CH_2-11), 28.8 (CH_2-12), 28.6 (CH_2-13), 25.4 (CH_3-19), 24.8 (CH_2-14). HRMS-ESI *m/z* $[M+H]^+$ and $[M-H]^-$ poor ionisation, LRMS only EI^+ 294 *m/z*. LCMS - Analytical MDAP 30-95% MeCN:Water (0.1% Formic), tR 13.34 min, $[M+H]^+$ 295.1 *m/z* (95%).

6-(3-Chloro-5-cyano-2-hydroxy-phenyl)-*N*,*N*-dimethyl-heptanamide (116)

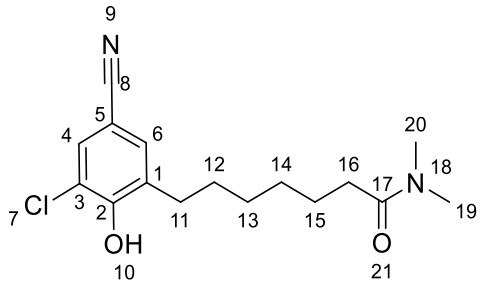

Sodium iodide (0.070 g, 0.500 mmol) was added to a solution of 6-(3-chloro-5-cyano-2-methoxy-phenyl)-*N,N*-dimethyl-heptanamide (**113**) (0.040 g, 0.120 mmol) and chloro(trimethyl)silane (0.060 mL, 0.500 mmol) in acetonitrile (1 mL). The reaction mixture was sealed and heated to 80 °C for 16 h. The cooled reaction mixture was partitioned between sodium thiosulfate (aq) (1 M, 10 mL) and ethyl acetate (2 x 20 mL). The combined organics were separated, dried over $MgSO_4$, filtered and concentrated under vacuum. The residue was purified by flash silica chromatography, eluting with CH_2Cl_2 to 5% methanol in CH_2Cl_2, then further purified by reverse phase flash chromatography eluting with water to methanol to provide the title compound as a colourless oil (0.005 g, 12%). m.p. 105-107 °C. IR (neat, vmax) cm^{-1} 2929, 2222, 1625, 1468, 1158. ^1H NMR (500 MHz, $CDCl_3$) δ_H 7.48 (s, 1H, CH-4) 7.31 (s, 1H, CH-6), 6.93 (br s, 1H, OH), 3.00 (s, 3H, CH_3-20/19), 2.96 (s, 3H, CH_3-20/19), 2.69-2.59 (m, 2H, CH_2-11), 2.34-2.24 (m, 2H, CH_2-16), 1.67-1.52 (m, 4H, CH_2-15/12), 1.42-1.29 (m, 4H, CH_2-13/14). ^{13}C NMR (126 MHz, $CDCl_3$) δ_C 173.2 (C17), 153.7 (C2), 132.6 (CH-6), 132.0 (C1), 130.5 (CH-4), 120.8 (C3), 118.2 (C8), 104.1 (C5), 37.3 (CH_3-19/20), 35.5 (CH_3-19/20), 33.1 (CH_2-16), 29.9 (CH_2-11), 28.83 (CH_2-12/13/14), 28.80 (CH_2-12/13/14), 28.75 (CH_2-12/13/14), 24.6 (CH_2-15). HRMS-ESI *m/z* $[M+H]^+$ calculated for $C_{16}H_{21}{}^{35}ClN_2NaO_2$ 331.1184, found 331.1183. LCMS - Analytical MDAP 30-95% MeCN:Water (0.1% Formic), tR 15.22 min, $[M+H]^+$ 309.1 *m/z* (95%).

Ethyl-(E)-3-5-cyano-2-hydroxy-4-methylphenyl)prop-2-enoate (117)

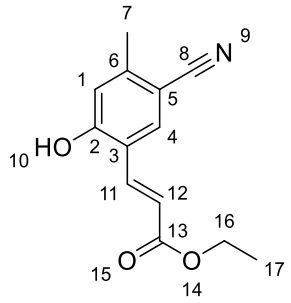

Potassium carbonate (0.98 g, 7.07 mmol) was added to a solution of 5-bromo-4-hydroxy-2-methyl-benzonitrile (**85**) (0.50 g, 2.36 mmol) and ethyl acrylate (0.77 mL, 7.07 mL) in 1-methyl-2-pyrrolidinone. [1,3-bis(2,4,6-trimethylphenyl)-2,3-dihydro-1H-imidazol-2-ylidene]({2-[(dimethylamino)methyl]phenyl})palladiumylium chloride was added to the suspension and the reaction was sealed under nitrogen and heated at 100 °C for 48 h. The reaction mixture was cooled to rt and diluted with ethyl acetate (50 mL) and filtered through a celite pad. The filtrate was washed with HCl (aq) (1 M, 25 mL), LiCl (aq) (0.5 M, 25 mL), brine (25 mL), dried over $MgSO_4$ filtered and concentrated under vacuum. The residue was purified by flash silica chromatography eluting with petroleum ether to 15% ethyl acetate in petroleum ether to provide the title compound as a white solid (0.16 g, 29%). m.p. 143-147 °C. IR (neat, vmax) cm^{-1} 2923, 2221, 1600, 1274. ^{1}H NMR (500 MHz, D_6-DMSO) δ_H 11.30 (br s, 1H, OH-10) 8.07 (s, 1H, CH-1), 7.73 (d, *J* = 16.0 Hz, 1H, CH-11), 6.90 (s, 1H, CH-2), 6.70 (d, *J* = 16.0 Hz, 1H, CH-12), 4.17 (q, *J* = 7.2 Hz, 2H, CH_2-16), 2.38 (s, 3H, CH_3-7), 1.24 (t, *J* = 7.2 Hz, 3H, CH_3-17). ^{13}C NMR (126 MHz, D_6-DMSO) δ_C 160.9 (C13), 160.6 (C2), 145.4 (C6), 138.2 (CH-11), 134.4 (CH-4), 120.3 (C3), 119.4 (CH-12), 118.5 (C8), 118.1 (CH-1), 103.19 (C8), 60.4 (CH_2-16), 20.5 (CH_3-7), 14.6 (CH_3-17). HRMS-ESI *m/z* $[M-H]^-$ calculated for $C_{13}H_{12}NO_3$ 230.0823, found 230.0814. LCMS - Analytical LCQ 7 min 30-90 Low MWt, Rt 3.18 min, $[M+H]^+$ 232.0, Analytical MDAP 30-95% MeCN:Water (0.1% Formic), tR 15.24 min, $[M+H]^+$ 230.1 (95%).

Ethyl 3-(5-cyano-2-hydroxy-4-methyl-phenyl)propanoate (118)

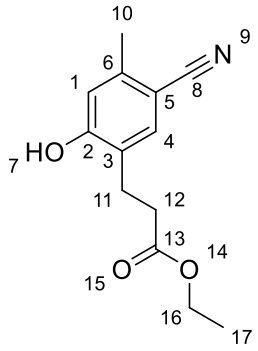

Triethylsilane (0.50 g, 4.32 mmol) was added to a solution ethyl (E)-3-(5-cyano-2-hydroxy-4-methyl-phenyl)prop-2-enoate (**117**) (0.10 g, 0.43 mmol) and 10% palladium on carbon (0.004 g, 0.04 mmol) in ethanol (5 mL). The reaction mixture was stirred at rt for 16 h. Further triethylsilane (0.50 g, 4.32 mmol) was added and the reaction mixture was stirred for a further 16 h. The reaction mixture was purged with nitrogen and was filtered through a pad of celite, the filtrate was partitioned between HCl (aq) (1 M, 10 mL) and ethyl acetate (2 x 20 mL). The combined organics were separated, dried over $MgSO_4$, filtered and concentrated under vacuum. The residue was purified by flash silica chromatography, eluting with petroleum ether to 50% ethyl acetate in petroleum ether to provide the title compound as a white solid (0.080 g, 77%). m.p. 78-80 °C. IR (neat, vmax) cm^{-1} 3496, 2927, 2225, 1716, 1199, 1250, 861. ^{1}H NMR (500 MHz, $CDCl_3$) δ_H 8.25 (s, 1H, CH-6/4), 7.32 (s, 1H, CH-6/4), 6.80 (s, 1H, OH-7), 4.16 (q, *J* = 7.3 Hz, CH_2-16), 2.84 (m, 2H, CH_2-11/12), 2.70 (m, 2H, CH_2-11/12), 2.44 (s, 3H, CH_3-10), 1.25 (t, *J* = 7.3 Hz, CH_3-17). ^{13}C NMR (126 MHz, $CDCl_3$) δ_C 175.9 (C13), 158.4 (C2), 142.5 (C6), 135.1 (CH-4), 125.8 (C3), 119.0 (CH-1), 118.6 (C8), 104.3 (C5), 61.8 (CH_2-16), 35.0 (CH_2-12), 24.0 (CH_2-11), 20.1 (CH_3-10), 14.0 (CH_3-17). HRMS-ESI *m/z* $[M+H]^+$ calculated for $C_{13}H_{15}NNaO_3$ 256.0944, found 256.0941. LCMS - Analytical MDAP 30-95% MeCN:Water (0.1% Formic), tR 14.34 min, $[M-H]^-$ 232.1 *m/z* (95%).

Ethyl 3-(3-chloro-5-cyano-2-hydroxy-4-methyl-phenyl)propanoate (119)

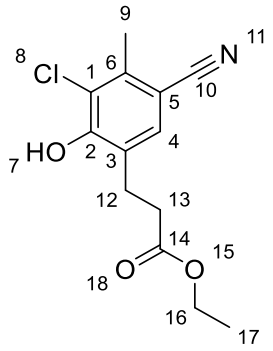

Sulfuryl chloride (0.02 mL, 0.26 mmol) was added to a solution ethyl 3-(5-cyano-2-hydroxy-4-methyl-phenyl)propanoate (**118**) (0.05 g, 0.21 mmol) in diethyl ether (1 mL). The reaction mixture was stirred at rt for 96 h. Further sulfuryl chloride (0.02 mL, 0.26 mmol) was added and the reaction mixture was stirred for a further 16 h. The reaction mixture was partitioned between HCl (aq) (1 M, 10 mL) and ethyl acetate (2 x 20 mL). The combined organics were separated, dried over $MgSO_4$, filtered and concentrated under reduced pressure. The residue was purified by flash silica chromatography, eluting with petroleum ether to 25% ethyl acetate in petroleum ether to provide the title compound as a white solid (0.043 g, 75%). m.p. 92-94 °C. IR (neat, vmax) cm^{-1} 3340, 2997, 2228, 1712, 1210, 1177, 880. ^{1}H NMR (500 MHz, $CDCl_3$) δ_H 7.33 (s, 1H, CH-4), 7.03 (s, 1H, OH-7), 4.14 (q, *J* = 7.1 Hz, 2H, CH_2-16), 2.94 (t, *J* = 7.1 Hz, 2H, CH_2-12), 2.65 (t, *J* = 7.1 Hz, 2H, CH_2-13), 2.55 (s, 3H, CH_3-9), 1.24 (t, *J* = 7.1 Hz, 3H, CH_3-17). ^{13}C NMR (126 MHz, $CDCl_3$) δ_C 173.6 (C14), 153.6 (C2), 139.4 (C6), 132.6 (CH-4), 126.7 (C10), 117.9 (C3), 105.3 (C5), 61.1 (CH_2-16), 33.7 (CH_2-12/13), 25.3 (CH_2-12/13), 18.9 (CH_3-17), 14.2 (CH_3-9). HRMS-ESI *m/z* $[M-H]^-$ calculated for $C_{13}H_{13}NO_3$ 266.0589, found 266.0576. LCMS - Analytical MDAP 30-95% MeCN:Water (0.1% Formic), tR 16.74 min, $[M-H]^-$ 265.9 *m/z* (95%).

_N_-Butyl-3-(3-chloro-5-cyano-2-hydroxy-4-methyl-phenyl)propenamide (120)

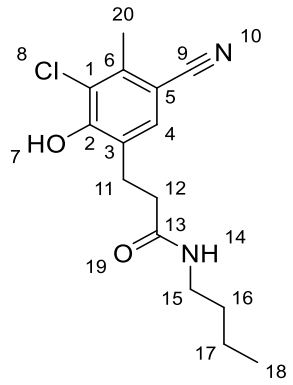

_N_-Butylamine (0.03 mL, 0.33 mmol) was added to a solution of 1,5,7-triazabicyclo[4.4.0]dec-5-ene (0.04 g, 0.26 mmol) and ethyl 3-(3-chloro-5-cyano-2-hydroxy-4-methyl-phenyl)propanoate (**119**) (0.04 g, 0.13 mmol) in acetonitrile (0.5 mL). The reaction was stirred at rt for 48 h. The reaction mixture was partitioned between ethyl acetate (25 mL) and water (25 mL). The organic layer was separated, washed with brine, dried over $MgSO_4$, filtered and concentrated under reduced pressure. The residue was purified by flash silica chromatography eluting with petroleum ether to 30% ethyl acetate in petroleum ether to provide the title compound as a colourless oil, that solidified upon standing (0.012 g, 31%). m.p. 141-143 °C. IR (neat, vmax) cm^{-1} 3369, 2928, 2220, 1632, 1562, 1157, 885. ^{1}H NMR - (500MHz, $CDCl_3$) δ_H 10.35 (br s, 1H, OH-7), 7.24 (s, 1H, CH-4), 5.55 (br s, 1H, NH-14), 3.26 (m, 2H, CH_2-15), 2.91 (m, 2H, CH_2-11), 2.59 (m, 2H, CH_2-12), 2.54 (s, 3H, CH_3-20), 1.45 (m, 2H, CH_2-16), 1.28 (m, 2H, CH_2-17), 0.90 (t, J = 7.5 Hz, 3H, CH_3-18). ^{13}C NMR - (126 MHz, $CDCl_3$) δ_C 173.6 (C13), 155.6 (C2), 140.0 (C6), 132.6 (CH-4), 127.4 (C3), 123.9 (C1), 118.3 (C9), 104.0 (C5), 39.9 (CH_2-15), 36.3 (CH_2-12), 31.4 (CH_2-16), 25.0 (CH_2-11), 19.9 (CH_2-17), 18.9 (CH_3-20), 13.6 (CH_3-18). HRMS-ESI *m/z* $[M+Na]^+$ calculated for $C_{15}H_{19}{}^{35}ClN_2NaO_2$ 317.1027, found 317.1019. LCMS - Analytical MDAP 30-95% MeCN:Water (0.1% Formic), tR 16.73 min, $[M+H]^+$ 295.0 (95%).

3-Chloro-5-heptyl-4-methoxy-2-methyl-benzonitrile (125)

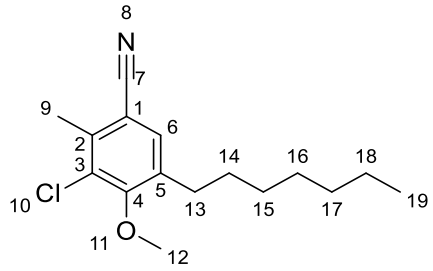

A solution of 1 M borane in THF (0.43 mL, 0.43 mmol) was added dropwise to 1-heptene (0.18 mL, 1.31 mmol) at 0 °C. This solution was warmed to rt and stirred for 15 min. The solution was quenched with the addition of water (1 mL) and diluted with toluene (5 mL). Potassium phosphate tribasic (0.25 g, 1.15 mmol), 5-bromo-3-chloro-4-methoxy-2-methyl-benzonitrile (**96**) (0.10 g, 0.38 mmol), palladium (II) acetate (0.02 g, 0.01 mmol) and 2-dicyclohexylphosphino-2'-6'-diisopropoxybiphenyl (0.09 g, 0.02 mmol) were added. The reaction mixture was sealed and heated 50 °C for 16 h. The cooled reaction mixture was filtered through a pad of celite, the filtrate partitioned between water (10 mL) and ethyl acetate (20 mL). The organic layer was separated, dried over $MgSO_4$, filtered and concentrated under vacuum. The residue was purified by flash silica chromatography, eluting with petroleum ether to 15% ethyl acetate, followed by further purification by reverse-phase chromatography eluting with 60% MeOH in water to 100% MeOH to provide the title compound as a colourless oil (0.040 g, 35%). IR (neat, vmax) cm^{-1} 2927, 2226, 1466, 1286. ^{1}H NMR (500 MHz, $CDCl_3$) δ_H 7.35 (s,1H, CH-6), 3.85 (s, 3H, CH_3-12), 2.60 (t, *J* = 7.9 Hz, 2H, CH_2-13), 2.54 (s, 3H, CH_3-9), 1.61-1.50 (m, 2H, CH_2-14), 1.38-1.11 (m, 8H, CH_2-15/16/17/18), 0.87 (t, *J* = 6.7 Hz, 3H, CH_3-19). ^{13}C NMR (126 MHz, $CDCl_3$) δ_C 158.1 (C4), 139.3 (C5), 136.3 (C2), 132.0 (CH-6), 129.6 (C3), 117.7 (C7), 109.3 (C1), 60.9 (CH_3-11), 31.7 (CH_2-17), 30.8 (CH_2-14), 29.7 (CH_2-13), 29.3 (CH_2-15/16) 29.0 (CH_2-15/16), 22.6 (CH_2-18), 18.8 (CH_3-9) 14.1 (CH_3-19). HRMS-ESI *m/z* $[M+Na]^+$ and $[M-H]^-$ poor ionisation LRMS only EI^+ 279 *m/z*. LCMS - Analytical MDAP 50-95% MeCN:Water (0.1% Formic), tR 26.21 min, no ionisation. (95%).

3-Chloro-5-hexyl-4-methoxy-2-methyl-benzonitrile (126)

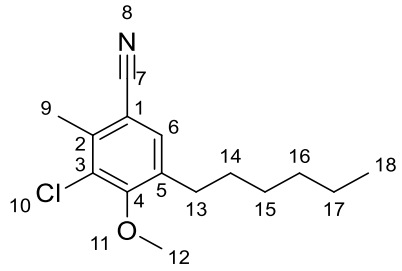

A solution of 1 M borane in THF (0.43 mL, 0.43 mmol) was added dropwise to 1-hexene (0.16 mL, 1.31 mmol) at 0 °C. This solution was warmed to rt and stirred for 15 min. The solution was quenched with the addition of water (1 mL) and diluted with toluene (5 mL). Potassium phosphate tribasic (0.25 g, 1.15 mmol), 5-bromo-3-chloro-4-methoxy-2-methyl-benzonitrile (96) (0.10 g, 0.38 mmol), palladium (II) acetate (0.02 g, 0.01 mmol) and 2-dicyclohexylphosphino-2'-6'-diisopropoxybiphenyl (0.09 g, 0.02 mmol) were added. The reaction mixture was sealed and heated 50 °C for 16 h. The cooled reaction mixture was filtered through a pad of celite, the filtrate partitioned between water (10 mL) and ethyl acetate (20 mL). The organic layer was separated, dried over $MgSO_4$, filtered and concentrated under vacuum. The residue was purified by flash silica chromatography, eluting with petroleum ether to 15% ethyl acetate, followed by further purification by reverse-phase chromatography eluting with 60% MeOH in water to 100% MeOH to provide the title compound as a colourless oil (0.040 g, 43%). IR (neat, vmax) cm^{-1} 2929, 2227, 1466, 1286. ^1H NMR (500 MHz, $CDCl_3$) δ_H 7.35 (s, 1H, CH-6), 3.85 (s, 3H, CH_3-12), 2.60 (t, *J* = 7.6 Hz, 2H, CH_2-13), 2.54 (s, 3H, CH_3-9), 1.61-1.48 (m, 2H, CH_2-14), 1.41-1.17 (m, 6H, CH_2-15/16/17), 0.87 (t, *J* = 6.8 Hz, 3H, CH_3-18). ^{13}C NMR (126 MHz, $CDCl_3$) δ_C 158.1 (C4), 139.3 (C5), 136.3 (C2), 132.0 (CH-6), 129.6 (C3), 117.7 (C1), 109.3 (C7), 60.9 (CH_3-12), 31.6 (CH_2-16), 30.1 (CH_2-14), 29.7 (CH_2-13), 29.1 (CH_2-15) 22.5 (CH_2-17), 18.8 (CH_3-9), 14.0 (CH_3-18). HRMS-ESI *m/z* $[M+Na]^+$ and $[M-H]^-$ poor ionisation LRMS only EI^+ 265 *m/z*. LCMS - Analytical MDAP 30-95% MeCN:Water (0.1% Formic), tR 28.32 min, no ionisation (95%).

3-Chloro-4-methoxy-2-methyl-5-pentyl-benzonitrile (127)

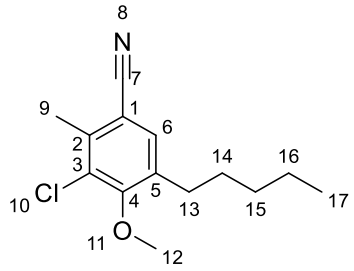

A solution of 1 M borane in THF (0.43 mL, 0.43 mmol) was added dropwise to 1-pentene (0.14 mL, 1.31 mmol) at 0 °C. This solution was warmed to rt and stirred for 15 min. The solution was quenched with the addition of water (1 mL) and diluted with toluene (5 mL). Potassium phosphate tribasic (0.25 g, 1.15 mmol), 5-bromo-3-chloro-4-methoxy-2-methyl-benzonitrile (96) (0.10 g, 0.38 mmol), palladium (II) acetate (0.02 g, 0.01 mmol) and 2-dicyclohexylphosphino-2'-6'-diisopropoxybiphenyl (0.09 g, 0.02 mmol) were added. The reaction mixture was sealed and heated 50 °C for 16 h. The cooled reaction mixture was filtered through a pad of celite, the filtrate partitioned between water (10 mL) and ethyl acetate (20 mL). The organic layer was separated, dried over $MgSO_4$, filtered and concentrated under vacuum. The residue was purified by flash silica chromatography, eluting with petroleum ether to 15% ethyl acetate, followed by further purification by reverse-phase chromatography eluting with 60% MeOH in water to 100% MeOH to provide the title compound as a colourless oil (0.03 g, 31%). IR (neat, vmax) cm^{-1} 2931, 2226, 1466, 1287. ^1H NMR (500 MHz, $CDCl_3$) δ_H 7.35 (s, 1H, CH-6), 3.85 (s, 3H, CH_3-12), 2.60 (t, *J* = 7.8 Hz, 2H, CH_2-13), 2.55 (s, 3H, CH_3-9), 1.57 (t, *J* = 7.5 Hz, 2H, CH_2-14), 1.41-1.18 (m, 4H, CH_2-15/16), 0.89 (t, *J* = 6.7 Hz, 3H, CH_3-17). ^{13}C NMR (126 MHz, $CDCl_3$) δ_C 158.1 (C4), 139.4 (C2), 136.3 (C5), 132.0 (CH-6), 129.6 (C3), 117.8 (C1), 109.3 (C7), 60.9 (CH_3-12), 31.5 (CH_2-15), 29.9 (CH_2-14), 29.7 (CH_2-13), 22.4 (CH_2-16), 18.8 (CH_3-9), 13.9 (CH_3-17). HRMS-ESI *m/z* $[M+Na]^+$ and $[M-H]^-$ poor ionisation LRMS only EI^+ 251 *m/z*. LCMS - Analytical MDAP 30-95% MeCN:Water (0.1% Formic), tR 26.44 min, no ionisation (95%).

5-Butyl-3-chloro-4-methoxy-2-methyl-benzonitrile (128)

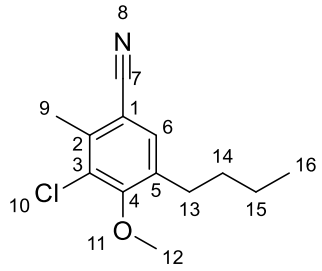

Palladium (II) acetate (0.02 g, 0.01 mmol) and 2-dicyclohexylphosphino-2'-6'-diisopropoxybiphenyl (0.09 g, 0.02 mmol) were added to a biphasic mixture of potassium phosphate tribasic (0.25 g, 1.15 mmol), 5-bromo-3-chloro-4-methoxy-2-methyl-benzonitrile (96) (0.10 g, 0.38 mmol) and 1-butaneboronic acid (0.06 g, 0.58 mmol) in water (1 mL) and diluted with toluene (5 mL). The reaction mixture was sealed and heated 50 °C for 16 h. The cooled reaction mixture was filtered through a pad of celite, the filtrate partitioned between water (10 mL) and ethyl acetate (20 mL). The organic layer was separated, dried over $MgSO_4$, filtered and concentrated under vacuum. The residue was purified by flash silica chromatography, eluting with petroleum ether to 15% ethyl acetate, followed by further purification by reverse-phase chromatography eluting with 60% MeOH in water to 100% MeOH to provide the title compound as a colourless oil (0.070 g, 65%). IR (neat, vmax) cm^{-1} 2944, 2226, 1466, 1285. ^{1}H NMR (500 MHz, $CDCl_3$) δ_H 7.35 (s, 1H, CH-6), 3.86 (s, 3H, CH3-9), 2.62 (t, *J* = 7.7 Hz, 2H, CH_2-13), 2.55 (s, 3H, CH_3-10), 1.59-1.51 (m, 2H, CH_2-14), 1.41-1.31 (m, 2H, CH_2-15), 0.93 (t, *J* = 6.7 Hz, 3H, CH_3-16). ^{13}C NMR (126 MHz, $CDCl_3$) δ_C 158.1 (C4), 139.4 (C2), 136.3 (C5), 132.1 (CH-6), 129.7 (C3), 117.8 (C11), 109.3 (C1), 60.9 (CH_3-9), 32.3 (CH_2-14), 31.7 (CH_2-13), 22.5 (CH_2-15), 18.8 (CH_3-10), 13.8 (CH_3-16). HRMS-ESI *m/z* $[M+Na]^+$ and $[M-H]^-$ poor ionisation LRMS only EI^+ 237 *m/z*. LCMS - Analytical MDAP 30-95% MeCN:Water (0.1% Formic), tR 24.85 min, no ionisation (95%).

3-Chloro-4-methoxy-2-methyl-5-propyl-benzonitrile (129)

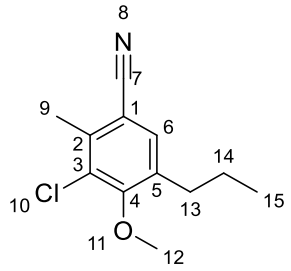

Palladium (II) acetate (0.02 g, 0.01 mmol) and 2-dicyclohexylphosphino-2'-6'-diisopropoxybiphenyl (0.09 g, 0.02 mmol) were added to a biphasic mixture of potassium phosphate tribasic (0.25 g, 1.15 mmol), 5-bromo-3-chloro-4-methoxy-2-methyl-benzonitrile (96) (0.10 g, 0.38 mmol) and 1-propylboronic acid (0.05 g, 0.58 mmol) in water (1 mL) and diluted with toluene (5 mL). The reaction mixture was sealed and heated 50 °C for 16 h. The cooled reaction mixture was filtered through a pad of celite, the filtrate partitioned between water (10 mL) and ethyl acetate (20 mL). The organic layer was separated, dried over $MgSO_4$, filtered and concentrated under reduced pressure. The residue was purified by flash silica chromatography, eluting with petroleum ether to 15% ethyl acetate, followed by further purification by reverse-phase chromatography eluting with 60% MeOH in water to 100% MeOH to provide the title compound as a colourless oil (0.07 g, 65%). IR (neat, vmax) cm^{-1} 2959, 2225, 1465, 1284. ^{1}H NMR (500 MHz, $CDCl_3$) δ_H 7.35 (s, 1H, CH-6), 3.86 (s, 3H, CH_3-9), 2.60 (t, *J* = 6.7 Hz, 2H, CH_2-13), 2.55 (s, 3H, CH_3-10), 1.66-1.56 (m, 2H, CH_2-14), 0.96 (t, *J* = 7.4 Hz, 3H, CH_3-15). ^{13}C NMR (126 MHz, $CDCl_3$) δ_C 158.2 (C4), 139.4 (C5), 136.0 (C2), 132.1 (CH-6), 129.7 (C3), 117.8 (C11), 109.3 (C1), 60.9 (CH_3-9), 31.7 (CH_2-13), 23.3 (CH_2-14), 18.9 (CH_3-10), 13.9 (CH_3-15). HRMS-ESI *m/z* $[M+Na]^+$ and $[M-H]^-$ poor ionisation LRMS only EI^+ 223 *m/z*. LCMS - Analytical MDAP 30-95% MeCN:Water (0.1% Formic), tR 24.85 min, no ionisation (95%).

3-Chloro-5-ethyl-4-methoxy-2-methyl-benzonitrile (130)

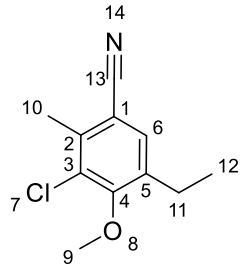

Palladium (II) acetate (0.02 g, 0.01 mmol) and 2-dicyclohexylphosphino-2'-6'-diisopropoxybiphenyl (0.09 g, 0.02 mmol) were added to a biphasic mixture of potassium phosphate tribasic (0.20 g, 0.96 mmol), 5-bromo-3-chloro-4-methoxy-2-methyl-benzonitrile (96) (0.10 g, 0.38 mmol) and triethylborane (0.42 mL, 0.42 mmol) in water (1 mL) and diluted with toluene (5 mL). The reaction mixture was sealed and heated 50 °C for 16 h. The cooled reaction mixture was filtered through a pad of celite, the filtrate partitioned between water (10 mL) and ethyl acetate (20 mL). The organic layer was separated, dried over $MgSO_4$, filtered and concentrated under reduced pressure. The residue was purified by flash silica chromatography, eluting with petroleum ether to 15% ethyl acetate, followed by further purification by reverse-phase chromatography eluting with 60% MeOH in water to 100% MeOH to provide the title compound as a colourless oil (0.020 g, 23%). IR (neat, vmax) cm^{-1} 2937, 2224, 1468, 1288. ^{1}H NMR (500 MHz, $CDCl_3$) δ_H 7.37 (s, 1H, CH-6), 3.86 (s, 3H, CH_3-9), 2.75-2.60 (m, 2H, CH_2-11), 2.56 (s, 3H, CH_3-10), 1.22 (t, *J* = 7.5 Hz, 3H, CH_3-12). ^{13}C NMR (126 MHz, $CDCl_3$) δ_C 158.0 (C4), 139.4 (C2), 137.5 (C5), 131.4 (CH-6), 129.6 (C3), 117.8 (C13), 109.5 (C1), 60.9 (CH_3-9), 22.3 (CH_2-11), 18.8 (CH_3-10), 14.4 (CH_3-12). HRMS-ESI *m/z* $[M+Na]^+$ and $[M-H]^-$ poor ionisation LRMS only EI^+ 209 *m/z*. LCMS - Analytical MDAP 30-95% MeCN:Water (0.1% Formic), tR 21.40 min, no ionisation (95%).

3-Chloro-4-methoxy-2,5-dimethyl-benzonitrile (131)

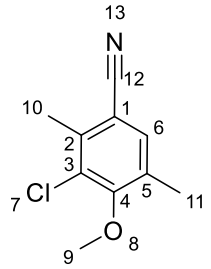

Bis[2-(di-tert-butylphosphanyl)cyclopenta-2,4-dien-1-yl]iron; dichloropalladium (0.01 g, 0.02 mmol) was added to a suspension of potassium phosphate tribasic (0.20 g, 0.96 mmol), 5-bromo-3-chloro-4-methoxy-2-methyl-benzonitrile (**96**) (0.10 g, 0.38 mmol) and trimethyl boroxine (0.12 mL, 0.42 mmol) in water (0.25 mL) and diluted with acetonitrile (1 mL). The reaction mixture was sealed and heated 100 °C for 16 h. The cooled reaction mixture was filtered through a pad of celite, the filtrate partitioned between water (10 mL) and ethyl acetate (20 mL). The organic layer was separated, dried over $MgSO_4$, filtered and concentrated under reduced pressure. The residue was purified by flash silica chromatography, eluting with petroleum ether to 15% ethyl acetate, followed by further purification by reverse-phase chromatography eluting with 60% MeOH in water to 100% MeOH to provide the title compound as a colourless oil (0.040 g, 57%). IR (neat, vmax) cm^{-1} 2935, 2223, 1468, 1288. ^{1}H NMR (500 MHz, $CDCl_3$) δ_H 7.35 (s, 1H, CH-6), 3.84 (s, 3H, CH_3-9), 2.55 (s, 3H, CH_3-10), 2.29 (s, 3H, CH_3-11). ^{13}C NMR (126 MHz, $CDCl_3$) δ_C 158.3 (C4), 139.5 (C2), 132.9 (CH-6), 131.5 (C5), 129.6 (C3), 117.6 (C12), 109.2 (C1), 60.2 (CH_3-9), 18.8 (CH_3-10), 16.0 (CH_3-11). HRMS-ESI *m/z* $[M+Na]^+$ and $[M-H]^-$ poor ionisation LRMS only EI^+ 195 *m/z*. LCMS - Analytical MDAP 30-95% MeCN:Water (0.1% Formic), tR 19.52 min, no ionisation (95%).

3-chloro-5-heptyl-4-hydroxy-2-methyl-benzonitrile (132)

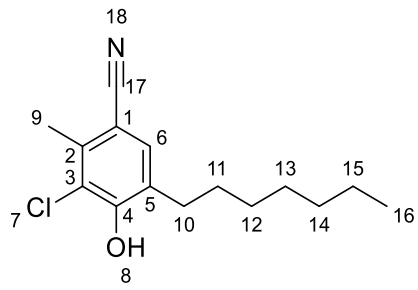

Sodium iodide (0.06 g, 0.43 mmol) was added to a solution of 3-chloro-5-heptyl-4-methoxy-2-methyl-benzonitrile (**125**) (0.03 g, 0.11 mmol) and chloro(trimethyl)silane (0.05 mL, 0.43 mmol) in acetonitrile (1 mL). The reaction mixture was sealed and heated to 80 °C for 16 h. The cooled reaction mixture was partitioned between sodium thiosulfate (aq) (1 M, 10 mL) and ethyl acetate (2 x 20 mL). The combined organics were separated, dried over $MgSO_4$, filtered and concentrated under vacuum. The residue was purified by reverse phase flash chromatography eluting with water to methanol to provide the title compound as a colourless oil (0.006 g, 22%). IR (neat, vmax) cm^{-1} 3335, 2928, 2225, 1466, 1155. ^1H NMR (500 MHz, $CDCl_3$) δ_H 7.30 (s, 1H, CH-6), 6.11 (br s, 1H, OH-8), 2.61 (t, *J* = 7.5, 2H, CH_2-10), 2.54 (s, 3H, CH_3-9), 1.61-1.53 (m, 2H, CH_2-11), 1.35-1.22 (m, 8H, CH_2-12/13/14/15), 0.88 (t, *J* = 6.2 Hz, CH_3-16). ^{13}C NMR (126 MHz, $CDCl_3$) δ_C 153.1 (C4), 138.2 (C2), 132.2 (CH-6), 128.9 (C5), 121.0 (C3), 118.1 (C17), 105.1 (C1), 31.7 (CH_2-14), 30.0 (CH_2-10), 29.2 (CH_2-12/13) 29.09 (CH_2-11/12/13), 29.06 (CH_2-11/12/13), 22.6 (CH_2-14), 18.8 (CH_3-9), 14.1 (CH_3-16). HRMS-ESI *m/z* $[M-H]^-$ calculated for $C_{15}H_{19}{}^{35}ClNO$ 264.1161, found 264.1152. LCMS - Analytical MDAP 30-95% MeCN : Water (0.1% Formic), tR 25.68 min, $[M-H]^-$ 264.0 (95%).

3-Chloro-5-hexyl-4-hydroxy-2-methyl-benzonitrile (133)

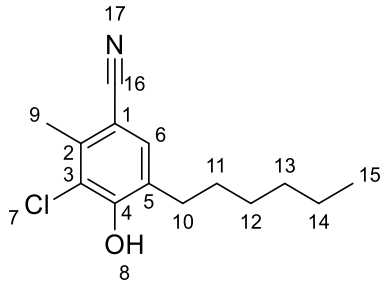

Sodium iodide (0.09 g, 0.60 mmol) was added to a solution of 3-chloro-5-hexyl-4-methoxy-2-methyl-benzonitrile (126) (0.04 g, 0.15 mmol) and chloro(trimethyl)silane (0.08 mL, 0.60 mmol) in acetonitrile (1 mL). The reaction mixture was sealed and heated to 80 °C for 16 h. The cooled reaction mixture was partitioned between sodium thiosulfate (aq) (1 M, 10 mL) and ethyl acetate (2 x 20 mL). The combined organics were separated, dried over $MgSO_4$, filtered and concentrated under vacuum. The residue was purified by reverse phase flash chromatography eluting with water to methanol to provide the title compound as a colourless oil (0.017 g, 45%). IR (neat, vmax) cm^{-1} 3339, 2932, 2223, 1601, 1466, 1163. ^1H NMR (500 MHz, $CDCl_3$) δ_H 7.29 (s, 1H, CH-6), 6.18 (br s, 1H, OH-8), 2.61 (t, *J* = 7.8 Hz, 2H, CH_2-10), 2.53 (s, 3H, CH_3-9), 1.61-1.50 (m, 2H, CH_2-11), 1.38-1.23 (m, 6H, CH_2-12/13/14), 0.92-0.84 (m, 3H, CH_3). ^{13}C NMR (126 MHz, $CDCl_3$) δ_C 153.1 (C4), 138.2 (C2), 132.2 (CH-6), 128.9 (C5), 121.0 (C3), 118.1 (C16), 105.0 (C1), 31.6 (CH_2-13), 30.0 (CH_2-10), 29.0 (CH_2-11), 28.9 (CH_2-12), 22.6 (CH_2-14), 18.8 (CH_3-9), 14.1 (CH_3-15). HRMS-ESI *m/z* $[M-H]^-$ calculated for $C_{14}H_{17}{}^{35}ClNO$ 250.1004, found 250.0995. LCMS - Analytical MDAP 30-95% MeCN:Water (0.1% Formic), tR 24.09 min, $[M-H]^-$ 249.9 *m/z* (95%).

3-Chloro-4-hydroxy-2-methyl-5-pentyl-benzonitrile (134)

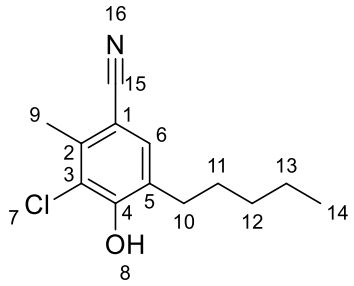

Sodium iodide (0.06 g, 0.40 mmol) was added to a solution of 3-chloro-4-methoxy-2-methyl-5-pentyl-benzonitrile (**127**) (0.03 g, 0.1 mmol) and chloro(trimethyl)silane (0.05 mL, 0.40 mmol) in acetonitrile (1 mL). The reaction mixture was sealed and heated to 80 °C for 16 h. The cooled reaction mixture was partitioned between sodium thiosulfate (aq) (1 M, 10 mL) and ethyl acetate (2 x 20 mL). The combined organics were separated, dried over $MgSO_4$, filtered and concentrated under vacuum. The residue was purified by reverse phase flash chromatography eluting with water to methanol to provide the title compound as a colourless oil (0.003 g, 13%). IR (neat, vmax) cm^{-1} 3334, 2931, 2226, 1600, 1468, 1158. ^{1}H NMR (500 MHz, $CDCl_3$) δ_H 7.30 (s, 1H, CH-6), 6.10 (br s, 1H, OH-8), 2.62 (t, *J* = 7.8 Hz, 2H, CH_2-10), 2.54 (s, 3H, CH_3-9), 1.65-1.52 (m, 2H, CH_2-11), 1.37-1.27 (m, 4H, CH_2s-11/13), 0.89 (t, *J* = 6.8 Hz, 3H, CH_3-14). ^{13}C NMR (126 MHz, $CDCl_3$) δ_C 153.1 (C4), 138.2 (C2), 132.2 (CH-6), 128.9 (C5), 121.0 (C3), 118.1 (C15), 105.1 (C1), 31.4 (CH_2-12), 29.9 (CH_2-10), 28.8 (CH_2-11), 22.4 (CH_2-13), 18.8 (CH_3-9), 14.0 (CH_3-14). HRMS-ESI *m/z* $[M-H]^-$ calculated for $C_{13}H_{15}{}^{35}ClNO$ 236.0848, found 236.0840. LCMS - Analytical MDAP 30-95% MeCN:Water (0.1% Formic), tR 22.41 min, $[M-H]^-$ 235.9 *m/z* (95%).

5-Butyl-3-chloro-4-hydroxy-2-methyl-benzonitrile (135)

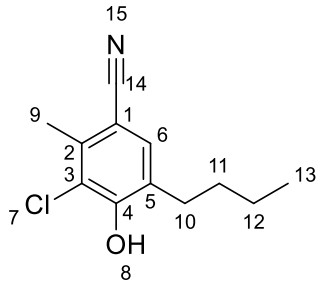

Sodium iodide (0.13 g, 0.84 mmol) was added to a solution of 5-butyl-3-chloro-4-methoxy-2-methyl-benzonitrile (**128**) (0.05 g, 0.21 mmol) and chloro(trimethyl)silane (0.11 mL, 0.84 mmol) in acetonitrile (1 mL). The reaction mixture was sealed and heated to 80 °C for 16 h. The cooled reaction mixture was partitioned between sodium thiosulfate (aq) (1 M, 10 mL) and ethyl acetate (2 x 20 mL). The combined organics were separated, dried over $MgSO_4$, filtered and concentrated under vacuum. The residue was purified by reverse phase flash chromatography eluting with water to methanol to provide the title compound as a colourless oil (0.029 g, 61%). ^{1}H NMR (500 MHz, $CDCl_3$) δ_H 7.29 (s, 1H, CH-6), 6.22 (br s, 1H, OH-8), 2.61 (t, *J* = 7.8 Hz, 2H, CH_2-10), 2.53 (s, 3H, CH_3-9), 1.60-1.50 (m, 2H, CH_2-11), 1.40-1.29 (m, 2H, CH_2-12), 0.92 (t, *J* = 7.3 Hz, 3H, CH_3-13). ^{13}C NMR (126 MHz, $CDCl_3$) δ_C 153.2 (C4), 138.2 (C2), 132.1 (CH-6), 128.9 (C5), 121.1 (C3), 118.1 (C14), 105.0 (C1), 31.2 (CH_2-11), 29.6 (CH_2-12), 22.3 (CH_2-12), 18.7 (CH_3-9), 13.8 (CH_3-13). HRMS-ESI *m/z* $[M-H]^-$ calculated for $C_{12}H_{13}{}^{35}ClNO$ 222.0691, found 222.0685. LCMS - Analytical MDAP 30-95% MeCN:Water (0.1% Formic), tR 20.71 min, $[M-H]^-$ 221.9 *m/z* (95%).

3-Chloro-4-hydroxy-2-methyl-5-propyl-benzonitrile (136)

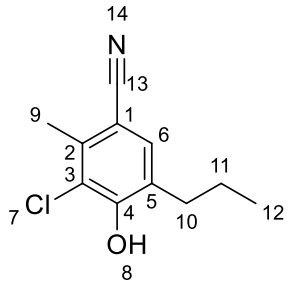

Sodium iodide (0.13 g, 0.89 mmol) was added to a solution of 3-chloro-4-methoxy-2-methyl-5-propyl-benzonitrile (**129**) (0.05 g, 0.22 mmol) and chloro(trimethyl)silane (0.11 mL, 0.89 mmol) in acetonitrile (1 mL). The reaction mixture was sealed and heated to 80 °C for 16 h. The cooled reaction mixture was partitioned between sodium thiosulfate (aq) (1 M, 10 mL) and ethyl acetate (2 x 20 mL). The combined organics were separated, dried over $MgSO_4$, filtered and concentrated under vacuum. The residue was purified by reverse phase flash chromatography eluting with water to methanol to provide the title compound as a colourless oil (0.022 g, 46%). IR (neat, vmax) cm^{-1} 3319, 2930, 2227, 1599, 1470, 1166. ^{1}H NMR (500 MHz, $CDCl_3$) δ_H 7.29 (s, 1H, CH-6), 6.21 (br s, 1H, OH-8), 2.60 (t, *J* = 7.7 Hz, 2H, CH_2-10), 2.53 (s, 3H, CH_3-9), 1.62-1.56 (m, 2H, CH_2-11), 0.94 (t, *J* = 7.3 Hz, 3H, CH_3-12). ^{13}C NMR (126 MHz, $CDCl_3$) δ_C 153.2 (C4), 138.3 (C5), 132.2 (CH-6), 128.7 (C5), 121.1 (C3), 118.1 (C13), 105.0 (C1), 31.9 (CH_2-10), 22.2 (CH_2-11), 18.8 (CH_3-9), 13.7 (CH_3-12). HRMS-ESI *m/z* $[M-H]^-$ calculated for $C_{11}H_{11}{}^{35}ClNO$ 208.0535, found 208.0528. LCMS - Analytical MDAP 30-95% MeCN:Water (0.1% Formic), tR 18.93 min, $[M-H]^-$ 207.9 *m/z* (95%).

3-Chloro-4-hydroxy-2,5-dimethyl-benzonitrile (138)

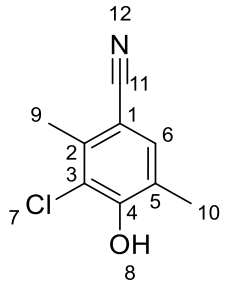

Sodium iodide (0.11 g, 0.72 mmol) was added to a solution of 3-chloro-4-methoxy-2,5-dimethyl-benzonitrile (**131**) (0.04 g, 0.18 mmol) and chloro(trimethyl)silane (0.09 mL, 0.72 mmol) in acetonitrile (1 mL). The reaction mixture was sealed and heated to 80 °C for 16 h. The cooled reaction mixture was partitioned between sodium thiosulfate (aq) (1 M, 10 mL) and ethyl acetate (2 x 20 mL). The combined organics were separated, dried over $MgSO_4$, filtered and concentrated under vacuum. The residue was purified by reverse phase flash chromatography eluting with water to methanol to provide the title compound as a colourless oil (0.015 g, 33%). IR (neat, vmax) cm^{-1} 3325, 2222, 1602, 1475, 1240, 1160. ^1H NMR (500 MHz, $CDCl_3$) δ_H 7.29 (s, 1H, CH-6), 6.21 (br s, 1H, OH-8), 2.53 (s, 3H, CH_3-9), 2.25 (s, 3H, CH_3-10). ^{13}C NMR (126 MHz, $CDCl_3$) δ_C 153.4 (C4), 138.3 (C2), 132.8 (CH-6), 124.2 (C5), 120.8 (C3), 118.0 (C11), 104.9 (C1), 18.7 (CH_3-9), 15.9 (CH_3-10). HRMS-ESI *m/z* $[M-H]^-$ calculated for $C_9H_7{}^{35}ClNO$ 180.0222, found 180.0217. LCMS - Analytical MDAP 30-95% MeCN:Water (0.1% Formic), tR 15.35 min, $[M-H]^-$ 179.9 *m/z* (95%).

5-Bromo-4-methoxy-2-methyl-benzonitrile (139)[261]

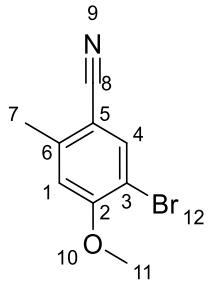

Dimethyl sulphate (0.19 mL, 1.98 mmol) was added to a suspension of potassium carbonate (0.29 g, 2.08 mmol) and 5-bromo-4-hydroxy-2-methyl-benzonitrile (**85**) (0.40 g 1.89 mmol)

in acetone (10 mL). The reaction mixture was heated to reflux for 1 h. The cooled reaction mixture was diluted with water (30 mL) and the resulting solid was filtered and air dried to provide the title compound as an off white solid (0.41 g, 95%). m.p. 88-90 °C. IR (neat, vmax) cm^{-1} 2223, 1686, 1594, 1488, 1258. ^{1}H NMR (500 MHz, D_6-DMSO) δ_H 7.99 (s, 1H, CH-4), 7.20 (s, 1H, CH-1), 3.91 (s, 3H, CH_3-11), 2.44 (s, 3H, CH_3-7). ^{13}C NMR (126 MHz, D_6-DMSO) δ_C 159.2 (C2), 144.3 (C6), 136.5 (CH-4), 117.5 (C3), 114.7 (CH-1), 108.5 (C8), 105.2 (C5), 57.3 (CH_3-11), 20.5 (CH_3-7). HRMS-ESI *m/z* $[M+Na]^+$ and $[M-H]^-$ poor ionisation LRMS only EI^+ 225 / 227 *m/z* (Br isotope). LCMS - Analytical MDAP 30-95% MeCN:Water (0.1% Formic), tR 20.20 min, no mass ion (95%).

5-(3-Fluorophenyl)-4-methoxy-2-methyl-benzonitrile (140)

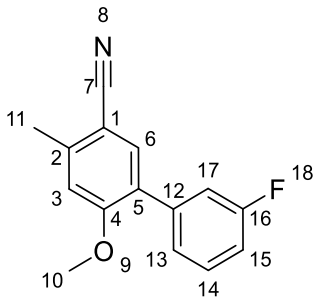

Palladium (II) acetate (0.003 g, 0.01 mmol), and 2-dicyclohexylphosphino-2'-6'-diisopropoxybiphenyl (0.01 g, 0.02 mmol) was added to a mixture of K_3PO_4 (0.29 g, 1.33 mmol), 5-bromo-4-methoxy-2-methyl-benzonitrile (**139**) (0.10 g, 0.44 mmol) and 3-fluorophenyl boronic acid (0.10 g, 0.66 mmol) in toluene (2 mL) and heated to 100 °C for 1 h. The reaction mixture was partitioned between CH_2Cl_2 (10 mL), and HCl (aq) (1 M, 10 mL), the chlorinated layer was separated through a phase separator and concentrated under reduced pressure. The residue was purified by flash silica chromatography, eluting with heptane to 20% ethyl acetate in heptane, to provide the title compound as a white solid (0.096 g, 90%). m. p. 107-108 °C. IR (neat, vmax) cm^{-1} 2924, 2209, 1600, 1471, 1255. ^{1}H NMR (500 MHz, $CDCl_3$) δ_H 7.52 (s, 1H, CH-6), 7.38 (dt, *J* = 8.1 Hz, 6.2 Hz, 1H, CH-14), 7.23-7.18 (m, 2H, CH-13/17), 7.05 (tdd, *J* = 8.4 Hz, 2.6 Hz, 1.0 Hz, 1H, CH-15), 6.87 (s, 1H, CH_3), 3.87 (s, 3H, CH_3-10), 2.59 (s, 3H, CH_3-11). ^{13}C NMR (126 MHz, $CDCl_3$) δ_C 162.5 (d, *J* = 246 Hz, C16), 159.4 (C4), 144.0 (C2), 138.4 (d, *J* = 8 Hz, C12), 134.4 (CH-6), 129.7 (d, *J* = 8 Hz, CH-14), 128.1 (d, *J*

= 3 Hz, C5), 124.9 (d, *J* = 4 Hz, CH-13), 118.3 (C7), 116.5 (d, *J* = 22 Hz, CH-15), 114.6 (d, *J* = 21 Hz, CH-17), 112.8 (CH-3), 104.8 (C1), 55.8 (CH_3-10), 20.8 (CH_3-11). HRMS-ESI *m/z* $[M+Na]^+$ calculated for $C_{15}H_{12}FNNaO$ 264.0795, found 264.0799. LCMS - Analytical UPLC 5-95% MeCN:Water (0.1% TFA), tR 0.88 min, $[M+H]^+$ 242.5 *m/z* (95%).

5-Benzyl-4-methoxy-2-methyl-benzonitrile (141)

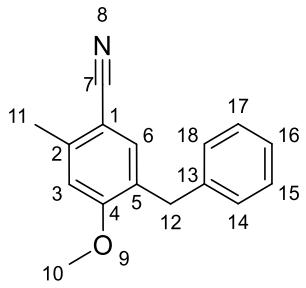

Palladium (II) acetate (0.003 g, 0.01 mmol), and 2-dicyclohexylphosphino-2'-6'-diisopropoxybiphenyl (0.01 g, 0.02 mmol) was added to a mixture of K_3PO_4 (0.29 g, 1.33 mmol), 5-bromo-4-methoxy-2-methyl-benzonitrile (**139**) (0.10 g, 0.44 mmol) and 2-benzyl-4,4,5,5-tetramethyl-1,3,2-dioxaborolane (0.14 g, 0.66 mmol) in toluene (2 mL) and water (0.2 mL) and heated to 100 °C for 1 h. The reaction mixture was partitioned between CH_2Cl_2 (10 mL), and HCl (aq) (1 M, 10 mL), the chlorinated layer was separated through a phase separator and concentrated under reduced pressure. The residue was purified by flash silica chromatography, eluting with heptane to 20% ethyl acetate in heptane, and further purified by reverse-phase (C18) chromatography eluting with 20% MeCN in water to 95% MeCN in water to provide the title compound as a white solid upon concentration (0.022 g, 21%). m. p. 111-112 °C. IR (neat, vmax) cm^{-1} 3302, 2922, 2223, 1600, 1454, 1170. ^1H NMR (500 MHz, $CDCl_3$) δ_H 7.36-7.17 (m, 6H, CH-6/14/15/16/17/18), 6.77 (s, 1H, CH-3), 3.93 (s, 2H, CH_2-12), 3.89 (s, 3H, CH_3-11), 2.54 (s, 3H, CH_3-9). ^{13}C NMR (126 MHz, $CDCl_3$) δ_C 160.4 (C4), 142.5 (C2), 139.6 (C13), 133.8 (CH-6), 128.9 (CH-14/18), 128.5 (CH-15/17&C5), 126.3 (CH-16), 118.8 (C7), 111.9 (CH-3), 104.0 (C1), 55.6 (CH_3-10), 35.2 (CH_2-12), 20.7 (CH_3-9). HRMS-ESI *m/z* $[M+Na]^+$ calculated for $C_{16}H_{15}NNaO$ 260.1046, found 260.1047. LCMS - Analytical UPLC 5-95% MeCN:Water (0.1% TFA), tR 0.90 min, $[M+H]^+$ 238.4 *m/z* (95%).

4-Methoxy-2-methyl-5-(2-phenylethyl)benzonitrile (142)

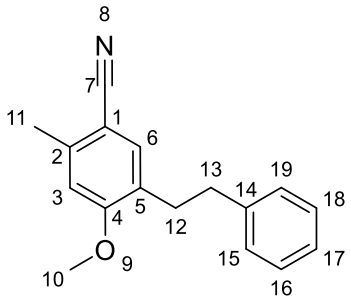

Palladium (II) acetate (0.003 g, 0.01 mmol), and 2-dicyclohexylphosphino-2'-6'-diisopropoxybiphenyl (0.01 g, 0.02 mmol) was added to a mixture of K_3PO_4 (0.29 g, 1.33 mmol), 5-bromo-4-methoxy-2-methyl-benzonitrile (139) (0.10 g, 0.44 mmol) and 2-phenylethylboronic acid (0.10 g, 0.66 mmol) in toluene (2 mL) and heated to 100 °C for 1 h. The reaction mixture was partitioned between CH_2Cl_2 (10 mL), and HCl (aq) (1 M, 10 mL), the chlorinated layer was separated through a phase separator and concentrated under reduced pressure. The residue was purified by flash silica chromatography, eluting with heptane to 20% ethyl acetate in heptane, to provide the title compound as a colourless oil (0.085 g, 76%). IR (neat, vmax) cm^{-1} 2927, 2216, 1607, 1501, 1457, 1256. ^1H NMR (500 MHz, $CDCl_3$) δ_H 7.31-7.24 (m, 3H, CH-6&16&18), 7.22-7.12 (m, 3H, CH-15&17&19), 6.72 (CH-3), 3.85 (s, 3H, 11), 2.90-2.80 (m, 4H, CH_2s-12&13), 2.51 (s, 3H, CH_3-9). ^{13}C NMR (126 MHz, $CDCl_3$) δ_C 160.6 (C4), 142.2 (C2/14), 141.5 (C2/14), 133.5 (CH-6), 128.7 (C5/CH-16/18/CH-15/19), 128.4 (C5/CH-16/18/CH-15/19), 128.3 (C5/CH-16/18/CH-15/19), 126.0 (CH-17), 118.8 (C7), 111.7 (CH-3), 103.8 (C1), 55.5 (CH_3-11), 35.7 (CH_2-13), 31.6 (CH_2-12) 20.6 (CH_3-9). HRMS-ESI *m/z* $[M+Na]^+$ calculated for $C_{17}H_{17}NNaO$ 274.1202, found 274.1211. LCMS - Analytical UPLC 5-95% MeCN:Water (0.1% TFA), tR 0.95 min, $[M+H]^+$ 252.4 *m/z* (95%).

5-Ethyl-4-methoxy-2-methyl-benzonitrile (143)

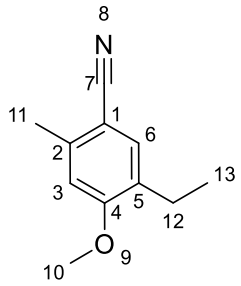

Palladium (II) acetate (0.01 g, 0.06 mmol), and 2-dicyclohexylphosphino-2'-6'-diisopropoxybiphenyl (0.06 g, 0.12 mmol) was added to a mixture of K_3PO_4 (1.52 g, 7.17 mmol), 5-bromo-4-methoxy-2-methyl-benzonitrile (**139**) (0.54 g, 2.39 mmol) and ethylboronic acid (0.27 g, 3.58 mmol) in toluene (10 mL) and heated to 100 °C for 16 h. The reaction mixture was partitioned between CH_2Cl_2 (50 mL), and HCl (aq) (1 M, 50 mL), the chlorinated layer was separated through a phase separator and concentrated under reduced pressure. The residue was purified by flash silica chromatography, eluting with heptane to 20% ethyl acetate in heptane, to provide the title compound as a colourless oil (0.41 g, 98%). IR (neat, vmax) cm^{-1} 2968, 2217, 1610, 1502, 1459, 1253. ^1H NMR (500 MHz, $CDCl_3$) δ_H 7.33 (s, 1H, CH-6), 6.70 (s, 1H, CH-3), 3.85 (s, 3H, CH_3-13), 2.57 (q, *J* = 7.5, 2H, CH_2-11), 2.50 (s, 3H, CH_3-9), 1.16 (t, *J* = 7.5 Hz, 3H, CH_3-12). ^{13}C NMR (126 MHz, $CDCl_3$) δ_C 160.5 (C4), 141.8 (C2), 132.4 (CH-6), 131.13 (C5), 119.0 (C7), 111.6 (CH-3), 103.8 (C1), 55.4 (CH_3-13), 22.5 (CH_2-11), 20.6 (CH_3-9), 13.6 (CH_3-9). HRMS-ESI *m/z* $[M+Na]^+$ and $[M-H]^-$ poor ionisation LRMS only EI^+ 175 *m/z*. LCMS - Analytical MDAP 30-95% MeCN:Water (0.1% Formic), tR 20.07 min, no mass ion (95%).

5-Isopentyl-4-methoxy-2-methyl-benzonitrile (144)

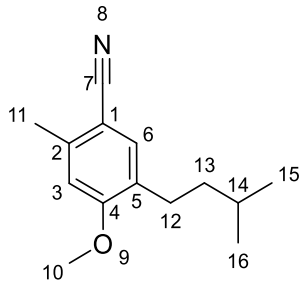

Palladium (II) acetate (0.003 g, 0.01 mmol), and 2-dicyclohexylphosphino-2'-6'-diisopropoxybiphenyl (0.01 g, 0.02 mmol) was added to a mixture of K_3PO_4 (0.23 g, 1.11 mmol), 5-bromo-4-methoxy-2-methyl-benzonitrile (**139**) (0.10 g, 0.44 mmol) and isopentylboronic acid (0.08 g, 0.66 mmol) in toluene (2 mL) and heated to 100 °C for 1 h. The reaction mixture was partitioned between CH_2Cl_2 (10 mL), and HCl (aq) (1 M, 10 mL), the chlorinated layer was separated through a phase separator and concentrated under reduced pressure. The residue was purified by flash silica chromatography, eluting with heptane to 20% ethyl acetate in heptane, to provide the title compound as a colourless oil (0.084 g, 87%). IR (neat, vmax) cm^{-1} 2953, 2218, 1609, 1461, 1255. ^1H NMR (500 MHz, $CDCl_3$) δ_H 7.32 (s, 1H, CH-6), 6.70 (s, 1H, CH-3), 3.85 (s, 3H, CH_3-11), 2.55 (t, *J* = 8.1 Hz, 2H, CH_2-12), 2.50 (s, 3H, CH_3-9), 1.61-1.54 (m, 1H, CH-14), 1.45-1.37 (m, 2H, CH_2-13), 0.93 (d, *J* = 6.6 Hz, 6H, CH_3's - 15 & 16). ^{13}C NMR (126 MHz, $CDCl_3$) δ_C 160.6 (C4), 141.7 (C2), 133.2 (CH-6), 130.1 (C5), 119.0 (C7), 111.7 (CH-3), 103.8 (C1), 55.5 (CH_3-11), 38.6 (CH_2-13), 27.9 (CH-14), 27.2 (CH_2-12), 22.5 (CH_3's - 15 & 16), 20.6 (CH_3-9). HRMS-ESI *m/z* $[M+Na]^+$ calculated for $C_{14}H_{19}NNaO$ 240.1359, found 240.1357. LCMS - Analytical UPLC 5-95% MeCN:Water (0.1% TFA), tR 1.00 min, $[M+H]^+$ 218.4 *m/z* (95%).

5-(3-Fluorophenyl)-4-hydroxy-2-methyl-benzonitrile (145)

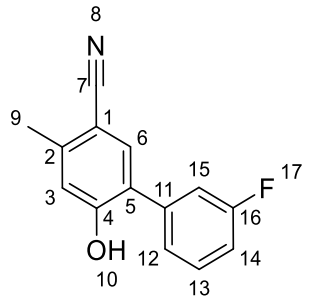

Iodo(trimethyl)silane (0.11 mL, 0.78 mmol) was added to a solution of 5-(3-fluorophenyl)-4-methoxy-2-methyl-benzonitrile (**140**) (0.075 g, 0.31 mmol) in acetonitrile (1 mL). The reaction mixture was sealed and heated to 90 °C in the microwave (Biotage Initiator®) for 1 h. The cooled reaction mixture was partitioned between sodium thiosulfate (aq) (0.1 M, 10 mL) and CH_2Cl_2 (2 x 20 mL). The chlorinated layers were separated through a phase separator and concentrated under reduced pressure. The residue was purified by flash silica chromatography eluting with heptane to 40% ethyl acetate in heptane to provide the title compound as a white solid (0.070 g, 99%). m.p. 157-159 °C. IR (neat, vmax) cm^{-1} 3225, 2223, 1578, 1390. ^1H NMR (500 MHz, $CDCl_3$) δ_H 7.54-7.47 (m, 2H, CH-6&14), 7.26-7.21 (m, 1H, CH-13), 7.21-7.13 (m, 2H, CH-15&16), 6.94 (s, 1H, CH-3), 5.65 (s, 1H, OH-11), 2.56 (s, 3H, CH_3-9). ^{13}C NMR (126 MHz, $CDCl_3$) δ_C 163.2 (d, *J* = 248 Hz, C17), 155.8 (C4), 144.1 (C2), 137.0 (d, *J* = 8 Hz, C12), 134.6 (CH-6), 131.2 (d, *J* = 8 Hz, C14), 125.6 (d, *J* = 2 Hz, C5), 124.5 (d, *J* = 3 Hz, C13), 118.1 (C7), 117.9 (CH-3), 116.2 (d, *J* = 21 Hz, C15), 115.7 (d, *J* = 21 Hz, C16), 105.2 (C1), 20.3 (CH_3-9). HRMS-ESI *m/z* $[M+Na]^+$ calculated for $C_{14}H_{10}FNNaO$ 250.0639, found 250.0638. LCMS - Analytical UPLC 2-98% MeCN:Water (0.1% TFA), tR 0.76 min, $[M+H]^+$ 228.3 *m/z* (95%).

5-Benzyl-4-hydroxy-2-methyl-benzonitrile (146)

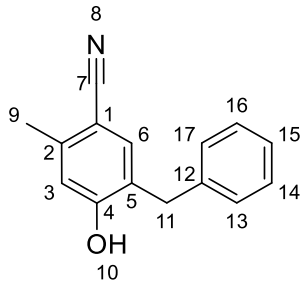

Iodo(trimethyl)silane (0.03 mL, 0.19 mmol) was added to a solution of 5-benzyl-4-methoxy-2-methyl-benzonitrile (**141**) (0.022 g, 0.09 mmol) in acetonitrile (1 mL). The reaction mixture was sealed and heated to 175 °C in the microwave (Biotage Initiator®) for 2 h. The cooled reaction mixture was partitioned between sodium thiosulfate (aq) (0.1 M, 10 mL) and CH_2Cl_2 (2 x 20 mL). The chlorinated layers were separated through a phase separator and concentrated under reduced pressure. The residue was purified by flash silica chromatography eluting with heptane to 40% ethyl acetate in heptane to provide the title compound as a white solid (0.021 g, 99%). m.p. 148-149 °C. IR (neat, vmax) cm^{-1} 3286, 2923, 2221, 1504, 1265. ^1H NMR (500 MHz, $CDCl_3$) δ_H 7.40-7.28 (m, 2H, CH-6/13/17/14/16/15), 7.28-7.14 (m, 2H, CH-6/13/17/14/16/15), 6.70 (s, 1H, CH-3), 5.22 (s, 1H, OH-10), 3.94 (s, 2H, CH_2-11), 2.46 (s, 3H, CH_3-9). ^{13}C NMR (126 MHz, $CDCl_3$) δ_C 157.2 (C4), 142.5 (C2), 138.4 (C12), 135.0 (CH-3), 128.9 (CH-13/17), 128.6 (CH-14/16), 126.8 (CH-15), 125.8 (C5), 118.5 (C7), 117.3 (CH-3), 104.7 (C1), 35.6 (CH_2-11), 20.1 (CH_3-9). HRMS-ESI *m/z* $[M+Na]^+$ calculated for $C_{15}H_{13}NNaO$ 246.0889, found 246.0892. LCMS - Analytical UPLC 2-98% MeCN:Water (0.1% TFA), tR 0.76 min, $[M+H]^+$ 224.4 *m/z* (95%).

4-Hydroxy-2-methyl-5-(2-phenylethyl)benzonitrile (147)

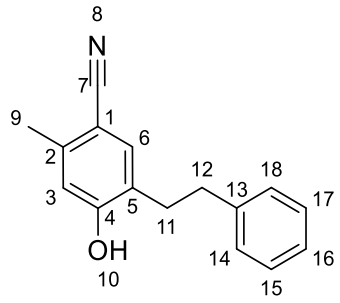

Iodo(trimethyl)silane (0.11 mL, 0.75 mmol) was added to a solution of 4-methoxy-2-methyl-5-(2-phenylethyl)benzonitrile (**142**) (0.075 g, 0.30 mmol) in acetonitrile (1 mL). The reaction mixture was sealed and heated to 90 °C in the microwave (Biotage Initiator®) for 1 h. The cooled reaction mixture was partitioned between sodium thiosulfate (aq) (0.1 M, 10 mL) and CH_2Cl_2 (2 x 20 mL). The chlorinated layers were separated through a phase separator and concentrated under reduced pressure. The residue was purified by flash silica chromatography eluting with heptane to 40% ethyl acetate in heptane to provide the title compound as a white solid (0.054 g, 76%). m.p. 108-109 °C. IR (neat, vmax) cm^{-1} 3329, 2925, 2218, 1608, 1264. ^{1}H NMR (500 MHz, $CDCl_3$) δ_H 7.34-7.29 (m, 3H, CH-6&16/17), 7.27-7.16 (m, 3H, CH-14/16/18), 6.69 (s, 1H, CH-3), 5.17 (s, 1H, OH-10), 2.95-2.86 (m, 4H, CH_2s-11&12), 2.47 (s, 3H, CH_3-9). ^{13}C NMR (126 MHz, $CDCl_3$) δ_C 157.2 (C4), 142.0 (C2), 141.1 (C13), 134.64 (CH-6), 128.6 (CH-16/17/14/18), 128.4 (CH-16/17/14/18), 126.3 (C5), 118.6 (C7), 117.0 (CH-3), 104.5 (C1), 35.8 (CH_2-12), 31.6 (CH_2-11), 20.1 (CH_3-9). HRMS-ESI *m/z* $[M+Na]^+$ calculated for $C_{16}H_{15}NNaO$ 260.1046, found 260.1046. LCMS - Analytical UPLC 2-98% MeCN:Water (0.1% TFA), tR 0.82 min, $[M+H]^+$ 238.4 *m/z* (95%).

5-Ethyl-4-hydroxy-2-methyl-benzonitrile (148)

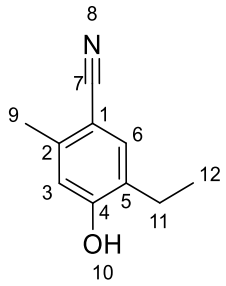

Chloro(trimethyl)silane (1.16 mL, 9.13 mmol) was added to a suspension of 5-ethyl-4-methoxy-2-methyl-benzonitrile (**143**) (0.40 g, 2.28 mmol) and sodium iodide (1.37 g, 9.13 mmol) in acetonitrile (10 mL). The reaction mixture was sealed and heated to 80 °C for 16 h. The cooled reaction mixture was partitioned between sodium thiosulfate (aq) (0.1 M, 100 mL) and ethyl acetate (2 x 100 mL). The combined organic layers were dried over $MgSO_4$, filtered and concentrated under reduced pressure. The residue was purified by flash silica chromatography eluting with heptane to 40% ethyl acetate in heptane to provide the title compound as a white solid (0.204 g, 55%). m.p. 99-100 °C. IR (neat, vmax) cm^{-1} 3277, 2221, 1610, 1409, 1255. ^{1}H NMR (500 MHz, $CDCl_3$) δ_H 7.35 (s, 1H, CH-6), 6.70 (s, 1H, CH-3), 6.02 (br s, 1H, OH-10), 2.59 (q, *J* = 7.6 Hz, 2H, CH_2-11), 2.44 (s, 3H, CH_3-9), 1.21 (t, *J* = 7.6 Hz, 3H, CH_3-12). ^{13}C NMR (126 MHz, $CDCl_3$) δ_C 157.5 (C4), 141.7 (C2), 133.5 (CH-6), 128.8 (C5), 118.9 (C7), 116.7 (CH-3), 103.9 (C1), 22.2 (CH_2-11), 20.0 (CH_3-9), 14.2 (CH_3-12). HRMS-ESI *m/z* $[M-H]^-$ calculated for $C_{10}H_{10}NO$ 160.0768, found 160.0766. LCMS - Analytical MDAP 30-95% MeCN:Water (0.1% Formic), tR 16.02 min, $[M-H]^-$ 160.1 *m/z* (95%).

4-Hydroxy-5-isopentyl-2-methyl-benzonitrile (149)

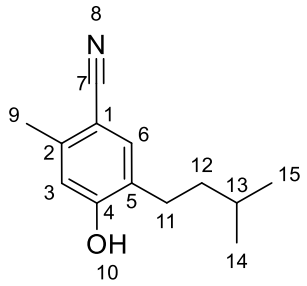

Iodo(trimethyl)silane (0.75 mL, 5.25 mmol) was added to a solution of 4-methoxy-5-isopentyl-2-methyl-benzonitrile (**144**) (0.290 g, 1.31 mmol) in acetonitrile (4 mL). The reaction mixture was sealed and heated to 90 °C in the microwave (Biotage Initiator®) for 1 h. The cooled reaction mixture was partitioned between sodium thiosulfate (aq) (0.1 M, 10 mL) and CH_2Cl_2 (2 x 20 mL). The chlorinated layers were separated through a phase separator and concentrated under reduced pressure. The residue was purified by flash silica chromatography eluting with heptane to 40% ethyl acetate in heptane to provide the title compound as a white solid (0.225 g, 84%). m.p. 69-71 °C. IR (neat, vmax) cm^{-1} 3253, 2953, 2223, 1607, 1416, 1267. ^1H NMR (500 MHz, $CDCl_3$) δ_H 7.37 (s, 1H, CH-6), 6.70 (s, 1H, CH-3), 5.38 (s, 1H, OH-10), 2.61-2.55 (m, 2H, CH_2-11), 2.47 (s, 3H, CH-9), 1.67-1.56 (m, 1H, CH-13), 1.52-1.45 (m, 2H, CH_2-12), 0.97 (d, *J* = 6.7 Hz, 6H, CH_3's-14&15). ^{13}C NMR (126 MHz, $CDCl_3$) δ_C 157.1 (C4). 141.6 (C2), 134.2 (CH-6), 127.6 (C5), 118.8 (C7), 116.8 (CH-3), 104.4 (C1), 38.5 (CH_2-12), 27.8 (CH-13), 27.0 (CH_2-11), 22.5 (CH_3's-14&15), 20.0 (CH_3-9). HRMS-ESI *m/z* $[M+Na]^+$ calculated for $C_{13}H_{17}NNaO$ 226.1202, found 226.1202. LCMS - Analytical UPLC 2-98% MeCN:Water (0.1% TFA), tR 0.86 min, $[M+H]^+$ 204.4 *m/z* (95%).

5-(3-Fluorophenyl)-4-hydroxy-2-methyl-benzonitrile (150)

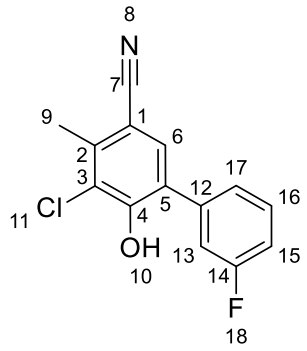

Sulfuryl chloride (0.02 mL, 0.39 mmol) was added to a solution of 5-(3-fluorophenyl)-4-hydroxy-2-methyl-benzonitrile (**145**) (0.04 g, 0.18 mmol) in diethyl ether (1 mL) and stirred for 16 h. The reaction mixture was partitioned between HCl (aq) (1 M, 5 mL) and CH_2Cl_2 (2 x 10 mL). The chlorinated layers were separated through a phase separator and concentrated under reduced pressure. The residue was purified by flash silica chromatography eluting with heptane to 40% ethyl acetate in heptane to provide the title compound as a white solid (0.026 g, 56%). m.p. 193-194 °C. IR (neat, vmax) cm^{-1} 3314, 2923, 2227, 1594, 1461, 1398, 1291. ^{1}H NMR (500 MHz, $CDCl_3$) δ_H 7.55 (s, 1H, CH-6), 7.50-7.41 (m, 1H, CH-16), 7.34-7.27 (m, 2H, CH-15&17), 7.17-7.09 (m, 1H, CH-13), 6.29 (s, 1H, OH-11), 2.66 (s, 3H, CH_3-9). ^{13}C NMR (126 MHz, $CDCl_3$) δ_C 162.6 (d, *J* = 230.4 Hz, CF-14), 152.0 (C4), 140.4 (C2), 137.2 (d, *J* = 8 Hz, C12), 132.8 (CH-6), 130.2 (d, *J* = 8 Hz, CH-16), 126.7 (d, *J* = 2 Hz, C5), 124.7 (d, *J* = 3 Hz, CH-17), 122.0 (C3 - observed HMBC), 117.5 (C7), 116.2 (d, *J* = 23 Hz, CH-15), 115.4 (d, *J* = 21 Hz, CH-13), 106.1 (C1), 19.1 (CH_3-9). HRMS-ESI *m/z* $[M-H]^-$ calculated for $C_{14}H_8{}^{35}ClFNO$ 260.0284, found 260.0275. LCMS - Analytical UPLC 2-98% MeCN:Water (0.1% TFA), tR 0.82 min, no mass ion observed, (95%).

5-Benzyl-3-chloro-4-hydroxy-2-methyl-benzonitrile (151)

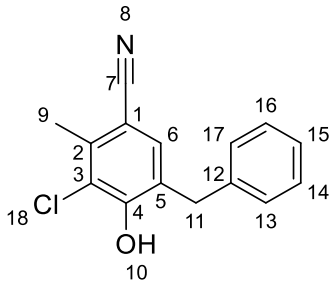

Sulfuryl chloride (0.01 mL, 0.18 mmol) was added to a solution of 5-benzyl-4-hydroxy-2-methyl-benzonitrile (**146**) (0.02 g, 0.09 mmol) in diethyl ether (1 mL) and stirred for 16 h. The reaction mixture was partitioned between HCl (aq) (1 M, 5 mL) and CH_2Cl_2 (2 x 10 mL). The chlorinated layers were separated through a phase separator and concentrated under reduced pressure. The residue was purified by flash silica chromatography eluting with heptane to 40% ethyl acetate in heptane to provide the title compound as a white solid (0.017 g, 74%). m.p. 151-153 °C. IR (neat, vmax) cm^{-1} 3320, 2226, 1595, 1414, 1240, 1157. ^1H NMR (500 MHz, $CDCl_3$) δ_H 7.37-7.30 (m, 2H, CH-14/16), 7.30-7.16 (m, 4H, CH-6/15/13/17), 6.20 (br, 1H, OH-11), 4.01 (s, 2H, CH_2-12), 2.58 (s, 3H, CH_3-9). ^{13}C NMR (126 MHz, $CDCl_3$) δ_C 153.0 (C4), 138.9 (C2), 138.6 (C12), 132.7 (CH-6), 128.9 (CH-13/17), 128.7 (CH-14/16), 127.6 (C5), 126.7 (CH-15), 121.3 (C3), 117.9 (C7), 105.4 (C1), 35.8 (CH_2-11), 18.9 (CH_3-9). HRMS-ESI *m/z* $[M+Na]^+$ calculated for $C_{15}H_{12}{}^{35}ClNNaO$ 280.0500, found 280.0502. LCMS - Analytical UPLC 2-98% MeCN:Water (0.1% TFA), tR 0.83 min, $[M+H]^+$ 258.4 *m/z*, (95%).

3-Chloro-4-hydroxy-2-methyl-5-(2-phenylethyl)benzonitrile (152)

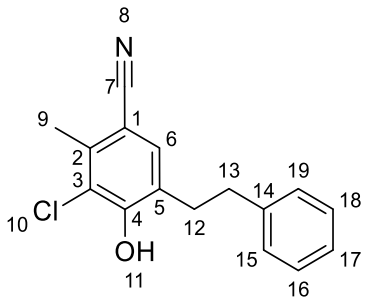

Sulfuryl chloride (0.04 mL, 0.50 mmol) was added to a solution of 4-hydroxy-2-methyl-5-(2-phenylethyl)benzonitrile (**147**) (0.05 g, 0.21 mmol) in diethyl ether (1 mL) and stirred for 16 h.

The reaction mixture was partitioned between HCl (aq) (1 M, 5 mL) and CH_2Cl_2 (2 x 10 mL). The chlorinated layers were separated through a phase separator and concentrated under reduced pressure. The residue was purified by flash silica chromatography eluting with heptane to 40% ethyl acetate in heptane to provide the title compound as a white solid (0.037 g, 65%). m.p. 144-145 °C. IR (neat, vmax) cm^{-1} 3304, 2923, 2228, 1600, 1320,1164. ^1H NMR (500 MHz, $CDCl_3$) δ_H 7.34-7.29 (m, 2H, CH-16/18), 7.27-7.16 (m, 4H, CH-6/17/15/19), 6.16 (OH-11), 3.00-2.88 (m, 4H, CH_2-12&13), 2.58 (s, 3H, CH_3-9). ^{13}C NMR (126 MHz, $CDCl_3$) δ_C 153.1 (C4), 141.0 (C14), 138.7 (C2), 132.4 (CH-6), 128.5 (CH's-15/16/18/19), 128.4 (CH-15/16/18/19), 127.8 (C5), 126.2 (CH-17), 121.2 (C3), 118.0 (C7), 105.2 (C1), 35.3 (CH_2-13), 32.2 (CH_2-12), 18.9 (CH_3-9). HRMS-ESI *m/z* $[M-H]^-$ calculated for $C_{16}H_{13}{}^{35}ClNO$ 270.0691, found 270.0682. LCMS - Analytical UPLC 2-98% MeCN:Water (0.1% TFA), tR 0.89 min, poor ionisation – no mass ion observed, (> 95%).

3-Chloro-5-ethyl-4-hydroxy-2-methyl-benzonitrile (153)

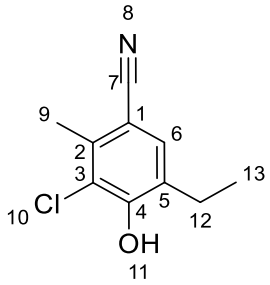

Sulfuryl chloride (0.1 mL, 1.16 mmol) was added to a solution of 5-ethyl-4-hydroxy-2-methyl-benzonitrile (**148**) (0.085 g, 0.53 mmol) in diethyl ether (1 mL) and stirred for 16 h. The reaction mixture was partitioned between HCl (aq) (1 M, 5 mL) and CH_2Cl_2 (2 x 10 mL). The chlorinated layers were separated through a phase separator and concentrated under reduced pressure. The residue was purified by flash silica chromatography eluting with heptane to 40% ethyl acetate in heptane to provide the title compound as a white solid (0.046 g, 45%). m.p. 95-97 °C. IR (neat, vmax) cm^{-1} 3336, 2966, 2219, 1601, 1413, 1313, 1166. ^1H NMR (500 MHz, $CDCl_3$) δ_H 7.32 (s, 1H, CH-6), 6.14 (s, 1H, OH-11), 2.66 (q, *J* = 7.6 Hz, 2H, CH_2-12), 2.54 (s, 3H, CH_3-9), 1.21 (t, *J* = 7.6 Hz, 3H, CH_3-13). ^{13}C NMR (126 MHz, $CDCl_3$) δ_C 153.0 (C4), 138.3 (C2), 131.4 (CH-6), 130.1 (C5), 121.0 (C3), 118.1 (C7), 105.2 (C1), 23.1 (CH_2-

12), 18.8 (CH_3-9), 13.4 (CH_3-13). HRMS-ESI *m/z* $[M-H]^-$ calculated for $C_{10}H_9{}^{35}ClNO$ 194.0378, found 194.0375. LCMS - Analytical MDAP 30-95% MeCN:Water (0.1% Formic), tR 21.64 min, $[M-H]^-$ 193.95 *m/z* (> 95%).

3-Chloro-4-hydroxy-5-isopentyl-2-methyl-benzonitrile (154)

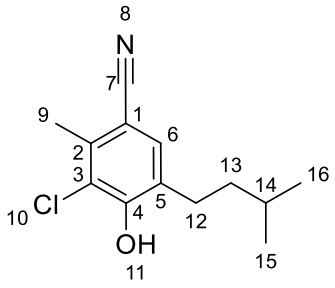

Sulfuryl chloride (0.16 mL, 2.06 mmol) was added to a solution of 4-hydroxy-5-isopentyl-2-methyl-benzonitrile (**149**) (0.175 g, 0.86 mmol) in diethyl ether (2 mL) and stirred for 16 h. The reaction mixture was partitioned between HCl (aq) (1 M, 5 mL) and CH_2Cl_2 (2 x 10 mL). The chlorinated layers were separated through a phase separator and concentrated under reduced pressure. The residue was purified by flash silica chromatography eluting with heptane to 40% ethyl acetate in heptane to provide the title compound as a white solid (0.185 g, 90%). m.p. 82-83 °C. IR (neat, vmax) cm^{-1} 3303, 2957, 2227, 1603, 1471,1319, 1245, 1170. ^1H NMR (500 MHz, $CDCl_3$) δ_H 7.34 (s, 1H, CH-6), 6.11 (s, 1H, OH-11), 2.66 (m, 2H, CH_2-12), 2.57 (s, 3H, CH_3-9), 1.62 (m, 1H, CH-14), 1.49 (m, 2H, CH_2-13), 0.97 (d, *J* = 6.6 Hz, 6H, CH_3-15&16). ^{13}C NMR (126 MHz, $CDCl_3$) δ_C 153.0 (C4), 138.2 (C2), 132.1 (CH-6), 129.1 (C5), 121.1 (C3), 118.1 (C7), 105.2 (C1), 38.3 (CH_2-13), 27.9 (CH_2-12), 27.8 (CH-14), 22.5 (CH_2s-15&16), 18.8 (CH_3-9). HRMS-ESI *m/z* $[M-H]^-$ calculated for $C_{13}H_{15}{}^{35}ClNO$ 236.0848, found 236.0840. LCMS - Analytical UPLC 2-98% MeCN:Water (0.1% Formic), tR 0.92 min, $[M+H]^+$ 238.3 *m/z* (95%).

5-(Cyclohexen-1-yl)-4-methoxy-2-methyl-benzonitrile (155)

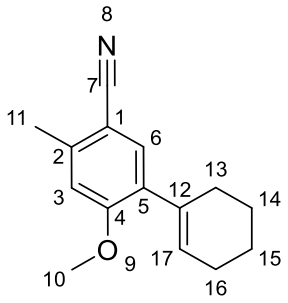

Palladium (II) acetate (0.006 g, 0.03 mmol), and 2-dicyclohexylphosphino-2'-6'-diisopropoxybiphenyl (0.025 g, 0.06 mmol) was added to a mixture of K_3PO_4 (0.59 g, 2.76 mmol), 5-bromo-4-methoxy-2-methyl-benzonitrile (**139**) (0.25 g, 1.11 mmol) and cyclohexen-1-yl boronic acid (0.21 g, 1.66 mmol) in toluene (5 mL) and heated to 100 °C for 16 h. The reaction mixture was partitioned between CH_2Cl_2 (10 mL), and HCl (aq) (1 M, 10 mL), the chlorinated layer was separated through a phase separator and concentrated under reduced pressure. The residue was purified by flash silica chromatography, eluting with heptane to 20% ethyl acetate in heptane, to provide the title compound as a yellow solid (0.187 g, 74%). m.p. 70-72 °C. IR (neat, vmax) cm^{-1} 2928, 2214, 1604, 1452, 1256. ^1H NMR (500 MHz, $CDCl_3$) δ_H 7.36 (s, 1H, CH-6), 6.74 (s, 1H, CH-3), 5.78 (tt, *J* = 3.8, 1.7 Hz, 1H, CH-17), 3.87 (s, 3H, CH_3-11), 2.53 (s, 3H, CH_3-9), 2.30 (m, 2H, CH_2-13), 2.20 (m, 2H, CH_2-16), 1.78-1.65 (m, 4H, CH_2s-14&15). ^{13}C NMR (126 MHz, $CDCl_3$) δ_C 159.9 (C4), 142.5 (C2), 135.6 (C12), 133.3 (CH-6), 132.3 (C5), 127.6 (CH-17), 118.7 (C7), 112.2 (CH-3), 104.1 (C1), 55.6 (CH_3-11), 28.6 (CH_2-13), 25.6 (CH-16), 22.8 (CH_2-14/15), 22.0 (CH_2-14/15) 20.6 (CH_3-9). HRMS-ESI *m/z* $[M+Na]^+$ calculated for $C_{15}H_{17}NNaO$ 250.1202, found 250.1206. LCMS - Analytical UPLC 2-98% MeCN:Water (0.1% TFA), tR 0.95 min, $[M+H]^+$ 228.4 *m/z*, (95%).

5-(Cyclopenten-1-yl)-4-methoxy-2-methyl-benzonitrile (156)

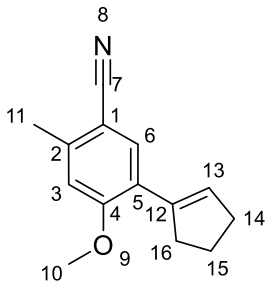

Palladium (II) acetate (0.006 g, 0.03 mmol), and 2-dicyclohexylphosphino-2'-6'-diisopropoxybiphenyl (0.025 g, 0.06 mmol) was added to a mixture of K_3PO_4 (0.59 g, 2.76 mmol), 5-bromo-4-methoxy-2-methyl-benzonitrile (**139**) (0.25 g, 1.11 mmol) and cyclopenten-1-yl boronic acid (0.19 g, 1.66 mmol) in toluene (5 mL) and heated to 100 °C for 16 h. The reaction mixture was partitioned between CH_2Cl_2 (10 mL), and HCl (aq) (1 M, 10 mL), the chlorinated layer was separated through a phase separator and concentrated under reduced pressure. The residue was purified by flash silica chromatography, eluting with heptane to 20% ethyl acetate in heptane, to provide the title compound as a yellow solid (0.212 g, 89%). m.p. 106-107 °C. IR (neat, vmax) cm^{-1} 2902, 2211, 1601, 1457, 1251. ^1H NMR (500 MHz, $CDCl_3$) δ_H 7.48 (s, 1H, CH-6), 6.79 (s, 1H, CH-3), 6.48-6.45, (m, 1H, CH-13), 3.93 (s, 3H, CH_3-11), 2.76-2.69 (m, 2H, CH_2-16), 2.61-2.54 (m, 5H, CH_2-14 & CH_3-9), 1.98 (tt, *J* = 8.3, 7.0 Hz, CH_2-15). ^{13}C NMR (126 MHz, $CDCl_3$) δ_C 160.4 (C4), 142.1 (C2), 137.2 (C12), 132.5 (CH-6), 132.1 (CH-13), 125.0 (C5), 118.8 (C7), 112.2 (CH-3), 104.1 (C1), 55.5 (CH_3-11), 35.0 (CH_2-16), 34.0 (CH_2-14), 22.7 (CH_2-15), 20.6 (CH_3-9). HRMS-ESI *m/z* $[M+Na]^+$ calculated for $C_{14}H_{15}NNaO$ 236.1046, found 236.1043. LCMS - Analytical UPLC 2-98% MeCN:Water (0.1% TFA), tR 0.92 min, $[M+H]^+$ 214.4 *m/z*, (95%).

5-[(E)-2-Cyclopropylvinyl]-4-methoxy-2-methyl-benzonitrile (157)

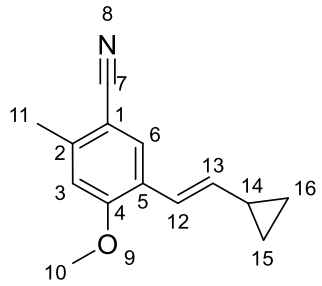

Palladium (II) acetate (0.006 g, 0.03 mmol), and 2-dicyclohexylphosphino-2'-6'-diisopropoxybiphenyl (0.025 g, 0.06 mmol) was added to a mixture of K_3PO_4 (0.59 g, 2.76 mmol), 5-bromo-4-methoxy-2-methyl-benzonitrile (**139**) (0.25 g, 1.11 mmol) and [(E)-2-cyclopropylvinyl]-(1,1,2,2-tetramethylpropoxy)boronic acid (0.35 g, 1.66 mmol) in toluene (5 mL) and water (0.5 mL) and heated to 100 °C for 16 h. The reaction mixture was partitioned between CH_2Cl_2 (10 mL), and HCl (aq) (1 M, 10 mL), the chlorinated layer was separated through a phase separator and concentrated under reduced pressure. The residue was purified by flash silica chromatography, eluting with heptane to 20% ethyl acetate in heptane, to provide the title compound as a yellow solid (0.209 g, 88%). m.p. 60-62 °C. IR (neat, vmax) cm^{-1} 2213, 1606, 1459, 1259. ^1H NMR (500 MHz, $CDCl_3$) δ_H 7.55 (s, 1H, CH-6), 6.74 (s, 1H, CH-3), 6.67, (d, *J* = 15.8 Hz, 1H, CH-12), 5.73 (dd, *J* = 15.8, 9.0 Hz, 1H, CH-13), 3.90 (s, 3H, CH_3-11), 2.52 (s, 3H, CH_3-9), 1.60 (m, 1H, CH-14), 0.91-0.79 (m, 2H, CH_2-15 & 16), 0.59-0.50 (m, 2H, CH_2-15&16). ^{13}C NMR (126 MHz, $CDCl_3$) δ_C 158.9 (C4), 141.9 (C2), 137.4 (CH-13), 130.0 (CH-6), 125.7 (C5), 120.0 (CH-12), 118.7 (C7), 112.1 (CH-3), 104.4 (C1) , 55.6 (CH_3-11), 20.7 (CH_3-9), 15.0 (CH-14), 7.5 (CH_2-15&16). HRMS-ESI *m/z* $[M+Na]^+$ calculated for $C_{14}H_{15}NNaO$ 236.1046, found 236.1048. LCMS - Analytical UPLC 2-98% MeCN:Water (0.1% TFA), tR 0.89 min, $[M+H]^+$ 214.4 *m/z*, (95%).

5-Cyclohexyl-4-methoxy-2-methyl-benzonitrile (158)

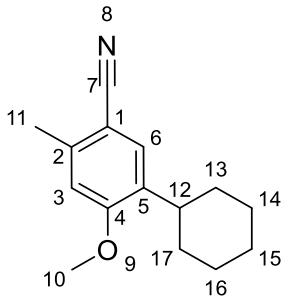

Triethylsilane (0.06 mL, 0.03 mmol) was added dropwise to a suspension of 5-(cyclohexen-1-yl)-4-methoxy-2-methyl-benzonitrile (**155**) (0.16 g, 0.70 mmol and palladium on carbon (10%, 0.08 g, 0.07 mmol) in ethanol (5 mL) stirred at rt for 16 h. The reaction mixture was filtered through a pad of celite and washed through with ethanol (2 × 10 mL), the filtrate was concentrated under reduced pressure. The residue was purified by flash silica chromatography, eluting with heptane to 20% ethyl acetate in heptane, to provide the title compound as a white solid (0.145 g, 90%). m.p. 94-96 °C. IR (neat, vmax) cm^{-1} 2924, 2214, 1603, 1455, 1249. ^{1}H NMR (500 MHz, $CDCl_3$) δ_H 7.39 (s, 1H, CH-6), 6.73 (s, 1H, CH-3), 3.88 (s, 3H, CH_3-11), 2.89 (tt, *J* = 11.0, 3.1 Hz, 1H, CH-12), 2.52 (s, 3H, CH_3-9), 1.88-1.78 (m, 5H, CH_2s 13/17/14/16/15), 1.48-1.20 (m, 4H, CH_2s 13/17/14/16), 1.03-0.94 (m, 1H, CH_2-15). ^{13}C NMR (126 MHz, $CDCl_3$) δ_C 159.9 (C4), 141.4 (C2), 134.9 (C5), 130.7 (CH-6), 119.1 (C7), 111.6 (CH-3), 104.0 (C1), 55.5 (CH_3-11), 36.3 (CH-12), 33.0 (CH_2s-13/17), 26.9 (CH_2s-13/14/16), 26.2 (CH_2s-13/14/16), 20.5 (CH_3-9). HRMS-ESI *m/z* $[M+Na]^+$ calculated for $C_{15}H_{19}NNaO$ 252.1359, found 252.1358. LCMS - Analytical UPLC 2-98% MeCN:Water (0.1% TFA), tR 1.01 min, $[M+H]^+$ 230.4 *m/z*, (95%).

5-Cyclopentyl-4-methoxy-2-methyl-benzonitrile (159)

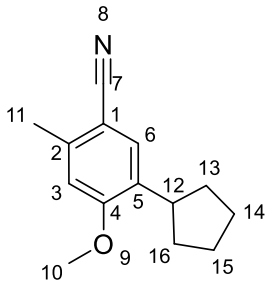

Triethylsilane (0.06 mL, 0.03 mmol) was added dropwise to a suspension of 5-(cyclopenten-1-yl)-4-methoxy-2-methyl-benzonitrile (**156**) (0.15 g, 0.70 mmol and palladium on carbon (10%, 0.08 g, 0.07 mmol) in ethanol (5 mL) stirred at rt for 16 h. The reaction mixture was filtered through a pad of celite and washed through with ethanol (2 × 10 mL), the filtrate was concentrated under reduced pressure. The residue was purified by flash silica chromatography, eluting with heptane to 20% ethyl acetate in heptane, to provide the title compound as a colourless oil (0.12 g, 79%). IR (neat, vmax) cm^{-1} 2950, 2217, 1608, 1501, 1458, 1251. ^{1}H NMR (500 MHz, $CDCl_3$) δ_H 7.41 (s, 1H, CH-6), 6.73 (s, 1H, CH-3), 3.88 (s, 3H, CH_3-11), 3.25 (p, *J* = 8.6, 2H, CH-12), 2.06-1.97 (m, 2H, CH_2-13/16), 1.85-1.64 (m, 4H, CH_2-14&15), 1.56-1.46 (m, 2H, CH_2-13/16). ^{13}C NMR (126 MHz, $CDCl_3$) δ_C 160.6 (C4), 141.5 (C2), 133.3 (C5), 130.6 (CH-6), 119.1 (C7), 111.7 (CH-3), 103.9 (C1), 55.5 (CH_3-11), 38.6 (CH-12), 32.7 (CH_2s-13&16), 25.2 (CH_2s-14&15), 20.5 (CH_3-9). HRMS-ESI *m/z* $[M+Na]^+$ calculated for $C_{14}H_{17}NNaO$ 238.1202, found 238.1202. LCMS - Analytical UPLC 2-98% MeCN:Water (0.1% TFA), tR 0.96 min, $[M+H]^+$ 216.4 *m/z*, (95%).

5-Cyclopentyl-4-methoxy-2-methyl-benzonitrile (160)

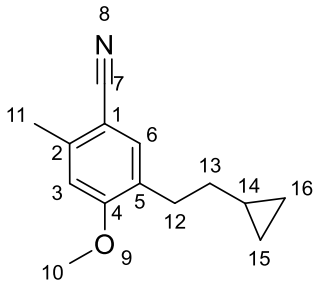

Triethylsilane (0.06 mL, 0.03 mmol) was added dropwise to a suspension of 5-(2-cyclopropylethyl)-4-methoxy-2-methyl-benzonitrile (**157**) (0.15 g, 0.70 mmol and palladium on carbon (10%, 0.08 g, 0.07 mmol) in ethanol (5 mL) stirred at rt for 16 h. The reaction mixture was filtered through a pad of celite and washed through with ethanol (2 × 10 mL), the filtrate was concentrated under reduced pressure. The residue was purified by flash silica chromatography, eluting with heptane to 20% ethyl acetate in heptane, to provide the title compound as a colourless oil (0.125 g, 83%). IR (neat, vmax) cm^{-1} 2926, 2217, 1609, 1503, 1459, 1255. ^{1}H NMR (500 MHz, $CDCl_3$) δ_H 7.36 (s, 1H, CH-6), 6.72 (s, 1H, CH-3), 3.88 (s, 3H, CH_3-11), 2.68 (t, *J* = 7.6 Hz, 2H, CH_2-12), 2.53 (s, 3H, CH_3-9), 1.49-1.42 (m, 2H, CH_2-13), 0.74-0.64 (m, 1H, CH-14), 0.46-0.41 (m, 2H, CH_2-15/16), 0.06-0.01 (m, 2H, CH_2-15/16). ^{13}C NMR (126 MHz, $CDCl_3$) δ_C 160.6 (C4). 141.9 (C2), 133.4 (CH-6), 129.6 (C5), 119.0 (C7), 111.7 (CH-3), 103.7 (C1), 55.5 (CH_3-11), 34.4 (CH_2-13), 29.6 (CH_2-12), 20.6 (CH_3-9), 10.8 (CH-14), 4.5 (CH_2-15/16). HRMS-ESI *m/z* $[M+Na]^+$ calculated for $C_{14}H_{17}NNaO$ 238.1202, found 238.1203. LCMS - Analytical UPLC 2-98% MeCN:Water (0.1% TFA), tR 0.94 min, $[M+H]^+$ 216.4 *m/z*, (> 95%).

5-Cyclohexyl-4-hydroxy-2-methyl-benzonitrile (161)

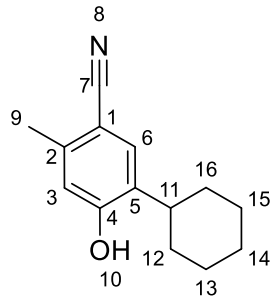

Iodo(trimethyl)silane (0.12 mL, 0.82 mmol) was added to a solution of 5-cyclohexyl-4-methoxy-2-methyl-benzonitrile (**158**) (0.075 g, 0.33 mmol) in acetonitrile (1 mL). The reaction mixture was sealed and heated to 90 °C in the microwave (Biotage Initiator®) for 1 h. The cooled reaction mixture was partitioned between sodium thiosulfate (aq) (0.1 M, 10 mL) and CH_2Cl_2 (2 x 20 mL). The chlorinated layers were separated through a phase separator and concentrated under reduced pressure. The residue was purified by flash silica chromatography eluting with heptane to 40% ethyl acetate in heptane to provide the title compound as a white solid (0.05 g, 71%). m.p. 158-159 °C. IR (neat, vmax) cm^{-1} 3249, 2927, 2223, 1609, 1411, 1258. ^1H NMR (500 MHz, $CDCl_3$) δ_H 7.41 (s, 1H, CH-6), 6.69 (s, 1H, CH-3), 5.29 (s, 1H, OH-10), 2.77 (tt, *J* = 11.5, 3.1 Hz, 1H, CH-11), 2.47 (s, 3H, CH_3-9), 1.92-1.84 (m, 4H, CH_2-12/16), 1.83-1.76 (m, 1H, CH-14), 1.49-1.23 (m, 5H, CH_2-13/15&CH-14). ^{13}C NMR (126 MHz, $CDCl_3$) δ_C 156.4 (C4), 141.2 (C2), 132.3 (C5), 131.7 (CH-6), 118.9 (C7), 116.9 (CH-3), 104.7 (C1), 36.7 (CH-11), 32.8 (CH_2-12/16), 26.8 (CH_2-13/15), 26.1 (CH_2-14), 20.0 (CH_3-9). HRMS-ESI *m/z* $[M+Na]^+$ calculated for $C_{14}H_{17}NNaO$ 238.1202, found 238.1204. LCMS - Analytical UPLC 2-98% MeCN:Water (0.1% TFA), tR 0.85 min, $[M+H]^+$ 216.4 *m/z* (95%).

5-Cyclopentyl-4-hydroxy-2-methyl-benzonitrile (162)

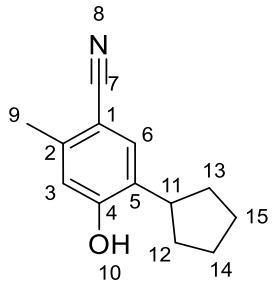

Iodo(trimethyl)silane (0.12 mL, 0.87 mmol) was added to a solution of 5-cyclopentyl-4-methoxy-2-methyl-benzonitrile (**159**) (0.075 g, 0.35 mmol) in acetonitrile (1 mL). The reaction mixture was sealed and heated to 90 °C in the microwave (Biotage Initiator®) for 1 h. The cooled reaction mixture was partitioned between sodium thiosulfate (aq) (0.1 M, 10 mL) and CH_2Cl_2 (2 x 20 mL). The chlorinated layers were separated through a phase separator and concentrated under reduced pressure. The residue was purified by flash silica chromatography eluting with heptane to 40% ethyl acetate in heptane to provide the title compound as a white solid (0.07 g, 99%). m.p. 96-97 °C. IR (neat, vmax) cm^{-1} 3254, 2949, 2224, 1609, 1412, 1286. ^1H NMR (500 MHz, $CDCl_3$) δ_H 7.43 (s, 1H, CH-6), 6.70 (s, 1H, CH-3), 5.36 (s, 1H, OH-10), 3.17 (p, *J* = 8.5 Hz, 1H, CH-11), 2.47 (s, 3H, CH_3-9), 2.11-2.03 (m, 2H, CH_2-12/15), 1.88-1.67 (m, 4H, CH_2-12/15, 13/14), 1.62-1.53 (m, 2H, CH_2-13/14). ^{13}C NMR (126 MHz, $CDCl_3$) δ_C 157.1 (C4), 141.4 (C2), 131.6 (CH-6), 130.7 (C5), 118.9 (C7), 116.9 (CH-3), 104.5 (C1), 38.5 (CH-11), 32.6 (CH_2-12&15), 25.2 (CH2-13&14), 20.0 (CH_3-9). HRMS-ESI *m/z* $[M+Na]^+$ calculated for $C_{13}H_{15}NNaO$ 224.1046, found 224.1044. LCMS - Analytical UPLC 2-98% MeCN:Water (0.1% TFA), tR 0.80 min, $[M+H]^+$ 202.4 *m/z* (> 95%).

3-Chloro-5-cyclohexyl-4-hydroxy-2-methyl-benzonitrile (163)

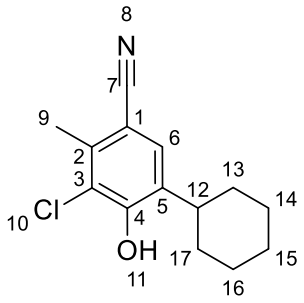

Sulfuryl chloride (0.04 mL, 0.44 mmol) was added to a solution of 5-cyclohexyl-4-hydroxy-2-methyl-benzonitrile (**161**) (0.04 g, 0.19 mmol) in diethyl ether (2 mL) and stirred for 16 h. The reaction mixture was partitioned between HCl (aq) (1 M, 5 mL) and CH_2Cl_2 (2 x 10 mL). The chlorinated layers were separated through a phase separator and concentrated under reduced pressure. The residue was purified by flash silica chromatography eluting with heptane to 40% ethyl acetate in heptane to provide the title compound as a white solid (0.031 g, 67%). m.p. 165-166 °C. IR (neat, vmax) cm^{-1} 3289, 2919, 2229, 1601, 1415, 1163. ^1H NMR (500 MHz, $CDCl_3$) δ_H 7.37 (s, 1H, CH-6), 6.13 (s, 1H, OH-11), 2.93 (tt, *J* = 11.7, 2.9 Hz, 1H, CH-12), 2.57 (s, 3H, CH_3-9), 1.91-1.85 (m, 4H, CH_2-13/17/14/16), 1.82-1.76 (m, 1H, CH_2-15), 1.50-1.22 (m, 5H, CH_2-13/14/15/16/17). ^{13}C NMR (126 MHz, $CDCl_3$) δ_C 152.4 (C4), 137.9 (C2), 133.8 (C5), 129.6 (CH-6), 121.1 (C3), 118.3 (C7), 105.4 (C1), 37.5 (CH-12), 32.6 (CH_2s-13&17), 26.7 (CH_2s-14&16), 26.1 (CH_2s-15), 18.8 (CH_2-15). HRMS-ESI *m/z* $[M-H]^-$ calculated for $C_{14}H_{15}{}^{35}ClNO$ 248.0848, found 248.0840. LCMS - Analytical UPLC 2-98% MeCN:Water (0.1% Formic), tR 0.93 min, poor ionisation, no mass ion observed (95%).

3-Chloro-5-cyclopentyl-4-hydroxy-2-methyl-benzonitrile (164)

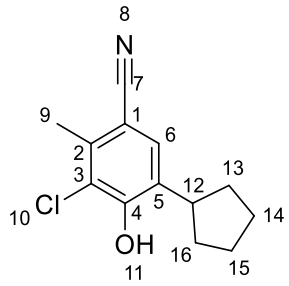

Sulfuryl chloride (0.04 mL, 0.44 mmol) was added to a solution of 5-cyclopentyl-4-hydroxy-2-methyl-benzonitrile (**162**) (0.04 g, 0.2 mmol) in diethyl ether (2 mL) and stirred for 16 h. The reaction mixture was partitioned between HCl (aq) (1 M, 5 mL) and CH_2Cl_2 (2 x 10 mL). The chlorinated layers were separated through a phase separator and concentrated under reduced pressure. The residue was purified by flash silica chromatography eluting with heptane to 40% ethyl acetate in heptane to provide the title compound as a white solid (0.028 g, 60%). m.p. 102-104 °C. IR (neat, vmax) cm^{-1} 3294, 2943, 2227, 1602, 1473, 1318, 1164. ^1H NMR (500 MHz, $CDCl_3$) δ_H 7.37 (s, 1H, CH-6), 6.13 (s, 1H, OH-11), 3.27 (p, *J* = 8.5 Hz, 1H, CH-12), 2.55 (s, 3H, CH_3-9), 2.09-2.01 (m, 2H, CH_2-13/16), 1.59-1.42 (m, 4H, CH_2-13/16/14/15), 1.59-1.49 (m, 2H, CH_2-14/15). ^{13}C NMR (126 MHz, $CDCl_3$) δ_C 153.0 (C4), 138.0 (C2), 132.4 (C5), 129.7 (CH-6), 121.1 (C3), 118.3 (C7), 105.2 (C1), 39.5 (CH-12), 32.5 (CH_2-13&16), 25.2 (CH_2-14&15), 18.8 (CH_3-9). HRMS-ESI *m/z* $[M-H]^-$ calculated for $C_{13}H_{13}{}^{35}ClNO$ 234.0691, found 234.0683. LCMS - Analytical UPLC 2-98% MeCN:Water (0.1% Formic), tR 0.88 min, poor ionisation, no mass ion observed (95%).

5-[(E)-2-Cyclopropylvinyl]-4-hydroxy-2-methyl-benzonitrile (165)

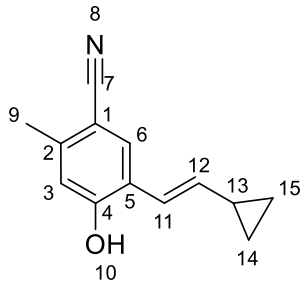

Palladium (II) acetate (0.013 g, 0.06 mmol), and 2-dicyclohexylphosphino-2'-6'-diisopropoxybiphenyl (0.055 g, 0.12 mmol) was added to a mixture of K_3PO_4 (1.25 g, 5.90 mmol), 5-bromo-4-hydroxy-2-methyl-benzonitrile (**85**) (0.50 g, 2.36 mmol) and [(E)-2-cyclopropylvinyl]-(1,1,2,2-tetramethylpropoxy)boronic acid (0.73 mL, 3.54 mmol) in toluene (8 mL) and water (0.8 mL) and heated to 100 °C for 16 h. The reaction mixture was partitioned between CH_2Cl_2 (10 mL), and HCl (aq) (1 M, 10 mL), the chlorinated layer was separated through a phase separator and concentrated under reduced pressure. The residue was purified by flash silica chromatography, eluting with heptane to 20% ethyl acetate in heptane, to provide the title compound as a yellow solid (0.226 g, 48%). m.p. 109-111 °C. IR (neat, vmax) cm^{-1} 3309, 2221, 1602, 1413, 1265. ^{1}H NMR (500 MHz, $CDCl_3$) δ_H 7.49 (s, 1H, CH-6), 6.70 (s, 1H, CH-3), 6.53, (d, *J* = 15.9 Hz, CH-11), 5.87 (br s, 1H, OH-10), 5.70 (dd, *J* = 15.9, 9.1 Hz, 1H, CH-12), 2.44 (s, 3H, CH_3-9), 1.65-1.57 (m, 1H, CH-13), 0.90-0.84 (m, 2H, CH_2-14/15), 0.58-0.53 (m, 2H, CH_2-14/15). ^{13}C NMR (126 MHz, $CDCl_3$) δ_C 156.1 (C4), 141.8 (C2), 138.8 (CH-12), 131.4 (CH-6), 124.0 (C5), 119.5 (CH-11), 118.7 (C7), 117.3 (CH-3), 104.2 (C1), 20.1 (CH_3-9), 15.0 (CH-13), 7.55 (CH_2-14/15). LCMS - Analytical MDAP LCMS 30-95% MeCN:Water (0.1% Formic), tR 17.18 min, $[M-H]^-$ 198.1 *m/z*, (95%).

5-Cyclopentyl-4-hydroxy-2-methyl-benzonitrile (166)

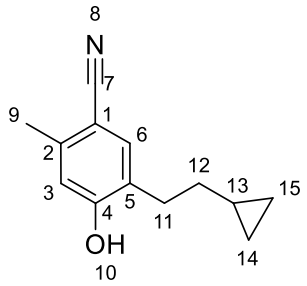

Triethylsilane (0.17 mL, 1.05 mmol) was added dropwise to a suspension of 5-[(E)-2-cyclopropylvinyl]-4-hydroxy-2-methyl-benzonitrile (**165**) (0.20 g, 1.00 mmol and palladium on carbon (10%, 0.010 g, 0.10 mmol) in ethanol (5 mL) stirred at rt for 16 h. The reaction mixture was filtered through a pad of celite and washed through with ethanol (2 × 10 mL), the filtrate was concentrated under reduced pressure. The residue was purified by flash silica chromatography, eluting with heptane to 20% ethyl acetate in heptane, then further purified by reverse-phase chromatography, eluting with 60% methanol in water to 95% methanol in water to provide the title compound as a white solid (0.060 g, 30%). m.p. 92-93 °C. IR (neat, vmax) cm^{-1} 3290, 2221, 1608, 1411, 1263. ^{1}H NMR (500 MHz, $CDCl_3$) δ_H 7.36 (s, 1H, CH-6), 6.69 (s, 1H, CH-3), 5.48 (br s, 1H, OH-10), 2.67 (t, *J* = 7.5 Hz, 2H, CH_2-11), 2.45 (s, 3H, CH_3-9), 1.52-1.46 (m, 2H, CH_2-12), 0.73-0.65 (m, 1H, CH-13), 0.47-0.43 (m, 2H, CH_2-14&15), 0.07-0.03 (m, 2H, CH_2-14'&15'). ^{13}C NMR (126 MHz, $CDCl_3$) δ_C 157.3 (C4), 141.7 (C2), 134.5 (CH-6), 127.0 (C5), 118.7 (C7), 116.9 (CH-3), 104.3 (C1), 34.4 (CH_2-12), 29.3 (CH_2-11), 20.03 (CH_3-9), 10.6 (CH-13), 4.55 (CH_2-14&15). HRMS-ESI *m/z* $[M+Na]^+$ and $[M-H]^-$ poor ionisation LRMS only EI^+ 201 *m/z*. LCMS - Analytical MDAP 30-95% MeCN:Water (0.1% Formic), tR 18.25 min, [M-H] 200.1 *m/z*, (95%).

3-Chloro-5-(2-cyclopropylethyl)-4-hydroxy-2-methyl-benzonitrile (167)

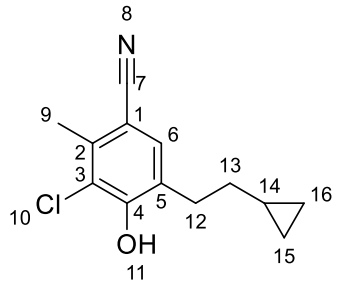

Sulfuryl chloride (0.09 mL, 1.12 mmol) was added to a solution of 5-(2-cyclopropylethyl)-4-hydroxy-2-methyl-benzonitrile (**166**) (0.045 g, 0.22 mmol) in diethyl ether (2 mL) and stirred for 16 h. The reaction mixture was partitioned between HCl (aq) (1 M, 5 mL) and CH_2Cl_2 (2 x 10 mL). The chlorinated layers were separated through a phase separator and concentrated under reduced pressure. The residue was purified by flash silica chromatography eluting with heptane to 40% ethyl acetate in heptane to provide the title compound as a white solid (0.048 g, 91%). m.p. 89-91 °C. IR (neat, vmax) cm^{-1} 3334, 2922, 2223, 1419, 1242, 1169. ^{1}H NMR (500 MHz, $CDCl_3$) δ_H 7.32 (s, 1H, CH-6), 6.10 (s, 1H, OH-11), 2.74 (t, *J* = 7.6 Hz, 2H, CH_2-12), 2.55 (s, 3H, CH_3-9), 1.51-1.46 (m, 2H, CH-14), 0.72-0.64 (m, 1H, CH-14), 0.46-0.40 (m, 2H, CH_2-14&15), 0.08-0.01 (m, 2H, CH_2-14'&15').^{13}C NMR (126 MHz, $CDCl_3$) δ_C 153.1 (C4), 138.3 (C2), 132.4 (CH-6), 128.6 (C5), 121.0 (C3), 118.1 (C7), 105.1 (C1), 34.1 (CH_2-13), 30.2 (CH_2-12), 18.8 (CH_3-9), 10.6 (CH-14), 4.5 (CH_2-15&16). HRMS-ESI *m/z* $[M-H]^-$ calculated for $C_{13}H_{13}{}^{35}ClNO$ 234.0691, found 234.0681. LCMS - Analytical MDAP 30-95% MeCN:Water (0.1% Formic), tR 20.66 min, $[M-H]^-$ 234.05 *m/z*, (95%).

5-(4,4-Diethoxybutyl)-4-methoxy-2-methyl-benzonitrile (168)

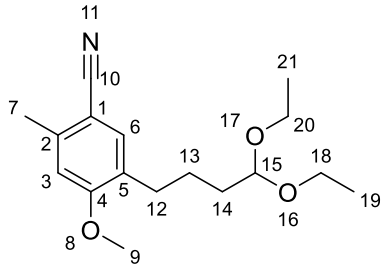

A solution of 1 M borane in THF (1.00 mL, 1.00 mmol) was added dropwise to 4,4-diethoxybut-1-ene (0.56 mL, 3.32 mmol) at 0 °C. This solution was warmed to rt and stirred for 15 min. The solution was quenched with the addition of water (1 mL) and diluted with toluene (5 mL). Potassium phosphate tribasic (1.17 g, 5.53 mmol), 5-bromo-4-methoxy-2-methyl-benzonitrile (**139**) (0.50 g, 2.21 mmol), palladium (II) acetate (0.012 g, 0.06 mmol) and 2-dicyclohexylphosphino-2'-6'-diisopropoxybiphenyl (0.05 g, 0.11 mmol) were added. The reaction mixture was sealed and heated 50 °C for 16 h. The cooled reaction mixture was filtered through a pad of celite, the filtrate partitioned between water (10 mL) and ethyl acetate (20 mL). The organic layer was separated, dried over $MgSO_4$, filtered and concentrated under vacuum. The residue was purified by flash silica chromatography, eluting with petroleum ether to 15% ethyl acetate, followed by further purification by reverse-phase chromatography eluting with 60% MeOH in water to 100% MeOH to provide the title compound as a colourless oil (0.376 g, 58%). IR (neat, vmax) cm^{-1} 2932, 2218, 1610, 1503, 1459, 1256. ^{1}H NMR (500 MHz, $CDCl_3$) δ_H 7.31 (s, 1H, CH-6), 6.69 (s, 1H, CH-3), 4.48 (m, 1H, CH-15), 3.84 (s, 3H, CH_3-9), 3.62 (m, 2H, CH_2-18/19), 3.47 (m, 2H, CH_2-18/19), 2.57 (m, 2H, CH_2-12), 2.49 (s, 3H, CH_3-7), 1.62 (m, 4H, CH_2s-13/14), 1.19 (t, *J* = 7.0 Hz, 6H, CH_3's-20/21). ^{13}C NMR (126 MHz, $CDCl_3$) δ_C 160.6 (C4), 142.0 (C2), 133.3 (CH-6), 129.3 (C5), 118.9 (C10), 111.7 (CH-3), 103.8 (C1), 102.7 (CH-15), 61.0 (CH_2-18/19), 55.4 (CH_3-9), 33.2 (CH_2-14), 29.1 (CH_2-12), 24.5 (CH_2-13), 20.6 (CH_3-7), 15.3 (CH_3-20/21). HRMS-ESI *m/z* $[M+Na]^+$ and $[M-H]^-$ poor ionisation LRMS only EI^+ 291 *m/z*. LCMS - Analytical MDAP 30-95% MeCN:Water (0.1% Formic), tR 21.79 min, no ionisation (95%).

5-(4,4-difluorobutyl)-4-methoxy-2-methyl-benzonitrile (169)

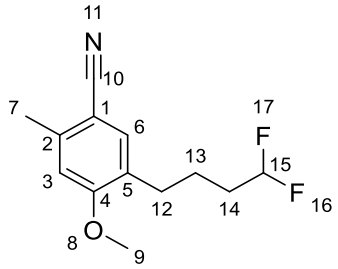

HCl (aq) (1 M, 1.17 mL, 5.83 mmol) was added to a solution of 5-(4,4-diethoxybutyl)-4-methoxy-2-methyl-benzonitrile (**168**) (0.17 g, 0.58 mmol) in tetrahydrofuran (5 mL) and stirred at rt for 2 h. The reaction mixture was diluted with water (20 mL) and extracted with ethyl acetate (2 × 30 mL), the organics were separated, dried over $MgSO_4$, filtered and concentrated under reduced pressure. The residue was dissolved in CH_2Cl_2 (3 mL) and transferred to a PTFE flask, a solution of bis(2-methoxyethyl)aminosulfur trifluoride (50% solution in toluene, 0.37 mL, 0.99 mmol) was added and the reaction sealed. Ethanol (5 µL) was added and the reaction was stirred at rt for 16 h. The reaction mixture was quenched with the addition of saturated $NaHCO_3$ (aq) (30 mL) and stirred at rt for 1 h. The resulting biphasic mixure was partitioned between water (20 mL) and CH_2Cl_2 (2 × 50 mL). The combined chlorinated layers were dried over $MgSO_4$, filtered and concentrated under vacuum. The residue was purified by flash silica chromatography, eluting with petroleum ether to 15% ethyl acetate to provide the title compound as a waxy white solid (0.094 g, 67%). m.p. 64-66 °C. IR (neat, vmax) cm^{-1} 2945, 2217, 1610, 1502, 1456, 1257. ^1H NMR (500 MHz, $CDCl_3$) δ_H 7.30 (s, 1H, CH-6), 6.72 (s, 1H, CH-3), 5.80 (tt, *J* = 56.8 Hz, 4.4 Hz, 1H, CH-15), 3.85 (s, 3H, CH_3-11), 2.60 (t, *J* = 7.6 Hz, 2H, CH_2-12), 2.50 (s, 3H, CH_3-9), 1.90-1.62 (m, 4H, CH_2s-13/14). ^{13}C NMR (126 MHz, $CDCl_3$) δ_C 160.6 (C4), 142.4 (C2), 133.4 (CH-6), 128.4 (C5), 118.7 (C7), 117.1 (t, *J* = 238.6 Hz, CH-15), 111.9 (CH-3), 103.9 (C1), 55.5 (CH_3-11), 33.5 (t, *J* = 21.2 Hz, CH_2-14), 28.8 (CH_2-12), 21.9 (t, *J* = 5.7 Hz, CH_2-13), 20.6 (CH_3-9). HRMS-ESI *m/z* $[M+Na]^+$ and $[M-H]^-$ poor ionisation LRMS only EI^+ 239 *m/z*. LCMS - Analytical MDAP 30-95% MeCN:Water (0.1% Formic), tR 19.87 min, no ionisation (95%).

5-(4,4-difluorobutyl)-4-hydroxy-2-methyl-benzonitrile (170)

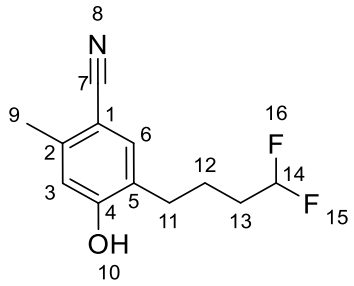

Chloro(trimethyl)silane (0.05 mL, 0.37 mmol) was added to a suspension of 5-(4,4-difluorobutyl)-4-methoxy-2-methyl-benzonitrile (169) (0.022 g, 0.09 mmol) and sodium iodide (0.20 g, 1.34 mmol) in acetonitrile (1 mL). The reaction mixture was sealed and heated to 80 °C for 16 h. The cooled reaction mixture was partitioned between sodium thiosulfate (aq) (0.1 M, 100 mL) and ethyl acetate (2 x 100 mL). The combined organic layers were dried over $MgSO_4$, filtered and concentrated under reduced pressure. The residue was purified by flash silica chromatography eluting with heptane to 30% ethyl acetate in heptane to provide the title compound as a white solid (0.016 g, 77%). m.p. 82-83 °C. IR (neat, vmax) cm^{-1} 3275, 2947, 2226, 1610, 1412, 1268. ^{1}H NMR (500 MHz, $CDCl_3$) δ_H 7.32 (s, 1H, CH-6), 7.24 (br s, 1H, OH-10), 6.74 (s, 1H, CH-3), 5.82 (tt, *J* = 56.8 Hz, 4.3 Hz, 1H, CH-14), 2.63 (t, *J* = 7.5 Hz, 2H, CH_2-11), 2.43 (s, 3H, CH_3-9), 1.92-1.69 (m, 4H, CH_2s-13/14). ^{13}C NMR (126 MHz, $CDCl_3$) δ_C 158.3 (C4), 142.1 (C2), 134.4 (CH-6), 126.7 (C5), 118.8 (C7), 117.2 (t, *J* = 239 Hz, C-14), 116.9 (CH-3), 103.2 (C1), 33.5 (t, *J* = 20.9 Hz, CH_2-13), 28.6 (CH_2-11), 21.9 (t, *J* = 5.5 Hz, CH_2-12), 14.1 (CH_3-9). HRMS-ESI *m/z* $[M-H]^-$ calculated for $C_{12}H_{12}F_2NO$ 224.0892, found 224.0887. LCMS - Analytical MDAP 30-95% MeCN:Water (0.1% Formic), tR 16.83 min, $[M-H]^-$ 223.95 *m/z* (95%).

3-Chloro-5-(4,4-difluorobutyl)-4-hydroxy-2-methyl-benzonitrile (171)

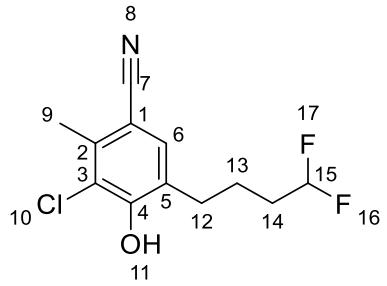

Sulfuryl chloride (0.02 mL, 0.26 mmol) was added to a solution of 5-(4,4-difluorobutyl)-4-hydroxy-2-methyl-benzonitrile (**170**) (0.02 g, 0.09 mmol) in diethyl ether (1 mL) and stirred for 16 h. The reaction mixture was partitioned between HCl (aq) (1 M, 5 mL) and CH_2Cl_2 (2 x 10 mL). The chlorinated layers were separated through a phase separator and concentrated under reduced pressure. The residue was purified by flash silica chromatography eluting with heptane to 40% ethyl acetate in heptane to provide the title compound as a white solid (0.009 g, 33%). m.p. 91-92 °C. ^{1}H NMR (500 MHz, $CDCl_3$) δ_H 7.31 (s, 1H, CH-6), 6.15 (s, 1H, OH-11), 5.83 (tt, *J* = 56.6 Hz, & 4.3 Hz, 1H, CH-15), 2.70 (t, *J* = 7.5 Hz, 2H, CH_2-12), 2.56 (s, 3H, CH_3-9), 1.97-1.74 (m, 4H, CH_2-13&14). ^{13}C NMR (126 MHz, $CDCl_3$) δ_C 153.1 (C4), 138.9 (C2), 132.3 (CH-6), 127.4 (C5), 117.8 (C7), 117.0 (t, *J* = 238 Hz, CH-15), 105.4 (C1), 33.5 (t, *J* = 21 Hz, CH_2-14), 29.4 (CH_2-12), 21.6 (CH_2-13), 18.8 (CH_3-9). HRMS-ESI *m/z* $[M-H]^-$ calculated for $C_{12}H_{11}{}^{35}ClF_2NO$ 258.0503, found 258.0495. LCMS - Analytical MDAP 30-95% MeCN:Water (0.1% Formic), tR 22.48 min, $[M-H]^-$ 257.95 *m/z*, (95%).

3-(5-Cyano-2-methoxy-4-methyl-phenyl)propanoate (172)

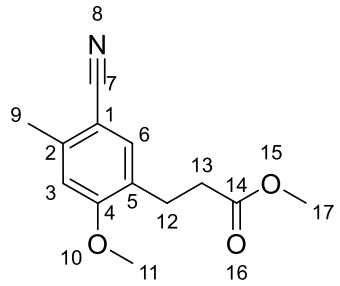

Palladium (II) acetate (0.062 g, 0.28 mmol), and 2-dicyclohexylphosphino-2'-6'-diisopropoxybiphenyl (0.26 g, 0.55 mmol) was added to a mixture of K_3PO_4 (7.04 g, 33.18 mmol), 5-bromo-4-methoxy-2-methyl-benzonitrile (**139**) (2.50 g, 11.06 mmol) and methyl 3-(4,4,5,5-tetramethyl-1,3,2-dioxaborolan-2-yl)propanoate (3.55 g, 16.59 mmol) in toluene (15 mL) and water (2 mL) and heated to 60 °C for 96 h. The reaction mixture was partitioned between CH_2Cl_2 (10 mL), and HCl (aq) (1 M, 10 mL), the chlorinated layer was separated through a phase separator and concentrated under reduced pressure. The residue was purified by flash silica chromatography, eluting with heptane to 20% ethyl acetate in heptane, to provide the title compound as a colourless oil (0.226 g, 48%). m.p. 109-111 °C. IR (neat, vmax) cm^{-1} 3345, 2219, 1612, 1437. ^1H NMR (500 MHz, $CDCl_3$) δ_H 7.34 (s, 1H, CH-6), 6.72 (s, 1H, CH-3), 3.86 (s, 3H, CH_3-11), 3.67 (s, 3H, CH_3-17), 2.88 (t, *J* = 7.6 Hz, 2H, CH_2-12), 2.57 (t, *J* = 7.6 Hz, 2H, CH_2-13), 2.50 (s, 3H, CH_3-9). ^{13}C NMR (126 MHz, $CDCl_3$) δ_C 173.2 (C14), 160.6 (C4), 142.7 (C2), 133.5 (CH-6), 127.4 (C5), 118.6 (C7), 111.8 (CH-3), 104.0 (C1), 55.5 (CH_3-11), 51.6 (CH_3-17), 33.4 (CH_2-12), 25.3 (CH_2-13), 20.6 (CH_3-9). HRMS-ESI *m/z* $[M+Na]^+$ and $[M-H]^-$ poor ionisation LRMS only EI^+ 233 *m/z*. LCMS - Analytical MDAP LCMS 30-95% MeCN:Water (0.1% Formic), tR 16.74 min, $[M+H]^+$ 233.95 *m/z*, (95%).

5-(3-Hydroxy-3-methyl-butyl)-4-methoxy-2-methyl-benzonitrile (173)

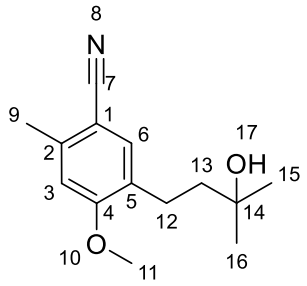

A solution of methylmagnesium bromide (3 M, 0.21 mL, 0.62 mmol), was added to a solution of 3-(5-cyano-2-methoxy-4-methyl-phenyl)propanoate (**172**) (0.07 g, 0.30 mmol) in tetrahydrofuran (0.5 mL) at -78 °C. The reaction mixture was warmed to rt and stirred for 2 h. The reaction mixture was quenched with the addition of HCl (aq), (1 M, 5 mL) and extracted with ethyl acetate (2 × 20 mL). The combined organic layers were dried over $MgSO_4$, filtered and concentrated under reduced pressure. The residue was purified by flash silica chromatography, eluting with heptane to 20% ethyl acetate in heptane, to provide the title compound as an orange oil (0.062 g, 89%). IR (neat, vmax) cm^{-1} 3436, 2968, 2218, 1610, 1503, 1461, 1256. ^{1}H NMR (500 MHz, $CDCl_3$) δ_H 7.31 (s, 1H, CH-3), 6.70 (s, 1H, CH-6), 3.84 (s, 3H, CH_3-11), 2.65-2.60 (m, 2H, CH_2-12), 2.47 (s, 3H, CH_3-9), 1.69-1.64 (m, 2H, CH_2-13), 1.26 (s, 6H, CH_3's-15&16). ^{13}C NMR (126 MHz, $CDCl_3$) δ_C 160.5 (C4), 142.0 (C2), 133.1 (CH-6), 129.7 (C5), 118.8 (C7), 111.8 (CH-3), 103.8 (C1), 70.8 (C14), 55.5 (CH_3-11), 43.3 (CH_2-13), 29.2 (CH_3's-15&16), 24.4 (CH_2-12), 20.5 (CH_3-9). HRMS-ESI *m/z* $[2M+Na]^+$ calculated for $C_{28}H_{38}N_2NaO_4$ 489.2724, found 489.2751 (dimer adduct). LCMS - Analytical MDAP LCMS 30-95% MeCN:Water (0.1% Formic), tR 14.99 min, $[M+Na]^+$ 257.00 *m/z*, (95%).

5-(3-Fluoro-3-methyl-butyl)-4-methoxy-2-methyl-benzonitrile (174)

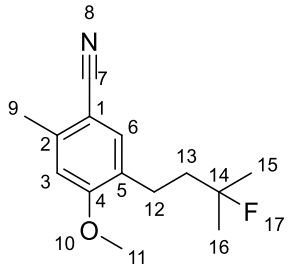

A solution of bis(2-methoxyethyl)aminosulfur trifluoride (50% solution in toluene, 0.37 mL, 0.99 mmol) was added to a solution of 5-(3-hydroxy-3-methyl-butyl)-4-methoxy-2-methyl-benzonitrile (**173**) (0.40 g, 1.71 mmol) in CH_2Cl_2 (8 mL) and the reaction was sealed. Ethanol (5 µL) was added and the reaction was stirred at rt for 16 h. The reaction mixture was quenched with the addition of saturated $NaHCO_3$ (aq) (30 mL) and stirred at rt for 1 h. The resulting biphasic mixture was partitioned between water (20 mL) and CH_2Cl_2 (2 × 50 mL). The combined chlorinated layers were dried over $MgSO_4$, filtered and concentrated under vacuum. The residue was purified by flash silica chromatography, eluting with petroleum ether to 15% ethyl acetate to provide the title compound as a colourless oil (0.34 g, 84%). IR (neat, vmax) cm^{-1} 2970, 2218, 1609, 1503, 1459, 1255. ^1H NMR (500 MHz, $CDCl_3$) δ_H 7.33 (s, 1H, CH-6), 6.72 (s, 1H, CH-3), 3.86 (s, 3H, CH_3-10), 2.68-2.62 (m, 2H, CH_2-12), 2.50 (s, 3H, CH3-9), 1.86-1.77 (m, 2H, CH_2-13), 1.40 (d, *J* = 21.4 Hz, 6H, CH_3's- 15&16). ^{13}C NMR (126 MHz, $CDCl_3$) δ_C 160.5 (C4), 142.2 (C2), 133.1 (CH-6) 129.1 (C5), 118.7 (C7), 111.8 (CH-3), 103.9 (C1), 95.2 (d, *J* = 166 Hz, C14), 55.5 (CH_3-11), 40.9 (d, *J* = 23 Hz, CH_2-13), 26.6 (d, *J* = 25 Hz, CH_3's-15&16), 24.1 (d, *J* = 6 Hz, CH_2-12), 20.6 (CH_3-9). HRMS-ESI *m/z* $[M+Na]^+$ and $[M-H]^-$ poor ionisation LRMS only EI^+ 235 *m/z*. LCMS - Analytical MDAP 30-95% MeCN:Water (0.1% Formic), tR 20.98 min, $[M+H+MeCN]^+$ 277.0 *m/z* (95%).

2,2,7-Trimethylchromane-6-carbonitrile (175)

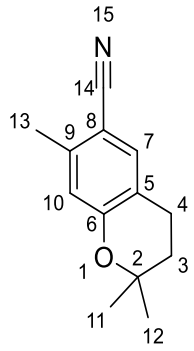

Chloro(trimethyl)silane (0.73 mL, 5.78 mmol) was added to a suspension of 5-(3-fluoro-3-methyl-butyl)-4-methoxy-2-methyl-benzonitrile (**174**) (0.34 g, 1.44 mmol) and sodium iodide (0.87 g, 5.78 mmol) in acetonitrile (4 mL). The reaction mixture was sealed and heated to 130 °C in the microwave (Biotage Initiator®) for 2 h. The cooled reaction mixture was partitioned between sodium thiosulfate (aq) (0.1 M, 100 mL) and ethyl acetate (2 x 100 mL). The combined organic layers were dried over $MgSO_4$, filtered and concentrated under reduced pressure. The residue was purified by flash silica chromatography eluting with heptane to 30% ethyl acetate in heptane to provide the title compound as a colourless oil (0.12 g, 42%). IR (neat, vmax) cm^{-1} 2934, 2217, 1619, 1562, 1495, 1449, 1291, 1251. ^{1}H NMR (500 MHz, $CDCl_3$) δ_H 7.30 (s, 1H, CH-7), 6.67 (s, 1H, CH-10), 2.74 (t, *J* = 6.8 Hz, 2H, CH_2-4), 2.42 (s, 3H, CH_3-13), 1.80 (t, *J* = 6.8 Hz, 2H, CH_2-3), 1.34 (s, 6H, CH_3's-11&12).^{13}C NMR (126 MHz, $CDCl_3$) δ_C 157.7 (C6), 141.3 (C9), 134.0 (CH-7), 119.3 (C5), 118.9 (C14), 118.8 (CH-10), 103.4 (C8), 75.6 (CH_2-4), 32.3 (CH_2-3), 26.8 (CH_3's-11&12), 21.7 (CH_2-4), 20.1 (CH_3-13). HRMS-ESI *m/z* $[M+Na]^+$ and $[M-H]^-$ poor ionisation LRMS only EI^+ 201 *m/z*. LCMS - Analytical MDAP 30-95% MeCN:Water (0.1% Formic), tR 20.65 min, $[M+H+MeCN]^+$ 242.95 *m/z* (95%).

4-Methoxy-2-methyl-5-pentyl-benzonitrile (176)

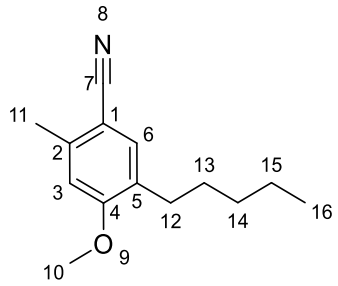

Palladium (II) acetate (0.10 g, 0.44 mmol), and 2-dicyclohexylphosphino-2'-6'-diisopropoxybiphenyl (0.41 g, 0.88 mmol) was added to a mixture of K_3PO_4 (18.78 g, 88.47 mmol), 5-bromo-4-methoxy-2-methyl-benzonitrile (**139**) (8.00 g, 35.39 mmol) and *n*-pentylboronic acid (6.16 g, 53.08 mmol) in toluene (200 mL) and heated to 100 °C for 1 h. The reaction mixture was filtered through a pad of celite and the filtrate was partitioned between ethyl acetate (300 mL), and HCl (aq) (1 M, 150 mL), the organic layer was separated an the aqueous layer was re-extracted with ethyl acetate (2 × 200 mL). The combined organic layers were dried over $MgSO_4$, filtered and concentrated under reduced pressure. The residue was purified by flash silica chromatography, eluting with heptane to 20% ethyl acetate in heptane to provide the title compound as a yellow oil (7.80 g, 90%). m. p. 111-112 °C. IR (neat, vmax) cm^{-1} 2929, 2218, 1609, 1503, 1460, 1209, 1255. ^1H NMR (500 MHz, $CDCl_3$) δ_H 7.34 (s, 1H, CH-6), 6.73 (s, 1H, CH-3), 3.88 (s, 3H, CH3-11), 2.59-2.54 (m, 2H, CH_2-12), 2.53 (s, 3H, CH_3-9), 1.59-1.51 (m, 2H, CH_2-13), 1.40-1.27 (m, 4H, CH_2s-14&15), 0.92 (t, *J* = 7.1 Hz, 3H, CH_3-16). ^{13}C NMR (126 MHz, $CDCl_3$) δ_C 160.6 (C4), 141.8 (C2), 133.3 (CH-6), 130.0 (C5), 119.0 (C7), 111.7 (CH-3), 103.7 (C1), 55.5 (CH_3-11), 31.6 (CH_2-14), 29.3 (CH_2-12), 29.0 (CH_2-13), 22.5 (CH_2-15), 20.6 (CH_3-16), 14.0 (CH_3-9). HRMS-ESI *m/z* $[M+Na]^+$ calculated for $C_{14}H_{19}NNaO$ 240.1359, found 240.1362. LCMS - Analytical UPLC 5-95% MeCN:Water (0.1% TFA), tR 1.01 min, $[M+H]^+$ 218.4 *m/z* (95%).

4-Hydroxy-2-methyl-5-pentyl-benzonitrile (177)

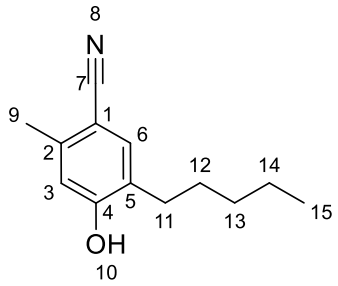

Iodo(trimethyl)silane (3.01 mL, 21.17 mmol) was added to a solution of 4-methoxy-2-methyl-5-pentyl-benzonitrile (**176**) (2.30 g, 10.58 mmol) in acetonitrile (30 mL). The reaction mixture was sealed and heated to 90 °C in the microwave in 2 vials (Biotage Initiator®) for 2 h. The cooled RM's were combined and partitioned between sodium thiosulfate (aq) (0.1 M, 100 mL) and CH_2Cl_2 (2 x 200 mL). The chlorinated layers were separated through a phase separator and concentrated under reduced pressure. The residue was purified by flash silica chromatography eluting with heptane to 30% ethyl acetate in heptane to provide the title compound as a white solid (2.20 g, 99%). m.p. 68-70 °C. IR (neat, vmax) cm^{-1} 3303, 2926, 2219, 1608, 1413, 1261. ^1H NMR (500 MHz, $CDCl_3$) δ_H 7.34 (s, 1H, CH-6), 6.67 (s, 1H, CH-3), 5.24 (s, 1H, OH-10), 2.55 (t, *J* = 7.8 H, 2H, CH_2-11), 2.45 (s, 3H, CH_3-9), 1.63-1.53 (m, 2H, CH_2-12), 1.38-1.28 (m, 4H, CH_2-13&14), 0.90 (t, *J* = 6.9 Hz, 3H, CH_3-15). ^{13}C NMR (126 MHz, $CDCl_3$) δ_C 157.0 (C4), 141.7 (C2), 143.3 (CH-6), 127.2 (C5), 118.7 (C7), 116.8 (CH-3), 104.4 (C1), 31.5 (CH_2-13), 29.1 (CH_2-11), 29.0 (CH_2-12), 22.5 (CH_2-14), 20.0 (CH_3-9), 14.0 (CH3-15). HRMS-ESI *m/z* $[M+Na]^+$ calculated for $C_{13}H_{17}NNaO$ 226.1202, found 226.1202. LCMS - Analytical UPLC 2-98% MeCN:Water (0.1% TFA), tR 0.85 min, $[M+H]^+$ 204.4 *m/z* (95%).

3-Bromo-4-hydroxy-2-methyl-5-pentyl-benzonitrile (178)

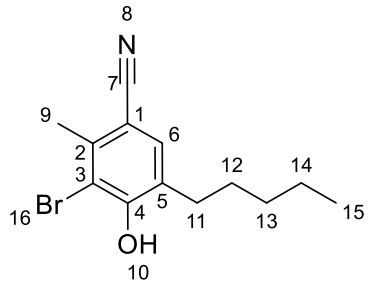

N-Bromosuccinimide (1.96 g, 11.00 mmol) was added to a solution of 4-hydroxy-2-methyl-5-pentyl-benzonitrile (**177**) (2.13 g, 10.48 mmol) in acetonitrile (50 mL). The reaction mixture was stirred at rt for 10 min. The reaction mixture was partitioned between HCl (aq) (1 M, 150 mL) and CH_2Cl_2 (2 × 200 mL), the chlorinated layers were combined and concentrated under reduced pressure. The residue was purified by flash silica chromatography eluting with heptane to 30% ethyl acetate in heptane to provide the title compound as a pale yellow solid (2.65 g, 90%). m.p. 74-75 °C. IR (neat, vmax) cm^{-1} 3333, 2932, 2225, 1598, 1464, 1147. ^1H NMR (500 MHz, $CDCl_3$) δ_H 7.36 (s, 1H, CH-6), 6.12 (s, 1H, OH-10), 2.66 (t, *J* = 7.8 Hz, 2H, CH_2-11), 2.61 (s, 3H, CH_3-9), 1.66-1.51 (m, 2H, CH_2-12), 1.42-1.30 (m, 3H, CH_2s-13&14), 0.92 (t, *J* = 6.8 Hz, 3H, CH_3-15). ^{13}C NMR (126 MHz, $CDCl_3$) δ_C 153.9 (C4), 140.1 (C2), 132.9 (CH-6), 128.8 (C5), 118.2 (C7), 113.9 (C3), 105.3 (C1), 31.5 (CH_2-13), 30.2 (CH_2-12), 28.8 (CH_2-11), 22.5 (CH_2-14), 21.9 (CH_3-9), 14.0 (CH_3-15). HRMS-ESI *m/z* $[M+Na]^+$ calculated for $C_{13}H_{16}{}^{79}BrNNaO$ 304.0307, found 304.0305. LCMS - Analytical UPLC 2-98% MeCN:Water (0.1% TFA), tR 0.95 min, $[M+H]^+$ 282.3 *m/z* (95%).

4-Hydroxy-2,3-dimethyl-5-pentyl-benzonitrile (179)

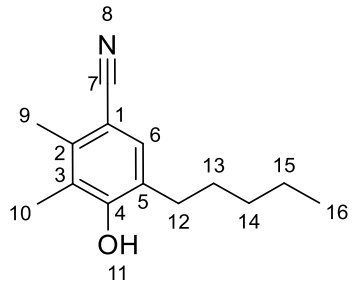

Palladium (II) acetate (0.002 g, 0.01 mmol), and 2-dicyclohexylphosphino-2'-6'-diisopropoxybiphenyl (0.01 g, 0.02 mmol) was added to a mixture of K_3PO_4 (0.10 g, 0.49 mmol), 3-bromo-4-hydroxy-2-methyl-5-pentyl-benzonitrile (**178**) (0.055 g, 0.19 mmol) and trimethylboroxine (0.072 g, 0.58 mmol) in toluene (1 mL) and water (0.1 mL) and heated to 100 °C for 16 h. The reaction mixture was partitioned between CH_2Cl_2 (10 mL), and HCl (aq) (1 M, 10 mL), the chlorinated layer was separated through a phase separator and concentrated under reduced pressure. The residue was purified by flash silica chromatography, eluting with heptane to 25% ethyl acetate in heptane to provide the title compound as a white solid upon concentration (0.041 g, 98%). m. p. 81-82 °C. IR (neat, vmax) cm^{-1} 3339, 2926, 2224, 1567, 1463, 1199. ^1H NMR (500 MHz, $CDCl_3$) δ_H 7.26 (s, 1H, CH-6), 5.12 (OH-11), 2.60-2.54 (m, 2H, CH_2-12), 2.47 (s, 3H, CH_3-9), 2.21 (s, 3H, CH_3-10), 1.65-1.58 (m, 2H, CH_2-13), 1.41-1.32 (m, 4H, CH_2-14&15), 0.95-0.90 (m, 3H, CH_3-16). ^{13}C NMR (126 MHz, $CDCl_3$) δ_C 155.4 (C4), 139.7 (C2), 131.3 (CH-6), 126.2 (C5), 123.2 (C3), 119.5 (C7), 104.6 (C1), 31.5 (CH_2-14), 29.6 (CH_2-12), 28.9 (CH_2-13), 22.5 (CH_2-15), 18.3 (CH_3-9), 14.0 (CH_3-16), 12.0 (CH_3-10). HRMS-ESI *m/z* $[M+Na]^+$ calculated for $C_{14}H_{19}NNaO$ 240.1359, found 240.1359. LCMS - Analytical UPLC 2-98% MeCN:Water (0.1% TFA), tR 0.89 min, $[M+H]^+$ 218.5 *m/z* (> 95%).

3-Ethyl-4-hydroxy-2-methyl-5-pentyl-benzonitrile (180)

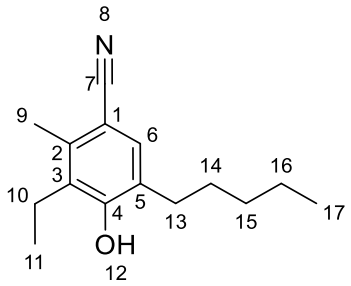

Palladium (II) acetate (0.001 g, 0.005 mmol), and 2-dicyclohexylphosphino-2'-6'-diisopropoxybiphenyl (0.003 g, 0.01 mmol) was added to a mixture of K_3PO_4 (0.056 g, 0.26 mmol), 3-bromo-4-hydroxy-2-methyl-5-pentyl-benzonitrile (**178**) (0.037 g, 0.13 mmol) and ethylboronic acid (0.015 g, 0.20 mmol) in toluene (0.5 mL) and water (0.05 mL) and heated to 100 °C for 16 h. The reaction mixture was partitioned between CH_2Cl_2 (10 mL), and HCl (aq) (1 M, 10 mL), the chlorinated layer was separated through a phase separator and concentrated under reduced pressure. The residue was purified by flash silica chromatography, eluting with heptane to 25% ethyl acetate in heptane to provide the title compound as a white solid upon concentration (0.012 g, 40%). m. p. 96-97 °C. IR (neat, vmax) cm^{-1} 3349, 2929, 2222, 1567, 1463, 1265, 1194. ^1H NMR (500 MHz, $CDCl_3$) δ_H 7.24 (s, 1H, CH-6), 5.15 (s, 1H, OH-12), 2.68 (q, *J* = 7.6 Hz, 2H, CH_2-10), 2.54 (t, *J* = 7.8 Hz, 2H, CH_2-13), 2.47 (s, 3H, CH_3-9), 1.63-1.56 (m, 2H, CH_2-14), 1.38-1.31 (m, 4H, CH_2s-15&16), 1.13 (t, *J* = 7.6 Hz, 3H, CH_3-11), 0.91 (t, *J* = 6.7 Hz, 3H, CH_3-17). ^{13}C NMR (126 MHz, $CDCl_3$) δ_C 155.0 (C4), 139.1 (C2), 131.5 (CH-6), 129.3 (C3), 126.3 (C5), 119.5 (C7), 104.9 (C1), 31.5 (CH_2-15), 29.5 (CH_2-13), 28.8 (CH_2-14), 22.5 (CH_2-16), 19.8 (CH_2-10). 17.4 (CH_3-9), 14.0 (CH_3-17), 13.01 (CH_3-11). HRMS-ESI *m/z* $[M-H]^-$ calculated for $C_{15}H_{20}NO$ 230.1550, found 230.1542. LCMS - Analytical MDAP 30-95% MeCN:Water (0.1% Formic), tR 22.35 min, $[M-H]^-$ 230.1 *m/z* (95%).

4-Hydroxy-2-methyl-5-pentyl-3-phenyl-benzonitrile (181)

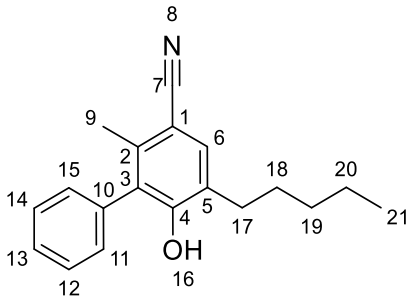

Palladium (II) acetate (0.001 g, 0.005 mmol), and 2-dicyclohexylphosphino-2'-6'-diisopropoxybiphenyl (0.004 g, 0.01 mmol) was added to a mixture of K_3PO_4 (0.094 g, 0.44 mmol), 3-bromo-4-hydroxy-2-methyl-5-pentyl-benzonitrile (178) (0.05 g, 0.18 mmol) and phenylboronic acid (0.032 g, 0.27 mmol) in toluene (0.75 mL) and heated to 100 °C for 16 h. The reaction mixture was partitioned between CH_2Cl_2 (10 mL), and HCl (aq) (1 M, 10 mL), the chlorinated layer was separated through a phase separator and concentrated under reduced pressure. The residue was purified by flash silica chromatography, eluting with heptane to 25% ethyl acetate in heptane, and further purified by reverse-phase chromatography, eluting with 30% MeCN in water to 95% MeCN to provide the title compound as a white solid upon concentration (0.014 g, 28%). m. p. 124-125 °C. IR (neat, vmax) cm^{-1} 3350, 2930, 2225, 1600, 1450, 1150. ^1H NMR (500 MHz, $CDCl_3$) δ_H 7.61-7.55 (m, 2H, CH-12&14), 7.55-7.47 (m, 1H, CH-13), 7.42 (s, 1H, CH-6), 7.30-7.25 (m, 2H, CH-11&15), 5.18 (s, 1H, OH-16), 2.63 (t, *J* = 7.8 Hz, 2H, CH_2-17), 2.23 (s, 3H, CH_3-9), 1.68-1.59 (m, 2H, CH_2-18), 1.42-1.33 (m, 4H, CH_2s-19&20), 0.96-0.89 (m, 3H, CH_3-21). ^{13}C NMR (126 MHz, $CDCl_3$) δ_C 154.4 (C4), 139.1 (C2), 133.6 (C10), 133.3 (CH-6), 130.2 (CH-11&15), 130.0 (CH-12&14), 129.1 (CH-13), 128.7 (C3), 127.9 (C5), 119.2 (C7), 104.5 (C1), 31.6 (CH_2-19), 29.7 (CH_2-17), 29.0 (CH_2-18), 22.5 (CH_2-20), 18.8 (CH_3-9), 14.0 (CH_3-21). HRMS-ESI *m/z* $[M+Na]^+$ calculated for $C_{19}H_{21}NNaO$ 302.1515, found 302.1517. LCMS - Analytical UPLC 2-98% MeCN:Water (0.1% Formic), tR 1.01 min, $[M+H]^+$ 280.5 *m/z* (95%).

Ethyl 5-cyano-2-hydroxy-6-methyl-3-pentyl-benzoate (182)

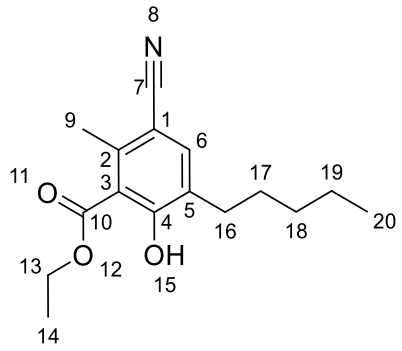

1,8-Diazabicyclo[5.4.0]undec-7-ene (0.28 mL, 1.86 mmol) was added to a suspension of *trans*-Bis(acetato)bis[o-(di-o-tolylphosphino)benzyl]dipalladium(II) (0.041 g, 0.04 mmol), molybdenum hexacarbonyl (0.23 g, 0.89 mmol) and 3-bromo-4-hydroxy-2-methyl-5-pentyl-benzonitrile (178) in ethanol (7.5 mL) and heated to 100 °C for 1 h. The reaction mixture was partitioned between CH_2Cl_2 (50 mL), and HCl (aq) (1 M, 20 mL), the chlorinated layer was separated through a phase separator and concentrated under reduced pressure. The residue was purified by flash silica chromatography, eluting with heptane to 25% ethyl acetate in heptane to provide the title compound as a colourless oil (0.38 g, 78%). IR (neat, vmax) cm^{-1} 2928, 2219, 1627, 1436, 1227, 1297. ^1H NMR (500 MHz, $CDCl_3$) δ_H 12.15 (s, 1H, OH-15), 7.48 (s, 1H, CH-6), 4.50 (q, *J* = 7.2 Hz, 2H, CH_2-13), 2.77 (s, 3H, CH_3-9), 2.63 (t, *J* = 7.7 Hz, 2H, CH_2-15), 1.65-1.57 (m, 2H, CH_2-17), 1.48 (t, *J* = 7.2 Hz, 3H, CH_3-14), 1.41-1.23 (m, 4H, CH_2s-18&19), 0.95-0.88 (m, 3H, CH_3-20). ^{13}C NMR (126 MHz, $CDCl_3$) δ_C 171.2 (C10), 164.1 (C4), 143.6 (C2), 137.1 (CH-6), 130.7 (C5), 118.8 (C7), 112.9 (C3), 105.0 (C1), 62.5 (CH_2-13), 31.6 (CH_2-18), 29.4 (CH_2-16), 28.5 (CH_2-17), 22.5 (CH_2-19), 21.7 (CH_3-9), 14.1 (CH_3-14), 14.0 (CH_3-20). HRMS-ESI *m/z* $[M+Na]^+$ calculated for $C_{16}H_{21}NNaO_3$ 298.1414, found 298.1416. LCMS - Analytical UPLC 2-98% MeCN:Water (0.1% Formic), tR 1.06 min, $[M+H]^+$ 276.4 *m/z* (95%).

5-Cyano-2-hydroxy-6-methyl-3-pentyl-benzoic acid (183)

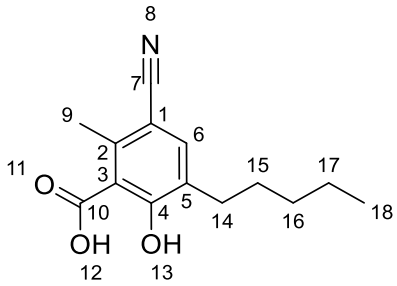

NaOH (aq) (4 M, 5.00 mL, 20.00 mmol) was added to a solution of ethyl 5-cyano-2-hydroxy-6-methyl-3-pentyl-benzoate (**182**) (0.50 g, 1.82 mmol) in methanol (2 mL) and tetrahydrofuran (10 mL) and heated to 60 °C for 120 h. The reaction mixture was partitioned between CH_2Cl_2 (50 mL), and NaOH (aq) (2 M, 20 mL), the chlorinated layer was washed with NaOH (aq) (2 M, 20 mL) the combined aqueous layers were acidified with HCl (aq) (5 M) to pH 1 and extracted with ethyl acetate (2 × 50 mL). The organics were dried over $MgSO_4$, filtered and concentrated under reduced pressure to provide the title compound as a white solid (0.43 g, 99%). m.p. 186-188 °C. IR (neat, vmax) cm^{-1} 3176, 2214, 1605, 1555, 1437, 1381, 1262. ^1H NMR (500 MHz, $CDCl_3$) δ_H 7.23 (s, 1H, CH-6), 7.19-6.98 (br, 2H, OH-12&13), 2.69 (s, 3H, CH_3-9), 2.44 (t, *J* = 7.7 Hz, 2H, CH_2-14), 1.56-1.45 (m, 2H, CH_2-15), 1.37-1.2 (m, 4H, CH_2-16&17), 0.87 (t, *J* = 7.0 Hz, 3H, CH_3-18). ^{13}C NMR (126 MHz, $CDCl_3$) δ_C 170.9 (C10), 169.5 (C4 observed in HMBC), 143.9 (C2), 133.4 (CH-6), 129.6 (C5), 121.0 (C7), 118.1 (C3), 98.3 (C1), 31.6 (CH_2-16), 29.7 (CH_2-14), 28.7 (CH_2-15), 22.5 (CH_2-17), 20.7 (CH_3-9), 14.4 (CH_3-9). HRMS-ESI *m/z* $[M+Na]^+$ calculated for $C_{14}H_{17}NNaO_3$ 270.1101, found 270.1106. LCMS - Analytical UPLC 2-98% MeCN:Water (0.1% Formic), tR 0.89 min, poor ionisation, no mass ion observed (95%).

5-Cyano-2-hydroxy-*N*,*N*,6-trimethyl-3-pentyl-benzamide (184)

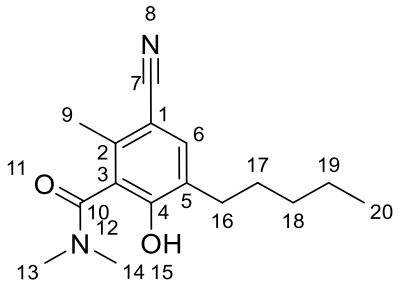

Oxalyl chloride (0.01 mL, 0.12 mmol) was added to a suspension of 5-cyano-2-hydroxy-6-methyl-3-pentyl-benzoic acid (**183**) (0.02 g, 0.08 mmol) in CH_2Cl_2 (0.5 mL), the reaction was added 1 drop of *N*,*N*-dimethylformamide. Once gas evolution had ceased, the reaction was added a solution of dimethylamine (2 M, 0.16 mL, 0.32 mmol) and stirred at rt for 16 h. The reaction mixture was partitioned between CH_2Cl_2 (20 mL), and HCl (aq) (1 M, 5 mL), the chlorinated layer was separated through a phase-separator and concentrated under reduced pressure. The residue was purified by flash silica chromatography eluting with heptane to 25% ethyl acetate in heptane to provide the title compound as a white solid (0.017 g, 77%). m.p. 87-89 °C. IR (neat, vmax) cm^{-1} 2925, 2217, 1580, 1460, 1399, 1321, 1259. ^1H NMR (500 MHz, $CDCl_3$) δ_H 8.70 (br, 1H, OH-15), 7.28 (s, 1H, CH-6), 3.29-2.73 (br m, 6H, CH_3-13&14), 2.50-2.34 (m, 5H, CH_2-16&CH_3-9), 1.53-1.41 (m, 2H, CH_2-17), 1.41-1.16 (m, 4H, CH_2-18&19), 0.91 (t, *J* = 7.0 Hz, 3H, CH_3-20). ^{13}C NMR (126 MHz, $CDCl_3$) δ_C 169.3 (C10), 155.2 (C4), 137.5 (C2), 134.3 (CH-6), 130.6 (C5), 123.9 (C3), 118.4 (C7), 104.6 (C1), 38.1 (br, CH_3-13/14), 35.1 (br, CH_3-13/14), 31.5 (CH_2-18), 29.3 (CH_2-16), 28.8 (CH_2-17), 22.4 (CH_2-19), 17.9 (CH_3-9), 14.0 (CH_3-20). HRMS-ESI *m/z* $[M+Na]^+$ calculated for $C_{16}H_{22}NNaO_2$ 297.1573, found 297.1579. LCMS - Analytical UPLC 2-98% MeCN:Water (0.1% Formic), tR 0.75 min, $[M+H]^+$ 275.4 *m/z* (95%).

3-Formyl-4-hydroxy-2-methyl-5-pentyl-benzonitrile (185)

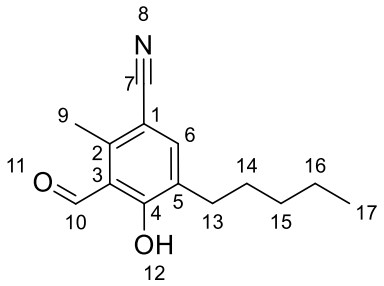

NaOH (aq) (4 M, 1.22 mL, 4.87 mmol) was added to a solution of 4-hydroxy-2-methyl-5-pentyl-benzonitrile (**177**) (0.20 g, 0.97 mmol) in $CHCl_3$ (3 mL), the reaction was heated at 100 °C in the microwave for 1 h. The reaction mixture was partitioned between CH_2Cl_2 (50 mL), and HCl (aq) (1 M, 30 mL), the chlorinated layer was separated through a phase-separator and concentrated under reduced pressure. The residue was purified by flash silica chromatography eluting with heptane to 25% ethyl acetate in heptane to provide the title compound as a white solid (0.054 g, 24%). m.p. 85-87 °C. ^{1}H NMR (500 MHz, $CDCl_3$) δ_H 12.75 (s, 1H, OH-12), 10.37 (s, 1H, CH-10), 7.55 (s, 1H, CH-6), 2.83 (s, 3H, CH_3-9), 2.64 (t, *J* = 7.8 Hz, 2H, CH_2-13), 1.68-1.54 (m, 2H, CH_2-14), 1.43-1.30 (m, 4H, CH_2s-15&16), 0.93 (t, *J* = 6.6 Hz, CH_3-17). ^{13}C NMR (126 MHz, $CDCl_3$) δ_C 195.0 (C10), 164.6 (C4), 144.7 (C2), 139.4 (CH-6), 131.7 (C5), 118.0 (C3), 117.8 (C7), 104.5 (C1), 31.5 (CH_2-15), 28.7 (CH_2-13), 28.5 (CH_2-14), 22.5 (CH_2-16), 16.1 (CH_3-9), 14.00 (CH_3-17). HRMS-ESI *m/z* $[M-H]^-$ calculated for $C_{14}H_{16}NO_2$ 230.1187, found 230.1179. LCMS - Analytical UPLC 2-98% MeCN:Water (0.1% Formic), tR 0.95 min, poor ionisation, no mass ion (95%).

4-Hydroxy-2-methyl-5-pentyl-benzaldehyde (187)

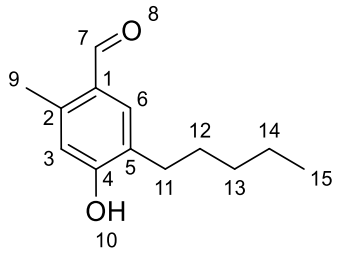

Palladium (II) acetate (0.20 g, 0.87 mmol), and 2-dicyclohexylphosphino-2'-6'-diisopropoxybiphenyl (0.81 g, 1.74 mmol) was added to a mixture of K_3PO_4 (18.5 g, 87.2 mmol), 5-bromo-4-hydroxy-2-methyl-benzaldehyde (**80**) (7.50 g, 34.9 mmol) and *n*-pentylboronic acid (6.07 g, 52.3 mmol) in toluene (150 mL) and water (15 mL) and heated to 85 °C for 96 h. The reaction mixture was filtered through a pad of celite and the filtrate was partitioned between ethyl acetate (300 mL), and HCl (aq) (1 M, 150 mL), the organic layer was separated, and the aqueous layer was re-extracted with ethyl acetate (2 × 200 mL). The combined organic layers were dried over $MgSO_4$, filtered and concentrated under reduced pressure. The residue was purified by flash silica chromatography, eluting with heptane to 20% ethyl acetate in heptane to provide the title compound as an orange oil (1.60 g, 22%). IR (neat, vmax) cm^{-1} 3131, 2927, 1650, 1574, 1430, 1394, 1258. ^1H NMR (500 MHz, $CDCl_3$) δ_H 10.08 (s, 1H, CH-7), 7.59 (s, 1H, CH-6), 6.64 (s, 1H, CH-3), 6.34 (br m, 1H, OH-10), 2.75-2.55 (m, 5H, CH_2-11 & CH_3-9), 1.66-1.58 (m, CH_2-12), 1.36-1.30 (m, 4H, CH_2s-13/14), 0.91-0.86 (m, 3H, CH_3-15). ^{13}C NMR (126 MHz, $CDCl_3$) δ_C 192.2 (CH-7), 158.8 (C4), 141.2 (C2), 134.8 (CH-6), 127.5 (C1), 118.1 (CH-3), 113.0 (C5), 31.6 (CH_2-13), 29.23 (CH_2-12), 29.17 (CH_2-11), 22.5 (CH_2-14), 19.1 (CH_3-9), 14.0 (CH_3-15). HRMS-ESI *m/z* $[M-H]^-$ calculated for $C_{13}H_{17}O_2$ 205.1234, found 205.1230. LCMS - Analytical MDAP 30-95% MeCN:Water (0.1% Formic), tR 19.70 min, $[M-H]^-$ 205.1 *m/z* (95%).

3-Chloro-4-hydroxy-2-methyl-5-pentyl-benzaldehyde (188)

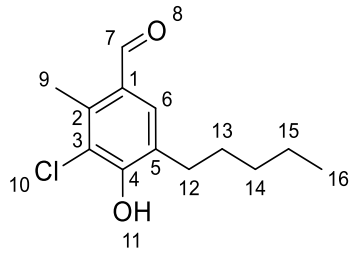

Sulfuryl chloride (1.18 mL, 14.5 mmol) was added to a solution of 4-hydroxy-2-methyl-5-pentyl-benzaldehyde (**187**) (1.00 g, 4.85 mmol) in diethyl ether (20 mL) and stirred for 30 min at rt. The reaction mixture was partitioned between HCl (aq) (1 M, 50 mL) and ethyl acetate (2 x 100 mL). The organic layers were combined, dried over $MgSO_4$, filtered and concentrated under reduced pressure. The residue was purified by flash silica chromatography eluting with heptane to 30% ethyl acetate in heptane to provide the title compound as a yellow solid (0.98 g, 84%). m.p. 69-71 °C. IR (neat, vmax) cm^{-1} 3228, 2918, 1674, 1600, 1549, 1320, 1223. ^1H NMR (500 MHz, $CDCl_3$) δ_H 10.11 (s, 1H, CH-7), 7.55 (s, 1H, CH-6), 6.24 (s, 1H, OH-11), 2.71-2.65 (m, 5H, CH_3-9& CH_2-12), 1.66-1.60 (m, 2H, CH_2-13), 1.36-1.30 (m, 4H, CH_2s-14&15), 0.90 (t, *J* = 6.8 Hz, 3H, CH_3-16). ^{13}C NMR (126 MHz, $CDCl_3$) δ_C 190.8 (C7), 153.8 (C4), 137.2 (C2), 132.5 (CH-6), 128.0 (C3/5), 127.9 (C3/5), 122.0 (C1), 31.6 (CH_2-14), 30.0 (CH_2-12), 29.0 (CH_2-13), 22.5 (CH_2-15), 15.2 (CH_3-9), 14.00 (CH_3-16). HRMS-ESI *m/z* $[M-H]^-$ calculated for $C_{13}H_{16}{}^{35}ClO_2$ 239.0844, found 239.0838. LCMS - Analytical MDAP 30-95% MeCN:Water (0.1% Formic), tR 21.88 min, $[M-H]^-$ 239.0 *m/z*, (95%).

5-Bromo-4-hydroxy-2-methyl-benzoic acid (189)

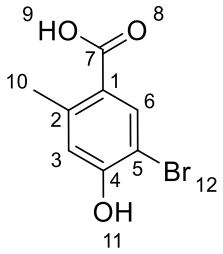

Sodium chlorite (2.94 g, 26.0 mmol) was added to a solution of 5-bromo-4-hydroxy-2-methyl-benzaldehyde (**80**) (4.00 g, 18.6 mmol) and sodium phosphate monobasic (3.01 g, 25.1 mmol) in *t*-BuOH (50 mL), 2-methyl-2-butene (1.98 mL, 18.6 mmol) and water (5 mL), and stirred at rt for 2 h. The reaction mixture was partitioned between HCl (aq) (1 M, 50 mL) and ethyl acetate (2 x 100 mL). The organic layers were combined, dried over $MgSO_4$, filtered and concentrated under reduced pressure to provide the title compound as a tan solid (4.31 g, 99%). m.p. 182-184 °C. IR (neat, vmax) cm^{-1} 2931, 2635, 1672, 1596,1554, 1434, 1271. ^1H NMR (500 MHz, D_6-DMSO) δ_H 12.59 (br s, 1H, OH-9), 10.87 (br s, 1H, OH-11), 7.94 (s, 1H, CH-6), 6.80 (s, 1H, CH-3), 2.42 (s, 3H, CH_3-10). ^{13}C NMR (126 MHz, D_6-DMSO) δ_C 167.3 (C7), 157.5 (C4), 141.9 (C2), 136.0 (CH-6), 122.4 (C1), 119.2 (CH-3), 106.3 (C5), 21.9 (CH_3-10). HRMS-ESI *m/z* $[M+Na]^+$ and $[M-H]^-$ poor ionisation LRMS only EI^+ 230 / 232 *m/z* (Br isotope). LCMS - Analytical MDAP 30-95% MeCN:Water (0.1% Formic), tR 11.01 min, $[M-H]^-$ 228.9 *m/z*, (95%).

Methyl 5-bromo-4-methoxy-2-methyl-benzoate (190)

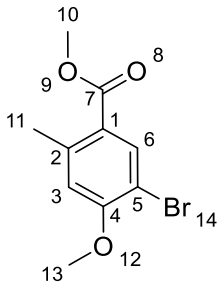

Dimethyl sulphate (1.02 mL, 10.8 mmol) was added to a suspension of potassium carbonate (1.87 g, 13.5 mmol) and 5-bromo-4-hydroxy-2-methyl-benzoic acid (**189**) (1.25 g 5.41 mmol) in acetone (50 mL). The reaction mixture was stirred at rt for 16 h, then diluted with water (200 mL) and the resulting solid was filtered and purified by flash silica chromatography

eluting with petroleum ether to 30% ethyl acetate in petroleum ether to provide the title compound as an off white solid (0.86 g, 61%). m.p. 93-95 °C. IR (neat, vmax) cm^{-1} 2946, 1712, 1593, 1315, 1233. ^{1}H NMR (500 MHz, $CDCl_3$) δ_H 8.15 (s, 1H, CH-6), 6.71 (s. 1H, CH-3), 3.93 (s, 3H, CH_3-13), 3.86 (s, 3H, CH_3-10), 2.59 (s, 3H, CH_3-11). ^{13}C NMR (126 MHz, $CDCl_3$) δ_C 166.3 (C7), 158.3 (C4), 142.5 (C2), 135.8 (CH-6), 122.6 (C1), 114.5 (CH-3), 108.1 (C5), 56.3 (CH_3-13), 51.7 (CH_3-10), 22.2 (CH_3-11). HRMS-ESI *m/z* $[M+Na]^+$ and $[M-H]^-$ poor ionisation LRMS only EI^+ 258 / 260 *m/z* (Br isotope). LCMS - Analytical MDAP 30-95% MeCN:Water (0.1% Formic), tR 19.56 min, $[M-H]^-$ 258.9 *m/z* (95%).

Methyl 5-isopentyl-4-methoxy-2-methyl-benzoate (191)

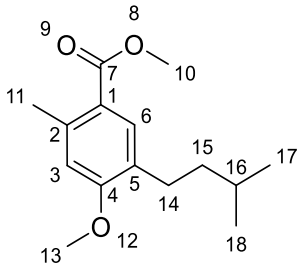

Palladium (II) acetate (0.052 g, 0.23 mmol), and 2-dicyclohexylphosphino-2'-6'-diisopropoxybiphenyl (0.216 g, 0.46 mmol) was added to a mixture of K_3PO_4 (3.93 g, 18.53 mmol), methyl 5-bromo-4-methoxy-2-methyl-benzoate (**190**) (2.40 g, 9.26 mmol) and (3-methylbutyl)boronic acid (1.61 g, 13.89 mmol) in toluene (50 mL) and heated to 100 °C for 3 h. The reaction mixture was filtered through a pad of celite and partitioned between ethyl acetate (100 mL), and HCl (aq) (1 M, 50 mL), the organic layer was separated, dried over $MgSO_4$, filtered and concentrated under reduced pressure. The residue was purified by flash silica chromatography, eluting with heptane to 15% ethyl acetate in heptane, to provide the title compound as a yellow oil (1.99 g, 86%). IR (neat, vmax) cm^{-1} 2952, 1712, 1445, 1253, 1141. ^{1}H NMR (500 MHz, $CDCl_3$) δ_H 7.74 (s, 1H, CH-6), 6.65 (s, 1H, CH-3), 3.85 (s, 6H, CH_3-10&13), 2.60 (s, 3H, CH_3-11), 2.59-2.55 (m, 2H, CH_2-14), 1.60-1.58 (m, 1H, CH-16), 1.47-1.41 (m, 2H, CH_2-15), 0.94 (d, *J* = 6.6 Hz, 6H, CH_3-17&18). ^{13}C NMR (126 MHz, $CDCl_3$) δ_C 167.8 (C7), 160.1 (C4), 140.5 (C2), 132.3 (CH-6), 128.8 (C5), 120.9 (C1), 113.1 (CH-3), 55.3 (CH_3-10/13), 51.4 (CH_3-10/13), 39.0 (CH_2-15), 28.0 (CH-16), 27.4 (CH_2-14), 22.6 (CH_3-17&18),

22.2 (CH_3-11). HRMS-ESI *m/z* $[M+Na]^+$ and $[M-H]^-$ poor ionisation LRMS only EI^+ 250 *m/z*. LCMS - Analytical MDAP 30-95% MeCN:Water (0.1% Formic), tR 26.11 min, $[M-H]^-$ 251.1 *m/z* (95%).

4-hydroxy-5-isopentyl-2-methyl-benzoic acid (192)

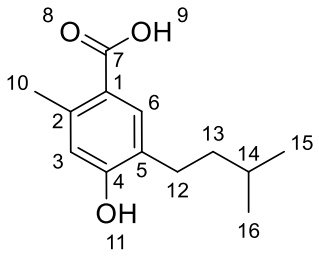

Chloro(trimethyl)silane (0.81 mL, 6.39 mmol) was added to a suspension of methyl 5-isopentyl-4-methoxy-2-methyl-benzoate (**191**) (0.40 g, 1.60 mmol) and sodium iodide (0.96 g, 6.39 mmol) in acetonitrile (2.4 mL). The reaction mixture was sealed and heated to 130 °C for 1 h. The cooled reaction mixture was partitioned between HCl (aq) (1 M, 50 mL) and ethyl acetate (2 x 50 mL). The combined organic layers were dried over $MgSO_4$, filtered and concentrated under reduced pressure. The residue was purified by flash silica chromatography eluting with heptane to 50% ethyl acetate in heptane to provide the title compound as a white solid (0.116 g, 33%). m.p. 119-122 °C. IR (neat, vmax) cm^{-1} 2956, 1679, 1567, 1447, 1398, 1273, 1210, 1150. ^1H NMR (500 MHz, $CDCl_3$) δ_H 7.92 (s, 1H, CH-6), 6.63 (s, 1H, CH-3), 2.62-2.55 (m, 5H, CH_2-12 & CH_3-10), 1.66-1.58 (m, 1H, CH-14), 1.53-1.47 (m, 2H, CH_2-13) 0.95 (d, *J* = 6.6 Hz, 6H, CH_3-15&16).^{13}C NMR (126 MHz, $CDCl_3$) δ_C 173.0 (C7), 157.5 (C4), 141.8 (C2), 134.3 (CH-6), 126.4 (C5), 120.3 (C1, 118.4 (CH-3), 38.7 (CH_2-13), 27.9 (CH-14), 27.1 (CH_2-12), 22.5 (CH_3-15&16) 22.0 (CH_3-9). HRMS-ESI *m/z* $[M+Na]^+$ and $[M-H]^-$ poor ionisation LRMS only EI^+ 222 *m/z*. LCMS - Analytical MDAP 30-95% MeCN:Water (0.1% Formic), tR 15.57 min, $[M-H]^-$ 221.1 *m/z*, (95%).

3-Chloro-4-hydroxy-5-isopentyl-2-methyl-benzoic acid (193)

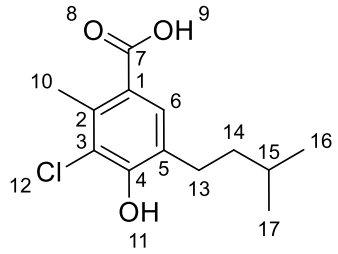

Sulfuryl chloride (0.14 mL, 1.75 mmol) was added to a solution of 4-hydroxy-2-methyl-5-pentyl-benzaldehyde (**192**) (0.13 g, 0.58 mmol) in diethyl ether (2 mL) and stirred at rt for 1 h. The reaction mixture was partitioned between HCl (aq) (1 M, 20 mL) and ethyl acetate (2 x 50 mL). The organic layers were combined, dried over $MgSO_4$, filtered and concentrated under reduced pressure. The residue was purified by flash silica chromatography eluting with heptane to 50% ethyl acetate in heptane to provide the title compound as a white solid (0.136 g, 91%). m.p. 116-118 °C. IR (neat, vmax) cm^{-1} 3470, 2954, 1674, 1604, 1395, 1270, 1157. ^{1}H NMR (500 MHz, $CDCl_3$) δ_H 12.28-11.53 (br, 1H, OH-9), 7.83 (s, 1H, CH-6), 6.13 (br s, 1H, OH-11), 2.70 (s, 3H, CH_3-10), 2.69-2.64 (m, 2H, CH_2-13), 1.64-1.57 (m, 1H, CH-15), 1.53-1.47 (m, 2H, CH_2-14), 0.95 (d, *J* = 6.6 Hz, 6H, CH_3's-16 & 17). ^{13}C NMR (126 MHz, $CDCl_3$) δ_C 172.1 (C7), 153.0 (C4), 137.5 (C2), 131.8 (CH-6), 127.43 (C5), 122.0 (C3), 121.3 (C1), 38.5 (CH_2-14), 28.0 (CH_2-13), 27.9 (CH-15), 22.5 (CH_3's-16 & 17), 18.0 (CH_3-9). HRMS-ESI *m/z* $[M+Na]^+$ and $[M-H]^-$ poor ionisation LRMS only EI^+ 256 *m/z*. LCMS - Analytical MDAP 30-95% MeCN:Water (0.1% Formic), tR 17.97 min, $[M-H]^-$ 255.0 *m/z*, (95%).

3-Chloro-4-hydroxy-5-isopentyl-*N*,*N*,2-trimethyl-benzamide (194)

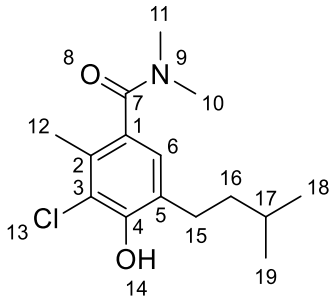

Triethylamine (0.05 mL, 0.35 mmol) was added to a solution of 3-chloro-4-hydroxy-5-isopentyl-2-methyl-benzoic acid (**193**) (0.03 g, 0.12 mmol), dimethylamine hydrochloride (0.014 g, 0.18 mmol) and 1-[bis(dimethylamino)methylene]-1H-1,2,3-triazolo[4,5-b]pyridinium 3-oxid hexafluorophosphate (0.053 g, 0.14 mmol) in acetonitrile (0.75 mL) and stirred at rt for 16 h. The reaction mixture was partitioned between HCl (aq) (1 M, 20 mL) and ethyl acetate (2 x 50 mL). The organic layers were combined, dried over $MgSO_4$, filtered and concentrated under reduced pressure. The residue was purified by flash silica chromatography eluting with heptane to 40% ethyl acetate in heptane, and further purified by reverse-phase chromatography (C18) eluting with 50% MeOH in water to 100% MeOH to provide the title compound as a white solid (0.014 g, 42%). m.p. 111-113 °C. IR (neat, vmax) cm^{-1} 2942, 1603, 1390, 1134, 1054. ^1H NMR (500 MHz, $CDCl_3$) δ_H 6.86 (s, 1H, CH-6), 5.91 (s, 1H, OH-14), 3.11 (s, 3H, CH_3-10/11), 2.83 (s, 3H, CH_3-10/11), 2.60 (t, *J* = 7.9 Hz, 2H, CH_2-15), 2.25 (s, 3H, CH_3-12), 1.61-1.53 (m, 1H, CH-17), 1.48-1.42 (m, 2H, CH_2-16), 0.92 (d, *J* = 6.6 Hz, 6H, CH_3's-18&19). ^{13}C NMR (126 MHz, $CDCl_3$) δ_C 170.9 (C7), 149.6 (C4), 130.1 (C2), 129.4 (C1), 128.3 (C5), 125.5 (CH-6), 121.1 (C3), 38.59 (CH_3-10/11/CH2-16), 38.55 (CH_3-10/11/CH2-16), 34.7 (CH_3-10/11), 28.1 (CH_2-15), 27.8 (CH-17), 22.5 (CH_3-18&19), 16.9 (CH_3-12). HRMS-ESI *m/z* $[M+Na]^+$ and $[M-H]^-$ poor ionisation LRMS only EI^+ 283 *m/z*. LCMS - Analytical MDAP 30-95% MeCN:Water (0.1% Formic), tR 17.33 min, $[M-H]^-$ 282.1 *m/z*, (95%).

3-Chloro-4-hydroxy-5-isopentyl-*N*,2-dimethyl-benzamide (195)

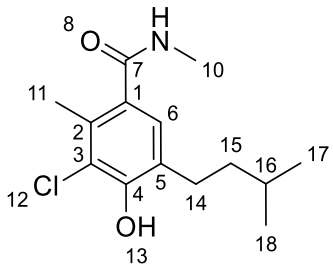

Triethylamine (0.05 mL, 0.35 mmol) was added to a solution of 3-chloro-4-hydroxy-5-isopentyl-2-methyl-benzoic acid (**193**) (0.03 g, 0.12 mmol), methylamine hydrochloride (0.012 g, 0.18 mmol) and 1-[bis(dimethylamino)methylene]-1H-1,2,3-triazolo[4,5-b]pyridinium 3-oxid hexafluorophosphate (0.053 g, 0.14 mmol) in acetonitrile (0.75 mL) and stirred at rt for 16 h. The reaction mixture was partitioned between HCl (aq) (1 M, 20 mL) and ethyl acetate (2 x 50 mL). The organic layers were combined, dried over $MgSO_4$, filtered and concentrated under reduced pressure. The residue was purified by flash silica chromatography eluting with heptane to 40% ethyl acetate in heptane, and further purified by reverse-phase chromatography (C18) eluting with 50% MeOH in water to 100% MeOH to provide the title compound as a white solid (0.012 g, 38%). m.p. 204-206 °C. IR (neat, vmax) cm^{-1} 3377, 2952, 1623, 1387, 1317, 1162. ^{1}H NMR (500 MHz, $CDCl_3$) δ_H 7.06 (s, 1H, CH-6), 5.82 (s, 1H, OH/NH), 5.68 (br s, 1H, OH/NH), 2.98 (s, 3H, CH_3-10), 2.61 (t, *J* = 8.1 Hz, 2H, CH_2-14), 2.43 (s, 3H, CH_3-11), 1.67-1.54 (m, 1H (over integration from water peak), CH-16), 1.50-1.39 (m, 2H, CH_2-15), 0.94 (d, *J* = 6.8 Hz, 6H, CH_3's-17&18). ^{13}C NMR (126 MHz, $CDCl_3$) δ_C 170.1 (C7), 150.3 (C4), 132.2 (C2), 129.8 (C3), 127.6 (C5), 126.6 (CH-6), 121.5 (C1), 38.7 (CH_2-13), 28.1 (CH_2-14), 27.9 (CH-16), 26.7 (CH_3-10), 22.5 (CH_3's-17&18), 17.2 (CH_3-11). HRMS-ESI *m/z* $[M+Na]^+$ and $[M-H]^-$ poor ionisation LRMS only EI^+ 269 *m/z*. LCMS - Analytical MDAP 30-95% MeCN:Water (0.1% Formic), tR 15.85 min, $[M-H]^-$ 268.1 *m/z*, (95%).

3-Chloro-4-hydroxy-5-isopentyl-2-methyl-benzamide (196)

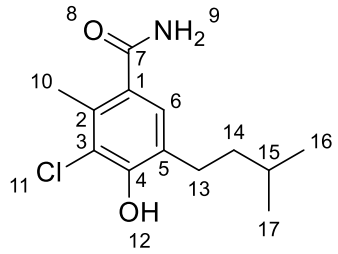

Triethylamine (0.05 mL, 0.35 mmol) was added to a solution of 3-chloro-4-hydroxy-5-isopentyl-2-methyl-benzoic acid (**193**) (0.03 g, 0.12 mmol), ammonium chloride (0.009 g, 0.18 mmol) and 1-[bis(dimethylamino)methylene]-1H-1,2,3-triazolo[4,5-b]pyridinium 3-oxid hexafluorophosphate (0.053 g, 0.14 mmol) in acetonitrile (0.75 mL) and stirred at rt for 16 h. The reaction mixture was partitioned between HCl (aq) (1 M, 20 mL) and ethyl acetate (2 x 50 mL). The organic layers were combined, dried over $MgSO_4$, filtered and concentrated under reduced pressure. The residue was purified by flash silica chromatography eluting with heptane to 40% ethyl acetate in heptane, and further purified by reverse-phase chromatography (C18) eluting with 50% MeOH in water to 100% MeOH to provide the title compound as a white solid (0.012 g, 38%). m.p. 167-169 °C. IR (neat, vmax) cm^{-1} 3376, 3193, 2952, 1630, 1385, 1161. ^{1}H NMR (500 MHz, $CDCl_3$) δ_H 7.17 (s, 1H, CH-6), 5.90 (s, 1H, OH-12), 5.72 (br, 2H, NH_2-9), 2.63 (t, *J* = 7.9 Hz, 2H, CH_2-13), 2.49 (s, 3H, CH_3-10), 1.65-1.56 (m, 1H (over intergrated with water peak), CH-15), 1.50-1.44 (m, 2H, CH_2-14), 0.94 (d, *J* = 6.6 Hz, 6H, CH_3's-16&17). ^{13}C NMR (126 MHz, $CDCl_3$) δ_C 171.2 (C7), 150.8 (C4), 132.6 (C2), 128.3 (C1), 127.6 (C5), 127.0 (CH-6), 121.8 (C3), 38.7 (CH_2-14), 28.1 (CH_2-13), 27.9 (CH-15), 22.5 (CH_3's-16&17), 17.3 (CH_3-10). HRMS-ESI *m/z* $[M+Na]^+$ and $[M-H]^-$ poor ionisation LRMS only EI^+ 255 *m/z*. LCMS - Analytical MDAP 30-95% MeCN:Water (0.1% Formic), tR 14.50 min, $[M-H]^-$ 256.0 *m/z*, (95%).

3-Bromo-4-hydroxy-5-isopentyl-2-methyl-benzonitrile (197)

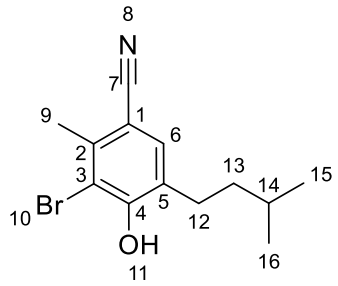

N-Bromosuccinimide (0.048 g, 0.27 mmol) was added to a solution of 4-hydroxy-5-isopentyl-2-methyl-benzonitrile (**149**) (0.05 g, 0.25 mmol) in acetonitrile (1 mL). The reaction mixture was stirred at rt for 10 min. The reaction mixture was partitioned between HCl (aq) (1 M, 10 mL) and CH_2Cl_2 (2 × 20 mL), the chlorinated layers were combined and concentrated under reduced pressure. The residue was purified by flash silica chromatography eluting with heptane to 30% ethyl acetate in heptane, and further purified by reverse-phase chromatography eluting with 30% MeCN in water to 100% MeCN to provide the title compound as a white solid (0.029 g, 42%). m.p. 91-92 °C. IR (neat, vmax) cm^{-1} 3310, 2934, 2221, 1598, 1464, 1410, 1320, 1246, 1153. ^{1}H NMR (500 MHz, $CDCl_3$) δ_H 7.36 (s, 1H, CH-6), 6.14 (br s, 1H, OH-4), 2.67 (t, *J* = 8.0 Hz, 2H, CH_2-12), 2.76 (s, 3H, CH_3-9), 1.66-1.55 (m, 1H, CH-14), 1.52-1.44 (m, 2H, CH_2-13), 0.96 (d, *J* = 6.7 Hz 6H, CH_3's-15&16). ^{13}C NMR (126 MHz, $CDCl_3$) δ_C 154.0 (C4), 140.0 (C2), 132.8 (CH-6), 129.0 (C5), 118.1 (C7), 113.9 (C3), 105.3 (C1), 38.3 (CH_2-13), 28.2 (CH_2-12), 27.7 (CH-14), 22.5 (CH_3's-15&16), 22.0 (CH_3-9). HRMS-ESI *m/z* $[M+Na]^+$ calculated for $C_{13}H_{16}{}^{79}BrNNaO$ 304.0307, found 304.0308. LCMS - Analytical UPLC 2-98% MeCN:Water (0.1% TFA), tR 0.93 min, poor ionisation, no mass ion observed (95%).

Bibliography

(1) World Health Organisation. *Control and surveillance of human African trypanosomiasis*; Geneva, 2013.

(2) Steverding, D. The history of African trypanosomiasis. *Parasit Vectors* 2008, *1* (3).

(3) Bruce, D. Preliminary report on the tsetse fly disease or nagana in Zululand. *Bennet & Davis. Durban* 1895, 28.

(4) Cox, F. E. . History of sleeping sickness (African trypanosomiasis). *Infect. Dis. Clin. North Am.* 2004, *18* (2), 231–245 DOI: 10.1016/j.idc.2004.01.004.

(5) Schultz, C. D. M. G. Image Public Health Image Library - 613. 1970.

(6) Fevre, E. M.; Wissmann, B. V.; Welburn, S. C.; Lutumba, P. The Burden of Human African Trypanosomiasis. *PLoS Negl. Trop. Dis.* 2008, *2* (12), e333 DOI: 10.1371/journal.pntd.0000333.

(7) Lejon, V.; Bentivoglio, M.; Franco, J. R. Human African trypanosomiasis. *Handb. Clin. Neurol.* 2013, *114* (0), 169–181 DOI: 10.1016/B978-0-444-53490-3.00011-X.

(8) Buguet, A.; Bisser, S.; Josenando, T.; Chapotot, F.; Cespuglio, R. Sleep structure: A new diagnostic tool for stage determination in sleeping sickness. *Acta Trop.* 2005, *93* (1), 107–117 DOI: 10.1016/j.actatropica.2004.10.001.

(9) Magnus, E.; Vervoort, T.; Van Meirvenne, N. A card-agglutination test with stained trypanosomes (C.A.T.T.) for the serological diagnosis of T. B. gambiense trypanosomiasis. *Ann Soc Belg Med Trop.* 1978, *58* (3), 169–176.

(10) Hasker, E.; Mitashi, P.; Baelmans, R.; Lutumba, P.; Jacquet, D.; Lejon, V.; Kande, V.; Declercq, J.; Van Der Veken, W.; Boelaert, M. A new format of the CATT test for the detection of Human African Trypanosomiasis, designed for use in peripheral health facilities. *Trop. Med. Int. Heal.* 2010, *15* (2), 263–267 DOI: 10.1111/j.1365-3156.2009.02446.x.

(11) WHO. Cases of sleeping sickness drop to lowest level in 75 years http://www.who.int/trypanosomiasis_african/cases_drop_to_lowest_since_75_years/en/ (accessed Jul 3, 2017).

(12) Nmorsi, O. P. G.; Isaac, C.; Igbinosa, I. B.; Umukoro, D. O.; Aitaikuru, D. P. Human African trypanosomiasis in endemic focus of Abraka, Nigeria. *Asian Pac. J. Trop. Med.* 2010, *3* (6), 448–450 DOI: 10.1016/S1995-7645(10)60107-1.

(13) Medicines Sans Frontiers. CAR: MSF denounces violence as teams are forced to suspend activities in Batangafo http://www.msf.org.uk/article/car-msf-denounces-violence-teams-are-forced-suspend-activities-batangafo (accessed May 26, 2015).

(14) Gilleman, Q.; Buscher, P.; Mertens, P.; Lecipteux, T. Development of a Rapid Diagnostic Test for active case detection in sleeping sickness contro: recHAT Sero-Strip. In *Poster presented at ISNTD-d3 Proceedings of the 3rd International Society of Neglected Tropical Diseases conference, 20-21 May 2015, London, UK*; 2015.

(15) Checchi, F.; Filipe, J. a N.; Barrett, M. P.; Chandramohan, D. The natural progression of Gambiense sleeping sickness: what is the evidence? *PLoS Negl. Trop. Dis.* 2008, *2* (12), e303 DOI: 10.1371/journal.pntd.0000303.

(16) Fairlamb, A. H. Chemotherapy of human African trypanosomiasis: Current and future prospects. *Trends in Parasitology*. 2003, pp 488–494.

(17) Lambrecht, F. L. Trypanosomes and Hominid Evolution. *Bioscience* 1985, *35* (10), 640–646 DOI: 10.2307/1309990.

(18) *African Animal Trypanosomiasis - Fact Sheet*; 2009.

(19) Van Vinh Chau, N.; Buu Chau, L.; Desquesnes, M.; Herder, S.; Phu Huong Lan, N.; Campbell, J. I.; Van Cuong, N.; Yimming, B.; Chalermwong, P.; Jittapalapong, S.; et al. A Clinical and Epidemiological Investigation of the First Reported Human Infection With the Zoonotic Parasite *Trypanosoma evansi* in Southeast Asia. *Clin. Infect. Dis.* 2016, *62*, ciw052 DOI: 10.1093/cid/ciw052.

(20) Nagana Disease information -PAAT http://www.fao.org/ag/againfo/programmes/en/paat/disease.html http://www.fao.org/ag/againfo/programmes/en/paat/disease.html (accessed Mar 16, 2015).

(21) Uilenberg, G. *A field guide for THE DIAGNOSIS, TREATMENT AND PREVENTION OF AFRICAN ANIMAL TRYPANOSOMOSIS*; FOOD AND AGRICULTURE ORGANIZATION OF THE UNITED NATIONS: Rome, 1998.

(22) OIE. OIE Terrestrial Manual 2013 Trypanosomosis (tsetse-transmitted). *www.oie.int/fileadmin/Home/eng/...in.../TRYPANO_TSETSE.pdf*. 2013, pp 1–11.

(23) Mihok, S.; Otieno, L. H.; Tarimo, C. S. Trypanosome infection rates in tsetse flies (Diptera: Glossinidae) and cattle during tsetse control operations in the Kagera River region of Rwanda. *Bulletin of Entomological Research*. 1992, p 361.

(24) McCord, P. F.; Messina, J. P.; Campbell, D. J.; Grady, S. C. Tsetse fly control in Kenya's spatially and temporally dynamic control reservoirs: A cost analysis. *Appl. Geogr.* 2012, *34* (517), 189–204 DOI: 10.1016/j.apgeog.2011.11.005.

(25) Ruggiero, M. A.; Gordon, D. P.; Orrell, T. M.; Bailly, N.; Bourgoin, T.; Brusca, R. C.; Cavalier-Smith, T.; Guiry, M. D.; Kirk, P. M. A higher level classification of all living organisms. *PLoS One* 2015, *10* (4), 1–60 DOI: 10.1371/journal.pone.0119248.

(26) Shapiro, T. A.; Englund, P. T. The structure and replication of kinetoplast DNA. *Annu.*

Rev. Microbiol. 1995, *49*, 117–143 DOI: 10.1146/annurev.mi.49.100195.001001.

(27) Magez, S.; Radwanska, M. *Trypanosomes and Trypanosomiasis*; Magez, S., Radwanska, M., Eds.; Springer, 2014.

(28) Gruby, M. Recherches et observations sur une nouvelle espece d'hematozoaire, Trypanosoma sanguinis. *C. R. Hebd. Seances Acad. Sci.* 1843, *t.17*, 1134.

(29) Vertommen, D.; Roy, J. Van; Szikora, J.; Rider, M. H.; Michels, P. A. M.; Opperdoes, F. R. Differential expression of glycosomal and mitochondrial proteins in the two major life-cycle stages of Trypanosoma brucei. *Mol Biochem Parasitol.* 2008, *158*, 189–201 DOI: 10.1016/j.molbiopara.2007.12.008.

(30) Sbicego, S.; Vassella, E.; Kurath, U.; Blum, B.; Roditi, I. The use of transgenic Trypanosoma brucei to identify compounds inducing the differentiation of bloodstream forms to procyclic forms. 1999, *104*, 311–322.

(31) Masocha, W.; Kristensson, K. Passage of parasites across the blood-brain barrier. *Virulence* 2012, *3* (2), 202–212.

(32) Amin, D. N.; Vodnala, S. K.; Masocha, W.; Sun, B.; Kristensson, K.; Rottenberg, M. E. Distinct toll-like receptor signals regulate cerebral parasite load and interferon α/β and tumor necrosis factor α-dependent T-cell infiltration in the brains of trypanosoma brucei-infected mice. *J. Infect. Dis.* 2012, *205* (2), 320–332 DOI: 10.1093/infdis/jir734.

(33) Masocha, W.; Rottenberg, M. E.; Kristensson, K. Migration of African trypanosomes across the blood-brain barrier. *Physiol. Behav.* 2007, *92* (1–2), 110–114 DOI: 10.1016/j.physbeh.2007.05.045.

(34) Horn, D.; McCulloch, R. Molecular mechanisms underlying the control of antigenic variation in African trypanosomes. *Current Opinion in Microbiology*. 2010, pp 700–705.

(35) Morrison, L. J.; Marcello, L.; McCulloch, R. Antigenic variation in the African trypanosome: molecular mechanisms and phenotypic complexity. *Cell. Microbiol.* 2009, *11* (12), 1724–1734 DOI: 10.1111/j.1462-5822.2009.01383.x.

(36) La Greca, F.; Magez, S. Vaccination against trypanosomiasis: Can it be done or is the trypanosome truly the ultimate immune destroyer and escape artist? *Human Vaccines*. 2011, pp 1225–1233.

(37) da Silva, A. J.; Moser, M. PHIL_3184 HAT lifecycle. CDC - DPDx 2003.

(38) Ravina, E. *The Evolution of Drug Discovery: From Traditional Medicines to Modern Drugs*; Wiley-VCH, 2011.

(39) Kuzoe, F. a. Current situation of African trypanosomiasis. *Acta Trop.* 1993, *54* (3–4), 153–162.

(40) Palm, K.; Stenberg, P.; Luthman, K.; Artursson1, P. Polar molecular surface properties predict the intestinal absorption of drugs in humans. *Pharm. Res.* 1997, *14* (5), 568–571 DOI: 10.1023/A:1012188625088.

(41) Hou, T. J.; Zhang, W.; Xia, K.; Qiao, X. B.; Xu, X. J. ADME evaluation in drug discovery. 5. Correlation of caco-2 permeation with simple molecular properties. *J. Chem. Inf. Comput. Sci.* 2004, *44* (5), 1585–1600 DOI: 10.1021/ci049884m.

(42) Hou, T. J.; Xu, X. J. ADME Evaluation in Drug Discovery. 3. Modeling Blood-Brain Barrier Partitioning Using Simple Molecular Descriptors. *J. Chem. Inf. Comput. Sci.* 2003, *43* (6), 2137–2152 DOI: 10.1021/ci034134i.

(43) Fairlamb, a H.; Bowman, I. B. Trypanosoma brucei: maintenance of concentrated suspensions of bloodstream trypomastigotes in vitro using continuous dialysis for measurement of endocytosis. *Exp. Parasitol.* 1980, *49* (3), 366–380 DOI: 10.1016/0014-4894(80)90072-7.

(44) Willson, M.; Callens, M.; Kuntz, D. a; Perie, J.; Opperdoes, F. R. Synthesis and activity of inhibitors highly specific for the glycolytic enzymes from Trypanosoma brucei. *Mol. Biochem. Parasitol.* 1993, *59* (2), 201–210 DOI: 10.1016/0166-6851(93)90218-M.

(45) Wang, C. C. Molecular Mechanisms and Therapeutic Approaches to the Treatment of African Trypanosomiasis. *Annu. Rev. Pharmacol. Toxicol.* 1995, *35* (1), 93–127 DOI: 10.1146/annurev.pa.35.040195.000521.

(46) Pépin, J.; Milord, F. The treatment of human African trypanosomiasis. *Adv. Parasitol.* 1994, *33*, 1–47 DOI: 1016/S0065-308X(08)60410-8.

(47) SCHAFTINGEN, E.; OPPERDOES, F. R.; HERS, H.-G. Effects of various metabolic conditions and of the trivalent arsenical melarsen oxide on the intracellular levels of fructose 2,6-bisphosphate and of glycolytic intermediates in Trypanosoma brucei. *Eur. J. Biochem.* 1987, *166* (3), 653–661 DOI: 10.1111/j.1432-1033.1987.tb13563.x.

(48) Carter, N. S.; Fairlamb, A. H. Arsenical-resistant trypanosomes lack an unusual adenosine transporter. *Nature* 1993, *361* (6408), 173–176 DOI: 10.1038/361173a0.

(49) Barrett, M. P.; Fairlamb, A. H. The biochemical basis of arsenical-diamidine crossresistance in African trypanosomes. *Parasitol. Today* 1999, *15* (4), 136–140 DOI: 10.1016/S0169-4758(99)01414-3.

(50) Baker, N.; de Koning, H. P.; Mäser, P.; Horn, D. Drug resistance in African trypanosomiasis: the melarsoprol and pentamidine story. *Trends Parasitol.* 2013, *29* (3), 110–118 DOI: 10.1016/j.pt.2012.12.005.

(51) Shapiro, T. a; Englund, P. T. Selective cleavage of kinetoplast DNA minicircles promoted by antitrypanosomal drugs. *Proc. Natl. Acad. Sci. U. S. A.* 1990, *87* (3), 950–954 DOI: 10.1073/pnas.87.3.950.

(52) Bray, P. G.; Barrett, M. P.; Ward, S. a.; De Koning, H. P. Pentamidine uptake and resistance in pathogenic protozoa: Past, present and future. *Trends Parasitol.* 2003, *19* (5), 232–239 DOI: 10.1016/S1471-4922(03)00069-2.

(53) Midgley, I.; Fitzpatrick, K.; Taylor, L. M.; Houchen, T. L.; Henderson, S. J.; Wright, S. J.; Cybulski, Z. R.; John, B. a; Mcburney, A.; Boykin, D. W.; et al. Pharmacokinetics and Metabolism of the Prodrug DB289 (2 , 5-Bis [4- (N-methoxyamidino) phenyl] furan Monomaleate) in Rat and Monkey and Its Conversion to the Antiprotozoal / Antifungal Drug DB75 (2 , 5-Bis (4-guanylphenyl) furan Dihydrochloride). *Drug Metab. Dispos.* 2007, *35* (6), 955–967 DOI: 10.1124/dmd.106.013391.treatments.

(54) Thuita, J. K.; Wolf, K. K.; Murilla, G. a.; Bridges, A. S.; Boykin, D. W.; Mutuku, J. N.; Liu, Q.; Jones, S. K.; Gem, C. O.; Ching, S.; et al. Chemotherapy of Second Stage Human African Trypanosomiasis: Comparison between the Parenteral Diamidine DB829 and Its Oral Prodrug DB868 in Vervet Monkeys. *PLoS Negl. Trop. Dis.* 2015, *9* (2), e0003409 DOI: 10.1371/journal.pntd.0003409.

(55) Wenzler, T.; Boykin, D. W.; Ismail, M. a.; Hall, J. E.; Tidwell, R. R.; Brun, R. New treatment option for second-stage African sleeping sickness: In vitro and in vivo efficacy of aza analogs of DB289. *Antimicrob. Agents Chemother.* 2009, *53* (10), 4185–4192 DOI: 10.1128/AAC.00225-09.

(56) Poulin, R.; Lu, L.; Ackermann, B.; Bey, P.; Pegg, a. E. Mechanism of the irreversible inactivation of mouse ornithine decarboxylase by ??-difluoromethylornithine. Characterization of sequences at the inhibitor and coenzyme binding sites. *J. Biol. Chem.* 1992, *267* (1), 150–158.

(57) Willert, E.; Phillips, M. a. Regulation and function of polyamines in African trypanosomes. *Trends in Parasitology*. Elsevier Ltd 2012, pp 66–72.

(58) Krauth-Siegel, R. L.; Comini, M. a. Redox control in trypanosomatids, parasitic protozoa with trypanothione-based thiol metabolism. *Biochimica et Biophysica Acta - General Subjects*. 2008, pp 1236–1248.

(59) Vincent, I. M.; Creek, D.; Watson, D. G.; Kamleh, M. a.; Woods, D. J.; Wong, P. E.; Burchmore, R. J. S.; Barrett, M. P. A molecular mechanism for eflornithine resistance in African trypanosomes. *PLoS Pathog.* 2010, *6* (11), 1–9 DOI: 10.1371/journal.ppat.1001204.

(60) Burri, C.; Brun, R. Eflornithine for the treatment of human African trypanosomiasis. *Parasitol. Res.* 2003, *90 Supp 1*, S49-52 DOI: 10.1007/s00436-002-0766-5.

(61) Alirol, E.; Schrumpf, D.; Amici Heradi, J.; Riedel, A.; De Patoul, C.; Quere, M.; Chappuis, F. Nifurtimox-eflornithine combination therapy for second-stage gambiense human African trypanosomiasis: Médecins Sans Frontières experience in the Democratic Republic of the Congo. *Clin. Infect. Dis.* 2013, *56* (2), 195–203 DOI: 10.1093/cid/cis886.

(62) Hall, B. S.; Bot, C.; Wilkinson, S. R. Nifurtimox activation by trypanosomal type I nitroreductases generates cytotoxic nitrile metabolites. *J. Biol. Chem.* 2011, *286* (15), 13088–13095 DOI: 10.1074/jbc.M111.230847.

(63) Yun, O.; Priotto, G.; Tong, J.; Flevaud, L.; Chappuis, F. NECT is next: implementing the new drug combination therapy for Trypanosoma brucei gambiense sleeping sickness. *PLoS Negl. Trop. Dis.* 2010, *4* (5), e720 DOI: 10.1371/journal.pntd.0000720.

(64) Iten, M.; Mett, H.; Evans, A.; Enyaru, J. C.; Brun, R.; Kaminsky, R. Alterations in ornithine decarboxylase characteristics account for tolerance of Trypanosoma brucei rhodesiense to D,L-alpha-difluoromethylornithine. *Antimicrob. Agents Chemother.* 1997, *41* (9), 1922–1925.

(65) DNDi. A fatal disease threatening millions in sub-Saharan Africa - HAT - Fact sheet. 2011, No. 1, 50055 DOI: 10.1371/journal.pmed.0050055.

(66) Eperon, G.; Balasegaram, M.; Potet, J.; Mowbray, C.; Valverde, O.; Chappuis, F. Treatment options for second-stage gambiense human African trypanosomiasis. *Expert Rev. Anti. Infect. Ther.* 2014, *12* (11), 1407–1417 DOI: 10.1586/14787210.2014.959496.

(67) Jennings, F. W.; Urquhart, G. M. The use of the 2 substituted 5-nitroimidazole, Fexinidazole (Hoe 239) in the treatment of chronic T. brucei infections in mice. *Z. Parasitenkd.* 1983, *69* (5), 577–581 DOI: 10.1007/BF00926669.

(68) Kaiser, M.; Bray, M. a.; Cal, M.; Trunz, B. B.; Torreele, E.; Brun, R. Antitrypanosomal activity of fexinidazole, a new oral nitroimidazole drug candidate for treatment of sleeping sickness. *Antimicrob. Agents Chemother.* 2011, *55* (12), 5602–5608 DOI: 10.1128/AAC.00246-11.

(69) Viodé, C. E.; Bettache, N.; Cenas, N.; Krauth-Siegel, R. L.; Chauvière, G. E.; Bakalara, N.; Périé, J. Enzymatic reduction studies of nitroheterocycles. *Biochem. Pharmacol.* 1999, *57* (5), 549–557 DOI: 10.1016/S0006-2952(98)00324-4.

(70) Wilkinson, S. R.; Taylor, M. C.; Horn, D.; Kelly, J. M.; Cheeseman, I. A mechanism for cross-resistance to nifurtimox and benznidazole in trypanosomes. *Proc. Natl. Acad. Sci. U. S. A.* 2008, *105* (13), 5022–5027 DOI: 10.1073/pnas.0711014105.

(71) Torreele, E.; Trunz, B. B.; Tweats, D.; Kaiser, M.; Brun, R.; Mazué, G.; Bray, M. a.; Pécoul, B. Fexinidazole - a new oral nitroimidazole drug candidate entering clinical development for the treatment of sleeping sickness. *PLoS Negl. Trop. Dis.* 2010, *4* (12), 1–15 DOI: 10.1371/journal.pntd.0000923.

(72) Mesu, V. K. B. K.; Kalonji, W. M.; Bardonneau, C.; Mordt, O. V.; Blesson, S.; Simon, F.; Delhomme, S.; Bernhard, S.; Kuziena, W.; Lubaki, J.-P. F.; et al. Oral fexinidazole for late-stage African Trypanosoma brucei gambiense trypanosomiasis: a pivotal multicentre, randomised, non-inferiority trial. *Lancet (London, England)* 2018, *391*

(10116), 144–154 DOI: 10.1016/S0140-6736(17)32758-7.

(73) Fexinidazole in Human African Trypanosomiasis Due to T.b. Gambiense at Any Stage https://www.clinicaltrials.gov/ct2/show/NCT03025789?term=Fexinidazole&rank=3 (accessed May 18, 2018).

(74) Mäser, P.; Wittlin, S.; Rottmann, M.; Wenzler, T.; Kaiser, M.; Brun, R. Antiparasitic agents: New drugs on the horizon. *Curr. Opin. Pharmacol.* 2012, *12* (5), 562–566 DOI: 10.1016/j.coph.2012.05.001.

(75) Jacobs, R.; Nare, B.; Wring, S.; Bacchi, C.; Brun, R.; Plattner, J.; Beaudet, B.; Bowling, T.; Chen, D.; Gaukel, E.; et al. Efficacy and Pharmacokinetics of SCYX-7158 (AN5568): a Novel and Potent Oxaborole-6-Carboxamide Selected as a Pre-Clinical Candidate for Once- Daily Oral Treatment for Stage 2 Human African Trypanosomiasis http://r4d.dfid.gov.uk/Output/185784/.

(76) Wring, S.; Gaukel, E.; Nare, B.; Jacobs, R.; Beaudet, B.; Bowling, T.; Mercer, L.; Bacchi, C.; Yarlett, N.; Randolph, R.; et al. Pharmacokinetics and pharmacodynamics utilizing unbound target tissue exposure as part of a disposition-based rationale for lead optimization of benzoxaboroles in the treatment of Stage 2 Human African Trypanosomiasis. *Parasitology* 2014, *141* (1), 104–118 DOI: 10.1017/S003118201300098X.

(77) DNDi. Clinical Trial SCYX-7158 launch announcement http://www.dndi.org/media-centre/press-releases/1169-oxa-phasei.html (accessed Apr 8, 2015).

(78) Prospective Study on Efficacy and Safety of SCYX-7158 in Patients Infected by Human African Trypanosomiasis Due to T.b. Gambiense (OXA002) https://www.clinicaltrials.gov/ct2/show/NCT03087955?term=SCYX-7158&rank=1 (accessed May 18, 2018).

(79) Bernardes, L. S. C.; Zani, C. L.; Carvalho, I. Trypanosomatidae diseases: from the current therapy to the efficacious role of trypanothione reductase in drug discovery. *Curr. Med. Chem.* 2013, *20* (21), 2673–2696 DOI: 10.2174/0929867311320210005.

(80) Bharate, S. B.; Khan, S. I.; Yunus, N. a M.; Chauthe, S. K.; Jacob, M. R.; Tekwani, B. L.; Khan, I. a; Singh, I. P. Antiprotozoal and antimicrobial activities of O-alkylated and formylated acylphloroglucinols. *Bioorganic Med. Chem.* 2007, *15* (1), 87–96 DOI: 10.1016/j.bmc.2006.10.006.

(81) Brand, S.; Norcross, N. R.; Thompson, S.; Harrison, J. R.; Smith, V. C.; Robinson, D. A.; Torrie, L. S.; McElroy, S. P.; Hallyburton, I.; Norval, S.; et al. Lead Optimization of a Pyrazole Sulfonamide Series of Trypanosoma brucei N -Myristoyltransferase Inhibitors: Identification and Evaluation of CNS Penetrant Compounds as Potential Treatments for Stage 2 Human African Trypanosomiasis. *J. Med. Chem.* 2014 DOI: 10.1021/jm500809c.

(82) Ferrins, L.; Gazdik, M.; Rahmani, R.; Varghese, S.; Sykes, M. L.; Jones, A. J.; Avery, V. M.; White, K. L.; Ryan, E.; Charman, S. A.; et al. Pyridyl benzamides as a novel class of potent inhibitors for the kinetoplastid Trypanosoma brucei. *J. Med. Chem.* 2014 DOI: 10.1021/jm500191u.

(83) Frearson, J. a; Brand, S.; McElroy, S. P.; Cleghorn, L. a T.; Smid, O.; Stojanovski, L.; Price, H. P.; Guther, M. L. S.; Torrie, L. S.; Robinson, D. a; et al. N-myristoyltransferase inhibitors as new leads to treat sleeping sickness. *Nature* 2010, *464* (7289), 728–732 DOI: 10.1038/nature08893.

(84) Grady, R. W.; Bienen, E. J.; Clarkson, A. B. Esters of 3,4-dihydroxybenzoic acid, highly effective inhibitors of the sn-glycerol-3-phosphate oxidase of Trypanosoma brucei brucei. *Mol. Biochem. Parasitol.* 1986, *21* (1), 55–63 DOI: 10.1016/0166-6851(86)90079-4.

(85) Grady, R. W.; Bienen, E. J.; Dieck, H. A.; Saric, M.; Clarkson, A. B. N-n-alkyl-3,4-dihydroxybenzamides as inhibitors of the trypanosome alternative oxidase: Activity in vitro and in vivo. *Antimicrob. Agents Chemother.* 1993, *37* (5), 1082–1085 DOI: 10.1128/AAC.37.5.1082.

(86) Nihei, C.; Fukai, Y.; Kita, K. Trypanosome alternative oxidase as a target of chemotherapy. *Biochim. Biophys. Acta* 2002, *1587* (2–3), 234–239.

(87) Ott, R.; Chibale, K.; Anderson, S.; Chipeleme, A.; Chaudhuri, M.; Guerrah, A.; Colowick, N.; Hill, G. C. Novel inhibitors of the trypanosome alternative oxidase inhibit Trypanosoma brucei brucei growth and respiration. *Acta Trop.* 2006, *100* (3), 172–184 DOI: 10.1016/j.actatropica.2006.10.005.

(88) Sharma, S.; Singha, U. K.; Chaudhuri, M. Role of Tob55 on mitochondrial protein biogenesis in Trypanosoma brucei. *Mol. Biochem. Parasitol.* 2010, *174* (2), 89–100 DOI: 10.1016/j.molbiopara.2010.07.003.

(89) Woodring, J. L.; Patel, G.; Erath, J.; Behera, R.; Lee, P. J.; Leed, S. E.; Rodriguez, A.; Sciotti, R. J.; Mensa-Wilmot, K.; Pollastri, M. P. Evaluation of aromatic 6-substituted thienopyrimidines as scaffolds against parasites that cause trypanosomiasis, leishmaniasis, and malaria. *Med. Chem. Commun.* 2015, *6* (2), 339–346 DOI: 10.1039/C4MD00441H.

(90) Price, H. P. Myristoyl-CoA:Protein N-Myristoyltransferase, an Essential Enzyme and Potential Drug Target in Kinetoplastid Parasites. *J. Biol. Chem.* 2003, *278* (9), 7206–7214 DOI: 10.1074/jbc.M211391200.

(91) Peterson, C.; Grinnage-Pulley, T. http://www.merckvetmanual.com/mvm/circulatory_system/blood_parasites/trypanosomiasis.html http://www.merckvetmanual.com/mvm/circulatory_system/blood_parasites/trypanosomiasis.html (accessed May 13, 2016).

(92) Dolan, R. B.; Okech, G.; Alushula, H.; Mutugi, M.; Stevenson, P.; Sayer, P. D.; Njogu, A. R. Homidium bromide as a chemoprophylactic for cattle trypanosomiasis in Kenya. *Acta Trop.* 1990, *47* (3), 137–144 DOI: 10.1016/0001-706X(90)90019-V.

(93) Browning, C. H.; Morgan, G. T.; Robb, J. V. M.; Walls, L. P. The trypanocidal action of certain phenanthridinium compounds. *J. Pathol. Bacteriol.* 1938, *46* (1), 203–204 DOI: 10.1002/path.1700460121.

(94) WATKINS, T. I.; WOOLFE, G. Effect of Changing the Quaternizing Group on the Trypanocidal Activity of Dimidium Bromide. *Nature* 1952, *169* (4299), 506.

(95) Wagner, T. E. Proceedings of the Research Symposium on Complexes of Biologically Active Substances with Nucleic Acids and Their Modes of Action: Held at the Walter Reed Army Institute of Research Washington, 16--19 March 1970; Hahn, F. E., Ed.; Springer Berlin Heidelberg: Berlin, Heidelberg, 1971; pp 152–162.

(96) Delespaux, V.; Dekoning, H. Drugs and drug resistance in African trypanosomiasis. *Drug Resist. Updat.* 2007, *10* (1–2), 30–50 DOI: 10.1016/j.drup.2007.02.004.

(97) Geerts, S. African bovine trypanosomiasis: the problem of drug resistance. *Parasitol. Today* 2001, *17* (1), 25–28 DOI: 10.1016/S0169-4758(00)01827-5.

(98) Shiferaw, S.; Muktar, Y.; Belina, D. A review on trypanocidal drug resistance in Ethiopia. 2015, *7* (May), 58–66 DOI: JPVB2015.0190.

(99) Peregrine, A. S.; Mamman, M. Pharmacology of diminazene: a review. *Acta Trop.* 1993, *54* (3–4), 185–203 DOI: 10.1016/0001-706X(93)90092-P.

(100) BAUER, F. [Trypanosomiasis and babesiasis in Africa and their treatment with the new preparation berenil]. *Zeitschrift für Tropenmedizin und Parasitol.* 1955, *6* (2), 129–140.

(101) Hu, S. H.; Weisz, K.; James, T. L.; Shafer, R. H. H-NMR studies on d(GCTTAAGC)2 and its complex with berenil. *Eur. J. Biochem.* 1992, *204* (1), 31–38 DOI: 10.1111/j.1432-1033.1992.tb16602.x.

(102) DAMPER, D.; PATTON, C. L. Pentamidine Transport and Sensitivity in brucei -Group Trypanosomes*. *J. Protozool.* 1976, *23* (2), 349–356 DOI: 10.1111/j.1550-7408.1976.tb03787.x.

(103) Boibessot, I.; Turner, C. M. R.; Watson, D. G.; Goldie, E.; Connel, G.; McIntosh, A.; Grant, M. H.; Skellern, G. G. Metabolism and distribution of phenanthridine trypanocides in Trypanosoma brucei. *Acta Trop.* 2002, *84* (3), 219–228 DOI: 10.1016/S0001-706X(02)00188-2.

(104) Whitelaw, D. D.; Bell, I. R.; Holmes, P. H.; Moloo, S. K.; Hirumi, H.; Urquhart, G. M.; Murray, M. Isometamidium chloride prophylaxis against Trypanosoma congolense challenge and the development of immune responses in Boran cattle. *Vet. Rec.* 1986, *118* (26), 722–726 DOI: 10.1136/vr.118.26.722.

(105) Delespaux, V.; Geysen, D.; Majiwa, P. A. O.; Geerts, S. Identification of a genetic marker for isometamidium chloride resistance in Trypanosoma congolense. *Int. J. Parasitol.* 2005, *35* (2), 235–243 DOI: 10.1016/j.ijpara.2004.11.009.

(106) CURD, F. H. S.; DAVEY, D. G. Antrycide, a new trypanocidal drug. *Br. J. Pharmacol. Chemother.* 1950, *5* (1), 25–32.

(107) ORMEROD, W. E. The mode of action of antrycide. *Br. J. Pharmacol. Chemother.* 1951, *6* (2), 325–333.

(108) ORMEROD, W. E. A study of resistance to antrycide in a strain of Trypanosoma equiperdum. *Br. J. Pharmacol. Chemother.* 1952, *7* (4), 674–684.

(109) ORMEROD, W. E.; SHAW, J. J. A STUDY OF GRANULES AND OTHER CHANGES IN PHASE-CONTRAST APPEARANCE PRODUCED BY CHEMOTHERAPEUTIC AGENTS IN TRYPANOSOMES. *Br. J. Pharmacol. Chemother.* 1963, *21* (2), 259–272 DOI: 10.1111/j.1476-5381.1963.tb01525.x.

(110) ORMEROD, W. E. A study of cytoplasmic inclusions in Trypanosoma lewisi and their relationship to the formation of antibody. *J. Gen. Microbiol.* 1959, *21* (1), 287–294 DOI: 10.1099/00221287-21-2-287.

(111) Liao, D.; Shen, J. Studies of quinapyramine-resistance of Trypanosoma brucei evansi in China. *Acta Trop.* 2010, *116* (3), 173–177 DOI: 10.1016/j.actatropica.2010.08.016.

(112) Freund, Y. R.; Akama, T.; Sanders, V.; Bu, W.; Jacob, J.; Easom, E.; Gillingwater, K.; Brun, R.; Napier, G. B.; Witty, M.; et al. Leveraging an Oxaborole in Clinical Trials for HAT to Develop Novel Compounds to Treat Animal African Trypanosomosis (AAT). Anacor Active in 12 Neglected Disease Research Programs and has a Long History with PDPs and the BMGF. In *ISCTRC*; Khartoum, Sudan, 2013.

(113) Clarkson, a. B.; Bienen, E. J.; Pollakis, G.; Grady, R. W. Respiration of bloodstream forms of the parasite Trypanosoma brucei brucei is dependent on a plant-like alternative oxidase. *J. Biol. Chem.* 1989, *264* (30), 17770–17776.

(114) Opperdoes, F. R.; Borst, P.; Bakker, S.; Leene, W. Localization of glycerol-3-phosphate oxidase in the mitochondrion and particulate NAD+-linked glycerol-3-phosphate dehydrogenase in the microbodies of the bloodstream form to Trypanosoma brucei. *Eur. J. Biochem.* 1977, *76* (1), 29–39 DOI: 10.1111/j.1432-1033.1977.tb11567.x.

(115) Minagawa, N.; Yabu, Y.; Kita, K.; Nagaid, K.; Ohtab, N.; Meguro, K.; Sakajo, S.; Yoshimoto, A. An antibiotic , ascofuranone , specifically inhibits respiration and in vitro growth of long slender bloodstream forms of Trypanosoma brucei brucei. *Mol. Biochem. Parasitol.* 1996, *81* (1), 127–136.

(116) Chaudhuri, M.; Ott, R. D.; Hill, G. C. Trypanosome alternative oxidase: from molecule to function. *Trends in Parasitology*. October 2006, pp 484–491.

(117) Chaudhuri, M.; Ajayi, W.; TEMPLE, S.; Hill, G. C. Identification and partial purification of a stage-specific 33 kDa mitochondrial protein as the alternative oxidase of the Trypanosoma brucei brucei bloodstream trypomastigotes. *J. Eukaryot. Microbiol.* 1995, *42* (5), 467–472 DOI: 10.1111/j.1550-7408.1995.tb05892.x.

(118) Chaudhuri, M.; Hill, G. C. Cloning, sequencing, and functional activity of the Trypanosoma brucei brucei alternative oxidase. *Mol. Biochem. Parasitol.* 1996, *83* (1), 125–129 DOI: 10.1016/S0166-6851(96)02754-5.

(119) Grant, P. T.; Sargent, J. R. L-alpha-Glycerophosphate dehydrogenase, a component of an oxidase system in Trypanosoma rhodesiense. *Biochem. J.* 1961, *81* (1959), 206–214.

(120) Kido, Y.; Sakamoto, K.; Nakamura, K.; Harada, M.; Suzuki, T.; Yabu, Y.; Saimoto, H.; Yamakura, F.; Ohmori, D.; Moore, A.; et al. Purification and kinetic characterization of recombinant alternative oxidase from Trypanosoma brucei brucei. *Biochim. Biophys. Acta - Bioenerg.* 2010, *1797* (4), 443–450 DOI: 10.1016/j.bbabio.2009.12.021.

(121) Fukai, Y.; Nihei, C.; Kawai, K.; Yabu, Y.; Suzuki, T.; Ohta, N.; Minagawa, N.; Nagai, K.; Kita, K. Overproduction of highly active trypanosome alternative oxidase in Escherichia coli heme-deficient mutant. *Parasitol. Int.* 2003, *52* (3), 237–241 DOI: 10.1016/S1383-5769.

(122) Nihei, C.; Fukai, Y.; Kawai, K.; Osanai, A.; Yabu, Y.; Suzuki, T.; Ohta, N.; Minagawa, N.; Nagai, K.; Kita, K. Purification of active recombinant trypanosome alternative oxidase. *FEBS Lett.* 2003, *538* (1–3), 35–40 DOI: 10.1016/S0014-5793(03)00120-0.

(123) Nakayashiki, T.; Nishimura, K.; Tanaka, R.; Inokuchi, H. Partial inhibition of protein synthesis accelerates the synthesis of porphyrin in heme-deficient mutants of Escherichia coli. *Mol. Gen. Genet.* 1995, *249* (2), 139–146 DOI: 10.1007/BF00290359.

(124) Chaudhuri, M.; Ajayi, W.; Hill, G. C. Biochemical and molecular properties of the Trypanosoma brucei alternative oxidase. *Mol. Biochem. Parasitol.* 1998, *95* (1), 53–68.

(125) Kido, Y.; Shiba, T.; Inaoka, D. K.; Sakamoto, K.; Nara, T.; Aoki, T.; Honma, T.; Tanaka, A.; Inoue, M.; Matsuoka, S.; et al. Crystallization and preliminary crystallographic analysis of cyanide-insensitive alternative oxidase from Trypanosoma brucei brucei. *Acta Crystallogr. Sect. F. Struct. Biol. Cryst. Commun.* 2010, *66* (Pt 3), 275–278 DOI: 10.1107/S1744309109054062.

(126) Fukai, Y.; Amino, H.; Hirawake, H.; Yabu, Y.; Ohta, N.; Minagawa, N.; Sakajo, S.; Yoshimoto, a; Nagai, K.; Takamiya, S.; et al. Functional expression of the ascofuranone-sensitive Trypanosoma brucei brucei alternative oxidase in the cytoplasmic membrane of Escherichia coli. *Comp. Biochem. Physiol. C. Pharmacol. Toxicol. Endocrinol.* 1999, *124* (2), 141–148.

(127) Mogi, T.; Ui, H.; Shiomi, K.; Omura, S.; Miyoshi, H.; Kita, K. Antibiotics LL-Z1272 identified as novel inhibitors discriminating bacterial and mitochondrial quinol

oxidases. *Biochim. Biophys. Acta* 2009, *1787* (2), 129–133 DOI: 10.1016/j.bbabio.2008.11.016.

(128) Saimoto, H.; Kido, Y.; Haga, Y.; Sakamoto, K.; Kita, K. Pharmacophore identification of ascofuranone, potent inhibitor of cyanide-insensitive alternative oxidase of Trypanosoma brucei. *J. Biochem.* 2013, *153* (3), 267–273 DOI: 10.1093/jb/mvs135.

(129) Shiba, T.; Kido, Y.; Sakamoto, K.; Inaoka, D. K.; Tsuge, C.; Tatsumi, R.; Takahashi, G.; Balogun, E. O.; Nara, T.; Aoki, T.; et al. Structure of the trypanosome cyanide-insensitive alternative oxidase. *Proc. Natl. Acad. Sci.* 2013, *110* (12), 4580–4585 DOI: 10.1073/pnas.1218386110.

(130) Nakamura, K.; Fujioka, S.; Fukumoto, S.; Inoue, N.; Sakamoto, K.; Hirata, H.; Kido, Y.; Yabu, Y.; Suzuki, T.; Watanabe, Y.; et al. Trypanosome alternative oxidase, a potential therapeutic target for sleeping sickness, is conserved among Trypanosoma brucei subspecies. *Parasitol. Int.* 2010, *59* (4), 560–564 DOI: 10.1016/j.parint.2010.07.006.

(131) Shibaa, T.; Kita, K.; Harada, S. Crystal structure of the trypanosome cyanide-insensitive alternative oxidase. *Spring 8 Res. Front. Life Sci. Stuctural Biol.* 2013, 10–11.

(132) Siedow, J. N.; Umbach, A. L.; Moore, A. L. The active site of the cyanide-resistant oxidase from plant mitochondria contains a binuclear iron center. *FEBS Lett.* 1995, *362* (1), 10–14 DOI: 10.1016/0014-5793(95)00196-G.

(133) Tsuda, A.; Witola, W. H.; Ohashi, K.; Onuma, M. Expression of alternative oxidase inhibits programmed cell death-like phenomenon in bloodstream form of Trypanosoma brucei rhodesiense. *Parasitol. Int.* 2005, *54* (4), 243–251 DOI: 10.1016/j.parint.2005.06.007.

(134) Fang, J.; Beattie, D. S. Alternative oxidase present in procyclic Trypanosoma brucei may act to lower the mitochondrial production of superoxide. *Arch. Biochem. Biophys.* 2003, *414* (2), 294–302 DOI: 10.1016/S0003-9861(03)00196-6.

(135) Jeacock, L.; Baker, N.; Wiedemar, N.; Mäser, P.; Horn, D. Aquaglyceroporin-null trypanosomes display glycerol transport defects and respiratory-inhibitor sensitivity. *PLoS Pathog.* 2017, *13* (3), 1–16 DOI: 10.1371/journal.ppat.1006307.

(136) Edwards, D. L.; Rosenberg, E.; Maroney, P. A. Induction of cyanide-insensitive Respiration in Neuropora crassa*. *J. Biochem.* 1974, *249* (11), 3551–3556.

(137) Lambowitz, A. M.; Slayman, C. W. Cyanide-resistant respiration in Neurospora crassa. *J. Bacteriol.* 1971, *108* (3), 1087–1096.

(138) Clarkson, A.; Brohn, F. Trypanosomiasis: an approach to chemotherapy by the inhibition of carbohydrate catabolism. *Science (80-.).* 1976, *194* (4261), 204–206 DOI: 10.1126/science.986688.

(139) Opperdoes, F. R.; Borst, P.; Fonck, K. The potential use of inhibitors of glycerol-3-

phosphate oxidase for chemotherapy of African trypanosomiasis. *FEBS Lett.* 1976, *62* (2), 169–172 DOI: 10.1016/0014-5793(76)80045-2.

(140) Bakker, B. M.; Michels, P. a M.; Opperdoes, R.; Westerhoff, H. V; Opperdoes, F. R. CELL BIOLOGY AND METABOLISM : What Controls Glycolysis in Bloodstream Form Trypanosoma brucei ? What Controls Glycolysis in Bloodstream Form Trypanosoma brucei ?*. 1999, *274* (21), 14551–14559.

(141) Hosokawa, T.; Sawada, M.; Ando, K. Isolation and Structure of Ascofuranone and Ascofuranol antibiotics with hypolipidemic activity. *J. Antibiot. (Tokyo).* 1973, *5* (I), 676–680.

(142) Sasaki, H.; Okutomi, T.; Hosokawa, T.; Nawata, Y.; Ando, K. Ascofuranone, a new antibiotic from ascochyta viciae. *Tetrahedron Lett.* 1972, *13* (25), 2541–2544 DOI: 10.1016/S0040-4039(01)84869-3.

(143) Tamura, G.; Suzuki, S.; Takatsuki, A.; Ando, K.; Arima, K. Ascochlorin, a new antibiotic, found by the paper-disc agar-diffusion method. I. Isolation, biological and chemical properties of ascochlorin. (Studies on antiviral and antitumor antibiotics. I). *J. Antibiot. (Tokyo).* 1968, *21* (9), 539–544 DOI: 10.7164/antibiotics.21.539.

(144) Mori, K.; Fujioka, T. Synthesis of (±)-ascofuranone, in antibiotic with hypolipidemic and antitumor protective properties. *Tetrahedron Lett.* 1983, *24* (14), 1547–1548 DOI: 10.1016/S0040-4039(00)81705-0.

(145) Mori, K.; Takechi, S. Synthesis of the natural enantiomers of ascochlorin, ascofuranone and ascofuranol. *Tetrahedron* 1985, *41* (15), 3049–3062 DOI: 10.1016/S0040-4020(01)96657-8.

(146) Magae, J.; Nagai, K.; Ando, K.; Tamura, G. Differentiation of Mouse and Human Myeloid Leukemia Cells Induced by an Antitumor Antibiotic, Ascofuranone. *Agric. Biol. Chem.* 1988, *52* (12), 3143–3147 DOI: 10.1080/00021369.1988.10869194.

(147) Fukai, Y.; Nihei, C.; Yabu, Y.; Suzuki, T.; Ohta, N.; Minagawa, N.; Nagai, K.; Kita, K. Strain-specific difference in amino acid sequences of trypanosome alternative oxidase. *Parasitol. Int.* 2002, *51* (2), 195–199.

(148) Kosuge, Y.; Suzuki, A.; Tamura, S. Structures of Colletochlorin C, Colletorin A and Colletorin C from Colletotrichum nicotianae. *Agric. Biol. Chem.* 1974, *38* (6), 1265–1267 DOI: 10.1080/00021369.1974.10861322.

(149) Mori, K.; Sato, K. A general synthetic method for prenylated phenols of microbial origin. *Tetrahedron* 1982, *38* (9), 1221–1225 DOI: 10.1016/0040-4020(82)85107-7.

(150) Takahashi, N.; Osada, H.; Numao, N.; Saimoto, H.; Kawabata, T.; Hiyama, T. Differentiation induction of human promyelocytic leukemia cells with colletochlorin B and its analogues. *Chem. Pharm. Bull. (Tokyo).* 1988, *36* (1), 452–455 DOI:

10.1248/cpb.36.452.

(151) Meco Navas, A.; Ebiloma, G. U.; Martín Domínguez, A.; Martínez Benayas, I.; cueto diaz, E.; Alhejely, A. S.; Balogun, E. O.; Saito, M.; Matsui, M.; Arai, N.; et al. SAR of 4-Alkoxybenzoic Acid Inhibitors of the Trypanosome Alternative Oxidase. *ACS Med. Chem. Lett.* 2018, acsmedchemlett.8b00282 DOI: 10.1021/acsmedchemlett.8b00282.

(152) Ebiloma, G. U.; Ayuga, T. D.; Balogun, E. O.; Gil, L. A.; Donachie, A.; Kaiser, M.; Herraiz, T.; Inaoka, D. K.; Shiba, T.; Harada, S.; et al. Inhibition of trypanosome alternative oxidase without its N-terminal mitochondrial targeting signal (ΔMTS-TAO) by cationic and non-cationic 4-hydroxybenzoate and 4-alkoxybenzaldehyde derivatives active against T. brucei and T. congolense. *Eur. J. Med. Chem.* 2018, *150*, 385–402 DOI: 10.1016/j.ejmech.2018.02.075.

(153) Fueyo González, F. J.; Ebiloma, G. U.; Izquierdo García, C.; Bruggeman, V.; Sánchez Villamañán, J. M.; Donachie, A.; Balogun, E. O.; Inaoka, D. K.; Shiba, T.; Harada, S.; et al. Conjugates of 2,4-Dihydroxybenzoate and Salicylhydroxamate and Lipocations Display Potent Antiparasite Effects by Efficiently Targeting the Trypanosoma brucei and Trypanosoma congolense Mitochondrion. *J. Med. Chem.* 2017, *60* (4), 1509–1522 DOI: 10.1021/acs.jmedchem.6b01740.

(154) Rosano, G. L.; Ceccarelli, E. A. Recombinant protein expression in Escherichia coli: advances and challenges. *Front. Microbiol.* 2014, *5* (APR), 1–17 DOI: 10.3389/fmicb.2014.00172.

(155) Hanahan, D. Studies on transformation of Escherichia coli with plasmids. *J. Mol. Biol.* 1983, *166* (4), 557–580 DOI: 10.1016/S0022-2836(83)80284-8.

(156) Goh, S.; Good, L. Plasmid selection in Escherichia coli using an endogenous essential gene marker. *BMC Biotechnol.* 2008, *8* (1), 61 DOI: 10.1186/1472-6750-8-61.

(157) Lewis, M. The lac repressor. *C. R. Biol.* 2005, *328* (6), 521–548 DOI: 10.1016/j.crvi.2005.04.004.

(158) Rigaut, G.; Shevchenko, A.; Rutz, B.; Wilm, M.; Mann, M.; Séraphin, B. A generic protein purification method for protein complex characterization and proteome exploration. *Nat. Biotechnol.* 1999, *17* (10), 1030–1032 DOI: 10.1038/13732.

(159) Ajayi, W. U.; Chaudhuri, M.; Hill, G. C. Site-directed mutagenesis reveals the essentiality of the conserved residues in the putative diiron active site of the trypanosome alternative oxidase. *J. Biol. Chem.* 2002, *277* (10), 8187–8193 DOI: 10.1074/jbc.M111477200.

(160) Oganesyan, N.; Ankoudinova, I.; Kim, S.-H.; Kim, R. Effect of osmotic stress and heat shock in recombinant protein overexpression and crystallization. *Protein Expr. Purif.* 2007, *52* (2), 280–285 DOI: 10.1016/j.pep.2006.09.015.

(161) Blackwell, J. R.; Horgan, R. A novel strategy for production of a highly expressed recombinant protein in an active form. *FEBS Lett.* 1991, *295* (1–3), 10–12 DOI: 10.1016/0014-5793(91)81372-F.

(162) Andersson, M. E.; Nordlund, P. A revised model of the active site of alternative oxidase. *FEBS Lett.* 1999, *449* (1), 17–22 DOI: S0014-5793(99)00376-2 [pii].

(163) Towbin, H.; Staehelin, T.; Gordon, J. Electrophoretic transfer of proteins from polyacrylamide gels to nitrocellulose sheets: procedure and some applications. *Proc. Natl. Acad. Sci.* 1979, *76* (9), 4350–4354 DOI: 10.1073/pnas.76.9.4350.

(164) Cardoza, J. D.; Parikh, J. R.; Ficarro, S. B.; Marto, J. A. Mass spectrometry-based proteomics: qualitative identification to activity-based protein profiling. *Wiley Interdiscip. Rev. Syst. Biol. Med.* 2012, *4* (2), 141–162 DOI: 10.1002/wsbm.166.

(165) Affourtit, C.; Albury, M. S.; Crichton, P. G.; Moore, A. L. Exploring the molecular nature of alternative oxidase regulation and catalysis. *FEBS Lett.* 2002, *510* (3), 121–126 DOI: 10.1016/S0014-5793(01)03261-6.

(166) Wilson, K.; Walker, J. *Principles and Techniques of Practical Biochemistry*; Principles and Techniques of Practical Biochemistry; Cambridge University Press, 2000.

(167) Suzuki, T.; Nihei, C.; Yabu, Y.; Hashimoto, T.; Suzuki, M.; Yoshida, A.; Nagai, K.; Hosokawa, T.; Minagawa, N.; Suzuki, S.; et al. Molecular cloning and characterization of Trypanosoma vivax alternative oxidase (AOX) gene, a target of the trypanocide ascofuranone. *Parasitol. Int.* 2004, *53* (3), 235–245 DOI: 10.1016/j.parint.2004.02.001.

(168) Hoefnagel, M.; Rich, P. R.; Zhang, Q.; Wiskich, J. T. Substrate Kinetics of the Plant Mitochondrial Alternative Oxidase and the Effects of Pyruvate. *Plant Physiol.* 1997, *115* (3), 1145–1153.

(169) Johnson, K. A.; Goody, R. S. The Original Michaelis Constant: Translation of the 1913 Michaelis–Menten Paper. *Biochemistry* 2011, *50* (39), 8264–8269 DOI: 10.1021/bi201284u.

(170) Lineweaver, H.; Burk, D. The Determination of Enzyme Dissociation Constants. *J. Am. Chem. Soc.* 1934, *56* (3), 658–666 DOI: 10.1021/ja01318a036.

(171) Ranaldi, F.; Vanni, P.; Giachetti, E. What students must know about the determination of enzyme kinetic parameters. *Biochem. Educ.* 1999, *27* (2), 87–91 DOI: 10.1016/S0307-4412(98)00301-X.

(172) Hoefnagel, M.; Rich, P. R.; Zhang, Q.; Wiskich, J. T. Substrate Kinetics of the Plant Mitochondrial Alternative Oxidase and the Effects of Pyruvate. *Plant Physiol.* 1997, *115* (3), 1145–1153.

(173) YOSHIKAWA, S.; ORII, Y. The Inhibition Mechanism of the Cytochrome Oxidase Reaction. *J. Biochem.* 1972, *71* (5), 859–872.

(174) Brooks, H. B.; Geeganage, S.; Kahl, S. D.; Montrose, C.; Sittampalam, S.; Smith, M. C.; Weidner, J. R. *Basics of Enzymatic Assays for HTS*; 2004.

(175) Iversen PW, Beck B, Chen YF, et al. HTS Assay Validation. Assay Guidance Manual. Bethesda (MD): Eli Lilly & Company and the National Center for Adv https://www.ncbi.nlm.nih.gov/books/NBK83783/ (accessed May 5, 2018).

(176) Simeonov, A.; Davis, M. I. Interference with Fluorescence and Absorbance Assay Guidance Manual. In *Assay Guidance Manual*; 2015; pp 1–12.

(177) Dahlin, J. L.; Walters, M. A. The essential roles of chemistry in high-throughput screening triage. *Future Med. Chem.* 2014, *6* (11), 1265–1290 DOI: 10.4155/fmc.14.60.

(178) West, R. A.; O'Doherty, O. G.; Askwith, T.; Atack, J.; Beswick, P.; Laverick, J.; Paradowski, M.; Pennicott, L. E.; Rao, S. P. S.; Williams, G.; et al. African trypanosomiasis: Synthesis & SAR enabling novel drug discovery of ubiquinol mimics for trypanosome alternative oxidase. *Eur. J. Med. Chem.* 2017, *141*, 676–689 DOI: 10.1016/j.ejmech.2017.09.067.

(179) Pryde, D. C.; Dalvie, D.; Hu, Q.; Jones, P.; Obach, R. S.; Tran, T.-D. Aldehyde Oxidase: An Enzyme of Emerging Importance in Drug Discovery. *J. Med. Chem.* 2010, *53* (24), 8441–8460 DOI: 10.1021/jm100888d.

(180) Kalgutkar, A. S. Liabilities Associated with the Formation of "Hard" Electrophiles in Reactive Metabolite Trapping Screens. *Chem. Res. Toxicol.* 2017, *30* (1), 220–238 DOI: 10.1021/acs.chemrestox.6b00332.

(181) Casey, M. L.; Kemp, D. S.; Paul, K. G.; Cox, D. D. Physical organic chemistry of benzisoxazoles. I. Mechanism of the base-catalyzed decomposition of benzisoxazoles. *J. Org. Chem.* 1973, *38* (13), 2294–2301 DOI: 10.1021/jo00953a006.

(182) Wager, T. T.; Hou, X.; Verhoest, P. R.; Villalobos, A. Moving beyond Rules: The Development of a Central Nervous System Multiparameter Optimization (CNS MPO) Approach To Enable Alignment of Druglike Properties. *ACS Chem. Neurosci.* 2010, *1* (6), 435–449 DOI: 10.1021/cn100008c.

(183) O'Doherty, O. G. Synthesis of novel trypanosome alternative oxidase inhibitors for the treatment of African trypanosomiasis, University of Sussex, 2016.

(184) Vilsmeier, A.; Haack, A. Über die Einwirkung von Halogenphosphor auf Alkyl-formanilide. Eine neue Methode zur Darstellung sekundärer und tertiärer p -Alkylamino-benzaldehyde. *Berichte der Dtsch. Chem. Gesellschaft (A B Ser.* 1927, *60* (1), 119–122 DOI: 10.1002/cber.19270600118.

(185) Masilamani, D.; Rogie, M. M. Sulfuryl Chloride as a Reagent for Selective Chlorination of Symmetrical Ketones and Phenols. *J. Org. Chem.* 1981, *46* (11), 4486–4489 DOI: 10.1021/jo00335a033.

(186) Harder, E.; Damm, W.; Maple, J.; Wu, C.; Reboul, M.; Xiang, J. Y.; Wang, L.; Lupyan, D.; Dahlgren, M. K.; Knight, J. L.; et al. OPLS3: A Force Field Providing Broad Coverage of Drug-like Small Molecules and Proteins. *J. Chem. Theory Comput.* 2016, *12* (1), 281–296 DOI: 10.1021/acs.jctc.5b00864.

(187) Kalkhambkar, R. G.; Yuvaraj, H. Triflic Anhydride: A Mild Reagent for Highly Efficient Synthesis of 1,2-Benzisoxazoles, Isoxazolo, and Isothiazolo Quinolines Without Additive or Base. *Synth. Commun.* 2014, *44* (4), 547–555 DOI: 10.1080/00397911.2013.821617.

(188) Thomas, B.; George, J.; Sugunan, S. Synthesis of benzoxazole via the Beckmann rearrangement of salicylaldoxime on protonated zeolites: A green continuous process. *Ind. Eng. Chem. Res.* 2009, *48* (2), 660–670 DOI: 10.1021/ie800913q.

(189) Miyaura, N.; Suzuki, A. Stereoselective synthesis of arylated (E)-alkenes by the reaction of alk-1-enylboranes with aryl halides in the presence of palladium catalyst. *J. Chem. Soc. Chem. Commun.* 1979, No. 19, 866 DOI: 10.1039/c39790000866.

(190) Miyaura, N.; Yamada, K.; Suzuki, A. A new stereospecific cross-coupling by the palladium-catalyzed reaction of 1-alkenylboranes with 1-alkenyl or 1-alkynyl halides. *Tetrahedron Lett.* 1979, *20* (36), 3437–3440 DOI: 10.1016/S0040-4039(01)95429-2.

(191) Mizoroki, T.; Mori, K.; Ozaki, A. Arylation of Olefin with Aryl Iodide Catalyzed by Palladium. *Bull. Chem. Soc. Jpn.* 1971, *44* (2), 581–581 DOI: 10.1246/bcsj.44.581.

(192) Heck, R. F.; Nolley, J. P. Palladium-catalyzed vinylic hydrogen substitution reactions with aryl, benzyl, and styryl halides. *J. Org. Chem.* 1972, *37* (14), 2320–2322 DOI: 10.1021/jo00979a024.

(193) Pourmousavi, S. A.; Salehi, P. Synthesis of Benzyl Triethyl Ammonium Tribromide and Its Application as a Highly Efficient and Regioselective Reagent for the Bromination of Activated Aromatic Compounds. *Acta Chim. Slov.* 2009, *3* (56), 734–739.

(194) Peh, G.-R.; Kantchev, E. A. B.; Zhang, C.; Ying, J. Y. N-heterocycle carbene (NHC)-ligated cyclopalladated N,N-dimethylbenzylamine: a highly active, practical and versatile catalyst for the Heck-Mizoroki reaction. *Org. Biomol. Chem.* 2009, *7* (10), 2110–2119 DOI: 10.1039/b821892g.

(195) Herrmann, W. A.; Köcher, C. N-Heterocyclic Carbenes. *Angew. Chemie Int. Ed. English* 1997, *36* (20), 2162–2187 DOI: 10.1002/anie.199721621.

(196) Hadei, N.; Kantchev, E. A. B.; O'Brie, C. J.; Organ, M. G. Electronic Nature of N-Heterocyclic Carbene Ligands: Effect on the Suzuki Reaction. *Org. Lett.* 2005, *7* (10), 1991–1994 DOI: 10.1021/ol050471w.

(197) Vatèle, J.-M. One-Pot Oxidative Conversion of Alcohols into Nitriles by Using a TEMPO/PhI(OAc)2/NH4OAc System. *Synlett* 2014, *25* (09), 1275–1278 DOI: 10.1055/s-

0033-1341124.

(198) Bag, S.; Tawari, N. R.; Degani, M. S. A new, mild and high yielding protocol for the preparation of nitriles from aldehydes using iodosobenzene diacetate in aqueous ammonia. *Arkivoc* 2009, *2009* (14), 118–123.

(199) Tamura, Y.; Yakura, T.; Tohma, H.; Ki-kuchi, K.; Kita, Y. Hypervalent Iodine Oxidation of p -Alkoxy- and Related Phenols: A Facile and Efficient Synthesis of p -Quinones. *Synthesis (Stuttg).* 1989, *1989* (02), 126–127 DOI: 10.1055/s-1989-27170.

(200) Pouységu, L.; Sylla, T.; Garnier, T.; Rojas, L. B.; Charris, J.; Deffieux, D.; Quideau, S. Hypervalent iodine-mediated oxygenative phenol dearomatization reactions. *Tetrahedron* 2010, *66* (31), 5908–5917 DOI: 10.1016/j.tet.2010.05.078.

(201) De Luca, L.; Giacomelli, G.; Porcheddu, A. Beckmann Rearrangement of Oximes under Very Mild Conditions. *J. Org. Chem.* 2002, *67* (17), 6272–6274 DOI: 10.1021/jo025960d.

(202) Mandal, P. K.; McMurray, J. S. Pd-C-induced catalytic transfer hydrogenation with triethylsilane. *J. Org. Chem.* 2007, *72* (17), 6599–6601 DOI: 10.1021/jo0706123.

(203) Suzuki, S.; Segawa, Y.; Itami, K.; Yamaguchi, J. Synthesis and characterization of hexaarylbenzenes with five or six different substituents enabled by programmed synthesis. *Nat. Chem.* 2015, *7* (3), 227–233 DOI: 10.1038/nchem.2174.

(204) Zhu, L.; Lu, L.; Wang, S.; Wu, J.; Shi, J.; Yan, T.; Xie, C.; Li, Q.; Hu, M.; Liu, Z. Oral Absorption Basics. In *Developing Solid Oral Dosage Forms*; Elsevier, 2017; pp 297–329.

(205) Lipinski, C. A.; Lombardo, F.; Dominy, B. W.; Feeney, P. J. Experimental and computational approaches to estimate solubility and permeability in drug discovery and development settings. *Adv. Drug Deliv. Rev.* 1997, *23* (1–3), 3–25 DOI: 10.1016/S0169-409X(96)00423-1.

(206) Egan, W. J.; Merz, K. M.; Baldwin, J. J. Prediction of drug absorption using multivariate statistics. *J. Med. Chem.* 2000, *43* (21), 3867–3877 DOI: 10.1021/jm000292e.

(207) Ghose, A. K.; Herbertz, T.; Salvino, J. M.; Mallamo, J. P. Knowledge-based chemoinformatic approaches to drug discovery. *Drug Discov. Today* 2006, *11* (23–24), 1107–1114 DOI: 10.1016/j.drudis.2006.10.012.

(208) Zmuidinavicius, D.; Didziapetris, R.; Japertas, P.; Avdeef, A.; Petrauskas, A. Classification Structure-Activity Relations (C-SAR) in Prediction of Human Intestinal Absorption. *J. Pharm. Sci.* 2003, *92* (3), 621–633 DOI: 10.1002/JPS.10321.

(209) Bergström, C. A. S.; Norinder, U.; Luthman, K.; Artursson, P. Experimental and Computational Screening Models for Prediction of Aqueous Drug Solubility. *Pharm. Res.* 2002, *19* (2), 182–188 DOI: 10.1023/A:1014224900524.

(210) Chen, X.; Cho, S. J.; Li, Y.; Venkatesh, S. Prediction of aqueous solubility of organic compounds using a quantitative structure–property relationship. *J. Pharm. Sci.* 2002, *91* (8), 1838–1852 DOI: 10.1002/jps.10178.

(211) Ishikawa, M.; Hashimoto, Y. Improvement in Aqueous Solubility in Small Molecule Drug Discovery Programs by Disruption of Molecular Planarity and Symmetry. *J. Med. Chem.* 2011, *54* (6), 1539–1554 DOI: 10.1021/jm101356p.

(212) Zanger, U. M.; Schwab, M. Cytochrome P450 enzymes in drug metabolism: Regulation of gene expression, enzyme activities, and impact of genetic variation. *Pharmacol. Ther.* 2013, *138* (1), 103–141 DOI: 10.1016/j.pharmthera.2012.12.007.

(213) Zhang, Z.; Tang, W. Drug metabolism in drug discovery and development. *Acta Pharm. Sin. B* 2018, No. 17 DOI: 10.1016/j.apsb.2018.04.003.

(214) Di, L.; Kerns, E. H.; Di, L.; Kerns, E. H. *Chapter 11 – Metabolic Stability*; 2016.

(215) Obach, R. S.; Walker, G. S.; Brodney, M. A. Biosynthesis of fluorinated analogs of drugs using human cytochrome P450 enzymes followed by deoxyfluorination and quantitative nuclear magnetic resonance spectroscopy to improve metabolic stability. *Drug Metab. Dispos.* 2016, *44* (5), 634–646 DOI: 10.1124/dmd.116.069310.

(216) Di, L.; Kerns, E. H. Lipophilicity. *Drug-like Prop. concepts, Struct. Des. methods from ADME to Toxic. Optim.* 2016, 39–50 DOI: 10.1016/B978-0-12-801076-1.00005-8.

(217) Nassar, A.-E. F.; Kamel, A. M.; Clarimont, C. Improving the decision-making process in the structural modification of drug candidates: enhancing metabolic stability. *Drug Discov. Today* 2004, *9* (23), 1020–1028 DOI: 10.1016/S1359-6446(04)03280-5.

(218) Lewis, D. F. V.; Jacobs, M. N.; Dickins, M. Compound lipophilicity for substrate binding to human P450s in drug metabolism. *Drug Discov. Today* 2004, *9* (12), 530–537 DOI: 10.1016/S1359-6446(04)03115-0.

(219) Freeman-Cook, K. D.; Hoffman, R. L.; Johnson, T. W. Lipophilic efficiency: the most important efficiency metric in medicinal chemistry. *Future Med. Chem.* 2013, *5* (2), 113–115 DOI: 10.4155/fmc.12.208.

(220) Shultz, M. D. The thermodynamic basis for the use of lipophilic efficiency (LipE) in enthalpic optimizations. *Bioorg. Med. Chem. Lett.* 2013, *23* (21), 5992–6000 DOI: 10.1016/j.bmcl.2013.08.030.

(221) Westergaard, E.; Brightman, M. W. Transport of proteins across normal cerebral arterioles. *J. Comp. Neurol.* 1973, *152* (1), 17–44 DOI: 10.1002/cne.901520103.

(222) Löscher, W.; Potschka, H. Blood-brain barrier active efflux transporters: ATP-binding cassette gene family. *NeuroRX* 2005, *2* (1), 86–98 DOI: 10.1602/neurorx.2.1.86.

(223) Clark, D. E. In silico prediction of blood–brain barrier permeation. *Drug Discov. Today*

2003, *8* (20), 927–933 DOI: 10.1016/S1359-6446(03)02827-7.

(224) Wager, T. T.; Hou, X.; Verhoest, P. R.; Villalobos, A. Central Nervous System Multiparameter Optimization Desirability: Application in Drug Discovery. *ACS Chem. Neurosci.* 2016, *7* (6), 767–775 DOI: 10.1021/acschemneuro.6b00029.

(225) Pardridge, W. M. The blood-brain barrier: Bottleneck in brain drug development. *NeuroRX* 2005, *2* (1), 3–14 DOI: 10.1602/neurorx.2.1.3.

(226) Di, L.; Kerns, E. H. Blood-Brain Barrier. In *Drug-Like Properties*; Elsevier, 2016; pp 141–159.

(227) Yabu, Y.; Minagawa, N.; Kita, K.; Nagai, K.; Honma, M.; Sakajo, S.; Koide, T.; Ohta, N.; Yoshimoto, A. Oral and intraperitoneal treatment of Trypanosoma brucei brucei with a combination of ascofuranone and glycerol in mice. *Parasitol. Int.* 1998, *47* (2), 131–137 DOI: 10.1016/S1383-5769(98)00011-7.

(228) Narang, A. S.; Mantri, R. V.; Raghavan, K. S. *Excipient compatibility and functionality*; Elsevier Inc., 2016.

(229) Yabu, Y.; Yoshida, A.; Suzuki, T.; Nihei, C.; Kawai, K.; Minagawa, N.; Hosokawa, T.; Nagai, K.; Kita, K.; Ohta, N. The efficacy of ascofuranone in a consecutive treatment on Trypanosoma brucei brucei in mice. *Parasitol. Int.* 2003, *52* (2), 155–164 DOI: 10.1016/S1383-5769(03)00012-6.

(230) Herman, M.; Pérez-Morga, D.; Schtickzelle, N.; Michels, P. A. M. Turnover of glycosomes during life-cycle differentiation of Trypanosoma brucei. *Autophagy* 2008, *4* (3), 294–308 DOI: 10.4161/auto.5443.

(231) Amiguet-Vercher, A.; Pérez-Morga, D.; Pays, A.; Poelvoorde, P.; Van Xong, H.; Tebabi, P.; Vanhamme, L.; Pays, E. Loss of the mono-allelic control of the VSG expression sites during the development of Trypanosoma brucei in the bloodstream. *Mol. Microbiol.* 2004, *51* (6), 1577–1588 DOI: 10.1111/j.1365-2958.2003.03937.x.

(232) Hughes, J. D.; Blagg, J.; Price, D. A.; Bailey, S.; Decrescenzo, G. A.; Devraj, R. V.; Ellsworth, E.; Fobian, Y. M.; Gibbs, M. E.; Gilles, R. W.; et al. Physiochemical drug properties associated with in vivo toxicological outcomes. *Bioorg. Med. Chem. Lett.* 2008, *18* (17), 4872–4875 DOI: 10.1016/j.bmcl.2008.07.071.

(233) Di, L.; Kerns, E. H. Solubility. In *Drug-Like Properties*; Elsevier, 2016; pp 61–93.

(234) Li, H.; Zhong, Y.-L.; Chen, C.; Ferraro, A. E.; Wang, D. A Concise and Atom-Economical Suzuki–Miyaura Coupling Reaction Using Unactivated Trialkyl- and Triarylboranes with Aryl Halides. *Org. Lett.* 2015, *17* (14), 3616–3619 DOI: 10.1021/acs.orglett.5b01720.

(235) Sabot, C.; Kumar, K. A.; Meunier, S.; Mioskowski, C. A convenient aminolysis of esters catalyzed by 1,5,7-triazabicyclo[4.4.0]dec-5-ene (TBD) under solvent-free conditions. *Tetrahedron Lett.* 2007, *48* (22), 3863–3866 DOI: 10.1016/j.tetlet.2007.03.146.

(236) Brown, H. C.; Keblys, K. A. Hydroboration. XXII. The Reaction of Unsaturated Esters with Diborane and Disiamylborane. *J. Am. Chem. Soc.* 1964, *86* (9), 1795–1801 DOI: 10.1021/ja01063a029.

(237) Colacot, T. J.; Shea, H. A. Cp 2 Fe(PR 2) 2 PdCl 2 (R = i -Pr, t -Bu) Complexes as Air-Stable Catalysts for Challenging Suzuki Coupling Reactions. *Org. Lett.* 2004, *6* (21), 3731–3734 DOI: 10.1021/ol048598t.

(238) Dreher, S. D.; Lim, S. E.; Sandrock, D. L.; Molander, G. A. Suzuki-miyaura cross-coupling reactions of primary alkyltrifluoroborates with aryl chlorides. *J. Org. Chem.* 2009, *74* (10), 3626–3631 DOI: 10.1021/jo900152n.

(239) Miller, E. J.; Mays, S. G.; Baillie, M. T.; Howard, R. B.; Culver, D. G.; Saindane, M.; Pruett, S. T.; Holt, J. J.; Menaldino, D. S.; Evers, T. J.; et al. Discovery of a Fluorinated Enigmol Analog with Enhanced in Vivo Pharmacokinetic and Anti-Tumor Properties. *ACS Med. Chem. Lett.* 2016, *7* (5), 537–542 DOI: 10.1021/acsmedchemlett.6b00113.

(240) Zhou, Y.; Wang, J.; Gu, Z.; Wang, S.; Zhu, W.; Aceña, J. L.; Soloshonok, V. A.; Izawa, K.; Liu, H. Next Generation of Fluorine-Containing Pharmaceuticals, Compounds Currently in Phase II–III Clinical Trials of Major Pharmaceutical Companies: New Structural Trends and Therapeutic Areas. *Chem. Rev.* 2016, *116* (2), 422–518 DOI: 10.1021/acs.chemrev.5b00392.

(241) Huchet, Q. A.; Kuhn, B.; Wagner, B.; Kratochwil, N. A.; Fischer, H.; Kansy, M.; Zimmerli, D.; Carreira, E. M.; Müller, K. Fluorination Patterning: A Study of Structural Motifs That Impact Physicochemical Properties of Relevance to Drug Discovery. *J. Med. Chem.* 2015, *58* (22), 9041–9060 DOI: 10.1021/acs.jmedchem.5b01455.

(242) Ritchie, T. J.; Macdonald, S. J. F.; Peace, S.; Pickett, S. D.; Luscombe, C. N. The developability of heteroaromatic and heteroaliphatic rings – do some have a better pedigree as potential drug molecules than others? *Medchemcomm* 2012, *3* (9), 1062 DOI: 10.1039/c2md20111a.

(243) Patel, K. D.; Prajapati, S. M.; Panchal, S. N.; Patel, H. D. Review of Synthesis of 1,3,4-Oxadiazole Derivatives. *Synth. Commun.* 2014, *44* (13), 1859–1875 DOI: 10.1080/00397911.2013.879901.

(244) Tokumaru, K.; Johnston, J. N. A convergent synthesis of 1,3,4-oxadiazoles from acyl hydrazides under semiaqueous conditions. *Chem. Sci.* 2017, *8* (4), 3187–3191 DOI: 10.1039/c7sc00195a.

(245) Wu, X.; Ekegren, J. K.; Larhed, M. Microwave-Promoted Aminocarbonylation of Aryl Iodides, Aryl Bromides, and Aryl Chlorides in Water. *Organometallics* 2006, *25* (6), 1434–1439 DOI: 10.1021/om051044p.

(246) Pineiro, M.; Dias, L. D.; Damas, L.; Aquino, G. L. B.; Calvete, M. J. F.; Pereira, M. M. Microwave irradiation as a sustainable tool for catalytic carbonylation reactions.

Inorganica Chim. Acta 2017, *455*, 364–377 DOI: 10.1016/j.ica.2016.06.043.

(247) Roberts, B.; Liptrot, D.; Alcaraz, L.; Luker, T.; Stocks, M. J. Molybdenum-mediated carbonylation of aryl halides with nucleophiles using microwave irradiation. *Org. Lett.* 2010, *12* (19), 4280–4283 DOI: 10.1021/ol1016965.

(248) Herrmann, W. A.; Brossmer, C.; Reisinger, C.-P.; Riermeier, T. H.; Öfele, K.; Beller, M. Palladacycles: Efficient New Catalysts for the Heck Vinylation of Aryl Halides. *Chem. - A Eur. J.* 1997, *3* (8), 1357–1364 DOI: 10.1002/chem.19970030823.

(249) Sangshetti, J. N.; Chabukswar, A. R.; Shinde, D. B. Microwave assisted one pot synthesis of some novel 2,5-disubstituted 1,3,4-oxadiazoles as antifungal agents. *Bioorg. Med. Chem. Lett.* 2011, *21* (1), 444–448 DOI: 10.1016/j.bmcl.2010.10.120.

(250) Reimer, K.; Tiemann, F. Ueber die Einwirkung von Chloroform auf Phenole und besonders aromatische Oxysäuren in alkalischer Lösung. *Berichte der Dtsch. Chem. Gesellschaft* 1876, *9* (2), 1268–1278 DOI: 10.1002/cber.18760090270.

(251) Wynberg, H. The reimer-tiemann reaction. *Chem. Rev.* 1960, *60* (2), 169–184 DOI: 10.1021/cr60204a003.

(252) Bal, B. S.; Childers, W. E.; Pinnick, H. W. Oxidation of α,β-un saturated aldehydes. *Tetrahedron* 1981, *37* (11), 2091–2096 DOI: 10.1016/S0040-4020(01)97963-3.

(253) Kraus, G. A.; Roth, B. toward Verrucarol. 2. 1980, *05*, 4825–4830 DOI: 10.1021/jo01312a004.

(254) Wilcken, R.; Zimmermann, M. O.; Lange, A.; Joerger, A. C.; Boeckler, F. M. Principles and Applications of Halogen Bonding in Medicinal Chemistry and Chemical Biology. *J. Med. Chem.* 2013, *56* (4), 1363–1388 DOI: 10.1021/jm3012068.

(255) Huang, K.; James, M. N. G.; Lu, W.; Laskowski, M.; Anderson, S. Water molecules participate in proteinase-inhibitor interactions: Crystal structures of Leu18, Ala18, and Gly18variants of turkey ovomucoid inhibitor third domain complexed with Streptomyces griseus proteinase B. *Protein Sci.* 1995, *4* (10), 1985–1997 DOI: 10.1002/pro.5560041004.

(256) Roberts, C. W.; Roberts, F.; Henriquez, F. L.; Akiyoshi, D.; Samuel, B. U.; Richards, T. A.; Milhous, W.; Kyle, D.; McIntosh, L.; Hill, G. C.; et al. Evidence for mitochondrial-derived alternative oxidase in the apicomplexan parasite Cryptosporidium parvum: a potential anti-microbial agent target. *Int. J. Parasitol.* 2004, *34* (3), 297–308 DOI: 10.1016/j.ijpara.2003.11.002.

(257) Williams, B. A. P.; Elliot, C.; Burri, L.; Kido, Y.; Kita, K.; Moore, A. L.; Keeling, P. J. A Broad Distribution of the Alternative Oxidase in Microsporidian Parasites. *PLoS Pathog.* 2010, *6* (2), e1000761 DOI: 10.1371/journal.ppat.1000761.

(258) Rodriguez, R.; Moses, J. E.; Adlington, R. M.; Baldwin, J. E. A new and efficient method

for o-quinone methide intermediate generation: application to the biomimetic synthesis of the benzopyran derived natural products (±)-lucidene and (±)-alboatrin. *Org. Biomol. Chem.* 2005, *3* (19), 3488 DOI: 10.1039/b508972g.

(259) Harris, T. M.; Harris, C. M.; Oster, T. A.; Brown, L. E.; Lee, J. Y. C. Biomimetic syntheses of pretetramides. 2. A synthetic route based on a preformed D ring. *J. Am. Chem. Soc.* 1988, *110* (18), 6180–6186 DOI: 10.1021/ja00226a037.

(260) Jiang, J. A.; Du, J. L.; Liao, D. H.; Wang, Z. G.; Ji, Y. F. Efficient Co(OAc)2-catalyzed aerobic oxidation of EWG-substituted 4-cresols to access 4-hydroxybenzaldehydes. *Tetrahedron Lett.* 2014, *55* (8), 1406–1411 DOI: 10.1016/j.tetlet.2013.12.077.

(261) Yokokawa, F.; Nilar, S.; Noble, C. G.; Lim, S. P.; Rao, R.; Tania, S.; Wang, G.; Lee, G.; Hunziker, J.; Karuna, R.; et al. Discovery of Potent Non-Nucleoside Inhibitors of Dengue Viral RNA-Dependent RNA Polymerase from a Fragment Hit Using Structure-Based Drug Design. *J. Med. Chem.* 2016, *59* (8), 3935–3952 DOI: 10.1021/acs.jmedchem.6b00143.

Appendix

European Journal of Medicinal Chemistry xxx (2017) 1–14

Contents lists available at ScienceDirect

European Journal of Medicinal Chemistry

journal homepage: http://www.elsevier.com/locate/ejmech

Research paper

African trypanosomiasis: Synthesis & SAR enabling novel drug discovery of ubiquinol mimics for trypanosome alternative oxidase

Ryan A. West [a, 1], Oran G. O'Doherty [a, 1], Trevor Askwith [a], John Atack [a, b], Paul Beswick [a], Jamie Laverick [a], Michael Paradowski [a], Lewis E. Pennicott [a], Srinivasa P.S. Rao [c], Gareth Williams [a], Simon E. Ward [a, b, *]

[a] Sussex Drug Discovery Centre, University of Sussex, Brighton, BN1 9QJ, UK
[b] Medicines Discovery Institute, Cardiff University, Park Place, Cardiff, CF10 3AT, UK
[c] Novartis Institutes for Tropical Diseases, 5300 Chiron Way, California, 94608-2916, USA

ARTICLE INFO

Article history:
Received 3 July 2017
Received in revised form
13 September 2017
Accepted 29 September 2017
Available online xxx

Keywords:
Antiprotozoal agents
Oxidoreductase
Medicinal chemistry
Synthesis design

ABSTRACT

African trypanosomiasis is a parasitic disease affecting 5000 humans and millions of livestock animals in sub-Saharan Africa every year. Current treatments are limited, difficult to administer and often toxic causing long term injury or death in many patients. Trypanosome alternative oxidase is a parasite specific enzyme whose inhibition by the natural product ascofuranone (AF) has been shown to be curative in murine models. Until now synthetic methods to AF analogues have been limited, this has restricted both understanding of the key structural features required for binding and also how this chemotype could be developed to an effective therapeutic agent. The development of 3 amenable novel synthetic routes to ascofuranone-like compounds is described. The SAR generated around the AF chemotype is reported with correlation to the inhibition of *T. b. brucei* growth and corresponding selectivity in cytotoxic assessment in mammalian HepG2 cell lines. These methods allow access to greater synthetic diversification and have enabled the synthesis of compounds that have and will continue to facilitate further optimisation of the AF chemotype into a drug-like lead.

1. Introduction

African Trypanosomiasis is a parasitic protozoan infection in mammals spread by the tsetse fly (*Glossina*) [1]. It is exclusively found in 36 sub-Saharan African countries between 14°N and 20°S [2]. *Trypanosoma brucei gambiense* and *T. b. rhodesiense* cause the chronic western and acute eastern infections respectively, these two species have developed strategies to neutralize the immunity conferred by apolipoprotein A1, a trypanosomal lytic factor (TLF) in normal human sera [3], and evade host immune response by antigenic variation of their variant surface glycoprotein coat [4]. 60 million people are at risk of human African trypanosomiasis (HAT) with 5000 new cases reported annually [5,6]. Stage 1 of the disease is haemolymphatic [7], subsequent penetration into the brain gives rise to stage 2 where meningoencephalitis and neuronal destruction produce a diverse range of symptoms including motor neuropathy, psychiatric disorders, sensory disturbances and the characteristic disruption of the diurnal cycle causing lethargy and insomnia that gives the disease its sleeping sickness title [8]. Without chemotherapeutic intervention the disease progresses to coma and death in almost all cases [9]. The high morbidity is evinced by the 1.79 million disability-adjusted life years (DALYs) calculated for HAT, over five times greater than that for the related disease leishmaniasis [10]. This infection is not limited to humans; animal African trypanosomiasis (AAT) is the single largest infection of cattle in Africa necessitating 35 million doses of trypanocidal agents, costing up to 140 million USD annually and impacting nutrition, livelihoods and development across sub-Saharan Africa. [11,12] Different trypanosome species affect cattle, predominantly *T. vivax*, *T. evansi* and *T. congolense* [13]. AAT is less often fatal but its characteristic anaemia [14] severely impairs the health and productivity of cattle.

Current treatments for HAT are far from ideal: stage 1 treatments pentamidine and suramin (Fig. 1) only treat one subspecies (*T.b. gambiense* and *T.b. rhodesiense* respectively) and require

* Corresponding author. Cardiff University, Park Place, Cardiff, CF10 3AT, UK.
E-mail address: wards10@cardiff.ac.uk (S.E. Ward).
[1] These authors contributed equally to this work.

https://doi.org/10.1016/j.ejmech.2017.09.067

intravenous/intramuscular (IV/IM) administration [15]. Similarly stage 2 is limited to nifurtimox-eflornithine combination therapy (NECT) and melarsoprol where NECT is ineffective in treating *T.b. rhodesiense* infection [15]. All current treatments are of limited utility due to significant toxicities; the organoarsenide melarsoprol even causes reactionary encephalitis in 10% of patients and death in 5%. [16,17] The treatments all require clinicians for IV/IM injections [15], which is a major practical impediment for a diffuse population over a sizable portion of continental Africa. Drug resistance for melarsoprol and pentamidine has been increasingly observed [18] and has been linked to mutated aquaglyceroproteins both *in vitro* and in field isolates, required for trypanosomal uptake of the compounds [19].

With such poor therapeutics currently available, it is imperative that new, improved drug agents are discovered. An excellent target for drug development is trypanosome alternative oxidase (TAO). TAO is a ubiquinol dependent terminal oxidase required for the long slender blood stream trypanosomes aerobic glucose metabolism converting oxygen into water [20]. It is a 38 kDa cyanide-insensitive mitochondrial inner-leaf protein with a di-iron core which is key for enzymatic activity [21]. Many factors make it an exciting drug development target: 1) TAO is expressed in only parasitic organisms with no mammalian homologues [22]; 2) biochemical assays are well established [23]; 3) the crystal structure has been determined [24]; 4) inhibition of TAO has demonstrated clear trypanocidal action [25]; 5) existence of potent natural product inhibitors of TAO, in particular ascofuranone (AF) with Ki = 0.13 nM [26]; 6) demonstration of efficacy with ascofuranone *in vitro* and murine *in vivo* models [25,27].

However, ascofuranone-like inhibitors have many undesirable qualities associated with their chemical structure. In particular, the electron rich aromatic ring, pendant aldehyde, phenols and lipophilic side chain contribute to the rapid observed clearance, low oral bioavailability and potential toxicity of this class. Furthermore, structure activity relationships (SAR) published around the geranyl tail clearly demonstrate that its effects are almost entirely due to non-specific lipophilic interactions.

Although TAO represents an attractive target for treating HAT, no real progress has been made in the development of potential drug agents from this chemical start point, despite the fact that AF has been known for over 20 years to be a potent inhibitor both *in vitro* and *in vivo*. [27,28] One of the major bottlenecks to this progress has been lack of versatility of the available synthetic routes to these templates. There are only a handful of published synthetic methods, all suffering from linear sequence of steps resulting in poor overall yields [29]. [30] Additionally, our group has not been able to reproduce all of the chemistry reported to date. One key limitation of the current methodologies is that they rely on pre-formation of the penta-substituted aromatic head group, which is low-yielding and has limited potential for SAR expansion.

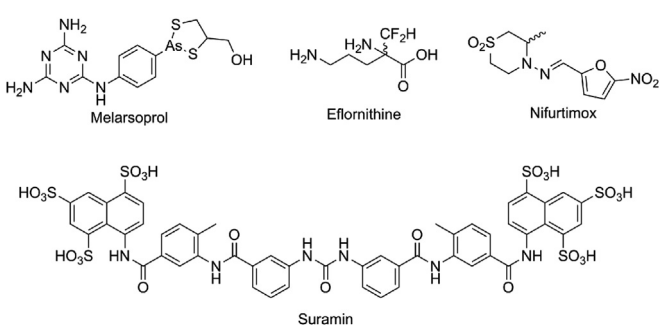

Fig. 1. Current HAT treatments.

The subsequent addition of the side chain is also capricious and low yielding. The reported deprotonation [31] with KOH followed by addition of geranyl bromide yielded only 5% product whilst other non-prenyl bromides preferably undergo O-alkylation. The selection of an appropriate protecting group for the bis-phenol **2** proved challenging as some silicon ethers or esters are labile in the presence of the *ortho*-aldehyde. The reported double SEM [32] protection of phenols in compound **3** with subsequent tail-chain addition *via* lithium halogen exchange was poor yielding, and subsequent removal of the SEM ethers proved impossible. Compound **2** does not undergo palladium-mediated coupling reactions, presumably due to the exposed phenols. Suzuki coupling is possible with methylated phenols but deprotection remains an impasse.

We report here a series of novel, simplified and improved synthetic routes to AF-like compounds. Two of the routes we have developed allow facile diversification of the head group that confers activity as well as alteration of the tail. We also report TAO inhibition data for the molecules prepared during these synthetic investigations. This will build upon the existing SAR platform around the active head group to help inform future development of AF-like TAO inhibitors for HAT.

2. Results and discussion

2.1. Synthetic chemistry

Previous attempts to deprotect the bis-protected phenol ethers (Fig. 2) was found to only remove protecting groups *ortho* to the aldehyde. This was likely due to an enhanced bidentate chelation of Lewis acids available to this motif, this chelation could destabilise the etheric C-O bond and allow for its removal. To take advantage of this, Lewis-acid mediated cationic rearrangement of the prenyl chain was employed [33]. It was necessary to mask the *para* phenol as the acetate, to enable the rearrangement, as the unprotected *para* phenol substrate did not rearrange. Compound **5** was rearranged to give colletochlorin B (CCB-**6**) a proven trypanocide and potent TAO inhibitor (IC_{50}–2 nM) in a yield which, although modest, was a significant improvement over past reports. This chemistry was subsequently employed to generate compounds in the following SAR investigation (see Scheme 1).

Exploiting the reactivity of the phenolic functionality had proven successful and was explored further. When starting from orcinol, double protection of the phenols as MOM ethers was required to allow the reaction of alkyl bromides *via* lithiation and subsequent electrophilic aromatic substitution (exemplified by DMF in Scheme 2) in excellent yields. This alkylation was attempted with the geranyl chain, giving an overall 48% yield *via* sequential one-pot additions. However, removal of the protecting groups was again challenging yielding only 15% product. This method for addition of the sidechain takes advantage of the symmetrical starting material thus removing the regioselectivity issues from the subsequent additions.

Further lithiation chemistry gave access to differentiated core structures through more flexible synthetic routes, however subsequent optimisation was required to improve both overall yields and increase structural diversity (Scheme 3). Starting from the

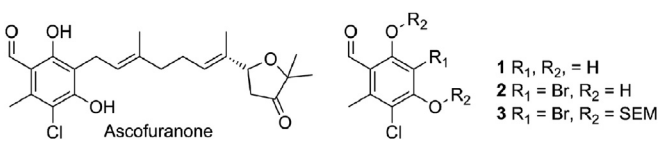

Fig. 2. Ascofuranone and previous synthetic starting points.

Please cite this article in press as: R.A. West, et al., African trypanosomiasis: Synthesis & SAR enabling novel drug discovery of ubiquinol mimics for trypanosome alternative oxidase, European Journal of Medicinal Chemistry (2017), https://doi.org/10.1016/j.ejmech.2017.09.067

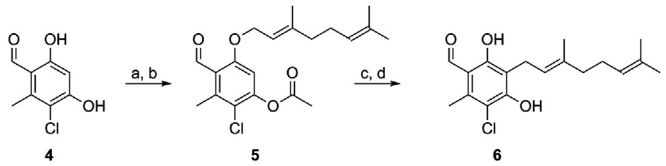

Scheme 1. Lewis acid catalysed synthesis: a) NEt_3, AcCl, CH_2Cl_2, 68%; b) geranyl bromide, K_2CO_3, KI, DMF, 50%; c) Florisil, toluene, 28%; d) NaOH, THF/MeOH, 97%.

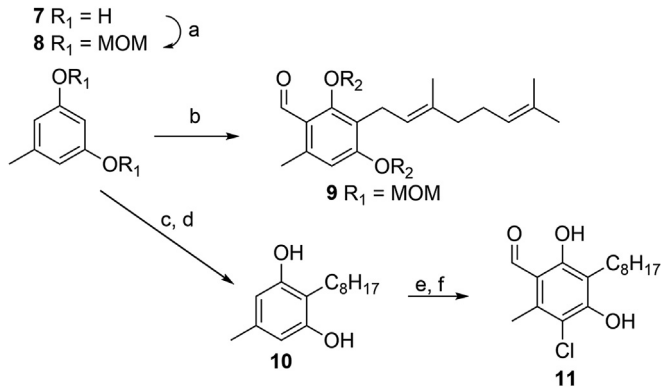

Scheme 2. *Ortho*-lithiation syntheses: a) NaH, MOMCl, DMF, 93%; b) 1) *n*-BuLi, geranyl bromide, THF 2) *n*-BuLi, DMF, 48%; c) *n*-BuLi, bromooctane, THF, 0 °C, 95%; d) ethylene glycol, mw 160 °C, 98%; e) $POCl_3$, DMF, 96%; f) SO_2Cl_2, CH_2Cl_2, quant.

diketone, various tails were installed, including those amenable to late stage diversification. Protection as the enol methyl ether **14** or **15** ensured clean formation of the desired enolate. This readily underwent substitution at the α-carbon. Oxidation by DDQ and subsequent de-protection afforded the AF-like analogues **18** and **19**.

A range of diverse analogues have been prepared with the chemistry described and are currently under biological investigation, data will be reported in future publications. These synthetic methods represent a significant improvement over previously reported methodologies and allow access to a range of diverse, novel AF-analogues. This work will facilitate the exploration of this chemotype to generate more drug like TAO inhibitors for future development.

2.2. Protein expression and purification

Recombinant TAO was expressed in Rosetta2® *E. coli* by transformation of plasmid containing complementary DNA for the overexpression of His-tagged trypanosome alternative oxidase, obtained from Anthony Moore, University of Sussex. Subsequent culture in LB broth, containing 120 g/L sorbitol and 250 mM betaine, 50 μg/mL ampicillin and 35 μg/mL chloramphenicol, grown at 37 °C until OD_{600} 0.2 then grown at 18 °C until OD_{600} 0.6 was reached. The culture was induced with the addition of Isopropyl β-D-1-thiogalactopyranoside 500 μM final concentration and the cultures continued overnight at 18 °C. The *E. coli* pellet was isolated by centrifugation 10000*g* for 20 min at 4 °C (Beckman Coulter Avanti J26S, JLA9.1000 rotor). Lysis was carried out by resuspension of the pellet in 50 mL of lysis buffer (50 mM Tris HCl, 20% (w/v) sucrose pH 7.4, 1 protease inhibitor cocktail tablet and 2 μL of Benzonase/DNAse® Sigma) and sonication (Sonics Vibracell, 13 mm probe, 35% intensity, 180 s, 5 s pulses). Cell debris and unbroken cells were removed by centrifugation (Beckman Coulter Avanti J26S, JA 25.50 rotor, 8000 *g*, 10 min, 4 °C) to provide the supernatant as the crude fraction for further purification.

Fractionation of the *E. coli* inner membranes was performed by isopycnic centrifugation. The crude supernatant was overlaid onto 45% sucrose solution (3 × 20 mL, 50 mM TrisHCl, 45% (w/v) sucrose, pH 7.4) and ultra-centrifuged (Beckman Coulter L-80, SW28, 141000 rcf max, 1 h, 4 °C) to isolate the *E. coli* inner membranes as the buoyant supernatant fraction. The supernatant from this was diluted 1:1 (50 mM Tris HCl, pH 7.4) to give a 15–20% sucrose solution reducing the density of the media and enabling the sedimentation of the inner membranes as a pellet by further ultracentrifugation (Beckman Coulter L-80, SW28, 141000 rcf max, 1 h, 4 °C). The inner membrane pellet was solubilised by resuspension with octylglucopyranoside (OG) buffer (37 mL, 50 mM TrisHCl, 1.4% OG (w/v), 20% glycerol (v/v), 200 mM $MgSO_4$, pH 7.4) followed by ultra-centrifugation (Beckman Coulter L-80, SW28, 141000 rcf max, 1 h, 4 °C) to remove non solubilised protein and debris. Purification of the solubilsed membrane fraction was performed by cobalt affinity chromatography (TALON® resin). The column was equilibrated with buffer (50 mL, 20 mM Tris HCl, 1.4% OG, 20% glycerol, 100 mM $MgSO_4$ pH 7.4). The resin was incubated with the solubilised supernatant for 30 min on a roller shaker at 4 °C. The flow through was collected and the resin was washed with buffer 1 (2 × 50 mL 20 mM TrisHCl, 20 mM imidazole, 0.042% (w/v) *n*-dodecyl-β-D-maltopyranoside (DDM), 20% (v/v) glycerol, 50 mM $MgSO_4$, pH 7.4) and buffer 2 (1 × 50 mL 20 mM TrisHCl, 160 mM imidazole, 0.042% (w/v) *n*-dodecyl-β-D-maltopyranoside (DDM), 20% (v/v) glycerol, 50 mM $MgSO_4$, pH 7.4). rTAO was then eluted with elution buffer (10 × 10 mL 20 mM TrisHCl, 200 mM imidazole, 0.042% (w/v) *n*-dodecyl-β-D-maltopyranoside (DDM), 20% (v/v) glycerol, 50 mM $MgSO_4$, 60 mM NaCl, pH 7.4). Concentration of these fractions through a 10 kDa molecular weight cut off Amicon Ultra-15 filter unit provided TAO enzyme for use in absorbance inhibition assay, lane 2 Fig. 4. AOX confirmed in Western Blot analysis using Polyclonal Ab from Agrisera (raised against plant AOX1/AOX2 (AS04 054) >70% homology to TAO) (lane 3 Fig. 3).

Both bands observed at 37 kDa and 74 kDa in SDS-PAGE (lane 2) were confirmed to be rTAO by in-gel trypsin digest and analysis by protein mass spec (data not shown).

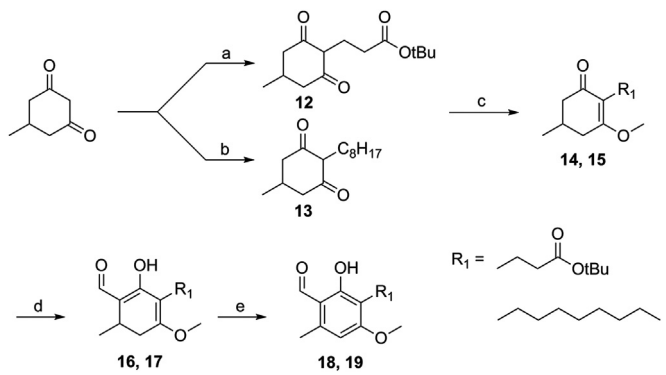

Scheme 3. Diversifiable synthesis: a) NaH, ^{t}Bu-acrylate, DMF, 80 °C, 95%, b) octanal, L-proline, $NaBH_3CN$, EtOH, quant; c) SO_4Me_2, NaH, THF, 95%; d) LDA, methyl formate, THF, −78 °C, 64%; e) DDQ, CH_2Cl_2, 84%.

2.3. TAO activity assay

The assessment of enzymatic activity of purified rTAO was carried out by monitoring the production of 1-ubiquinone from the substrate 1-ubiquinol. This modified substrate was used over the endogenous substrate as it has a higher aqueous solubility and allows assessment of enzyme activity at higher substrate concentrations. The measurement of 1-ubiquinone production was carried out kinetically by absorbance readings at the substrates lambda

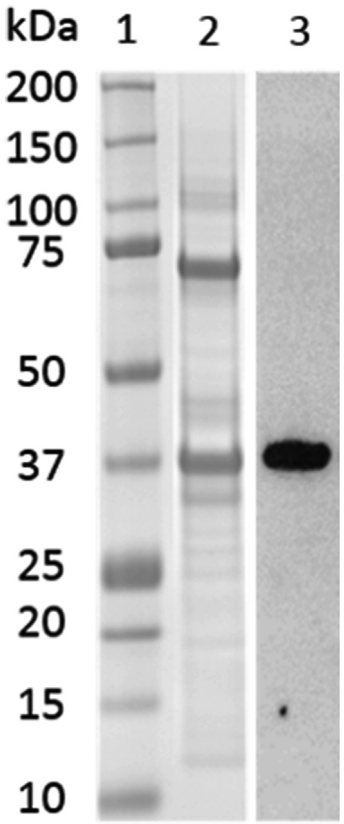

Fig. 3. SDS-PAGE and Western analysis of rTAO with Quick Coomassie stain (Generon QC154201/008). 1 Molecular weight markers, 2 Concentrated purified rTAO protein, 3 WB 100 ng protein load. Polyclonal Ab from Agrisera (raised against plant AOX1/AOX2 (AS04 054) >70% homology to TAO).

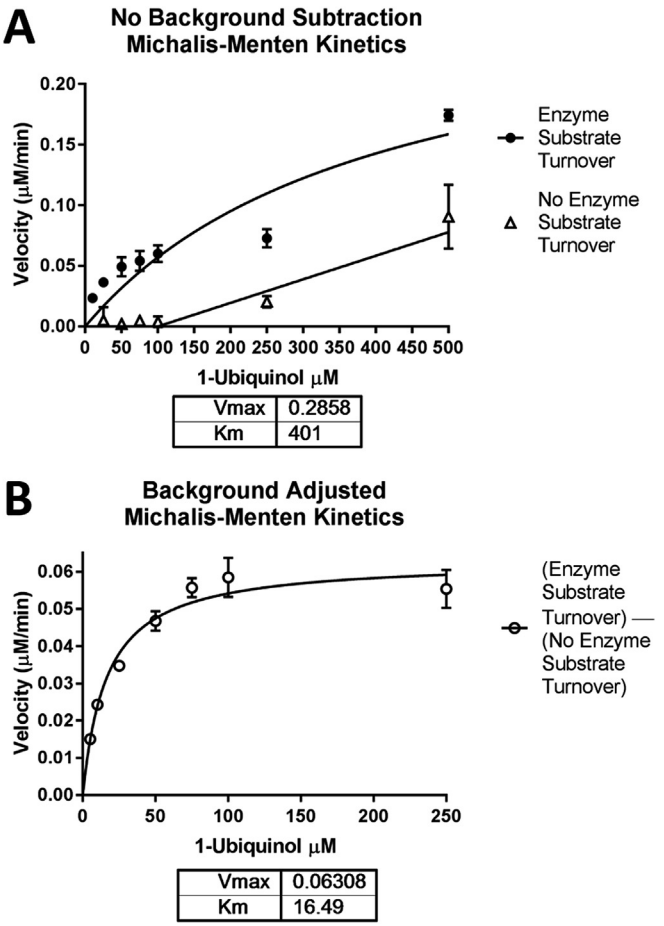

Fig. 4. Michalis-Menten kinetics of rTAO. Data plotted is the mean of 3 independent experiments each with triplicate points for each condition. The error plotted is the SEM of the 3 independent experiments. The relative background turnover of substrate without enzyme was subtracted from each condition internally generated within each experiment in triplicate. 3 nM of purified rTAO was used. Graph generated in GraphPad Prism®.

max at 278 nm over time. Measurements were taken using assay buffer containing detergent C10E8 previously identified in assay optimisation experiments reported by Kido et al. [23] and 50 mM Tris buffer.

The Michalis-Menten kinetics of the purified enzyme was measured to determine the most suitable substrate concentration for use in screening activities. Interestingly we observed a Km of 16.5 μM which is notably lower than previous reports [23,34]. Within our experiments we observed that kinetic measurements of product formation at high substrate concentrations (>250 μM) showed substantial rates of turnover. This was also observed in control experiments of substrate turnover without enzyme. If background subtractions of substrate turnover without enzyme were not performed calculations of Km showed to be in line with the previously reported figures for Km (**A** - Fig. 4). We therefore carried out background subtractions of turnover without enzyme at each concentration of substrate to generate Michalis-Menten Km calculations of enzyme alone (**B** - Fig. 4).

In IC_{50} determination and in screening activities final concentrations of 3 nM of purified rTAO were used with 15 μM 1-ubiquinol for a sufficient window to assess the inhibitory activity of synthesised analogues. Using a substrate concentration close to the measured Km also enables the identification of competitive, non-competitive and uncompetitive types of inhibitors. We carried out ten-point IC_{50} determinations with purified rTAO protein to try to understand the action of these compounds. Example data for the natural product CCB – **6** is shown below (Fig. 5). With correlation to the *ex vivo* of inhibition of the growth of *T. b. brucei.* (Fig. 6).

To understand the mechanism of TAO inhibition by

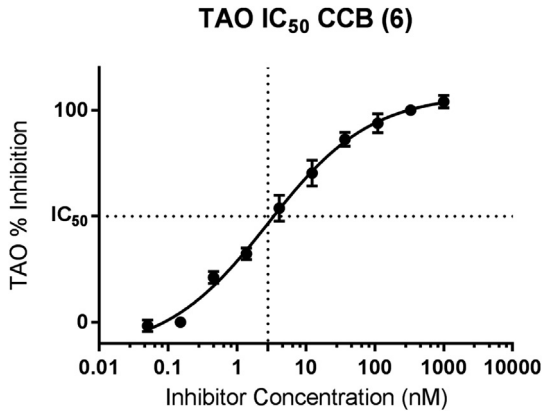

Fig. 5. IC_{50} data for colletochlorin B from 4 parameter logistic regression of 10 point inhibitory concentration data. Data from 3 independent experiments reported concentrations run in duplicate per experiment, SEM plotted of experiments. 3 nM of purified rTAO was used.

Please cite this article in press as: R.A. West, et al., African trypanosomiasis: Synthesis & SAR enabling novel drug discovery of ubiquinol mimics for trypanosome alternative oxidase, European Journal of Medicinal Chemistry (2017), https://doi.org/10.1016/j.ejmech.2017.09.067

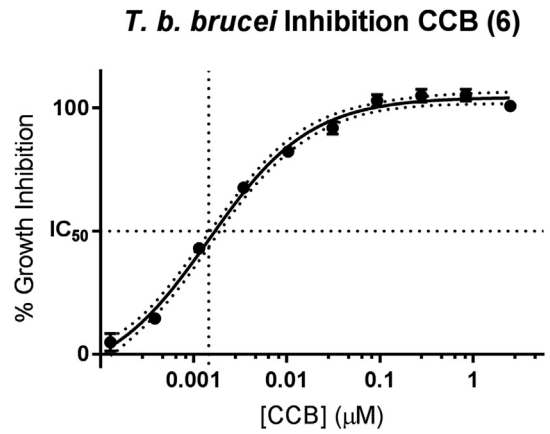

Fig. 6. IC_{50} data for concentration of colletochlorin B required to inhibit 50% growth of *T. b. brucei* Lister427, following incubation with compound for 48 h. Growth inhibition was measured by quantifying ATP levels. 4 parameter logistic regression of 10 point inhibitory concentration data. Data from 3 independent experiments reported concentrations run in duplicate per experiment, SEM plotted of experiments.

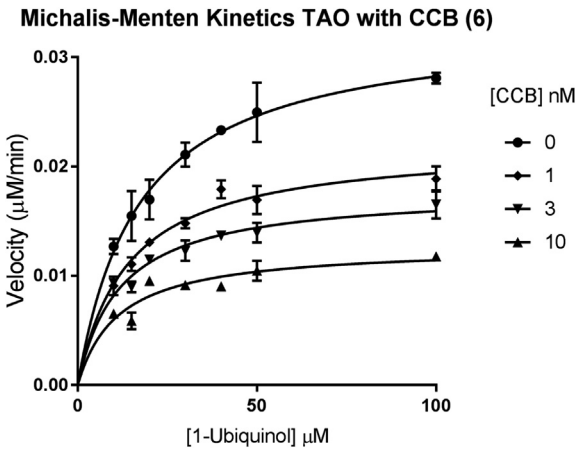

Fig. 7. Michalis-Menten inhibitor kinetics of rTAO, in presence of increasing concentration of inhibitor CCB. Data plotted is the mean of 3 independent experiments each with triplicate points for each condition. The error plotted is the SEM of the 3 independent experiments. The relative background turnover of substrate without enzyme was subtracted from each condition internally generated within each experiment in triplicate. 2 nM of purified rTAO was used. Graph generated in GraphPad Prism®.

colletochlorin B, more thorough experiments were performed, measuring the velocity of 1-ubiquinol turn over with increasing concentrations of colletochlorin B at different concentrations of substrate (Fig. 7). Interestingly this data suggests a mixed type non-competitive inhibition profile with regard to 1-ubiquinol substrate, that is in accordance with previous reports by Kido et al. [23] The apparent affinity of 1-ubiquinol is not affected by increasing concentrations of inhibitor as the calculated Km remains similar with increasing inhibitor concentration. Furthermore the V_{max} is reduced with increasing inhibitor concentration, which together with the Km observation are suggestive of non-competitive binding with regards to 1-ubiquinol.

2.4. Structure-activity relationships

At the outset of our research, there was not only a lack of robust synthetic routes to AF analogues but the basic SAR around the aromatic head group was under explored. Consequently, it was unclear which substituents were necessary for activity. Interestingly

Table 1
Summary of modifications to the aromatic head group.

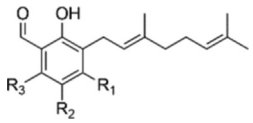

#	R_1	R_2	R_3	TAO inhibition (pIC_{50})[a]	*T.b.b.* Growth Inhibition (pIC_{50})[b]	HepG2 Cytotox (pCC_{50})[c]
6	OH	Cl	Me	8.4 ± 0.3	8.5 ± 0.1	5.1 ± 0.1
20	OAc	Cl	Me	6.5 ± 0.2	7.4 ± 0.7	4.8 ± 0.1
21	OH	Cl	H	7.0 ± 0.2	6.6 ± 0.1	<4.8
22	OAc	Cl	H	6.3 ± 0.1	6.2 ± 0.1	4.6 ± 0.1
23	OH	H	Me	5.5 ± 0.2	5.8 ± 0.1	4.4 ± 0.1
24	OAc	H	Me	5.4 ± 0.1	–	–
25	OH	H	H	5.4 ± 0.2	–	–
26	OAc	H	H	5.5 ± 0.1	–	–
27	H	Cl	H	5.4 ± 0.1	–	–
28	OH	H	OH	5.5 ± 0.1	–	–

[a] Negative log concentration and standard deviation of compounds required for 50% inhibition of trypanosome alternative oxidase.
[b] Negative log concentration and standard deviation of compounds required for 50% growth inhibition of *T. b. brucei* Lister427.
[c] Negative log concentration and standard deviation of compounds required for 50% growth inhibition of HepG2 cell line.

chlorination at R_2 contributes a great deal to the inhibition of TAO. The des-chloro modifications to compounds **6** and **20**–**26** (Table 1) result in a reduction of 1–3 pIC_{50} units of potency against the enzyme, and diminishes selectivity for the growth of the trypanosome. Compound **23** shows 30 fold selectivity for inhibition of trypanosome growth compared to that of compound **6** that shows >500 fold selectivity over HepG2 cytotoxicity. Similarly the presence of a methyl group at R_3 contributes significantly to the inhibition of TAO albeit to a lesser extent than that of chloro at R_2. Compound **21** shows reduced inhibition of TAO that results in lower efficacy for trypanosome growth inhibition and consequently reduces the selectivity against the mammalian HepG2 cell to ~60 fold.

Previously published work had shown that electron withdrawing groups were preferred at R_4 [26]. Our results confirm this with the exception of compound **30** where R_4 is methyl. Direct comparison to compound **20** shows an order loss in potency suggesting that it is not only electron withdrawing groups could be tolerated in this position. Interestingly replacement of the benzaldehyde with nitrile **29** and **30** appeared to be a well-tolerated modification showing similar inhibition against TAO, however a drop in efficacy was observed against the trypanosome (see Table 2). One further divergence from the reported pharmacophore is compound **33** where the hydrogen bond donor of the phenol of C_5 has been removed whilst retaining a modest inhibition of TAO, suggesting that the interaction with the enzyme at this position may not be *via* an essential hydrogen bond (see Fig. 8). This is supported by inhibition data of compound **35** where the point of

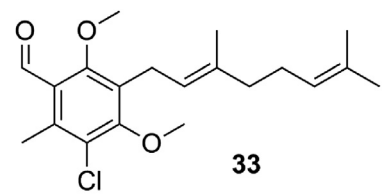

Fig. 8. Dimethoxy analogue.

Table 2
Summary of modifications to the aldehyde.

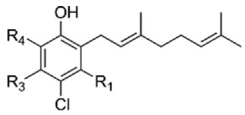

#	R_1	R_3	R_4	TAO inhibition (pIC_{50})[a]	*T.b.b.* Growth inhibition (pIC_{50})[b]	HepG2 Cytotox (pCC_{50})[c]
29	OH	Me	CN	8.4 ± 0.2	6.4 ± 0.1	4.9 ± 0.1
6	OH	Me	C=O	8.5 ± 0.3	8.4 ± 0.1	5.1 ± 0.1
20	OAc	Me	C=O	6.5 ± 0.2	7.4 ± 0.7	4.8 ± 0.1
30	OAc	Me	Me	5.7 ± 0.1	–	–
21	OH	H	C=O	7.0 ± 0.2	6.6 ± 0.1	<4.8
31	OH	H	CN	7.6 ± 0.3	5.2 ± 0.1	4.4 ± 0.1
32	OH	H	C=NOH	6.1 ± 0.3	5.7 ± 0.1	5.0 ± 0.1

[a] Negative log concentration and standard deviation of compounds required for 50% inhibition of trypanosome alternative oxidase.
[b] Negative log concentration and standard deviation of compounds required for 50% growth inhibition of *T. b. brucei* Lister427.
[c] Negative log concentration and standard deviation of compounds required for 50% growth inhibition of HepG2 cell line.

attachment of the lipophilic tail was explored. The compound retains activity against TAO supporting the hypothesis that the necessity for a hydrogen bond donor at R_5 is not a requirement for TAO inhibition. Ether-linked tails could thus reasonably represent a group of underexplored TAO inhibitors that are more synthetically amenable (see Table 3).

In general a reasonable correlation was observed between the inhibition of TAO and the inhibition of growth of the parasite. The OAc masked phenol in compound **20** showed higher inhibitory activity against *T. b. brucei* than expected. This higher than expected potency could be from the cleavage of the acetate to the free phenol compound **6** under the conditions of the assay. The majority of the compounds synthesised showed greater than 20 fold selectivity for *T. b. brucei* growth inhibition over mammalian HepG2 cytotoxicity. In general compounds that showed more potent inhibition of TAO showed better a better selectivity index over mammalian HepG2 cells (see Table 3).

3. Conclusions

Despite current efforts, HAT remains a considerable threat to the health and well-being of those infected. Currently available treatments are far from safe with increasing incidences of drug resistance being reported. Ascofuranone was described as a nanomolar inhibitor of TAO in the late 1990s [27], however exploitation of this opportunity has been severely limited due to the availability of robust synthetic routes to these molecules. With the potential to assist future drug development of the ascofuranone chemotype we present 3 novel and versatile synthetic approaches, together with the SAR findings developed during our synthetic exploration. These routes offer significantly improved yields over previous methods and importantly, allow late stage diversification of the crucial aromatic head group that is responsible for both the affinity for the enzyme and the undesirable, non-drug-like functionality. The SAR presented builds on that previously published [26], demonstrating that the aromatic pharmacophore is more amenable to alteration than previously reported. These synthetic and SAR findings provide the foundations for onward exploitation of this chemotype towards novel treatments for HAT *via* inhibition of TAO and our onward investigation further aims to develop CNS drug-like leads from these challenging chemical starting points.

4. Experimental section

Experimental Details. ChemAxon Calculator Plugins were used for structure property prediction and calculation (clogP), Marvin 15.5.4, 2015, ChemAxon (http://www.chemaxon.com). All commercial reagents were purchased from Sigma-Aldrich, Alfa Aesar, Apollo Scientific, Fluorochem or Tokyo Chemical Industry and of the highest available purity. Unless otherwise stated, chemicals were used as supplied without further purification. Anhydrous solvents were purchased from Acros (AcroSeal™) or Sigma-Aldrich (SureSeal™) and were stored under nitrogen. 40–60 petrol ether refers to the fraction with a boiling point between 40 °C and 60 °C. Anhydrous solvents and reagents were used as purchased. Thin layer chromatography (TLC) was carried out using glass plates pre-

Table 3
Alkylation of phenols.

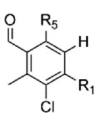

#	R_1	R_5	TAO inhibition (pIC_{50})[a]	*T.b.b.* Growth inhibition (pIC_{50})[b]	HepG2 Cytotox (pCC_{50})[c]
34	*O*-Geranyl	OH	6.0 ± 0.1	5.5 ± 0.1	4.7 ± 0.1
35	OH	*O*-Geranyl	6.6 ± 0.2	4.9 ± 0.1	5.0 ± 0.1

[a] Negative log concentration and standard deviation of compounds required for 50% inhibition of trypanosome alternative oxidase.
[b] Negative log concentration and standard deviation of compounds required for 50% growth inhibition of *T. b. brucei* Lister427.
[c] Negative log concentration and standard deviation of compounds required for 50% growth inhibition of HepG2 cell line.

Please cite this article in press as: R.A. West, et al., African trypanosomiasis: Synthesis & SAR enabling novel drug discovery of ubiquinol mimics for trypanosome alternative oxidase, European Journal of Medicinal Chemistry (2017), https://doi.org/10.1016/j.ejmech.2017.09.067

coated with Merck silica gel 60 F254. Melting points were determined using an OptiMelt apparatus and are uncorrected. Proton nuclear magnetic resonance spectra were recorded at 500 MHz on a Varian VNMRS 500 MHz spectrometer (at 30 °C), using residual isotopic solvent ($CHCl_3$, $\delta_H = 7.27$ ppm, DMSO $\delta_H = 2.50$ ppm, MeOH $\delta_H = 3.31$ ppm) as an internal reference. Chemical shifts are quoted in parts per million (ppm). Coupling constants (J) are recorded in Hertz (Hz). Carbon nuclear magnetic resonance spectra were recorded at 125 MHz on a Varian 500 MHz spectrometer and are proton decoupled, using residual isotopic solvent ($CHCl_3$, $\delta_C = 77.00$ ppm, DMSO $\delta_C = 39.52$ ppm, MeOH $\delta_C = 49.00$ ppm) as an internal reference. Proton and carbon spectra assignments are supported by DEPT editing. Chemical shifts (δ_C) are quoted in ppm. High resolution mass spectrometry (HRMS) data (ESI) was recorded on Bruker Daltonics, Apex III, ESI source: Apollo ESI with methanol as spray solvent. Only molecular ions, fractions from molecular ions and other major peaks are reported as mass/charge (m/z) ratios. LCMS data was recorded on a Waters 2695 HPLC using a Waters 2487 UV detector and a Thermo LCQ ESI-MS. Samples were eluted through a Phenomenex Lunar 3 μm C18 50 mm × 4.6 mm column, using water and acetonitrile acidified by 0.1% formic acid at 1 ml/min and detected at 254 nm. The gradient employed was a 7 min method 30–90% MeCN over a 5 min gradient, held at 90% MeCN for 1 min, then re-equilibrated to 30% MeCN over 1 min. All experiments were carried out under an inert atmosphere of N_2 unless otherwise stated.

Absorbance Assay. 1-Ubiquinol turnover was measured by recording the increase in absorbance at 278 nm (Greiner 96-well UV star flat bottom plates with BMG PHERAstar FS photo spectrometer) to monitor the increase of 1-Ubiquinone concentration kinetically over 6 min with purified rTAO (3 nM), The Michalis-Menten derived Km of 1-Ubiquinol showed to be 16.5 μM, kinetic measurements at high (>250 μM) concentrations of substrate showed higher rates of enzyme product formation, this was also observed with high substrate concentrations without enzyme. It was therefore necessary to carry out a background subtraction of substrate turnover without enzyme to generate accurate Michalis-Menten Km calculations. A final concentration of 15 μM 1-Ubiquinol was used under the following conditions: 50 mM Tris-HCl; 0.05% (w/v) C10E8; pH 7.4; 25 °C). The sigmoidal curve of the inhibition was observed by 10-point 3 fold serial dilution of test compounds to generate IC_{50} values.

Growth inhibition assays. Bloodstream form *Trypanosoma brucei brucei* Lister 427 parasites were continuously passaged in HMI-9 medium formulated from IMDM medium (Invitrogen), 10% heat-inactivated fetal bovine serum, 10% Serum Plus medium supplement (SAFC Biosciences), 1 mM hypoxanthine (Sigma-Aldrich), 50 μM bathocuproine disulfonic acid (Sigma-Aldrich), 1.5 mM cysteine (Sigma-Aldrich), 1 mM pyruvic acid (Sigma-Aldrich), 39 μg/mL thymidine (Sigma-Aldrich), and 14 μL/L beta-mercapthoethanol (Sigma-Aldrich); all concentrations of added components refer to that in complete HMI-9 medium. The parasites were cultured in 10 mL of HMI-9 medium in T75 CELL-STAR tissue culture flasks at 37 °C/5% CO_2.

To determine growth inhibitory potency of compounds against *T. b. brucei* bloodstream form parasites, 200 nL of 10-point, 3 fold serially diluted compounds in DMSO were transferred to the wells of white, solid bottom 384-well plates (Greiner Bio-One) by either Echo 555 acoustic liquid handling system or Mosquito. Then, 10^4 of *T. b. brucei* parasites in 40 μL of HMI-9 medium were added to each well, and the plates were incubated for 48 h at 37 °C in 5% CO_2 incubators. Parasite numbers in individual plate wells were determined through quantification of intracellular ATP amount. The CellTiter-Glo luminescent cell viability reagent (Promega) was added to plate wells, and ATP-dependent luminescence signal was measured on Tecan M1000 plate Reader after 30 min incubation. Suramin an *anti*-trypanosomal drug was used positive control and DMSO was used as negative control. pIC_{50} values were calculated using Graph Pad Prism software by plotting the luminescence values in sigmoidal dose response curves. Suramin was used as a positive control in screening. (pIC_{50}–6.7 ± 0.1).

Hep-G2 Cytotoxicity Assay. Human hepatocellular carcinoma (HepG2) cells were obtained from ATCC and grown in RPMI media. 25 μL of 1.6 × 10^4 cells/mL were dispensed into sterile 384 well Griener clear plates and incubated at 37 °C in 5% CO_2 incubator for 24 h. Once the cells adhered, 125 nL of 10-point, 3 fold serially diluted compounds in DMSO were transferred on to cells. After incubating for additional 96 h at 37 °C in 5% CO_2 incubator, cells were added with CCK-8 reagent to each well. Plates were further incubated for 3 h followed by absorbance reading at 450 nM using Envision reader. Absorbance values were used for determination of cytotoxic concentration (pCC_{50}) required to inhibit 50% growth. Purmycin was used as positive control in screening (pIC_{50}–6.3 ± 0.1).

4.1. Synthesis

4.1.1. 2-Chloro-5-{[(2E)-3,7-dimethylocta-2,6-dien-1-yl]oxy}-4-formyl-3-methylphenyl acetate **(5)**

To a suspension of 3-chloro-4,6-dihydroxy-2-methylbenzaldehyde (**4**) [35] [36] (11.8 g, 63.2 mmol) in DCM (300 mL) was added trimethylamine (8.8 mL, 63.2 mmol) at room temperature. This mixture was stirred for 15 min during which time the suspension had dissolved. Acetyl chloride (4.5 mL, 63.3 mmol) was added to the reaction mixture dropwise at room temperature over 20 min and this was stirred for a further 5 h. Deionised water (200 mL) was added and the phases were separated. The aqueous layer was extracted with ethyl acetate (3 × 100 mL) and the combined organic extracts were dried over magnesium sulfate, filtered and concentrated under reduced pressure. Purification 2 times by flash column chromatography (100 g silica), eluting with a gradient of petrol ether: ethyl acetate (95: 5) to (90: 10), gave 2-chloro-4-formyl-5-hydroxy-3-methylphenyl acetate as an off-white solid (9.9 g, 68%): R_f 0.46 (10% ethyl acetate/90% 40–60 petrol ether); ^{1}H NMR (500 MHz, Chloroform-*d*) δ 12.16 (s, 1H), 10.31 (s, 1H), 6.70 (s, 1H), 2.68 (s, 3H), 2.37 (s, 3H).

To a solution of 2-chloro-4-formyl-5-hydroxy-3-methylphenyl acetate (1.30 g, 5.7 mmol) and geranyl bromide (1.35 mL, 6.8 mmol) in dimethylformamide (10 mL) was added potassium iodide (85 mg, 0.6 mmol) followed by potassium carbonate (2.35 g, 17.1 mmol). The reaction mixture was stirred at room temperature for 16 h before being diluted with deionised water (50 mL). This mixture was extracted with diethyl ether (3 × 30 mL) and the combined organic extracts were dried over magnesium sulfate, filtered and concentrated under reduced pressure. Purification by flash column chromatography (25 g silica), eluting with a gradient of petrol ether: ethyl acetate (100: 0) to (90: 10), gave the title compound as a yellow oil (1.04 g, 50%) and 4-chloro-5-{[(2E)-3,7-dimethylocta-2,6-dien-1-yl]oxy}-2-formyl-3-methylphenyl acetate (710 mg, 41%).

4.1.2. 2-Chloro-5-{[(2E)-3,7-dimethylocta-2,6-dien-1-yl]oxy}-4-formyl-3-methylphenyl acetate **(5)**

R_f 0.46 (10% ethyl acetate/90% 40–60 petrol ether) ^{1}H NMR (500 MHz, Chloroform-*d*) δ 10.56 (s, 1H), 6.71 (s, 1H), 5.51–5.40 (m, 1H), 5.13–5.05 (m, 1H), 4.60 (d, J = 6.6 Hz, 2H), 2.67 (s, 3H), 2.38 (s, 3H), 2.22–1.97 (m, 4H), 1.73 (s, 3H), 1.69 (s, 3H), 1.62 (s, 3H). LCMS (ESI) retention time 6.64 min, m/z 365.77/367.26.

Please cite this article in press as: R.A. West, et al., African trypanosomiasis: Synthesis & SAR enabling novel drug discovery of ubiquinol mimics for trypanosome alternative oxidase, European Journal of Medicinal Chemistry (2017), https://doi.org/10.1016/j.ejmech.2017.09.067

4.1.3. 4-Chloro-5-{[(2E)-3,7-dimethylocta-2,6-dien-1-yl]oxy}-2-formyl-3-methylphenyl acetate (5)

R_f 0.28 (10% ethyl acetate/90% 40–60 petrol ether) ^{1}H NMR (500 MHz, Chloroform-*d*) δ 10.26 (s, 1H), 6.58 (s, 1H), 5.57–5.41 (m, 1H), 5.09 (t, $J = 6.1$ Hz, 1H), 4.67 (d, $J = 6.5$ Hz, 2H), 2.72 (s, 3H), 2.38 (s, 3H), 2.18–2.07 (m, 4H), 1.76 (s, 3H), 1.69 (s, 3H), 1.62 (s, 3H). LCMS (ESI) retention time 6.64 min, *m/z* 365.59/367.66.

*4.1.4. 3-Chloro-5-[(2E)-3,7-dimethylocta-2,6-dien-1-yl]-4,6-dihydroxy-2-methylbenzaldehyde **(6)***

(colletochlorin B) To a solution of 2-chloro-5-{[(2E)-3,7-dimethylocta-2,6-dien-1-yl]oxy}-4-formyl-3-methylphenyl acetate (**5**) (757 mg, 2.1 mmol) in toluene (7.5 mL) was added Fluorosil (100–200 mesh, 2.3 g). The reaction mixture was heated at reflux for 3 h before being allowed to cool to room temperature and being filtered. The Fluorosil was washed with ethyl acetate (3 × 15 mL) and the combined filtrate was concentrated under reduced pressure. Purification by flash column chromatography (25 g silica), eluting with a gradient of petrol ether: ethyl acetate (100: 0) to (95: 5), gave 2-chloro-6-[(2E)-3,7-dimethylocta-2,6-dien-1-yl]-4-formyl-5-hydroxy-3-methylphenyl acetate as a colourless oil (212 mg, 28%): R_f 0.67 (5% ethyl acetate/95% 40–60 petrol ether); ^{1}H NMR (500 MHz, Chloroform-*d*) δ 12.53 (s, 1H), 10.31 (s, 1H), 5.21–4.96 (m, 2H), 3.35–3.25 (m, 2H), 2.66 (s, 3H), 2.38 (s, 3H), 2.09–2.01 (m, 2H), 2.01–1.93 (m, 2H), 1.75 (s, 3H), 1.66 (s, 3H), 1.59 (s, 2H).

To a solution of 2-chloro-6-[(2E)-3,7-dimethylocta-2,6-dien-1-yl]-4-formyl-5-hydroxy-3-methylphenyl acetate (110 mg, 0.3 mmol) in THF (4 mL) and MeOH (1 mL) was added 1 M aqueous sodium hydroxide (1.5 mL, 1.5 mmol). The reaction mixture was stirred at room temperature for 3 h during which time the reaction mixture turned deep purple. The reaction mixture was acidified to pH 1 with 1 M aqueous HCl and the reaction colour faded to yellow. This mixture was extracted with ethyl acetate (3 × 10 mL) and the combined organic extracts were dried over magnesium sulfate, filtered and concentrated under reduced pressure. Purification by flash column chromatography (10 g silica), eluting with a gradient of petrol ether: ethyl acetate (100: 0) to (95: 5), gave the title compound as an off-white solid (93 mg, 97%): R_f 0.48 (5% ethyl acetate/95% 40–60 petrol ether); ^{1}H NMR (500 MHz, Chloroform-*d*) δ 12.70 (s, 1H), 10.16 (s, 1H), 6.42 (s, 1H), 5.29–5.17 (m, 1H), 5.09–5.05 (m, 1H), 3.42 (d, $J = 7.1$ Hz, 2H), 2.61 (s, 3H), 2.13–2.03 (m, 2H), 2.03–1.97 (m, 2H), 1.80 (s, 3H), 1.66 (d, $J = 1.4$ Hz, 3H), 1.59 (s, 3H).

*4.1.5. 1,3-Bis(methoxymethoxy)-5-methylbenzene **(8)***

60% Sodium hydride in mineral oil (742 mg, 18.5 mmol) was added in three portions to a stirred solution of orcinol (**7**) (1.00 g, 8.1 mmol) in DMF (20 mL) at 0 °C. This was stirred for 40 min and methyl chloromethoxy ether (1.35 mL, 17.7 mmol) added dropwise. The reaction was stirred for 16 h and then diluted with water (100 mL) and extracted with diethyl ether (3 × 100 mL). The combined ether fractions were washed with 1 M sodium hydroxide solution (50 mL), saturated brine solution (50 mL), dried over sodium sulfate, filtered and concentrated under reduced pressure. Purification by flash column chromatography (20 g silica), eluting with a gradient of 40–60 petrol ether: ethyl acetate (100: 0) to (95: 5), gave the title compound as a clear oil (1.59 g, 93%): ^{1}H NMR (500 MHz, chloroform-d) δ 6.56 (1 H, s), 6.54 (2H, s), 5.15 (4 H, s), 3.49 (6 H, s), 2.31 (3 H, s); HRMS (ESI) calcd 212.1049 for $C_{11}H_{16}O_4$ [M+H]+, found 212.1047 *m/z*.

*4.1.6. (E)-3-(3,7-Dimethylocta-2,6-dienyl)-2,4-bis(methoxymethoxy)-6-methylbenzaldehyde **(9)***

3-Bis(methoxymethoxy)-5-methylbenzene (**8**) (2.50 g, 11.8 mmol) was dissolved in dry tetrahydrofuran (90 mL) and cooled to 0 °C. 2.1 M *n*-butyl lithium (8.41 mL, 17.7 mmol) was added drop-wise and the reaction was left to stir for 1 h at 0 °C. Geranyl bromide (4.48 g, 20.6 mmol) was added to the reaction mixture in a drop-wise manner. This was stirred for 1 h and allowed to come to room temperature. The reaction was cooled to 0 °C again and 2.1 M *n*-butyl lithium (8.41 mL, 17.7 mmol) added followed by another 1 h stirring at 0 °C. Excess dry DMF was added and the reaction was allowed to come to room temperature over 1 h. The reaction was diluted with water (300 mL) and extracted with diethyl ether (3 × 200 mL). The combined organics were dried over sodium sulfate, filtered and concentrated under reduced pressure. Purification by flash column chromatography (50 g silica), eluting with a gradient of 40–60 petrol ether: ethyl acetate (100:0) to (95:5), gave the title compound as a yellow tinted clear oil (1.28 g, 31%): ^{1}H NMR (500 MHz, chloroform-d) δ 10.38 (1 H, s), 6.74 (1 H, s), 5.24 (2 H, s), 5.17 (1 H, t, $J = 6.6$ Hz), 5.04 (2 H, s), 5.01 (1 H, t, $J = 6.4$ Hz), 3.57 (3 H, s), 3.46 (3 H, s), 3.36 (2 H, d, $J = 6.7$ Hz), 2.57 (3 H, s), 2.05 (2 H, m), 1.97 (2 H, m), 1.76 (3 H, s), 1.63 (3 H, s), 1.56 (3 H, s); IR (neat, ν_{max}) cm^{-1} 2932, 1682, 1595, 1560, 1440, 1375, 1315, 1284, 1220, 1152, 1039, 1007, 924; HRMS (ESI) calcd 399.2142 for $C_{23}H_{32}NaO_5$ [M+Na]+, found: 399.2147 *m/z*.

*4.1.7. 5-Methyl-2-octylbenzene-1,3-diol **(10)***

3-Bis(methoxymethoxy)-5-methylbenzene (**8**) (2.00 g, 9.4 mmol) was dissolved in dry tetrahydrofuran (60 mL) and cooled to 0 °C. 2.5 M *n*-butyl lithium (4.90 mL, 12.3 mmol) was added dropwise and the reaction was left to stir for 1 h at 0 °C. Iodooctane (2.55 mL, 14.1 mmol) was added to the reaction mixture and this was stirred for 1 h before being allowed to come to room temperature. The reaction was diluted with water (300 mL) and extracted with diethyl ether (3 × 200 mL). The organic fractions were dried over sodium sulfate, filtered and concentrated under reduced pressure. Purification by flash column chromatography (25 g silica), eluting 40–60 petrol ether: ethyl acetate (100: 0) to (95: 5), gave 1,3-bis(methoxymethoxy)-5-methyl-2-octylbenzene as a colourless oil (2.54 g, 83%): R_f 0.79 (10% ethyl acetate/90% 40–60 petrol ether); ^{1}H NMR (500 MHz, chloroform-d) δ 6.59 (2 H, s), 5.17 (4 H, s), 3.49 (6 H, s), 2.64 (2 H, t, $J = 8.0$ Hz), 2.30 (3 H, s), 1.50 (2 H, m), 1.32 (10 H, m), 0.89 (3 H, t, $J = 6.8$ Hz); ^{13}C NMR (126 MHz, chloroform-d) δ 155.7, 136.6, 118.4, 108.7, 94.5, 75.4, 56.0, 31.9, 29.8, 29.7, 29.5, 29.3, 23.2, 22.7, 21.8, 14.1; IR (neat, ν_{max}) cm^{-1} 2924, 2854, 1612, 1586, 1463, 1394, 1154, 1122, 1036, 923, 823; HRMS (ESI): calcd. 347.2198 for $C_{19}H_{32}NaO_4$ [M+Na]$^+$, found 347.2187 *m/z*.

1,3-Bis(methoxymethoxy)-5-methyl-2-octylbenzene (350 mg, 1.1 mmol) was suspended in ethylene glycol (10 mL) and heated to 160 °C by microwave irradiation for 5 h in sealed vial. The reaction mixture was diluted with water (40 mL) and extracted with diethyl ether (3 × 30 ml). The combined extracts were washed with water (30 mL), dried over magnesium sulfate, filtered and concentrated under reduced pressure. Purification by flash column chromatography (10 g silica), eluting 40–60 petrol ether: ethyl acetate (100: 0) to (70: 30), gave the title compound as an orange/white powder (220 mg, 86%, m.p. 63–66 °C): R_f 0.32 (10% ethyl acetate/90% 40–60 petrol ether); ^{1}H NMR (500 MHz, chloroform-d) δ 6.23 (2 H, s), 4.69 (2 H, s), 2.59 (2 H, t, $J = 7.9$ Hz), 2.22 (3 H, s), 1.60–1.51 (2 H, m), 1.43–1.23 (10 H, m), 0.89 (3 H, t, $J = 6.8$ Hz); ^{13}C NMR (126 MHz, chloroform-d) δ 154.4, 137.0, 112.4, 108.7, 75.4, 31.9, 29.8, 29.5, 29.3, 23.0, 22.7, 21.0, 14.1. IR (neat, ν_{max}) cm^{-1} 3427, 3280, 2956, 2918, 2850, 1635, 1584, 1522, 1467, 1328, 1268, 1160, 1112, 829, 534; HRMS (ESI): calcd. 237.1849 for $C_{15}H_{25}O_2$ [M+H]+, found 237.1853 *m/z*.

*4.1.8. 3-Chloro-4,6-dihydroxy-2-methyl-5-octylbenzaldehyde **(11)***

5-Methyl-2-octyl-benzene-1,3-diol (**10**) (500 mg, 2.1 mmol) was dissolved in dry DMF (4.08 mL, 52.9 mmol) and cooled to 0 °C.

Please cite this article in press as: R.A. West, et al., African trypanosomiasis: Synthesis & SAR enabling novel drug discovery of ubiquinol mimics for trypanosome alternative oxidase, European Journal of Medicinal Chemistry (2017), https://doi.org/10.1016/j.ejmech.2017.09.067

Phosphorous oxychloride (0.39 mL, 4.2 mmol) was added slowly by syringe and the reaction was then allowed to come to room temperature. The reaction was followed by thin layer chromatography (20% ethyl acetate in 40–60 petroleum ether) and upon completion after 2 h the reaction was cooled to 0 °C and diluted with 1 M aqueous sodium hydroxide solution (10 mL). This was stirred for 5 min then acidified with 1 M aqueous hydrogen chloride solution (30 mL) and transferred to a separating funnel. The mixture was then extracted with diethyl ether (3 × 20 mL). The combined organic layers were washed with water (50 mL) and brine (50 mL). The organics were dried over magnesium sulfate and concentrated to dryness under reduced pressure. Purification by flash column chromatography (10 g silica), eluting 40–60 petrol ether: ethyl acetate (100: 0) to (80: 20), gave 2,4-dihydroxy-6-methyl-3-octylbenzaldehyde as an orange/white powder (559 mg, 95%, m.p. 101–103 °C): R_f 0.18 (10% ethyl acetate/90% 40–60 petrol ether); ^{1}H NMR (500 MHz, chloroform-d) δ 12.63 (1 H, s), 10.09 (1 H, s), 6.20 (1 H, s), 5.52 (1 H, s), 2.60 (2 H, d, J = 7.1 Hz), 2.50 (3 H, s), 1.59–1.47 (2 H, m), 1.42–1.21 (10 H, m), 0.89 (3 H, d, J = 6.9 Hz); ^{13}C NMR (126 MHz, chloroform-d) δ 193.0, 164.2, 161.0, 141.5, 114.0, 113.4, 110.2, 31.9, 29.7, 29.5, 29.3, 28.7, 22.6, 22.0, 17.9, 14.1; IR (neat, ν_{max}) cm^{-1} 3111, 2916, 2849, 1605, 1509, 1466, 1284, 1250, 1216, 1135, 829, 773, 644, 567; HRMS (ESI): calcd. 265.1804 for $C_{16}H_{25}O_3$ $[M+H]^+$, found 265.1805 *m/z*.

2,4-Dihydroxy-6-methyl-3-octylbenzaldehyde (70 mg, 0.3 mmol) was dissolved in dry diethyl ether (5 mL) and sulfuryl chloride (32 μL, 0.4 mmol) added. The reaction was stirred for 1 h at room temperature before being quenched with 1 M aqueous sodium hydroxide (5 mL). The mixture was then extracted with diethyl ether (2 × 15 mL). The combined organic phases were dried over magnesium sulfate, filtered and concentrated on celite (1 g). Purification by flash column chromatography over silica (10 g) eluting 40–60 petrol ether: ethyl acetate (100: 0) to (80: 20) gave the title compound as a white powder (65 mg, 81%, m.p. 65 °C): R_f 0.58 (10% ethyl acetate/90% 40–60 petrol ether); ^{1}H NMR (500 MHz, chloroform-d) δ 12.65 (1 H, s), 10.14 (1 H, s), 6.34 (1 H, s), 2.69 (2 H, d, J = 7.1 Hz), 2.60 (3 H, s), 1.54–1.47 (2 H, m), 1.30–1.23 (10 H, m), 0.88 (3 H, d, J = 6.9 Hz); ^{13}C NMR (126 MHz, chloroform-d) δ 193.1, 162.5, 156.2, 137.2, 115.8, 113.5, 113.0, 31.9, 29.6, 29.5, 29.3, 28.4, 22.9, 22.6, 14.4, 14.1; IR (neat, ν_{max}) cm^{-1} 3327, 2924, 2856, 1606, 1452, 1416, 1374, 1233, 1132, 791, 767, 710, 555; HRMS (ESI): calcd. 299.1414 for $C_{16}H_{24}ClO_3$ $[M+H]^+$, found 299.1421 *m/z*.

4.1.9. Tert-butyl-3-(4-methyl-2,6-dioxocyclohexyl)propanoate **(12)**

5-Methylcyclohexane-1,3-dione (2.00 g, 15.9 mmol) and *t*-butyl acrylate (2.55 mL, 17.4 mmol) were dissolved in *N*,*N*-dimethylformamide (10 mL) and sodium hydride (635 mg, 15.8 mmol) added slowly. The reaction was stirred for 1 h at room temperature then heated to 80 °C for 16 h. The reaction was allowed cool to room temperature, acidified to pH 4 with acetic acid then neutralised and diluted with saturated aqueous sodium hydrogen carbonate solution (30 mL). This was extracted with ethyl acetate (3 × 30 mL). The combined organics were washed with saturated aqueous sodium hydrogen carbonate (30 mL), dried over magnesium sulfate, filtered and concentrated under reduced pressure onto celite (4 g). Purification by flash column chromatography over silica (25 g) eluting 40–60 petrol ether: ethyl acetate (100:0) to (60:40) gave the title compound as a pale yellow powder (2.94 g, 73%). Product was unstable, full characterisation after subsequent reaction to *tert*-butyl 3-(2-methoxy-4-methyl-6-oxocyclohex-1-en-1-yl)propanoate (**14**): ^{1}H (500 MHz, chloroform-d) δ 2.49–2.36 (6 H, m), 2.18–2.02 (3 H, m), 1.42 (9 H, s), 1.02 (3 H, d, J = 6 Hz); HRMS (ESI) calcd 277.1410 for $C_{14}H_{22}NaO_4$ $[M+Na]^+$, found: 277.1415 *m/z*.

4.1.10. 5-Methyl-2-octylcyclohexane-1,3-diol **(13)**

5-Methylcyclohexane-1,3-dione (10.3 g, 81.9 mmol), octanal (8.54 mL, 54.6 mmol) and L-proline (1.26 g, 10.9 mmol) were dissolved in ethanol (150 mL) and stirred for 1 h. Sodium cyanoborohydride (3.43 g, 54.6 mmol) and molecular sieves (350 mg per mmol of aldehyde) were added and the reaction heated to 80 °C for 2 h. The reaction was poured onto ice (100 g) and the white solid suspension that formed was vacuum filtered. The solids were dissolved in ethyl acetate (40 mL) and washed with water (2 × 40 mL). The organics were dried over magnesium sulfate, filtered and concentrated under reduced pressure to give the title compound as a white powder (11.9 g, 91%) Product was a complex mixture of isomers and full characterisation was confirmed after successful subsequent reaction to 3-methoxy-5-methyl-2-octylcyclohex-2-enone (**15**): R_f 0.12 (20% ethyl acetate/80% 40–60 petrol ether); HRMS (ESI) calcd 277.1410 for $C_{15}H_{27}O_2$ $[M+H]^+$: found: 239.2005 *m/z*.

4.1.11. Tert-butyl-3-(2-methoxy-4-methyl-6-oxocyclohex-1-en-1-yl)propanoate **(14)**

Tert-butyl 3-(2-hydroxy-4-methyl-6-oxo-cyclohexen-1-yl) propanoate (**12**) (16.00 g, 62.9 mmol) and dimethyl sulfate (7.14 mL, 75.5 mmol) were dissolved in tetrahydrofuran (200 mL) and sodium hydride (3.02 g, 75.5 mmol) added slowly. The reaction was stirred at room temperature for 3 h then the reaction was concentrated under reduced pressure and re-diluted with ethyl acetate (25 mL) and water (25 mL). This mixture was neutralised using excess sodium phosphate monobasic. The ethyl acetate was separated and the aqueous layer extracted with more ethyl acetate (2 × 30 mL). The combined organics were dried over magnesium sulfate, filtered and concentrated under reduced pressure onto celite (2 g). Purification by flash column chromatography over silica (100 g) eluting 40–60 petrol ether: ethyl acetate (100:0) to (80:20) gave the title compound as a clear colourless oil (15.20 g, 90%). ^{1}H (600 MHz, choroform-d) δ 3.78 (3 H, s), 2.69–2.58 (1 H, m), 2.55–2.43 (2 H, m), 2.43–2.34 (1 H, m), 2.24–2.17 (2 H, m), 2.17–2.09 (2 H, m), 2.05–1.93 (1 H, m), 1.40 (9 H, s), 1.07 (3 H, d, J 6.1).^{13}C NMR (126 MHz, chloroform-d) δ 197.6, 172.9, 171.5, 117.7, 79.6, 55.1, 44.7, 34.3, 33.0, 28.4, 28.1, 21.1, 17.8; IR (neat, ν_{max}) cm^{-1} 2973, 1723, 1611, 1367, 1233, 1148, 1084, 846; HRMS (ESI): calcd. 291.1572 for $C_{15}H_{24}NaO_4$ $[M+Na]+$, found 291.1572 *m/z*.

4.1.12. 3-Methoxy-5-methyl-2-octylcyclohex-2-enone **(15)**

5-methyl-2-octyl-cyclohexane-1,3-dione (**13**) (567 mg, 2.4 mmol) was dissolved in dry methyl alcohol (5 mL) with 3 Å molecular sieves (0.5 g) and 4-methylbenzenesulfonic acid (20 mg, 0.1 mmol) was added. The reaction was stirred for 24 h and then was concentrated onto celite (2 g). Purification by flash column chromatography over silica (10 g) eluting 40–60 petrol ether: ethyl acetate (100:0) to (90:10) gave the title compound as a yellow oil (257 mg, 43%): R_f 0.26 (20% ethyl acetate/80% 40–60 petrol ether); ^{1}H (500 MHz, chloroform-d) δ 3.80 (3 H, s), 2.71–2.61 (1 H, m), 2.44 (1 H, dd, J = 15.7, 3.2 Hz), 2.28–2.11 (4 H, m), 2.07–1.98 (1 H, m), 1.26 (12 H, s), 1.10 (3 H, d, J = 6.0 Hz), 0.88 (3 H, t, J = 6.9 Hz); ^{13}C NMR (126 MHz, chloroform-d) δ 198.0, 170.8, 119.6, 54.9, 44.8, 33.0, 31.8, 29.6, 29.4, 29.2, 28.6, 28.4, 22.6, 21.9, 21.1, 13.9. IR (neat, ν_{max}) cm^{-1} 2924, 1709, 1377, 1230, 1128, 1061, 1033, 722; HRMS (ESI): calcd. 253.2168 for $C_{16}H_{29}O_2$ $[M+H]+$, found 253.2163 *m/z*.

4.1.13. Tert-butyl-3-(5-(hydroxymethylene)-2-methoxy-4-methyl-6-oxocyclohex-1-en-1-yl)propanoate **(16)**

Diisopropylamine (4.62 mL, 32.9 mmol) was dissolved in dry tetrahydrofuran (550 mL) and cooled to −78 °C and 2.5 M *n*-butyllithium (12.16 mL, 30.4 mmol) added. The reaction was warmed to room temperature then cooled to −78 °C and *tert*-butyl

Please cite this article in press as: R.A. West, et al., African trypanosomiasis: Synthesis & SAR enabling novel drug discovery of ubiquinol mimics for trypanosome alternative oxidase, European Journal of Medicinal Chemistry (2017), https://doi.org/10.1016/j.ejmech.2017.09.067

3-(2-methoxy-4-methyl-6-oxo-cyclohexen-1-yl)propanoate (**14**) (6.8 g, 25.3 mmol) added. The reaction was stirred for 1 h at −78 °C then methyl formate (2.34 mL, 38.0 mmol) was added and it was allowed to warm to room temperature overnight. The reaction was concentrated under reduced pressure, diluted water (50 mL) and neutralised by careful addition of 1 M aqueous hydrogen chloride solution. The organics were dried over magnesium sulfate, filtered and concentrated under reduced pressure onto celite (5 g). Purification by flash column chromatography over silica (100 g) eluting 40–60 petrol ether: ethyl acetate (100:0) to (70:30) gave the title compound as a yellow oil (4.41 g, 58.6%): R_f 0.22 (20% ethyl acetate/80% 40–60 petrol ether); ^{1}H NMR (500 MHz, chloroform-d) δ 7.21–7.07 (1 H, m), 3.79 (3 H, s), 2.76–2.69 (1 H, m), 2.67–2.60 (1 H, m), 2.60–2.56 (2 H, m), 2.35–2.25 (3 H, m), 1.41 (9 H, s), 1.16 (3 H, d, J = 6.8 Hz); ^{13}C NMR (126 MHz, chloroform-d) δ 191.7, 172.7, 170.0, 160.3, 116.5, 111.2, 79.7, 55.2, 34.3, 32.0, 28.3, 28.1, 20.3, 17.5. IR (neat, ν_{max}) cm^{-1} 2972, 1721, 1607, 1366, 1241, 1146, 1080, 998, 847; HRMS (ESI): calcd. 319.1521 for $C_{16}H_{24}NaO_5$ [M+Na]$^+$, found 319.1521 *m/z*.

4.1.14. 6-(Hydroxymethylene)-3-methoxy-5-methyl-2-octylcyclohex-2-enone (17)

Diisopropylamine (2.67 mL, 19.0 mmol) was dissolved in dry tetrahydrofuran (150 mL) and cooled to −78 °C and *n*-butyllithium (6.18 mL, 15.5 mmol) added. The mixture was allowed to warm to room temperature and stirred for 30 min. This was cooled to −78 °C and a solution of 3-methoxy-5-methyl-2-octyl-cyclohex-2-en-1-one (**15**) (3.00 g, 11.9 mmol) in dry tetrahydrofuran (5 mL) was added *via* syringe. This was stirred for 1 h and dry methyl formate (1.47 mL, 23.77 mmol) was added, the reaction was allowed to warm to room temperature overnight slowly in the dry ice acetone bath. The reaction mixture was concentrated under reduced pressure and diluted with ethyl acetate (30 mL) and water (30 mL). This was neutralised with 1 M aqueous hydrogen chloride, the ethyl acetate separated and washed with water (30 mL). The organics were dried over magnesium sulfate, filtered and concentrated under reduced pressure onto celite (2 g). Purification by flash column chromatography over silica (25 g) eluting 40–60 petrol ether: ethyl acetate (100:0) to (90:10) gave the title compound as a clear yellow oil (2.25 g, 68%): Rf 0.46 (20% ethyl acetate/80% 40–60 petrol ether) ^{1}H (500 MHz, chloroform-d) δ 7.19 (1 H, d, J = 1.2 Hz), 3.79 (3 H, s), 2.75 (1 H, q, J = 6.7 Hz), 2.65 (1 H, dd, J = 16.6, 6.1 Hz), 2.37–2.27 (3 H, m), 1.34 (2 H, m), 1.27 (10 H, m), 1.18 (3 H, d, J = 6.8 Hz), 0.88 (3 H, t, J = 6.8 Hz); ^{13}C NMR (126 MHz, chloroform-d) δ 191.9, 169.3, 160.5, 111.3, 55.0, 31.9, 31.8, 29.6, 29.4, 29.2, 28.6, 28.3, 22.6, 21.6, 20.4, 14.0. IR (neat, ν_{max}) cm^{-1} 2923, 1608, 1378, 1238, 1159, 1130, 1006, 953; HRMS (ESI): calcd. 281.2117 for $C_{17}H_{29}O_3$ [M+H]+, found 281.2113 *m/z*.

4.1.15. Tert-butyl-3-(3-formyl-2-hydroxy-6-methoxy-4-methylphenyl)propanoate (18)

(Z)-^{t}Butyl 3-(5-(hydroxymethylene)-2-methoxy-4-methyl-6-oxocyclohex-1-en-1-yl)propanoate (**16**) (1.00 g, 3.4 mmol) and 2,3-dichloro-5,6-dicyano-1,4-benzoquinone (0.92 g, 4.1 mmol) were dissolved in toluene (100 mL) and stirred for 16 h at room temperature. The reaction was diluted with diethyl ether (200 mL), the organics were washed with water (6 × 100 mL), dried over magnesium sulfate, filtered and concentrated under reduced pressure onto celite (2 g). Purification by flash column chromatography over silica (25 g) eluting 40–60 petrol ether: ethyl acetate (100:0) to (70:30) gave the title compound as a white solid (835 mg, 84%, m.p. 58–59 °C): R_f 0.36 (20% ethyl acetate/80% 40–60 petrol ether); ^{1}H (500 MHz, chloroform-d) δ 12.41 (1 H, s), 10.13 (1 H, s), 6.28 (1 H, s), 3.89 (3 H, s), 2.95–2.86 (2 H, m), 2.57 (3 H, s), 2.45–2.38 (2 H, m), 1.44 (9 H, s). ^{13}C NMR (126 MHz, chloroform-d) δ 193.1, 172.7, 164.1, 162.9, 142.3, 114.1, 113.6, 105.2, 79.9, 55.7, 34.2, 28.1, 18.4, 17.8. IR (neat, ν_{max}) cm^{-1} 2967, 1722, 1637, 1366, 1248, 1125, 1004, 816, 644; HRMS (ESI): calcd. 317.1365 for $C_{16}H_{22}NaO_5$ [M+Na]+, found 317.1363 *m/z*.

4.1.16. 2-Hydroxy-4-methoxy-6-methyl-3-octylbenzaldehyde (19)

6-(Hydroxymethylene)-3-methoxy-5-methyl-2-octylcyclohex-2-enone (**17**) (77 mg, 0.3 mmol) and 2,3-dichloro-5,6-dicyano-1,4-benzoquinone (73 mg, 4.1 mmol) were dissolved in toluene (20 mL) and stirred for 16 h at room temperature. The reaction was diluted with diethyl ether (50 mL), the organics were washed with water (6 × 50 mL), dried over magnesium sulfate, filtered and concentrated under reduced pressure onto celite (2 g). Purification by flash column chromatography over silica (25 g) eluting 40–60 petrol ether: ethyl acetate (100:0) to (70:30) gave the title compound as a white solid (835 mg, 84%, m.p. 58–59 °C): Rf 0.24 (20% ethyl acetate/80% 40–60 petrol ether); ^{1}H (500 MHz, chloroform-d) δ 12.41 (1 H, s), 10.13 (1H, s), 6.28 (1H, s), 3.89 (3H, s), 2.95–2.86 (2H, m), 2.57 (3H, s), 2.45–2.38 (2H, m), 1.44 (9H, s). ^{13}C NMR (126 MHz, chloroform-d) δ 193.1, 172.7, 164.1, 162.9, 142.3, 114.1, 113.6, 105.2, 79.9, 55.7, 34.2, 28.13, 18.4, 17.8. HRMS (ESI): calcd. 279.1955 for $C_{17}H_{27}O_3$ [M+H]+, found 279.1948 *m/z*.

4.1.17. 2-Chloro-6-[(2E)-3,7-dimethylocta-2,6-dien-1-yl]-4-formyl-5-hydroxy-3-methylphenyl acetate (20)

To a solution of 2-chloro-5-{[(2E)-3,7-dimethylocta-2,6-dien-1-yl]oxy}-4-formyl-3-methylphenyl acetate (**5**) (757 mg, 2.07 mmol) in toluene (7.5 mL) was added Fluorosil (100–200 mesh, 2.3 g). The reaction mixture was heated at reflux for 3 h before being allowed to cool to room temperature and being filtered. The Fluorosil was washed with ethyl acetate (3 × 15 mL) and the combined filtrate was concentrated under reduced pressure. Purification by flash column chromatography (25 g silica), eluting with a gradient of petrol ether: ethyl acetate (100: 0) to (95: 5), gave the title compound as a colourless oil (212 mg, 28%): R_f 0.67 (5% ethyl acetate/95% 40–60 petrol ether) ^{1}H NMR (500 MHz, Chloroform-*d*) δ 12.53 (s, 1H), 10.31 (s, 1H), 5.21–4.96 (m, 2H), 3.35–3.25 (m, 2H), 2.66 (s, 3H), 2.38 (s, 3H), 2.09–2.01 (m, 2H), 2.01–1.93 (m, 2H), 1.75 (s, 3H), 1.66 (s, 3H), 1.59 (s, 2H). LCMS (ESI) retention time 6.83 min, *m/z* 365.43/367.21.

4.1.18. 5-Chloro-3-[(2E)-3,7-dimethylocta-2,6-dien-1-yl]-2,4-dihydroxybenzaldehyde (21)

To a solution of 6-chloro-2-[(2E)-3,7-dimethylocta-2,6-dien-1-yl]-4-formyl-3-hydroxyphenyl acetate (**22**) (70.0 mg, 0.200 mmol) in tetrahydrofuran (4 mL) and methanol (1 mL) was added 1 M aqueous sodium hydroxide (1.0 mL, 1.00 mmol). The reaction mixture was stirred at room temperature for 6 h before being quenched with 1 M aqueous hydrochloric acid (5 mL) and extracted with ethyl acetate (3 × 10 mL). The combined organic fractions dried over magnesium sulfate, filtered and concentrated under reduced pressure. Purification by flash column chromatography (10 g silica), eluting with a gradient of petrol ether: ethyl acetate (100: 0) to (90: 10), gave the title compound as an off-white solid (55 mg, 89%): R_f 0.40 (5% ethyl acetate/95% 40–60 petrol ether) ^{1}H NMR (500 MHz, Chloroform-*d*) δ 11.53 (s, 1H), 9.67 (s, 1H), 7.39 (s, 1H), 6.38 (s, 1H), 5.29–5.19 (m, 1H), 5.10–5.02 (m, 1H), 3.44 (d, J = 7.2 Hz, 2H), 2.13–2.04 (m, 2H), 2.04–1.97 (m, 2H), 1.81 (d, J = 1.5 Hz, 3H), 1.66 (d, J = 1.7 Hz, 3H), 1.58 (s, 3H).

4.1.19. 6-Chloro-2-[(2E)-3,7-dimethylocta-2,6-dien-1-yl]-4-formyl-3-hydroxyphenyl acetate (22)

To a solution of 2-chloro-5-{[(2E)-3,7-dimethylocta-2,6-dien-1-yl]oxy}-4-formylphenyl acetate (synthesised using the same method to make **5**) (430 mg, 1.22 mmol) in toluene (6.5 mL) was

Please cite this article in press as: R.A. West, et al., African trypanosomiasis: Synthesis & SAR enabling novel drug discovery of ubiquinol mimics for trypanosome alternative oxidase, European Journal of Medicinal Chemistry (2017), https://doi.org/10.1016/j.ejmech.2017.09.067

added Fluorosil (100–200 mesh, 2.2 g). The reaction mixture was heated at reflux for 3 h before being allowed to cool to room temperature and being filtered. The Fluorosil was washed with ethyl acetate (3 × 15 mL) and the combined filtrate was concentrated under reduced pressure. Purification 3 times by flash column chromatography (10 g silica), eluting with a gradient of petrol ether: ethyl acetate (100: 0) to (95: 5), gave the title compound as a pale yellow oil (78 mg, 18%): R_f 0.59 (5% ethyl acetate/95% 40–60 petrol ether) ^{1}H NMR (500 MHz, Chloroform-*d*) δ 11.41 (s, 1H), 9.82 (s, 1H), 7.51 (s, 1H), 5.13–5.08 (m, 1H), 5.08–5.04 (m, 1H), 3.34 (d, *J* = 7.0 Hz, 2H), 2.38 (s, 3H), 2.13–2.01 (m, 2H), 2.01–1.91 (m, 2H), 1.76 (s, 3H), 1.66 (s, 3H), 1.59 (s, 3H). LCMS (ESI) retention time 6.64 min, *m/z* 351.59/353.19.

4.1.20. 3-[(2E)-3,7-Dimethylocta-2,6-dien-1-yl]-2,4-dihydroxy-6-methylbenzaldehyde **(23)**

To a solution of 2-[(2E)-3,7-dimethylocta-2,6-dien-1-yl]-4-formyl-3-hydroxy-5-methylphenyl acetate (**24**) (6.0 mg, 0.018 mmol) in tetrahydrofuran (0.5 mL) and methanol (0.12 mL) was added 4 M aqueous sodium hydroxide (9 μL, 1.00 mmol). The reaction mixture was stirred at room temperature for 3 h before being acidified to pH 2 with 1 M aqueous hydrochloric acid and extracted with ethyl acetate (3 × 3 mL). The combined organic fractions dried over magnesium sulfate, filtered and concentrated under reduced pressure. Purification by flash column chromatography (1 g silica), eluting with a gradient of petrol ether: ethyl acetate (100: 0) to (90: 10), gave the title compound as a white solid (2.7 mg, 51%): R_f 0.15 (10% ethyl acetate/90% 40–60 petrol ether) ^{1}H NMR (500 MHz, Chloroform-*d*) δ 12.78 (s, 1H), 10.09 (s, 1H), 6.22 (s, 1H), 6.15 (s, 1H), 5.31–5.22 (m, 1H), 5.12–5.00 (m, 1H), 3.42 (d, *J* = 7.2 Hz, 2H), 2.51 (s, 3H), 2.19–2.01 (m, 4H), 1.82 (d, *J* = 1.5 Hz, 3H), 1.69 (d, *J* = 1.6 Hz, 3H), 1.60 (s, 3H). LCMS (ESI) retention time 5.73 min, *m/z* 289.67.

4.1.21. 2-[(2E)-3,7-Dimethylocta-2,6-dien-1-yl]-4-formyl-3-hydroxy-5-methylphenyl acetate **(24)**

To a solution of 3-{[(2E)-3,7-dimethylocta-2,6-dien-1-yl]oxy}-4-formyl-5-methylphenyl acetate (synthesised using the same method to make **5**) (300 mg, 0.908 mmol) in toluene (9.0 mL) was added Fluorosil (100–200 mesh, 3.0 g). The reaction mixture was heated at reflux for 3 h before being allowed to cool to room temperature and being filtered. The Fluorosil was washed with ethyl acetate (3 × 10 mL) and the combined filtrate was concentrated under reduced pressure. Purification by flash column chromatography (10 g silica), eluting with a gradient of petrol ether: ethyl acetate (100: 0) to (80: 20) then by prep HPLC, gave the title compound as a pale yellow oil (12 mg, 4%): R_f 0.28 (10% ethyl acetate/90% 40–60 petrol ether) ^{1}H NMR (500 MHz, Chloroform-*d*) δ 12.45 (s, 1H), 10.25 (s, 1H), 6.47 (s, 1H), 5.17–5.09 (m, 1H), 5.08–5.01 (m, 1H), 3.28 (d, *J* = 7.0 Hz, 2H), 2.57 (s, 3H), 2.31 (s, 3H), 2.10–2.00 (m, 2H), 2.01–1.95 (m, 2H), 1.75 (s, 3H), 1.65 (d, *J* = 1.6 Hz, 3H), 1.58 (s, 3H). LCMS (ESI) retention time 6.44 min, *m/z* 331.72.

4.1.22. 3-[(2E)-3,7-Dimethylocta-2,6-dien-1-yl]-2,4-dihydroxybenzaldehyde **(25)**

To a solution of 2-[(2E)-3,7-dimethylocta-2,6-dien-1-yl]-4-formyl-3-hydroxyphenyl acetate (**26**) (130 mg, 0.411 mmol) in tetrahydrofuran (4.0 mL) and methanol (1.0 mL) was added 4 M aqueous sodium hydroxide (308 μL, 1.23 mmol). The reaction mixture was stirred at room temperature for 3 h before being diluted with deionised water (10 mL), acidified to pH 1 with 1 M aqueous hydrochloric acid and extracted with ethyl acetate (3 × 10 mL). The combined organic fractions dried over magnesium sulfate, filtered and concentrated under reduced pressure. Purification by flash column chromatography (10 g silica), eluting with a gradient of petrol ether: ethyl acetate (100: 0) to (80: 20), gave the title compound as a cream coloured solid (83 mg, 73%): R_f 0.36 (20% ethyl acetate/80% 40–60 petrol ether) ^{1}H NMR (500 MHz, Chloroform-*d*) δ 11.79 (s, 1H), 9.70 (s, 1H), 7.32 (d, *J* = 8.7 Hz, 1H), 6.49 (d, *J* = 8.5 Hz, 1H), 6.21 (s, 1H), 5.34–5.21 (m, 1H), 5.11–4.98 (m, 1H), 3.47 (d, *J* = 7.2 Hz, 2H), 2.18–2.02 (m, 4H), 1.83 (s, 3H), 1.68 (d, *J* = 1.7 Hz, 3H), 1.60 (s, 3H). LCMS (ESI) retention time 5.57 min, *m/z* 275.64.

4.1.23. 2-[(2E)-3,7-Dimethylocta-2,6-dien-1-yl]-4-formyl-3-hydroxyphenyl acetate **(26)**

To a solution of 3-{[(2E)-3,7-dimethylocta-2,6-dien-1-yl]oxy}-4-formylphenyl acetate (synthesised using the same method to make **5**) (520 mg, 1.64 mmol) in toluene (7.5 mL) was added Fluorosil (100–200 mesh, 2.6 g). The reaction mixture was heated at reflux for 3 h before being allowed to cool to room temperature and being filtered. The Fluorosil was washed with ethyl acetate (3 × 20 mL) and the combined filtrate was concentrated under reduced pressure. Purification 2 times by flash column chromatography (10 g silica), eluting with a gradient of petrol ether: ethyl acetate (100: 0) to (90: 10), gave the title compound as a pale yellow oil (133 mg, 26%): R_f 0.50 (10% ethyl acetate/90% 40–60 petrol ether) ^{1}H NMR (500 MHz, Chloroform-*d*) δ 11.54 (s, 1H), 9.85 (s, 1H), 7.44 (d, *J* = 8.5 Hz, 1H), 6.76 (d, *J* = 8.4 Hz, 1H), 5.17–5.10 (m, 1H), 5.09–5.02 (m, 1H), 3.33 (d, *J* = 7.0 Hz, 2H), 2.33 (s, 3H), 2.10–2.02 (m, 2H), 2.02–1.94 (m, 2H), 1.77 (s, 3H), 1.65 (d, *J* = 1.8 Hz, 3H), 1.58 (s, 3H).

4.1.24. 5-Chloro-3-[(2E)-3,7-dimethylocta-2,6-dien-1-yl]-2-hydroxybenzaldehyde **(27)**

To a solution of 5-chloro-2-{[(2E)-3,7-dimethylocta-2,6-dien-1-yl]oxy}benzaldehyde (synthesised using the same method to make **5**) (300 mg, 1.02 mmol) in toluene (5.0 mL) was added Fluorosil (100–200 mesh, 3.0 g). The reaction mixture was heated at reflux for 3 h before being allowed to cool to room temperature and being filtered. The Fluorosil was washed with ethyl acetate (3 × 10 mL) and the combined filtrate was concentrated under reduced pressure. Purification 2 times by flash column chromatography (10 g silica), eluting with a gradient of petrol ether: ethyl acetate (100: 0) to (99: 1), gave the title compound as a pale yellow oil (45 mg, 15%): R_f 0.12 (100% 40–60 petrol ether) ^{1}H NMR (500 MHz, Chloroform-*d*) δ 11.22 (s, 1H), 9.84 (d, *J* = 0.8 Hz, 1H), 7.39 (d, *J* = 2.6 Hz, 1H), 7.35 (d, *J* = 2.6 Hz, 1H), 5.37–5.23 (m, 1H), 5.17–5.05 (m, 1H), 3.37 (d, *J* = 7.4 Hz, 2H), 2.21–2.02 (m, 4H), 1.76–1.65 (m, 6H), 1.62 (s, 3H).

4.1.25. 3-[(2E)-3,7-Dimethylocta-2,6-dien-1-yl]-2,4,6-trihydroxybenzaldehyde **(28)**

To a solution of 2,4,6-trihydroxybenzaldehyde (500 mg, 3.24 mmol) and geranyl bromide (536 μL, 2.70 mmol) in acetone (30 mL) was added potassium carbonate (224 mg, 1.62 mmol). The reaction mixture was heated at reflux for 5 h before being allowed to cool to room temperature and being concentrated under reduced pressure. Purification by flash column chromatography (10 g silica), eluting with a gradient of petrol ether: ethyl acetate (100: 0) to (60: 40), gave the title compound as a yellow solid (102 mg, 13%): R_f 0.36 (40% ethyl acetate/60% 40–60 petrol ether) ^{1}H NMR (500 MHz, Chloroform-*d*) δ 12.25 (s, 1H), 10.04 (s, 1H), 7.65 (d, 1H), 7.22 (s, 1H), 5.90 (s, 1H), 5.29–5.23 (m, 1H), 5.05 (t, *J* = 6.7 Hz, 1H), 3.33 (d, *J* = 7.3 Hz, 2H), 2.21–1.97 (m, 4H), 1.80 (s, 3H), 1.67 (s, 3H), 1.59 (s, 3H).

4.1.26. 3-Chloro-5-[(2E)-3,7-dimethylocta-2,6-dien-1-yl]-4,6-dihydroxy-2-methylbenzonitrile **(29)**

To a solution of 5-chloro-7-[(2E)-3,7-dimethylocta-2,6-dien-1-yl]-4-methyl-1,2-benzoxazol-6-ol (synthesised using the same

Please cite this article in press as: R.A. West, et al., African trypanosomiasis: Synthesis & SAR enabling novel drug discovery of ubiquinol mimics for trypanosome alternative oxidase, European Journal of Medicinal Chemistry (2017), https://doi.org/10.1016/j.ejmech.2017.09.067

method to make **31**) (45 mg, 0.141 mmol) in ethanol (4.5 mL) at room temperature was added 1 M aqueous sodium hydroxide (1.4 mL, 1.4 mmol). The reaction mixture was stirred at room temperature for 1 h before being acidified to pH 1 with 1 M aqueous hydrochloric acid. Ethyl acetate (10 mL) was added and the phases were separated. The aqueous phase was extracted with ethyl acetate (2 × 10 mL) and the combined organic fractions were dried over magnesium sulfate, filtered and concentrated under reduced pressure. Purification by flash column chromatography (5 g silica), eluting with a gradient of petrol ether: ethyl acetate (100: 0) to (90: 10), gave the title compound as a colourless oil (17 mg, 38%): R_f 0.40 (10% ethyl acetate/90% 40–60 petrol ether) ^{1}H NMR (500 MHz, Chloroform-*d*) δ 6.24 (s, 1H), 6.17 (s, 1H), 5.28–5.19 (m, 1H), 5.09–5.02 (m, 1H), 3.46 (d, J = 7.2 Hz, 2H), 2.52 (s, 3H), 2.21–2.02 (m, 4H), 1.86–1.78 (m, 3H), 1.70 (d, J = 1.3 Hz, 3H), 1.61 (d, J = 1.6 Hz, 3H). LCMS (ESI) retention time 5.43 min, *m/z* 320.15/322.07.

4.1.27. 2-Chloro-6-[(2E)-3,7-dimethylocta-2,6-dien-1-yl]-5-hydroxy-3,4-dimethylphenyl acetate **(30)**

To a solution of 2-chloro-6-[(2E)-3,7-dimethylocta-2,6-dien-1-yl]-4-formyl-5-hydroxy-3-methylphenyl acetate (**20**) (100 mg, 0.274 mmol) in dichloromethane (5 mL) was added triethylamine (76 μL, 0.548 mmol) and acetyl chloride (39 μL, 0.548 mmol) at room temperature. The reaction mixture was stirred at room temperature for 3 h before being concentrated under reduced pressure. Purification by flash column chromatography (10 g silica), eluting with a gradient of petrol ether: ethyl acetate (100: 0) to (80: 20), 3-(acetyloxy)-6-chloro-2-[(2E)-3,7-dimethylocta-2,6-dien-1-yl]-4-formyl-5-methylphenyl acetate as a pale yellow oil (30 mg, 27%): R_f 0.40 (10% ethyl acetate/90% 40–60 petrol ether) ^{1}H NMR (500 MHz, Chloroform-*d*) δ 10.27 (s, 1H), 5.12–5.01 (m, 1H), 5.01–4.91 (m, 1H), 3.21 (d, J = 6.6 Hz, 2H), 2.68 (s, 3H), 2.37 (s, 3H), 2.36 (s, 3H), 2.09–2.01 (m, 2H), 2.01–1.94 (m, 2H), 1.73 (d, J = 1.5 Hz, 3H), 1.67 (d, J = 1.7 Hz, 3H), 1.59 (d, J = 1.4 Hz, 3H). LCMS (ESI) retention time 6.44 min, *m/z* no ionisation.

To a solution of 3-(acetyloxy)-6-chloro-2-[(2E)-3,7-dimethylocta-2,6-dien-1-yl]-4-formyl-5-methylphenyl acetate (30 mg, 0.073 mmol) in tetrahydrofuran (1.0 mL) was added sodium borohydride (11 mg, 0.295 mmol). The reaction mixture was stirred at room temperature for 3 h before being diluted with deionised water (1 mL), quenched with 1 M aqueous hydrochloric acid (3 mL) and extracted with ethyl acetate (3 × 10 mL). The combined organic extracts were dried over magnesium sulfate, filtered and concentrated under reduced pressure. Purification by flash column chromatography (10 g silica), eluting with a gradient of petrol ether: ethyl acetate (100: 0) to (90: 10), gave the title compound as an off-white solid (15 mg, 58%): R_f 0.57 (10% ethyl acetate/90% 40–60 petrol ether) ^{1}H NMR (500 MHz, Chloroform-*d*) δ 5.43 (s, 1H), 5.22–5.12 (m, 1H), 5.09–4.97 (m, 1H), 3.28 (d, J = 7.6 Hz, 2H), 2.36 (s, 3H), 2.33 (s, 3H), 2.18 (s, 3H), 2.15–2.04 (m, 4H), 1.81 (s, 3H), 1.69 (d, J = 1.4 Hz, 3H), 1.61 (s, 3H). LCMS (ESI) retention time 6.43 min, *m/z* no ionisation.

4.1.28. 5-Chloro-3-[(2E)-3,7-dimethylocta-2,6-dien-1-yl]-2,4-dihydroxybenzonitrile **(31)**

To a solution of triphenylphosphine (42 mg, 0.162 mmol) in dichloromethane (2 mL) was added 2,3-dichloro-5,6-dicyano-*p*-benzoquinone (37 mg, 0.162 mmol). The dark reaction mixture was stirred at room temperature for 1 min during which time the colour faded. 4-Chloro-2-2E)-3,7-dimethylocta-2,6-dien-1-yl]-6-[(hydroxyimino)methyl]benzene-1,3-diol (**32**) (35 mg, 0.108 mmol) in dichloromethane (0.5 mL) was added to the reaction mixture in 1 portion and this was stirred for 1 min before being concentrated under reduced pressure. Purification by flash column chromatography (10 g silica), eluting with a gradient of petrol ether: ethyl acetate (100: 0) to (90: 10), gave 5-chloro-7-[(2E)-3,7-dimethylocta-2,6-dien-1-yl]-1,2-benzoxazol-6-ol as a white solid (24 mg, 72%).

To a solution of 5-chloro-7-[(2E)-3,7-dimethylocta-2,6-dien-1-yl]-1,2-benzoxazol-6-ol in ethanol (2.1 mL) at room temperature was added 1 M aqueous sodium hydroxide (0.69 mL, 0.69 mmol). The reaction mixture was stirred at room temperature for 1 h before being acidified to pH 1 with 1 M aqueous hydrochloric acid. Ethyl acetate (10 mL) was added and the phases were separated. The aqueous phase was extracted with ethyl acetate (2 × 10 mL) and the combined organic fractions were dried over magnesium sulfate, filtered and concentrated under reduced pressure. Purification by flash column chromatography (5 g silica), eluting with a gradient of petrol ether: ethyl acetate (100: 0) to (90: 10), gave the title compound as a light green oil (12 mg, 57%): R_f 0.09 (5% ethyl acetate/95% 40–60 petrol ether) ^{1}H NMR (500 MHz, Chloroform-*d*) δ 7.38 (s, 1H), 6.31 (s, 1H), 6.11 (s, 1H), 5.33–5.17 (m, 1H), 5.11–4.97 (m, 1H), 3.49 (d, J = 7.4 Hz, 3H), 2.20–2.01 (m, 4H), 1.82 (s, 3H), 1.70 (s, 3H), 1.61 (s, 3H). LCMS (ESI) retention time 4.98 min, *m/z* 306.09.

4.1.29. 4-Chloro-2-[(2E)-3,7-dimethylocta-2,6-dien-1-yl]-6-[(hydroxyimino)methyl]benzene-1,3-diol **(32)**

To a solution of 3-[(2E)-3,7-dimethylocta-2,6-dien-1-yl]-2,4-dihydroxy-6-methylbenzaldehyde (**23**) (44 mg, 0.142 mmol) in ethanol/deionised water/tetrahydrofuran (3:2:2, 0.5 mL) was added sodium acetate (17 mg, 0.214 mmol) and hydroxylamine hydrochloride (11 mg, 0.157 mmol). The reaction mixture was stirred for 16 h before being concentrated under reduced pressure. Purification by flash column chromatography (5 g silica), eluting with a gradient of petrol ether: ethyl acetate (100: 0) to (90: 10), gave the title compound as a white solid (37 mg, 80%): R_f 0.30 (5% ethyl acetate/95% 40–60 petrol ether) ^{1}H NMR (500 MHz, Chloroform-*d*) δ 9.31 (s, 1H), 8.10 (s, 1H), 7.08 (s, 1H), 7.02 (s, 1H), 5.88 (s, 1H), 5.35–5.18 (m, 1H), 5.14–5.00 (m, 1H), 3.46 (d, J = 7.2 Hz, 2H), 2.12–2.04 (m, 2H), 2.04–1.96 (m, 2H), 1.81 (d, J = 1.5 Hz, 3H), 1.66 (s, 3H), 1.59 (s, 3H). LCMS (ESI) retention time 5.40 min, *m/z* 324.09/326.11.

4.1.30. 3-Chloro-5-[(2E)-3,7-dimethylocta-2,6-dien-1-yl]-4,6-dimethoxy-2-methylbenzaldehyde **(33)**

To a solution of 3-chloro-5-[(2E)-3,7-dimethylocta-2,6-dien-1-yl]-4,6-dihydroxy-2-methylbenzaldehyde (**6**) (30 mg, 0.0929 mmol) and potassium carbonate (128 mg, 0.929 mmol) in acetone (2 ml) was added methyl iodide (57 μL, 0.929 mmol). The reaction mixture was stirred at room temperature for 16 h before being concentrated under reduced pressure. The residue was dissolved in ethyl acetate (5 mL) and deionised water (5 mL). The phases were separated and the aqueous phase was extracted with ethyl acetate (2 × 5 mL). The combined organic extracts were dried over magnesium sulfate, filtered and concentrated under reduced pressure. Purification by flash column chromatography (5 g silica), eluting with a gradient of petrol ether: ethyl acetate (100: 0) to (95: 5), gave the title compound as a yellow oil (16 mg, 49%): R_f 0.71 (5% ethyl acetate/95% 40–60 petrol ether) ^{1}H NMR (500 MHz, Chloroform-*d*) δ 10.43 (s, 1H), 5.24–5.12 (m, 1H), 5.12–5.00 (m, 1H), 3.88 (s, 3H), 3.83 (s, 3H), 3.42 (d, J = 7.0 Hz, 2H), 2.65 (s, 3H), 2.12–2.04 (m, 2H), 2.04–1.96 (m, 2H), 1.80 (s, 3H), 1.64 (s, 3H), 1.60–1.55 (m, 3H).

4.1.31. 3-Chloro-4-{[(2E)-3,7-dimethylocta-2,6-dien-1-yl]oxy}-6-hydroxy-2-methylbenzaldehyde **(34)**

To a solution of 4-chloro-5-{[(2E)-3,7-dimethylocta-2,6-dien-1-yl]oxy}-2-formyl-3-methylphenyl acetate (50 mg, 0.137 mmol) in tetrahydrofuran (2 mL) and methanol (0.5 ml) was added 4 M aqueous sodium hydroxide (68 μL, 0.274 mmol). The reaction

Please cite this article in press as: R.A. West, et al., African trypanosomiasis: Synthesis & SAR enabling novel drug discovery of ubiquinol mimics for trypanosome alternative oxidase, European Journal of Medicinal Chemistry (2017), https://doi.org/10.1016/j.ejmech.2017.09.067

mixture was stirred at room temperature for 2 h before being diluted with deionised water (2 mL) and acidified to pH 2 with 1 M aqueous hydrochloric acid. The reaction mixture was extracted with ethyl acetate (3 × 3 mL). The combined organic extracts were dried over magnesium sulfate, filtered and concentrated under reduced pressure. Purification by flash column chromatography (10 g silica), eluting with a gradient of petrol ether: ethyl acetate (100: 0) to (95: 5), gave the title compound as a white solid (31 mg, 70%): R_f 0.16 (5% ethyl acetate/95% 40–60 petrol ether) ^{1}H NMR (500 MHz, Chloroform-*d*) δ 12.59 (s, 1H), 10.16 (s, 1H), 6.36 (s, 1H), 5.53–5.43 (m, 1H), 5.14–5.03 (m, 1H), 4.67 (d, J = 6.5 Hz, 2H), 2.63 (s, 3H), 2.22–2.05 (m, 4H), 1.76 (d, J = 1.4 Hz, 3H), 1.68 (d, J = 1.6 Hz, 3H), 1.61 (d, J = 1.5 Hz, 3H). LCMS (ESI) retention time 6.88 min, *m/z* 323.72/325.95.

4.1.32. 3-Chloro-6-{[(2E)-3,7-dimethylocta-2,6-dien-1-yl]oxy}-4-hydroxy-2-methylbenzaldehyde (**35**)

To a solution of 2-chloro-5-{[(2E)-3,7-dimethylocta-2,6-dien-1-yl]oxy}-4-formyl-3-methylphenyl acetate (**5**) (50 mg, 0.137 mmol) in tetrahydrofuran (2 mL) and methanol (0.5 ml) was added 4 M aqueous sodium hydroxide (68 μL, 0.274 mmol). The reaction mixture was stirred at room temperature for 2 h before being diluted with deionised water (2 mL) and acidified to pH 2 with 1 M aqueous hydrochloric acid. The reaction mixture was extracted with ethyl acetate (3 × 3 mL). The combined organic extracts were dried over magnesium sulfate, filtered and concentrated under reduced pressure. Purification by flash column chromatography (10 g silica), eluting with a gradient of petrol ether: ethyl acetate (100: 0) to (90: 10), gave the title compound as a white solid (39 mg, 88%): R_f 0.23 (10% ethyl acetate/90% 40–60 petrol ether) ^{1}H NMR (500 MHz, Chloroform-*d*) δ 10.50 (s, 1H), 6.56 (s, 1H), 6.14 (s, 1H), 5.51–5.43 (m, 1H), 5.14–5.04 (m, 1H), 4.61 (d, J = 6.5 Hz, 2H), 2.69 (s, 3H), 2.21–2.04 (m, 3H), 1.75 (d, J = 1.5 Hz, 3H), 1.69 (d, J = 1.8 Hz, 3H), 1.62 (s, 3H). LCMS (ESI) retention time 5.88 min, *m/z* 323.22/325.21.

Acknowledgements

With thanks to Professor Anthony Moore at the University of Sussex for the supply of the plasmid containing complementary DNA for the over expression of Trypanosome Alternative Oxidase.

This work was supported by the Biotechnology and Biological Sciences Research Council [Grant Ref: BB/L017180/1] iCASE with Novartis Institute for Tropical Diseases.

Appendix A. Supplementary data

Supplementary data related to this article can be found at https://doi.org/10.1016/j.ejmech.2017.09.067.

References

[1] R. Brun, J. Blum, F. Chappuis, C. Burri, Human African trypanosomiasis, Lancet 375 (2010) 148–159, https://doi.org/10.1016/S0140-6736(09)60829-1.
[2] WHO Trypanosomiasis, Human African (factsheet). http://www.who.int/mediacentre/factsheets/fs259/en/, 2017. (Accessed 3 July 2017).
[3] R. Thomson, G. Genovese, C. Canon, D. Kovacsics, M.K. Higgins, M. Carrington, C.A. Winkler, J. Kopp, C. Rotimi, A. Adeyemo, A. Doumatey, G. Ayodo, S.L. Alper, M.R. Pollak, D.J. Friedman, J. Raper, Evolution of the primate trypanolytic factor APOL1, Proc. Natl. Acad. Sci. 111 (2014) E2130–E2139, https://doi.org/10.1073/pnas.1400699111.
[4] L.J. Morrison, L. Marcello, R. McCulloch, Antigenic variation in the African trypanosome: molecular mechanisms and phenotypic complexity, Cell. Microbiol. 11 (2009) 1724–1734, https://doi.org/10.1111/j.1462-5822.2009.01383.x.
[5] N. Baker, H.P. de Koning, P. Mäser, D. Horn, Drug resistance in African trypanosomiasis: the melarsoprol and pentamidine story, Trends Parasitol. 29 (2013) 110–118, https://doi.org/10.1016/j.pt.2012.12.005.
[6] WHO, Cases of Sleeping Sickness Drop to Lowest Level in 75 Years, 2015. http://www.who.int/trypanosomiasis_african/cases_drop_to_lowest_since_75_years/en/. (Accessed 3 July 2017).
[7] P.G.E. Kennedy, Clinical features, diagnosis, and treatment of human African trypanosomiasis (sleeping sickness), Lancet Neurol. 12 (2013) 186–194, https://doi.org/10.1016/S1474-4422(12)70296-X.
[8] J. Blum, C. Schmid, C. Burri, Clinical aspects of 2541 patients with second stage human African trypanosomiasis, Acta Trop. 97 (2006) 55–64, https://doi.org/10.1016/j.actatropica.2005.08.001.
[9] R.T. Jacobs, B. Nare, M.A. Phillips, State of the art in African trypanosome drug discovery, Curr. Top. Med. Chem. 11 (2011) 1255–1274, https://doi.org/10.2174/156802611795429167.
[10] E.M. Fevre, B.V. Wissmann, S.C. Welburn, P. Lutumba, The burden of human African trypanosomiasis, PLoS Negl. Trop. Dis. 2 (2008) e333, https://doi.org/10.1371/journal.pntd.0000333.
[11] African Trypanosomiasis-Disease Database, 2016. http://www.discontools.eu/Diseases/Detail/61. (Accessed 3 July 2017).
[12] S.G. Wilson, K.R.S. Morris, I.J. Lewis, E. Krog, The effects of trypanosomiasis on rural economy, Bull. World Health Organ 28 (5-6) (1963) 595–613.
[13] D. Muhanguzi, K. Picozzi, J. Hattendorf, M. Thrusfield, J.D. Kabasa, C. Waiswa, S.C. Welburn, The burden and spatial distribution of bovine African trypanosomes in small holder crop-livestock production systems in Tororo District, south-eastern Uganda, Parasit. Vectors 7 (2014) 603, https://doi.org/10.1186/s13071-014-0603-6.
[14] B.S. Salgado, C.T. Battaglia, R.S. Stuchi, F.A. Cadioli, D.B. Rozza, G.F. Machado, What is your diagnosis? Lymphadenopathy in a cow with severe anemia. Bovine trypanosomiasis, Vet. Clin. Pathol. 40 (2011) 103–104, https://doi.org/10.1111/j.1939-165X.2011.00295.x.
[15] A. Stich, A. Ponte-Sucre, U. Holzgrabe, Do we need new drugs against human African trypanosomiasis? Lancet Infect. Dis. 13 (2013) 733–734, https://doi.org/10.1016/S1473-3099(13)70191-9.
[16] I. The, R. Societyoftropical, J. Pbpin, F. Milord, A.N. Khonde, T. Niyonsenga, L. Loko, B. Mpia, D. Wals, Risk factors for encephalopathy Trypanosoma brucei gambiense and mortality during sleeping sickness melarsoprol treatment of, Trans. R. Soc. Trop. Med. Hyg. 89 (1995) 92–97.
[17] J. Blum, S. Nkunku, C. Burri, Clinical description of encephalopathic syndromes and risk factors for their occurrence and outcome during melarsoprol treatment of human African trypanosomiasis, Trop. Med. Int. Heal 6 (2001) 390–400, https://doi.org/10.1046/j.1365-3156.2001.00710.x.
[18] I.M. Rollo, J. Williamson, Acquired resistance to “Melarsen”, Tryparsamide and Amidines in pathogenic trypanosomes after treatment with “Melarsen” alone, Nature 167 (1951) 147–148, https://doi.org/10.1038/167147a0.
[19] S. Alsford, S. Eckert, N. Baker, L. Glover, A. Sanchez-Flores, K.F. Leung, D.J. Turner, M.C. Field, M. Berriman, D. Horn, High-throughput decoding of antitrypanosomal drug efficacy and resistance, Nature 482 (2012) 232–236, https://doi.org/10.1038/nature10771.
[20] G.C. Vanlerberghe, L. McIntosh, Alternative oxidase: from gene to function, Annu. Rev. Plant Physiol. Plant Mol. Biol. 48 (1997) 703–734, https://doi.org/10.1146/annurev.arplant.48.1.703.
[21] T. Shiba, Y. Kido, K. Sakamoto, D.K. Inaoka, C. Tsuge, R. Tatsumi, G. Takahashi, E.O. Balogun, T. Nara, T. Aoki, T. Honma, A. Tanaka, M. Inoue, S. Matsuoka, H. Saimoto, A.L. Moore, S. Harada, K. Kita, Structure of the trypanosome cyanide-insensitive alternative oxidase, Proc. Natl. Acad. Sci. 110 (2013) 4580–4585, https://doi.org/10.1073/pnas.1218386110.
[22] C. Nihei, Y. Fukai, K. Kita, Trypanosome alternative oxidase as a target of chemotherapy, Biochim. Biophys. Acta 1587 (2002) 234–239. http://www.ncbi.nlm.nih.gov/pubmed/12084465.
[23] Y. Kido, K. Sakamoto, K. Nakamura, M. Harada, T. Suzuki, Y. Yabu, H. Saimoto, F. Yamakura, D. Ohmori, A. Moore, S. Harada, K. Kita, Purification and kinetic characterization of recombinant alternative oxidase from Trypanosoma brucei brucei, Biochim. Biophys. Acta Bioenerg. 1797 (2010) 443–450, https://doi.org/10.1016/j.bbabio.2009.12.021.
[24] Y. Kido, T. Shiba, D.K. Inaoka, K. Sakamoto, T. Nara, T. Aoki, T. Honma, A. Tanaka, M. Inoue, S. Matsuoka, A. Moore, S. Harada, K. Kita, Crystallization and preliminary crystallographic analysis of cyanide-insensitive alternative oxidase from Trypanosoma brucei brucei, Acta Crystallogr. Sect. F. Struct. Biol. Cryst. Commun. 66 (2010) 275–278, https://doi.org/10.1107/S1744309109054062.
[25] Y. Yabu, N. Minagawa, K. Kita, K. Nagai, M. Honma, S. Sakajo, T. Koide, N. Ohta, A. Yoshimoto, Oral and intraperitoneal treatment of Trypanosoma brucei brucei with a combination of ascofuranone and glycerol in mice, Parasitol. Int. 47 (1998) 131–137, https://doi.org/10.1016/S1383-5769(98)00011-7.
[26] H. Saimoto, Y. Kido, Y. Haga, K. Sakamoto, K. Kita, Pharmacophore identification of ascofuranone, potent inhibitor of cyanide-insensitive alternative oxidase of Trypanosoma brucei, J. Biochem. 153 (2013) 267–273, https://doi.org/10.1093/jb/mvs135.
[27] N. Minagawa, Y. Yabu, K. Kita, K. Nagai, N. Ohta, K. Meguro, S. Sakajo, A. Yoshimoto, Erratum to “An antibiotic, ascofuranone, specifically inhibits respiration and in vitro growth of long slender bloodstream forms of Trypanosoma brucei brucei”, Mol. Biochem. Parasitol. 84 (1997) 271–280, https://doi.org/10.1016/S0166-6851(96)02797-1.
[28] Y. Yabu, A. Yoshida, T. Suzuki, C. Nihei, K. Kawai, N. Minagawa, T. Hosokawa, K. Nagai, K. Kita, N. Ohta, The efficacy of ascofuranone in a consecutive treatment on Trypanosoma brucei brucei in mice, Parasitol. Int. 52 (2003) 155–164. http://www.ncbi.nlm.nih.gov/pubmed/12798927.
[29] H. Saimoto, Y. Kusano, T. Hiyama, A mild procedure for hydrolysis of

alkoxymethyl aryl ethers to give hydroxyarenes. A rational synthesis of ascofuranone, Tetrahedron Lett. 27 (1986) 1607–1610, https://doi.org/10.1016/S0040-4039(00)84326-9.
[30] K. Mori, T. Fujioka, Synthesis of (±)-ascochlorin, (±)-ascofuranone and LL-Z1272, Tetrahedron 40 (1984) 2711–2720, https://doi.org/10.1016/S0040-4020(01)96890-5.
[31] C. Kau-Ming, M.M. Joullié, A simple total synthesis of (±)-ascofuranone, Tetrahedron Lett. 25 (1984) 3795–3796, https://doi.org/10.1016/S0040-4039(01)91169-4.
[32] H. Saimoto, T. Hiyama, A general highly efficient access to prenylated phenolic natural products. Synthesis of colletochlorins B and D, Tetrahedron Lett. 27 (1986) 597–600, https://doi.org/10.1016/S0040-4039(00)84050-2.
[33] F.X. Talamás, D.B. Smith, A. Cervantes, F. Franco, S.T. Cutler, D.G. Loughhead, D.J. Morgans, R.J. Weikert, The Florisil® catalyzed [1,3]-sigmatropic shift of allyl phenyl ethers — an entryway into novel mycophenolic acid analogues, Tetrahedron Lett. 38 (1997) 4725–4728, https://doi.org/10.1016/S0040-4039(97)00949-0.
[34] C. Nihei, Y. Fukai, K. Kawai, A. Osanai, Y. Yabu, T. Suzuki, N. Ohta, N. Minagawa, K. Nagai, K. Kita, Purification of active recombinant trypanosome alternative oxidase, FEBS Lett. 538 (2003) 35–40, https://doi.org/10.1016/S0014-5793(03)00120-0.
[35] L. Xie, Y. Takeuchi, L.M. Cosentino, A.T. McPhail, K.-H. Lee, Anti-AIDS agents. 42. Synthesis and anti-HIV activity of disubstituted (3' R ,4' R)-3',4'-Di- O -(S)-camphanoyl-(+)- cis -khellactone analogues, J. Med. Chem. 44 (2001) 664–671, https://doi.org/10.1021/jm000070g.
[36] K.M. Chen, J.E. Semple, M.M. Joullie, Total syntheses of fungal metabolites and functionalized furanones, J. Org. Chem. 50 (1985) 3997–4005, https://doi.org/10.1021/jo00221a009.

Please cite this article in press as: R.A. West, et al., African trypanosomiasis: Synthesis & SAR enabling novel drug discovery of ubiquinol mimics for trypanosome alternative oxidase, European Journal of Medicinal Chemistry (2017), https://doi.org/10.1016/j.ejmech.2017.09.067

ACS Infectious Diseases

Article

Cite This: ACS Infect. Dis. 2018, 4, 592−604

pubs.acs.org/journal/aidcbc

Toward More Drug Like Inhibitors of Trypanosome Alternative Oxidase

Ryan A. West,[†] Thomas Cunningham,[†] Lewis E. Pennicott,[†] Srinivasa P. S. Rao,[‡] and Simon E. Ward*[,†,§]

[†]Sussex Drug Discovery Centre, University of Sussex, Brighton, BN1 9QJ, United Kingdom

[‡]Novartis Institutes for Tropical Diseases, 5300 Chiron Way, Emeryville, California 94608-2916, United States

[§]Medicines Discovery Institute, Cardiff University, Park Place, Cardiff, CF10 3AT, United Kingdom

ABSTRACT: New tools are required to ensure the adequate control of the neglected tropical disease human African trypanosomiasis. Annual reports of infection have recently fallen to fewer than 5000 cases per year; however, current therapies are hard to administer and have safety concerns and, hence, are far from ideal. Trypanosome alternative oxidase is an exciting target for controlling the infection; it is unique to the parasite, and inhibition of this enzyme with the natural product ascofuranone has shown to clear *in vivo* infections. We report the synthesis and associated structure activity relationships of inhibitors based upon this natural product with correlation to *T. b. brucei* growth inhibition in an attempt to generate molecules that possess improved physicochemical properties and potential for use as new treatments for human African trypanosomiasis.

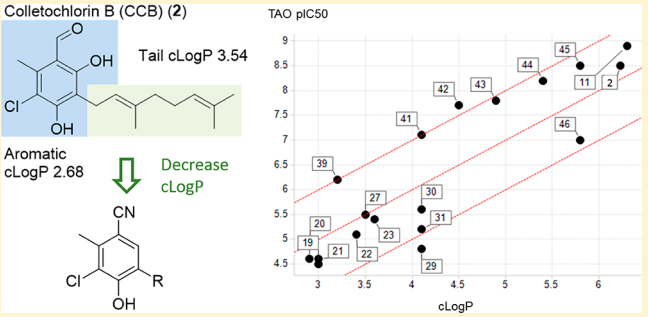

KEYWORDS: *medicinal chemistry, drug design, multiparameter optimization, human African trypanosomiasis*

Human African trypanosomiasis (HAT), otherwise known as African sleeping sickness, is a neglected tropical disease caused by human infection by the protozoan parasites *T. b. gambiense* or *T. b. rhodesiense*, transmitted by tsetse flies in sub-Saharan Africa.[1] Without treatment, HAT is invariably fatal;[2] the drugs that are currently approved for treatment of both the hemolymphatic (stage 1) and encenphalitic (stage 2) phases of the disease either have toxic side effects or require complex administration procedures.[3] Resistant strains of the parasites have been observed in the clinic, and there is a requirement for new treatment options to guarantee the successful control of the disease.[4,5] In 2009, it was estimated that occurrences of the disease had fallen below 20 000 incidences a year and that 65 million people are at risk of transmission.[1]

The trypanosome, first discovered by Sir David Bruce in 1895,[6] undergoes diverse lifecycle adaptations conferring viability in both the tsetse fly vector and mammalian host.[7,8] A predominant feature of *Trypanosoma brucei* is that it is capable of successfully evading host immune responses, predominantly due to its capacity to diversify the surface antigens that it presents to its host;[9] this ability has been a major factor for preventing the development of an efficacious vaccine against the pathogen.[10] *T. b. gambiense* is responsible for >95% of cases of HAT and is a zoonotic disease, residing in a variety of domestic animals and livestock.[11] Trypanosome infection in cattle and other livestock also has a large burden on the health and associated economic output of animals; the cost of delivering trypanocidal agents to control "Nagana" or African animal trypanosomiasis (AAT) is estimated to be 140 million USD per year.[12]

Current treatments for HAT are far from ideal. Stage 1 of the disease is treated with suramin for *T. b. rhodesiense* or pentamidine for *T. b. gambiense*; both compounds display undesired toxic side effects in the clinic.[13] Resistance against pentamidine has also been observed and linked to mutations in the P2 amino purine and other trypanosome uptake transporters.[5] Both suramin and pentamidine are unable to permeate into the central nervous system (CNS) to sufficient levels and, thus, are ineffective against stage 2 infections.[14] The organoarsenide melarsoprol and the more recent combination therapy of nifurtimox and eflornithine (NECT) are currently used to treat infections of *T. b. gambiense* and *T. b. rhodesiense*, respectively. Both treatments have their limitations. Melarsoprol shows significant toxic effects in those treated, causing encephalopathy in 5−10% of people treated with the drug.[15] Incidences of resistance to melarsoprol are becoming more commonplace, again linked to mutations in the P2 amino purine uptake transporters; associated failure rates in the clinic have been reported to be between 20% and 30% in the early 2000s.[5] NECT requires the administration of eflornithine via

Special Issue: Drug Discovery for Global Health

Received: November 6, 2017
Published: January 21, 2018

DOI: 10.1021/acsinfecdis.7b00218
ACS Infect. Dis. 2018, 4, 592−604

slow intravenous infusion of 200 mg/kg every 12 h for 7 days as it is only trypanostatic, thus requiring trypanocidal action by the coadministered nifurtimox and innate host clearance mechanisms.[16]

With the limitations of the currently approved medicines for treating HAT and the increasing reports of resistance to these therapies, it is vital to discover new and improved treatments against the pathogen. An ideal target for drug discovery for HAT is the trypanosome alternative oxidase (TAO).[17] TAO is the sole terminal oxidase enzyme in the aerobic respiratory pathway for the long slender blood stage form of *Trypanosoma brucei* subspecies. The enzyme utilizes oxygen and ubiquinol as substrates for the efficient generation of cellular ATP as the parasite does not express regular cytochrome respiratory complexes.[18] TAO is a di-iron (nonheme) oxidoreductase that is located in the inner-mitochondrial membrane of the trypanosome.[19] As TAO is not found in mammalian systems, there is a unique opportunity to attain compounds with enhanced selectivity and circumvent on-target toxicity.[19] It has recently been reported that the pentamidine and melarsoprol drug resistant parasites have an increased sensitivity to inhibition of TAO, as these parasites have a reduced capacity to efflux cellular glycerol that is produced as the result of anaerobic respiration.[20] The crystal structure of TAO has been reported, allowing a structure based design approach to new molecules.[21] Nanomolar inhibition of TAO has been reported with the natural product ascofuranone (AF (**1**)) and its analogues in validated biochemical assays,[22] demonstrating correlation in *ex vivo* growth inhibition[23] and efficacy in *in vivo* clearance models.[24]

Our previous work identified robust synthetic routes to close analogues of AF (**1**) and structure activity relationships of the synthesized molecules, highlighting the requirement of both the chloro and methyl substituents on the aromatic ring for high potency (Figure 1).[23] With these routes in place, we set out to

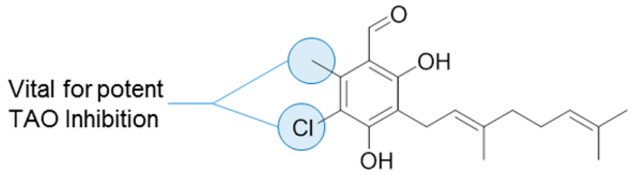

Figure 1. Summary of previous work[23]

further explore structurally similar analogues with the aim to reduce lipophilicity and improve the drug like properties of these molecules. Our aim of reducing lipophilicity was to specifically improve aqueous solubility, decrease metabolism, and improve the potential to achieve efficacious CNS concentrations, as new compounds for HAT must be effective against both stages of the disease.

There are many hurdles preventing permeability of organic drug molecules to the brain. The blood–brain barrier provides significant protection to xenobiotics; tight junctions around capillaries prevent permeation, and the expression of ABC-transporters actively transport solubilized organic molecules out and away from the barrier and the brain.[25] Compounds that traverse readily into the CNS tend to have high passive permeability, have low efflux from ABC-transporters like P-glyco-protein (P-gp), and have low metabolic turnover in human liver microsomes, providing the basis for the generation of a predictive scoring tool for CNS penetration.[26]

A major contribution to the poor multiparameter optimization (MPO)[26] predicted a CNS-penetration score for AF (**1**), and colletochlorin B (CCB (**2**)) is attributed to its high lipophilicity. Clearly, the major contributor to the high lipophilicity of CCB (**2**) is from the geranyl "lipophilic tail" (Figure 2). Compounds with a cLogP above 5 are commonly

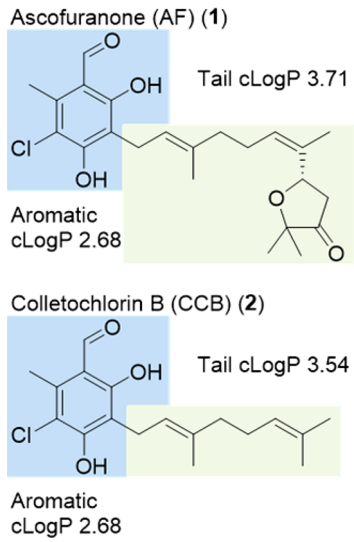

Figure 2. Per atom contribution to lipophilicity of ascofuranone (AF) (**1**) and colletochlorin B (CCB) (**2**).

observed to be P-gp substrates and tend to have a high metabolic liability. We herein report the synthesis and SAR investigation of analogues focused on reducing the lipophilicity of the tail region of structural analogues of AF (**1**) and CCB (**2**), with an aim to improve physicochemical properties and increase the predicted CNS penetration MPO score.

RESULTS AND DISCUSSION

The biochemical assessment of the bicyclic 1,2-isoxazole intermediate prepared to access the aldehyde replacement with the nitrile analogue of CCB (**2**) had shown unexpectedly high potency for inhibiting TAO. Previous reports had postulated that a hydrogen bond donor was needed at this position for potent inhibition of TAO.[22] To confirm this result, a synthetic route to the monophenolic compound (**11**) was devised (Scheme 1), to rule out the activity arising from an *in situ* formation of nitrile compound via a Kemp elimination (Figure 3).[27]

Selective bromination of the phenolic aldehyde was achieved by treatment with trimethylbenzylammonium tribromide at 0 °C; nonselective and over bromination was observed using *N*-bromosuccinimide.[28] The aldehyde (**6**) could be successfully converted to the nitrile (**7**) by oxime formation with hydroxylamine hydrochloride and subsequent *in situ* dehydration. Protection of the phenol (**8**) to the anisole (**9**) with dimethylsulfate was required to facilitate a high yielding Suzuki-Miyaura cross-coupling using tri-*n*-octylborane as the coupling partner that was formed *in situ* by reacting 1-octene with a solution of 1 M borane in THF.[29] Final deprotection of the anisol (**10**) to the free phenol using trimethylsilyl chloride and sodium iodide provided the monophenol analogue (**11**) for biochemical and *ex vivo* assessment (Table 1).[30]

Interestingly, the monophenol analogue (**11**) retained high potency against TAO that corresponded to the most potent

DOI: 10.1021/acsinfecdis.7b00218
ACS Infect. Dis. 2018, 4, 592–604

Scheme 1. Monophenol Analogue Synthesis[a]

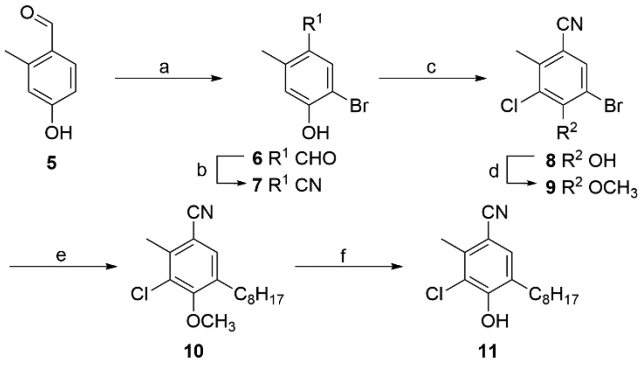

[a]Reaction conditions: (a) trimethylphenylammonium tribromide, CH_2Cl_2/MeOH rt, 3 h, 77%, (b) $NH_2OH{\cdot}HCl$, EtOH, reflux, 16 h, 90%, (c) NCS, Et_3N, MeCN, 0 °C to rt, 16 h, 70%, (d) dimethyl sulfate, acetone, rt, 16 h, 98%, (e) (i) $BH_3{\cdot}THF$, 1-octene, 0 °C, 20 min, (ii) toluene, H_2O, K_3PO_4, RuPhos, $Pd(OAc)_2$, 50 °C, 16 h, 90%, and (f) TMS-Cl, NaI, MeCN, 80 °C, 16 h, 65%.

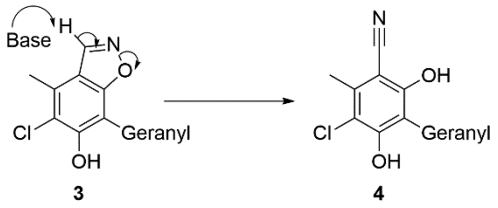

Figure 3. Isoxazole Kemp elimination.

inhibition of *T. b. brucei* growth for a compound not containing the benzaldehyde functionality present in AF and CCB. The removal of one of the flanking substituents *ortho* to the brominated coupling position facilitated its reactivity and thus exploration of this tail. This synthetic route was adopted for further diversification of this tail region. The des-methyl starting material was accessible from commercially available sources and was used to initially investigate tail modifications.

The introduction of polarity into the lipophilic tail was devised to reduce cLogP and improve upon the predicted CNS penetration MPO score (>4 required for high predicted CNS exposure). The introduction of amide functionality in alternate positions in the chain were planned to mimic the *n*-octyl (C_8H_{17}) or geranyl chain. The inclusion of the amide functionality had the largest predicted improvement to both cLogP and MPO score (Row C, Table 2). 1-Alkene esters were converted to trialkylboranes using the methodology previously employed to access the *n*-octyl analogues (Scheme 2). These were then coupled with the brominated intermediate (**14**). The esters were converted to the desired amides by either *in situ* hydrolysis under the demethylation conditions, with subsequent HATU amide coupling with the required alkylamine, or a direct aminolysis of the ester by using 1,5,7-triazabicyclo[4.4.0]-dec-5-ene (TBD) and the desired alkylamine with subsequent anisole deprotection with TMSCl/NaI to provide the amide chain compounds for biological assessment (Table 3).[31]

The acrylic ester could not be successfully coupled under these conditions; we postulate that the required trialkylborane may not form as the alkene is too electron deficient. The desired ester was synthesized by a Heck-Mizoroki cross-coupling and subsequent reduction of the double bond, before chlorination and amide formation with TBD (Scheme 3).

A selection of ether chain analogues was also planned and synthesized (D, Table 2); these were expected to be more chemically similar to that of the aliphatic chain with a smaller amount of polarity introduced in comparison to the amide. These compounds were less chemically tractable; in our hands, the anisole deprotection to the phenol proved challenging. The deprotection conditions that we explored led to the cleavage of the desired ether functionality present in the chain to the terminal alcohol. To mitigate this synthetic hurdle, alternative protecting groups were investigated. Bulkier silyl protecting groups hindered the cross-coupling and failed to provide the desired ether tail analogues. Reaction with the phenolic ester (**27**) provided some cross-coupled product; the stability of this protecting group perhaps, unsurprisingly, proved to be labile under the reaction coupling conditions. The deacetylated products (**29** to **31**) were observed and isolated from the reactions; however, significant proportions of the starting material ester (**28**) saponified before cross-coupling providing a major byproduct of the deacetylated phenol (**14**) thus resulting in lower isolated yields (Scheme 4).

Assessment of these less lipophilic analogues showed a large decrease in potency compared to the *n*-octyl analogues, highlighting that even minor increases in polarity in this part of the lipophilic tail were not tolerated. The most promising analogues included polarity at the terminal of the chain (**22** and **23**); however, disappointingly, these compounds resulted in no measurable inhibition of *T. b. brucei* growth (Table 3).

This data suggested that a lipophilic tail was required for the potent inhibition of TAO. To further probe this observation, analogues were prepared to assess the length of tail needed for potent inhibition of TAO and whether total lipophilicity could be decreased by reduction of the carbon chain length (E, Table 2). Previous reports had shown large decreases in potency against TAO at carbon chain length below 3. The C1−7 analogues (**39** to **45**) were prepared in a similar fashion to that of the *n*-octyl analogue (**11**); C1−4 analogues were, however, prepared directly using the alkyl boronic acid or trimeric alkyl boroxines as the volatile alkene hydrocarbons were not accessible (Scheme 5).

Interestingly, the reduced carbon chain length analogues showed good potency against TAO (Table 4), until a notable decrease in enzymatic inhibition was observed at compounds with C3 or below, corroborating previous reports.[22] What was more evident was the decrease observed in efficacy against *T. b. brucei* growth inhibition as chain length and cLogP decreased. Compounds showed a distinct drop off in potency against *T. b. brucei* for each carbon reduction. To interrogate this data, further correlations of cLogP and biochemical and cellular potency were carried out (Figure 4).

Biochemical potency for these compounds track to a lipophilic ligand efficiency of 3. Cellular potency, however, correlates to a lipophilic ligand efficiency of 1, relating to a 100-fold decrease in potency from the biochemical activity to the cellular assay. The 2 log decrease in cellular potency observed here could be due a combination of reasons that we are currently investigating; it is of interest that CCB (**2**) shows a smaller decrease in potency from the biochemical to cellular assay. The permeability of the compounds through the cell and mitochondrial membranes of the trypanosome may be reduced as the lipophilicity decreases. The compounds could be substrates for efflux transport, that may reduce the intracellular concentration. The TAO inhibition kinetics of the compounds may be altered with the reduction in carbon chain length that

DOI: 10.1021/acsinfecdis.7b00218
ACS Infect. Dis. 2018, 4, 592−604

Table 1. Biological Assay Assessment of Isoxazole and Monophenol Analogues

#	Structure	TAO pIC_{50}[a]	*T. b. b.* pEC_{50}[b]	HepG2 pCC_{50}[c]
2	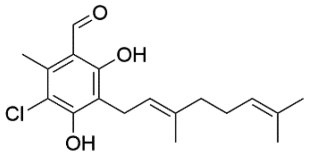	8.5 ± 0.3	8.4 ± 0.1	5.1 ± 0.1
4	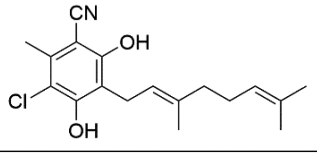	8.4 ± 0.2	6.4 ± 0.1	4.9 ± 0.1
3	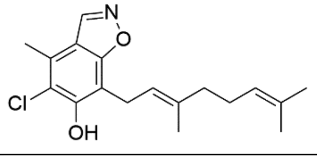	8.3 ± 0.4	7.0 ± 0.2	5.3 ± 0.2
11	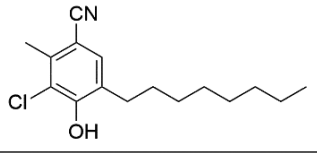	8.9 ± 0.3	7.6 ± 0.1	5.1 ± 0.1
46	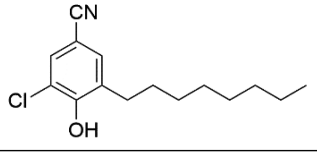	7.0 ± 0.1	5.1 ± 0.2	4.7 ± 0.1
10	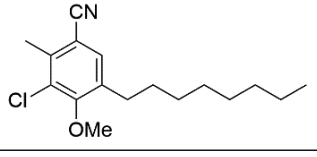	4.5 ± 0.1	< 4.3	< 4.3

[a]Negative log concentration and standard deviation of compounds required for 50% inhibition of trypanosome alternative oxidase. [b]Negative log concentration and standard deviation of compounds required for 50% growth inhibition of *T. b. brucei* Lister427. [c]Negative log concentration and standard deviation of compounds required for 50% cytotoxicity of HepG2 cell line ($n \geq 2$ in all assays).

could result in faster dissociation, resulting in reduced efficacy on target. The compounds may not locate to the desired cell compartment as lipophilicity may be required for the inhibitors to be retained in the inner mitochondrial membrane where the enzyme is located. Colletochlorin B could be acting on an unknown complementary antiparasitic target. On-going studies to better understand these data will aid future analogue design and synthesis to identify more drug like inhibitors of TAO.

We also noticed positive correlation between cLogP and both biochemical and cellular activity (Figure 4). Examples of potency correlating to high lipophilicity have previously been observed with other membrane proteins and enzymes requiring lipophilic substrates.[33,34]

CONCLUSIONS

HAT continues to provide a challenge for the development of new therapies; cases continue to be reported with resistance more frequently observed. Discoveries of new brain penetrant *T. b. gambiense* and *T. b. rhodesiense* trypanocides are vital for ensuring the adequate control of HAT in the future. Our work in this area has been to identify potent inhibitors of TAO that possess improved physicochemical properties compared to that of the natural products from which they are derived. Our exploration in this area has previously shown the requirement for the methyl and chloro substituents on the aromatic ring for high potency inhibition of TAO. Our efforts reported here for modulating the lipophilicity of this molecule by the introduction of polar functionality in the tail region of this chemotype has proved challenging. Polar functionality in this region of the molecule was shown to not be tolerated with large decreases in potency against TAO observed. The reduction in the carbon chain length of the tail resulted in identifying analogues that retained high inhibitory activity of TAO; however, *ex vivo* efficacy against *T. b. brucei* growth was diminished. We will continue to try to understand this disconnect and use this generated data for future compound design toward more drug like inhibitors of TAO.

MATERIALS AND METHODS

Experimental Details. ChemAxon Calculator Plugins were used for structure property prediction and calculation (cLogP), Marvin 15.5.4, 2015, ChemAxon (http://www.chemaxon.com). All commercial reagents were purchased from Sigma-Aldrich, Alfa Aesar, Apollo Scientific, Fluorochem, or Tokyo Chemical Industry and of the highest available purity. Unless otherwise stated, chemicals were used as supplied without further

DOI: 10.1021/acsinfecdis.7b00218
ACS Infect. Dis. 2018, 4, 592−604

Table 2. cLogP and Predicted MPO Scores for Planned Analogues[a]

Row	Structure	cLogP	MPO Score[26]
A (**4**)	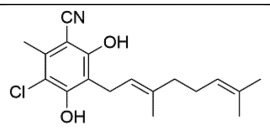	6.2	3.5
B (**11**)	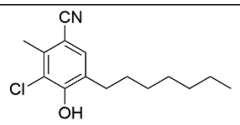	6.3	3.8
C	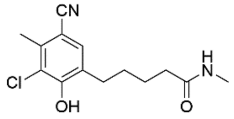	3.5	5.5
D	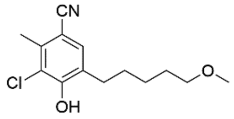	4.6	4.8
E (**43**)	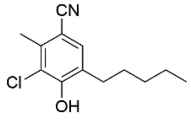	4.9	4.2

[a]cLogP calculated from ChemAxon Marvin Sketch; calculated MPO as described by Wager et al.[26]

Scheme 2. Amide Tail Linker Synthesis[a]

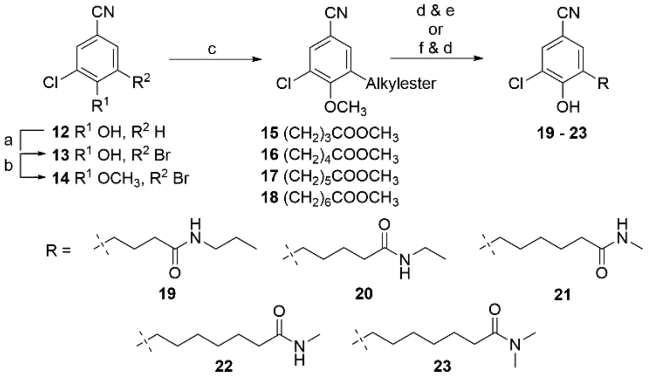

[a]Reaction conditions: (a) NBS, MeCN, rt, 16 h, 85%, (b) dimethyl sulfate, acetone, reflux, 3 h, 90%, (c) (i) BH_3·THF, 1-alkene ester, 0 °C, 20 min, (ii) toluene, H_2O, K_3PO_4, RuPhos, $Pd(OAc)_2$, 16 h, 50 °C, 90%, (d) TMSCl, NaI, MeCN, 80 °C, 16 h, 35−85%, (e) HATU, Et_3N, R^1R^2NH, MeCN, rt, 3 h, 60−90%, and (f) TBD, R^1R^2NH, MeCN, rt, 1−16 h 70−85%.

purification. Anhydrous solvents were purchased from Acros (AcroSeal) or Sigma-Aldrich (SureSeal) and were stored under nitrogen. 40−60 petrol ether refers to the fraction with a boiling point between 40 and 60 °C. Anhydrous solvents and reagents were used as purchased. Thin layer chromatography (TLC) was carried out using glass plates precoated with Merck silica gel 60 F254. Melting points were determined using an OptiMelt apparatus and are uncorrected. Proton nuclear magnetic resonance spectra were recorded at 500 MHz on a Varian VNMRS 500 MHz spectrometer (at 30 °C), using residual isotopic solvent ($CHCl_3$, δ = 7.27 ppm, DMSO δ = 2.50 ppm, MeOH δ = 3.31 ppm) as an internal reference. Chemical shifts are quoted in parts per million (ppm). Coupling constants (J) are recorded in Hertz (Hz). Carbon nuclear magnetic resonance spectra were recorded at 125 MHz on a Varian 500 MHz spectrometer and are proton decoupled, using residual isotopic solvent ($CHCl_3$, δ = 77.00 ppm, DMSO δ = 39.52 ppm, MeOH δ = 49.00 ppm) as an internal reference. Proton and carbon spectra assignments are supported by DEPT editing. High resolution mass spectrometry (HRMS) data (ESI) was recorded on Bruker Daltonics, Apex III, ESI source: Apollo ESI with methanol as spray solvent. Only molecular ions, fractions from molecular ions, and other major peaks are reported as mass/charge (m/z) ratios. LCMS data was recorded on a Waters 2695 HPLC using a Waters 2487 UV detector and a Thermo LCQ ESI-MS. Samples were eluted through a Phenomenex Lunar 3 μm C18 50 mm × 4.6 mm column, using water and acetonitrile acidified by 0.1% formic acid at 1 mL/min and detected at 254 nm. The gradient employed was a 7 min method 30−90% MeCN over a 5 min gradient, held at 90% MeCN for 1 min, and then re-equilibrated to 30% MeCN over 1 min. All experiments were carried out under an inert atmosphere of N_2 unless otherwise stated.

TAO Absorbance Assay. 1-Ubiquinol turnover was measured by recording the increase in absorbance at 278 nm (Greiner 96-well UV star flat bottom plates with BMG PHERAstar FS photo spectrometer) to monitor the increase of 1-ubiquinone concentration kinetically over 6 min with purified rTAO (3 nM). A final concentration of 15 μM 1-ubiquinol was used under the following conditions: 50 mM Tris-HCl; 0.05% (w/v) C10E8; pH 7.4; 25 °C. The sigmoidal curve of the inhibition was observed by 10-point 3-fold serial dilution of test compounds to generate IC_{50} values.

Growth Inhibition Assays. Bloodstream form *Trypanosoma brucei brucei* (*T. b. brucei* or *T. b. b.*) Lister 427 parasites were continuously passaged in HMI-9 medium formulated from IMDM medium (Invitrogen), 10% heat-inactivated fetal bovine serum, 10% Serum Plus medium supplement (SAFC Biosciences), 1 mM hypoxanthine (Sigma-Aldrich), 50 μM bathocuproine disulfonic acid (Sigma-Aldrich), 1.5 mM cysteine (Sigma-Aldrich), 1 mM pyruvic acid (Sigma-Aldrich), 39 μg/mL thymidine (Sigma-Aldrich), and 14 μL/L β-mercapthoethanol (Sigma-Aldrich); all concentrations of added components refer to that in complete HMI-9 medium. The parasites were cultured in 10 mL of HMI-9 medium in T75 CELL-STAR tissue culture flasks at 37 °C/5% CO_2.

To determine growth inhibitory potency of compounds against *T. b. brucei* bloodstream form parasites, 200 nL of 10-point, 3-fold serially diluted compounds in DMSO were transferred to the wells of white, solid bottom 384-well plates (Greiner Bio-One) by either Echo 555 acoustic liquid handling system or Mosquito. Then, 104 of *T. b. brucei* parasites in 40 μL of HMI-9 medium were added to each well, and the plates were incubated for 48 h at 37 °C in 5% CO_2 incubators. Parasite numbers in individual plate wells were determined through quantification of intracellular ATP amount. The CellTiter-Glo luminescent cell viability reagent (Promega) was added to plate wells, and ATP-dependent luminescence signal was measured on a Tecan M1000 plate Reader after 30 min of incubation. Suramin an antitrypanosomal drug was used as positive control, and DMSO was used as negative control. pIC_{50} values were calculated using Graph Pad Prism software by plotting the luminescence values in sigmoidal dose response curves.

DOI: 10.1021/acsinfecdis.7b00218
ACS Infect. Dis. 2018, 4, 592−604

Table 3. Biological Assessment of Polar Tail Analogues

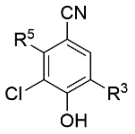

#	R^3	R^5	cLogP	TAO pIC_{50}[a]	*T. b. b.* pEC_{50}[b]
11		CH_3	6.3	8.9 ± 0.3	7.6 ± 0.1
46		H	5.8	7.0 ± 0.1	5.1 ± 0.2
27	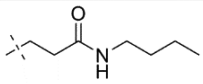	CH_3	3.5	5.5 ± 0.2	<4.3
19	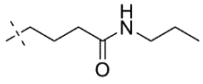	H	3.0	<4.5	-
20	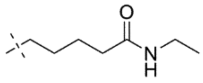	H	2.9	4.6 ± 0.1	-
21	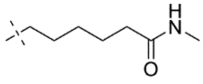	H	3.0	4.6 ± 0.1	-
22	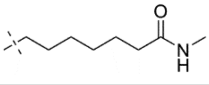	H	3.4	5.1 ± 0.1	<4.3
23	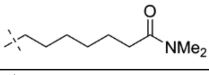	H	3.6	5.4 ± 0.2	<4.3
29	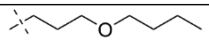	H	4.1	4.8 ± 0.1	4.7 ± 0.1
30		H	4.1	5.6 ± 0.1	4.6 ± 0.1
31	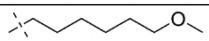	H	4.1	5.2 ± 0.1	<4.3

[a]Negative log concentration and standard deviation of compounds required for 50% inhibition of trypanosome alternative oxidase. [b]Negative log concentration and standard deviation of compounds required for 50% growth inhibition of *T. b. brucei* Lister427 ($n \geq 2$ in all assays performed).

Scheme 3. Heck Cross-Coupled Amide Tail Linker Synthesis[a]

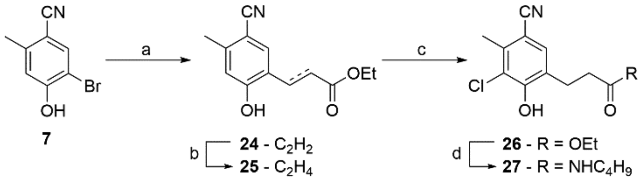

[a]Reaction conditions: (a) ethyl acrylate, SingaCycle, K_2CO_3, NMP, 100 °C, 16 h, 30%, (b) triethylsilane, Pd/C, EtOH, rt, 16 h, 78%, (c) SO_2Cl_2, Et_2O, rt, 96 h, 57%, and (d) TBD, *n*-butylamine, MeCN, 16h, 39%.

Scheme 4. Ether Tail Linker Synthesis[a]

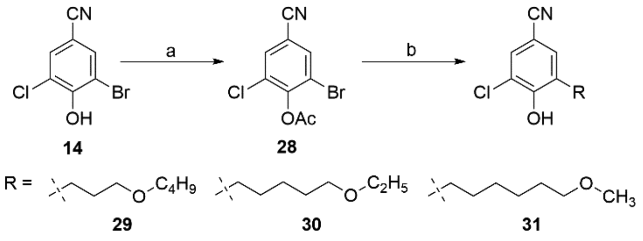

[a]Reaction conditions: (a) Ac_2O, pyridine, DCM, rt, 16 h, 74% and (b) (i) BH_3·THF, 1-alkene ether, 0 °C, 20 min, (ii) toluene, H_2O, K_3PO_4, RuPhos, $Pd(OAc)_2$, 16 h, 50 °C, 7−24%.

Suramin was used as a positive control in screening (pIC_{50} 6.7 ± 0.1).

Hep-G2 Cytotoxicity Assay. Human hepatocellular carcinoma (HepG2) cells were obtained from ATCC and grown in RPMI media. Twenty-five μL of 1.6 × 104 cells/mL were dispensed into sterile 384 well Griener clear plates and incubated at 37 °C in a 5% CO_2 incubator for 24 h. Once the cells adhered, 125 nL of 10-point, 3-fold serially diluted compounds in DMSO was transferred onto the cells. After incubating for an additional 96 h at 37 °C in 5% CO_2 incubator, cells were added with CCK-8 reagent to each well. Plates were further incubated for 3 h followed by absorbance reading at 450 nM using Envision reader. Absorbance values were used for determination of cytotoxic concentration (pCC_{50}) required to inhibit 50% growth. Purmycin was used as positive control in screening (pCC_{50} 6.3 ± 0.1).

Synthesis. *5-Chloro-7-[(2E)-3,7-dimethylocta-2,6-dien-1-yl]-1,2-benzoxazol-6-ol (**3**).* To a solution of triphenylphosphine (42 mg, 0.16 mmol) in dichloromethane (2 mL) was added 2,3-dichloro-5,6-dicyano-*p*-benzoquinone (37 mg, 0.16 mmol). The dark reaction mixture was stirred at room temperature for 1 min during which time the color faded. 4-Chloro-2-[(2E)-3,7-dimethylocta-2,6-dien-1-yl]-6-[(hydroxyimino)m ethyl]benzene-1,3-diol (35 mg, 0.10 mmol)

DOI: 10.1021/acsinfecdis.7b00218
ACS Infect. Dis. 2018, 4, 592−604

Scheme 5. Carbon Chain Length Analogue Synthesis[a]

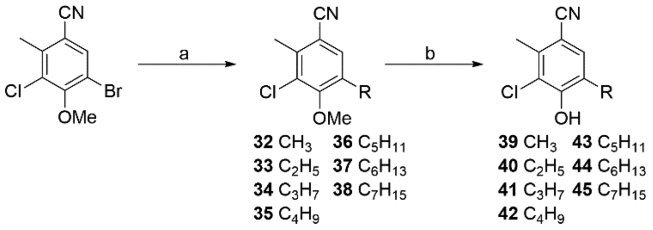

[a]Reaction conditions: (a) (i) BH_3·THF, 1-alkene, 0 °C, 20 min, (ii) toluene, H_2O, K_3PO_4, RuPhos, $Pd(OAc)_2$, 16 h, 50 °C, 65−90%, or 1-boronic acid/boroxine, K_3PO_4, RuPhos, $Pd(OAc)_2$, 16 h, 80 °C and (b) TMSCl, NaI, MeCN, 80 °C, 16 h, 35−85%.

Table 4. Biological Assessment of Carbon Chain Length Analogues

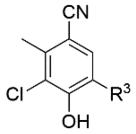

#	R^3	cLogP	TAO pIC_{50}[a]	*T. b. b.* pEC_{50}[b]
11	*n*-C_8H_{17}	6.3	8.9 ± 0.3	7.6 ± 0.1
45	*n*-C_7H_{15}	5.8	8.5 ± 0.1	6.6 ± 0.2
44	*n*-C_6H_{13}	5.4	8.2 ± 0.1	6.1 ± 0.1
43	*n*-C_5H_{11}	4.9	7.8 ± 0.1	6.0 ± 0.1
42	*n*-C_4H_9	4.5	7.7 ± 0.1	5.3 ± 0.1
41	*n*-C_3H_7	4.1	7.1 ± 0.1	4.7 ± 0.1
39	*n*-CH_3	3.2	6.2 ± 0.1	4.7 ± 0.1

[a]Negative log concentration and standard deviation of compounds required for 50% inhibition of trypanosome alternative oxidase. [b]Negative log concentration and standard deviation of compounds required for 50% growth inhibition of *T. b. brucei* Lister427 ($n \geq 2$ for all assays performed).

in dichloromethane (0.5 mL) was added to the reaction mixture in 1 portion, and this was stirred for 1 min before being concentrated under reduced pressure. Purification by flash column chromatography (10 g silica), eluting with a gradient of petrol ether/ethyl acetate (100:0) to (90:10), gave the title compound as a white solid (24 mg, 72%). ^{1}H NMR (500 MHz, Chloroform-*d*) δ 8.60 (s, 1H), 6.10 (s, 1H), 5.42−5.32 (m, 1H), 5.10−5.01 (m, 1H), 3.66 (d, J = 7.3 Hz, 2H), 2.58 (s, 3H), 2.11−2.05 (m, 2H), 2.05−1.98 (m, 2H), 1.84 (d, J = 1.2 Hz, 3H), 1.64 (d, J = 1.4 Hz, 3H), 1.57 (d, J = 1.2 Hz, 3H).

*2-Methyl-4-hydroxy-5-bromo-benzaldehyde (**6**).* To a solution of 2-methyl-4-hydroxy-benzaldehyde (10 g, 73.45 mmol) in CH_2Cl_2 (100 mL) and methanol (50 mL) was added a solution of phenyltrimethylammonium tribromide (30.07 g, 77.12 mmol) in CH_2Cl_2/methanol (1:1, 100 mL) at −5 °C. The reaction was warmed to ambient temperature and stirred for 16 h. The reaction was concentrated under reduced pressure, and the residue was added to 1 M HCl (aq) (200 mL) to precipitate a white solid; the solid was collected by filtration and dried under reduced pressure to give the title compound as a cream precipitate (14.67 g, 94%): mp 160−165 °C, (methanol/water). IR (neat, ν_{max}) cm^{-1}, 3063, 1384, 1310, 1136. ^{1}H NMR (500 MHz, DMSO-d_6) δ 11.35 (1H, br s), 9.95 (1H, s), 7.91 (1H, s), 6.83 (1H, s), 2.49 (3H, s). ^{13}C NMR (126 MHz, DMSO-d_6) δ 190.8 (CH), 159.2 (C), 142.3 (C), 137.1 (CH), 128.0 (C), 119.1 (CH), 107.4 (C), 19.1 (CH_3). HRMS (ESI^-) m/z $[M - H]^-$ calculated for $C_8H_6BrO_2$ 212.9557, found 212.9550.

*5-Bromo-4-hydroxy-2-methyl-benzonitrile (**7**).* A solution of 2-methyl-4-hydroxy-5-bromo-benzaldehyde (20.00 g, 93.0 mmol) in acetonitrile (300 mL) was added to hydroxylamine hydrochloride (6.92 g, 99.5 mmol). The reaction mixture was heated to reflux and stirred for 16 h. The reaction mixture was cooled to 50 °C, and further hydroxylamine hydrochloride (1.5 g, 21.5 mmol) was added. The reaction mixture was heated to reflux for a further 3 h. This was collected by filtration and dried under vacuum to give 13.08 g of an off-white solid. Analysis showed a good purity product. The filtrate was concentrated under vacuum. The residue was triturated in MeCN/water (1:2) and sonicated; the solid was collected by filtration and dried under vacuum, to provide a further 6.67 g (19.75, quant.). mp 194−199 °C (MeCN/water). IR (neat, ν_{max}) cm^{-1} 3203, 2232 (CN), 1595, 1402, 1386, 1260, 1221. ^{1}H NMR (500 MHz, DMSO-d_6) δ 11.38 (1H, br s), 7.90 (1H, s), 6.92 (1H, s),

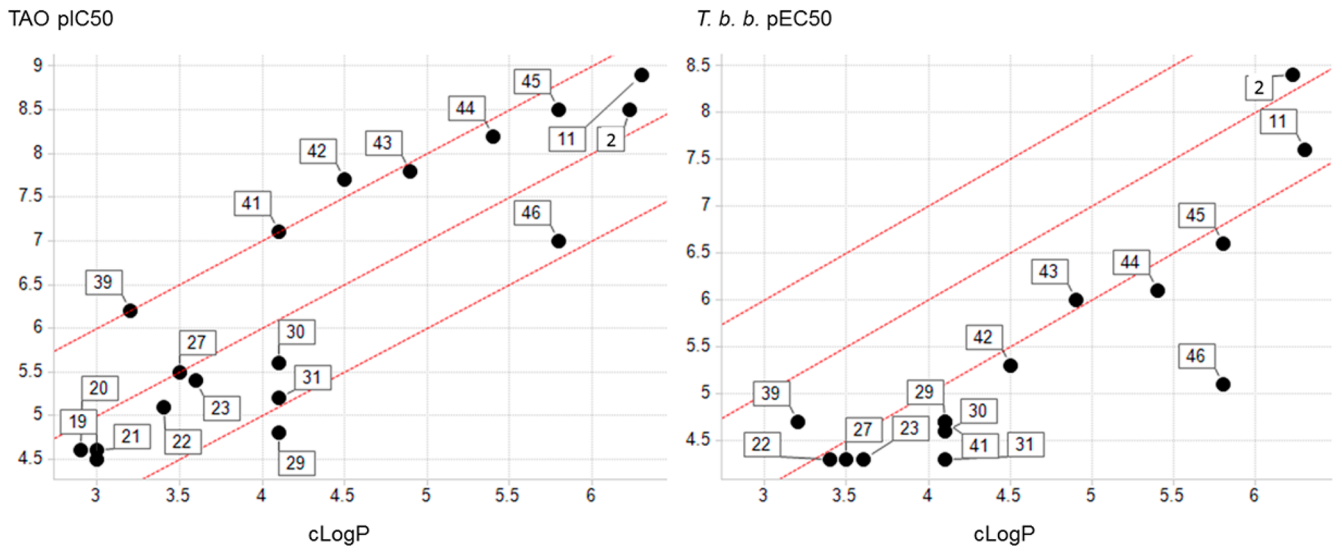

Figure 4. Correlations of cLogP vs TAO inhibition pIC_{50} (left) and cLogP vs *T. b. b.* pIC_{50} growth inhibition (right). LipE is lipophilic ligand efficiency (pIC50 − cLogP).[32]

DOI: 10.1021/acsinfecdis.7b00218
ACS Infect. Dis. 2018, 4, 592−604

2.49 (3H, s). ^{13}C NMR (126 MHz, DMSO-d_6) δ 158.6 (C), 143.4 (C), 137.1 (CH), 117.9 (CH), 117.7 (C), 107.3 (C), 103.8 (C), 19.1 (CH_3). HRMS (ESI^-) m/z $[M - H]^-$ calculated for C_8H_5BrNO 209.9560, found 209.9554.

*5-Bromo-3-chloro-4-hydroxy-2-methyl-benzonitrile (**8**).* Triethylamine (0.83 mL, 5.97 mmol) was added to a solution of 5-bromo-2-methyl-4-hydroxybenzonitrile (1.15 g, 5.42 mmol) in acetonitrile (50 mL). 1-Chloropyrorolidine-2,5-dione (1.52 g, 11.38 mmol) was added portionwise to the stirring solution. To the reaction mixture was added water (50 mL), precipitating a pale-yellow solid that was collected by filtration to provide the title compound (1.11 g, 83%). mp 166−169 °C, IR (neat, ν_{max}), cm^{-1} 3239, 2236 (CN), 1581, 1468, 1384, 1294, 1224, 1147. ^{1}H NMR (500 MHz, $CDCl_3$) δ 7.70 (s, 1H), 6.39 (s, 1H), 2.58 (s, 3H). ^{13}C NMR (126 MHz, $CDCl_3$) δ 152.5 (C), 140.9 (C), 134.4 (CH), 122.1 (CH), 116.4 (C), 107.5 (CH), 106.9 (C), 19.0 (CH_3). HRMS (ESI^-) m/z $[M - H]^-$ calcd for $C_8H_4BrClNO$ 243.9170, found 243.9165.

*5-Bromo-3-chloro-4-methoxy-2-methyl-benzonitrile (**9**).* Dimethyl sulfate (0.85 mL, 8.95 mmol) was added to a suspension of 5-bromo-3-chloro-4-hydroxy-benzonitrile (2.10 g, 8.52 mmol) and potassium carbonate (1.41 g, 10.22 mmol) in acetone (80 mL). The reaction mixture was heated to reflux for 3 h; the reaction was cooled to RT, and water (160 mL) was added to precipitate a white solid that was collected by vacuum filtration to give the title compound (2.07 g, 93%). mp 119−120 °C, IR (neat, ν_{max}), cm^{-1} 2229 (CN), 1457, 1372, 1275, 1048. ^{1}H NMR (500 MHz, $CDCl_3$) δ 7.74 (s, 1H), 3.94 (s, 3H), 2.58 (s, 3H). ^{13}C NMR (126 MHz, $CDCl_3$) δ 157.4 (C), 141.7 (C), 134.9 (CH), 131.3 (C), 116.3 (C), 116.0 (C), 111.0 (C), 61.0 (CH_3), 19.2 (CH_3). LRMS EI^+ 261 m/z.

*3-Bromo-5-chloro-4-hydroxybenzonitrile (**13**).* *N*-Bromosuccinimide (0.30 g, 1.71 mmol) was added to a solution of 3-chloro-4-hydroxybenzonitrile (0.25g, 1.63 mmol) in acetonitrile (5 mL). To the reaction mixture was added water (15 mL), precipitating a white solid; this was collected by filtration and dried under reduced pressure to provide the title compound as a white solid (0.36 g, 84%). mp 166−169 °C. IR (neat, ν_{max}), cm^{-1} 3411, 2229, 1471, 1327, 1294, 1245, 1204, 1156. ^{1}H NMR (500 MHz, $CDCl_3$) δ 7.75 (s, 1H), 7.64 (s, 1H) 6.37 (s, 1H). ^{13}C NMR (126 MHz, $CDCl_3$) δ 152.8 (C), 135.0 (C), 132.6 (CH), 121.7 (C), 116.3 (C), 110.9 (C), 106.1 (C). HRMS (ESI^-) m/z $[M - H]^-$ calcd for $C_7H_2BrClNO$ 229.9014, found 231.8984.

*3-Bromo-5-chloro-4-methoxybenzonitrile (**14**).* Dimethyl sulfate (0.15 mL, 1.61 mmol) was added to a suspension of potassium carbonate (0.22 g, 1.61 mmol) and 3-bromo-5-chloro-4-hydroxy-benzonitrile (0.30 g, 1.29 mmol) in acetone (10 mL). The reaction mixture was heated to reflux for 30 min and cooled to RT; water was added. The resulting precipitate was collected by filtration and dried under reduced pressure to provide the title compound as a white solid (0.29 g, 90%). mp 115−116 °C, IR (neat, ν_{max}), cm^{-1} 2236 (CN), 1539, 1470, 1419, 1272. ^{1}H NMR (500 MHz, $CDCl_3$) δ 7.78 (s, 1H), 7.66 (s, 1H), 3.97 (s, 3H). ^{13}C NMR (126 MHz, $CDCl_3$) δ 157.6 (C), 135.4 (CH), 133.2 (CH), 130.4 (C), 119.5 (C), 116.0 (C), 109.9 (C), 61.0 (CH_3). HRMS (ESI^-) m/z $[M - H]^-$ calcd for $C_8H_3BrClNO$ 243.9170, found 243.9165.

*(2-Bromo-6-chloro-4-cyano-phenyl) Acetate (**28**).* 3-Bromo-5-chloro-4-hydroxy-benzonitrile (500 mg, 2.15 mmol) was dissolved in dichloromethane (10 mL), before pyridine (0.26 mL, 3.23 mmol) and acetic anhydride (0.24 mL, 2.58 mmol) were added. The reaction mixture was stirred at room temperature for 12 h. The reaction mixture was taken up in water (10 mL), and the organic components were washed with water (2 × 10 mL). The chlorinated layer was separated, washed with brine (1 × 10 mL), dried over $MgSO_4$, filtered and concentrated in vacuo, to give the title compound as a granular white solid (462 mg, 74%). mp 116−119 °C, IR (neat, ν_{max}, cm^{-1}) 3088, 2238, 1774. ^{1}H NMR (500 MHz, $CDCl_3$) δ 7.83 (s, 1H), 7.72 (s, 1H), 2.44 (s, 3H). ^{13}C (126 MHz, $CDCl_3$) δ 166.3 (C), 149.3 (C), 135.0 (CH), 132.7 (CH), 130.3 (C), 119.3 (C), 115.7 (C), 112.2 (C), 20.3 (CH_3). LRMS EI^+ 275 m/z.

General Protocol for Alkene Cross-Couplings. 1-Alkene (2.54 mmol) was dropwise added to an ice cooled solution of 1 M borane in THF (0.91 mmol). This solution was warmed to room temperature and stirred for 15 min. The solution was quenched with the addition of water (0.25 mL) and diluted with toluene (2.5 mL). Potassium phosphate tribasic (0.43 g, 2.03 mmol), aromatic bromide (1.01 mmol), palladium(II) acetate (0.01 g, 0.025 mmol), and 2-dicyclohexylphosphino-2′-6′-diisopropoxybiphenyl (0.02 g, 0.05 mmol) were added. The reaction mixture was sealed and heated to 100 °C for 16 h. The reaction mixture was partitioned between water (10 mL) and EtOAc (20 mL). The organic layer was separated, dried over $MgSO_4$, filtered, and concentrated under vacuum. The residue was purified by flash silica chromatography, eluting with petroleum ether to 10−50% EtOAc followed by purification by preparative HPLC 50% MeCN in water to 100% MeCN to provide the title compounds (11−90%).

*3-Chloro-4-methoxy-2-methyl-5-octyl-benzonitrile (**10**).* IR (neat, ν_{max}) cm^{-1} 2913, 2849, 2226 (CN), 1468, 1291, 1074. ^{1}H NMR (500 MHz, $CDCl_3$) δ 7.36 (s, 1H), 3.87 (s, 3H), 2.62 (t, J = 7.9 Hz, 2H), 2.57 (s, 3H), 1.61−1.55 (m, 2H), 1.36−1.27 (m, 10H), 0.89 (t, J = 6.8 Hz, 3H).^{13}C NMR (126 MHz, $CDCl_3$) δ 158.2 (C), 139.4 (C), 136.3 (C), 132.0 (CH), 129.7 (C), 117.7 (C), 109.4 (C), 60.9 (CH_3), 31.8 (CH_2), 30.2 (CH_2), 29.7 (CH_2), 29.4 (CH_2), 29.3 (CH_2), 29.1 (CH_2), 22.6 (CH_2), 18.8 (CH_3), 14.0 (CH_3). LRMS EI^+ 293 m/z.

*5-Chloro-4-methoxy-5-octylbenzonitrile (**46** Intermediate).* IR (neat, ν_{max}) cm^{-1} 2925, 2854, 2232 (CN), 1470, 1426, 1275. ^{1}H NMR (500 MHz, $CDCl_3$) δ 7.53 (s, 1H), 7.40 (s, 1H), 3.90 (s, 3H), 2.66 (t, J = 7.9 Hz, 2H), 1.60 (m, 2H), 1.40−1.26 (m, 10H), 0.90 (t, J = 6.8 Hz, 3H). ^{13}C NMR (126 MHz, $CDCl_3$) δ 158.2 (C), 139.7 (C), 132.4 (CH), 131.7 (CH), 128.9 (C), 117.7 (C), 108.5 (C), 61.1 (CH_3), 31.8 (CH_2), 30.2 (CH_2), 30.0 (CH_2), 29.4 (CH_2), 29.3 (CH_2), 29.1 (CH_2), 22.6 (CH_2), 14.0 (CH_3). HRMS (ESI^-) m/z $[M - H]^-$ calcd for $C_{15}H_{19}ClNO$ 264.1161, found 264.1153.

*Methyl 4-(3-chloro-5-cyano-2-methoxy-phenyl)butanoate (**15**).* IR (neat, ν_{max}), cm^{-1} 2952, 2231 (CN), 1732, 1427, 1276, 993, 877. ^{1}H NMR (500 MHz, $CDCl_3$) δ 7.55 (d, J = 2.1 Hz, 1H), 7.40 (d, J = 2.1 Hz, 1H), 3.90 (s, 3H), 3.68 (s, 3H), 2.70 (t, J = 7.7 Hz, 2H), 2.36 (t, J = 7.3 Hz, 2H), 1.92 (m, 2H). ^{13}C NMR (126 MHz, CDCl3) δ 158.2 (C), 139.7 (C), 132.4 (CH), 131.7 (CH), 128.9 (C), 117.7 (C), 108.5 (C), 61.1 (CH_3), 31.8 (CH_2), 30.2 (CH_2), 30.0 (CH_2), 29.4 (CH_2), 29.3 (CH_2), 29.1 (CH_2), 22.6 (CH_2), 14.0 (CH_3). LRMS EI^+ 267 m/z.

*Methyl 5-(3-chloro-5-cyano-2-methoxy-phenyl)-pentanoate (**16**).* IR (neat, ν_{max}), cm^{-1} 2951, 2233 (CN), 1733, 1472, 1275. ^{1}H NMR (500 MHz, $CDCl_3$) δ 7.53 (s, 1H), 7.38 (s, 1H), 3.89 (s, 3H), 3.67 (s, 3H), 2.67 (m, 2H), 2.35 (m, 2H), 1.65 (m, 4H). ^{13}C NMR (126 MHz, $CDCl_3$) δ 173.8 (C),

DOI: 10.1021/acsinfecdis.7b00218
ACS Infect. Dis. 2018, 4, 592−604

158.2 (C), 139.9 (C), 132.4 (C), 132.0 (C), 128.9 (C), 117.6 (C), 108.5 (C), 61.1 (CH_3), 51.6 (CH_3), 33.7 (CH_2), 29.7 (CH_2), 29.5 (CH_2), 24.6 (CH_2). LRMS EI$^+$ 281 m/z.

*Methyl 6-(3-chloro-5-cyano-2-methoxy-phenyl)hexanoate (**17**).* IR (neat, ν_{max}), cm^{-1} 2948, 2232 (CN), 1733, 1472, 1275. ^{1}H NMR (500 MHz, $CDCl_3$) δ 7.53 (s, 1H), 7.38 (s, 1H), 3.89 (s, 3H), 3.67 (s, 3H), 2.65 (m, 2H), 2.32 (m, 2H), 1.70−1.57 (m, 4H), 1.39 (m, 2H). ^{13}C NMR (126 MHz, $CDCl_3$) δ 174.0 (C), 158.2 (C), 139.2 (C), 132.4 (CH), 131.9 (CH), 128.9 (C), 117.7 (C), 108.5 (C), 61.1 (CH_3), 51.5 (CH_3), 33.8 (CH_2), 29.82 (CH_2), 29.80 (CH_2), 28.8 (CH_2), 24.6 (CH_2). LRMS EI$^+$ 295 m/z.

*Methyl 7-(3-chloro-5-cyano-2-methoxy-phenyl)-heptanoate (**18**).* IR (neat, ν_{max}), cm^{-1} 2933, 2232 (CN), 1734, 1472, 1276. ^{1}H NMR (500 MHz, $CDCl_3$) δ 7.52 (s, 1H), 7.38 (s, 1H), 3.88 (s, 3H), 3.66 (s, 3H), 2.64 (m, 2H), 2.31 (m, 2H), 1.66−1.55 (m, 4H), 1.36 (m, 4H). ^{13}C NMR (126 MHz, $CDCl_3$) δ 174.3 (C), 158.4 (C), 139.6 (C), 132.6 (CH), 132.0 (CH), 129.1 (C), 117.9 (C), 108.6 (C), 61.3 (CH_3), 51.7 (CH_3), 34.1 (CH_2), 30.14 (CH_2), 30.08 (CH_2), 29.2 (CH_2), 29.0 (CH_2), 24.9 (CH_2). HRMS (ESI$^+$) m/z [M + Na]$^+$ calcd for $C_{16}H_{20}ClNNaO_3$ 332.1024, found 332.1019.

*3-(3-Butoxypropyl)-5-chloro-4-hydroxy-benzonitrile (**29**).* IR (neat, ν_{max}, cm^{-1}) 2923, 2236. ^{1}H NMR (500 MHz, $CDCl_3$) 7.51 (s, 1H), 7.31 (s, 1H), 3.50 (t, J = 6.6 Hz, 2H), 3.43 (t, J = 5.9 Hz, 2H), 2.76 (t, J = 6.9 Hz, 2H), 1.90 (p, J = 6.4 Hz, 2H), 1.62(p, J = 7.1 Hz, 2H), 1.40 (h, J = 7.5 Hz, 2H), 0.95 (t, J = 7.5 Hz, 3H); ^{13}C NMR (126 MHz, $CDCl_3$) δ 154.9 (C), 133.0 (CH), 131.5 (CH), 130.4 (C), 121.8 (C), 118.2 (C), 104.0 (C), 71.1 (CH_2), 68.5 (CH_2), 31.5 (CH_2), 29.0 (CH_2), 26.4 (CH_2), 19.3 (CH_2), 13.9 (CH_3); HRMS (ESI$^-$) m/z [M − H]$^-$ calcd for $C_{14}H_{17}ClNO_2$ 266.0953, found 266.0953.

*3-Chloro-5-(5-ethoxypentyl)-4-hydroxy-benzonitrile (**30**).* ^{1}H (500 MHz, $CDCl_3$) δ 7.49 (s, 1H), 7.33 (s, 1H), 3.47 (q, J = 7.1 Hz, 2H), 3.41 (t, J = 6.3 Hz, 2H), 2.66 (t, J = 7.8 Hz, 2H), 1.62 (p, J = 8 Hz, 4H), 1.40 (p, J = 7.8 Hz, 2H), 1.20 (t, J = 7.0 Hz, 3H). ^{13}C (126 MHz, $CDCl_3$) δ 153.6 (C), 132.6 (CH), 130.4, (CH), 120.5 (C), 118.1 (C), 104.1 (C), 88.2 (C), 70.5 (CH_2), 66.2 (CH_2), 30.2 (CH_2), 29.4 (CH_2), 28.7 (CH_2), 26.0 (CH_2), 15.1 (CH_3). HRMS (ESI$^-$) m/z [M − H]$^-$ calcd for $C_{14}H_{17}ClNO_2$ 266.0953, found 266.0942.

*3-Chloro-4-hydroxy-5-(6-methoxyhexyl)benzonitrile (**31**).* IR (neat, ν_{max}, cm^{-1}) 2932, 2860, 2233 (CN), 1174, 1116. ^{1}H NMR (500 MHz, $CDCl_3$) δ 7.49 (s, 1H), 7.33 (s, 1H), 3.55 (s, 3H) 3.36 (t, J = 6.6 Hz, 2H), 2.65 (t, J = 7.8 Hz, 2H), 1.57 (p, J = 7.4 Hz, 4H), 1.37 (m, 4H). ^{13}C (126 MHz, $CDCl_3$) δ 153.3 (C), 132.7 (CH), 130.3, (CH), 120.4 (C), 110.0 (C), 100.2 (C), 88.3 (C), 72.8 (C), 58.6 (C), 30.1 (CH_2), 29.5 (CH_2), 29.1 (CH_2), 28.9 (CH_2), 25.9 (CH_3). HRMS (ESI$^-$) m/z [M − H]$^-$, calcd for $C_{14}H_{17}ClNO_2$ 266.0953, found 266.0941.

*3-Chloro-4-methoxy-2-methyl-5-pentyl-benzonitrile (**36**).* ^{1}H NMR (500 MHz, $CDCl_3$) δ 7.35 (s, 1H), 3.85 (s, 3H), 2.60 (t, J = 7.8 Hz, 2H), 2.55 (s, 3H), 1.57 (t, J = 7.5 Hz, 2H), 1.41−1.18 (m, 4H), 0.89 (t, J = 6.7 Hz, 3H). ^{13}C NMR (126 MHz, $CDCl_3$) δ 158.1 (C), 139.4 (C), 136.3 (C), 132.0 (CH), 129.6 (C), 117.8 (C), 109.3 (C), 60.9 (CH_3), 31.5 (CH_2), 29.9 (CH_2), 29.7 (CH_2), 22.4 (CH_2), 18.8 (CH_3), 13.9 (CH_3).

*3-Chloro-5-hexyl-4-methoxy-2-methyl-benzonitrile (**37**).* ^{1}H NMR (500 MHz, $CDCl_3$) δ 7.35 (s, 1H), 3.85 (s, 3H), 2.60 (t, J = 7.6 Hz, 2H), 2.54 (s, 3H), 1.61−1.48 (m, 2H), 1.41−1.17 (m, 6H), 0.87 (t, J = 6.8 Hz, 3H). ^{13}C NMR (126 MHz, $CDCl_3$) δ 158.1 (C), 139.3 (C), 136.3 (C), 132.0 (CH), 129.6 (C), 117.7 (C), 109.3 (C), 60.9 (CH_3), 31.6 (CH_2), 30.1 (CH_2), 29.7 (CH_2), 29.1 (CH_2) 22.5 (CH_2), 18.8 (CH_3), 14.0 (CH_3).

*3-Chloro-5-heptyl-4-methoxy-2-methyl-benzonitrile (**38**).* ^{1}H NMR (500 MHz, $CDCl_3$) δ 7.35 (s, 1H), 3.85 (s, 3H), 2.60 (t, J = 7.9 Hz, 2H), 2.54 (s, 3H), 1.61−1.50 (m, 2H), 1.38−1.11 (m, 8H), 0.87 (t, J = 6.7 Hz, 3H). ^{13}C NMR (126 MHz, $CDCl_3$) δ 158.1 (C), 139.3 (C), 136.3 (C), 132.0 (CH), 129.6 (C), 117.7 (C), 109.3 (C), 60.9 (CH_3), 31.7 (CH_2), 30.8 (CH_2), 29.7 (CH_2), 29.3 (CH_2) 29.0 (CH_2), 22.6 (CH_2), 18.8 (CH_3), 14.1 (CH_3).

General Protocol for Alkylboronic Acid Suzuki-Miyaura Cross-Coupling. Dicyclohexyl-[2-(2,6-diisopropoxyphenyl)phenyl]phosphane (9 mg, 0.02 mmol) and palladium(II) acetate (2 mg, 0.01 mmol) were added to a degassed suspension of 5-bromo-3-chloro-4-methoxy-2-methyl-benzonitrile (100 mg, 0.38 mmol), boronic acid or trialkylboroxine (0.58 mmol), and tripotassium phosphate (244 mg, 1.15 mmol) in toluene (2 mL). The reaction mixture was sealed, degassed, put under a nitrogen atmosphere, and heated to 100 °C for 16−72 h. The reaction mixture was filtered through a pad of Celite; the filtrate was partitioned between ethyl acetate and water, and the organics were separated, washed with brine, dried over $MgSO_4$, filtered, and concentrated under vacuum. The residue was purified by flash chromatography eluting with petroleum ether to 10−25% ethyl acetate in petroleum ether. Material was further purified by reverse phase flash chromatography, eluting with water to MeOH if required to provide the cross-coupled analogues described (36−67%).

*3-Chloro-4-methoxy-2,5-dimethyl-benzonitrile (**32**).* ^{1}H NMR (500 MHz, $CDCl_3$) δ 7.35 (s, 1H), 3.84 (s, 3H), 2.55 (s, 3H), 2.29 (s, 3H). ^{13}C NMR (126 MHz, $CDCl_3$) δ 158.3 (C), 139.5 (C), 132.9 (CH), 131.5 (C), 129.6 (C), 117.6 (C), 109.2 (C), 60.2 (CH_3), 18.8 (CH_3), 16.0 (CH_3).

*3-Chloro-5-ethyl-4-methoxy-2-methyl-benzonitrile (**33**).* ^{1}H NMR (500 MHz, $CDCl_3$) δ 7.37 (s, 1H), 3.86 (s, 3H), 2.75−2.60 (m, 2H), 2.56 (s, 3H), 1.22 (t, J = 7.5 Hz, 3H). ^{13}C NMR (126 MHz, $CDCl_3$) δ 158.0 (C), 139.4 (C), 137.5 (C), 131.4 (CH), 129.6 (C), 117.8 (C), 109.5 (C), 60.9 (CH_3), 22.3 (CH_2), 18.8 (CH_3), 14.4 (CH_3).

*3-Chloro-4-methoxy-2-methyl-5-propyl-benzonitrile (**34**).* ^{1}H NMR (500 MHz, $CDCl_3$) δ 7.35 (s, 1H), 3.86 (s, 3H), 2.60 (t, J = 6.7 Hz, 2H), 2.55 (s, 3H), 1.66−1.56 (m, 2H), 0.96 (t, J = 7.4 Hz, 3H). ^{13}C NMR (126 MHz, $CDCl_3$) δ 158.2 (C), 139.4 (C), 136.0 (C), 132.1 (CH), 129.7 (C), 117.8 (C), 109.3 (C), 60.9 (CH_3), 31.7 (CH_2), 23.3 (CH_2), 18.9 (CH_3), 13.9 (CH_3).

*5-Butyl-3-chloro-4-methoxy-2-methyl-benzonitrile (**35**).* ^{1}H NMR (500 MHz, $CDCl_3$) δ 7.35 (s, 1H), 3.86 (s, 3H), 2.62 (t, J = 7.7 Hz, 2H), 2.55 (s, 3H), 1.59−1.51 (m, 2H), 1.41−1.31 (m, 2H), 0.93 (t, 3H). ^{13}C NMR (126 MHz, $CDCl_3$) δ 158.1 (C), 139.4 (C), 136.3 (C), 132.1 (CH), 129.7 (C), 117.8 (C), 109.3 (C), 60.9 (CH_3), 32.3 (CH_2), 31.7 (CH_2), 22.5 (CH_2), 18.8 (CH_3), 13.8 (CH_3).

General Protocol for Demethylation with Trimethylsilyl Iodide. Chloro(trimethyl)silane (0.26 mL, 2.0 mmol) was added to a suspension of sodium iodide (0.31 g, 2.0 mmol) and anisole (0.51 mmol) in acetonitrile (2 mL). The reaction mixture was heated to reflux for 4−96 h. The cooled reaction mixture was partitioned between 0.1 M sodium thiosulfate (10

DOI: 10.1021/acsinfecdis.7b00218
ACS Infect. Dis. 2018, 4, 592−604

mL) and ethyl acetate (2 × 20 mL). The organic layers were separated, combined dried over $MgSO_4$, filtered, and concentrated under vacuum. The residue was purified by flash silica chromatography, eluting with petroleum ether to 30% ethyl acetate to provide the phenolic compounds (28−80%).

*3-Chloro-4-hydroxy-2-methyl-5-octyl-benzonitrile (**11**).* IR (neat, ν_{max}) cm^{-1} 3360, 2928, 2850, 2222 (CN), 1601, 1473, 1461, 1163. ^1H NMR (500 MHz, $CDCl_3$) δ 7.31 (s, 1H), 6.08 (s, 1H), 2.64 (t, J = 7.7 Hz, 2H), 2.56 (s, 3H), 1.59 (m, 2H), 1.45−1.20 (m, 10H) 0.91 (t, J = 7.2 Hz, 3H). ^{13}C NMR (126 MHz, $CDCl_3$) δ 153.0 (C), 138.2 (C), 132.2 (CH), 128.9 (C), 121.0 (C), 118.0 (C), 110.0 (C), 31.8 (CH_2), 29.9 (CH_2), 29.3 (CH_2), 29.3 (CH_2), 29.2 (CH_2), 29.1 (CH_2), 22.6 (CH_2), 18.7 (CH_2), 14.0 (CH_3). HRMS (ESI^-) m/z $[M - H]^-$ calculated for $C_{16}H_{21}ClNO$ 278.1317, found 278.1303.

*4-(3-Chloro-5-cyano-2-hydroxy-phenyl)butanoic Acid (**19a**).* IR (neat, ν_{max}) cm^{-1} 3345, 2569, 2228 (CN), 1691, 1474, 1253. ^1H NMR (500 MHz, $CDCl_3$) δ 12.06 (br s, 1H), 10.43 (br s, 1H), 7.81 (d, J = 2.0 Hz, 1H), 7.51 (d, J = 2.0 Hz, 1H), 2.61 (t, J = 7.5 Hz, 2H), 2.19 (t, J = 7.5 Hz, 2H), 1.73 (quintet, J = 7.5 Hz, 2H). ^{13}C NMR (126 MHz, $CDCl_3$) δ 174.6 (C), 155.6 (C), 133.1 (CH), 132.4 (C), 131.9 (CH), 121.6 (C), 118.7 (C), 102.8 (C), 33.6 (CH_2), 29.5 (CH_2), 24.5 (CH_2). HRMS (ESI^-) m/z $[M - H]^-$ calcd for $C_{11}H_9ClNO_3$ 238.0276, found 238.0266.

*5-(3-Chloro-5-cyano-2-hydroxy-phenyl)pentanoic Acid (**20a**).* IR (neat, ν_{max}), cm^{-1} 3093, 2867, 2243 (CN), 1723, 1471, 1105. ^1H NMR (500 MHz, $CDCl_3$) δ 11.98 (br s, 1H), 10.40 (br s, 1H), 7.78 (d, J = 2.0 Hz, 1H), 7.53 (d, J = 2.0 Hz, 1H), 2.59 (t, J = 7.2 Hz, 2H), 2.20 (m, 2H), 1.49 (m, 4H). ^{13}C NMR (126 MHz, $CDCl_3$) δ 174.8 (C), 155.6 (C), 133.8 (C), 133.0 (C), 131.8 (C), 121.5 (C), 118.8 (C), 102.7 (C), 33.9 (CH_2), 29.8 (CH_2), 28.7 (CH_2), 24.5 (CH_2). HRMS (ESI^-) m/z $[M - H]^-$ calcd for $C_{12}H_{11}ClNO_3$ 252.0433, found 252.0423.

*6-(3-Chloro-5-cyano-2-hydroxy-phenyl)-N-methyl-hexanamide (**21b**).* IR (neat, ν_{max}), cm^{-1} 3395, 2941, 2226 (CN), 1638, 1559, 1291, 1271. ^1H NMR (500 MHz, DMSO-d_6) δ 10.37 (br s, 1H), 7.76 (s, 1H), 7.67 (br s, 1H), 7.51 (s, 1H), 2.56 (t, J = 7.14 Hz, 2H), 2.52 (m, 3H), 2.01 (t, J = 7.2 Hz, 2H), 1.47 (m, 4H), 1.22 (m, 2H). ^{13}C NMR (126 MHz, DMSO-d_6) δ 172.9 (C), 155.6 (C), 133.2 (C), 133.0 (CH), 131.7 (CH), 121.5 (C), 118.8 (C), 102.6 (C5), 35.6 (CH_2), 29.9 (CH_2, 29.0 (CH_2), 28.8 (CH_2), 25.8 (CH_3), 25.5 (CH_2). HRMS-ESI m/z $[M + H]^+$ calcd for $C_{14}H_{17}ClN_2NaO_2$ 303.0871, found 303.0865.

*7-(3-Chloro-5-cyano-2-hydroxy-phenyl)-N-methyl-heptanamide (**22b**).* ^1H NMR (500 MHz, $CDCl_3$) δ 7.57 (d, J = 2.0 Hz, 1H), 7.40 (d, J = 2.0 Hz, 1H), 2.69 (s, 3H), 2.66 (t, J = 7.4 Hz, 2H), 2.16 (t, J = 7.6 Hz, 2H), 1.70−1.50 (m, 4H), 1.44−1.22 (m, 4H). ^{13}C NMR (126 MHz, $CDCl_3$) δ 172.4 (C), 155.2 (C), 132.9 (C), 132.1 (CH), 130.8 (CH), 121.0 (C), 117.8 (C), 102.8 (C). LRMS (ESI^+) $[M + H]^+$ 295.1 m/z.

*7-(3-Chloro-5-cyano-2-hydroxy-phenyl)-N,N-dimethyl-heptanamide (**23b**).* ^1H NMR (500 MHz, $CDCl_3$) δ 7.48 (s, 1H) 7.31 (s, 1H), 6.93 (br s, 1H), 3.00 (s, 3H), 2.96 (s, 3H), 2.69−2.59 (m, 2H), 2.34−2.24 (m, 2H), 1.67−1.52 (m, 4H), 1.42−1.29 (m, 4H). ^{13}C NMR (126 MHz, $CDCl_3$) δ 173.2 (C), 153.7 (C), 132.6 (CH), 132.0 (C), 130.5 (CH), 120.8 (C), 118.2 (C), 104.1 (C), 37.3 (CH_3), 35.5 (CH_3), 33.1 (CH_2), 29.9 (CH_2), 28.83 (CH_2), 28.80 (CH_2), 28.75 (CH_2), 24.6 (CH_2). LRMS (ESI^+) $[M + H]^+$ 309.1 m/z.

*3-Chloro-4-hydroxy-2,5-dimethyl-benzonitrile (**39**).* ^1H NMR (500 MHz, $CDCl_3$) δ 7.29 (s, 1H), 6.21 (br s, 1H), 2.53 (s, 3H), 2.25 (s, 3H). ^{13}C NMR (126 MHz, $CDCl_3$) δ 153.4 (C), 138.3 (C), 132.8 (CH), 124.2 (C), 120.8 (C), 118.0 (C), 104.9 (C), 18.7 (CH_3), 15.9 (CH_3). LRMS (ESI^-) $[M - H]^-$ 179.9 m/z.

*3-Chloro-5-ethyl-4-hydroxy-2-methyl-benzonitrile (**40**).* ^1H NMR (500 MHz, $CDCl_3$) δ 7.32 (s, 1H), 6.14 (s, 1H), 2.66 (q, J = 7.6 Hz, 2H), 2.54 (s, 3H), 1.21 (t, J = 7.6 Hz, 3H). ^{13}C NMR (126 MHz, $CDCl_3$) δ 153.0 (C), 138.3 (C), 131.4 (CH), 130.1 (C), 121.0 (C), 118.1 (C), 105.2 (C), 23.1 (CH_2), 18.8 (CH_3), 13.4 (CH_3). LRMS (ESI^-) $[M - H]^-$ 194.0 m/z.

*3-Chloro-4-hydroxy-2-methyl-5-propyl-benzonitrile (**41**).* ^1H NMR (500 MHz, $CDCl_3$) δ 7.29 (s, 1H), 6.21 (br s, 1H), 2.60 (t, J = 7.7 Hz, 2H), 2.53 (s, 3H), 1.62−1.56 (m, 2H), 0.94 (t, J = 7.3 Hz, 3H). ^{13}C NMR (126 MHz, $CDCl_3$) δ 153.2 (C), 138.3 (C), 132.2 (CH), 128.7 (C), 121.1 (C), 118.1 (C), 105.0 (C), 31.9 (CH_2), 22.2 (CH_2), 18.8 (CH_3), 13.7 (CH_3). LRMS (ESI^-) $[M - H]^-$ 207.9 m/z.

*5-Butyl-3-chloro-4-hydroxy-2-methyl-benzonitrile (**42**).* ^1H NMR (500 MHz, $CDCl_3$) δ 7.29 (s, 1H), 6.22 (br s, 1H), 2.61 (t, J = 7.8 Hz, 2H), 2.53 (s, 3H), 1.60−1.50 (m, 2H), 1.40−1.29 (m, 2H), 0.92 (t, J = 7.3 Hz, 3H). ^{13}C NMR (126 MHz, $CDCl_3$) δ 153.2 (C), 138.2 (C), 132.1 (CH), 128.9 (C), 121.1 (C), 118.1 (C), 105.0 (C), 31.2 (CH_2), 29.6 (CH_2), 22.3 (CH_2), 18.7 (CH_3), 13.8 (CH_3). LRMS (ESI^-) $[M - H]^-$ 221.9 m/z.

*3-Chloro-4-hydroxy-2-methyl-5-pentyl-benzonitrile (**43**).* ^1H NMR (500 MHz, $CDCl_3$) δ 7.30 (s, 1H), 6.10 (br s, 1H), 2.62 (t, J = 7.8 Hz, 2H), 2.54 (s, 3H), 1.65−1.52 (m, 2H), 1.37−1.27 (m, 4H), 0.89 (t, J = 6.8 Hz, 3H). ^{13}C NMR (126 MHz, $CDCl_3$) δ 153.1 (C), 138.2 (C), 132.2 (CH), 128.9 (C), 121.0 (C), 118.1 (C), 105.1 (C), 31.4 (CH_2), 29.9 (CH_2), 28.8 (CH_2), 22.4 (CH_2), 18.8 (CH_3), 14.0 (CH_3). LRMS (ESI^-) $[M - H]^-$ 235.9 m/z.

*3-Chloro-5-hexyl-4-hydroxy-2-methyl-benzonitrile (**44**).* ^1H NMR (500 MHz, $CDCl_3$) δ 7.29 (s, 1H), 6.18 (br s, 1H), 2.61 (t, J = 7.8 Hz, 2H), 2.53 (s, 3H), 1.61−1.50 (m, 2H), 1.38−1.23 (m, 6H), 0.92−0.84 (m, 3H). ^{13}C NMR (126 MHz, $CDCl_3$) δ 153.1 (C), 138.2 (C), 132.2 (CH), 128.9 (C), 121.0 (C), 118.1 (C), 105.0 (C), 31.6 (CH_2), 30.0 (CH_2), 29.0 (CH_2), 28.9 (CH_2), 22.6 (CH_2), 18.8 (CH_3), 14.1 (CH_3). LRMS (ESI^-) $[M - H]^-$ 249.9 m/z.

*3-Chloro-5-heptyl-4-hydroxy-2-methyl-benzonitrile (**45**).* ^1H NMR (500 MHz, $CDCl_3$) δ 7.30 (s, 1H), 6.11 (br s, 1H), 2.61 (t, J = 7.5, 2H), 2.54 (s, 3H), 1.61−1.53 (m, 2H), 1.35−1.22 (m, 8H), 0.88 (t, J = 6.2 Hz, 3H). ^{13}C NMR (126 MHz, $CDCl_3$) δ 153.1 (C), 138.2 (C), 132.2 (CH), 128.9 (C), 121.0 (C), 118.1 (C), 105.1 (C), 31.7 (CH_2), 30.0 (CH_2), 29.2 (CH_2), 29.09 (CH_2), 29.06 (CH_2), 22.6 (CH_2), 18.8 (CH_3), 14.1 (CH_3). LRMS (ESI^-) $[M - H]^-$ 264.0 m/z.

*5-Chloro-4-hydrox-5-octylbenzonitrile (**46**).* mp 60.1−61.8 °C. IR (neat, ν_{max}) cm^{-1} 3362, 2927, 2849, 2230 (CN), 1595, 1471, 1316, 1241, 1168. ^1H NMR (500 MHz, $CDCl_3$) δ 7.49 (s, 1H), 7.34 (s, 1H), 6.07 (s, 1H), 2.66 (m, 2H), 1.59 (m, 2H), 1.49−1.17 (m, 10H), 0.88 (m, 3H). ^{13}C NMR (126 MHz, $CDCl_3$) δ 153.4 (C), 132.9 (C), 132.2 (CH), 130.4 (CH), 120.5 (C), 118.2 (CH), 104.6 (C), 32.0 (CH_2), 30.3 (CH_2), 29.5 (CH_2), 29.5 (CH_2), 29.4 (CH_2), 29.2 (CH_2), 22.8 (CH_2), 14.3 (CH_3). HRMS (ESI^-) m/z $[M - H]^-$ calcd for $C_{15}H_{19}ClNO$ 264.1161, found 264.1151.

DOI: 10.1021/acsinfecdis.7b00218
ACS Infect. Dis. 2018, 4, 592−604

General Protocol for HATU Amide Coupling. Triethylamine (0.07 mL, 0.49 mmol) was added to a solution of carboxylic acid (0.2 mmol), HATU (0.08 g, 0.22 mmol), and amine (0.3 mmol) in acetonitrile (0.5 mL). The reaction was stirred at RT for 16 h. The reaction mixture was partitioned between ethyl acetate (5 mL) and water (5 mL). The organic layer was separated, washed with brine, dried over $MgSO_4$, filtered, and concentrated under reduced pressure. The residue was purified by flash silica chromatography eluting with petroleum ether to ethyl acetate in petroleum ether and then further purified by reverse phase chromatography eluting with water to MeOH if necessary to provide the amides described (29−67%).

*4-(3-Chloro-5-cyano-2-hydroxy-phenyl)-N-propyl-butanamide (**19b**).* ^{1}H NMR (500 MHz, $CDCl_3$) δ 10.73 (br s, 1H), 7.95 (br t, 1H), 7.73 (s, 1H), 7.45 (s, 1H), 2.97, (m, 2H), 2.56 (t, J = 7.4 Hz, 2H), 2.04 (t, J = 7.4 Hz, 2H), 1.71 (m, 2H), 1.37 (m, 2H), 0.81 (t, J = 7.4 Hz, 3H). ^{13}C NMR (126 MHz, $CDCl_3$) δ 172.0 (C), 155.4 (C), 132.8 (CH), 131.9 (C), 131.4 (CH), 121.2 (C), 118.3 (C), 102.12 (C), 40.3 (CH_2), 34.3 (CH_2), 29.1 (CH_2), 25.0 (CH_2), 22.3 (CH_2), 11.4 (CH_3). LRMS (ESI$^-$) $[M - H]^-$ 281.0 m/z.

*5-(3-Chloro-5-cyano-2-hydroxy-phenyl)-N-ethyl-pentanamide (**20b**).* IR (neat, ν_{max}) cm^{-1} 3353, 2945, 2231 (CN), 1649, 1560, 1462, 1174. ^{1}H NMR (500 MHz, DMSO-d_6) δ 10.16 (br 1H), 7.76−7.72 (br m, 2H), 7.49 (s, 1H), 3.02 (m, 2H), 2.58 (t, J = 6.3 Hz, 2H), 2.02 (t, J = 6.3 Hz, 2H), 1.45 (m, 4H), 0.96 (t, J = 7.2 Hz, 3H). ^{13}C NMR (126 MHz, DMSO-d_6) δ 172.1 (C), 156.0 (C), 133.0 (C), 132.9 (C), 131.7 (C), 121.6 (C), 118.9 (C), 102.1 (C), 35.7 (CH_2), 33.6 (CH_2), 29.9 (CH_2), 28.9 (CH_2), 25.4 (CH_2), 15.2 (CH_3). HRMS (ESI$^+$) m/z $[M + Na]^+$ calcd for $C_{14}H_{17}ClN_2NaO_2$ 303.0871, found 303.0865.

*Ethyl(2E)-3-5-cyano-2-hydroxy-4-methylphenyl)prop-2-enoate (**24**).* Potassium carbonate (0.98 g, 7.07 mmol) was added to a solution of 5-bromo-4-hydroxy-2-methyl-benzonitrile (0.50 g, 2.36 mmol) and ethyl acrylate (0.77 mL, 7.07 mL) in 1-methyl-2-pyrrolidinone (10 mL). [1,3-Bis(2,4,6-trimethylphenyl)-2,3-dihydro-1*H*-imidazol-2-ylidene]({2-[(dimethylamino)methyl]phenyl})palladiumylium chloride (SingaCycle) was added to the suspension, and the reaction was sealed under nitrogen and heated at 100 °C for 48 h. The reaction mixture was cooled to RT and diluted with ethyl acetate (50 mL) and filtered through a Celite pad. The filtrate was washed with 1 M HCl (aq) (25 mL), 0.5 M LiCl (aq) (25 mL), and brine (25 mL), dried over $MgSO_4$, filtered, and concentrated under vacuum. The residue was purified by flash silica chromatography eluting with petroleum ether to 15% ethyl acetate in petroleum ether to provide the title compound as a white solid (0.16 g, 29%). mp 142.6−149.8 °C. IR (neat, ν_{max}), cm^{-1} 2923, 2221, 1600, 1274. ^{1}H NMR (500 MHz, DMSO-d_6) δ 11.30 (br s, 1H) 8.07 (s, 1H), 7.73 (d, J = 16 Hz, 1H), 6.90 (s, 1H), 6.70 (d, J = 16 Hz, 1H), 4.17 (d, J = 7.2 Hz, 2H), 2.38 (s, 3H), 1.24 (t, J = 7.2 Hz, 3H). ^{13}C NMR (126 MHz, DMSO-d_6) δ 160.9 (C), 160.6 (C), 145.4 (C), 138.2 (CH), 134.4 (CH), 120.3 (C), 119.4 (CH), 118.5 (C), 118.1 (CH), 103.19 (CN), 60.4 (CH_2), 20.5 (CH_3), 14.6 (CH_3). HRMS (ESI$^-$) m/z $[M - H]^-$ calcd for $C_{13}H_{12}NO_3$ 230.0823, found 230.0814.

*Ethyl 3-(5-Cyano-2-hydroxy-4-methyl-phenyl)propanoate (**25**).* Triethylsilane (0.50 g, 4.32 mmol) was added to a solution ethyl (*E*)-3-(5-cyano-2-hydroxy-4-methyl-phenyl)-prop-2-enoate (0.10 g, 0.43 mmol) and 10% palladium on carbon (4 mg, 0.04 mmol) in ethanol (5 mL). The reaction mixture was stirred at RT for 16 h. Further triethylsilane (0.50 g, 4.32 mmol) was added, and the reaction mixture was stirred for a further 16 h. The nitrogen purged reaction mixture was filtered through a pad of Celite; the filtrate was partitioned between 1 M HCl (aq) (10 mL) and ethyl acetate (2 × 20 mL). The combined organics were separated, dried over $MgSO_4$, filtered, and concentrated under vacuum. The residue was purified by flash silica chromatography, eluting with petroleum ether to 50% ethyl acetate in petroleum ether to provide the title compound as a white solid (0.08 g, 77%). IR (neat, ν_{max}) cm^{-1} 3496, 2927, 2225 (CN), 1716, 1199, 1250. ^{1}H NMR (500 MHz, $CDCl_3$) δ 8.25 (s, 1H), 7.32 (s, 1H), 6.80 (s, 1H), 4.16 (q, J = 7.3 Hz, 2H), 2.84 (m, 2H), 2.70 (m, 2H), 2.44 (s, 3H), 1.25 (t, J = 7.3 Hz). ^{13}C NMR (126 MHz, CDCl3) δ 175.9 (C), 158.4 (C), 142.5 (C), 135.1 (CH), 125.8 (C), 119.0 (CH), 118.6 (C), 104.3 (C), 61.8 (CH_2), 35.0 (CH_2), 24.0 (CH_2), 20.1 (CH_3), 14.0 (CH_3). HRMS (ESI$^+$) m/z $[M + H]^+$ calcd for $C_{13}H_{15}NNaO_3$ 256.0944, found 256.0941.

*Ethyl 3-(3-Chloro-5-cyano-2-hydroxy-4-methyl-phenyl)-propanoate (**26**).* Sulfuryl chloride (0.02 mL, 0.26 mmol) was added to a solution of ethyl 3-(5-cyano-2-hydroxy-4-methyl-phenyl)propanoate (0.05 g, 0.21 mmol) in diethyl ether (1 mL). The reaction mixture was stirred at RT for 96 h. Further sulfuryl chloride (0.02 mL, 0.26 mmol) was added, and the reaction mixture was stirred for a further 16 h. The reaction mixture was partitioned between 1 M HCl (aq) (10 mL) and ethyl acetate (2 × 20 mL). The combined organics were separated, dried over $MgSO_4$, filtered, and concentrated under vacuum. The residue was purified by flash silica chromatography, eluting with petroleum ether to 25% ethyl acetate in petroleum ether to provide the title compound as a white solid (0.043 g, 75%). IR (neat, ν_{max}) cm^{-1} 3340, 2997, 2228 (CN), 1712, 1210, 1177. ^{1}H NMR (500 MHz, $CDCl_3$) δ 7.33 (s, 1H), 7.03 (s, 1H), 4.14 (q, J = 7.1 Hz, 2H), 2.94 (t, J = 7.1 Hz, 2H), 2.65 (t, J = 7.1 Hz, 2H), 2.55 (s, 3H), 1.24 (t, J = 7.1 Hz, 3H). ^{13}C NMR (126 MHz, CDCl3) δ 173.6 (C), 153.6 (C), 139.4 (C), 132.6 (CH), 126.7 (C), 117.9 (C), 105.3 (C), 61.1 (CH_2), 33.7 (CH_2), 25.3 (CH_2), 18.9 (CH_3), 14.2 (CH_3). HRMS (ESI$^-$) m/z $[M - H]^-$ calcd for $C_{13}H_{13}NO_3$ 266.0589, found 266.0576.

General Protocol for 1,5,7-Triazabicyclo[4.4.0]dec-5-ene Amide Formation. Amine (0.33 mmol) was added to a solution of 1,5,7-triazabicyclo[4.4.0]dec-5-ene (0.04 g, 0.26 mmol) and ester (0.13 mmol) in acetonitrile (0.5 mL). The reaction was stirred at RT for 5−40 h. The reaction mixture was partitioned between ethyl acetate (25 mL) and water (25 mL). The organic layer was separated, washed with brine, dried over $MgSO_4$, filtered, and concentrated under reduced pressure. The residue was purified by flash silica chromatography eluting with petroleum ether to 30−50% ethyl acetate in petroleum ether to provide the amides described (27−80%).

*6-(3-Chloro-5-cyano-2-methoxy-phenyl)-N-methyl-hexanamide (**21a**).* IR (neat, ν_{max}) cm^{-1} 3300, 2938, 2230 (CN), 1639, 1557, 1281. ^{1}H NMR (500 MHz, $CDCl_3$) δ 7.52 (d, J = 2.0 Hz, 1H), 7.37 (d, J = 2.0 Hz, 1H), 5.44 (br s, 1H), 3.88 (s, 3H), 2.80 (d, J = 5.0 Hz, 3H), 2.65 (t, J = 7.6 Hz, 2H), 2.17 (t, J = 7.6 Hz, 2H), 1.68 (m, 2H), 1.59 (m, 2H), 1.37 (m, 2H). ^{13}C NMR (126 MHz, $CDCl_3$) δ 173.5 (C), 158.4 (C), 139.4 (C), 132.6 (CH), 132.0 (CH), 129.1 (C), 117.8 (C), 108.6 (C), 61.3 (CH_3), 36.6 (CH_2), 30.1 (CH_2), 30.0 (CH_2), 29.1 (CH_2), 26.4 (CH_2), 25.5 (CH_3). HRMS (ESI$^+$) m/z $[M + Na]^+$ calcd for $C_{15}H_{19}ClN_2NaO_2$ 317.1027, found 317.1019.

DOI: 10.1021/acsinfecdis.7b00218
ACS Infect. Dis. 2018, 4, 592−604

*7-(3-Chloro-5-cyano-2-methoxy-phenyl)-N-methyl-heptanamide (**22a**).* ^{1}H NMR (500 MHz, $CDCl_3$) δ 7.52 (d, J = 2.0 Hz, 1H), 7.37 (d, J = 2.0 Hz, 1H), 5.41 (br s, 1H), 3.88 (s, 3H), 2.80 (d, J = 5.0 Hz, 3H), 2.64 (t, J = 7.9 Hz, 2H), 2.16 (t, J = 7.6 Hz, 2H), 1.69−1.52 (m, 4H), 1.42−1.28 (m, 4H). ^{13}C NMR (126 MHz, $CDCl_3$) δ 173.5 (C), 158.2 (C), 139.4 (C), 132.4 (C), 131.8 (C), 128.9 (C), 117.7 (C), 108.4 (C), 61.1 (CH_3), 36.6 (CH_2), 30.0 (CH_2), 29.9 (CH_2), 29.1 (CH_2), 29.0 (CH_2), 26.3 (CH_3), 25.5 (CH_2). LRMS (ESI$^+$) $[M + H]^+$ 309.1 m/z.

*7-(3-Chloro-5-cyano-2-methoxy-phenyl)-N,N-dimethyl-heptanamide (**23a**).* ^{1}H NMR (500 MHz, $CDCl_3$) δ 7.52 (s, 1), 7.37 (s, 1H), 3.88 (s, 3H), 2.99 (s, 3H), 2.94 (s, 3H), 2.64 (m, 2H), 2.30 (m, 2H), 1.70−1.53 (m, 4H), 1.43−1.32 (m, 4H). ^{13}C NMR (126 MHz, $CDCl_3$) δ 173.0 (C), 158.2 (C), 139.5 (C), 132.4 (C), 131.8 (C), 128.9 (C), 117.7 (C), 108.4 (C), 61.1 (CH_3), 37.3 (CH_3), 35.4 (CH_3), 33.2 (CH_2), 30.1 (CH_2), 29.9 (CH_2), 29.2 (CH_2), 29.2 (CH_2), 25.0 (CH_2). LRMS (ESI$^+$) $[M + H]^+$ 323.1 m/z.

*N-Butyl-3-(3-chloro-5-cyano-2-hydroxy-4-methyl-phenyl)-propenamide (**27**).* IR (neat, ν_{max}) cm^{-1} 3369, 2928, 2220 (CN), 1632, 1562, 1157. ^{1}H NMR (500 MHz, $CDCl_3$) δ 10.35 (br s, 1H), 7.24 (s, 1H), 5.55 (br s, 1H), 3.26 (m, 2H), 2.91 (m, 2H), 2.59 (m, 2H), 2.54 (s, 3H), 1.45 (m, 2H), 1.28 (m, 2H), 0.90 (t, J = 7.5 Hz, 3H). ^{13}C NMR (126 MHz, $CDCl_3$) δ 173.6 (C), 155.6 (C), 140.0 (C), 132.6 (CH), 127.4 (C), 123.9 (C), 118.3 (C), 104.0 (C), 39.9 (CH_2), 36.3 (CH_2), 31.4 (CH_2), 25.0 (CH_2), 19.9 (CH_2), 18.9 (CH_3), 13.6 (CH_3). HRMS (ESI$^+$) m/z $[M + Na]^+$ calcd for $C_{15}H_{19}ClN_2NaO_2$ 317.1027, found 317.1019.

AUTHOR INFORMATION

Corresponding Author

*E-mail: wards10@cardiff.ac.uk.

ORCID

Ryan A. West: 0000-0002-8068-9180

Author Contributions

All authors have given approval to the final version of the manuscript.

Notes

The authors declare no competing financial interest.

ACKNOWLEDGMENTS

We would like to acknowledge and thank Rima Palkar and Nahdiyah Ghafar for carrying out the *T. b. brucei* growth inhibition assays. This work was supported by the Biotechnology and Biological Sciences Research Council [Grant ref: BB/L017180/1] iCASE with Novartis Institute for Tropical Diseases.

ABBREVIATIONS

AAT, African animal trypanosomiasis; AF, ascofuranone; CCB, colletochlorin B; CNS, central nervous system; HAT, human African trypanosomiasis; LipE, lipophilic efficiency; MPO, multiparameter optimization; NECT, nifurtimox and eflornithine combination therapy; TAO, trypanosome alternative oxidase; *T. b. b.*, *Trypanosoma brucei brucei*; TBD, 1,5,7-triazabicyclo[4.4.0]dec-5-ene

REFERENCES

(1) World Health Organisation. (2013) *Control and surveillance of human African trypanosomiasis*, WHO, Geneva.

(2) Jacobs, R. T., Nare, B., and Phillips, M. A. (2011) State of the Art in African Trypanosome Drug Discovery. *Curr. Top. Med. Chem. 11* (10), 1255−1274.

(3) Stich, A., Ponte-Sucre, A., and Holzgrabe, U. (2013) Do we need new drugs against human African trypanosomiasis? *Lancet Infect. Dis. 13* (9), 733−734.

(4) Delespaux, V., and Dekoning, H. (2007) Drugs and drug resistance in African trypanosomiasis. *Drug Resist. Updates 10* (1−2), 30−50.

(5) Baker, N., de Koning, H. P., Mäser, P., and Horn, D. (2013) Drug resistance in African trypanosomiasis: the melarsoprol and pentamidine story. *Trends Parasitol. 29* (3), 110−118.

(6) Bruce, D. (1895) *Preliminary report on the tsetse fly disease or nagana in Zululand*, p 28, Bennet & Davis, Durban.

(7) Nagle, A. S., Khare, S., Kumar, A. B., Supek, F., Buchynskyy, A., Mathison, C. J. N., Chennamaneni, N. K., Pendem, N., Buckner, F. S., Gelb, M. H., et al. (2014) Recent Developments in Drug Discovery for Leishmaniasis and Human African Trypanosomiasis. *Chem. Rev. 114*, 11305.

(8) Matthews, K. R. (2005) The developmental cell biology of Trypanosoma brucei. *J. Cell Sci. 118*, 283−290.

(9) Wang, C. C. (1995) Molecular Mechanisms and Therapeutic Approaches to the Treatment of African Trypanosomiasis. *Annu. Rev. Pharmacol. Toxicol. 35* (1), 93−127.

(10) Barry, J. D., and McCulloch, R. (2001) Antigenic variation in trypanosomes: Enhanced phenotypic variation in a eukaryotic parasite. *Advances in Parasitology 49*, 1−70.

(11) Fevre, E. M., Wissmann, B. V., Welburn, S. C., and Lutumba, P. (2008) The Burden of Human African Trypanosomiasis. *PLoS Neglected Trop. Dis. 2* (12), e333.

(12) Wilson, S. G., Morris, K. R. S., Lewis, I. J., and Krog, E. (1963) The effects of trypanosomiasis on rural economy*. *Bull World Health Organ 28*, 595−613.

(13) Fairlamb, A. H. (2003) Chemotherapy of human African trypanosomiasis: Current and future prospects. *Trends Parasitol. 19*, 488−494.

(14) Pépin, J., and Milord, F. (1994) The treatment of human African trypanosomiasis. *Adv. Parasitol. 33*, 1−47.

(15) Kennedy, P. G. (2013) Clinical features, diagnosis, and treatment of human African trypanosomiasis (sleeping sickness). *Lancet Neurol. 12* (2), 186−194.

(16) Burri, C., and Brun, R. (2003) Eflornithine for the treatment of human African trypanosomiasis. *Parasitol. Res. 90* (S1), S49−S52.

(17) Menzies, S. K., Tulloch, L. B., Florence, G. J., and Smith, T. K. (2016) The trypanosome alternative oxidase: a potential drug target? *Parasitology*, 1−9, DOI: 10.1017/S0031182016002109.

(18) Nihei, C., Fukai, Y., and Kita, K. (2002) Trypanosome alternative oxidase as a target of chemotherapy. *Biochim. Biophys. Acta, Mol. Basis Dis. 1587* (2−3), 234−239.

(19) Chaudhuri, M., Ajayi, W., and Hill, G. C. (1998) Biochemical and molecular properties of the Trypanosoma brucei alternative oxidase. *Mol. Biochem. Parasitol. 95* (1), 53−68.

(20) Jeacock, L., Baker, N., Wiedemar, N., Mäser, P., and Horn, D. (2017) Aquaglyceroporin-null trypanosomes display glycerol transport defects and respiratory-inhibitor sensitivity. *PLoS Pathog. 13* (3), e1006307.

(21) Kido, Y., Shiba, T., Inaoka, D. K., Sakamoto, K., Nara, T., Aoki, T., Honma, T., Tanaka, A., Inoue, M., Matsuoka, S., et al. (2010) Crystallization and preliminary crystallographic analysis of cyanide-insensitive alternative oxidase from Trypanosoma brucei brucei. *Acta Crystallogr., Sect. F: Struct. Biol. Cryst. Commun. 66* (Pt 3), 275−278.

(22) Saimoto, H., Kido, Y., Haga, Y., Sakamoto, K., and Kita, K. (2013) Pharmacophore identification of ascofuranone, potent inhibitor of cyanide-insensitive alternative oxidase of Trypanosoma brucei. *J. Biochem. 153* (3), 267−273.

(23) West, R. A., Doherty, O. G. O., Askwith, T., Atack, J., Beswick, P., Laverick, J., Pennicott, L. E., Williams, G., and Ward, S. E. (2017) African trypanosomiasis : Synthesis & SAR enabling novel drug

DOI: 10.1021/acsinfecdis.7b00218
ACS Infect. Dis. 2018, 4, 592−604

discovery of ubiquinol mimics for trypanosome alternative oxidase. *Eur. J. Med. Chem. 141*, 676−689.
(24) Yabu, Y., Suzuki, T., Nihei, C. I., Minagawa, N., Hosokawa, T., Nagai, K., Kita, K., and Ohta, N. (2006) Chemotherapeutic efficacy of ascofuranone in Trypanosoma vivax-infected mice without glycerol. *Parasitol. Int. 55* (1), 39−43.
(25) Pardridge, W. M. (2005) The blood-brain barrier: Bottleneck in brain drug development. *NeuroRx 2* (1), 3−14.
(26) Wager, T. T., Hou, X., Verhoest, P. R., and Villalobos, A. (2010) Moving beyond Rules: The Development of a Central Nervous System Multiparameter Optimization (CNS MPO) Approach To Enable Alignment of Druglike Properties. *ACS Chem. Neurosci. 1* (6), 435−449.
(27) Casey, M. L., Kemp, D. S., Paul, K. G., and Cox, D. D. (1973) Physical organic chemistry of benzisoxazoles. I. Mechanism of the base-catalyzed decomposition of benzisoxazoles. *J. Org. Chem. 38* (13), 2294−2301.
(28) Kajigaeshi, S., Kakinami, T., Okamoto, T., Nakamura, H., and Fujikawa, M. (1987) Halogenation Using Quaternary Ammonium Polyhalides. IV. Selective Bromination of Phenols by Use of Tetraalkylammonium Tribromides. *Bull. Chem. Soc. Jpn. 60* (11), 4187−4189.
(29) Li, H., Zhong, Y.-L., Chen, C., Ferraro, A. E., and Wang, D. (2015) A Concise and Atom-Economical Suzuki−Miyaura Coupling Reaction Using Unactivated Trialkyl- and Triarylboranes with Aryl Halides. *Org. Lett. 17* (14), 3616−3619.
(30) Enache, L. A., Kennedy, I., Sullins, D. W., Chen, W., Ristic, D., Stahl, G. L., Dzekhtser, S., Erickson, R. A., Yan, C., Muellner, F. W., et al. (2009) Development of a Scalable Synthetic Process for DG-051B, A First-in-Class Inhibitior of LTA4H. *Org. Process Res. Dev. 13* (6), 1177−1184.
(31) Sabot, C., Kumar, K. A., Meunier, S., and Mioskowski, C. (2007) A convenient aminolysis of esters catalyzed by 1,5,7-triazabicyclo[4.4.0]dec-5-ene (TBD) under solvent-free conditions. *Tetrahedron Lett. 48* (22), 3863−3866.
(32) Ryckmans, T., Edwards, M. P., Horne, V. A., Correia, A. M., Owen, D. R., Thompson, L. R., Tran, I., Tutt, M. F., and Young, T. (2009) Rapid assessment of a novel series of selective CB2 agonists using parallel synthesis protocols: A Lipophilic Efficiency (LipE) analysis. *Bioorg. Med. Chem. Lett. 19* (15), 4406−4409.
(33) Kondreddi, R. R., Jiricek, J., Rao, S. P. S., Lakshminarayana, S. B., Camacho, L. R., Rao, R., Herve, M., Bifani, P., Ma, N. L., Kuhen, K., et al. (2013) Design, Synthesis, and Biological Evaluation of Indole-2-carboxamides: A Promising Class of Antituberculosis Agents. *J. Med. Chem. 56* (21), 8849−8859.
(34) Ng, P. S., Manjunatha, U. H., Rao, S. P. S., Camacho, L. R., Ma, N. L., Herve, M., Noble, C. G., Goh, A., Peukert, S., Diagana, T. T., et al. (2015) Structure activity relationships of 4-hydroxy-2-pyridones: A novel class of antituberculosis agents. *Eur. J. Med. Chem. 106*, 144−156.

DOI: 10.1021/acsinfecdis.7b00218
ACS Infect. Dis. 2018, 4, 592−604